frontiers | Research Topics

Brain stimulation: from basic research to clinical use

Edited by
Alia Benali, Ken-Ichiro Tsutsui, Friederike Pfeiffer and Masaki Sekino

Published in
Frontiers in Human Neuroscience
Frontiers in Behavioral Neuroscience

ISSN 1664-8714
ISBN 978-2-83250-757-5
DOI 10.3389/978-2-83250-757-5

About Frontiers

Frontiers is more than just an open access publisher of scholarly articles: it is a pioneering approach to the world of academia, radically improving the way scholarly research is managed. The grand vision of Frontiers is a world where all people have an equal opportunity to seek, share and generate knowledge. Frontiers provides immediate and permanent online open access to all its publications, but this alone is not enough to realize our grand goals.

Frontiers journal series

The Frontiers journal series is a multi-tier and interdisciplinary set of open-access, online journals, promising a paradigm shift from the current review, selection and dissemination processes in academic publishing. All Frontiers journals are driven by researchers for researchers; therefore, they constitute a service to the scholarly community. At the same time, the *Frontiers journal series* operates on a revolutionary invention, the tiered publishing system, initially addressing specific communities of scholars, and gradually climbing up to broader public understanding, thus serving the interests of the lay society, too.

Dedication to quality

Each Frontiers article is a landmark of the highest quality, thanks to genuinely collaborative interactions between authors and review editors, who include some of the world's best academicians. Research must be certified by peers before entering a stream of knowledge that may eventually reach the public - and shape society; therefore, Frontiers only applies the most rigorous and unbiased reviews. Frontiers revolutionizes research publishing by freely delivering the most outstanding research, evaluated with no bias from both the academic and social point of view. By applying the most advanced information technologies, Frontiers is catapulting scholarly publishing into a new generation.

What are Frontiers Research Topics?

Frontiers Research Topics are very popular trademarks of the *Frontiers journals series*: they are collections of at least ten articles, all centered on a particular subject. With their unique mix of varied contributions from Original Research to Review Articles, Frontiers Research Topics unify the most influential researchers, the latest key findings and historical advances in a hot research area.

Find out more on how to host your own Frontiers Research Topic or contribute to one as an author by contacting the Frontiers editorial office: frontiersin.org/about/contact

Brain stimulation: from basic research to clinical use

Topic editors

Alia Benali — Department of Cognitive Neurology, Hertie Institute for Clinical Brain Research, Germany

Ken-Ichiro Tsutsui — Tohoku University, Japan

Friederike Pfeiffer — University of Tübingen, Germany

Masaki Sekino — The University of Tokyo, Japan

Citation

Benali, A., Tsutsui, K.-I., Pfeiffer, F., Sekino, M., eds. (2022). *Brain stimulation: from basic research to clinical use*. Lausanne: Frontiers Media SA.

doi: 10.3389/978-2-83250-757-5

Table of contents

frontiers | Frontiers in Human Neuroscience

TYPE Editorial
PUBLISHED 28 November 2022
DOI 10.3389/fnhum.2022.1092165

OPEN ACCESS

EDITED AND REVIEWED BY
Mingzhou Ding,
University of Florida, United States

*CORRESPONDENCE
Alia Benali
alia.benali@uni-tuebingen.de

SPECIALTY SECTION
This article was submitted to Brain Imaging and Stimulation, a section of the journal Frontiers in Human Neuroscience

RECEIVED 07 November 2022
ACCEPTED 09 November 2022
PUBLISHED 28 November 2022

CITATION
Benali A, Tsutsui K-I, Sekino M and Pfeiffer F (2022) Editorial: Brain stimulation: From basic research to clinical use.
Front. Hum. Neurosci. 16:1092165.
doi: 10.3389/fnhum.2022.1092165

Editorial: Brain stimulation: From basic research to clinical use

Alia Benali[1]*, Ken-Ichiro Tsutsui[2], Masaki Sekino[3] and Friederike Pfeiffer[4]

[1]Section Computational Sensomotorics, Hertie Institute for Clinical Brain Research and Centre for Integrative Neurocience, University of Tuebingen, Tuebingen, Germany, [2]Laboratory of Systems Neuroscience, Graduate School of Life Sciences, Tohoku University, Sendai, Japan, [3]Department of Bioengineering, School of Engineering, The University of Tokyo, Tokyo, Japan, [4]Department of Neurophysiology, Institute of Physiology, Eberhard Karls University of Tuebingen, Tuebingen, Germany

KEYWORDS

TMS (transcranial magnetic stimulation), rTMS (repetitive transcranial magnetic stimulation), tDCS, vagus nerve stimulation, noninvasive, neuromodulation

Editorial on the Research Topic
Brain stimulation: From basic research to clinical use

The aim of this Research Topic was to show how broad the field of brain stimulation has become recently, including basic research and clinical application. Numerous brain stimulation methods are being investigated to serve as neuromodulatory techniques, treating a variety of neuropsychiatric or neurological disorders (Antal et al., 2022; Camacho-Conde et al., 2022; Siebner et al., 2022). They can be divided into noninvasive and invasive methods. Non-invasive brain stimulation includes transcranial magnetic stimulation (TMS), transcranial direct current stimulation (tDCS) and transcranial alternating current stimulation (tACS), transcranial electrical stimulation (tES) and non-invasive vagus nerve stimulation (VNS). Invasive brain stimulation consists of intracortical microstimulation (ICMS) and deep brain stimulation (DBS).

Most of the original articles published here focused on brain stimulation using TMS. This section started with an overview article by Ueno, the inventor of the figure-of-eight coil, who, together with Masaki Sekino, provided an overview on figure-of-eight coils and their geometric variations. Figure-of-eight coils are advantageous for focal, localized stimulation, and are therefore already widely used in clinical applications. In addition, it is possible to achieve stimulation of deeper brain regions with different geometries of the coils. In general, a trade-off between depth and focality must be made. Tan et al. used a special double-cone coil to stimulate the cerebellar vermis with iTBS and study cerebral cortical excitability in healthy subjects exerting a balance task. The results showed, that even a single iTBS session increased HbO2 concentration measured with fNIRS, in the supplementary motor area but not in the dorsal lateral prefrontal cortex, although both structures are crucial during balance tasks. Mori et al. used a figure-of-eight coil to stimulate the superficially located primary motor cortex (M1). They investigated the differences in analgesic effects of applying rTMS to M1 to treat neuropathic pain. Results from three extracted clinical trials showed that rTMS was more effective in patients with neuropathic pain in the upper limb than in patients with neuropathic pain in the lower

limb and face, thus the location of pain influences the analgesic effect of rTMS. Overall, TMS and various designs of figure-eight coils are a powerful tool to noninvasively investigate human neural networks. In daily clinical practice, attempts are made not only to stimulate focally or deeply with TMS, but also to shorten the duration of stimulation-time for the patient. This is more comfortable for the patient and economically favorable. One way to shorten the duration of stimulation was shown by the work of Matilainen et al., where active muscle contraction canceled the modulating effect of the interpulse intervals (IPIs) that are present in a resting muscle. The result suggested that IPIs as short as 2 s can be used to accelerate motor mapping with TMS in active muscles.

In general, most rTMS studies published here indicate that rTMS has a transient, short-lived effect on the network and that patient follow-up is necessary. Izuno et al. showed that the locally and transiently increased density of frontal sleep spindle activity in patients with major depressive episodes could be downregulated to baseline levels during the last half period of 10 consecutive rTMS sessions. The authors hypothesized that the increase was initially triggered by the high activity elicited by the high-frequency rTMS sessions and was then restored to baseline levels by an intrinsic homeostatic regulatory system between the cortex and thalamic loops. The clinico-cognitive correlation of this study with the rTMS-induced changes in sleep spindle density sheds light on the neuromodulatory effects of daily rTMS sessions on nocturnal sleep spindle activity.

A similar transient rTMS effect was observed by Fu et al., attempting to modulate network disorders in patients with refractory epilepsy with low-frequency rTMS over the vertex to achieve an antiepileptic effect. Almost all patients had visible motor seizures more than once per week during the ictal period. After stimulation, a positive result was obtained at the first follow-up, but it disappeared during the observation periods, indicating temporary antiepileptic efficacy for the patient and a necessity for sustained treatment.

Concerning rehabilitation, Brihmat et al. investigated 20 different rTMS protocols for their potential to improve functional outcomes after spinal cord injury. Preliminary results suggest benefits for motor and sensory recovery and are thought to be due to changes in corticospinal excitability and connectivity as well as cortical inhibition, altogether altering spinal circuits. Safety, tolerability and persistency need to be determined, and individually targeted rTMS interventions designed.

Could the rTMS therapy be improved in the long term by combining different brain stimulation techniques? Tang et al. demonstrated that electroacupuncture (EA) and TMS can modulate cerebral cortical excitability. Before EA, the right swallowing motor cortex of healthy subjects was more excitable by TMS than the left cortex at rest. After the EA, however, both cortices showed a modulation, with effects being more pronounced the right swallow motor cortex, and absent in the sham treatment group.

Geffen et al. investigated the effects of slow oscillatory (SO) tACS on motor cortical excitability with TMS, showing a significant increase in TMS-induced motor evoked potential amplitudes that persisted throughout the stimulation period. The increase was not simply due to anodal stimulation, because the acute effects of SO tACS were independent of phase and therefore do not support entrainment of endogenous slow oscillations as an underlying mechanism. These two studies showed that TMS can be combined with other brain stimulation methods, but the extent to which the combination prolongs the effects remains to be elucidated.

Importantly, not only positive effects and results supporting the hypothesis should be reported. The work of Rittweger et al. is a well-conceptualized paper, including the effects of sham treatment. In this study, rodent models of maternal immune activation (MIA) were used to answer the question: Is rTMS an alternative therapy for schizophrenia? MIA offspring are primarily impaired in behaviors requiring attentional decisions. iTBS reduced some behavioral deficits in MIA rats, but was not superior to sham stimulation, thus the handling itself had an effect. The authors describe small differences in processing experience between sham and MIA rats in the novel object recognition task but only when MIA rats were treated at juvenile age.

The second part of the publications dealed with non-invasive tES. Thereby, electrical currents are delivered to the brain with the aim of modulating neuronal activity. tDCS is widely used and applied to the left prefrontal cortex to elicit wide-ranging behavioral effects, including improved learning ability and vigilance. The neural mechanisms and repetitive stimulation have not yet been adequately explored. In their work, Sherwood et al., have investigated the effects of repetition and stimulation intensity of tDCS on cerebral perfusion [cerebral blood flow (CBF)]. Three groups (sham, tDCS of 1 or 2-mA) were stimulated and measured on three consecutive days. Resting CBF was quantified before and after stimulation using arterial spin-labeling MRI and then compared with the sham-condition. A distinct increase in CBF was only observed in the stimulation groups, depending on stimulation strength and number of pulses, suggesting that the neuronal effects of stimulation persisted for at least 24 h. Like rTMS, the tDCS-effects appear to be short-lived after a single stimulation but may produce a cumulative effect with repeated stimulation.

tDCS is a promising tool to improve and accelerate motor rehabilitation after stroke, but variability in clinical trials makes evidence-based clinical application difficult. One factor of its variability has been attributed to the unknown effects of stroke lesion conductance on stimulation intensity in targeted brain regions. Volume conductance models are promising tools for determining optimal stimulation settings, but the lesion volume is not considered in these models. Van der Cruijsen et al.

proposed a method combining MRI, EEG, and transcranial stimulation to experimentally estimate the conductance of cortical stroke lesions. They developed and tested an algorithm to estimate the conductance of stroke lesions. This development will increase the accuracy of models of volume conductance of stroke patients and may lead to improved and more effective configurations of transcranial electrical stimulation for this group of patients.

Markovic et al., summarized 30 articles considering tDCS and rTMS to modulate fear memory and extinction. Fear memory and extinction are impaired in anxiety disorders, post-traumatic stress disorder and obsessive-compulsive disorders. Studies in either healthy humans or the clinical population as well as animal models addressing tDCS or rTMS as therapeutic approaches to treat these disorders are discussed. Pattern, timing, and location of the stimulation are important parameters to consider in future noninvasive therapies to treat these disorders.

Nooristani et al., discussed the parameters of tES that need to be defined before applying tES to patients with difficulties in hearing, such as electrode positioning and stimulation patterns, and their effect on specific aspects of hearing, such as temporal and spectral processing or binaural integration and speech comprehension.

Mitsutake et al., reviewed the feasibility of noninvasive M1 anodal transcranial direct current stimulation to improve gait performance in stroke patients. Nine studies using comparable stimulation parameters, patients and readouts were analyzed for their efficiency when combining tDCS with repetitive gait training vs. subsequent gait training after the application of tDCS. The authors concluded that simultaneous application of anodal tDCS during repetitive gait training seems to improve walking abilities more.

Has brain stimulation been discussed with regards to aging? Siegert et al., screened a database of published articles on tDCS and analyzed 16 studies for their reported effects on cognitive abilities, declarative and working memory, in older patients. Depending on the task that should be improved and the condition of the patient, the area of the brain as well as stimulation parameters should be carefully chosen. Anodal tDCS applied to the left cortical hemisphere is recommended to improve age-associated cognitive decline. In addition, combination with cognitive training seems promising.

A third method of brain stimulation is the cranial nerve stimulation. Cranial nerves transmit information from the environment or sensations directly to the brain, determining and modulating brain function (Adair et al., 2020). Invasive and noninvasive methods of electrical cranial nerve stimulation are already being used in clinical, behavioral, and cognitive areas. Compared to previous methods, cranial nerve stimulation is unique in that it allows axon pathway-specific manipulation of brain circuits, including thalamo-cortical networks. VNS is already approved in the EU and US for the treatment of drug-resistant epilepsy, cluster headache, and depressive disorders.

Von Wrede et al. investigated the effect of taVNS in focal and generalized types of epilepsy and a control group. The results showed that short-term taVNS affects the global characteristics of EEG-derived functional brain networks differently in the epilepsy groups than in the control group, and taVNS-induced changes in global network characteristics differed significantly between epilepsy types. No discernible spatial pattern was detected on the local network scale, indicating a rather nonspecific and generalized change in brain activity. The effects of such a nonpharmaceutical intervention need further investigation.

taVNS is unapproved as a treatment for stroke-associated dysphagia. After stroke, dysphagia may occur and is probably the most important factor for aspiration pneumonia, malnutrition, and dehydration. The vagus nerve, along with other cranial nerves, plays an important motor and sensory role in the regulation of swallowing. Long et al. investigated the effect of taVNS on cortical white matter and dysphagia symptoms in a rodent stroke model (cerebral ischemia). The results revealed that taVNS effectively improves dysphagia symptoms, increases remyelination, induces angiogenesis, and inhibits inflammatory response in the white matter.

Yu et al. reviewed the potential of closed-loop taVNS systems to influence and balance the central and peripheral nervous systems as well as the autonomic nervous system. taVNS is already applied in a disease-oriented way: motor-activated taVNS for upper limb rehabilitation, and respiratory-gated auricular vagal afferent nerve stimulation for pain/migraine patients. The authors further discussed the potential of additional future applications to treat neurological disorders, cardiovascular diseases, or diabetes.

Unlike noninvasive brain stimulation methods, invasive stimulation methods are more focal but require neurosurgery. Li et al. addressed the prevention and treatment of hardware-related infections during DBS surgery. The authors showed that the intraoperative irrigation with hydrogen dioxide solution during the implantation of the implantable pulse generator (IPG) reduced the incidence of primary infections. For late-infections (after 3 months), the authors developed a strategy called Isa that helps to prevent the occurrence of secondary IPG infections.

The other two publications focused on ICMS in humans and rats.

Investigations on humans are not ethically approved and can only be performed with restrictions. In the present case study by Long et al., intracranial electrodes were implanted in a 30-year-old female patient to localize the source of drug-resistant seizures. The results of the direct cortical stimulations were recorded with a stereo-EEG. The authors were able to elicit two types of auditory hallucinations and confirmed hierarchical processing of auditory information in humans.

The goal of cortical neuroprosthetics is to feed sensory information directly into the cortical network as precisely as possible. However, sensory processing is dependent on behavioral context. Therefore, a particular behavioral context may alter stimulation effects and thus perception. In the study by Butovas and Schwarz, rats were operantly conditioned to move a whisker in a target-specific manner. The authors were able to investigate the effect of a passive or active touch (the absence or presence of a whisker movement) at the cortical level and gain a deeper understanding of the underlying mechanism.

Finally, Liu et al. summarized recent advances in adjusting second-generation brain stimulation techniques that aim at neuromodulation in humans. Noninvasive focused ultrasound did not only alter neuronal activity and influenced behavior but was also shown to cause responses at the molecular level. Temporal interference stimulation can reach deep brain regions noninvasively and is feasible to precisely regulate subcortical structures, influence several cell types and is a promising future alternative for deep brain stimulation. Near-infrared optogenetic stimulation requires the insertion of responsive nanoparticles in the target cells that respond to the near-infrared light. Thus, it is minimally invasive but offers the possibility to activate specific cells. These approaches would provide the possibility to modulate neural activity in a more targeted way, but still need a lot of investigation before application in humans would be possible.

Overall, noninvasive methods of brain stimulation are already used as therapy for certain neurological disorders but hold promise for many additional and more specific applications in the future. Researchers are working hard to improve the techniques, refine the results, and understand the underlying mechanisms.

Author contributions

All authors listed have made a substantial, direct, and intellectual contribution to the work and approved it for publication.

Funding

This work was supported by DFG, Germany, Grant No. BE 6048/2-1 (to AB). FP has received funding from the European Union's Horizon 2020 research and innovation program under the Marie Sklodowska-Curie grant agreement No. 845336 NG2-cells.

Conflict of interest

The authors declare that the research was conducted in the absence of any commercial or financial relationships that could be construed as a potential conflict of interest.

Publisher's note

All claims expressed in this article are solely those of the authors and do not necessarily represent those of their affiliated organizations, or those of the publisher, the editors and the reviewers. Any product that may be evaluated in this article, or claim that may be made by its manufacturer, is not guaranteed or endorsed by the publisher.

References

Adair, D., Truong, D., Esmaeilpour, Z., Gebodh, N., Borges, H., Ho, L., et al. (2020). Electrical stimulation of cranial nerves in cognition and disease. *Brain Stimul.* 13, 717–750. doi: 10.1016/j.brs.2020.02.019

Antal, A., Luber, B., Brem, A.K., Bikson, M., Brunoni, A.R., Cohen Kadosh, R., et al. (2022). Non-invasive brain stimulation and neuroenhancement. *Clin. Neurophysiol. Pract* 7, 1.46–165. doi: 10.1016/j.cnp.2022.05.002

Camacho-Conde, J. A., Del Rosario Gonzalez-Bermudez, M., Carretero-Rey, M., and Khan, Z. U. (2022). Therapeutic potential of brain stimulation techniques in the treatment of mental, psychiatric, and cognitive disorders. *CNS Neurosci. Ther.* 28, 5–18. doi: 10.1111/cns.13769

Siebner, H.R., Funke, K., Aberra, A.S., Antal, A., Bestmann, S., Chen, R., et al. (2022). Transcranial magnetic stimulation of the brain: what is stimulated? - A consensus and critical position paper. *Clin. Neurophysiol.* 140, 59–97. doi: 10.1016/j.clinph.2022.04.022

frontiers in Human Neuroscience

SYSTEMATIC REVIEW
published: 22 March 2021
doi: 10.3389/fnhum.2021.655947

A Systematic Review on the Effect of Transcranial Direct Current and Magnetic Stimulation on Fear Memory and Extinction

Vuk Marković[1,2], *Carmelo M. Vicario*[3*†], *Fatemeh Yavari*[1], *Mohammad A. Salehinejad*[1] and *Michael A. Nitsche*[2,4†]

[1] Department of Psychology and Neurosciences, Leibniz Research Centre for Working Environment and Human Factors, Dortmund, Germany, [2] International Graduate School of Neuroscience, Ruhr-University-Bochum, Bochum, Germany, [3] Department of Cognitive Science, University di Messina, Messina, Italy, [4] Department of Neurology, University Medical Hospital Bergmannsheil, Bochum, Germany

OPEN ACCESS

Edited by:
Ken-Ichiro Tsutsui,
Tohoku University, Japan

Reviewed by:
Joaquim Pereira Brasil-Neto,
Unieuro, Brazil
Vera Moliadze,
University Medical Center
Schleswig-Holstein, Germany

***Correspondence:**
Carmelo M. Vicario
cvicario@unime.it

[†] These authors have contributed equally to this work

Specialty section:
This article was submitted to Brain Imaging and Stimulation, a section of the journal Frontiers in Human Neuroscience

Received: 19 January 2021
Accepted: 25 February 2021
Published: 22 March 2021

Citation:
Marković V, Vicario CM, Yavari F, Salehinejad MA and Nitsche MA (2021) A Systematic Review on the Effect of Transcranial Direct Current and Magnetic Stimulation on Fear Memory and Extinction. Front. Hum. Neurosci. 15:655947. doi: 10.3389/fnhum.2021.655947

Anxiety disorders are among the most prevalent mental disorders. Present treatments such as cognitive behavior therapy and pharmacological treatments show only moderate success, which emphasizes the importance for the development of new treatment protocols. Non-invasive brain stimulation methods such as repetitive transcranial magnetic stimulation (rTMS) and transcranial direct current stimulation (tDCS) have been probed as therapeutic option for anxiety disorders in recent years. Mechanistic information about their mode of action, and most efficient protocols is however limited. Here the fear extinction model can serve as a model of exposure therapies for studying therapeutic mechanisms, and development of appropriate intervention protocols. We systematically reviewed 30 research articles that investigated the impact of rTMS and tDCS on fear memory and extinction in animal models and humans, in clinical and healthy populations. The results of these studies suggest that tDCS and rTMS can be efficient methods to modulate fear memory and extinction. Furthermore, excitability-enhancing stimulation applied over the vmPFC showed the strongest potential to enhance fear extinction. We further discuss factors that determine the efficacy of rTMS and tDCS in the context of the fear extinction model and provide future directions to optimize parameters and protocols of stimulation for research and treatment.

Keywords: non-invasive brain stimulation, fear memory, dorsolateral prefrontal cortex, ventromedial prefrontal cortex, repetitive transcranial magnetic stimulation, fear extinction

INTRODUCTION

Anxiety disorders are among the most prevalent mental disorders (Kessler et al., 2009; Bandelow and Michaelis, 2015). With 3.4% (264 million) of the global population affected (WHO, 2017), 16.6% lifetime prevalence (Remes et al., 2016), and an increased number of affected patients due to population aging and growth (WHO, 2017), anxiety disorders have a relevant impact on patients and societies worldwide. Accordingly, disease burden led to a total of 24.6 million years lived with this disability (YLD) in 2015 (WHO, 2017), unemployment and loss of productivity at work,

reduced quality of life (Kessler et al., 2009; Simpson et al., 2010; Remes et al., 2016; Martino et al., 2019), higher risk of mortality (Van Hout et al., 2004), and vast financial burden (Andlin-Sobocki and Wittchen, 2005; Kessler et al., 2009; Wittchen et al., 2011). Analysis of the efficacy of currently available routine treatments, such as pharmacological treatment with serotonin reuptake inhibitors (SRIs), and cognitive-behavioral therapy, shows that about a fifth of the patients terminate treatment prematurely, one third is classified as non-responders, and complete recovery is uncommon (Taylor et al., 2012). The development of more efficient therapies is thus required, which could in turn lead to improved well-being of the patients, and reduction of societal costs.

A large number of studies use the fear extinction model as a model for studying the psychopathology of anxiety disorders, and therapeutic mechanisms (Milad et al., 2014; VanElzakker et al., 2014). In this model, which is based on Pavlovian fear conditioning, participants undergo different phases of learning. During the acquisition phase, a neutral stimulus (e.g., blue light) is paired with a biologically potent aversive stimulus (unconditioned stimulus (US), e.g., electrical shock) which provokes a fear response. After repeated presentation and pairing, the neutral stimulus becomes the conditioned stimulus (CS), with a potential to provoke the respective fear response on its own. In the extinction phase, participants are exposed to the CS without US, and gradually, fear responses decline and, at the end, are extinguished. Extinction recall, as the final phase, is assessed typically the following day. In this phase, participants are again exposed to the CS without US presentation in order to evaluate the retention of extinction memory. Beyond these classical protocols, recently virtual reality (VR) approaches have been introduced, which have the potential to improve the ecological validity of respective procedures (Huff et al., 2010; Maples-Keller et al., 2017).

Fear extinction is most often measured by several psychophysiological parameters, such as skin-conductance response (SCR), heart rate response (HRR), or fear-potentiated startle (FPS; electromyography), which monitor vegetative responses, i.e., enhanced sympathetic tone, to the respective stimuli. SCR, HRR, and FPS are enhanced during fear acquisition, but reduced by fear extinction (Hamm and Vaitl, 1996; Milad et al., 2005; Norrholm et al., 2006; Hein et al., 2011). Beyond these vegetative parameters, also psychological measures, such as US-expectancy ratings (i.e., the prediction that the CS would be followed by the US) are obtained, which add a cognitive component to respective outcome measures (Zuj et al., 2018). In animal models, the fear response is often measured through freezing behavior as an indicator of anxiety-like behavior (Richmond et al., 1998; Chang et al., 2009; Roelofs, 2017).

Providing an exhaustive overview of the neural circuits involved in fear acquisition and extinction is beyond the scope of this review and we will focus only on the core brain structures and their role in the above-mentioned process. More elaborated overviews can be found elsewhere (see, Herry et al., 2010; Knapska et al., 2012; Milad and Quirk, 2012; Tovote et al., 2015). Neural circuits of fear acquisition and extinction include several areas of the brain, such as the amygdala, ventromedial prefrontal cortex (vmPFC), dorsolateral prefrontal cortex (dlPFC), dorsal anterior cingulate cortex (dACC), insula and hippocampus. Different parts of the amygdala are considered as crucial for the acquisition, expression and extinction of fear (Barad et al., 2006; Myers and Davis, 2007). Signals from the US and CS converge in the basolateral complex (BLA) of the amygdala, which processes those stimuli and sends its output to the central nucleus (CEA) (Barad et al., 2006). Neurons in the central nucleus initiate physiological and behavioral response characteristics of fear (Sah and Westbrook, 2008). The intercalated (ITC) amygdala neurons are relevant for extinction of conditioned fear (i.e., ITC neurons receive information about the CS from the BLA and have inhibitory projections to the CEA) (Likhtik et al., 2008). In accordance, neuroimaging studies in humans show enhanced activation of the amygdala during acquisition of a conditioned fear response, whereas during extinction training, its activity gradually diminishes (Phelps et al., 2004; Milad et al., 2007). Therefore, it can be concluded that inputs from the US and CS converge in the BLA during fear conditioning, are processed and sent to the CEA, which initiates fear-related physiological and behavioral responses. ICT neurons of the amygdala contribute to fear extinction via their inhibitory projections to the CEA.

Apart from the amygdala, the anterior cingulate cortex (ACC) has a role in expression of fear responses. Multichannel unit recordings in animal models showed that activity of pre-limbic cortex (PL) neurons, the homolog of the dorsal ACC (dACC) in humans, correlates with the expression of fear (Burgos-Robles et al., 2009). Furthermore, the resting state metabolism of this area predicts the magnitude of conditioned fear responses (Linnman et al., 2011) in humans. In accordance, the persistence of PL responses after extinction training was associated with a failure to express extinction memory in rats (Burgos-Robles et al., 2009). Furthermore, ontogenetic methods have shown that PL activity is not critical for the expression of extinction memory (Kim et al., 2016). For the insula, higher BOLD reactivity was related to greater SCRs (Linnman et al., 2011) and greater thickness of this area was related to larger conditioned responses during fear acquisition (Hartley et al., 2011). Moreover, a meta-analysis by Stark et al. (2015) suggests that the right anterior insula could be a core region of the network undergoing changes after experiencing a traumatic or painful event.

In summary, amygdala, the ACC, and the insular cortex are crucial structures in the acquisition of aversive conditioning (see, Sehlmeyer et al., 2009). Furthermore, the hippocampus is involved in fear conditioning. It is activated during contextual and simple cue fear conditioning in humans and animals, and activates or inhibits fear expression depending on the context of learning (VanElzakker et al., 2014; Sevenster et al., 2018). Regarding the prefrontal cortex, research in animal models suggests that the dlPFC is important to promote the expression of learned fear (Morgan et al., 1993; Quirk et al., 2006).Furthermore, a recent study (Kroes et al., 2019) in six patients with dlPFC lesions and 19 control participants provided evidence that the dlPFC might be essential in providing a cognitive regulation of subjective fear to threatening stimuli. Moreover, it was suggested that the dlPFC has a role in detection of uncertainty, and

similar to the insula and ACC, shows higher activity during fear conditioning, since higher activity in these areas is detected when the CS-US pairing is uncertain (Dunsmoor et al., 2007, 2008).

The vmPFC is a central area involved in mediating mechanisms of extinction learning and recall. It is activated during fear extinction, but not acquisition (Phelps et al., 2004; Milad et al., 2007). Moreover, a lesion of the infralimbic (IL) cortex, the homolog of the human vmPFC, impairs recall of fear extinction in rodents (Quirk et al., 2000), and the IL is activated during extinction recall in rats (Milad et al., 2007). In accordance, a recently conducted optogenetics study by Do-Monte et al. (2015) showed that activation, contrary to silencing, of the IL during extinction learning improves subsequent retrieval and, further, this structure is relevant for controlling the expression of fear after extinction (Kim et al., 2016). The vmPFC/IL sends direct projections to ICT neurons, and thus controls the output of the amygdala during extinction (Quirk and Gehlert, 2003; Sah and Westbrook, 2008). In accordance, Motzkin et al. (2015) found that vmPFC lesions of patients were associated with increased right amygdala reactivity to aversive stimuli, suggesting disinhibition of the amygdala. Therefore, it has been proposed that the vmPFC is responsible for top-down regulation of the amygdala (Milad et al., 2007), and that dysfunctions of vmPFC-amygdala connectivity may mediate the susceptibility to and/or maintenance of anxiety disorders (Milad et al., 2014). Moreover, the vmPFC is an important target of the hippocampus in context-dependent expression of fear extinction memory (Kalisch et al., 2006; Milad et al., 2007).

Anxiety disorders, post-traumatic stress disorder (PTSD) and obsessive-compulsive disorder (OCD), show deficits in fear extinction and functionality of the neural circuits discussed above (Milad et al., 2014). Patients with panic disorder (PD) exhibit larger SCR in response to conditioned stimuli during extinction, and maintain a more negative evaluation of CSs, as compared to healthy controls (Michael et al., 2007). In accordance, individuals with PTSD show larger responses to CSs during acquisition and extinction with respect to SCR, EMG and HRR in comparison to healthy individuals (see, Milad et al., 2014; VanElzakker et al., 2014). Impaired extinction recall is documented also in OCD patients (Milad et al., 2013; McLaughlin et al., 2015). Several studies have found alterations of specific fear- and extinction-relevant neural circuits in these diseases. For patients with generalized anxiety disorder (GAD), deficient vmPFC activity has been observed during fear-related task performance (Greenberg et al., 2013; Via et al., 2018). Individuals with PTSD show structural and functional deficits of various fear-related areas of the brain, including amygdala, PFC and hippocampus. Amygdala responsivity is positively associated with symptom severity in PTSD (Shin et al., 2006), and a smaller volume of the amygdala has been described in individuals with PTSD (Morey et al., 2012). Furthermore, during extinction recall, PTSD patients show reduced activation of the vmPFC and hippocampus, but increased activation of the dACC (Milad et al., 2009). With respect to specific phobias, patients with spider phobia show increased activity of the insula and reduced activity of the vmPFC in automatic emotion regulation (Hermann et al., 2009). In accordance, extinction-based exposure therapy of specific phobias reduces amygdala hyperactivity (Goossens et al., 2007).

Advances in neuroscience methods have the potential to enrich our understanding of the basic neural mechanisms of anxiety disorders and, consequently, lead to the development of new treatment options, and protocols. The above-mentioned studies enable the identification of candidate areas critically involved in respective processes, and thus identification of targets for new interventions such as brain stimulation approaches. In this connection, recent reviews showed that non-invasive methods of brain stimulation (NIBS), including transcranial direct current stimulation (tDCS) and repetitive transcranial magnetic stimulation (rTMS), are promising therapeutic approaches for anxiety disorders (Vicario et al., 2019, 2020a) as well as other psychiatric conditions including pediatric populations (see Vicario and Nitsche, 2013a,b, 2019; Salehinejad et al., 2019, 2020).

tDCS modulates cortical excitability with direct electrical currents that pass through the cerebral cortex (Nitsche and Paulus, 2000; Nitsche et al., 2003, 2008). Electrical currents (1 $\sim$ 2 mA) are delivered via two or more electrodes of opposite polarities (i.e., anode and cathode) placed on the scalp. tDCS does not generate action potentials, but instead modulates resting neuronal membrane potentials at subthreshold levels (Nitsche and Paulus, 2000). Anodal stimulation increases cortical excitability, while cathodal stimulation decreases it (Stagg and Nitsche, 2011) during stimulation, and stimulation within a certain duration and intensity range elicits after-effects, which can last from 90 min to more than 24 h (Nitsche and Paulus, 2001; Monte-Silva et al., 2013; Agboada et al., 2020). Even though physiological mechanisms of tDCS-induced plasticity are not yet fully understood, it is assumed that its effects are based on long-term potentiation–(LTP) and long-term depression-like (LTD) mechanisms, with primarily glutamatergic processes involved, and that GABA modulation has a gating function on respective plasticity (Stagg and Nitsche, 2011; Yavari et al., 2018). tDCS has a potential to modulate cognitive, motor, perceptual and emotional processes, based on respective physiological alterations (Yavari et al., 2018).

rTMS is another non-invasive brain stimulation method for studying neuroplasticity and modulating cortical excitability (Pascual-Leone et al., 1998; Hallett, 2007). Unlike tDCS, rTMS uses magnetic fields to induce electrical discharges of respective target areas of the brain. Trains of magnetic pulses at varying frequencies are delivered via a coil positioned on the scalp. In general, low frequency stimulation ($</=$1 Hz) has inhibitory effects, while high frequency stimulation ($>$5 Hz) results in excitatory effects (Klomjai et al., 2015). Similar to tDCS, it is assumed that rTMS after-effects are based on LTP- and LTD-like mechanisms of synaptic plasticity (Hallett, 2007; Lefaucheur et al., 2014). Deep TMS is similar to conventional rTMS, but stimuli are conducted via an H-coil, which is suggested to enable stimulation of deeper cerebral regions (Levkovitz et al., 2015). Theta burst stimulation (iTBS) is a form of patterned rTMS with stimulation delivered in repetitive bursts of 50 Hz five times per second, which delivers similar plasticity responses as rTMS, but via shorter stimulation protocols (Huang et al., 2005; Di Lazzaro

et al., 2011; Bakker et al., 2015). Due to improved knowledge of the neural circuits outlined above, the availability of interventions to tackle respective circuits in humans, and considering the need for adjunctive treatment protocols, NIBS methods are attractive candidates for modulating fear and extinction memory. Here we review studies related to fear and extinction memory and NIBS in clinical and non-clinical samples, as well as in human and animal models, to give an overview about the state of the art, and derive hypotheses about future developments in this field, with respect to optimization and mechanisms involved.

METHODS

Inclusion and Exclusion Criteria

To select papers with sound quality, only peer-reviewed published papers were included in this review. Inclusion criteria were: (1) research articles in healthy and clinical samples, as well as research in animal models published in English language; (2) research articles based on fear memory and extinction (including studies that used exposure therapy protocols), which employed non-invasive brain stimulation methods (i.e., tDCS, and TMS); (3) research articles with a sufficiently detailed description of respective intervention protocols (e.g., duration, intensity/frequency, experimental design), and also case studies. Exclusion criteria: (1) research articles in other than English language; (2) research articles that are not based on fear extinction and exposure protocols in combination with NIBS methods; (3) review articles, abstracts and commentaries.

Search Strategy, Information Sources, and Study Selection

The procedure was conducted by one of the authors (VM) in accordance with the guidelines of Preferred reporting items for systematic reviews and meta-analyses (PRISMA) (Moher et al., 2009) (for details, see **Figure 1**). An extensive search was conducted via PubMed and Google Scholar databases. Key words used in the search were: "transcranial direct current stimulation" OR "transcranial magnetic stimulation" AND "fear extinction" OR "fear memory" OR "exposure therapy," which led to six pairs of key words. Initially, 1,078 records were identified. After screening and removing duplicates, 88 studies remained eligible for the review. "Transcranial direct current stimulation" and "fear memory" led to eight results (six of these were excluded; four did not use fear conditioning/extinction or exposure protocols, and two were reviews). "Transcranial magnetic stimulation" and "fear memory" led to four results, three studies were excluded because they were not based on fear conditioning/extinction or exposure protocols, and one was a review; "transcranial direct current stimulation" and "fear extinction" led to 33 results (21 of these were excluded; six did not use fear extinction or exposure protocols, two did not use brain stimulation methods, two of these were abstracts, two were commentaries, one was not written in English, and eight were reviews), "transcranial magnetic stimulation" and "fear extinction" lead to 22 results (14 of these were excluded; two were abstracts, eight did not use fear conditioning/extinction or exposure protocols, and four were reviews), "transcranial direct current stimulation" and "exposure therapy" led to five results (four were excluded; one did not use fear conditioning/extinction or exposure protocols, one did not use brain stimulation methods and two were reviews). "Transcranial magnetic stimulation" and "exposure therapy" led to 15 results (13 were excluded; five studies did not use fear conditioning/extinction or exposure protocols, four were reviews, three did not use brain stimulation methods, and one was an abstract). Five more studies were identified through other sources (i.e., research articles) resulting in 30 studies included in this review. Research of the records was conducted until 1st of March 2020. In addition, a study by Ney et al. (2021) was published recently and included in the review.

Outcome Variables

Major outcome variables in fear memory studies (both tDCS and TMS studies) were skin-conductance response (SCR), self-reported fear, anxiety and stress inventories, visual analog scales and approach-avoidance tasks (see **Table 1** for more details). In animal studies, fear memory (short-term and long-term contextual memory, auditory fear memory) was measured by freezing and latency to freezing behaviors (see **Table 2**). In fear extinction studies conducted in healthy humans (both tDCS and TMS studies), respective outcome measures were again SCR, fear potentiated startle, approach-avoidance tasks, and self-report scales of fear. In the clinical population, outcome variables were most frequently the symptoms measured by self-report scales and inventories of respective disorders (PTSD, OCD, specific phobia) (see **Tables 1**, **3**, for details). In animal studies, fear extinction was measured similarly to fear memory by freezing and latency to freezing as well as the sensitized fear test and object recognition task (see **Table 4** for details).

RESULTS

Effects of tDCS on Fear Memory

Effects of tDCS on Fear Memory in Animal Models

Four studies applied tDCS in animal models with the aim to modulate fear memory (**Table 2**). Abbasi et al. (2017) performed a study in mice that received anodal, or cathodal tDCS for 20 or 30 min at an intensity of 0.2 mA, or sham stimulation over the left prefrontal cortex. tDCS was delivered a few minutes before fear conditioning with an electrical shock. Twenty-four hours later, animals were tested in a contextual fear memory test (absence of CS and US, but context of fear conditioning), and a cued fear memory test (different context, CS presented). Several measures of anxiety-like behaviors were assessed (i.e., latency to freezing, duration of freezing, locomotor activity). Anodal and cathodal tDCS impaired acquisition of contextual and cued fear memory, largely independent from the respective stimulation duration (**Table 2**).

In three other studies, the impact of priming tDCS 1 day before fear conditioning or application of tDCS after fear conditioning was explored, with a specific dedication to the re-establishment of fear memory compromised by pharmacological interventions. Manteghi et al. (2017) applied anodal or sham

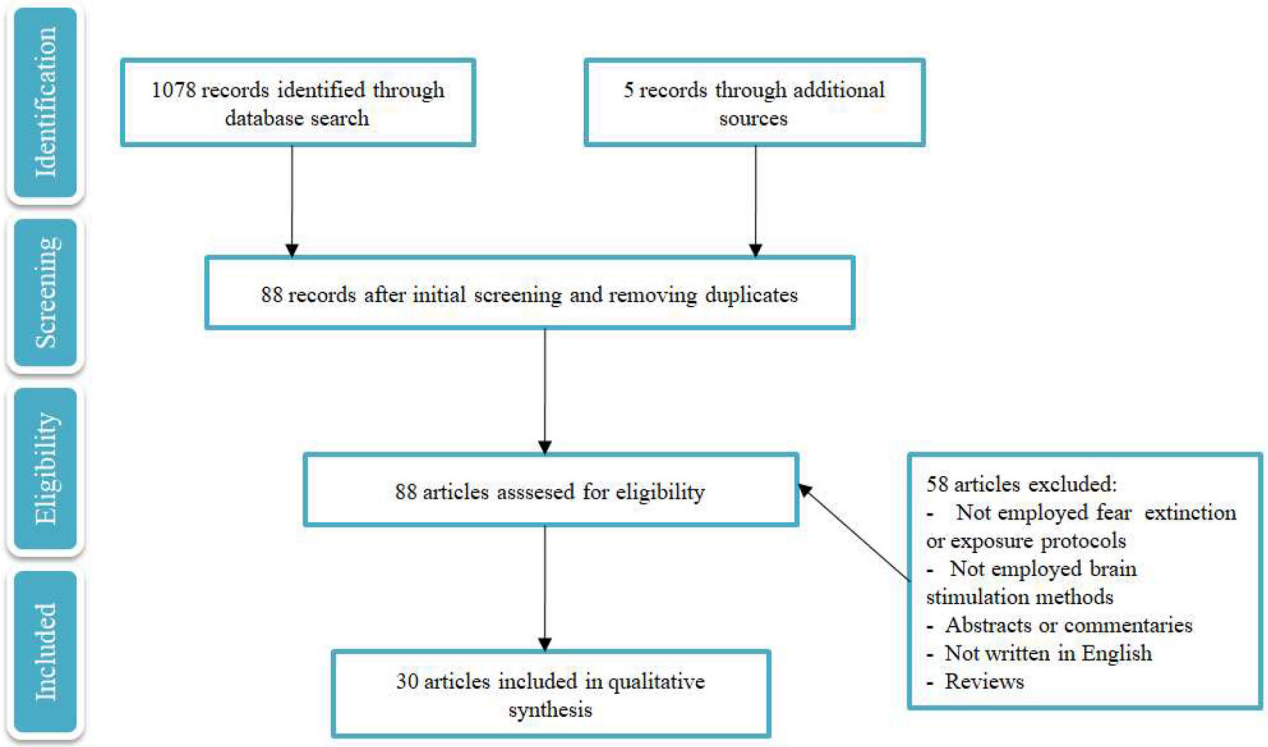

FIGURE 1 | PRISMA flow diagram selected for qualitative analysis of the respective studies.

tDCS in combination with the cannabinoid receptor agonist arachidonylcyclopropylamide (ACPA; 0.01, 0.05, 0.1 mg/kg, or vehicle). ACPA was injected 15 min before fear conditioning to impair fear learning and memory (Nasehi et al., 2016). tDCS was delivered over the right frontal region (i.e., 1 mm anterior and 1 mm to the right from the Bregma) for 20 min at an intensity of 0.2 mA 1 day before auditory fear conditioning. Twenty-four hours, and 2 weeks after training, animals were tested with a contextual associative memory test (i.e., same conditioning context, but without US and CS) and an auditory associative memory test (i.e., different context than training, but exposed to the CS). tDCS selectively improved drug-induced impairments of short-term contextual fear memory, but it did not affect short-term contextual and auditory memory in the absence of ACPA. After 14 days, tDCS restituted all memory functions which were compromised by ACPA. Nasehi et al. (2017b) tested the influence of tDCS on fear memory on mice. Animals received anodal, cathodal, or sham tDCS for 20 min over the right frontal cortex at an intensity of 0.2 mA 1 day before or immediately post-training (fear conditioning), without or with pre- and post-training administration of propranolol, which reduces fear memory (Lonergan et al., 2013). On the next day, animals were tested for contextual fear memory and 1 h later for auditory fear memory. When propranolol was applied prior to the training, and anodal stimulation prior or after the training, contextual fear memory retrieval increased, and the drug-induced impairment of auditory fear memory was reversed. Moreover, when stimulation was applied prior to the training and propranolol was administered after training, a selective improvement of contextual, but not of auditory fear memory retrieval was observed. Cathodal stimulation abolished the effects of propranolol on auditory fear memory only when performed prior to the training.

Using an otherwise identical experimental design, Nasehi et al. (2017a) applied tDCS over the left frontal cortex. The main result shows that pre- or post-training anodal tDCS applied when propranolol was administered prior to training reversed the effect of propranolol on contextual fear memory acquisition (Nasehi et al., 2017a). Moreover, regardless of the specific timing of cathodal stimulation, and administration of propranolol, stimulation re-established the propranolol-induced diminution of contextual memory retrieval.

Overall, the results of these studies show that tDCS can alter fear memories. However, specific effects are heterogeneous. Prefrontal stimulation immediately before fear acquisition reduced, whereas post-training cathodal enhanced fear memory. Moreover, tDCS applied 1 day before fear acquisition restituted pharmacologically compromised fear memory. An important limitation of the examined literature is that, in most cases, no sufficient information is reported about which specific portion of the prefrontal cortex was stimulated. This makes it problematic to provide mechanistic explanations of the available data. Other potential limitations of the respective studies, which make interpretation of the data difficult, are related to the adopted

TABLE 1 | Effect of tDCS on fear memory and fear extinction in healthy and clinical groups.

References	Study type	N/Groups	Gender M/F (Mean age ± SD)	Target area	Target/return electrode position	Polarity	Size	Online/offline stimulation	Intensity/ duration	Type of CS/ US	Reinforcement rate	Outcome measures	Outcome direction
FEAR MEMORY													
Asthana et al. (2013)	RCT, sham controlled, single blind	49 healthy participants/ anodal, cathodal and sham	24/25 (22.58 ± 2.24)	Left dlPFC	F3/left mastoid	Anodal/ cathodal	35 cm^2	Offline, after acquisition and break (10–20 min)	1 mA/12 min	Colored blue and yellow squares/ Scream	75%	SCR	Diminution of fear memory
Mungee et al. (2014)	RCT, sham controlled, single blind	50 healthy participants/ active and sham tDCSgroups	28/22 (N.R.)	Right dlPFC/ vmPFC	F4/ contralateral supraorbital area	Anodal	15 cm^2	Offline, on day 2 immediately after reminding	1 mA/20 min	Blue and yellow squares/ Electrical shock	38%	SCR	- Enhancement of fear memory
Mungee et al. (2016)	RCT, sham controlled, single blind	17 healthy participants/ active and sham tDCS groups	5/12 (N.R.)	Right dlPFC/ vmPFC	F4/ contralateral supraorbital area	Cathodal	15 cm^2	Offline, on day 2 immediately after reminding,	1 mA/20 min	Blue and yellow squares/ Electrical shock	38%	SCR	- No effect on fear memory
FEAR EXTINCTION													
Abend et al. (2016)	RCT, sham controlled, double blind	45 healthy participants/ tDCS, tACS and sham groups	24/21 (25.2 ± 5.7)	mPFC	Between Fpz and Fp1/ occipital bone (Oz)	Anodal	35 cm^2	Online, during extinction	1.5 mA/20 min	Two female faces/ Scream	80%	SCR, self-reported fear	- Anodal tDCS led to overgeneralization
van't Wout et al. (2016)	RCT, sham controlled, single blind	44 healthy participants/ active and sham tDCS groups	23/21 (27.34 ± 8.18)	Left vmPFC	AF3/ contralateral mastoid	Anodal	15 cm^2	Online, started before and continued during extinction	2 mA/10 min	Red, blue and yellow lights/ Electrical shock	60%	SCR	- tDCS during the first extinction block enhanced late extinction of the second extinction block
Dittert et al. (2018)	RCT, sham controlled, double blind	84 healthy participants/two active and two sham tDCS groups	38/46 (24.25 ± 4.07)	Right and left vmPFC	Electrodes positions: M20, M21, I20, I21, J13, J14 for the left and M9, M10, I9, I10, J6, J7 for the right electrode pad (slightly below F7 and F8)	Anodal	16 cm^2	Online, started during the break between acquisition and extinction and lasted until the end of the extinction	1.5 mA/20 min	Two female faces/ Scream	80%	SCR, self-report measures (valence, arousal and CS-US contingency STAI-X1, PANAS)	-Enhancement of early extinction - No differential effect of current flow direction on early extinction - left anodal tDCS reduced state anxiety
Ganho-Ávila et al. (2019)	RCT, sham controlled, single blind	41 healthy participants/ cathodal and sham tDCS groups	0/41 (20.42 ± 4.99)	Right dlPFC	F4/ contralateral deltoid	Cathodal	24.75cm^2	Offline, on day 2, after verbal recall of CS+ color	1 mA/20 min	Blue and yellow squares/ Scream	75%	SCR, self-report measures (valence, arousal, contingency and expectancy), STAI-S, AAT.	- No short-term effect on fear extinction - Enhancement of fear memory retention - Enhancement of stimuli discrimination
Vicario et al. (2020b)	RCT, sham controlled, single blind	23 healthy participants/ anodal and sham tDCS groups	10/13 (24.15 ± 4.92)	Left vmPFC	AF3/ contralateral mastoid	Anodal	25 cm^2	Online, during extinction	2 mA/20 min	Colored circles/ Electrical shock	71%	SCR	-Enhanced fear extinction and recall
Ney et al. (2021)	RCT, sham controlled, single blind	30 healthy participants/ anodal and sham tDCS groups	10/20 (24.60 ± 7.30)	Left vmPFC	AF3/ contralateral mastoid	Anodal	25 cm^2	Offline, after extinction	2 mA/10 min	Colored circles/ Electrical shock	62.5%	SCR	- Anodal tDCS impaired fear extinction retention on day 2

(Continued)

TABLE 1 | Continued

References	Study type	N/Groups	Gender M/F (Mean age ± SD)	Target area	Target/return electrode position	Polarity	Size	Online/offline stimulation	Intensity/ duration	Type of CS/ US	Reinforcement rate	Outcome measures	Outcome direction
CLINICAL GROUPS													
van't Wout et al. (2017)	RCT, sham controlled Blinding mode not reported	28 PTSD/two groups (stimulation during extinction learning vs after extinction)	28/0 (56.25 ± 12.3)	Left vmPFC	AF3/ contralateral mastoid process	Anodal	25 cm^2	Online and offline, during and after extinction	2 mA/10 min (single-session)	Red, blue and yellow light./ Electrical shock	60%	SCR	- Enhanced early fear extinction recall when tDCS was applied after extinction
Todder et al. (2018)	RCT, within-subject sham controlled, double blind	12 refractory OCD patients/ one group	7/5 (38.5 ± 12)	mPFC	Fpz/right shoulder	Anodal/ cathodal	35 mm^2	Offline, after exposure and between presentation of obsession provoking stimuli	2 mA/20 min (3 sessions for each polarity)	Individualized anxiety provoking stimuli	N/A	7-point VAS, Y-BOCS, HAMA, MADRS	- Reduction of obsession-induced anxiety after cathodal stimulation
van't Wout-Frank et al. (2019)	RCT, sham controlled, single blind	12 PTSD patients	12/0 (40.5 ± 8.8)	Left vmPFC	AF3/right posterior occipital (PO8)	Anodal	25 cm^2	tDCS started simultaneously with VR, online	2 mA/25 min (6 sessions)	N/A	N/A	SCR, self-reported PTSD symptoms	- Greater decrease in SCR in real tDCS group - RealtDCS group continued to improve during the 1-month follow-up.

DlPFC, dorsolateral prefrontal cortex; Mpfc, medial prefrontal cortex; vmPFC, ventromedial prefrontal cortex; VR, virtual reality; OCD, Obsessive-Compulsive disorder; PTSD, Posttraumatic stress disorder; SCR, Skin conductance response; STAI-X1, State-trait anxiety inventory-state form; PANAS, Positive and Negative Affect Schedule; VAS, visual analog scale; AAT, approach avoidance task; MADRS, Montgomery-Åsberg Depression Rating Scale; Y-BOCS, Yale-Brown Obsessive-Compulsive Scale; HAMA, Hamilton Anxiety Rating Scale; N/A = not applicable.

protocols, which could have induced metaplastic effects. Finally, the absence of online stimulation studies, which would probably have provided fewer complex effects, and rTMS studies for comparison with the currently available tDCS literature, is another limitation.

Effects of tDCS on Fear Memory in Healthy Humans

The database research identified 3 tDCS studies performed in healthy humans that aimed to affect fear memory (**Table 5**). Asthana et al., 2013 performed a study to investigate the effect of anodal and cathodal tDCS on fear memory consolidation. Participants received anodal, cathodal or sham tDCS over the left dlPFC (return electrode over left mastoid) with 1 mA for 12 min in connection with a 2-day fear conditioning protocol. During the first day, participants went through the habituation and fear acquisition phase. Colored circles were used as CS and a scream as US. Stimulation was started 10 to 20 min after the acquisition phase. On the second day, participants were again exposed to the CS without US to assess consolidation of fear memory. Fear conditioning was assessed by SCR. Cathodal stimulation resulted in significantly lower SCR values compared to anodal and sham, suggesting a role of the left dlPFC in fear memory consolidation. Mungee et al. (2014) aimed to assess the effects of tDCS on fear memory reconsolidation in a 3-day protocol. Fear acquisition was performed on the first day with colored squares as CS and an electrical shock as US. On the second day, participants were first reminded of the CS+ (presentation of one CS+ that was combined with electrical shock on day 1) and stimulated with tDCS immediately afterwards for 20 min with an intensity of 1 mA, with the anode placed over the right dlPFC, and the cathode over the left supraorbital area. Assessment of fear memory was performed on the third day via presentation of the CS stimuli without US. Fear memory was assessed with SCR. The results showed an enhancement of fear memory by tDCS, suggesting a role of the right dlPFC and/or left vmPFC in fear memory reconsolidation. In a second study of the same group (Mungee et al., 2016), the participants performed the same protocol as in the previous study, but with reversed electrode positions for tDCS (i.e., right dorsolateral prefrontal–cathodal, left supraorbital–anodal). The results showed no change in SCR.

Although preliminary, tDCS appears to modulate fear memory in human subjects. Specifically, cathodal stimulation of the left dlPFC led to disruption of fear memory consolidation, while anodal stimulation of the right dlPFC (which however might have also involved effects of cathodal tDCS over left mesio-frontal areas) enhanced fear memory retrieval. Furthermore, the mentioned studies targeted different memory consolidation processes, i.e., consolidation (Asthana et al., 2013) vs. reconsolidation (Mungee et al., 2014, 2016).

Effects of rTMS on Fear Memory in Healthy Humans

Only one recently published study has tested the effects of low-frequency excitability-diminishing rTMS (1 Hz, 110% RMT, stimulation duration 15 min) on fear memory in healthy humans (Borgomaneri et al., 2020) by targeting, in separate groups, the left or right dlPFC in a 3-day—sham controlled–protocol. During the first day, participants conducted a fear conditioning task [two

TABLE 2 | Effects of tDCS on fear memory in animal models.

References	Study type	Subjects and groups	Target area	Target electrode position	Return electrode position	Stimulation polarity	Size of target and return electrodes	Online/offline stimulation	Intensity (mA)	Duration (minutes)	Drug/doses	CS/UCS	Outcome measures	Outcome
Manteghi et al. (2017)	RCT, placebo and sham controlled	64 male NMRI mice, 8 groups	Prefrontal region(right)	1 mm anterior and 1 mm right to the Bregma	Chest	Anodal	3.5 mm^2, 9.5 cm^2	Offline, 24 h before conditioning	0.2	20	ACPA/0.01, 0.05, and 0.1 mg/kg	Tone/foot shock	- Freezing duration and latency - Grooming and rearing duration	- tDCS improved short-term contextual fear memory (0.01 and 0.05 doses of ACPA) and long-term contextual and auditory fear memory formation (all doses of ACPA)
Abbasi et al. (2017)	RCT, sham controlled	41 male NMRI mice, 5 groups	Prefrontal region(left)	1 mm anterior and 1 mm left to the Bregma	Chest	Anodal, cathodal	3.5 mm^2, 9.5 cm^2	Offline, immediately before fear conditioning	0.2	20 and 30	No drugs	Tone/foot shock	Freezing duration and latency	- tDCS impaired acquisition of contextual and cued fear memory (Contextual: 20 and 30 min of anodal, 30 min cathodal; Cued: 20 min anodal, 30 min cathodal)
Nasehi et al. (2017b)	RCT, placebo and sham controlled	120 male NMRI mice, 9 groups	Prefrontal region (right)	1 mm anterior and 1 mm right to the Bregma	Chest	Anodal, cathodal	3.5 mm^2, 9.5 cm^2	Offline, 1 day before/ immediately after fear conditioning	0.2	20	Propranolol/0.1 mg/kg	Tone/foot shock	Freezing duration and latency	- Post-training cathodal stimulation itself facilitated contextual and auditory fear memory retrieval - Pre-training application of cathodal tDCS combined with pre- or post- training propranolol restored auditory fear memory retrieval - Pre- and post-cathodal tDCS in combination with pre-training propanolol increased fear memory retrieval and combined with post-training propanolol increased contextual fear memory - Pre- or post-training anodal tDCS in combination with pre-training propranolol increased contextual and reversed auditory fear memory retrieval - Pre-training anodal combined with post-training propranolol increased contextual fear memory retrieval
Nasehi et al. (2017a)	RCT, placebo and sham controlled	120 male NMRI mice, 9 groups	Prefrontal cortex (left)	1 mm anterior and 1 mm left to the Bregma	Chest	Anodal, cathodal	3.5 mm^2, 9.5 cm^2	Offline, 1 day before/ immediately after fear conditioning	0.2	20	Propranolol/0.1 mg/kg	Tone/foot shock	Freezing duration and latency	- Pre-training cathodaltDCS itself increased contextual fear memory retrieval - Pre- and post-training cathodal tDCS in combination with propanolol pre-training increased fear memory retrieval - Pre- and post-training cathodal tDCSwith post-training propanolol increased contextual fear memory - Pre- and post-training anodal tDCS with pre-training propanolol increased contextual memory retrieval - Pre-training anodal tDCS with pre-training propranolol increased auditory fear memory retrieval

TABLE 3 | Effect of rTMS on fear extinction in clinical groups.

References	Study type	N/Groups	Syndrome	Gender, M/F (age, Mean ± SD)	Target area	Coil position	Online/ offline stimulation	Pulses per session/ duration	Frequency/ Intensity/ Coil shape	Outcome measures	Outcome direction
Notzon et al. (2015)	RCT, Single blind, active (control site) and sham controlled	83/4	Spider phobia	1) 4/37 (27.51 ± 9.4) 2) 5/37 (25.43 ± 7.37) 3) 4/36 (25.85 ± 7.65) 4) 5/38 (27.02 ± 9.23)	Left dlPFC	F3	Offline, before the VR challenge	iTBS/600/ 3 min	15 Hz/80% RMT/figure of 8	FSQ, SPQ, ASI, psychophysiological measures (HR, HRV, SCR)	iTBS - had no general effect of on anxiety, disgust, HR and SCR. - significantly increased sympathetic activity
Herrmann et al. (2017)	RCT, Double blind, sham controlled	39/2	Acrophobia	1) 6/13 (46.6 ± 13.7) 2) 7/13 13/26 (43.2 ± 12.6)	mPFC	Fpz	Offline, before exposure	rTMS/1560/ 2 × 20 minutes	10 Hz/100% RMT/Round	AQ, BAT	- rTMS reduced phobic anxiety immediately after two sessions of VR exposure therapy. - No differences between active and sham rTMS stimulation at follow up.
Osuch et al. (2009)	Double-blind, sham controlled	9/1	PTSD	1/8 (41.4 ± 12.3)	Right dlPFC	5 cm rostral to APB muscle hotspot	Online, during exposure to emotionally provoking memories.	rTMS/1800/ 30 min per session/20 sessions	1 Hz/100% RMT/figure of 8	CAPS, IES, HDRS	- Active rTMS showed a larger improvement of hyperarousal symptoms compared to sham
Isserles et al. (2013)	RCT, Double-blind, sham controlled, controlled for traumatic event as well	26/3	PTSD	1) 7/2 (49 ± 12.5) 2) 8/1 (40.4 ± 10.5) 3) 5/3 (40.5 ± 9.8)	mPFC	H-Coil designed tostimulate the mPFC.	Offline, after exposure to the traumatic event	Deep rTMS/ 1680/ 15.5 min per session/ 12 sessions	20 Hz/120% RMT/H-coil	CAPS, PSS-SR, HDRS, BDI, psychophysiological data (HR)	-Symptom improvement by dTMS (revealed by changes in CAPS, PSS-SR, HDRS, BDI and HR)
Fryml et al. (2019)	RCT, Double blind, sham controlled	8/2	PTSD	1) 2/1 (30 ± 2.6) 2) 5/0 (27 ± 2.1)	Leftor right dlPFC	6 cm anterior to the right hand motor thumb area	Online, duringprolonged exposure therapy	rTMS/6000/ 30 min per session/8 sessions	10Hz/120% RMT/figure of 8	CAPS, HRSD	- Change in HRSD showed antidepressant benefit of rTMS. - CAPS scores showed no significant improvement
Carmi et al. (2018)	RCT, Double blind, sham controlled	41/3	OCD	1) 9/7 (36 ± 2.1) 2) 4/4 (28 ± 3.1) 3) 7/7 (35 ± 3.5)	mPFCand ACC	4 cm anterior to theleg motor spot at midline	Offline, following symptom provocation	Deep rTMS/ HF: 2000 LF: 900/25 sessions	HF: 20 Hz, LF: 1 Hz/HF: 100% RMT, LF: 110% RMT/H7 Coil	YBOCS, CGI-I	- Symptoms improved by high frequency deep rTMS (YBOCS, CGI-I)
Carmi et al. (2019)	RCT, Double blind, sham controlled	94/2	OCD	1) 20/27; (41.1 ± 11.97) 2) 19/28 (36.5 ± 11.38)	mPFCand ACC	4 cm anterior to the foot motor spot	Offline, following symptom provocation	Deep rTMS/ 2,000/29 sessions	20 Hz/100% RMT/H7 coil	YBOCS, CGI-I, CGI-S, and Sheehan Disability Scale scores	- Symptom improvement by dTMS (YBOCS, CGI-I, CGI-S)

(Continued)

TABLE 3 | Continued

References	Study type	N/Groups	Syndrome	Gender, M/F (age, Mean ± SD)	Target area	Coil position	Online/ offline stimulation	Pulses per session/ duration	Frequency/ Intensity/ Coil shape	Outcome measures	Outcome direction
Adams et al. (2014)	Case study, Single blind	1	OCD	1/0 (52 yo)	Pre-supplementary motor area	50% of the distance between the Fz and FCz	Offline, immediately prior ERP exercises	rTMS/1200/ 20 min per session/15 sessions	1 Hz/110% RMT/figure of 8	YBOCS,PHQ-9,GAD-7, DOCS	- Symptom improvement in YBOCS, DOCS, GAD-7, and PHQ-9
Grassi et al. (2015)	Case study	1	OCD	0/1 (32 yo)	Left dlPFC	N.R.	Offline, immediately prior ERP exercises.	rTMS/1800/ N.A./10 sessions	10 Hz/80% RMT/NR	Y-BOCS, CGI-I, HAM-D, GAF	- Symptomimprovement in Y-BOCS, CGI-I, GAF

ACC, Anterior cingulate cortex; dlPFC, dorsolateral prefrontal cortex; mPFC, medial prefrontal cortex; vmPFC, ventromedial prefrontal cortex; iTBS, intermittent theta burst stimulation; rTMS, repetitive transcranial magnetic stimulation; LF, low frequency; HF, high frequency; MEP, motor evoked potential; RMT, resting motor threshold; PTSD, Posttraumatic stress disorder; OCD, Obsessive-Compulsive disorder; HR, heart rate; HRV, heart rate variability; SCR, Skin conductance response; EEG, electroencephalography; FPS, Fear potentiated startle; fNIRS, Functional near-infrared spectroscopy; CAPS, Clinician Administered PTSD Scale; IES, The Impact of Event Scale; SPQ, Spider Phobia Questionnaire; FSQ, Fear of Spiders Questionnaire; ASI, Anxiety Sensitivity Index; AQ, acrophobia questionnaire; BAT, Behavioral Avoidance Test; BDI, Beck Depression Inventory; HDS, Hamilton Depression scale; HDRS, Hamilton Rating Scale for Depression; PGI-T, Patient Global Impression of Improvement; Y-BOCS, Yale-Brown Obsessive-Compulsive Scale; GAF, Global Assessment of Functioning; GAD-7, General Anxiety Disorder Scale; PHQ-9, Patient Health Questionnaire; DOCS, Dimensional Obsessive-Compulsive Scale; CGI-S, Clinical Global Impression—severity scale; CGI-I, The CGI—improvement scale; ERP, Exposure Response Prevention; N/A, not applicable; N.R., not reported.

TABLE 4 | Effect of rTMS on extinction in animal models.

References	Study type	Subjects and groups	Target area	Coil position	Online/ offline stimulation	Pulses per session/ duration	Frequency/ Intensity/ coil shape	Drug/ doses	Reinforcement rate	CS/US	Outcome measure	Outcome direction
Baek et al. (2012)	RCT, sham controlled	35 rats, 2 experiments, active and sham group in each experiment;	Infralimbic cortex	3 mm anterior to bregma	Offline and online, rTMS was finished either 5 min before or applied during extinction	1,000 pulses/ 10 min	10 Hz/90% MT/Modified figure-of-eight coil,	None	100%	Sound/Foot shock	Freezing duration	- rTMS paired with CS significantly facilitated fear extinction
Legrand et al. (2019)	RCT, sham and vehicle controlled study	140 mice, 8 groups	Infralimbic cortex	2 mm anterior to the bregma	Offline, from day 7 to 12, five rTMS sessions or sham sessions were applied 24 h apart	750 pulses/ 7 min and 48 s × 5 sessions	12 Hz/115% MT/Circular coil	Fluoxetine/ 15 mg/kg	N/A	Chamber/ Foot shock	- Freezing duration and latency - Performance in object recognition task - c-Fos neuronal expression	rTMS - enhanced fear extinction. - reversed short-term memory impairments. - evoked c-Fos activity in the vmPFC (infralimbic cortex), the basolateral amygdala and the ventral CA1

TABLE 5 | Effect of rTMS on fear memory and extinction in healthy participants.

References	Study type	N/ Groups	Gender, M/F (age, Mean ± SD)	Target area	Coil position	Online/ offline stimulation	Pulses per session/ duration	Frequency/ Intensity/ Coil shape	Type of CS/ US	Reinforcement rate	Outcome measures	Outcome direction
Borgomaneri et al. (2020)	RCT, Single-blind, active (control site) and sham controlled	84/6	1.6/8 (23.9 ± 2.3) 5/9 (23.1 ± 2.6) 3/11 (21.6 ± 2.0) 8/6 (22.4 ± 3.7) 6/8 (23.2 ± 1.8) 6. 5/9 (24.4 ± 3.1)	Left and right dlPFC	F3 and F4	Online, during reconsolidation of fear memory	900/15 min	1 Hz/110% RMT/figure of 8	Room pictures/ electrical shocks	60%	SCR, contingency ratings	Both l- and r-dlPFCrTMS -diminished expression of fear response - prevented return of fear response
Guhn et al. (2014)	RCT, Single-blind, sham controlled	85/2	Active group: 21/19 (23.9 ± 3.0); Sham: 22/23 (24.6 ± 4.5)	mPFC	Fpz	Offline, between acquisition and extinction	1,560/20 min	10 Hz/110% RMT/Round	Two male faces/ scream	50%	SCR, FPS, fNIRS, and self-report scales	rTMS - enhanced fear extinction learning - Improved extinction recall
Raij et al. (2018)	Single-blind, active (control site) controlled	28/2	23/5 (28yo;19-51)	vmPFC	Left posterior PFCwith strong or weak vmPFC connectivity	Online, during extinction	28/4 trains, 7 pulses per train	20 Hz/100% RMT/figure of 8	Red, blue and yellow lights/ Electrical shocks	62.5%	SCR	rTMS enhanced fear extinction recall

pictures of a room (CS), one paired with an electrical shock (US)]. Twenty-four hours afterwards, fear memory reactivation was induced via a reminder cue (two times presentation of the CS+ without US), and then rTMS was conducted. On day 3, memory recall, extinction and reinstatement measures were performed. Compared to the sham rTMS group, participants of the left and right dlPFCrTMS groups exhibited decreased physiological expression of fear in the memory recall test (i.e., reduced SCR), only when rTMS was administered within the reconsolidation time window (i.e., 10 min after the exposure to a reminder cue that reactivated a fear memory acquired 1 day before). Moreover, dlPFC-rTMS prevented subsequent return of fear after extinction training.

Since no effects were reported in participants tested immediately after dlPFC-rTMS or dlPFC-rTMS without preceding fear-memory reactivation, the authors suggest a specific role of dlPFC in fear-memory reconsolidation. Overall, this result is in line with previous evidence from tDCS studies (Mungee et al., 2014) documenting a modulation of fear memory with anodal tDCS of the right dlPFC applied in the context of fear memory reconsolidation.

Effects of NIBS Methods on Fear Extinction

Effects of rTMS on Fear Extinction in Animal Models

Two studies were identified that fulfilled the inclusion criteria (**Table 4**). Baek et al. (2012) conducted a 3-day protocol in rats to assess the effect of excitability-enhancing rTMS on fear extinction with real or sham stimulation applied before or during extinction. The coil was positioned over the PFC (∼3 mm anterior to Bregma, in a region that would be able to target vmPFC, according to the authors aim) and stimulation was applied for 10 min at 10 Hz frequency. On the first day, rats were exposed to auditory stimuli for habituation, and then exposed to auditory stimuli (CS) paired with a foot shock (US). The next day, in experiment 1, rTMS or sham stimulation were finished 5 min before the extinction process. In experiment 2, stimulation was applied simultaneously with the extinction protocol. On day 3, the CS was presented without the US to assess fear extinction memory. Freezing behavior served as dependent variable. Rats who received rTMS during, but not before extinction showed significantly less freezing behavior than the sham group, during, and 1 day after extinction. Legrand et al. (2019) conducted a study in an experimental mouse PTSD model to assess the effect of rTMS on fear extinction and related neurocircuits. The mice were split into non-stressed and stressed (PTSD) groups, and received sham or real rTMS, combined with the serotonin reuptake inhibitor fluoxetine, which is used for PTSD treatment (Ariel et al., 2017), or vehicle. Facilitatory 12 Hz rTMS was applied over the vmPFC (the coil was positioned latero-medial to promote bilateral effects) for 7 min and 48 s per session. On the first day, the PTSD mice were exposed to foot shocks to induce stress-like effects. From the second day on, a treatment with fluoxetine or vehicle was conducted. From day 7 to 12, five rTMS or sham stimulation sessions were applied. At day 17 and 18, the mice underwent object recognition tasks and at day 22, the mice were re-exposed to the conditioning chamber. Object recognition task (ORT) performance, duration of freezing and latency to

freezing were used as indicators of anxiety-like behaviors. PTSD rTMS mice explored novel objects significantly more than the PTSD sham group and showed a decreased duration of freezing. rTMS furthermore increased c-Fos activity in the infralimbic cortex, basolateral amygdala and the ventral CA1. Taken together, results suggest that rTMS enhanced fear extinction and reversed short-term memory impairments, which was associated with early gene expression in extinction-related areas. In summary, these studies suggest that application of facilitatory rTMS over the PFC can influence fear extinction via modulation of specific brain circuits involved in extinction, such as the IL, amygdala, and hippocampus.

Effects of rTMS on Fear Extinction in Healthy Humans

Two studies related to the application of rTMS to influence fear extinction were identified (**Table 5**). Guhn et al. (2014) conducted a study to assess the influence of high frequency rTMS on fear extinction in a 2-day sham-controlled protocol. Stimulation was delivered with 10 Hz frequency (110% RMT) for 20 min over the bilateral mPFC. On the first day, participants were familiarized with the stimuli (habituation), and subsequently fear acquisition took place. Human faces served as CS, and a scream as US. rTMS was applied immediately before extinction. On the second day, extinction recall was assessed. SCR, fear potentiated startle (FPS), functional near-infrared spectroscopy (fNIRS), and subjective ratings were obtained to assess fear responses. Active rTMS enhanced fear extinction, as measured by FPS, SCR, and subjective valence and arousal ratings. Furthermore, the active rTMS group showed significantly reduced FPS magnitudes during extinction recall. Raij et al. (2018) assessed effects of rTMS on fear extinction in healthy subjects in a 3-day protocol. Stimulation (20 Hz, 100% RMT) was applied over two spots of the PFC with strong or weak connections with the vmPFC, as revealed by fMRI. On the first day, participants were conditioned to two colors (CS+) associated with an electrical shock (US), while another color (CS-) was not paired with the electrical shock. On the second day, the extinction protocol was applied with only one CS+ paired with online rTMS. rTMS was applied four times for 300 ms after each CS+. SCR during extinction recall was significantly reduced when the cue was paired with rTMS over the area that exhibited strong functional connectivity with the vmPFC.

Although preliminary, these results show a potential of high frequency rTMS to enhance fear extinction and recall when applied over the mPFC, and areas which are strongly connected with the vmPFC.

Effects of tDCS on Fear Extinction in Healthy Humans

Five studies were identified that meet the inclusion criteria. Four of these studies applied tDCS over the mPFC or vmPFC, and one over the dlPFC (**Table 3**). Abend et al. (2016) assessed the effect of tDCS on fear extinction and recall. Participants received anodal tDCS or sham stimulation over the mPFC (return electrode over occipital bone) for 20 min with a constant current of 1.5 mA in a 3-day protocol. On the first day, participants underwent classical conditioning, where one of two female faces (CS) was combined with a scream (US). During extinction on the second day, the CS was presented without the US, except for the first CS+ trial, which was reinforced as a reminder of the conditioned association from day 1. tDCS was applied during extinction. On the third day, stimuli were again presented without the US to assess extinction recall. SCR and self-reported fear served as indicators of conditioned fear. No significant effects of the intervention were detected during the extinction phase. During the recall phase, the results showed significant changes in SCR and self-report measures. The SCR response to CS+ in the anodal tDCS group was comparable to the CS- response, and furthermore, self-reported fear showed retention of fear related to the CS+, as compared to sham. Thus, tDCS led to overgeneralization of the vegetative fear response to non-reinforced stimuli. van't Wout et al. (2016) conducted a two-day protocol study to assess the impact of tDCS on fear extinction and recall. The anodal electrode was placed over the left vmPFC (return electrode over contralateral mastoid), and stimulation was conducted with 2 mA for 10 min. Participants underwent habituation, acquisition, and extinction phases during the first day. Each participant was conditioned to two CS+, and each CS+ was presented in one of two consecutive extinction blocks. The CS were presented in different contexts according to phase of the protocol (i.e., one context during acquisition and another during extinction and recall). An electrical shock served as US, the conditioned stimuli were colored lights. The first group received 5 min of tDCS before extinction, and stimulation continued the next 5 min during the first extinction block. In the second block, sham stimulation started 5 min before the second extinction block and continued during extinction. The second group received the reversed order of stimulation. In this design, each participant received anodal tDCS during the extinction of one CS+ and sham stimulation during the extinction of the other CS+. During the second day, extinction recall was assessed. SCR was used as a dependent measure. Participants who received tDCS during the first extinction block showed lower SCR during late extinction of the second extinction block. No effect of tDCS on extinction recall was observed. Another study that assessed the effect of tDCS on fear extinction was conducted by Dittert et al. (2018). Participants received bilateral stimulation (i.e., right anodal- left cathodal tDCS, and vice versa) or respective sham stimulation over the vmPFC in a one-day protocol (i.e., habituation, acquisition, and extinction performed on the same day). Duration of stimulation was 20 min, and the intensity of the applied stimulation was 1.5 mA. Two neutral female faces served as CS, and a female scream simultaneously presented with a fearful expression of the face was used as the US. Two active stimulation groups were treated with the same electrode positions, but opposite current flow directions. The stimulation started during a 10 min break between acquisition and extinction and went on until the end of extinction. SCR, self-report measures [subjective ratings of arousal, valence, and CS-US contingency, STAI-X1 (Laux et al., 1981) and PANAS (Watson et al., 1988)] served as dependent variables. tDCS accelerated early extinction learning in both real stimulation groups. Furthermore, the significant decrease of reaction toward the CS+ was accompanied by an increased reaction toward the CS– in the active tDCS groups. Furthermore, the left anodal

tDCS group showed a higher decrease in subjectively rated state anxiety. Vicario et al. (2020b) conducted a sham-controlled study with a 2-day fear extinction protocol to investigate the effect of anodal tDCS on fear extinction. Anodal tDCS was applied over the left vmPFC (return electrode over controlateral mastoid) with an intensity of 2 mA for 10 min. During the first day participants underwent habituation, acquisition, and extinction stages. Two colored circles were used as a CS and one of them was followed by a highly uncomfortable electrical stimulus. Stimulation was applied during the whole extinction phase. Fear responses were assessed by SCR. Anodal tDCS over the left vmPFC reduced fear reactions during extinction recall in participants that acquired fear responses during fear acquisition. Results of electrical field simulations showed that the AF3-contralateral mastoid montage used in this study is better suited than other protocols to tackle the vmPFC, and amygdala, which are both crucial for extinction learning. Ney et al. (2021) conducted a sham-controlled study with a 2-day fear extinction protocol to investigate how timing of tDCS will influence fear extinction retention. The fear conditioning/extinction protocol and stimulation parameters were identical to those in the previous study (Vicario et al., 2020b), but tDCS or sham stimulation were applied 10 min after fear extinction to target consolidation processes. Fear responses were assessed by SCR. In that study, anodal stimulation led to impaired fear extinction retention.

One study has targeted the dlPFC to modulate fear extinction. Ganho-Ávila et al. (2019) conducted a study in female participants using a 3-day paradigm to investigate the effects of cathodal tDCS on fear extinction. Cathodal stimulation was delivered over the right dlPFC (return electrode over contralateral deltoid) for 20 min at 1 mA intensity. On the first day, habituation and fear acquisition were conducted. The authors used two colors as CS and a female scream as the US. On the second day, before tDCS, participants were asked to verbally recall the CS+, and afterwards stimulation was applied. Then extinction learning was conducted. After 1 to 3 months, participants participated in follow-up sessions. Participants were asked to recall the CS+, and were again exposed to four unsignaled USs. The re-extinction phase started immediately after reinstatement. To assess fear conditioning/extinction learning, SCR, and self-reports (valence, arousal, contingency, and expectancy) were conducted. Furthermore, the State-trait anxiety inventory (STAI-S; Spielberger, 1984) and Approach avoidance task (AAT; Krypotos et al., 2014), which is designed to assess implicit avoidance tendencies, were employed. Cathodal tDCS had no immediate effect on SCR and self-report measures. The delayed after-measures showed however increased CS+ retention, suggesting a reduction of extinction efficacy by cathodal tDCS. Moreover, cathodal tDCS enhanced CS+/CS– stimuli discrimination, as measured by the AAT task, via establishing a positive bias toward the CS–, leading to a decreased generalization effect.

Taken together, the results of these studies suggest that tDCS over the vmPFC can influence fear extinction and recall in healthy humans. Specifically, studies suggest that anodal tDCS over the vmPFC leads to enhanced fear extinction memory consolidation, but these effects seem to critically depend on experimental protocol characteristics, as well as timing and area of stimulation. Diminution of activity of the dlPFC seems to reduce extinction and enhance CS+/CS– discrimination.

Effects of tDCS on Fear Extinction in the Clinical Population

One study was identified that meets the described criteria (**Table 3**). van't Wout et al. (2017) conducted a 2-day fear extinction protocol in male veterans with posttraumatic stress disorder (PTSD) to assess effects of tDCS, and timing of stimulation (i.e., during or after extinction) on fear extinction memory. Anodal tDCS was conducted over the left vmPFC (return electrode over controlateral mastoid) for 10 min with an intensity of 2 mA. On the first day, participants underwent habituation, acquisition and extinction. Different contexts were used for acquisition on the one hand, and extinction and recall on the other, and each participant was conditioned to two different CS. An electrical shock was used as US. Half of the participants were stimulated with tDCS during extinction and half of them immediately after extinction. On the second day, extinction recall was performed. SCR served as dependent measure. Veterans who received anodal tDCS after fear extinction showed trendwise lower SCR on early recall, compared to those who received stimulation during extinction learning.

NIBS and Exposure Therapy

rTMS and Exposure Therapy

Nine articles were identified which met the inclusion criteria (**Table 5**). Two studies adopted rTMS and exposure protocols in patients with specific phobias, three in patients with PTSD and four in patients with OCD. Notzon et al. (2015) conducted a sham-controlled study on patients with spider phobia to assess the combined effect of intermittent Theta Burst Stimulation (iTBS) and exposure on symptoms. Participants received facilitatory iTBS or sham stimulation over the left dlPFC before VR spider exposure. For assessment of spider fear symptoms, the Fear of Spiders Questionnaire (FSQ; Szymanski and O'Donohue, 1995), and Spider Phobia Questionnaire (SPQ; Olatunji et al., 2009) were used. Besides that, the Anxiety Sensitivity Index (ASI; Reiss et al., 1986), the questionnaire for the assessment of disgust sensitivity (disgust scale: DS; Haidt et al., 1994), the Subjective Units of Discomfort Scale (SUDS; Wolpe, 1973), and also electrophysiological measures of HR, heart rate variability (HRV) and SCR were conducted. The results showed no effect of iTBS on self-report measures of anxiety and disgust of spiders, HR, and SCR. Regarding HRV, iTBS significantly increased sympathetic activity during the spider scene. Herrmann et al. (2017) conducted a sham-controlled study to investigate the effects of rTMS on height phobia. Participants were exposed to two virtual reality scenarios within a period of 2 weeks, and before each VR session, facilitatory rTMS (10 Hz, 100% RMT), or sham stimulation was applied bilaterally over the mPFC for 20 min. The Acrophobia Questionnaire (AQ; Cohen, 1977), and Behavioral Avoidance Test served as outcome measures. The results show a significant reduction of phobic anxiety and avoidance measured by the AQ in active-,

as compared to sham-stimulated patients immediately but not 3 months after intervention.

Osuch et al. (2009) performed a study to assess the potential of rTMS to reduce symptoms in patients with chronic PTSD. In a sham-controlled crossover design, patients received one block of 20 sham rTMS and exposure sessions and one block of 20 active rTMS and exposure sessions. Low-frequency inhibitory rTMS (1 Hz, 100% RMT) was delivered over the right dlPFC. Before the treatment, each participant completed a list of 10 events or cues that were used during the exposure session (i.e., experience 0–referred to something calming, experience 1–referred to a neutral experience, experiences 2–9 were related to the trauma). During the first and second sessions in each condition, subjects were instructed to talk about item number 0 and item number 1, respectively, for 5 min in order to become habituated to the experimental setting. In subsequent sessions, subjects could freely choose to speak 5 min about any of the 10 items on their list or remain silent, but they could talk more if they wanted. Stimulation was delivered 5 min before participants started to speak about the events and lasted for 30 min. As outcome measures, the Clinician Administered PTSD Scale (CAPS; Blake et al., 1995), the Impact of Event Scale (IES; Sundin and Horowitz, 2002), and the Hamilton Depression Rating Scale (HDRS; Hamilton, 1960) were applied at baseline and after treatment. Combination of active rTMS and exposure led to a moderate improvement of hyperarousal symptoms assessed by the CAPS. A study by Isserles et al. (2013) assessed the effect of deep rTMS on symptom improvement in pharmaco- and psychotherapy-resistant PTSD patients. Facilitatory stimulation was delivered over the mPFC at 20 Hz frequency (120% RMT). One group received deep rTMS after script-driven imagery of a traumatic experience, the second group received deep rTMS after script-driven imagery of a positive experience, and the third group received sham rTMS after script-driven imagery of traumatic experiences. The participants received 3 treatment sessions per week during a period of 4 weeks. Each session lasted for around 20 min with ∼4 min of script-driven imagery followed by 15.5 min of deep rTMS. The authors performed the Clinically Administered PTSD Scale (CAPS; Blake et al., 1995) at baseline, and at the 5th, 7th and 13th week as primary outcome measure for assessing PTSD symptoms. Additionally, the PTSD-symptoms scale-self report (PSS-SR; Foa et al., 1993), HDRS-24 (Hamilton, 1960), and the Beck Depression Inventory-II (BDI-II; Beck et al., 1996) were conducted at baseline, once weekly at the beginning of each treatment week, at the end of the treatment phase at week 5, and at 7th and 13th week for follow up. Furthermore, HR was recorded before, during and after each script imagery period. The traumatic experience imagery group exposed to active rTMS significantly improved in total CAPS and corresponding domain scores (i.e., intrusion, avoidance/numbness, and arousal), compared to the other two groups. This beneficial effect was preserved during the follow-up period. Even for the secondary outcome measures (i.e., PSS-SR, HDRS-24, and BDI-II), symptom improvements were obtained in the traumatic experience imagery group exposed to active rTMS during treatment and follow-up periods. Furthermore, HR was significantly reduced throughout treatment in the traumatic experience imagery group exposed to active rTMS. Fryml et al. (2019) performed a study in which facilitatory rTMS (10 Hz, 120% RMT) was performed over the left or right dlPFC. Participants were furthermore divided into active rTMS and sham groups and treated one time per week (for 5 weeks), combined with imaginal exposure to traumatic situations. The whole session lasted around 40 min with rTMS started 5 min after the begin of exposure for a total duration of 30 min. The Clinically Administered PTSD Scale (CAPS; Blake et al., 1995) and Hamilton Rating Scale for Depression (HRSD; Hamilton, 1960) were applied as outcome measures. CAPS scores showed a trend toward improvement in the real vs. sham rTMS condition after the treatment. Interestingly, the active rTMS group had furthermore significantly lower depression scores at the fourth and fifth sessions relative to baseline and compared to sham. The authors did not report whether any differences were found regarding the area of the stimulation (i.e., right vs. left dlPFC).

Carmi et al. (2018) performed a study on OCD patients to assess whether high or low frequency deep rTMS affects symptoms. Three groups of patients received high frequency rTMS (20 Hz, 100% RMT), low frequency rTMS (1 Hz, 110% RMT), or sham rTMS applied bilaterally to tackle the mPFC and ACC. Each treatment session began with a 3–5 min provocation of personalized obsessive-compulsive cues and stimulation was delivered afterwards. Patients were treated five times per week for 5 weeks (25 sessions in total). As outcome measures, the Yale-Brown Obsessive-Compulsive Scale (YBOCS; Goodman et al., 1989), and Clinical Global Impression Scale-Improvement (CGI-I; Guy, 1976) were performed at baseline (pre-treatment), during and up to 1 month after intervention. YBOCS and CGI-I scores improved by high-frequency deep rTMS in contrast to low frequency and sham interventions, and the effect was significant for 1 week, but not for 1 month after intervention. In another sham-controlled study, Carmi et al. (2019) assessed the effect of high frequency deep rTMS for the treatment of OCD patients. Parameters and area of rTMS, and the exposure protocol were identical to those described in the previous study, except that the treatment lasted for 6 weeks, and included a 4-week follow-up. The Yale-Brown Obsessive-Compulsive Scale (YBOCS; Goodman et al., 1989), Clinical Global Impression Scale-Improvement (CGI-I; Guy, 1976), Clinical Global Impressions Severity scale (CGI-S; Guy, 1976), and Sheehan Disability Scale (Sheehan et al., 1996) were applied for obtaining outcome measures. The results showed a significant reduction of OCD symptoms in the active as compared to the sham rTMS group at the posttreatment assessment and the 4-week follow-up. Furthermore, global functioning was improved by active rTMS, as compared to sham treatment at the posttreatment assessment. Furthermore, two case studies combined rTMS and exposure protocols to reduce OCD symptoms. Adams et al. (2014) combined exposure and response prevention (ERP, see Foa et al., 2005) with low frequency rTMS (1 Hz pulses, 110% RMT) over the pre-supplementary motor area to treat a male patient that showed minimal response to medication. Low-frequency rTMS was delivered immediately prior to ERP for 3 weeks. The results showed improvement in OCD (YBOCS; Goodman et al., 1989, DOCS; Abramowitz et al., 2010), generalized anxiety (GAD-7;

Spitzer et al., 2006) and depression symptoms (PHQ-9; Kroenke et al., 2001). Grassi et al. (2015) investigated the effects of high-frequency rTMS (10 Hz frequency, 80% of RMT) applied over the left dlPFC for 10 session of a treatment-resistant OCD patient. Each exposure session was immediately preceded by stimulation. Authors reported a reduction of symptom severity measured by the Y-BOCS (Goodman et al., 1989), CGI-I (Guy, 1976) and Global Assessment of Functioning (GAF) scales. The clinical improvement was maintained, and the global level of functioning increased for up to 24 months after intervention.

In general, the results of the above-mentioned studies suggest a potential of rTMS in combination with exposure protocols to reduce symptoms in individuals with specific phobias, PTSD and OCD. In patients with specific phobias, results suggest that high frequency rTMS over the mPFC might be promising. For PTSD treatment, stimulation over the dlPFC and mPFC have shown effects. High frequency deep rTMS over the mPFC and ACC shows promising results for treatment of OCD patients. Here, pre-supplementary motor area and left dlPFC stimulation might also be promising.

tDCS and Exposure Therapy

Two studies explored the effect of exposure therapy combined with tDCS (**Table 3**). van't Wout-Frank et al. (2019) assessed anxiolytic effects of tDCS combined with Virtual reality (VR) exposure in veterans with warzone-related PTSD. Anodal tDCS was applied over the left vmPFC (return electrode over the contralateral mastoid) for 25 min at an intensity of 2 mA. Participants received active or sham tDCS in 6 sessions during exposure to three VR driving scenarios (8 min duration), in which 12 warzone events were presented. A head-mounted display with integrated head tracking and stereo earphones presented combat-related multisensory information (visual, auditory, olfactory, and haptic). Measures of SCR and self-reported PTSD symptoms (at baseline, after VR sessions, and 1 month later) were obtained. SCR was reduced to a larger extent in the active tDCS group, as compared to sham. Both groups showed furthermore a significant reduction in PTSD symptom severity after treatment, but only the active tDCS group continued to improve during the 1-month follow-up. Todder et al. (2018) performed a sham-controlled crossover study in refractory OCD patients i to assess whether anodal or cathodal tDCS applied bilaterally over the mPFC (return electrode over right shoulder) for 20 min per session at an intensity of 2 mA reduces obsession-induced anxiety. During the 5 weeks of treatment (first, third and fifth week were treatment sessions), participants received anodal, cathodal, or sham tDCS three times a week with 48-h intervals in-between. Before the first session, obsession-provoking stimuli (OPS) were individualized for each patient. In all following sessions, patients were first exposed to OPS, and then to tDCS for 20 min. Participants rated their level of anxiety via a Visual Analog Scale (VAS) immediately after OPS and tDCS. Additionally, the clinical scales CGI (Guy, 1976), Montgomery-Åsberg Depression Rating Scale (MADRS; Montgomery and Åsberg, 1977), HAM-A (Hamilton, 1960), Y-BOCS (Goodman et al., 1989) were rated by the patients at the beginning of each stimulation week. Cathodal tDCS reduced obsession-induced anxiety, as compared to anodal and sham stimulation.

In summary, these results suggest that the combination of tDCS over the mPFC and exposure has potential to reduce PTSD, and OCD symptoms. The effect of tDCS over other areas on respective symptoms has however not been explored, and the efficient stimulation protocols differed between diseases, and timing of stimulation.

DISCUSSION

We systematically reviewed 30 research articles conducted in animal models and healthy humans, but also clinical patient groups that aimed to influence fear and extinction memory processes via NIBS methods. In summary, the reviewed articles show a potential of NIBS to influence fear memory, enhance fear extinction and reduce clinical symptoms in various fear-related disorders. The potential and limitations of these studies will be discussed in the next paragraphs.

Fear Memory

The prefrontal cortex plays an important role in controlling several cognitive and affective functions (e.g., Ridderinkhof et al., 2004). In this regard, the dlPFC is assumed to be critically involved in up-/down regulation of the cortico-meso-limbic network (Vicario et al., 2019), and shows activity enhancement during fear conditioning (Dunsmoor et al., 2007, 2008). In contrast, the vmPFC is relevant for the up-regulation of reward seeking behavior (Hutcherson et al., 2012), down-regulation of negative affective responses (Diekhof et al., 2011), and critically involved in extinction learning and recall (Phelps et al., 2004; Milad et al., 2007). Accordingly, in most of the studies the dlPFC was selected as target area for modulation of fear memory.

In general, the examined literature on fear memory is limited in terms of studies which tackled specific areas. Regarding animal studies, it offers only investigations with tDCS over the PFC, with limited specification of different subregions of this cortical target. Overall, the main results suggest that tDCS can alter fear memories, but specific effects are intervention timing- and brain state-related. PFC stimulation (both anodal and cathodal) immediately before fear acquisition reduced fear memory (i.e., Abbasi et al., 2017). In other studies, stimulation effects were reported also when tDCS was performed after conditioning. Moreover, for pharmacologically impaired fear learning, tDCS restituted learning, when stimulation was performed 24 h before conditioning, which shows a dependency of the directionality of effects on brain states.

In humans, excitability-diminishing cathodal tDCS over the left dlPFC disrupted fear memory consolidation, while excitability-enhancing anodal tDCS had no effects (Asthana et al., 2013). This result is in accordance with an rTMS study showing that inhibitory rTMS over the left dlPFC disrupts fear memory consolidation (Borgomaneri et al., 2020). In contrast, excitability-enhancing anodal, but not cathodal tDCS over the right dlPFC enhanced fear memory (Mungee et al., 2014, 2016) when applied during the reconsolidation period. However, in the latter study the return electrode was placed over the vmPFC, another cortical

region relevant for memory consolidation (Nieuwenhuis and Takashima, 2011), which makes interpretation of the results of that study complex.

Mechanistically, the impact of left dlPFC modulation on fear memory can be explained by referral to the neuroimaging literature on memory consolidation. It has been suggested that the dlPFC is functionally connected with the hippocampus (Wang and Morris, 2010). Liu et al. (2016) reported that an attenuated hippocampal functional connectivity with the left dlPFC was predictive of more effective suppression of overnight consolidation of aversive memories. Accordingly, inhibitory tDCS, and rTMS over the left dlPFC might have resulted in attenuated hippocampal activity, and thus impaired consolidation. On the other hand, the enhanced fear memory following excitatory right dlPFC stimulation (Mungee et al., 2014) is in line with evidence for higher activation of the right dlPFC during memory retrieval processes (Sakai et al., 1998). Overall, these studies suggest that the dlPFC can be a relevant cortical target for fear memory consolidation.

A limitation of the NIBS literature on fear memory is the absence of "online" stimulation protocols, that should have also tackled the fear acquisition stage, besides consolidation, and re-consolidation. Future research should close this gap, although consolidation studies might be particularly promising from a clinical point of view (e.g., early intervention after trauma). Moreover, studies are needed to more systematically explore functional differences between the left and the right hemisphere, to clarify the optimal timing of stimulation with respect to the considered process (i.e., acquisition, consolidation, reconsolidation) and clarify the underlying specific mechanism. Finally, comparability between studies conducted in animal models and humans is currently limited because of relevant differences between the respective protocols (including targeted cortical sites, and the use of pharmacological manipulations in animal models).

Fear Extinction

Studies on human and animal models have demonstrated that rTMS and tDCS can lead to enhancement of fear extinction and affect related fear circuits. Previous imaging studies have shown that the vmPFC is specifically activated during fear extinction (Phelps et al., 2004; Milad et al., 2007), and this area is assumed to be involved in the top-down regulation of the amygdala during extinction learning (Milad et al., 2007). Therefore, inducing LTP-like plasticity over the vmPFC by NIBS methods is assumed to enhance regulation of the amygdala and lead to reduction of fear expression.

tDCS

Area of Stimulation

In most studies (five out of six that have employed a fear extinction protocol), application of tDCS in healthy humans over the vmPFC and mPFC resulted in enhanced fear extinction learning and memory. In accordance, anodal tDCS over the vmPFC improved fear extinction and recall in healthy humans (van't Wout et al., 2016; Dittert et al., 2018; Vicario et al., 2020b), and PTSD patients (van't Wout et al., 2017). In contrast to these results, Abend et al. (2016) reported detrimental effects of anodal tDCS over the mPFC, i.e., an overgeneralization of fear response by tDCS. Dittert et al. (2018) also reported a gradual enhancement of the vegetative reaction to the non-reinforced stimuli in addition to the extinction enhancement induced by tDCS, which stresses the importance of further research for optimizing stimulation parameters. The specific electrode arrangement used in the Abend et al. (2016) study might explain its deviating results. Computational modeling results (Vicario et al., 2020b) suggest that the AF3/Mastoid electrode montage, which was applied in the studies conducted by van't Wout et al. (2016), and Vicario et al. (2020b) result in stronger electrical fields at the level of the vmPFC and amygdala, as compared to the FPz/Iz montage used by Abend et al. (2016).

Only one study is available that applied cathodal tDCS over the right dlPFC for extinction modulation (Ganho-Ávila et al., 2019). The results of this study show a delayed enhancement of fear memory and CS+/CS– discrimination, which suggest a positive effect of this stimulation protocol with respect to specification of a stimulus as dangerous, or not. This enhanced discrimination by cathodal tDCS might be related to attentional processes that improved signal to noise discrimination, as shown already for visuo-motor learning.

In line with anatomical, optogenetic, lesion and imaging studies (Quirk et al., 2000; Phelps et al., 2004; Milad et al., 2007; Motzkin et al., 2015; Kim et al., 2016), available tDCS studies favor the vmPFC as target for stimulation in order to enhance fear extinction and recall. Studies on other areas are largely missing due to conceptual reasons, or because these areas are not surface-near, and thus no suitable target for NIBS approaches. The at least partial heterogeneity of the results of different studies is likely caused by protocol differences, and we will focus on relevant parameters in the next sections.

Timing of Stimulation

An important factor that affects the results of stimulation is whether tDCS is delivered during extinction (i.e., online) or before or after extinction (i.e., offline), because the timing of stimulation determines how respective stimulation- and task-dependent physiological effects interact. The three studies conducted in humans (i.e., three anodal tDCS protocols–van't Wout et al., 2016; Dittert et al., 2018; Vicario et al., 2020b), that have applied online stimulation over the vmPFC or areas closely connected with the vmPFC improved extinction. Ney et al. (2021) showed detrimental effects of anodal tDCS over the vmPFC on fear extinction retention, when the consolidation window was targeted, which further emphasizes the importance of appropriate timing of stimulation. This general pattern of results is supported by optogenetic studies (Do-Monte et al., 2015). In general accordance, online tDCS, compared with offline tDCS, has been shown to have a superior impact on various tasks (Stagg et al., 2011; Martin et al., 2014; Dedoncker et al., 2016; Oldrati et al., 2018). Therefore, enhancing LTP-like plasticity of fear-related brain circuits during extinction learning might be advantageous. In contrast (van't Wout et al., 2017), one study in PTSD patients, that tested whether anodal tDCS over the vmPFC has better effects when applied online

or offline, showed enhanced extinction recall when tDCS was applied after extinction, as compared to online stimulation. The lack of a control group, small sample size and recruitment of exclusively male participants in this study limits conclusions, but it might be that stimulation after extinction leads to enhanced consolidation of fear extinction memory, which should be tested in future studies. Given the partially heterogeneous study results, a systematic evaluation of the optimal timing of intervention is still warranted. Specifically, research protocols are needed to clarify the different role of encoding and consolidation of fear extinction memory (Vicario et al., 2017) and directly test, in otherwise identical protocols, the effect of online vs. offline stimulation. Here, an important point regarding consolidation of fear and extinction memory is the time interval between acquisition and extinction (Abend and van't Wout, 2018). If not sufficiently temporally discerned, stimulation might modulate fear related memory that is not yet consolidated, which could lead to mixed effects. For example, traumatic events are usually separated, and therefore consolidated, prior to pharmacological or psychotherapeutic interventions. Therefore, using protocols where acquisition of fear is not immediately followed by extinction might lead to more ecologically valid results.

Duration and Intensity of Stimulation

Especially for tDCS, duration and intensity of interventions varied relevantly between studies. Positive effects on fear extinction and recall were observed with anodal tDCS at an intensity of 2 mA (van't Wout et al., 2016, 2017; Vicario et al., 2020b) applied for 10 min, but also 1.5 mA (Dittert et al., 2018) applied for 20 min, and with different electrode sizes. Since duration and intensity of stimulation influence cortical excitability in a partially non-linear manner (Batsikadze et al., 2013; Jamil et al., 2017; Agboada et al., 2019; Samani et al., 2019), further research should address the relationship between these factors and fear extinction. Furthermore, none of the studies have applied anodal stimulation with an intensity of 3 mA over the vmPFC, that according to recent studies might be more efficient than lower stimulation intensities (Agboada et al., 2019). Since the vmPFC is not a surface-near structure, increasing stimulation intensity might lead to better activation of this area that could in turn lead to enhanced extinction and retrieval of fear extinction memory. Furthermore, the tDCS studies varied with respect to the applied current densities, which could have an impact on the results. Future studies should test systematically how different intensities and durations of applied current relate to fear extinction.

Hemispheric Lateralization

Only one study has directly compared the effect of left anodal—right cathodal, and vice versa tDCS stimulation protocols and provided some insights into prefrontal hemispheric lateralization (Dittert et al., 2018). No current flow direction-dependent effects on early extinction were detected but left anodal tDCS reduced additionally state anxiety in that study. Furthermore, three more studies (van't Wout et al., 2016, 2017; Vicario et al., 2020b) that have applied anodal tDCS over the left vmPFC (anode over the AF3 and cathode over the contralateral mastoid process). A hemispheric lateralization of the PFC in emotion regulation has been previously documented, relating activity of the left PFC to the ability to adequately regulate emotions (Kim and Bell, 2006). In accordance, it has been demonstrated that the metabolic activity of the left PFC is increased in persons that use reappraisal strategies, which is positively related to greater experience and behavioral expression of positive emotion and increased sense of well-being, while suppression of emotional expressions was negatively associated with reduced right-hemispheric glucose metabolism (Kim et al., 2012). Furthermore, emotion regulation is accompanied by enhanced left hemispheric connectivity between the amygdala, and the vmPFC, OFC, dmPFC, and dlPFC in persons with high reappraisal use (Eden et al., 2015). Therefore, it might be assumed that anodal tDCS over the left vmPFC leads to enhanced emotion regulation. In contrast, Dittert et al. (2018) found that right anodal-left cathodal stimulation might be advantageous in reducing fear responses in late extinction blocks. Considering these preliminary and partially conflicting results, further research is required to explore if hemispheric lateralization is an important factor in regulating extinction.

rTMS

Area of Stimulation

The rTMS studies document enhanced fear extinction learning and memory following stimulation of the vmPFC and mPFC in healthy humans. Specifically, high-frequency, excitability-enhancing rTMS (Klomjai et al., 2015) over the mPFC and vmPFC reduced fear responses (Guhn et al., 2014; Raij et al., 2018).This pattern of results is supported by studies in animal models which showed that apart from enhancing fear extinction (Baek et al., 2012; Legrand et al., 2019), application of high frequency rTMS over the PFC induced structural changes, and alterations of early gene expression in the infralimbic cortex (functionally related to the human vmPFC), the basolateral amygdala and the ventral CA1, which are relevant for extinction of fear memories (Legrand et al., 2019).Overall, the results from the examined rTMS study corroborates those of respective tDCS studies.

Timing of Stimulation

One excitatory rTMS study–(Raij et al., 2018) with online stimulation over the vmPFC (however with an indirect approach with direct stimulation of a lateral PFC area closely connected with the vmPFC) report improved extinction. This result is supported by a rTMS study in an animal model, where online stimulation of the vmPFC had better outcomes as compared to offline stimulation (Baek et al., 2012).On the other hand, Guhn et al. (2014) provide evidence of effective fear extinction following excitatory stimulation over the mPFC, and thus with offline stimulation.

Overall, the results from the available rTMS studies suggest that both online and offline stimulation can be effective in boosting fear extinction, depending on the considered cortical target. More research is needed to explore the effectiveness of online and offline interventions regarding different cortical targets.

Duration and Intensity of Stimulation

Two rTMS studies have applied relevantly different facilitatory stimulation protocols with respect to intensity and duration, but also timing (Guhn et al., 2014; Raij et al., 2018). Since duration and intensity of stimulation influence cortical excitability (Fitzgerald et al., 2006; Lang et al., 2006), further research should address the relationship between these factors and fear extinction systematically.

Hemispheric Lateralization

Only one study (Raij et al., 2018) suggests an impact of hemispheric lateralization on rTMS results. In that study, application of rTMS over the left posterior PFC reduced fear reactions. This finding is in line with tDCS studies on fear extinction and recall. Lateralized effects thus might be assumed, but were not systematically studied with rTMS. Overall, these results are preliminary, and more work is needed to explore the relevance of hemispheric lateralization with respect to fear extinction.

Methodological Considerations

Fear memory and extinction studies vary relevantly with respect to fear conditioning-extinction protocol characteristics, which complicate interpretation of outcomes. Reinforcement rates in studies discussed here vary from 38 to 80%. It has been previously demonstrated that different reinforcement rates can relevantly influence fear responses (Chin et al., 2016), and therefore, this might be a factor that influences the results of interventions. Also, the modality of US stimuli (i.e., scream vs. electrical shock) that was used for fear conditioning might affect results. Larger startle responses are exhibited in the electrical shock task, and the respective US shock and overall task are rated as more aversive than the scream (Glenn et al., 2012). Furthermore, some studies used CS+ reminders before extinction (Abend et al., 2016; Ganho-Ávila et al., 2019), which could affect the outcomes of extinction learning by re-activation of fear memories. Intervals between acquisition and extinction varied between studies, which could further influence results via an effect of stimulation on respective re-activated memory traces. Considering that stimuli and procedures used in fear extinction protocols cannot encompass all aspects and the complexity of fear emotion and anxiety in the real world, moving toward more ecologically valid protocols might lead to more relevant outcomes. Virtual reality might be a promising tool as it combines the experimental control of laboratory measures with real life scenarios providing immersion, presence, impact on different sensory modalities, control of actions and interactions (Parsons, 2015; Carl et al., 2019).

NIBS and Exposure Protocols

Studies exploring the effect of rTMS and tDCS combined with exposure protocols show a potential to improve symptoms in specific phobias, PTSD and OCD. Similar to what was discussed in the previous section, however also here heterogeneities of protocols make it difficult to come to definite conclusions.

For specific phobias, one study that applied facilitatory rTMS over the vmPFC combined with exposition reduced symptoms in patients with height phobia (Herrmann et al., 2017). Notzon et al. (2015), on the contrary, did not find a significant symptom improvement in patients with spider phobia by excitability-enhancing iTBS over the dlPFC. Reasons for these discrepant results could be that Herrmann et al. (2017) applied repeated stimulation over the vmPFC, while Notzon et al. (2015) conducted a single session approach over the left dlPFC, and that the vmPFC, but not the dlPFC is assumed to have a critical role in extinction. Moreover, the specific stimulation protocol differed between studies.

A couple of studies has been conducted in PTSD patients. Facilitatory (Isserles et al., 2013) rTMS over the mPFC and inhibitory (Osuch et al., 2009) rTMS applied over the dlPFC combined with exposure have shown to improve symptoms. Fryml et al. (2019) did not find an effect of facilitatory rTMS over the dlPFC on PTSD symptoms. Beyond rTMS, also anodal tDCS over the left vmPFC combined with VR exposition reduced SCR and symptoms in veterans with warzone-related PTSD (van't Wout-Frank et al., 2019). This study supports findings that online and left vmPFC application of tDCS is a promising way for enhancing fear extinction. Overall, these studies show that enhancing LTP-like plasticity over the vmPFC with rTMS and tDCS, leads to enhanced fear extinction and symptom improvement. Furthermore, inhibitory stimulation over the dlPFC might improve symptoms. Due to the preliminary and partially mixed results of the available data, and missing comparative studies, firm conclusions about the efficacy of specific stimulation parameters are difficult to make, and future studies should explore these aspects systematically.

For OCD treatment, preliminary results suggest furthermore that high frequency deep rTMS targeting the mPFC and ACC reduces symptoms in these patients (Carmi et al., 2018, 2019). Additionally, in two case studies, symptoms improved after low frequency rTMS over the pre-supplementary motor area (SMA) and high frequency rTMS over the left dlPFC (Adams et al., 2014; Grassi et al., 2015). Interestingly, in difference to the respective rTMS-studies, where excitability-enhancing stimulation over the mPFC reduced symptoms, cathodal, but not anodal tDCS over the mPFC reduced obsession-induced anxiety in OCD patients (Todder et al., 2018). One explanation for these seemingly conflicting results might be application of different NIBS methods (i.e., deep rTMS might lead to deeper penetration of the brain) and different areas of stimulation. Furthermore, case studies suggest that excitatory stimulation over the left dlPFC might lead to enhanced cognitive control in OCD, while inhibition of the pre-SMA, whose hyperactivity underlies cognitive control deficits in OCD (Adams et al., 2014), lead to symptom reduction. Therefore, inducing LTP- or LTD-like plasticity with tDCS and rTMS over the PFC might be a promising way to alleviate symptoms in OCD, however available data are scarce. Future studies should further explore and optimize parameters of stimulation (e.g., area, frequency, duration, excitation, or inhibition inducing methods) to develop more efficient treatments.

For mechanisms of these effects, exposure protocols might lead to activation of symptom-related neural circuits (Carmi

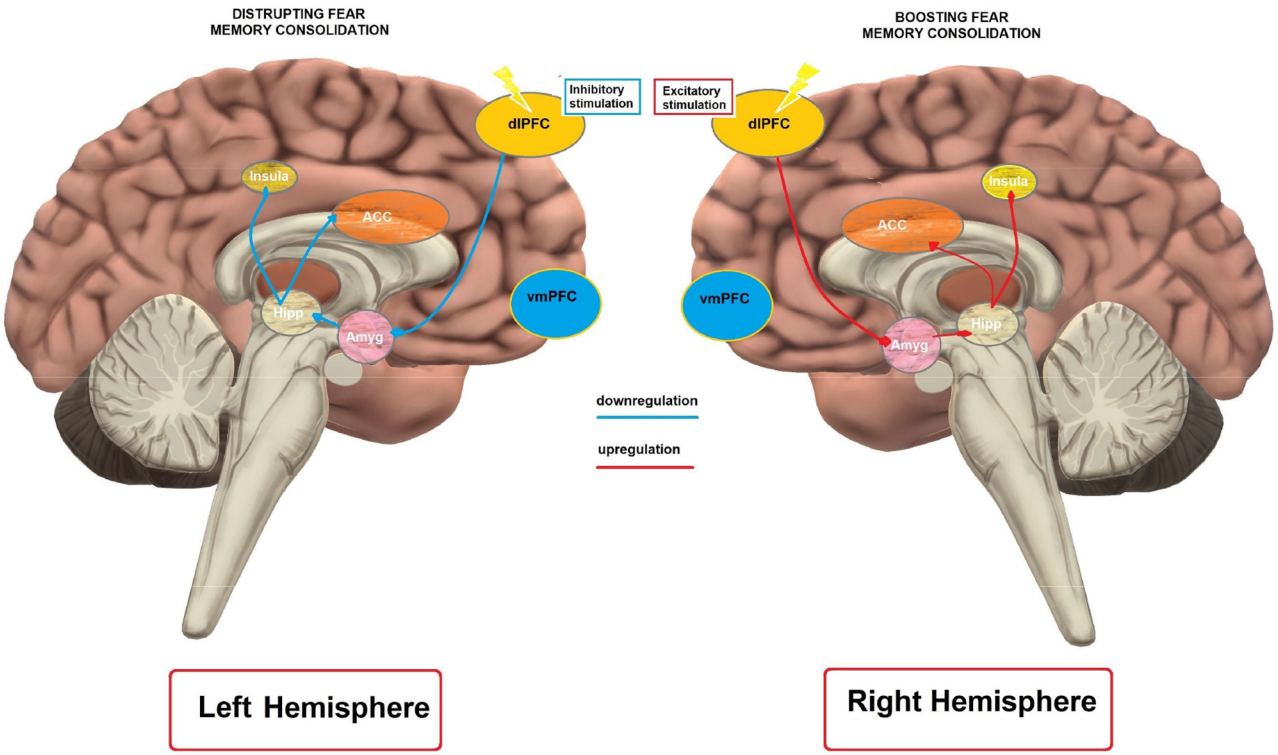

FIGURE 2 | Model on how NIBS is thought to influence fear memory formation. Inhibitory NIBS of left dlPFC interferes with fear memory consolidation by downregulating the activity of the amygdala which, in turn, downregulates the hippocampus, which is responsible for memory consolidation, and ACC/insula, which are involved in the expression of fear responses. Excitatory NIBS of the right dlPFC boosts fear memory consolidation by upregulating the activity of amygdala, which, in turn, upregulates the activity of hippocampus and ACC/Insula.

et al., 2018, 2019) engaged in dysfunctional cognition, which are then susceptible to change via application of NIBS. In line with previous claims that online stimulation might have advantages as compared to offline interventions, combining exposure protocols with simultaneous NIBS might have a better outcome than application of stimulation alone, or conducted before exposure. On the other side, previous studies have shown that application of rTMS or tDCS also without exposure can lead to symptom reduction (Vicario et al., 2019) and, therefore, future studies should compare effects of these two approaches. Furthermore, disease-related hyper- or hypo-activation of specific brain areas might depend critically on the respective disease, and therefore designing stimulation parameters optimized for specific disorders, or symptoms, is important. For example, based on the results mentioned above, enhancing excitability in medial parts of the PFC, and reducing it in pre-SMA might lead to better outcomes in patients with OCD.

GENERAL REMARKS

The present review provides evidence that NIBS methods are promising to influence fear memory and fear extinction processes and have potential for the treatment of various clinical fear-related syndromes. Our work provides preliminary evidence linking the dlPFC with fear memory in humans (**Figure 2**), probably at the level of consolidation/reconsolidation processes. However, results from research with animal models provide a mixed picture, which might be due to substantial protocol differences (including differences of cortical stimulation sites and use of pharmacological manipulation).

Regarding fear extinction, the results of the reviewed studies are in line with previous conclusions about the role of the vmPFC for top-down regulation of the amygdala (Milad et al., 2007), and that dysfunctions of vmPFC-amygdala connectivity may mediate the susceptibility to and/or maintenance of anxiety disorders (Milad et al., 2014). A model on how NIBS over the left vmPFC is suggested to improve fear extinction is shown in **Figure 3**. However, the field is only at its beginning, and some steps are required to make further advances.

Systematic studies are required to deliver information about the optimal area (including laterality), duration, intensity, polarity/frequency, and timing of stimulation. Here enhanced knowledge about physiological mechanisms of action of NIBS on fear and extinction memory would be helpful as a foundation for optimization; most of the studies in the field are purely behavioral. In this line, current NIBS protocols affect mostly superficial areas, and network effects on deeper structures remain largely unexplored. The adoption of other brain stimulation approaches such as transcranial focused ultrasound stimulation might help to overcome these limitations in future, in line

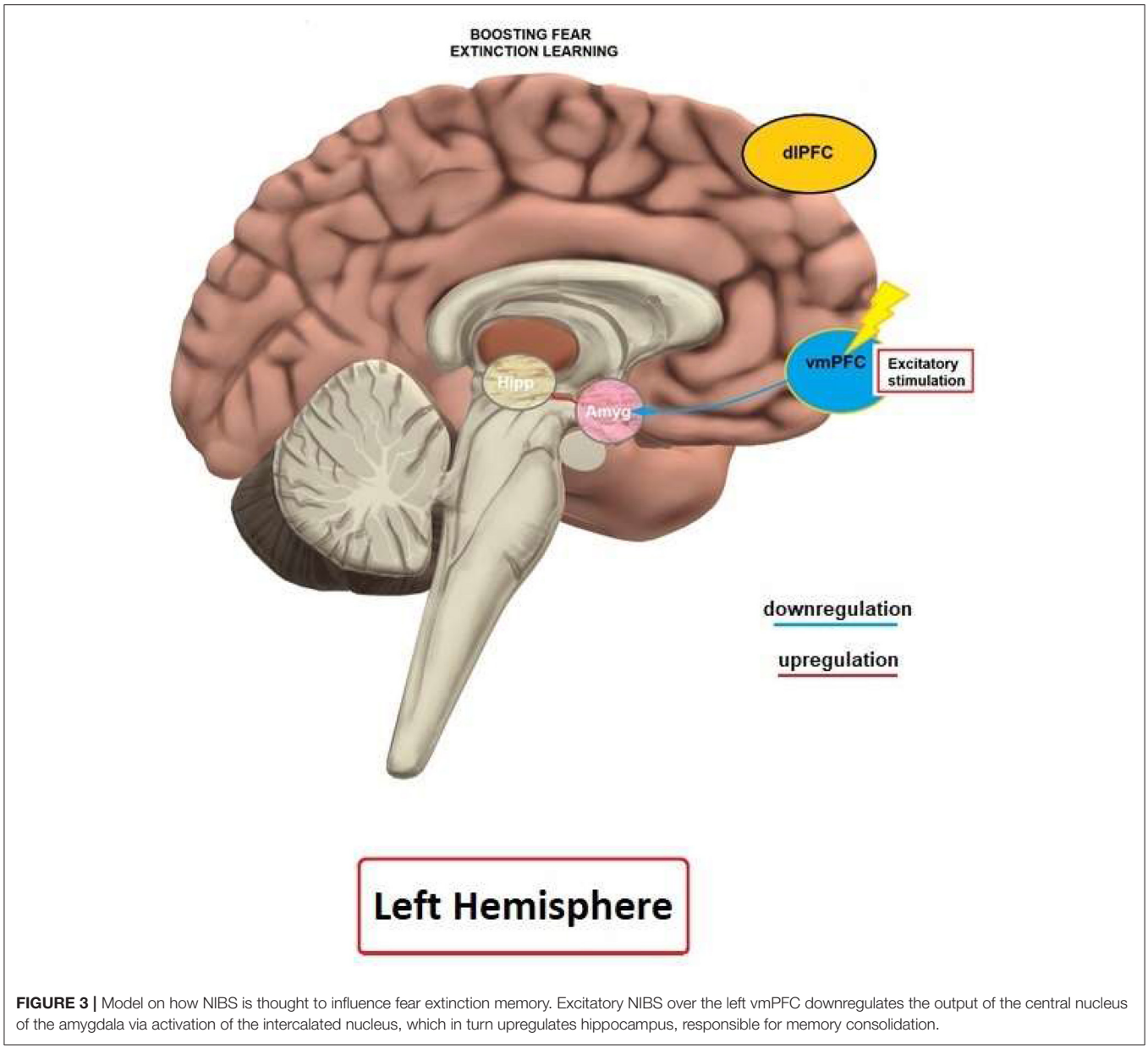

FIGURE 3 | Model on how NIBS is thought to influence fear extinction memory. Excitatory NIBS over the left vmPFC downregulates the output of the central nucleus of the amygdala via activation of the intercalated nucleus, which in turn upregulates hippocampus, responsible for memory consolidation.

with evidence from non-human primates (e.g., Folloni et al., 2019) suggesting that this method might be suited to modulate subcortical neural structures which are critical for fear processing and extinction. Another critical factor is the adoption of a more systematic procedure for fear conditioning/extinction protocols, as the variability of results in the examined literature might have been caused at least partially by task heterogeneities. Finally, the sample sizes in most of the studies in clinical populations are rather small, and future studies should employ larger groups. Large-scale studies are especially needed for protocols optimized for routine application in the clinical field. An overview of key variables to be systematically explored to investigate the effect of NIBS on fear memory/fear extinction learning is shown in **Figure 4**.

In summary, our review shows preliminary evidence that NIBS is a relevant method to modulate fear-related processes in humans. The main limitations of the available literature in the field, which should be addressed in future investigations, can be summarized as follows: (i) the low number of double blind, sham controlled studies (i.e., only about 14% of the available research); (ii) the absence of systematic titration of stimulation parameters such as duration, repetition, intensity and cortical target for optimization; (iii) the absence of systematic protocols which combine standard therapies with NIBS; (iv) a limited number of follow-up studies aiming at investigating the long-term effects of NIBS on fear memory and/or fear extinction learning processes; (v) the lack of mechanistic studies exploring the physiological foundation of NIBS effects.

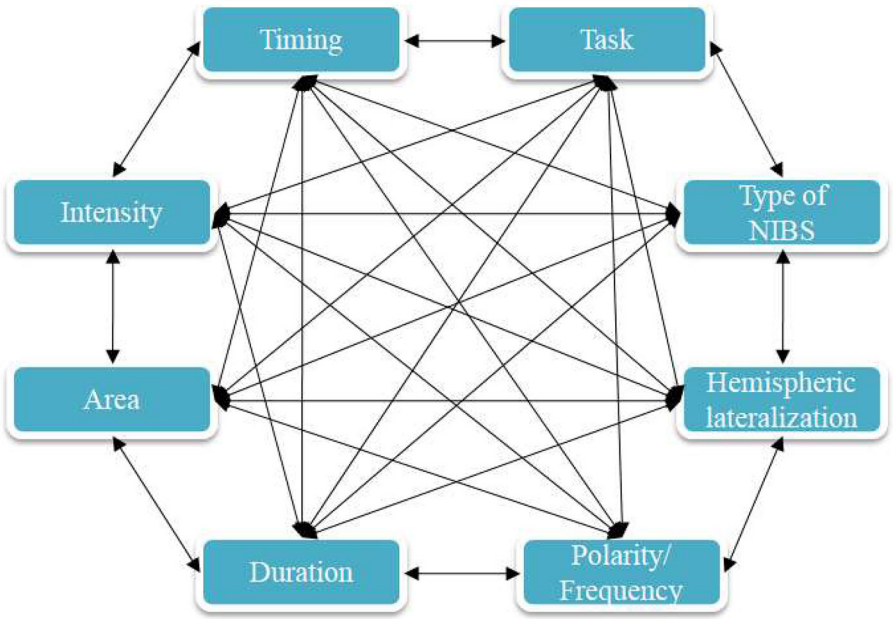

FIGURE 4 | Complex and mutual relationships between various factors mediating the effects of NIBS methods on fear and extinction memory. *Type of NIBS*- refers to which NIBS method is applied, e.g., rTMS, tDCS; *Hemispheric lateralization* refers to whether stimulation is dominantly applied over the left or right hemisphere; *Polarity/frequency* refers to whether anodal or cathodal tDCS is applied, or low or high frequency rTMS; *Duration* refers to duration of the applied stimulation; *Area*- refers to which area is intended to be targeted for the stimulation; *Intensity* refers to the intensity of applied stimulation; *Timing* refers to whether stimulation is applied before, simultaneously or after the extinction/exposure; *Task*- refers to specifics of the fear conditioning/extinction protocol (e.g., reinforcement rate, modality of the US, using CS+ reminders).

DATA AVAILABILITY STATEMENT

The original contributions presented in the study are included in the article/supplementary material, further inquiries can be directed to the corresponding author/s.

AUTHOR CONTRIBUTIONS

CV and MN conceived the work. VM wrote the early version of the manuscript. FY, MS, and VM prepared tables. All authors revised and approved the final version of the manuscript.

FUNDING

This work was supported by Deutscher Akademischer Austauschdienst (DAAD), BIAL foundation (Prot. Number 160/18), and the Deutsche Forschungsgemeinschaft (DFG, German Research Foundation)- Projektnummer 316803389 - SFB 1280.

REFERENCES

Abbasi, S., Nasehi, M., Lichaei, H. R. S., and Zarrindast, M. R. (2017). Effects of left prefrontal transcranial direct current stimulation on the acquisition of contextual and cued fear memory. *Iran. J. Basic Med. Sci.* 20:623.

Abend, R., Jalon, I., Gurevitch, G., Sar-El, R., Shechner, T., Pine, D. S., et al. (2016). Modulation of fear extinction processes using transcranial electrical stimulation. *Transl. Psychiatry* 6, e913–e913. doi: 10.1038/tp.2016.197

Abend, R., and van't Wout, M. (2018). Commentary: augmentation of fear extinction by Transcranial Direct Current Stimulation (tDCS). *Front. Behav. Neurosci.* 12:121. doi: 10.3389/fnbeh.2018.00121

Abramowitz, J. S., Deacon, B. J., Olatunji, B. O., Wheaton, M. G., Berman, N. C., Losardo, D., et al. (2010). Assessment of obsessive-compulsive symptom dimensions: development and evaluation of the dimensional obsessive-compulsive scale. *Psychol. Assess* 22:180. doi: 10.1037/a0018260

Adams, J. T., Badran, B. W., and George, M. S. (2014). Integration of cortical brain stimulation and exposure and response prevention for obsessive-compulsive disorder (OCD). *Brain Stimul.* 7, 764–765. doi: 10.1016/j.brs.2014.06.010

Agboada, D., Mosayebi-Samani, M., Kuo, M. F., and Nitsche, M. A. (2020). Induction of long-term potentiation-like plasticity in the primary motor cortex with repeated anodal transcranial direct current stimulation - Better effects with intensified protocols? *Brain Stimul.* 13, 987–997. doi: 10.1016/j.brs.2020.04.009

Agboada, D., Samani, M. M., Jamil, A., Kuo, M. F., and Nitsche, M. A. (2019). Expanding the parameter space of anodal transcranial direct current stimulation of the primary motor cortex. *Sci. Rep.* 9, 1–11. doi: 10.1038/s41598-019-54621-0

Andlin-Sobocki, P., and Wittchen, H. U. (2005). Cost of anxiety disorders in Europe. *Eur. J. Neurol.* 12(Suppl. 1), 39–44. doi: 10.1111/j.1468-1331.2005.01196.x

Ariel, L., Inbar, S., Edut, S., and Richter-Levin, G. (2017). Fluoxetine treatment is effective in a rat model of childhood-induced post-traumatic stress disorder. *Transl. Psychiatry* 7:1260. doi: 10.1038/s41398-017-0014-5

Asthana, M., Nueckel, K., Mühlberger, A., Neueder, D., Polak, T., Domschke, K., et al. (2013). Effects of transcranial direct current stimulation on consolidation of fear memory. *Front. Psychiatry* 4:107. doi: 10.3389/fpsyt.2013.00107

Baek, K., Chae, J. H., and Jeong, J. (2012). The effect of repetitive transcranial magnetic stimulation on fear extinction in rats. *Neuroscience* 200, 159–165. doi: 10.1016/j.neuroscience.2011.09.050

Bakker, N., Shahab, S., Giacobbe, P., Blumberger, D. M., Daskalakis, Z. J., Kennedy, S. H., et al. (2015). rTMS of the dorsomedial prefrontal cortex for major depression: safety, tolerability, effectiveness, and outcome predictors for 10 Hz versus intermittent theta-burst stimulation. *Brain Stimul.* 8, 208–215. doi: 10.1016/j.brs.2014.11.002

Bandelow, B., and Michaelis, S. (2015). Epidemiology of anxiety disorders in the 21st century. *Dialogues Clin. Neurosci.* 17, 327–335. doi: 10.31887/DCNS.2015.17.3/bbandelow

Barad, M., Gean, P. W., and Lutz, B. (2006). The role of the amygdala in the extinction of conditioned fear. *Biol. Psychiatry* 60, 322–328. doi: 10.1016/j.biopsych.2006.05.029

Batsikadze, G., Moliadze, V., Paulus, W., Kuo, M. F., and Nitsche, M. A. (2013). Partially non-linear stimulation intensity-dependent effects of direct current stimulation on motor cortex excitability in humans. *J. Physiol.* 591, 1987–2000. doi: 10.1113/jphysiol.2012.249730

Beck, A. T., Steer, R. A., and Brown, G. K. (1996). *Manual for the Beck Depression Inventory-II*. San Antonio, TX: Psychological Corporation, 1, 82.

Blake, D. D., Weathers, F. W., Nagy, L. M., Kaloupek, D. G., Gusman, F. D., Charney, D. S., et al. (1995). The development of a clinician-administered PTSD scale. *J. Trauma. Stress* 8, 75–90. doi: 10.1002/jts.2490080106

Borgomaneri, S., Battaglia, S., Garofalo, S., Tortora, F., Avenanti, A., and di Pellegrino, G. (2020). State-dependent TMS over prefrontal cortex disrupts fear-memory reconsolidation and prevents the return of fear. *Curr. Biol.* 30, 3672–3679.e4. doi: 10.1016/j.cub.2020.06.091

Burgos-Robles, A., Vidal-Gonzalez, I., and Quirk, G. J. (2009). Sustained conditioned responses in prelimbic prefrontal neurons are correlated with fear expression and extinction failure. *J. Neurosci.* 29, 8474–8482. doi: 10.1523/JNEUROSCI.0378-09.2009

Carl, E., Stein, A. T., Levihn-Coon, A., Pogue, J. R., Rothbaum, B., Emmelkamp, P., et al. (2019). Virtual reality exposure therapy for anxiety and related disorders: a meta-analysis of randomized controlled trials. *J. Anxiety Disord.* 61, 27–36. doi: 10.1016/j.janxdis.2018.08.003

Carmi, L., Alyagon, U., Barnea-Ygael, N., Zohar, J., Dar, R., and Zangen, A. (2018). Clinical and electrophysiological outcomes of deep TMS over the medial prefrontal and anterior cingulate cortices in OCD patients. *Brain Stimul.* 11, 158–165. doi: 10.1016/j.brs.2017.09.004

Carmi, L., Tendler, A., Bystritsky, A., Hollander, E., Blumberger, D. M., Daskalakis, J., et al. (2019). Efficacy and safety of deep transcranial magnetic stimulation for obsessive-compulsive disorder: a prospective multicenter randomized double-blind placebo-controlled trial. *Am. J. Psychiatry* 176, 931–938. doi: 10.1176/appi.ajp.2019.18101180

Chang, C. H., Knapska, E., Orsini, C. A., Rabinak, C. A., Zimmerman, J. M., and Maren, S. (2009). Fear extinction in rodents. *Curr. Protoc. Neurosci.* 47, 8–23. doi: 10.1002/0471142301.ns0823s47

Chin, B., Nelson, B. D., Jackson, F., and Hajcak, G. (2016). Intolerance of uncertainty and startle potentiation in relation to different threat reinforcement rates. *Int. J. Psychophysiol.* 99, 79–84. doi: 10.1016/j.ijpsycho.2015.11.006

Cohen, D. C. (1977). Comparison of self-report and overt-behavioral procedures for assessing acrophobia. *Behav. Ther.* 8, 17–23. doi: 10.1016/S0005-7894(77)80116-0

Dedoncker, J., Brunoni, A. R., Baeken, C., and Vanderhasselt, M. A. (2016). A systematic review and meta-analysis of the effects of transcranial direct current stimulation (tDCS) over the dorsolateral prefrontal cortex in healthy and neuropsychiatric samples: influence of stimulation parameters. *Brain Stimul.* 9, 501–517. doi: 10.1016/j.brs.2016.04.006

Di Lazzaro, V., Dileone, M., Pilato, F., Capone, F., Musumeci, G., Ranieri, F., et al. (2011). Modulation of motor cortex neuronal networks by rTMS: comparison of local and remote effects of six different protocols of stimulation. *J. Neurophysiol.* 105, 2150–2156. doi: 10.1152/jn.00781.2010

Diekhof, E. K., Geier, K., Falkai, P., and Gruber, O. (2011). Fear is only as deep as the mind allows: a coordinate-based meta-analysis of neuroimaging studies on the regulation of negative affect. *Neuroimage* 58, 275–285. doi: 10.1016/j.neuroimage.2011.05.073

Dittert, N., Hüttner, S., Polak, T., and Herrmann, M. J. (2018). Augmentation of fear extinction by transcranial direct current stimulation (tDCS). *Front. Behav. Neurosci.* 12:76. doi: 10.3389/fnbeh.2018.00076

Do-Monte, F. H., Manzano-Nieves, G., Quiñones-Laracuente, K., Ramos-Medina, L., and Quirk, G. J. (2015). Revisiting the role of infralimbic cortex in fear extinction with optogenetics. *J. Neurosci.* 35, 3607–3615. doi: 10.1523/JNEUROSCI.3137-14.2015

Dunsmoor, J. E., Bandettini, P. A., and Knight, D. C. (2007). Impact of continuous versus intermittent CS-UCS pairing on human brain activation during Pavlovian fear conditioning. *Behav. Neurosci.* 121:635. doi: 10.1037/0735-7044.121.4.635

Dunsmoor, J. E., Bandettini, P. A., and Knight, D. C. (2008). Neural correlates of unconditioned response diminution during Pavlovian conditioning. *Neuroimage* 40, 811–817. doi: 10.1016/j.neuroimage.2007.11.042

Eden, A. S., Schreiber, J., Anwander, A., Keuper, K., Laeger, I., Zwanzger, P., et al. (2015). Emotion regulation and trait anxiety are predicted by the microstructure of fibers between amygdala and prefrontal cortex. *J. Neurosci.* 35, 6020–6027. doi: 10.1523/JNEUROSCI.3659-14.2015

Fitzgerald, P. B., Fountain, S., and Daskalakis, Z. J. (2006). A comprehensive review of the effects of rTMS on motor cortical excitability and inhibition. *Clin. Neurophysiol.* 117, 2584–2596. doi: 10.1016/j.clinph.2006.06.712

Foa, E. B., Liebowitz, M. R., Kozak, M. J., Davies, S., Campeas, R., Franklin, M. E., et al. (2005). Randomized, placebo-controlled trial of exposure and ritual prevention, clomipramine, and their combination in the treatment of obsessive-compulsive disorder. *Am. J. Psychiatry* 162, 151–161. doi: 10.1176/appi.ajp.162.1.151

Foa, E. B., Riggs, D. S., Dancu, C. V., and Rothbaum, B. O. (1993). Reliability and validity of a brief instrument for assessing post-traumatic stress disorder. *J. Trauma. Stress* 6, 459–473. doi: 10.1002/jts.2490060405

Folloni, D., Verhagen, L., Mars, R. B., Fouragnan, E., Constans, C., Aubry, J. F., et al. (2019). Manipulation of subcortical and deep cortical activity in the primate brain using transcranial focused ultrasound stimulation. *Neuron* 101, 1109–1116. doi: 10.1016/j.neuron.2019.01.019

Fryml, L. D., Pelic, C. G., Acierno, R., Tuerk, P., Yoder, M., Borckardt, J. J., et al. (2019). Exposure therapy and simultaneous repetitive transcranial magnetic stimulation: a controlled pilot trial for the treatment of posttraumatic stress disorder. *J. ECT* 35, 53–60. doi: 10.1097/YCT.0000000000000505

Ganho-Ávila, A., Gonçalves, Ó. F., Guiomar, R., Boggio, P. S., Asthana, M. K., Krypotos, A. M., et al. (2019). The effect of cathodal tDCS on fear extinction: a cross-measures study. *PLoS ONE* 14:e0221282. doi: 10.1371/journal.pone.0221282

Glenn, C. R., Lieberman, L., and Hajcak, G. (2012). Comparing electric shock and a fearful screaming face as unconditioned stimuli for fear learning. *Int. J. Psychophysiol.* 86, 214–219. doi: 10.1016/j.ijpsycho.2012.09.006

Goodman, W. K., Price, L. H., Rasmussen, S. A., Mazure, C., Fleischmann, R. L., Hill, C. L., et al. (1989). The Yale-Brown obsessive compulsive scale: I. Development, use, and reliability. *Arch. General Psychiatry* 46, 1006–1011. doi: 10.1001/archpsyc.1989.01810110048007

Goossens, L., Sunaert, S., Peeters, R., Griez, E. J., and Schruers, K. R. (2007). Amygdala hyperfunction in phobic fear normalizes after exposure. *Biol. Psychiatry* 62, 1119–1125. doi: 10.1016/j.biopsych.2007.04.024

Grassi, G., Godini, L., Grippo, A., Piccagliani, D., and Pallanti, S. (2015). Enhancing cognitive-behavioral therapy with repetitive transcranial magnetic stimulation in refractory obsessive-compulsive-disorder: a case report. *Brain Stimul.* 8:160. doi: 10.1016/j.brs.2014.10.007

Greenberg, T., Carlson, J. M., Cha, J., Hajcak, G., and Mujica-Parodi, L. R. (2013). Ventromedial prefrontal cortex reactivity is altered in generalized

anxiety disorder during fear generalization. *Depress. Anxiety* 30, 242–250. doi: 10.1002/da.22016

Guhn, A., Dresler, T., Andreatta, M., M?ller, L. D., Hahn, T., Tupak, S. V., et al. (2014). Medial prefrontal cortex stimulation modulates the processing of conditioned fear. *Front. Behav. Neurosci.* 8:44. doi: 10.3389/fnbeh.2014.00044

Guy, W. (1976). *ECDEU assessment manual for Psychopharmacology*. US Department of Health, Education, and Welfare, Public Health Service, Alcohol, Drug Abuse, and Mental Health Administration, National Institute of Mental Health, Psychopharmacology Research Branch, Division of Extramural Research Programs.

Haidt, J., McCauley, C., and Rozin, P. (1994). Individual differences in sensitivity to disgust: A scale sampling seven domains of disgust elicitors. *Pers. Individ. Dif.* 16, 701–713. doi: 10.1016/0191-8869(94)90212-7

Hallett, M. (2007). Transcranial magnetic stimulation: a primer. *Neuron* 55, 187–199. doi: 10.1016/j.neuron.2007.06.026

Hamilton, M. (1960). The hamilton depression scale—accelerator or break on antidepressant drug discovery. *Psychiatry* 23, 56–62. doi: 10.1136/jnnp.23.1.56

Hamm, A. O., and Vaitl, D. (1996). Affective learning: awareness and aversion. *Psychophysiology* 33, 698–710. doi: 10.1111/j.1469-8986.1996.tb02366.x

Hartley, C. A., Fischl, B., and Phelps, E. A. (2011). Brain structure correlates of individual differences in the acquisition and inhibition of conditioned fear. *Cerebral Cortex* 21, 1954–1962. doi: 10.1093/cercor/bhq253

Hein, G., Lamm, C., Brodbeck, C., and Singer, T. (2011). Skin conductance response to the pain of others predicts later costly helping. *PLoS ONE* 6:e22759. doi: 10.1371/journal.pone.0022759

Hermann, A., Schäfer, A., Walter, B., Stark, R., Vaitl, D., and Schienle, A. (2009). Emotion regulation in spider phobia: role of the medial prefrontal cortex. *Soc. Cogn. Affect. Neurosci.* 4, 257–267. doi: 10.1093/scan/nsp013

Herrmann, M. J., Katzorke, A., Busch, Y., Gromer, D., Polak, T., Pauli, P., et al. (2017). Medial prefrontal cortex stimulation accelerates therapy response of exposure therapy in acrophobia. *Brain Stimul.* 10, 291–297. doi: 10.1016/j.brs.2016.11.007

Herry, C., Ferraguti, F., Singewald, N., Letzkus, J. J., Ehrlich, I., and Lüthi, A. (2010). Neuronal circuits of fear extinction. *Eur. J. Neurosci.* 31, 599–612. doi: 10.1111/j.1460-9568.2010.07101.x

Huang, Y. Z., Edwards, M. J., Rounis, E., Bhatia, K. P., and Rothwell, J. C. (2005). Theta burst stimulation of the human motor cortex. *Neuron* 45, 201–206. doi: 10.1016/j.neuron.2004.12.033

Huff, N. C., Zielinski, D. J., Fecteau, M. E., Brady, R., and LaBar, K. S. (2010). Human fear conditioning conducted in full immersion 3-dimensional virtual reality. *JoVE* 42:e1993. doi: 10.3791/1993

Hutcherson, C. A., Plassmann, H., Gross, J. J., and Rangel, A. (2012). Cognitive regulation during decision making shifts behavioral control between ventromedial and dorsolateral prefrontal value systems. *J. Neurosci.* 32, 13543–13554. doi: 10.1523/JNEUROSCI.6387-11.2012

Isserles, M., Shalev, A. Y., Roth, Y., Peri, T., Kutz, I., Zlotnick, E., et al. (2013). Effectiveness of deep transcranial magnetic stimulation combined with a brief exposure procedure in post-traumatic stress disorder–a pilot study. *Brain Stimul.* 6, 377–383. doi: 10.1016/j.brs.2012.07.008

Jamil, A., Batsikadze, G., Kuo, H. I., Labruna, L., Hasan, A., Paulus, W., et al. (2017). Systematic evaluation of the impact of stimulation intensity on neuroplastic after-effects induced by transcranial direct current stimulation. *J. Physiol.* 595, 1273–1288. doi: 10.1113/JP272738

Kalisch, R., Korenfeld, E., Stephan, K. E., Weiskopf, N., Seymour, B., and Dolan, R. J. (2006). Context-dependent human extinction memory is mediated by a ventromedial prefrontal and hippocampal network. *J. Neurosci.* 26, 9503–9511. doi: 10.1523/JNEUROSCI.2021-06.2006

Kessler, R. C., Aguilar-Gaxiola, S., Alonso, J., Chatterji, S., Lee, S., Ormel, J., et al. (2009). The global burden of mental disorders: an update from the WHO World Mental Health (WMH) surveys. *Epidemiol. Psichiatr. Soc.* 18:23. doi: 10.1017/S1121189X00001421

Kim, H. S., Cho, H. Y., Augustine, G. J., and Han, J. H. (2016). Selective control of fear expression by optogenetic manipulation of infralimbic cortex after extinction. *Neuropsychopharmacology* 41, 1261–1273. doi: 10.1038/npp.2015.276

Kim, K. J., and Bell, M. A. (2006). Frontal EEG asymmetry and regulation during childhood. *Ann. N. Y. Acad. Sci.* 1094, 308–312. doi: 10.1196/annals.1376.040

Kim, S. H., Cornwell, B., and Kim, S. E. (2012). Individual differences in emotion regulation and hemispheric metabolic asymmetry. *Biol. Psychol.* 89, 382–386. doi: 10.1016/j.biopsycho.2011.11.013

Klomjai, W., Katz, R., and Lackmy-Vallée, A. (2015). Basic principles of transcranial magnetic stimulation (TMS) and repetitive TMS (rTMS). *Ann. Phys. Rehabil. Med.* 58, 208–213. doi: 10.1016/j.rehab.2015.05.005

Knapska, E., Macias, M., Mikosz, M., Nowak, A., Owczarek, D., Wawrzyniak, M., et al. (2012). Functional anatomy of neural circuits regulating fear and extinction. *Proc. Natl. Acad. Sci. U.S.A.* 109, 17093–17098. doi: 10.1073/pnas.1202087109

Kroenke, K., Spitzer, R. L., and Williams, J. B. (2001). The PHQ-9: validity of a brief depression severity measure. *J. Gen. Intern. Med.* 16, 606–613. doi: 10.1046/j.1525-1497.2001.016009606.x

Kroes, M. C., Dunsmoor, J. E., Hakimi, M., Oosterwaal, S., NYU PROSPEC collaboration, Meager, M. R., and Phelps, E. A. (2019). Patients with dorsolateral prefrontal cortex lesions are capable of discriminatory threat learning but appear impaired in cognitive regulation of subjective fear. *Soc. Cogn. Affect. Neurosci.* 14, 601–612. doi: 10.1093/scan/nsz039

Krypotos, A. M., Effting, M., Arnaudova, I., Kindt, M., and Beckers, T. (2014). Avoided by association: Acquisition, extinction, and renewal of avoidance tendencies toward conditioned fear stimuli. *Clin. Psychol. Sci.* 2, 336–343. doi: 10.1177/2167702613503139

Lang, N., Harms, J., Weyh, T., Lemon, R. N., Paulus, W., Rothwell, J. C., et al. (2006). Stimulus intensity and coil characteristics influence the efficacy of rTMS to suppress cortical excitability. *Clin. Neurophysiol.* 117, 2292–2301. doi: 10.1016/j.clinph.2006.05.030

Laux, L., Glanzmann, P., Schaffner, P., and Spielberger, C.D. (1981). *Das State-Trait-Angstinventar (Testmappe mit Handanweisung, Fragebogen STAI-G Form X 1 und Fragebogen STAI-G Form X 2).* Weinheim: Beltz

Lefaucheur, J. P., André-Obadia, N., Antal, A., Ayache, S. S., Baeken, C., Benninger, D. H., et al. (2014). Evidence-based guidelines on the therapeutic use of repetitive transcranial magnetic stimulation (rTMS). *Clin. Neurophysiol.* 125, 2150–2206. doi: 10.1016/j.clinph.2014.05.021

Legrand, M., Troubat, R., Brizard, B., Le Guisquet, A. M., Belzung, C., and El-Hage, W. (2019). Prefrontal cortex rTMS reverses behavioral impairments and differentially activates c-Fos in a mouse model of post-traumatic stress disorder. *Brain Stimul.* 12, 87–95. doi: 10.1016/j.brs.2018.09.003

Levkovitz, Y., Isserles, M., Padberg, F., Lisanby, S. H., Bystritsky, A., Xia, G., et al. (2015). Efficacy and safety of deep transcranial magnetic stimulation for major depression: a prospective multicenter randomized controlled trial. *World Psychiatry* 14, 64–73. doi: 10.1002/wps.20199

Likhtik, E., Popa, D., Apergis-Schoute, J., Fidacaro, G. A., and Paré, D. (2008). Amygdala intercalated neurons are required for expression of fear extinction. *Nature* 454, 642–645. doi: 10.1038/nature07167

Linnman, C., Rougemont-Bücking, A., Beucke, J. C., Zeffiro, T. A., and Milad, M. R. (2011). Unconditioned responses and functional fear networks in human classical conditioning. *Behav. Brain Res.* 221, 237–245. doi: 10.1016/j.bbr.2011.02.045

Liu, Y., Lin, W., Liu, C., Luo, Y., Wu, J., Bayley, P. J., et al. (2016). Memory consolidation reconfigures neural pathways involved in the suppression of emotional memories. *Nat. Commun.* 7, 1–12. doi: 10.1038/ncomms13375

Lonergan, M. H., Olivera-Figueroa, L. A., Pitman, R. K., and Brunet, A. (2013). Propranolol's effects on the consolidation and reconsolidation of long-term emotional memory in healthy participants: a meta-analysis. *J. Psychiatry Neurosci.* 38:222. doi: 10.1503/jpn.120111

Manteghi, F., Nasehi, M., and Zarrindast, M. R. (2017). Precondition of right frontal region with anodal tDCS can restore the fear memory impairment induced by ACPA in male mice. *EXCLI J.* 16, 1–13. doi: 10.17179/excli2016-693

Maples-Keller, J. L., Yasinski, C., Manjin, N., and Rothbaum, B. O. (2017). Virtual reality-enhanced extinction of phobias and post-traumatic stress. *Neurotherapeutics* 14, 554–563. doi: 10.1007/s13311-017-0534-y

Martin, D. M., Liu, R., Alonzo, A., Green, M., and Loo, C. K. (2014). Use of transcranial direct current stimulation (tDCS) to enhance cognitive training: effect of timing of stimulation. *Exp. Brain Res.* 232, 3345–3351. doi: 10.1007/s00221-014-4022-x

Martino, G., Catalano, A., Bellone, F., Russo, G. T., Vicario, C. M., Lasco, A., et al. (2019). As time goes by: anxiety negatively affects the perceived quality

of life in patients with type 2 diabetes of long duration. *Front. Psychol.* 10:1779. doi: 10.3389/fpsyg.2019.01779

McLaughlin, N. C. R., Strong, D., Abrantes, A., Garnaat, S., Cerny, A., O'Connell, C., et al. (2015). Extinction retention and fear renewal in a lifetime obsessive–compulsive disorder sample. *Behav. Brain Res.* 280, 72–77. doi: 10.1016/j.bbr.2014.11.011

Michael, T., Blechert, J., Vriends, N., Margraf, J., and Wilhelm, F. H. (2007). Fear conditioning in panic disorder: enhanced resistance to extinction. *J. Abnorm. Psychol.* 116:612. doi: 10.1037/0021-843X.116.3.612

Milad, M. R., Furtak, S. C., Greenberg, J. L., Keshaviah, A., Im, J. J., Falkenstein, M. J., et al. (2013). Deficits in conditioned fear extinction in obsessive-compulsive disorder and neurobiological changes in the fear circuit. *JAMA Psychiatry* 70, 608–618. doi: 10.1001/jamapsychiatry.2013.914

Milad, M. R., Orr, S. P., Pitman, R. K., and Rauch, S. L. (2005). Context modulation of memory for fear extinction in humans. *Psychophysiology* 42, 456–464. doi: 10.1111/j.1469-8986.2005.00302.x

Milad, M. R., Pitman, R. K., Ellis, C. B., Gold, A. L., Shin, L. M., Lasko, N. B., et al. (2009). Neurobiological basis of failure to recall extinction memory in posttraumatic stress disorder. *Biol. Psychiatry* 66, 1075–1082. doi: 10.1016/j.biopsych.2009.06.026

Milad, M. R., and Quirk, G. J. (2012). Fear extinction as a model for translational neuroscience: ten years of progress. *Annu. Rev. Psychol.* 63, 129–151. doi: 10.1146/annurev.psych.121208.131631

Milad, M. R., Rosenbaum, B. L., and Simon, N. M. (2014). Neuroscience of fear extinction: implications for assessment and treatment of fear-based and anxiety related disorders. *Behav. Res. Ther.* 62, 17–23. doi: 10.1016/j.brat.2014.08.006

Milad, M. R., Wright, C. I., Orr, S. P., Pitman, R. K., Quirk, G. J., and Rauch, S. L. (2007). Recall of fear extinction in humans activates the ventromedial prefrontal cortex and hippocampus in concert. *Biol. Psychiatry* 62, 446–454. doi: 10.1016/j.biopsych.2006.10.011

Moher, D., Liberati, A., Tetzlaff, J., Altman, D. G., and PRISMA, Group (2009). Preferred reporting items for systematic reviews and meta-analyses: the PRISMA statement. *PLoS Med.* 6:e1000097. doi: 10.1371/journal.pmed.1000097

Monte-Silva, K., Kuo, M. F., Hessenthaler, S., Fresnoza, S., Liebetanz, D., Paulus, W., et al. (2013). Induction of late LTP-like plasticity in the human motor cortex by repeated non-invasive brain stimulation. *Brain Stimul.* 6, 424–432. doi: 10.1016/j.brs.2012.04.011

Montgomery, S., and Åsberg, M. A. R. I. E. (1977). *A New Depression Scale Designed to be Sensitive to Change*. London: Acad. Department of Psychiatry, Guy's Hospital.

Morey, R. A., Gold, A. L., LaBar, K. S., Beall, S. K., Brown, V. M., Haswell, C. C., et al. (2012). Amygdala volume changes in posttraumatic stress disorder in a large case-controlled veterans group. *Arch. Gen. Psychiatry* 69, 1169–1178. doi: 10.1001/archgenpsychiatry.2012.50

Morgan, M. A., Romanski, L. M., and LeDoux, J. E. (1993). Extinction of emotional learning: contribution of medial prefrontal cortex. *Neurosci. Lett.* 163, 109–113. doi: 10.1016/0304-3940(93)90241-C

Motzkin, J. C., Philippi, C. L., Wolf, R. C., Baskaya, M. K., and Koenigs, M. (2015). Ventromedial prefrontal cortex is critical for the regulation of amygdala activity in humans. *Biol. Psychiatry* 77, 276–284. doi: 10.1016/j.biopsych.2014.02.014

Mungee, A., Burger, M., and Bajbouj, M. (2016). No effect of cathodal transcranial direct current stimulation on fear memory in healthy human subjects. *Brain Sci.* 6:55. doi: 10.3390/brainsci6040055

Mungee, A., Kazzer, P., Feeser, M., Nitsche, M. A., Schiller, D., and Bajbouj, M. (2014). Transcranial direct current stimulation of the prefrontal cortex: a means to modulate fear memories. *Neuroreport* 25, 480–484. doi: 10.1097/WNR.0000000000000119

Myers, K. M., and Davis, M. (2007). Mechanisms of fear extinction. *Mol. Psychiatry* 12, 120–150. doi: 10.1038/sj.mp.4001939

Nasehi, M., Hajian, M., Ebrahimi-Ghiri, M., and Zarrindast, M. R. (2016). Role of the basolateral amygdala dopamine receptors in arachidonylcyclopropylamide-induced fear learning deficits. *Psychopharmacology* 233, 213–224. doi: 10.1007/s00213-015-4096-6

Nasehi, M., Khani-Abyaneh, M., Ebrahimi-Ghiri, M., and Zarrindast, M. R. (2017a). The effect of left frontal transcranial direct-current stimulation on propranolol-induced fear memory acquisition and consolidation deficits. *Behav. Brain Res.* 331, 76–83. doi: 10.1016/j.bbr.2017.04.055

Nasehi, M., Soltanpour, R., Ebrahimi-Ghiri, M., Zarrabian, S., and Zarrindast, M. R. (2017b). Interference effects of transcranial direct current stimulation over the right frontal cortex and adrenergic system on conditioned fear. *Psychopharmacology* 234, 3407–3416. doi: 10.1007/s00213-017-4722-6

Ney, L. J., Vicario, C. M., Nitsche, M. A., and Felmingham, K. L. (2021). Timing matters: Transcranial direct current stimulation after extinction learning impairs subsequent fear extinction retention. *Neurobiol. Learn. Mem.* 177:107356. doi: 10.1016/j.nlm.2020.107356

Nieuwenhuis, I. L., and Takashima, A. (2011). The role of the ventromedial prefrontal cortex in memory consolidation. *Behav. Brain Res.* 218, 325–334. doi: 10.1016/j.bbr.2010.12.009

Nitsche, M. A., Cohen, L. G., Wassermann, E. M., Priori, A., Lang, N., Antal, A., et al. (2008). Transcranial direct current stimulation: state of the art 2008. *Brain Stimul.* 1, 206–223. doi: 10.1016/j.brs.2008.06.004

Nitsche, M. A., Liebetanz, D., Lang, N., Antal, A., Tergau, F., and Paulus, W. (2003). Safety criteria for transcranial direct current stimulation (tDCS) in humans. *Clin. Neurophysiol.* 114, 2220–2223. doi: 10.1016/S1388-2457(03)00235-9

Nitsche, M. A., and Paulus, W. (2000). Excitability changes induced in the human motor cortex by weak transcranial direct current stimulation. *J. Physiol.* 527:633. doi: 10.1111/j.1469-7793.2000.t01-1-00633.x

Nitsche, M. A., and Paulus, W. (2001). Sustained excitability elevations induced by transcranial DC motor cortex stimulation in humans. *Neurology* 57, 1899–1901. doi: 10.1212/WNL.57.10.1899

Norrholm, S. D., Jovanovic, T., Vervliet, B., Myers, K. M., Davis, M., Rothbaum, B. O., et al. (2006). Conditioned fear extinction and reinstatement in a human fear-potentiated startle paradigm. *Learn. Memory* 13, 681–685. doi: 10.1101/lm.393906

Notzon, S., Deppermann, S., Fallgatter, A., Diemer, J., Kroczek, A., Domschke, K., et al. (2015). Psychophysiological effects of an iTBS modulated virtual reality challenge including participants with spider phobia. *Biol. Psychol.* 112, 66–76. doi: 10.1016/j.biopsycho.2015.10.003

Olatunji, B. O., Woods, C. M., de Jong, P. J., Teachman, B. A., Sawchuk, C. N., and David, B. (2009). Development and initial validation of an abbreviated Spider Phobia Questionnaire using item response theory. *Behav. Ther.* 40, 114–130. doi: 10.1016/j.beth.2008.04.002

Oldrati, V., Colombo, B., and Antonietti, A. (2018). Combination of a short cognitive training and tDCS to enhance visuospatial skills: a comparison between online and offline neuromodulation. *Brain Res.* 1678, 32–39. doi: 10.1016/j.brainres.2017.10.002

Osuch, E. A., Benson, B. E., Luckenbaugh, D. A., Geraci, M., Post, R. M., and McCann, U. (2009). Repetitive TMS combined with exposure therapy for PTSD: a preliminary study. *J. Anxiety Disord.* 23, 54–59. doi: 10.1016/j.janxdis.2008.03.015

Parsons, T. D. (2015). Virtual reality for enhanced ecological validity and experimental control in the clinical, affective and social neurosciences. *Front. Hum. Neurosci.* 9:660. doi: 10.3389/fnhum.2015.00660

Pascual-Leone, A., Tarazona, F., Keenan, J., Tormos, J. M., Hamilton, R., and Catala, M. D. (1998). Transcranial magnetic stimulation and neuroplasticity. *Neuropsychologia* 37, 207–217. doi: 10.1016/S0028-3932(98)00095-5

Phelps, E. A., Delgado, M. R., Nearing, K. I., and LeDoux, J. E. (2004). Extinction learning in humans: role of the amygdala and vmPFC. *Neuron* 43, 897–905. doi: 10.1016/j.neuron.2004.08.042

Quirk, G. J., Garcia, R., and González-Lima, F. (2006). Prefrontal mechanisms in extinction of conditioned fear. *Biol. Psychiatry* 60, 337–343.. doi: 10.1016/j.biopsych.2006.03.010

Quirk, G. J., and Gehlert, D. R. (2003). Inhibition of the amygdala: key to pathological states? *Ann. N. Y. Acad. Sci.* 985, 263–272. doi: 10.1111/j.1749-6632.2003.tb07087.x

Quirk, G. J., Russo, G. K., Barron, J. L., and Lebron, K. (2000). The role of ventromedial prefrontal cortex in the recovery of extinguished fear. *J. Neurosci.* 20, 6225–6231. doi: 10.1523/JNEUROSCI.20-16-06225.2000

Raij, T., Nummenmaa, A., Marin, M. F., Porter, D., Furtak, S., Setsompop, K., et al. (2018). Prefrontal cortex stimulation enhances fear extinction memory in humans. *Biol. Psychiatry* 84, 129–137. doi: 10.1016/j.biopsych.2017.10.022

Reiss, S., Peterson, R. A., Gursky, D. M., and McNally, R. J. (1986). Anxiety sensitivity, anxiety frequency and the prediction of fearfulness. *Behav. Res. Ther.* 24, 1–8. doi: 10.1016/0005-7967(86)90143-9

Remes, O., Brayne, C., Van Der Linde, R., and Lafortune, L. (2016). A systematic review of reviews on the prevalence of anxiety disorders in adult populations. *Brain Behav.* 6:e00497. doi: 10.1002/brb3.497

Richmond, M. A., Murphy, C. A., Pouzet, B., Schmid, P., Rawlins, J. N. P., and Feldon, J. (1998). A computer controlled analysis of freezing behaviour. *J. Neurosci. Methods* 86, 91–99. doi: 10.1016/S0165-0270(98)00150-2

Ridderinkhof, K. R., Van Den Wildenberg, W. P., Segalowitz, S. J., and Carter, C. S. (2004). Neurocognitive mechanisms of cognitive control: the role of prefrontal cortex in action selection, response inhibition, performance monitoring, and reward-based learning. *Brain Cogn.* 56, 129–140. doi: 10.1016/j.bandc.2004.09.016

Roelofs, K. (2017). Freeze for action: neurobiological mechanisms in animal and human freezing. *Philos. Trans. Royal Soc. B* 372:20160206. doi: 10.1098/rstb.2016.0206

Sah, P., and Westbrook, R. F. (2008). The circuit of fear. *Nature* 454, 589–590. doi: 10.1038/454589a

Sakai, K., Hikosaka, O., Miyauchi, S., Takino, R., Sasaki, Y., and Pütz, B. (1998). Transition of brain activation from frontal to parietal areas in visuomotor sequence learning. *J. Neurosci.* 18, 1827–18-40. doi: 10.1523/JNEUROSCI.18-05-01827.1998

Salehinejad, M. A., Nejati, V., Mosayebi-Samani, M., Mohammadi, A., Wischnewski, M., Kuo, M. F., et al. (2020). Transcranial Direct Current Stimulation in ADHD: a systematic review of efficacy, safety, and protocol-induced electrical field modeling results. *Neurosci. Bull* 36, 1191–1212. doi: 10.1007/s12264-020-00501-x

Salehinejad, M. A., Wischnewski, M., Nejati, V., Vicario, C. M., and Nitsche, M. A. (2019). Transcranial direct current stimulation in attention-deficit hyperactivity disorder: a meta-analysis of neuropsychological deficits. *PLoS ONE* 14:e0215095. doi: 10.1371/journal.pone.0215095

Samani, M. M., Agboada, D., Jamil, A., Kuo, M. F., and Nitsche, M. A. (2019). Titrating the neuroplastic effects of cathodal transcranial direct current stimulation (tDCS) over the primary motor cortex. *Cortex* 119, 350–361. doi: 10.1016/j.cortex.2019.04.016

Sehlmeyer, C., Schöning, S., Zwitserlood, P., Pfleiderer, B., Kircher, T., Arolt, V., et al. (2009). Human fear conditioning and extinction in neuroimaging: a systematic review. *PLoS ONE* 4:e5865. doi: 10.1371/journal.pone.0005865

Sevenster, D., Visser, R. M., and D'Hooge, R. (2018). A translational perspective on neural circuits of fear extinction: current promises and challenges. *Neurobiol. Learn. Mem.* 155, 113–126. doi: 10.1016/j.nlm.2018.07.002

Sheehan, D. V., Harnett-Sheehan, K., and Raj, B. A. (1996). The measurement of disability. *Int. Clin. Psychopharmacol.* 11(Suppl. 3), 89–95. doi: 10.1097/00004850-199606003-00015

Shin, L. M., Rauch, S. L., and Pitman, R. K. (2006). Amygdala, medial prefrontal cortex, and hippocampal function in PTSD. *Ann. N. Y. Acad. Sci.* 1071, 67–79. doi: 10.1196/annals.1364.007

Simpson, H. B., Neria, Y., Lewis-Fernández, R., and Schneier, F. (Eds.). (2010). *Anxiety Disorders: Theory, Research and Clinical Perspectives*. Cambridge: Cambridge University Press.

Spielberger, C. D. (1984). *State-Trait Inventory: A Comprehensive Bibliography*. Palo Alto.

Spitzer, R. L., Kroenke, K., Williams, J. B., and Löwe, B. (2006). A brief measure for assessing generalized anxiety disorder: the GAD-7. *Arch. Intern. Med.* 166, 1092–1097. doi: 10.1001/archinte.166.10.1092

Stagg, C. J., Jayaram, G., Pastor, D., Kincses, Z. T., Matthews, P. M., and Johansen-Berg, H. (2011). Polarity and timing-dependent effects of transcranial direct current stimulation in explicit motor learning. *Neuropsychologia* 49, 800–804. doi: 10.1016/j.neuropsychologia.2011.02.009

Stagg, C. J., and Nitsche, M. A. (2011). Physiological basis of transcranial direct current stimulation. *Neuroscientist* 17, 37–53. doi: 10.1177/1073858410386614

Stark, E. A., Parsons, C. E., Van Hartevelt, T. J., Charquero-Ballester, M., McManners, H., Ehlers, A., et al. (2015). Post-traumatic stress influences the brain even in the absence of symptoms: a systematic, quantitative meta-analysis of neuroimaging studies. *Neurosci. Biobehav. Rev.* 56, 207–221. doi: 10.1016/j.neubiorev.2015.07.007

Sundin, E. C., and Horowitz, M. J. (2002). Impact of Event Scale: psychometric properties. *British J. Psychiatry* 180, 205–209. doi: 10.1192/bjp.180.3.205

Szymanski, J., and O'Donohue, W. (1995). Fear of spiders questionnaire. *J. Behav. Ther. Exp. Psychiatry* 26, 31–34. doi: 10.1016/0005-7916(94)00072-T

Taylor, S., Abramowitz, J. S., and McKay, D. (2012). Non-adherence and non-response in the treatment of anxiety disorders. *J. Anxiety Disord.* 26, 583–589. doi: 10.1016/j.janxdis.2012.02.010

Todder, D., Gershi, A., Perry, Z., Kaplan, Z., Levine, J., and Avirame, K. (2018). Immediate effects of transcranial direct current stimulation on obsession-induced anxiety in refractory obsessive-compulsive disorder: a pilot study. *J. ECT* 34, e51–e57. doi: 10.1097/YCT.0000000000000473

Tovote, P., Fadok, J. P., and Lüthi, A. (2015). Neuronal circuits for fear and anxiety. *Nat. Rev. Neurosci.* 16, 317–331. doi: 10.1038/nrn3945

Van Hout, H. P., Beekman, A. T., De Beurs, E., Comijs, H., Van Marwijk, H., De Haan, M., et al. (2004). Anxiety and the risk of death in older men and women. *Br. J. Psychiatry* 185, 399–404. doi: 10.1192/bjp.185.5.399

VanElzakker, M. B., Dahlgren, M. K., Davis, F. C., Dubois, S., and Shin, L. M. (2014). From Pavlov to PTSD: the extinction of conditioned fear in rodents, humans, and anxiety disorders. *Neurobiol. Learn. Mem.* 113, 3–18. doi: 10.1016/j.nlm.2013.11.014

van't Wout, M., Longo, S. M., Reddy, M. K., Philip, N. S., Bowker, M. T., and Greenberg, B. D. (2017). Transcranial direct current stimulation may modulate extinction memory in posttraumatic stress disorder. *Brain Behav.* 7:e00681. doi: 10.1002/brb3.681

van't Wout, M., Mariano, T. Y., Garnaat, S. L., Reddy, M. K., Rasmussen, S. A., and Greenberg, B. D. (2016). Can transcranial direct current stimulation augment extinction of conditioned fear? *Brain Stimul.* 9, 529–536. doi: 10.1016/j.brs.2016.03.004

van't Wout-Frank, M., Shea, M. T., Larson, V. C., Greenberg, B. D., and Philip, N. S. (2019). Combined transcranial direct current stimulation with virtual reality exposure for posttraumatic stress disorder: feasibility and pilot results. *Brain Stimul.* 12, 41–43. doi: 10.1016/j.brs.2018.09.011

Via, E., Fullana, M. A., Goldberg, X., Tinoco-González, D., Martínez-Zalacaín, I., Soriano-Mas, C., et al. (2018). Ventromedial prefrontal cortex activity and pathological worry in generalised anxiety disorder. *Br. J. Psychiatry* 213, 437–443. doi: 10.1192/bjp.2018.65

Vicario, C. M., and Nitsche, M. A. (2013a). Non-invasive brain stimulation for the treatment of brain diseases in childhood and adolescence: state of the art, current limits and future challenges. *Front. Syst. Neurosci.* 7:94. doi: 10.3389/fnsys.2013.00094

Vicario, C. M., and Nitsche, M. A. (2013b). Transcranial direct current stimulation: a remediation tool for the treatment of childhood congenital dyslexia? *Front. Hum. Neurosci.* 7:139. doi: 10.3389/fnhum.2013.00139

Vicario, C. M., Nitsche, M. A., and Felmingham, K. (2017). Forgetting fear associations through tES: which memory process might be critical? *Transl. Psychiatry* 7, e1046–e1046. doi: 10.1038/tp.2017.26

Vicario, C. M., Nitsche, M. A., Hoysted, I., Yavari, F., Avenanti, A., Salehinejad, M. A., et al. (2020b). Anodal transcranial direct current stimulation over the ventromedial prefrontal cortex enhances fear extinction in healthy humans: a single blind sham-controlled study. *Brain Stimul.* 13, 489–491. doi: 10.1016/j.brs.2019.12.022

Vicario, C. M., and Nitsche, M. A., (2019). "tDCS in pediatric neuropsychiatric disorders," in *Neurotechnology and Brain Stimulation in Pediatric Psychiatric and Neurodevelopmental Disorders*, eds L.M. Oberman, P.G. Enticott (Cambridge, MA: Academic Press), 217–35. doi: 10.1016/B978-0-12-812777-3.00009-X

Vicario, C. M., Salehinejad, M. A., Avenanti, A., and Nitsche, M. A. (2020a). "Transcranial Direct Current Stimulation (tDCS) in anxiety disorders," in *Non Invasive Brain Stimulation in Psychiatry and Clinical Neurosciences* (Cham: Springer), 301–317. doi: 10.1007/978-3-030-43356-7_21

Vicario, C. M., Salehinejad, M. A., Felmingham, K., Martino, G., and Nitsche, M. A. (2019). A systematic review on the therapeutic effectiveness of non-invasive brain stimulation for the treatment of anxiety disorders. *Neurosci. Biobehav.Rev.* 96, 219–231. doi: 10.1016/j.neubiorev.2018.12.012

Wang, S. H., and Morris, R. G. (2010). Hippocampal-neocortical interactions in memory formation, consolidation, and reconsolidation. *Annu. Rev. Psychol.* 61, 49–79. doi: 10.1146/annurev.psych.093008.100523

Watson, D., Clark, L. A., and Tellegen, A. (1988). Development and validation of brief measures of positive and negative affect: the PANAS scales. *J. Pers. Soc. Psychol.* 54:1063. doi: 10.1037/0022-3514.54.6.1063

WHO (2017). *Depression and Other Common Mental Disorders: Global Health Estimates*. Geneva: World Health Organization, 1–24.

Wittchen, H. U., Jacobi, F., Rehm, J., Gustavsson, A., Svensson, M., Jönsson, B., et al. (2011). The size and burden of mental disorders and other disorders of the brain in Europe 2010. *Eur. Neuropsychopharmacol.* 21, 655–679. doi: 10.1016/j.euroneuro.2011.07.018

Wolpe, J. (1973). *The Practice of Behavior Therapy*. (2nd ed.). Oxford: Pergamon.

Yavari, F., Jamil, A., Samani, M. M., Vidor, L. P., and Nitsche, M. A. (2018). Basic and functional effects of transcranial Electrical Stimulation (tES)—an introduction. *Neurosci. Biobehav. Rev.* 85, 81–92. doi: 10.1016/j.neubiorev.2017.06.015

Zuj, D. V., Palmer, M. A., Malhi, G. S., Bryant, R. A., and Felmingham, K. L. (2018). Greater sleep disturbance and longer sleep onset latency facilitate SCR-specific fear reinstatement in PTSD. *Behav. Res. Ther.* 110, 1–10. doi: 10.1016/j.brat.2018.08.005

Conflict of Interest: MN is a member of the Scientific Advisory Boards of Neuroelectrics and NeuroDevice.

The remaining authors declare that the research was conducted in the absence of any commercial or financial relationships that could be construed as a potential conflict of interest.

frontiers in Behavioral Neuroscience

ORIGINAL RESEARCH
published: 21 April 2021
doi: 10.3389/fnbeh.2021.670699

Effects of iTBS-rTMS on the Behavioral Phenotype of a Rat Model of Maternal Immune Activation

*Nadine Rittweger[1], Tanja Ishorst[1], Gleb Barmashenko[1,2], Verena Aliane[1], Christine Winter[3,4] and Klaus Funke[1]**

[1]Department of Neurophysiology, Medical Faculty, Ruhr-University, Bochum, Germany, [2]AIO-Studien-gGmbH, Berlin, Germany, [3]Department of Psychiatry and Psychotherapy, Charité University Medicine Berlin, Berlin, Germany, [4]Department of Psychiatry and Psychotherapy, Medical Faculty Carl Gustav Carus, Technische Universität Dresden, Dresden, Germany

Repetitive transcranial magnetic stimulation (rTMS) is considered a promising therapeutic tool for treating neuropsychiatric diseases. Previously, we found intermittent theta-burst stimulation (iTBS) rTMS to be most effective in modulating cortical excitation-inhibition balance in rats, accompanied by improved cortical sensory processing and sensory learning performance. Using an animal schizophrenia model based on maternal immune activation (MIA) we tested if iTBS applied to either adult or juvenile rats can affect the behavioral phenotype in a therapeutic or preventive manner, respectively. In a sham-controlled fashion, iTBS effects in MIA rats were compared with rats receiving vehicle NaCl injection instead of the synthetic viral strand. Prior to iTBS, adult MIA rats showed deficits in sensory gating, as tested with prepulse inhibition (PPI) of the acoustic startle reflex, and deficits in novel object recognition (NOR). No differences between MIA and control rats were evident with regard to signs of anxiety, anhedonia and depression but MIA rats were somewhat superior to controls during the training phase of Morris Water Maze (MWM) test. MIA but not control rats significantly improved in PPI following iTBS at adulthood but without significant differences between verum and sham application. If applied during adolescence, verum but not sham-iTBS improved NOR at adulthood but no difference in PPI was evident in rats treated either with sham or verum-iTBS. MIA and control rat responses to sham-iTBS applied at adulthood differed remarkably, indicating a different physiological reaction to the experimental experiences. Although verum-iTBS was not superior to sham-iTBS, MIA rats seemed to benefit from the treatment procedure in general, since differences—in relation to control rats declined or disappeared.

OPEN ACCESS

Edited by:
Alia Benali, Hertie Institute for Clinical Brain Research, Germany

Reviewed by:
Jennifer Rodger, University of Western Australia, Australia
Vera Moliadze, University Medical Center Schleswig-Holstein, Germany

***Correspondence:**
Klaus Funke
klaus.funke@rub.de

Specialty section:
This article was submitted to Pathological Conditions, a section of the journal Frontiers in Behavioral Neuroscience

Received: *03 March 2021*
Accepted: *30 March 2021*
Published: *21 April 2021*

Citation:
Rittweger N, Ishorst T, Barmashenko G, Aliane V, Winter C and Funke K (2021) Effects of iTBS-rTMS on the Behavioral Phenotype of a Rat Model of Maternal Immune Activation. Front. Behav. Neurosci. 15:670699. doi: 10.3389/fnbeh.2021.670699

Abbreviations: ANOVA, analysis of variance; ASR, acoustic startle response; DAT+, dopamine transporter overexpressing rat; DBS, deep brain stimulation; EPM, elevated plus maze; GD, gestational day; iTBS, intermittent theta-burst stimulation; MIA, maternal immune activation; MK-801, NMDA receptor antagonist dizolcilpine; mPFC, medial prefrontal cortex; MWM, Morris water maze; NIBS, non-invasive brain stimulation; NOR, novel object recognition; PFST, Porsolt forces swim test; PolyI:C, polyinosinic:polycytidylic acid; PPI, prepulse inhibition; PV, parvalbumin; rTMS, repetitive transcranial magnetic stimulation; SCT, sucrose consumption test; tDCS, transcranial direct current stimulation.

Even if classical placebo effects can be excluded, motor or cognitive challenges or the entire handling procedure during the experiments appear to alleviate the behavioral impairments of MIA rats.

Keywords: maternal immune stimulation, schizophrenia, animal model, behavioral phenotypes, rTMS, iTBS, sham stimulation, history of experience

INTRODUCTION

Schizophrenia is considered a neurodevelopmental disorder originating from disturbed neuronal maturation at prenatal stage and/or during adolescence (Insel, 2010; Selemon and Zecevic, 2015). Epidemiological studies demonstrate a relationship between infections during pregnancy and increased risk of the offspring to develop a schizophrenic phenotype during early adulthood (Mednick et al., 1988; Brown et al., 2004; Brown, 2012; Estes and McAllister, 2016). Based on these findings rodent maternal immune activation (MIA) models have been launched which use injections of either viral or bacterial pathogens to pregnant dams at a particular state of gestation (Zuckerman et al., 2003; Zuckerman and Weiner, 2005; Meyer, 2014; for review see Bergdolt and Dunaevsky, 2019).

Converging evidence obtained from patient studies and MIA models suggests aberrant synchrony of long-range neuronal network oscillations as a major cause of psychotic states and cognitive deficits as observed in schizophrenia and other psychiatric disorders (for reviews see Sukhodolsky et al., 2007; Lisman and Buzsáki, 2008; Uhlhaas and Singer, 2010; Başar, 2013). Disturbed local and long-range synchronization of neuronal activity is likely a result of maldevelopment of neurons and/or their connections (Insel, 2010; Selemon and Zecevic, 2015) leading to a misbalance of excitatory and inhibitory processes, most strikingly evidenced by a reduced function of the interneurons expressing the calcium-binding protein parvalbumin (PV; for review of knowledge obtained from clinical studies and animal models see Lewis et al., 2012; Ferguson and Gao, 2018).

Pharmacological treatment of schizophrenia in the adult is still unsatisfying since alleviation is mostly restricted to the positive symptoms of the disease but less improves the cognitive deficits. And, often a pharmacoresistance develops due to a plastic response of the neuronal system, e.g., changes in the number of receptors targeted by the drug, further limiting the efficiency of drug treatment. Furthermore, neuronal malfunctions resulting from a disturbed development are even more difficult to treat at adult state. Currently, preventive interventions in the pharmacological, social and cognitive-behavioral regime are discussed (Reisinger et al., 2015; Millan et al., 2016). As non-invasive brain stimulation (NIBS) techniques, like transcranial direct current stimulation (tDCS) and repetitive transcranial magnetic stimulation (rTMS), have been shown to modulate cortical excitability and plasticity (Huang et al., 2005; Ziemann and Siebner, 2008; Ridding and Ziemann, 2010; Dayan et al., 2013), they may also be considered as alternative therapeutic or possible preventive tools (Post and Keck, 2001; Padberg and George, 2009; Rajji et al., 2013; Kuo et al., 2017; Iimori et al., 2019; Hadar et al., 2020) in the context of schizophrenia (Hadar et al., 2018, 2020).

We previously demonstrated that rTMS, and particularly the intermittent theta-burst stimulation (iTBS; Huang et al., 2005) protocol, is effective in modulating cortical excitability in rats. In this line, iTBS reduced expression of inhibitory activity markers like GAD67, PV and calbindin (CB; Trippe et al., 2009; Benali et al., 2011), increased evoked sensory responses (Thimm and Funke, 2015), and improved tactile associative learning (Mix et al., 2010). In a recent study we could further demonstrate that iTBS is able to alleviate aberrant synchrony of oscillatory brain activity within the limbic system of MIA offspring (Lippmann et al., 2021).

To evaluate its therapeutic and preventive potential, we applied iTBS either to adult or juvenile MIA rats, respectively, and tested the rats with regard to changes in behavioral phenotypes possibly induced by MIA, like deficits in attentional directing or spatial orientation/learning, or depression- and anxiety-like behaviors. With regard to the findings of previous experiments showing iTBS to modulate molecular and electrical neuronal activity markers as well as behavior, as mentioned above, we expected iTBS to have either a beneficial or detrimental effect on behavioral performance, depending on how it modulates inhibitory cortical activity and that application during adolescence has more profound effects. According to the effects of MIA, we expected different iTBS effects compared to controls. Given the many reports on sham-stimulation effects in humans we further expected to find additional effects related to testing and treatment, in particular in the groups of adult rats being re-tested, although pure placebo effects can be excluded. We found iTBS to reduce some of the behavioral deficits of MIA rats, like with sensory gating and novel object recognition (NOR), however, the effects of verum stimulation were largely not superior to sham stimulation, indicating a general beneficial effect of the cognitive and motor activity related to the testing and handling procedure. Interestingly, sham effects were different in MIA and control rats indicating differences in the processing of experiences related to the experimental conditions.

MATERIALS AND METHODS

Animals

Pregnant Wistar rats were delivered by Charles-River (Sulzfeld, Germany) on gestational day (GD) 13 for the purpose of MIA at GD15. Prior to iTBS and behavioral testing the dams and their offspring were housed within the central experimental animal facility of the medical faculty with free access to food pellets (V1534-000, Ssniff Spezialdiäten GmbH, Soest, Germany) and tap water and with a light-dark cycle of 12/12 h (light on at

6 am). On postnatal day 21, offspring were separated from their mothers with females and males housed separately in groups of four per cage (Macrolon type IV). To avoid additional variability due to varying hormone status of the females and for better comparability to other NIBS studies on male MIA offspring, we included only males in this study. One week before starting the experimental procedures the rats were moved to ventilated cabinets within the department and randomly allocated to the different experimental groups (see below) while still housed in the same groups of 4 animals per cage (Macrolon type IV). All experiments were performed in compliance with German laws and the directive of the European Community (2010/63/EU, Sept. 22th, 2010) for the use of animals in research and were approved by the local ethics committee (State Office for Nature, Environment and Consumer Protection, LANUV, Section 81-Animal Welfare, Az. 84-02.04.2014.A294).

Experimental Groups

We conducted two experimental series with sham or verum-iTBS applied to MIA offspring (termed MIA rats in the following) and age-matched controls either at adulthood (3–4 months old, *Exp. I*), or during adolescence (6 weeks old, *Exp. II*). To evaluate a possible therapeutic effect of iTBS (*Exp. I*) the behavioral phenotype of the adult rats was determined before and after stimulation. To test a possible preventive action, stimulation was applied during adolescence and behavioral testing followed when rats were adult. The offspring of each litter (MIA or controls) were randomly attributed to these experimental series and subgroups (sham or verum-iTBS) by a technician to achieve blinding, with each group composed of offspring originating from five different MIA and five different control litters.

Induction of MIA

To induce MIA, polyinosinic:polycytidylic acid (PolyI:C, 4 mg/kg, Sigma–Aldrich P1530, Steinheim, Germany dissolved in 1 ml 0.9% sterile NaCl) was injected in the tail vein at GD 15 as has been done in previous studies (see Hadar et al., 2020). To avoid stress and to enable a safe and precise injection, rats were transiently sedated by placing them within a desiccator equipped with an isoflurane (Forene® Abbvie GmbH, Ludwigshafen, Germany) soaked sponge. Control animals received 1 ml/kg NaCl vehicle in the same way.

rTMS (iTBS)

iTBS was applied to conscious rats as previously described in more detail (e.g., Mix et al., 2014; Kloosterboer and Funke, 2019): after the animals had been adapted to the handling (manual restrain) and the noise and skin sensations of iTBS over a period of about a week, daily iTBS (Monday to Friday) was applied using a Magstim rapid^2 and a 2 × 70 mm figure-of-eight coil (Magstim Limited, Whitland, Dyfed, UK). In a manner of accelerated rTMS (for review see Sonmez et al., 2019), each rat received three iTBS blocks of 600 pulses per day at 15–20 min intervals (1,800 pulses/day). This inter-block interval was chosen because it had been shown to amplify molecular iTBS effects in rat models (Volz et al., 2013) and effects on motor cortex in humans (Nettekoven et al., 2014). One iTBS block consisted of 20 trains, with each train consisting of 10 bursts (three pulses @ 50 Hz) repeated at 5 Hz. The trains were applied at intervals of 10 s (2 s ON/8 s OFF). Thus, one block lasted 192 s in total and was well tolerated by the animals without obvious discomfort or extensive movements. With regard to the fast maturation of rats and because of the higher succeptability of the juvenile brain to plasticity-inducing stimulation procedures we applied iTBS sessions only at 10 days (2 weeks) to the juvenile rats but stimulated the adult rats at 20 days (4 weeks). Stimulus intensity was set to 21–23% of maximal machine output for the adult rats as done in the previous studies. In case of the juvenile rats, stimulus intensity had to be increased to 30% due to the smaller brain size (Weissman et al., 1992) to achieve comparable stimulation efficiency as estimated by induced muscle twitches. Finally, for each individual animal the distance between coil and head of the animals varied between 5 and 10 mm to determine the optimal position to just prevent activation of body and limbs muscle, thus stimulation strength was below motor threshold. Stimulation intensity was re-adjusted if muscle twitches occurred at a coil-to-brain distance closer as 10 mm. The coil was placed in a way to induce a mediolateral oriented electric field suitable to activate cortical areas *via* the callosal axons while preventing stimulation of deeper structures (see Kloosterboer and Funke, 2019; Murphy et al., 2016, for more details). In case of sham stimulation the coil was lifted by 10 cm to prevent magnetic stimulation but exposing the animal to the sound of the TMS coil while manually restraining it in the same way.

Behavioral Testing Procedures

Prepulse Inhibition (PPI)

Prepulse Inhibition (PPI) test is based on the acoustic startle response (ASR) and estimates sensory gating by applying a prepulse of lower intensity (69, 73 and 83 dB) 100 ms prior to the startle stimulus (100 dB) (Swerdlow et al., 2008). PPI of the ASR was measured in a sound-shielded chamber equipped with a small mesh-wire cage (220 × 90 × 90 mm) mounted on a motion-sensitive transducer platform (TSE, Bad Homburg, Germany) to register the strength of the rat's flinch response. All sounds had durations of 20 ms and were applied *via* two loudspeakers as broad-band (white) noise signals on a continuous noise level of 60 dB SPL. Following acclimatization for 5 min, first a sequence of 10 startle stimuli (100 dB) was applied in isolation. Then, during the testing phase either the startle stimulus alone, one of the three pre-pulses alone, or a combination of one of the three pre-pulses with the startle pulse were quasi-randomly applied 10 times *via* custom software control. Stimuli were applied at intervals of 25 s with a jitter of ±5 s. PPI was calculated as 100 − mean prepulse-startle response/mean startle response separately, for each prepulse intensity.

Sucrose Consumption Test (SCT)

The Sucrose Consumption Test (SCT) is used as a measure of anhedonia if rats show a decreased preference of sweet solution over tap water (decreased ability to experience pleasure and reward; Papp et al., 1991). Rats were first habituated to the sweet test solution (Nestlé, Milchmädchen gezuckerte Kondensmilch, 1:3 diluted with tap water) and adapted to the test cage and

the bottle two days prior to testing. One day before testing, rats were restricted to 15 g food pellets per animal but with water *ad libitum*. On the test day itself rats had free access to the test solution for 15 min. The amount of consumed solution was determined by weighting the bottles before and after testing and by normalization to the individual body weight prior to testing.

Elevated Plus Maze (EPM)

Elevated plus maze (EPM) is a test for anxiety and determines how long rats stay on an open arm of a cross-shaped maze compared to arms enclosed by walls (Pellow et al., 1985). Each arm had a length of 90 cm and a width of 20 cm for the open arms and 8 cm for the closed. Two opposing arms were equipped with walls of 19 cm height starting at 10 cm from the center of the cross. The maze was placed in a brightly illuminated room at a height of 62 cm from bottom. The 5 min procedure which was video-recorded from top was started by placing the rat at the center of the maze with the head facing one of the open arms in a random order. Percent of time the rat spent in one of the open arms (full body out of the walls) was determined off-line by video analysis (Pinnacle Studio 10.6). Rats staying all the time at the central platform without moving to the open or closed arms were excluded from analysis.

Novel Object Recognition (NOR)

This procedure tests if rats are aware of either novel objects or changed places of objects (Ennaceur and Delacour, 1988). We tested for the recognition of novel objects 1 and 24 h after a previous configuration. Prior to the testing, rats were familiarized with the testing box (85 × 85 cm, 45 cm height) for 45 min. Three of four different objects were used in a random order. The acrylic objects were 20 cm in height and about 10 cm in diameter and had a different shapes (cylindrical, quadratic, triangular and hexagonal) and colors (red, yellow, blue, green inlays). The position of the objects to be replaced by a new object was changed from rat to rat to exclude place preferences according to room landmarks. After the two objects were placed equidistantly from the walls within the test arena, a rat was placed between the two objects facing one wall. The rat was allowed to explore the objects for 5 min while the process was video-recorded. The time the rat inspected each object with the criterion that at least one whisker or another part of the body was in close contact with the object was determined by off-line video analysis. A preference index (PI) was calculated as the ratio of the difference between time spent for new and old object to the sum of both $[(T_{new} - T_{old})/(T_{new} + T_{old})]$ yielding a range of −1 (only old object) to +1 (only new object).

Morris Water Maze (MWM)

The test was conducted according to Terry et al. (2011). A pool of 180 cm in diameter and 60 cm height was filled to a height of 30 cm with water at 22°C. For the purpose of video tracking/analysis, we have chosen a black pool to achieve a better contrast to the white body of the rats. The platform (12 cm in diameter) was made of transparent acryl to obtain invisibility if hidden by the water. When raised above water level during first trial, the platform was equipped by a bright signal red circumference to enhance visibility against transparent water by the rat. The pool was virtually divided into four cardinal sectors and the platform area. Automatic tracing of the rat's position was achieved by custom software video analysis based on the open source routines provided by Aguiar et al. (2007). The position of the white body of the rat against the black background can be reliably traced if preventing light reflections on the water surface, e.g., by using indirect illumination of the room. In addition to landmarks of the room, the walls of the pool were equipped with four different high contrast patterns at each cardinal direction.

MWM training sessions of four trials each were performed on four subsequent days while final place memory test happened on the 5th day with the platform removed. The platform was always located in the middle of the north quadrant, equidistantly from the wall and the center of the basin (45 cm). Only in case the MWM was performed a second time (rats having received iTBS in adult state) the platform location was switched to the south quadrant. The platform was above water level and thus visible for the rats for the four trials on day 1, but hidden below water surface on days 2–4. The platform was removed for the final memory test on day 5. For each of the four trials of one session the rat was released at a different quadrant facing the wall of the basin. The order of quadrants was randomized for each session. Rats were given a relaxing phase between trials (30–60 min) by testing the rats in an interleaved fashion. After each trial, rats were dried by a towel and placed in a cage under a red heat lamp. Each trial lasted for 90 s and the rat was guided by hand to the platform if not hitting the platform within this time. After the rat climbed the platform it was allowed to visually explore and memories the environment before being put back in the cage. The path of the rat was continuously tracked by the software and used to calculate the following parameters: total time to reach the platform, time spent in each quadrant (incl. platform area) and the number of entries to each quadrant online. Offline analysis further included total path length, mean swimming speed and mean distance from platform and pool center to further calculate five behavioral types (1 = thigmotaxis, 2 = cycling, 3 = random, 4 = corrected and 5 = direct, see Illouz et al., 2016) with the value indicating worst (1) to best (5) grade. In case of the final memory trial (with the platform removed) percent of time the rat spent within each quadrant for the first 30 s was calculated and time spent in the target quadrant was set in relation to the non-target quadrants.

Porsolt Forced Swim Test (PFST)

The Porsolt Forced Swim Test (PFST) had been developed as a paradigm to test the efficiency of antidepressive substances in rodents. It measures the time the animals spends in actively trying to escape from the aversive situation (swimming, struggling) vs. passive behavior, with the latter interpreted as a sign of depression-like behavior (Porsolt et al., 1977). In the test rats were placed for 5 min in transparent acrylic cylinders of 52 cm height and 19 cm in diameter, filled with water at 22°C up to a level of 35 cm. The procedure was video-recorded from aside to determine off-line the time spent with struggling, swimming, diving and floating. Floating was classified as being "immobile"

while the other behaviors were classified as "active." Finally, the ratio of immobile to active behavior was calculated. The rats were immediately removed from the water if they showed signs of respiratory distress and near-drowning. Afterward, rats were dried with a towel and placed in a cage with red light warming.

Statistical Analysis

All data sets were first tested for normal distribution using Shapiro–Wilk test. Two rats, one of the sham-iTBS control group and one of the MIA sham-iTBS group, did not move at all during EPM test. To avoid falsification of group means these data were excluded but imputated by group means. It turned out that all data sets appeared to be normally distributed after correction of these two outliers and were subjected to parametric tests. Two-factorial analysis of variance (ANOVA) using factors GROUP (MIA vs. Controls) and iTBS with either pre vs. post data for sham- and verum-iTBS in case of the adult rats, or sham vs. verum in case of the juvenile rats not tested before iTBS. Pairwise comparison of MIA vs. control groups and sham vs. verum groups was done using *t*-test for independent samples, while paired *t*-test was applied to compare pre- vs. post-iTBS data within a group. A difference was considered being statistically significant with $p < 0.05$. Partial eta^2 (η^2) was calculated as effect size in case of ANOVA while Cohen's-d (d) was calculated for *t*-test results on the basis of common SD.

RESULTS

Exp. Series I: iTBS Applied to Adult Rats (Therapeutic Approach)

Application of iTBS to adult MIA rats aimed at testing a possible therapeutic effect of this method. Therefore, the behavioral testing battery was conducted once before (data set pre-iTBS) and once after 4 weeks of daily iTBS (Monday–Friday, 3 blocks/day, data sets sham and verum-iTBS). This series was conducted in six blocks with each block consisting of two MIA offspring, with one receiving verum-iTBS, the other receiving sham-iTBS, and two corresponding controls (all male and from one litter).

PPI

ANOVA conducted with factors GROUP (Controls, MIA) and PREPULSE (69, 73, 83 dB) for PPI measurements prior to iTBS revealed a significant effect of both factors (GROUP: $F_{(1,71)} = 10.364$, $p = 0.002$, $\eta^2 = 0.136$; PREPULSE: $F_{(2,71)} = 71.568$, $p < 0.001$, $\eta^2 = 0.684$) indicating not only significant differences in PPI as induced by different prepulse strength but also a difference in PPI between MIA rats and controls. *Post hoc t*-test (for independent samples) revealed significantly less PPI in MIA rats compared to controls in case of 73 and 83 dB prepulse (73 dB: $T_{(22)} = 3.565$, $p = 0.0017$; $d = 1.46$; 83 dB: $T_{(22)} = 3.915$, $p < 0.001$; $d = 1.60$; **Figure 1A**).

MIA and control rats were then split into two groups, with one receiving sham-iTBS and the other verum-iTBS. ANOVA conducted with factors GROUP (Controls, MIA) and iTBS (pre, post) revealed no significant effects of both factors when analyzing sham and verum-iTBS groups tested with 73 and 83 dB prepulse but a highly significant interaction of both factors in case of sham- and verum-iTBS when tested with 73 dB prepulse and with verum-iTBS when tested with 83 dB prepulse (for further details see **Table 1**). A comparison of post-iTBS to pre-iTBS PPI values using paired *t*-test revealed a significant increase in PPI for MIA rats after sham and verum-iTBS both, in case of 73 dB and 83 dB prepulse (see **Table 1** and **Figure 1B**, orange asterisks). Differently, the controls showed a significant decrease in PPI after sham-iTBS when tested with 73 dB prepulse (**Table 1**, **Figure 1B**, blue asterisks). Post-iTBS data further showed a significant difference of PPI values between the sham-iTBS treated MIA and control rats ($T_{(10)} = -2{,}710$, $p = 0.026$, $d = 1.34$).

EPM

MIA rats did not differ from Control rats with regard to percent time spent in the open arms during EPM test when tested prior to iTBS ($p = 0.911$; **Figure 1C**). ANOVA conducted with the factors GROUP (Controls, MIA) and iTBS (pre, post) after sham- or verum-iTBS had been applied revealed no significant effect of factor GROUP but a significant effect of factor iTBS in case of sham-iTBS ($F_{(1,25)} = 5.824$, $p = 0.025$, $\eta^2 = 0.209$) and a strong trend in case of verum-iTBS ($F_{(1,25)} = 3.569$, $p = 0.073$, $\eta^2 = 0.151$). Paired *t*-test yielded a significant decrease in open arm stays for the control rats after sham-iTBS ($T_{(6)} = 2.495$, $p = 0.047$, $d = 1.17$) but no significant difference after verum-iTBS. In case of MIA rats, neither sham- nor verum-iTBS had a significant effect.

NOR

MIA rats appeared to show a lower performance in NOR when tested 24 h after first presentation of objects. A comparison of MIA and control rats using *t*-test revealed a statistically significant difference ($T_{(23)} = 2.130$, $p = 0.044$, $d = 0.85$; **Figure 1D**). ANOVA conducted with the factors GROUP and iTBS revealed no significant effects of each factor and no interaction between both when applied to the sham- or verum-iTBS treated groups.

PFST and SCT

In case of PFST and SCT neither differences between MIA and control rats nor effects of iTBS were found (**Figures 1E,F**).

MWM

All rats learned to find and remember the hidden platform during the first training phase prior to iTBS (days 1–4), evident by the progressive shortening of the time and the path to reach the platform when analyzed per day and for the individual trials of the first day (T 1–4). Also an increase in swimming speed and behavioral type was evident (see **Figure 2**). ANOVA conducted with the factors GROUP (MIA, controls) and either DAY (days 1–4) or TRIAL (trials 1–4 of day 1) revealed a significant effect of factors DAY and TRIAL for all measures (see **Tables 1–3**), as could be expected. Furthermore, factor GROUP appeared to be effective for time-to-reach platform (target) and mean swimming speed when ANOVA was applied to days 1–4 (**Table 2**), and a significant interaction between TRAIL and GROUP was evident in case of performance type (**Table 3**). A pairwise comparison of MIA and control rats using *t*-test revealed better performance

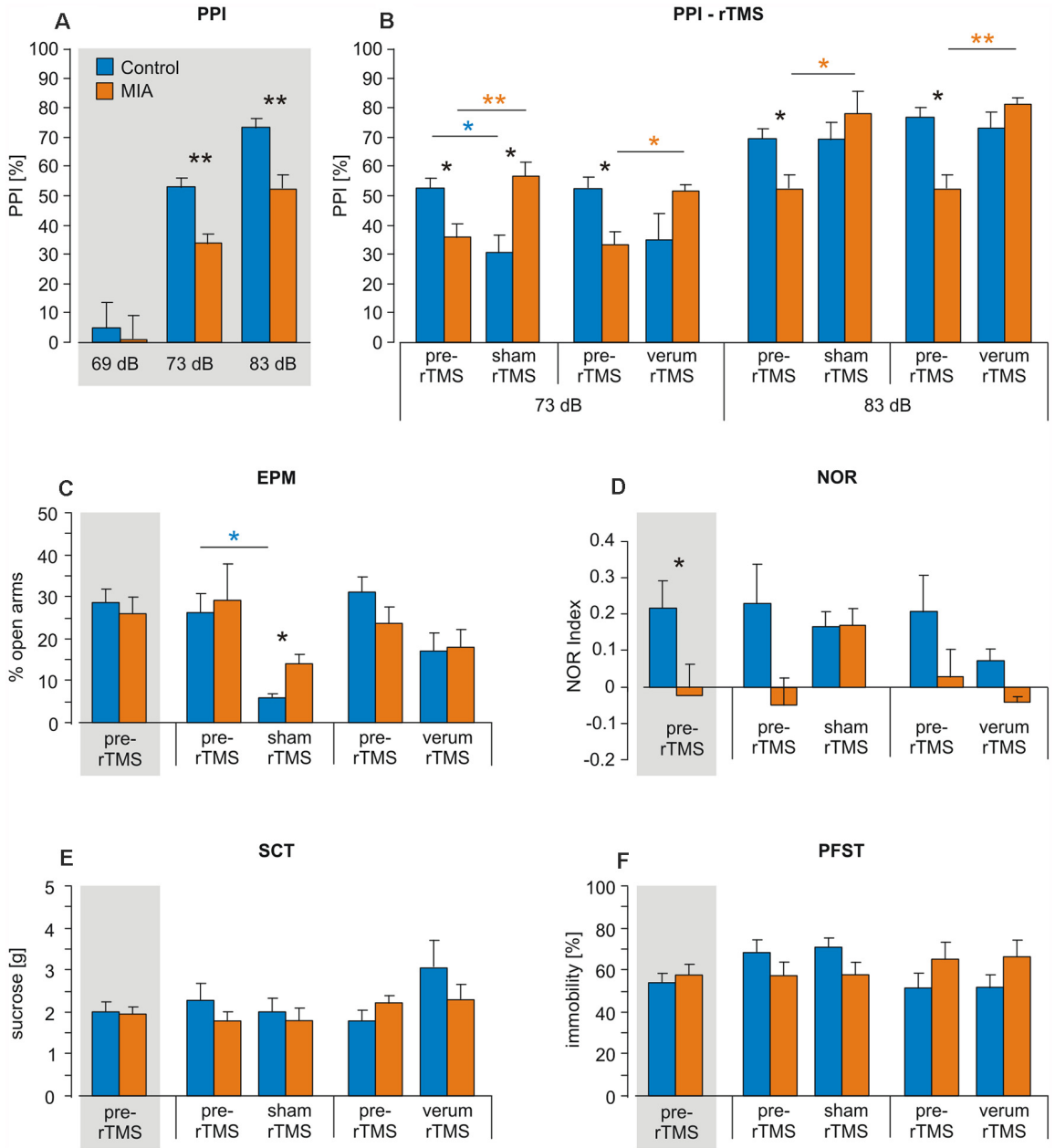

FIGURE 1 | Intermittent theta-burst stimulation (iTBS) applied to adult rats: effects on prepulse inhibition (PPI), elevated plus maze (EPM), novel object recognition (NOR), sucrose consumption test (SCT) and porsolt forced swim test (PFST). Maternal immune activation (MIA) and control rats (n = 12 + 12) were tested for **(A,B)** PPI, **(C)** EPM, **(D)** NOR, **(E)** SCT and **(F)** PFST once before iTBS (pre-iTBS, gray shading: all pre-iTBS measures pooled) and a second time after either sham-iTBS or verum-iTBS (n = 6 per group). Colored asterisks above lines indicate statistically significant differences between pre- and post-iTBS (sham or verum) data determined by paired t-test (controls: blue, MIA: orange, here pre-iTBS data shown separately for sham and verum groups) while black asterisks indicate significant differences between MIA and control rats as revealed by t-test for independent samples (two-sided). $^{*}p < 0.05$, $^{**}p < 0.01$. Data are shown as group means ± SEM.

of MIA rats on days 1, 2 and 4 for time-to-platform (**Table 2**, **Figure 2B**) and for the trials 3 and 4 of day 1 (**Table 3**, **Figure 2A**, T3, T4). A significantly better performance of MIA rats was also evident for behavioral type on trial 4 of day 1 and a higher mean speed on day 3.

Following sham- or verum-iTBS, all groups started at a high level of performance for the second block of training sessions with the position of the platform now changed from north to south (**Figures 2C–L**). No significant differences for any kind of measure were evident between the groups MIA-sham, MIA-verum, control-sham and control-verum. Place memory test (% time in target sector, first 30 s) with the platform removed on day 5 revealed no differences between MIA and control rats prior to iTBS and performance increased both, after sham

TABLE 1 | Analysis of variance (ANOVA and *post hoc t*-test results of the analysis of prepulse inhibition (PPI) data in case of ntermittent theta-burst stimulation (iTBS) applied to adult rats, using factors Group (maternal immune activation, MIA, controls) and iTBS (pre, post).

		ANOVA				*t*-test pre vs. post iTBS (sign. cases)			
Parameter	**Factor**	**DF**	***F*-value**	***p*-value**	η^2	**Case**	**DF**	***T*-value**	***p*-value**	***d***
Verum-iTBS										
73 dB prepulse	Group	1		n.s.		MIA	5	−3.014	**0.03**	1.62
	itbs	1		n.s.						
	Group × iTBS	1	6.522	**0.019**	0.246					
Sham-iTBS										
73 dB prepulse	Group	1		n.s.		MIA	5	−4.887	**0.005**	1.10
	iTBS	1		n.s.		controls	5	3.070	**0.028**	1.56
	Group × iTBS	1	9.812	**0.005**	0.329					
Verum-iTBS										
83 dB prepulse	Group	1		n.s.		MIA	5	−3.651	**0.015**	2.18
	iTBS	1		n.s.						
	Group × iTBS	1	10.385	**0.004**	0.342					
Sham-iTBS										
83 dB prepulse	Group	1		n.s.		MIA	5	−3.913	**0.011**	1.26
	iTBS	1		n.s.						
	Group × iTBS	1		n.s.						

DF, degrees of freedom; η^2, partial ETA; d, Cohen's d; n.s. -, not significant; p-values of significant cases (<0.05) are shown in bold font.

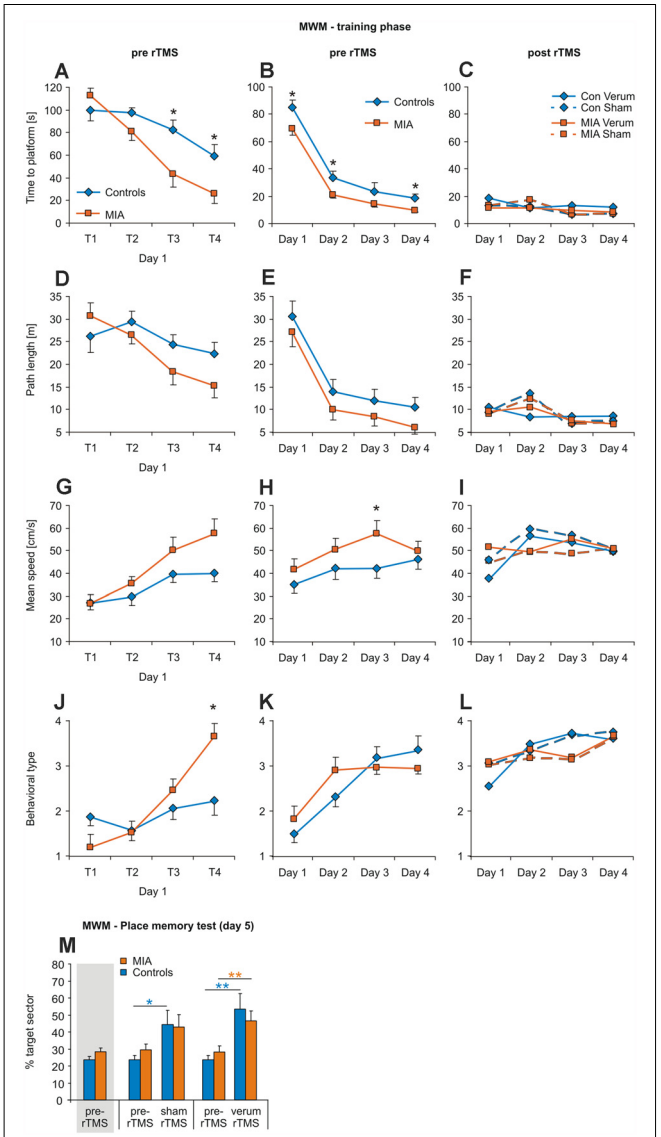

FIGURE 2 | iTBS applied to adult rats: effects on morris water maze (MWM). Measures of time to platform **(A–C)**, total path length **(D–F)**, mean swimming speed **(G–I)** and behavioral type **(J–L)** are separately shown for the four trials of the first training day (left column), for the means of days 1–4 (middle column) and for the days 1–4 when repeating MWM after sham or verum-iTBS (right column) with the platform position now shifted from north to south quadrant. **(M)** Results of the place memory test conducted on day 5 with the platform removed. Shown are percent time spent within the target quadrant during the first 30 s of testing both, for the test prior to iTBS and after either verum- or sham-iTBS. Colored asterisks: paired *t*-test [controls: blue, MIA: orange, in this case pre-iTBS data shown separately for sham and verum groups but pooled in case of the leftmost columns (gray shading)], black asterisks: *t*-test for independent samples (MIA vs. controls, 2-sided). $^*p < 0.05$, $^{**}p < 0.01$. Data are shown as group means ± SEM. For clarity, SEMs are not shown for the post-iTBS samples. *n*/groups as in **Figure 1**.

and verum-iTBS, although somewhat better after verum-iTBS (**Figure 2M**). ANOVA conducted with factors iTBS and GROUP resulted in a significant effect of factor iTBS only ($F_{(2,42)} = 12.697$; $p < 0.001$; $\eta^2 = 0.377$) without interaction between these factors.

Post hoc paired *t*-test indicated a significant increase in time spent in target sector after sham- ($T_{(6)} = -2.931$, $p = 0.033$, $d = 1.29$) and verum-iTBS ($T_{(6)} = -4.040$, $p = 0.009$, $d = 1.71$) for the controls and a significant increase after verum-iTBS ($T_{(6)} = -3.388$, $p = 0.01$, $d = 1.31$) in case of the MIA rats.

Exp. Series II: iTBS Applied to Juvenile Rats (Preventive Approach)

Application of iTBS to juvenile MIA rats aimed at testing a possible preventive iTBS effect. Therefore, rats received 2 weeks of daily iTBS (Monday–Friday, 3 blocks/day, either sham or verum-iTBS) at an age of 6 weeks without prior behavioral testing. Behavioral testing was conducted when the rats were 12–13 weeks old. This experimental series was conducted in seven blocks with litters of MIA and control rats randomly assigned to the sham or verum-iTBS groups (all male), meaning that each of the four groups included offspring cumulating from seven different litters ($n = 12–14$).

PPI

PPI test revealed no significant differences between the four experimental groups when tested with prepulse intensities of 69 dB, 73 dB and 83 dB (**Figure 3A**). Factors GROUP (MIA, Controls) and iTBS (sham, verum) tested with ANOVA appeared to be both ineffective and without interaction.

EPM

EPM test revealed no significant effects of factors GROUP and iTBS when tested with ANOVA but a significant interaction between these factors ($F_{(1,47)} = 7.520$, $p = 0.009$, $\eta^2 = 0.143$). A pairwise comparison of MIA vs. control groups (**Figure 3B**) and sham vs. verum-iTBS groups revealed a significant difference between sham- and verum-iTBS treated MIA groups ($T_{(22)} = 2.520$, $p = 0.018$, $d = 0.99$).

NOR

NOR test conducted with 24 h interval showed poor performance of MIA rats compared to controls (**Figure 3C**). ANOVA with factors GROUP and iTBS revealed significant effects of both factors but without interaction (GROUP: $F_{(1,47)} = 6.998$, $p = 0.011$, $\eta^2 = 0.13$; iTBS: $F_{(1,47)} = 5.615$, $p = 0.022$, $\eta^2 = 0.11$). Pairwise comparison indicated a significant difference between MIA and control groups subjected to sham-iTBS ($T_{(23)} = 2.910$, $p = 0.008$, $d = 1.16$) and between sham- and verum-iTBS treated MIA rats ($T_{(25)} = 2.612$, $p = 0.015$, $d = 1.00$).

PFST and SCT

Also in case of the rats treated with iTBS during adolescence no differences between MIA and control rats and no effects of iTBS were evident for PFST and SCT (**Figures 3D,E**).

MWM

No principal difference in learning performance was evident between the four groups during the training phase (**Figures 4A–H**). ANOVA conducted with factors GROUP, iTBS and either TRIALS (trials 1–4 of the first day), or DAYS (days 1–4), revealed only factors TRIALS and DAYS as being effective in any case of measure (see **Tables 4**, **5**). However, a pairwise comparison of the data of the MIA and control groups revealed a

TABLE 2 | ANOVA and *post hoc t*-test results of the analysis of Morris water maze (MWM) data in case of iTBS applied to adult rats, using factors Group (MIA, controls) and Days (1–4).

		ANOVA					*t*-test MIA vs. controls (sign. cases)			
Parameter	**Factor**	**DF**	***F*-value**	***p*-value**	η^2	**Parameter**	**DF**	***T*-value**	***p*-value**	***d***
Time to target										
	Day	3	76.993	**<0.001**	0.384	Day 1	22	2.149	**0.043**	0.88
	Group	1	4.897	**0.028**	0.013	Day 2	22	2.336	**0.029**	0.96
	Day × Group	3	0.1	0.960	0.001	Day 4	22	2.162	**0.041**	0.88
Path length										
	Day	3	68.915	**<0.001**	0.357					
	Group	1	2.866	0.091	0.008					
	Day × Group	3	0.198	0.898	0.002					
Mean Speed										
	Day	3	3.383	**0.018**	0.027	Day 3	22	3.464	**0.002**	1.41
	Group	1	10.074	**0.002**	0.027					
	Day × Group	3	1.565	0.198	0.013					
Perform. type										
	Day	3	34.741	**<0.001**	0.239					
	Group	1	3.192	0.075	0.01					
	Day × Group	3	0.523	0.667	0.005					

DF, degrees of freedom; η^2, partial ETA; d, Cohen's d; p-values of significant cases (<0.05) are shown in bold font.

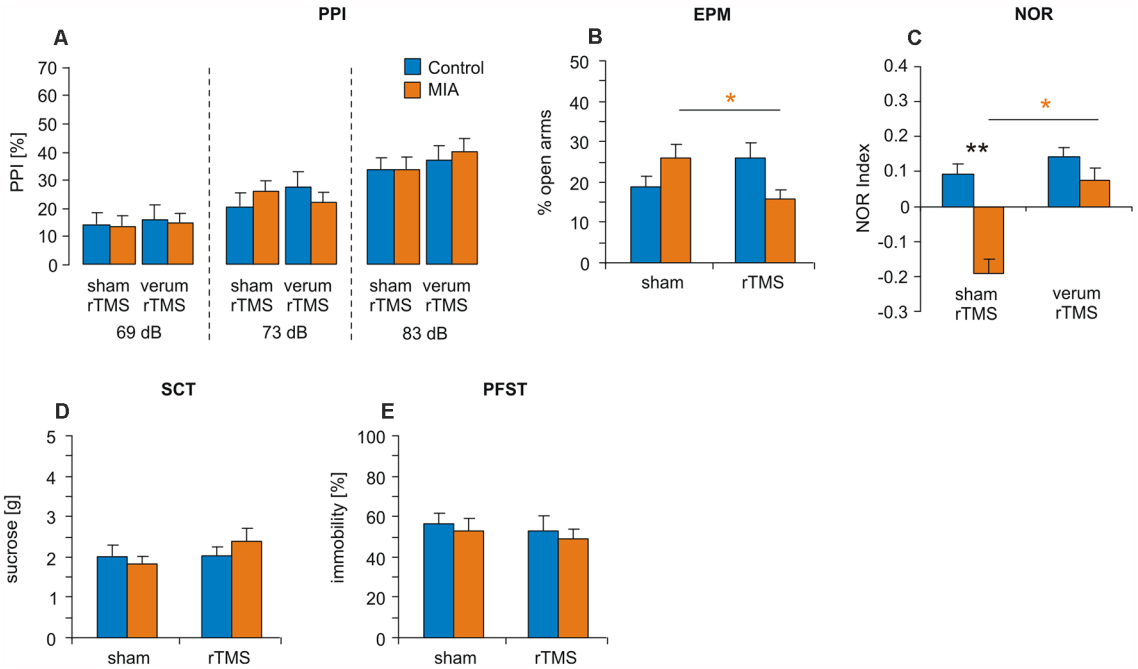

FIGURE 3 | iTBS applied to juvenile rats: effects on PPI, EPM, NOR, SCT and PFST. MIA and control rats were tested at adulthood for **(A)** PPI, **(B)** EPM, **(C)** NOR, **(D)** SCT and **(E)** PFST after iTBS-rTMS (sham or verum) had been applied during adolescence. Colored asterisks: *t*-test comparing sham and verum-iTBS groups (controls: blue, MIA: orange), black asterisks: *t*-test comparing MIA and control groups. $^{*}p < 0.05$, $^{**}p < 0.01$. Data are shown as group means ± SEM. *N* = 12 control-sham, *N* = 12 control-verum, *N* = 13 MIA-sham, *N* = 14 MIA-verum.

better performance of MIA rats with measure time-to-platform (target) at days 2 and 4 (**Table 4**). Furthermore, MIA rats showed better performance in path length, mean speed and behavioral type on training day 4 (**Table 4**). No differences between the four groups were evident for the first four trials on day 1.

In case of final place memory test on day 5 (**Figure 4I**), no difference was found between MIA and control rats for the time spent in the target sector (first 30 s) but verum-iTBS treated groups showed a lower performance than sham-treated groups. Only factor iTBS but not factor GROUP tested with ANOVA appeared to be effective ($F_{(1,53)} = 8.955$, $p = 0.004$, $\eta^2 = 0.145$). *T*-test revealed a significant difference between sham- and verum-iTBS treated MIA rats ($T_{(25)} = 2.091$, $p = 0.047$, $d = 0.80$).

DISCUSSION

Summary of Findings—Differences Between MIA Offspring and Controls

The primary goal of this study was to test the potential of iTBS to treat the behavioral symptoms of schizophrenia either as a therapeutic tool applied during adulthood when the pathological phenotype is already established, or in a preventive fashion during development of the juvenile brain. For this reason, we had chosen the rat MIA model of schizophrenia because it is mainly based on developmental perturbations allowing possible modulation of misbalanced neuronal networks. Behavioral tests comprised PPI, the "gold standard" to test deficits in sensory gating in animal models of schizophrenia (Swerdlow et al., 2008) complemented by standard testing of anxiety, depression, anhedonia and cognitive performance (e.g., see Bergdolt and Dunaevsky, 2019) because iTBS had not been tested before on these behavioral phenotypes and because schizophrenia and MIA are often associated with anhedonia and depressed states (Buckley et al., 2009; Pelizza and Ferrari, 2009). Our data show that the MIA offspring perform better during the training phase of MWM, which had not been described so far, and confirm previously described deficits of MIA rats in sensory gating (PPI; Wolff and Bilkey, 2008; Hadar et al., 2015) and NOR performance (Ito et al., 2010; Wolff et al., 2011; Gray et al., 2019; Saunders et al., 2020). Most studies testing classical MWM found no effects of MIA on performance with regard to acquisition and remembering the platform location (Zuckerman and Weiner, 2005; Piontkewitz et al., 2009; Vorhees et al., 2015). Interestingly, Wolff and Bilkey (2015) reported that, compared to controls, MIA offspring exhibit smaller receptive fields of hippocampal place cells, indicating that local spatial orientation may be increased but contextual orientation requiring integration of a wider space may be impaired (Wolff et al., 2011).

Reports on anxiety-related behavior of MIA offspring are contradictory with some describing increased anxiety (Shi et al., 2003; Abazyan et al., 2010; Yee et al., 2011; Canetta et al., 2016) while others found no difference (Ratnayake et al., 2012; Li et al., 2014; Vorhees et al., 2015) or even reduced anxiety (Ozawa et al., 2006). Our tests revealed no differences between MIA

TABLE 3 | ANOVA and *post hoc t*-test results of the analysis of MWM data in case of iTBS applied to adult rats, using factors Group (MIA, controls) and trials (1–4).

	ANOVA					*t*-test MIA vs. controls (sign. cases)				
Parameter	**Factor**	**DF**	***F*-value**	***p*-value**	η^2	**Parameter**	**DF**	***T*-value**	***p*-value**	***d***
Time to target										
	Trial	3	14.063	**<0.001**	0.327	Trial 3	22	2.553	**0.019**	1.04
	Group	1	2.109	0.150	0.024	Trial 4	22	2.474	**0.022**	1.01
	Trial × Group	3	1.619	0.191	0.053					
Path length										
	Trial	3	4.780	**0.004**	0.143					
	Group	1	1.190	0.278	0.014					
	Trial × Group	3	0.667	0.575	0.023					
Mean Speed										
	Trial	3	6.721	**<0.001**	0.192					
	Group	1	1.298	0.258	0.015					
	Trial × Group	3	0.711	0.548	0.024					
Perform. type										
	Trial	3	13.171	**<0.001**	0.354	Trial 4	22	2.12	**0.046**	0.86
	Group	1	2.076	0.154	0.028					
	Trial × Group	3	2.493	**0.043**	0.106					

DF, degrees of freedom; η^2, partial ETA; d, Cohen's d; p-values of significant cases (<0.05) are shown in bold font.

TABLE 4 | ANOVA and *post hoc t*-test results of the analysis of MWM data in case of iTBS applied to juvenile rats, using factors Group (MIA, controls) and Days (1–4).

	ANOVA					*t*-test MIA vs. controls (sign. cases)				
Parameter	**Factor**	**DF**	***F*-value**	***p*-value**	η^2	**Parameter**	**DF**	***T*-value**	***p*-value**	***d***
Time to target										
	Day	3	32.796	**<0.001**	0.384	Day 2	23	2.672	**0.009**	0.59
	Group	3	1.184	0.315	0.013	Day 4	23	2.239	**0.028**	0.37
	Day × Group	9	0.748	0.665	0.001					
Path length										
	Day	3	99.787	**<0.001**	0.272	Day 4	23	2.323	**0.022**	0.46
	Group	3	2.294	0.077	0.009					
	Day × Group	9	0.913	0.513	0.010					
Mean Speed										
	Day	3	8.730	**<0.001**	0.033	Day 4	23	2.134	**0.035**	0.45
	Group	3	0.976	0.404	0.004					
	Day × Group	9	1.431	0.170	0.017					
Perform. type										
	Day	3	69.950	**<0.001**	0.223	Day 4	23	2.362	**0.020**	0.48
	Group	3	0.613	0.606	0.003					
	Day × Group	9	1.001	0.437	0.012					

DF, degrees of freedom; η^2, partial ETA; d, Cohen's d; p-values of significant cases (<0.05) are shown in bold font.

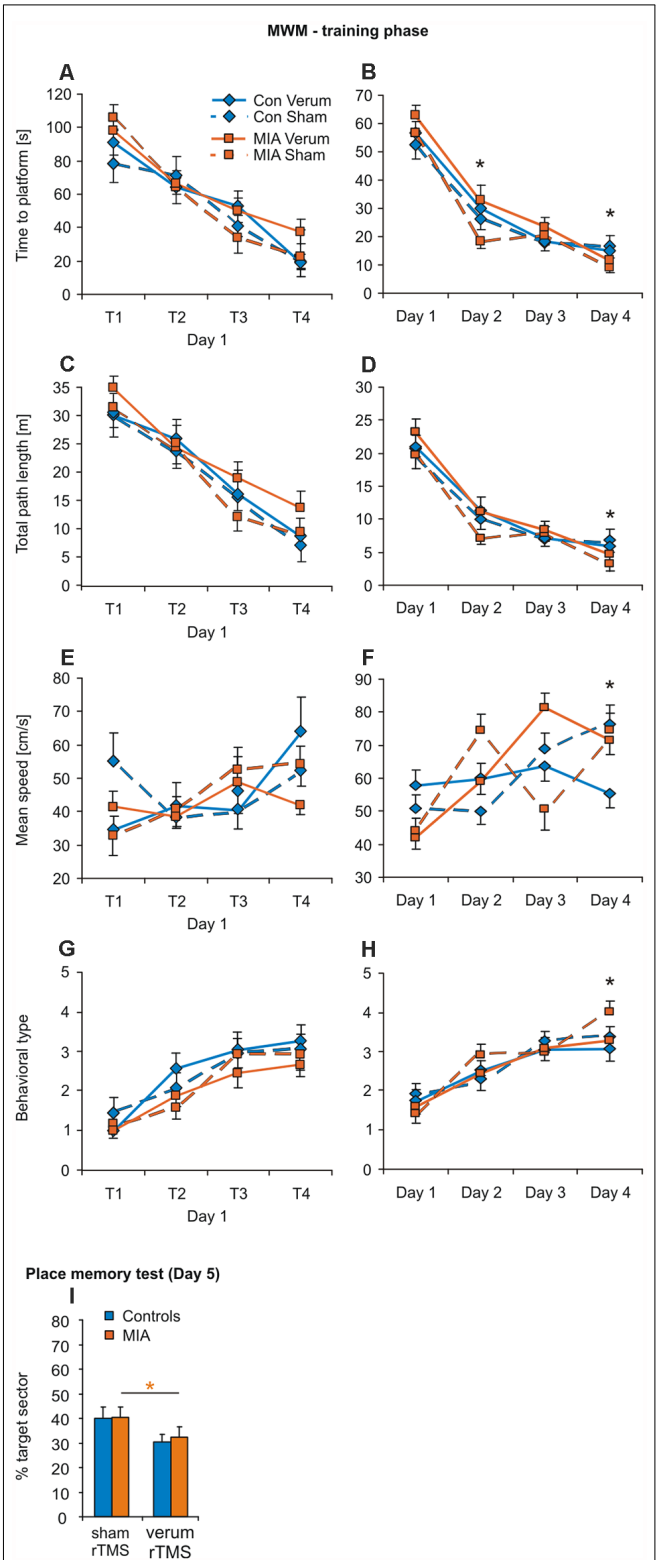

FIGURE 4 | iTBS applied to juvenile rats: effects on MWM. Training phase of MWM with the trials of day 1 **(A,C,E,G)** separately shown from the means of the trials for day 1–4 **(B,D,F,H)** for the measures: time to platform, total path length, mean swimming speed and behavioral type. **(I)** Results of the place (*Continued*)

FIGURE 4 | Continued
memory test conducted on day 5 with the platform removed. Shown are percent time spent within the target quadrant during the first 30 s of testing. Colored asterisks: *t*-test comparing sham vs. verum-iTBS groups (controls: blue, MIA: orange), black asterisks: *t*-test comparing sham-iTBS treated MIA and control groups. *$p < 0.05$. Data are shown as group means ± SEM. $N = 12$ control-sham, $N = 12$ control-verum, $N = 13$ MIA-sham, $N = 14$ MIA verum.

and controls rats in EPM test, neither if tested in adult rats prior to iTBS, nor after having received iTBS during adolescence. We further found no signs of depression, like anhedonia or early surrender in PFST, as has been described as a possible co-morbidity of schizophrenia and a further consequence of MIA (Samsom and Wong, 2015). However, specific changes of the behavioral phenotype in MIA offspring are highly dependent on the kind and timing of interference of genetic and environmental factors (see Missault et al., 2014; Ronovsky et al., 2016).

Like others, our study confirms that MIA offspring are primarily impaired in behavior requiring attentional decision as with PPI and NOR. Canetta et al. (2016) and Wallace et al. (2014) demonstrated MIA offspring being deficient in attentional set shifting and reversal learning (Wallace et al., 2014) but no signs of deficits in working memory were evident (Canetta et al., 2016; Nakamura et al., 2021), the latter being in accordance with the lack of deficits we found with MWM test. Canetta et al. (2016) further demonstrated an impaired GABAergic transmission in the mPFC of adult MIA offspring which was selective for PV-expressing interneurons. This class of interneurons has gained interest as they are essential for the generation of cortical oscillations in the gamma frequency (30–80 Hz; Cardin et al., 2009), assumed to support cognitive processes including working memory and attentional set shifting (Tallon-Baudry et al., 1998; Uhlhaas and Singer, 2010; Cho et al., 2015).

Summary of Findings—Effects of iTBS at Adolescence or Adulthood

According to the changes in oscillatory activity we observed after of iTBS in MIA rats (Lippmann et al., 2021) we also expected to find changes at the behavioral level. Deficits in PPI declined if MIA rats received iTBS at adulthood. However, sham-iTBS was as effective as verum-iTBS, indicating little or no *specific* effects of the brain stimulation itself. Surprisingly, control rats showed a clear decrease in PPI following sham and verum-iTBS while the MIA rats improved. MIA offspring receiving iTBS during adolescence did not show PPI values different from control rats, regardless of verum or sham treatment, a further indication that sham and verum-iTBS were similarly effective. However, for unknown reasons, these rats exhibited generally lower PPI values (ca. −20%, MIA and controls) compared to adult control rats not being stimulated before. It cannot be excluded that early experiences deviating from the conventional housing conditions may alter the rat's behavioral phenotype as determined by standard testing. This impression is supported by the findings of Kentner et al. (2016) and Zhao et al. (2020), demonstrating that housing MIA

TABLE 5 | ANOVA results of the analysis of MWM data in case of iTBS applied to juvenile rats, using factors Group (MIA, controls) and trials (1–4).

Parameter	Factor	DF	*F*-value	*p*-value	η^2
Time to target					
	Trial	3	14.063	**<0.001**	0.327
	Group	1	2.109	0.150	0.024
	Trial × Group	3	1.619	0.191	0.053
Path length					
	Trial	3	4.780	**0.004**	0.143
	Group	1	1.190	0.278	0.014
	Trial × Group	3	0.667	0.575	0.023
Mean Speed					
	Trial	3	6.721	**<0.001**	0.192
	Group	1	1.298	0.258	0.015
	Trial × Group	3	0.711	0.548	0.024
Perform. type					
	Trial	3	13.171	**<0.001**	0.354
	Group	1	2.076	0.154	0.028
	Trial × Group	3	2.493	**0.043**	0.106

DF, degrees of freedom; η^2, partial ETA; p-values of significant cases (<0.05) are shown in bold font.

offspring in an enriched environment (EE) reverses the cognitive deficits in spatial discrimination and the down-regulation of genes critical to synaptic transmission and plasticity. Similarly, rodent studies using NMDA receptor antagonist dizolcilpine (MK-801) injection to induce a schizophrenia-like state demonstrated beneficial effects of EE, reversing the MK-801 induced deficits in NOR and PPI (Murueta-Goyena et al., 2018; Huang et al., 2021), accompanied by recovery of PV immunoreactivity. Interestingly, the same effect could be achieved by selective chemogenetic activation of PV-expressing interneurons within frontal association cortex (Huang et al., 2021). On the other hand, a study investigating the effects of an enriched environment on the behavior of normal Wistar rats in EPM, radial maze, operant conditioning, ASR and PPI showed no clear differences to rats housed at standard conditions (Hoffmann et al., 2009), indicating that experience of an enriched environment is not directly comparable with the experience of testing and handling. However, it cannot be excluded that MIA offspring react in a different way than normal rats.

On the other hand, a specific stimulation effect was evident for NOR if iTBS had been applied during adolescence, since improvement was evident only after verum-iTBS. Interventions modulating cortical excitability and the interplay of excitatory and inhibitory synaptic activities appear to be effective if applied to the juvenile brain (Huang et al., 2021). Of note, phenotype specific, i.e., pathology dependent effects of NIBS during adolescence have previously been reported both in the MIA (Hadar et al., 2020) and the dopamine transporter overexpressing rat (DAT+) model of repetitive symptoms (Edemann-Callesen et al., 2018). tDCS of frontal cortex prevented the schizophrenia-like symptoms of MIA rats when applied during adolescence and ameliorated repetitive symptoms when applied to adult DAT+ rats (Edemann-Callesen et al., 2018). We recently described that MIA rats show disturbed long-range synchrony of neuronal theta-oscillations, in particular between medial prefrontal cortex (mPFC) and ventral hippocampus, aberrant prefrontal gamma-theta phase coupling and an overall increase in the ratio of low to high frequency oscillations of brain activity (Lippmann et al., 2021). rTMS with iTBS protocol and deep brain stimulation (DBS) within mPFC were able to normalize these activity patterns at least acutely. Similar disturbances of limbic brain oscillations have been observed in psychiatric diseases including schizophrenia and are assumed to be a neuronal counterpart of cognitive deficits related to malfunction of attention (see Leicht et al., 2016; Northoff and Duncan, 2016; Hunt et al., 2017). Hence, deficits in sensory gating (PPI) and NOR as found in the MIA rats, and also the partial improvement of both measures following iTBS well match the effects on oscillatory limbic brain activity as described above.

Sham-iTBS Effects vs. Re-test Effects and Differences Between MIA and Control Rats

Results obtained for PPI, EPM and in part NOR revealed strong changes when adult rats were re-tested after iTBS, not only after verum but also after sham-iTBS. Since classical placebo effects as in humans can be excluded, the history of handling and testing appears to be a relevant factor, in particular when re-testing animals with the same paradigm. The decrease in time spent on the open arms of the EPM after iTBS could be interpreted as increased anxiety. However, others discuss the reduced open arm visits in the re-test condition as less exploratory drive due to previous experience (see Carobrez and Bertoglio, 2005). In case of PPI, no data on re-test effects appear to be available to separate re-test effects from effects related to the iTBS procedure when tested under sham condition. Remarkably, clear differences between MIA and control rats were evident when re-tested after sham-iTBS, indicating that the experimental experiences affected the behavioral phenotype of MIA and control rats differently, and obviously more than verum stimulation: PPI performance significantly increased in case of MIA rats but decreased in controls after sham-iTBS. And, open arm stays in EPM generally decreased after sham-iTBS but significantly more in controls.

The significance of the history of experiences has been well documented not only for the after-effects of rTMS in humans (Ridding and Ziemann, 2010; Smith et al., 2010; Karabanov et al., 2015; Suppa et al., 2016). Donato et al. (2013) demonstrated that, compared to non-fearful experiences (enriched environment), a fearful experience (foot-shock fear conditioning) weakens the performance of rats in subsequent cognition tests. Since changes in the activity of hippocampal inhibitory interneurons expressing the calcium-binding protein PV are involved in this process and are also considered in the pathology of psychiatric diseases (Chung et al., 2016), MIA and control rats likely differ also in the way of experience-dependent responses (Canetta et al., 2016). As one limitation of our study we have to submit that an additional group of adult animals receiving neither verum- nor sham-iTBS would have be useful to clarify whether not only repeated testing but also the procedures of applying rTMS influence the behavior. However, given that real placebo effects due to expectations in the procedure can be excluded, we decided to omit such a group. Nevertheless, future studies of this kind may consider such an additional control group.

FINAL CONCLUSIONS

Our study aimed at investigating the possible therapeutic and preventive effect of iTBS applied with iTBS protocol in a rat schizophrenia model. It turned out that verum-iTBS had little specific beneficial effect related to changes in behavioral phenotype. If applied during adolescence, improvement was found only for NOR. Improvement in sensory gating (PPI) of MIA rats—but worsening performance of controls—was evident both, after verum- and sham-iTBS applied in a therapeutic manner, indicating that effects of environmental factors are superior to iTBS effect in the Wistar rats used in this study and, most importantly, affect MIA and control rats differently. In translational terms these findings support the importance of experiences, like physical exercise, social and cognitive training and even enriched environments, as adjunct therapeutic interventions in treating schizophrenia symptoms in humans (Spielman et al., 2016; Girdler et al., 2019; Gómez-Rubio and Trapero, 2019; Maurus et al., 2019) besides the hopeful experiences originating from the care by a medical doctor and the clinical facilities.

DATA AVAILABILITY STATEMENT

The original contributions presented in the study are included in the article, further inquiries can be directed to the corresponding author.

ETHICS STATEMENT

The animal study was reviewed and approved by State Office for Nature, Environment and Consumer Protection, LANUV, Section 81-Animal Welfare, Az. 84-02.04.2014.A294.

AUTHOR CONTRIBUTIONS

KF, CW and VA designed the experiments. NR, TI, GB and VA conducted the experiments. NR, TI, VA and KF did the data analysis. KF wrote the first draft of the manuscript. All authors contributed to the article and approved the submitted version.

FUNDING

This work was supported by the Federal Ministry of Education and Research (Bundesministerium für Bildung und Forschung; BMBF) of Germany (grant number: 01EE1403B to KF) as part of the German Center for Brain Stimulation (GCBS). We acknowledge support by the Open Access Publication Funds of the Ruhr-Universität Bochum.

ACKNOWLEDGMENTS

We like to further thank the Federal Ministry of Education and Research (BMBF) of Germany for the financial support (grant number: 01EE1403B to KF).

REFERENCES

Abazyan, B., Nomura, J., Kannan, G., Ishizuka, K., Tamashiro, K. L., Nucifora, F., et al. (2010). Prenatal interaction of mutant DISC1 and immune activation produces adult psychopathology. *Biol. Psychiatry* 68, 1172–1181. doi: 10.1016/j.biopsych.2010.09.022

Aguiar, P., Mendonca, L., and Galhardo, V. (2007). OpenControl: a free opensource software for video tracking and automated control of behavioral mazes. *J. Neurosci. Methods* 166, 66–72. doi: 10.1016/j.jneumeth.2007.06.020

Başar, E. (2013). Brain oscillations in neuropsychiatric disease. *Dialogues Clin. Neurosci.* 15, 291–300. doi: 10.1002/bio.4047

Benali, A., Trippe, J., Weiler, E., Mix, A., Petrasch-Parwez, E., Girzalsky, W., et al. (2011). Theta-burst transcranial magnetic stimulation alters cortical inhibition. *J. Neurosci.* 31, 1193–1203. doi: 10.1523/JNEUROSCI.1379-10.2011

Bergdolt, L., and Dunaevsky, A. (2019). Brain changes in a maternal immune activation model of neurodevelopmental brain disorders. *Prog. Neurobiol.* 175, 1–19. doi: 10.1016/j.pneurobio.2018.12.002

Brown, A. S. (2012). Epidemiologic studies of exposure to prenatal infection and risk of schizophrenia and autism. *Dev. Neurobiol.* 72, 1272–1276. doi: 10.1002/dneu.22024

Brown, A. S., Begg, M. D., Gravenstein, S., Schaefer, C. A., Wyatt, R. J., Bresnahan, M., et al. (2004). Serologic evidence of prenatal influenza in the etiology of schizophrenia. *Arch. Gen. Psychiatry* 61, 774–780. doi: 10.1001/archpsyc.61.8.774

Buckley, P. F., Miller, B. J., Lehrer, D. S., and Castle, D. J. (2009). Psychiatric comorbidities and schizophrenia. Schizophr. *Bull* 35, 383–402. doi: 10.1093/schbul/sbn135

Canetta, S., Bolkan, S., Padilla-Coreano, N., Song, L. J., Sahn, R., Harrison, N. L., et al. (2016). Maternal immune activation leads to selective functional deficits in offspring parvalbumin interneurons. *Mol. Psychiatry* 21, 956–968. doi: 10.1038/mp.2015.222

Cardin, J. A., Carlén, M., Meletis, K., Knoblich, U., Zhang, F., Deisseroth, K., et al. (2009). Driving fast-spiking cells induces gamma rhythm and controls sensory responses. *Nature* 459, 663–667. doi: 10.1038/nature08002

Carobrez, A. P., and Bertoglio, L. J. (2005). Ethological and temporal analyses of anxiety-like behavior: the elevated plus-maze model 20 years on. *Neurosci. Biobehav. Rev.* 29, 1193–1205. doi: 10.1016/j.neubiorev.2005.04.017

Cho, K. K., Hoch, R., Lee, A. T., Patel, T., Rubenstein, J. L., and Sohal, V. S. (2015). Gamma rhythms link prefrontal interneuron dysfunction with cognitive inflexibility in dlx5/6(+/−) mice. *Neuron* 85, 1332–1343. doi: 10.1016/j.neuron.2015.02.019

Chung, D. W., Fish, K. N., and Lewis, D. A. (2016). Pathological basis for deficient excitatory drive to cortical parvalbumin interneurons in schizophrenia. *Am. J. Psychiatry* 173, 1131–1139. doi: 10.1176/appi.ajp.2016.16010025

Dayan, E., Censor, N., Buch, E. R., Sandrini, M., and Cohen, L. G. (2013). Noninvasive brain stimulation: from physiology to network dynamics and back. *Nat. Neurosci.* 16, 838–844. doi: 10.1038/nn.3422

Donato, F., Rompani, S. B., and Caroni, P. (2013). Parvalbumin-expressing basket-cell network plasticity induced by experience regulates adult learning. *Nature* 504, 272–276. doi: 10.1038/nature12866

Edemann-Callesen, H., Habelt, B., Wieske, F., Jackson, M., Khadka, N., Mattei, D., et al. (2018). Non-invasive modulation reduces repetitive behavior in a rat model through the sensorimotor cortico-striatal circuit. *Transl. Psychiatry* 8:11. doi: 10.1038/s41398-017-0059-5

Ennaceur, A., and Delacour, J. (1988). A new one-trial test for neurobiological studies of memory in rats. 1. Behavioral data. *Behav. Brain Res.* 31, 47–59. doi: 10.1016/0166-4328(88)90157-x

Estes, M. L., and McAllister, A. K. (2016). Maternal immune activation: implications for neuropsychiatric disorders. *Science* 353, 772–777. doi: 10.1126/science.aag3194

Ferguson, B. R., and Gao, W. J. (2018). PV interneurons: critical regulators of E/I balance for prefrontal cortex-dependent behavior and psychiatric disorders. *Front. Neural Circuits* 12:37. doi: 10.3389/fncir.2018.00037

Girdler, S. J., Confino, J. E., and Woesner, M. E. (2019). Exercise as a treatment for schizophrenia: a review. *Psychopharmacol. Bull.* 49, 56–69.

Gómez-Rubio, P., and Trapero, I. (2019). The effects of exercise on IL-6 levels and cognitive performance in patients with schizophrenia. *Diseases* 7:11. doi: 10.3390/diseases7010011

Gray, A., Tattoli, R., Dunn, A., Hodgson, D. M., Michie, P. T., and Harms, L. (2019). Maternal immune activation in mid-late gestation alters amphetamine sensitivity and object recognition, but not other schizophrenia-related behaviors in adult rats. *Behav. Brain Res.* 356, 358–364. doi: 10.1016/j.bbr.2018.08.016

Hadar, R., Bikovski, L., Soto-Montenegro, M. L., Schimke, J., Maier, P., Ewing, S., et al. (2018). Early neuromodulation prevents the development of brain and behavioral abnormalities in a rodent model of schizophrenia. *Mol. Psychiatry* 23, 943–951. doi: 10.1038/mp.2017.52

Hadar, R., Soto-Montenegro, M. L., Götz, T., Wieske, F., Sohr, R., Desco, M., et al. (2015). Using a maternal immune stimulation model of schizophrenia to study behavioral and neurobiological alterations over the developmental course. *Schizophr. Res.* 166, 238–247. doi: 10.1016/j.schres.2015.05.010

Hadar, R., Winter, R., Edemann-Callesen, H., Wieske, F., Habelt, B., Khadka, N., et al. (2020). Prevention of schizophrenia deficits *via* non-invasive adolescent frontal cortex stimulation in rats. *Mol. Psychiatry* 25, 896–905. doi: 10.1038/s41380-019-0356-x

Hoffmann, L. C., Schütte, S. R., Koch, M., and Schwabe, K. (2009). Effect of ''enriched environment'' during development on adult rat behavior and response to the dopamine receptor agonist apomorphine. *Neuroscience* 158, 1589–1598. doi: 10.1016/j.neuroscience.2008.11.035

Huang, Y., Jiang, H., Zheng, Q., Fok, A. H. K., Li, X., Lau, C. G., et al. (2021). Environmental enrichment or selective activation of parvalbumin-expressing interneurons ameliorates synaptic and behavioral deficits in animal models with schizophrenia-like behaviors during adolescence. *Mol. Psychiatry* doi: 10.1038/s41380-020-01005-w. [Online ahead of print].

Huang, Y. Z., Edwards, M. J., Rounis, E., Bhatia, K. P., and Rothwell, J. C. (2005). Theta burst stimulation of the human motor cortex. *Neuron* 45, 201–206. doi: 10.1016/j.neuron.2004.12.033

Hunt, M. J., Kopell, N. J., Traub, R. D., and Whittington, M. A. (2017). Aberrant network activity in schizophrenia. *Trends Neurosci.* 40, 371–382. doi: 10.1016/j.tins.2017.04.003

Iimori, T., Nakajima, S., Miyazaki, T., Tarumi, R., Ogyu, K., Wada, M., et al. (2019). Effectiveness of the prefrontal repetitive transcranial magnetic stimulation on cognitive profiles in depression, schizophrenia and Alzheimer's disease: a systematic review. *Prog. Neuropsychopharmacol. Biol. Psychiatry* 88, 31–40. doi: 10.1016/j.pnpbp.2018.06.014

Illouz, T., Madar, R., Louzoun, Y., Griffioen, K. J., and Okun, E. (2016). Unraveling cognitive traits using the Morris water maze unbiased strategy classification (MUST-C) algorithm. *Brain Behav. Immun.* 52, 132–144. doi: 10.1016/j.bbi.2015.10.013

Insel, T. R. (2010). Rethinking schizophrenia. *Nature* 468, 187–193. doi: 10.1038/nature09552

Ito, H. T., Smith, S. E., Hsiao, E., and Patterson, P. H. (2010). Maternal immune activation alters nonspatial information processing in the hippocampus of the adult offspring. *Brain Behav. Immun.* 24, 930–941. doi: 10.1016/j.bbi.2010.03.004

Karabanov, A., Ziemann, U., Hamada, M., George, M. S., Quartarone, A., Classen, J., et al. (2015). Consensus article: probing homeostatic plasticity of human cortex with non-invasive transcranial brain stimulation. *Brain Stimul.* 8, 993–1006. doi: 10.1016/j.brs.2015.01.404

Kentner, A. C., Khoury, A., Lima Queiroz, E., and MacRae, M. (2016). Environmental enrichment rescues the effects of early life inflammation on markers of synaptic transmission and plasticity. *Brain Behav. Immun.* 57, 151–160. doi: 10.1016/j.bbi.2016.03.013

Kloosterboer, E., and Funke, K. (2019). Repetitive transcranial magnetic stimulation recovers cortical map plasticity induced by sensory deprivation due to deafferentiation. *J. Physiol.* 597, 4025–4051. doi: 10.1113/JP277507

Kuo, M. F., Chen, P. S., and Nitsche, M. A. (2017). The application of tDCS for the treatment of psychiatric diseases. *Int. Rev. Psychiatry* 29, 146–167. doi: 10.1080/09540261.2017.1286299

Leicht, G., Vauth, S., Polomac, N., Andreou, C., Rauh, J., Mußmann, M., et al. (2016). EEG-informed fMRI reveals a disturbed gamma-band-specific network in subjects at high risk for psychosis. *Schizophr. Bull.* 42, 239–249. doi: 10.1093/schbul/sbv092

Lewis, D. A., Curley, A. A., Glausier, J. R., and Volk, D. W. (2012). Cortical parvalbumin interneurons and cognitive dysfunction in schizophrenia. *Trends Neurosci.* 35, 57–67. doi: 10.1016/j.tins.2011.10.004

Li, W. Y., Chang, Y. C., Lee, L. J., and Lee, L. J. (2014). Prenatal infection affects the neuronal architecture and cognitive function in adult mice. *Dev. Neurosci.* 36, 359–370. doi: 10.1159/000362383

Lippmann, B., Barmashenko, G., and Funke, K. (2021). Effects of repetitive transcranial magnetic and deep brain stimulation on long-range synchrony of oscillatory activity in a rat model of developmental schizophrenia. *Eur. J. Neurosci.* doi: 10.1111/ejn.15125. [Online ahead of print].

Lisman, J., and Buzsáki, G. (2008). A neural coding scheme formed by the combined function of gamma and theta oscillations. *Schizophr. Bull.* 34, 974–980. doi: 10.1093/schbul/sbn060

Maurus, I., Hasan, A., Röh, A., Takahashi, S., Rauchmann, B., Keeser, D., et al. (2019). Neurobiological effects of erobic exercise, with a focus on patients with schizophrenia. *Eur. Arch. Psychiatry Clin. Neurosci.* 269, 499–515. doi: 10.1007/s00406-019-01025-w

Mednick, S. A., Machon, R. A., Huttunen, M. O., and Bonett, D. (1988). Adult schizophrenia following prenatal exposure to an influenza epidemic. *Arch. Gen. Psychiatry* 45, 189–192. doi: 10.1001/archpsyc.1988.01800260109013

Meyer, U. (2014). Prenatal poly (I:C) exposure and other developmental immune activation models in rodent systems. *Biol. Psychiatry* 75, 307–315. doi: 10.1016/j.biopsych.2013.07.011

Millan, M. J., Andrieux, A., Bartzokis, G., Cadenhead, K., Dazzan, P., Fusar-Poli, P., et al. (2016). Altering the course of schizophrenia: progress and perspectives. *Nat. Rev. Drug Discov.* 15, 485–515. doi: 10.1038/nrd.2016.28

Missault, S., Van den Eynde, K., Vanden Berghe, W., Fransen, E., Weeren, A., Timmermans, J. P., et al. (2014). The risk for behavioral deficits is determined by the maternal immune response to prenatal immune challenge in a neurodevelopmental model. *Brain Behav. Immun.* 42, 138–146. doi: 10.1016/j.bbi.2014.06.013

Mix, A., Benali, A., Eysel, U. T., and Funke, K. (2010). Continuous and intermittent transcranial magnetic theta-burst stimulation differently modify tactile learning performance and cortical protein expression in the rat. *Eur. J. Neurosci.* 32, 1575–1586. doi: 10.1111/j.1460-9568.2010.07425.x

Mix, A., Benali, A., and Funke, K. (2014). Strain differences in the effect of rTMS on cortical expression of calcium-binding proteins in rats. *Exp. Brain Res.* 232, 435–442. doi: 10.1007/s00221-013-3751-6

Murphy, S. C., Palmer, L. M., Nyffeler, T., Müri, R. M., and Larkum, M. E. (2016). Transcranial magnetic stimulation (TMS) inhibits cortical dendrites. *eLife* 5:e13598. doi: 10.7554/eLife.13598

Murueta-Goyena, A., Ortuzar, N., Gargiulo, P.Á., Lafuente, J. V., and Bengoetxea, H. (2018). Short-term exposure to enriched environment in adult rats restores MK-801-induced cognitive deficits and GABAergic interneuron immunoreactivity loss. *Mol. Neurobiol.* 55, 26–41. doi: 10.1007/s12035-017-0715-z

Nakamura, J. P., Gillespie, B., Gibbons, A., Jaehne, E. J., Du, X., Chan, A., et al. (2021). Maternal immune activation targeted to a window of parvalbumin interneuron development improves spatial working memory: Implications for autism. *Brain Behav. Immun.* 91, 339–349. doi: 10.1016/j.bbi.2020.10.012

Nettekoven, C., Volz, L. J., Kutscha, M., Pool, E. M., Rehme, A. K., Eickhoff, S. B., et al. (2014). Dose-dependent effects of theta burst rTMS on cortical excitability and resting-state connectivity of the human motor system. *J. Neurosci.* 34, 6849–6859. doi: 10.1523/JNEUROSCI.4993-13.2014

Northoff, G., and Duncan, N. W. (2016). How do abnormalities in the brain's spontaneous activity translate into symptoms in schizophrenia? From an overview of resting state activity findings to a proposed spatiotemporal psychopathology. *Prog. Neurobiol.* 145, 26–45. doi: 10.1016/j.pneurobio.2016.08.003

Ozawa, K., Hashimoto, K., Kishimoto, T., Shimizu, E., Ishikura, H., and Iyo, M. (2006). Immune activation during pregnancy in mice leads to dopaminergic hyperfunction and cognitive impairment in the offspring: a neurodevelopmental animal model of schizophrenia. *Biol. Psychiatry* 59, 546–554. doi: 10.1016/j.biopsych.2005.07.031

Padberg, F., and George, M. S. (2009). Repetitive transcranial magnetic stimulation of the prefrontal cortex in depression. *Exp. Neurol.* 219, 2–13. doi: 10.1016/j.expneurol.2009.04.020

Papp, M., Willner, P., and Muscat, R. (1991). An animal model of anhedonia: attenuation of sucrose consumption and place preference conditioning by chronic unpredictable mild stress. *Psychopharmacology* 104, 255–259. doi: 10.1007/BF02244188

Pelizza, L., and Ferrari, A. (2009). Anhedonia in schizophrenia and major depression: state or trait? *Ann. Gen. Psychiatry* 8:22. doi: 10.1186/1744-859X-8-22

Pellow, S., Chopin, P., File, S. E., and Briley, M. (1985). Validation of open:closed arm entries in an elevated plusmaze as a measure of anxiety in the rat. *J. Neurosci. Methods* 14, 149–167. doi: 10.1016/0165-0270(85)90031-7

Piontkewitz, Y., Assaf, Y., and Weiner, I. (2009). Clozapine administration in adolescence prevents postpubertal emergence of brain structural pathology in an animal model of schizophrenia. *Biol. Psychiatry* 66, 1038–1046. doi: 10.1016/j.biopsych.2009.07.005

Porsolt, R. D., Le Pichon, M., and Jalfre, M. (1977). Depression: a new animal model sensitive to antidepressant treatments. *Nature* 266, 730–732. doi: 10.1038/266730a0

Post, A., and Keck, M. E. (2001). Transcranial magnetic stimulation as a therapeutic tool in psychiatry: what do we know about the neurobiological mechanisms? *J. Psychiatr. Res.* 35, 193–215. doi: 10.1016/s0022-3956(01)00023-1

Rajji, T. K., Rogasch, N. C., Daskalakis, Z. J., and Fitzgerald, P. B. (2013). Neuroplasticity-based brain stimulation interventions in the study and treatment of schizophrenia: a review. *Can. J. Psychiatry* 58, 93–98. doi: 10.1177/070674371305800206

Ratnayake, U., Quinn, T. A., Castillo-Melendez, M., Dickinson, H., and Walker, D. W. (2012). Behavior and hippocampus-specific changes in spiny mouse neonates after treatment of the mother with the viral-mimetic poly I:C at mid-pregnancy. *Brain Behav. Immun.* 26, 1288–1299. doi: 10.1016/j.bbi.2012.08.011

Reisinger, S., Khan, D., Kong, E., Berger, A., Pollak, A., and Pollak, D. D. (2015). The poly(I:C)-induced maternal immune activation model in preclinical neuropsychiatric drug discovery. *Pharmacol. Ther.* 149, 213–226. doi: 10.1016/j.pharmthera.2015.01.001

Ridding, M. C., and Ziemann, U. (2010). Determinants of the induction of cortical plasticity by non-invasive brain stimulation in healthy subjects. *J. Physiol.* 588, 2291–2304. doi: 10.1113/jphysiol.2010.190314

Ronovsky, M., Berger, S., Molz, B., Berger, A., and Pollak, D. D. (2016). Animal models of maternal immune activation in depression research. *Curr. Neuropharmacol.* 14, 688–704. doi: 10.2174/1570159x14666151215095359

Samsom, J. N., and Wong, A. H. (2015). Schizophrenia and depression co-morbidity: what we have learned from animal models. *Front. Psychiatry* 6:13. doi: 10.3389/fpsyt.2015.00013

Saunders, J. M., Moreno, J. L., Ibi, D., Sikaroodi, M., Kang, D. J., Muñoz-Moreno, R., et al. (2020). Gut microbiota manipulation during the prepubertal period shapes behavioral abnormalities in a mouse neurodevelopmental disorder model. *Sci. Rep.* 10:4697. doi: 10.1038/s41598-020-61635-6

Selemon, L. D., and Zecevic, N. (2015). Schizophrenia: a tale of two critical periods for prefrontal cortical development. *Transl. Psychiatry* 5:e623. doi: 10.1038/tp.2015.115

Shi, L., Fatemi, S. H., Sidwell, R. W., and Patterson, P. H. (2003). Maternal influenza infection causes marked behavioral and pharmacological changes in the offspring. *J. Neurosci.* 23, 297–302. doi: 10.1523/JNEUROSCI.23-01-00297.2003

Smith, S. E. P., Hsiao, E., and Patterson, P. H. (2010). "Activation of the maternal immune system as a risk factor for neuropsychiatric disorders," in *Maternal Influences on Fetal Neurodevelopment: Clinical and Research Aspects.* eds A. W. Zimmerman, and S. L. Connors (NewYork, NY: Springer), 97–115.

Sonmez, A. I., Camsari, D. D., Nandakumar, A. L., Voort, J. L. V., Kung, S., Lewis, C. P., et al. (2019). Accelerated TMS for depression: a systematic review and meta-analysis. *Psychiatry Res.* 273, 770–781. doi: 10.1016/j.psychres.2018.12.041

Spielman, L. J., Little, J. P., and Klegeris, A. (2016). Physical activity and exercise attenuate neuroinflammation in neurological diseases. *Brain Res. Bull.* 125, 19–29. doi: 10.1016/j.brainresbull.2016.03.012

Sukhodolsky, D. G., Leckman, J. F., Rothenberger, A., and Scahill, L. (2007). The role of abnormal neural oscillations in the pathophysiology of co-occurring tourette syndrome and attention-deficit/hyperactivity disorder. *Eur. Child Adolesc. Psychiatry* 1, 51–59. doi: 10.1007/s00787-007-1007-3

Suppa, A., Huang, Y. Z., Funke, K., Ridding, M. C., Cheeran, B., Di Lazzaro, V., et al. (2016). Ten years of theta burst stimulation in humans: established knowledge, unknowns and prospects. *Brain Stimul.* 9, 323–335. doi: 10.1016/j.brs.2016.01.006

Swerdlow, N. R., Weber, M., Qu, Y., Light, G. A., and Braff, D. L. (2008). Realistic expectations of prepulse inhibition in translational models for schizophrenia research. *Psychopharmacology* 199, 331–388. doi: 10.1007/s00213-008-1072-4

Tallon-Baudry, C., Bertrand, O., Peronnet, F., and Pernier, J. (1998). Induced gamma-band activity during the delay of a visual short-term memory task in humans. *J. Neurosci.* 18, 4244–4254. doi: 10.1523/JNEUROSCI.18-11-04244.1998

Terry, A. V., Jr., Kutiyanawalla, A., and Pillai, A. (2011). Age-dependent alterations in nerve growth factor (NGF)-related proteins, sortilin and learning and memory in rats. *Physiol. Behav.* 102, 149–157. doi: 10.1016/j.physbeh.2010.11.005

Thimm, A., and Funke, K. (2015). Multiple blocks of intermittent and continuous theta-burst stimulation applied *via* transcranial magnetic stimulation differently affect sensory responses in rat barrel cortex. *J. Physiol.* 593, 967–985. doi: 10.1113/jphysiol.2014.282467

Trippe, J., Mix, A., Aydin-Abidin, S., Funke, K., and Benali, A. (2009). Theta burst and conventional low frequency rTMS differentially affect GABAergic neurotransmission in the rat cortex. *Exp. Brain Res.* 199, 411–421. doi: 10.1007/s00221-009-1961-8

Uhlhaas, P. J., and Singer, W. (2010). Abnormal neural oscillations and synchrony in schizophrenia. *Nat. Rev. Neurosci.* 11, 100–113. doi: 10.1038/nrn2774

Volz, L. J., Benali, A., Mix, A., Neubacher, U., and Funke, K. (2013). Dose-dependence of changes in cortical protein expression induced with repeated transcranial magnetic theta-burst stimulation in the rat. *Brain Stimul.* 6, 598–606. doi: 10.1016/j.brs.2013.01.008

Vorhees, C. V., Graham, D. L., Braun, A. A., Schaefer, T. L., Skelton, M. R., Richtand, N. M., et al. (2015). Prenatal immune challenge in rats: effects

of polyinosinic-polycytidylic acid on spatial learning, prepulse inhibition, conditioned fear and responses to MK-801 and amphetamine. *Neurotoxicol. Teratol.* 47, 54–65. doi: 10.1016/j.ntt.2014.10.007

Wallace, J., Marston, H. M., McQuade, R., and Gartside, S. E. (2014). Evidence that aetiological risk factors for psychiatric disorders cause distinct patterns of cognitive deficits. *Eur. Neuropsychopharmacol.* 24, 879–889. doi: 10.1016/j.euroneuro.2013.12.005

Weissman, J. D., Epstein, C. M., and Davey, K. R. (1992). Magnetic brain stimulation and brain size: relevance to animal studies. *Electroencephalogr. Clin. Neurophysiol.* 85, 215–219. doi: 10.1016/0168-5597(92)90135-x

Wolff, A. R., and Bilkey, D. K. (2008). Immune activation during mid-gestation disrupts sensorimotor gating in rat offspring. *Behav. Brain Res.* 190, 156–159. doi: 10.1016/j.bbr.2008.02.021

Wolff, A. R., and Bilkey, D. K. (2015). Prenatal immune activation alters hippocampal place cell firing characteristics in adult animals. *Brain Behav. Immun.* 48, 232–243. doi: 10.1016/j.bbi.2015.03.012

Wolff, A. R., Cheyne, K. R., and Bilkey, D. K. (2011). Behavioral deficits associated with maternal immune activation in the rat model of schizophrenia. *Behav. Brain Res.* 225, 382–387. doi: 10.1016/j.bbr.2011.07.033

Yee, N., Ribic, A., de Roo, C. C., and Fuchs, E. (2011). Differential effects of maternal immune activation and juvenile stress on anxiety-like behaviour and physiology in adult rats: no evidence for the ''double-hit hypothesis''. *Behav. Brain Res.* 224, 180–188. doi: 10.1016/j.bbr.2011.05.040

Zhao, X., Rondón-Ortiz, A. N., Lima, E. P., Puracchio, M., Roderick, R. C., and Kentner, A. C. (2020). Therapeutic efficacy of environmental enrichment on behavioral, endocrine and synaptic alterations in an animal model of maternal immune activation. *Brain Behav. Immun. Health* 3:100043. doi: 10.1016/j.bbih.2020.100043

Ziemann, U., and Siebner, H. R. (2008). Modifying motor learning through gating and homeostatic metaplasticity. *Brain Stimul.* 1, 60–66. doi: 10.1016/j.brs.2007.08.003

Zuckerman, L., Rehavi, M., Nachman, R., and Weiner, I. (2003). Immune activation during pregnancy in rats leads to a postpubertal emergence of disrupted latent inhibition, dopaminergic hyperfunction and altered limbic morphology in the offspring: a novel neurodevelopmental model of schizophrenia. *Neuropsychopharmacology* 28, 1778–1789. doi: 10.1038/sj.npp.1300248

Zuckerman, L., and Weiner, I. (2005). Maternal immune activation leads to behavioral and pharmacological changes in the adult offspring. *J. Psychiatr. Res.* 39, 311–323. doi: 10.1016/j.jpsychires.2004.08.008

Conflict of Interest: GB was employed by the company AIO-Studien-gGmbH.

The remaining authors declare that the research was conducted in the absence of any commercial or financial relationships that could be construed as a potential conflict of interest.

frontiers in Human Neuroscience

ORIGINAL RESEARCH
published: 13 May 2021
doi: 10.3389/fnhum.2021.667619

Antiepileptic Efficacy and Network Connectivity Modulation of Repetitive Transcranial Magnetic Stimulation by Vertex Suppression

Cong Fu[1], Aikedan Aisikaer[2], Zhijuan Chen[1], Qing Yu[3], Jianzhong Yin[2] and Weidong Yang[1]**

[1]*Department of Neurosurgery, Tianjin Medical University General Hospital, Tianjin Medical University, Tianjin, China,* [2]*Department of Radiology, Tianjin First Central Hospital, Tianjin Medical University, Tianjin, China,* [3]*Department of Neurology, Tianjin Medical University General Hospital, Tianjin Medical University, Tianjin, China*

A core feature of drug-resistant epilepsy is hyperexcitability in the motor cortex, and low-frequency repetitive transcranial magnetic stimulation (rTMS) is a suitable treatment for seizures. However, the antiepileptic effect causing network reorganization has rarely been studied. Here, we assessed the impact of rTMS on functional network connectivity (FNC) in resting functional networks (RSNs) and their relation to treatment response. Fourteen patients with medically intractable epilepsy received inhibitive rTMS with a figure-of-eight coil over the vertex for 10 days spread across two weeks. We designed a 6-week follow-up phase divided into four time points to investigate FNC and rTMS-induced timing-dependent plasticity, such as seizure frequency and abnormal interictal discharges on electroencephalography (EEG). For psychiatric comorbidities, the Hamilton Depression Scale (HAM-D) and the Hamilton Anxiety Scale (HAM-A) were applied to measure depression and anxiety before and after rTMS. FNC was also compared to that of a cohort of 17 healthy control subjects. The after-effects of rTMS included all subjects that achieved the significant decrease rate of more than 50% in interictal epileptiform discharges and seizure frequency, 12 (14) patients with the reduction rate above 50% compared to the baseline, as well as emotional improvements in depression and anxiety ($p < 0.05$). In the analysis of RSNs, we found a higher synchronization between the sensorimotor network (SMN) and posterior default-mode network (pDMN) in epileptic patients than in healthy controls. In contrast to pre-rTMS, the results demonstrated a weaker FNC between the anterior DMN (aDMN) and SMN after rTMS, while the FNC between the aDMN and dorsal attention network (DAN) was greater ($p < 0.05$, FDR corrected). Importantly, the depressive score was anticorrelated with the FNC of the aDMN-SMN ($r = -0.67$, $p = 0.0022$), which was markedly different in the good and bad response groups treated with rTMS ($p = 0.0115$). Based on the vertex suppression by rTMS, it is possible to achieve temporary clinical efficacy by modulating network reorganization in the DMN and SMN for patients with refractory epilepsy.

Keywords: rTMS, refractory epilepsy, BOLD fMRI, functional network connectivity, sensorimotor network, default mode network

OPEN ACCESS

Edited by:
Friederike Pfeiffer, University of Tübingen, Germany

Reviewed by:
Giovanni Assenza, Campus Bio-Medico University, Italy
Gianluca Mingoia, RWTH Aachen University, Germany

****Correspondence:***
Weidong Yang
yangweidongshine@sina.com
Jianzhong Yin
jianzhongyin@gmail.com

Specialty section:
This article was submitted to Brain Imaging and Stimulation, a section of the journal Frontiers in Human Neuroscience

Received: *14 February 2021*
Accepted: *12 April 2021*
Published: *13 May 2021*

Citation:
Fu C, Aisikaer A, Chen Z, Yu Q, Yin J and Yang W (2021) Antiepileptic Efficacy and Network Connectivity Modulation of Repetitive Transcranial Magnetic Stimulation by Vertex Suppression. Front. Hum. Neurosci. 15:667619. doi: 10.3389/fnhum.2021.667619

INTRODUCTION

Transcranial magnetic stimulation (TMS) is a safe and well-tolerated noninvasive focal cortical stimulation technique (Pereira et al., 2016; Tsuboyama et al., 2020) based on the theory of Faraday electromagnetic induction (Barker, 1999). Through a series of magnetic pulses acting on the cerebral cortex, neural activity is inhibited under low-frequency stimulation. Because of its hypothesized mechanism of action with enhancement of GABAergic activity (Pascual-Leone et al., 1994) and a decrease in synaptic transmission (Chen et al., 1997; Ye and Kaszuba, 2019), low-frequency repetitive TMS (rTMS) might be ideally suited to epilepsy pathophysiology. An important characteristic of the epileptic brain is cortical hyperexcitability due to disruption of brain networks (Cantello et al., 2000) and abnormal imbalance of cortical excitability and sensitivity (Tombini et al., 2013), which supports excitation-inhibiting rTMS as a potential therapeutic approach (Badawy et al., 2012; Kramer and Cash, 2012).

For refractory patients with multiple foci or diffuse epileptiform foci, the vertex region (in SMN) was used as the untargeted rTMS site, which could be located in Cz according to the 10-20 electroencephalography (EEG) system (Tergau et al., 1999). In a randomized, double-blind, crossover design study for 43 new cortex focal epilepsy patients selected for 26 weeks trial, TMS therapeutic targeted a vertex area and results showed that the true stimulus group compared with sham stimulus clinical performance with no significant difference, but the EEG detected that a third of the patients gained improvement on epileptiform discharge (Cantello et al., 2007). Kinoshita et al. (2005) found that compared with vertex stimulation of simple focal seizures, complex focal seizures were more obvious in the improvement of seizure, which explained that the vertex inhibitory stimulus did not prevent the occurrence of epileptic activity but prevented the proliferation of abnormal brain activity (Kinoshita et al., 2005). Therefore, as observed in the beneficial result from patients with diffuse or multiple foci epilepsy, it might be that the vertex caused the network effect, making the whole epilepsy network excitatory downgrade (Tergau et al., 2003; Joo et al., 2007). A recent study from Yun and colleagues suggested that SMN may have implications for intervention in generalized epilepsy due to SMN in the subcortical-cortical circuit (Qin et al., 2020). The above studies provide theoretical and practical support for the regulation of excitation-inhibitory rTMS, and the vertex areas (in SMN) are regarded as an untargeted site to modulate the functional network for an antiepileptic effect.

Functional network connectivity (FNC) is a technique based on resting-state fMRI that identifies connectivity between contributed resting-state networks (RSNs) based on correlations over time in the blood oxygenation level-dependent (BOLD) signal. TMS has been combined extensively with FNC to identify abnormalities in brain connectivity in different neurologic and psychiatric diseases (Fox et al., 2012a,b; Chou et al., 2015). However, there are few studies about the rTMS vertex-suppressive effect causing FNC reorganization in refractory epilepsy.

Here, the first aim of the study was to examine the effect of vertex desynchronization by rTMS in terms of seizure frequency, abnormal EEG discharges, and depressive and anxious scores. The second aim was to use FNC analysis to identify network connectivity reorganization that was modulated by the rTMS intervention and assess whether rTMS-induced functional connectivity modulation was associated with changes in clinical symptoms.

MATERIALS AND METHODS

Subjects

Seventeen right-handed drug-resistant epilepsy patients who were not eligible for surgical treatment were recruited from the outpatient and inpatient department of neurology and neurosurgery. Drug resistance was defined in agreement with commonly accepted criteria (Schmidt and Löscher, 2005; Kwan et al., 2010). According to the criteria of the International League Against Epilepsy (ILAE) Board, epileptic syndrome and seizure type were definitively diagnosed (ILAE, 1989). We excluded three patients with serious structural abnormalities. Eventually, 14 patients were included in our baseline assessment {six females, age 26.72 (8.13) years [mean (standard deviation)]}. During the experiment, there were four dropout patients due to individual reasons. In the end, 10 patients finished the whole experiment (see **Supplementary Figure 1**). The diagnostic and clinical characteristics of the patient group are described in **Table 1**. Additionally, 17 age- and sex-matched healthy adults [nine females, age 25.29 (1.86) years] were recruited from the local community. All subjects were eligible for MRI based on standard MRI safety screening; all patients passed the TMS adult safety–screening questionnaire (TASS; Keel et al., 2001; except for the epilepsy-related questions). All subjects gave written and informed consent.

Research Protocol

There were 10 weeks for patients to participate (see **Figure 1A**). We performed rTMS in 10 sessions over 2 weeks, one session per day for five consecutive weekdays each week. The baseline assessment T0 occurred 2 weeks prior to the stimulation

TABLE 1 | Patients' clinical characteristics.

Clinical characteristic	Patients (No.)
Seizures	
Motor seizures	14
Focal	2
Generalized	12
Epilepsy	
Focal	2
Multifocal	2
Generalized	12
Multifocal	12
Comorbidities	
Depression	
Intellectual dysfunction	3
Motor deficits	
Gait	2
Movement disorders	3

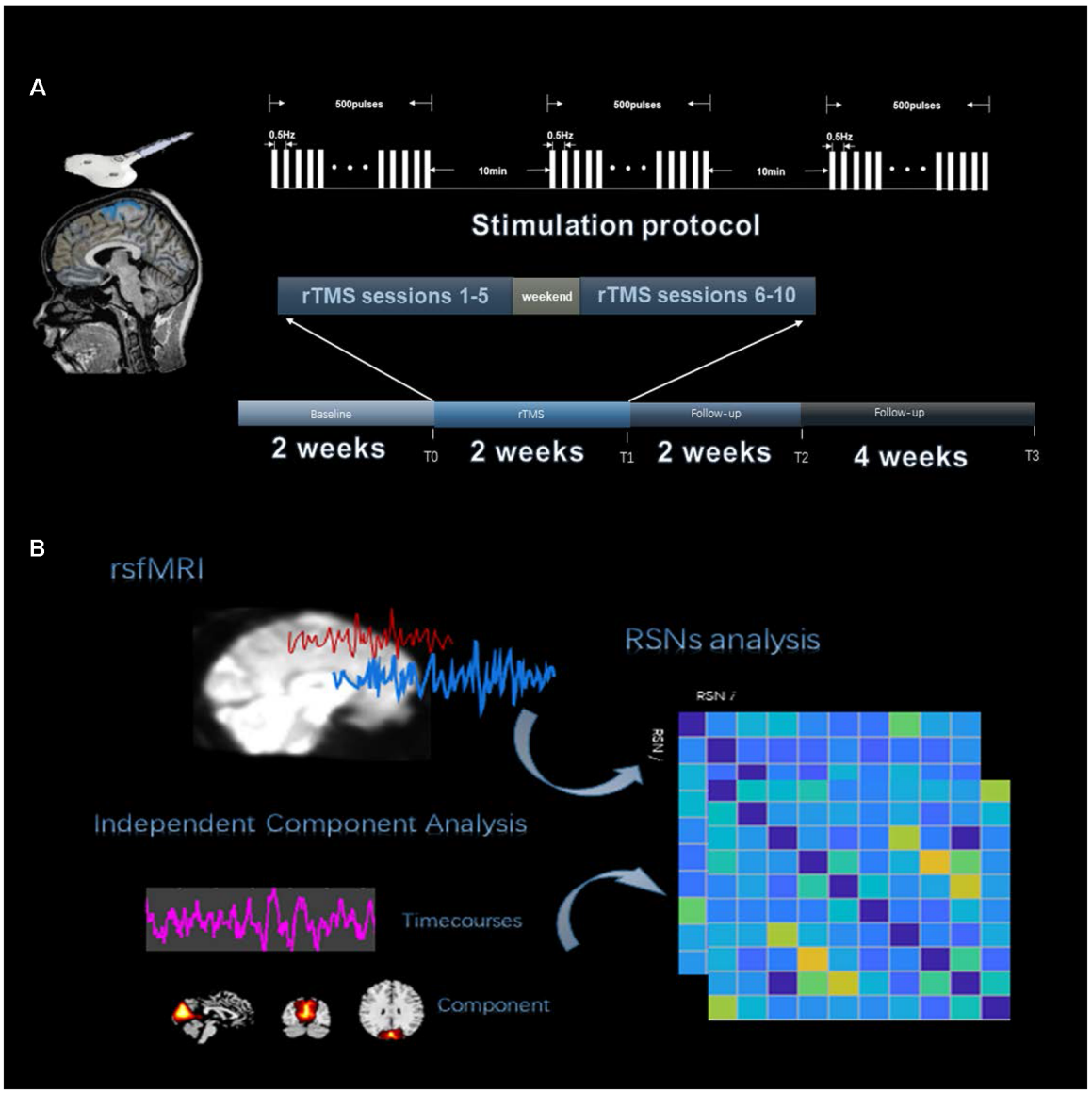

FIGURE 1 | Experiment procedure. **(A)** The four time points were designed into the timeline of the study, which were T0, T1, T2, and T3. Repetitive transcranial magnetic stimulation (rTMS) 10 sessions with the stimulation protocol are shown above the timeline. **(B)** The analysis process of functional network connectivity (FNC) divided into three steps, including fMRI data preprocessing, resting-state network (RSN) identification by independent component analysis (ICA) and extracting RSN time courses to calculate Pearson's correlation.

session, and there were 10 daily stimulation sessions. Post-rTMS assessment, T1, T2, and T3 occurred on the first day, the end of the 2nd week, and the 6th week after the final stimulation session. At each time point, we monitored patients' seizure frequency. Imaging data were collected, including structural MRI and blood oxygen level-dependent (BOLD) fMRI, for each time point (T0–T3) using the parameters indicated below. Following MRI scanning, subjects underwent video electroencephalography (VEEG) and emotional assessment, as described below. Each healthy subject participated in imaging data collection, including structural MRI and BOLD fMRI.

Repetitive Transcranial Magnetic Stimulation (rTMS)

rTMS was applied to the stimulation location using a CCY-IA TMS instrument (YIRUIDE Limited, China). A 70 mm figure-of-eight coil was used. For the stimulation condition, rTMS was applied at a 100% motor threshold, which was necessary to generate a visible contraction of the right thumb (abductor pollicis brevis) for 5 out of 10 consecutive pulses, to the stimulation site for 1,500 pulses of 0.5 Hz pulses for every 500 pulses followed by 10 min of interval stimulation (see **Figure 1A**). A coil was positioned over the motor cortex (at Cz),

which was targeted using a 10-20 EEG standard location system. Each patient received rTMS at the same time every afternoon (2:00 PM). During the study period, antiepileptic medications were kept constant.

Clinical Evaluation and Rating Scales

At the T0–T3 phases, patients underwent medical and neuropsychological examinations. The mean number of weekly seizures (MNWS) could represent the main indicator of the antiepileptic effect on rTMS. All patients and their families documented every seizure before and after the low-frequency rTMS treatment. To compare the MNWS of three phases immediately subsequent to the rTMS treatment, we performed a one-way analysis of variance (ANOVA) and time (T0, T1, T2 and T3) as a repeated factor. Similarly, EEG comparisons were performed for the absolute number of interictal epileptiform discharges (IEDs) within the second 30 min of 1.5 h of detection (Varrasi et al., 2004). The Hamilton Depression Scale (HAM-D) and Hamilton Anxiety Scale (HAM-A) were used by a skilled psychologist (M.M.) to measure the patients' emotions, and the mean value of the total score was recorded as a statistical indicator. The significance level was set to $p < 0.05$.

Imaging Protocol

All MRI scanning data were obtained on a 3-tesla MRI scanner (Siemens Prisma). High-resolution T1-weighted data images were acquired using a magnetization–prepared rapid gradient–echo (MPRAGE) sequence (repetition time (TR) = 1,550 ms, echo time (TE) = 2.98 ms, field of view (FOV) = 256 mm ×256 mm, slice thickness 1.00 mm, 176 volumes). Resting-state functional BOLD (Bonilha et al., 2010) data images were acquired using an echo planar imaging (Wiebe et al., 2001) sequence (TR = 2,000 ms, TE = 30.00 ms, flip angle 40°, FOV = 220 mm ×220 mm, slice thickness 2.5 mm, 380 volumes). The patients were asked to not move and to stay with their eyes closed and resting. Headphones and cushions were used to reduce noise interference and prevent excessive head movement.

fMRI Data Analysis

Preprocessing of the data was performed according to graph-theoretical network analysis. The toolkit (GRETNA[1]) fMRI preprocessing pipeline included slice-timing correction, head motion correction, spatial normalization, and smoothing. The following denoising steps were performed with the unsmoothed images (Wang et al., 2015): detrending, temporal bandpass filtering, and removal of nuisance signals by regression on head motion effect, white matter, and cerebrospinal fluid signals, and an indispensable "scrubbing" procedure. Finally, no patient had fewer than 300 volumes. Additional preprocessing information is described in the **Supplementary Material**.

We used the group independent component analysis (GICA) method to extract the spatial components of nine defined RSNs as shown in **Figure 1B**. The GICA of the fMRI toolbox[2] was used for each group of participants for their respective

[1]http://www.nitrc.org/projects/gretna/
[2]https://www.nitrc.org/projects/gift

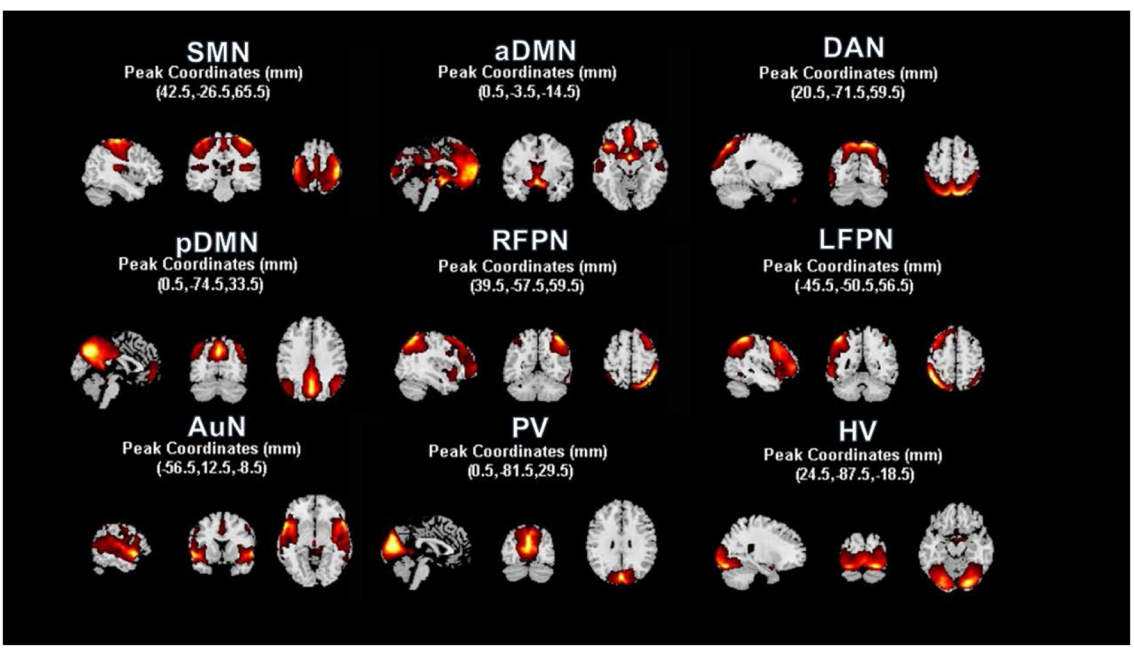

FIGURE 2 | Resting state functional networks identified by ICA. We identified nine meaningful RSNs and extracted the corresponding mean time courses. In each RSN, peak coordinates in Montreal Neurological Institute (MNI) space helped us to verify the location of these nine built networks. A one-sample *t*-test was used to find the significant voxels within their networks ($p < 0.01$, voxel correlation *via* FDR).

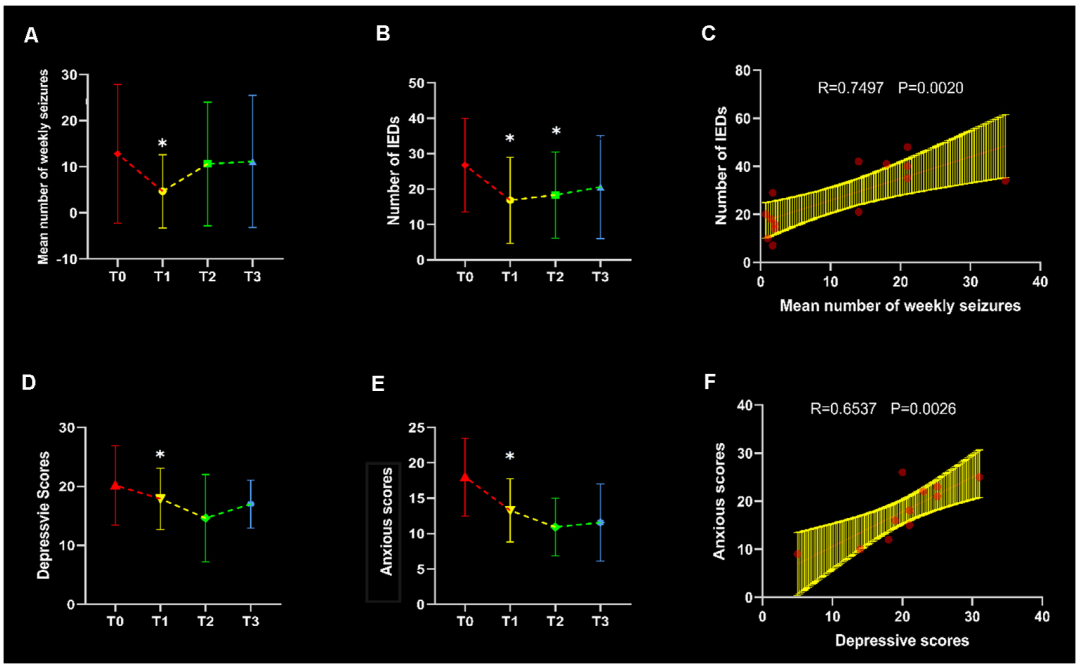

FIGURE 3 | Clinical evaluation and correlation. Line graphs were plotted in terms of the comparisons between three follow-up time points and baseline ($p < 0.05$), with asterisks indicating significant changes. The mean number of weekly seizures (MNWS), interictal epileptiform discharges (IEDs), depressive scores and anxious scores in each time points were shown in panels **(A,B,D)** and **(E)** respectively. In the T0 baseline, IEDs showed an increased association with MNWS in **(C)**, and a positive correlation was found between depressive and anxious scores in **(F)**.

group spatial ICA, and more details are provided in the **Supplementary Material**. Spatial components of nine cortical RSNs were gathered across each group by one-sample *t*-tests, including Attention Network (AN), Anterior Default Modal Network (DMN), Posterior Default Modal Network (DMN), Sensorimotor Network (SMN), Right Frontoparietal Network (RFPN), Left Frontoparietal Network (LFPN), Prim-visual Network (PV), High-visual Network (HV) and Auditory Network (AuN), as shown in **Figure 2** ($p < 0.01$ for multiple comparisons corrected *via* false discovery rate). The abbreviation rules of nine RSNs were in terms of the Stanford brain functional template[3] and prior studies (Corbetta and Shulman, 2002). Finally, 36 statistical maps were converted to 36 binary masks and were shown with BrainNet Viewer (Xia et al., 2013) in MATLAB.

The corresponding mean time series of the 36 RSNs were extracted with REST software (Song et al., 2011), and FNCs in the epilepsy groups (T0, T1, T2, and T3) and healthy control group were calculated. We obtained 9 × 9 FNC mean matrices of all the subjects and performed Fisher's *r* to *z* transformation. We compared FNC results in four time windows: "baseline" before treatment (T0) and the two to four phases of "posttreatment follow-up" after treatment (T1–T3). Four pairwise comparisons were performed using two-sample *t*-tests between patients and HCs ($p < 0.05$, FDR corrected), with age, sex, and head motion (mean FD) as nuisance covariates. The significance level was set at $p < 0.05$ and corrected for multiple comparisons using the false discovery rate (FDR). The three follow-up groups were compared to the pretreatment groups using two-sample *t*-tests ($p < 0.05$, FDR corrected).

[3]http://findlab.stanford.edu/functional_ROIs.html

RESULTS

Subject Characterization and Antiepileptic Effects of rTMS

Fourteen patients with refractory epilepsy were enrolled in this study, and all completed the 2-week course of rTMS over the vertex. There was no adverse effect on rTMS treatment reported from patients. Patients and healthy controls ($N = 17$) did not differ significantly in terms of age ($t = 0.70$, $p = 0.49$), sex ($\chi^2 = 0.31$, $p = 0.58$) or handedness (**Supplementary Table 1**).

After rTMS treatment, the mean number of weekly seizure (MNWS) across the patients for T1, T2, and T3 was 4.67 ± 7.94, 10.61 ± 13.42, and 11.17 ± 14.30 (mean ± standard deviation). Compared with 12.82 ± 15.06 in T0, 12 (14) patients exhibited a decreased MNWS with a statistical significance, $F_{(1.11, 14.48)} = 10.15$, $p = 0.01$. After Bonferroni *post hoc* test, we found there was a noticeable reduction in T1 ($p = 0.03$) while no significant change was found in T2 ($p = 0.05$) and T3 ($p = 0.10$) as shown in **Figure 3A**.

All patients showed a decreased IEDs and an ANOVA of the IEDs yielded a significant main effect of time points, $F_{(2.04, 26.51)} = 8.81$, $p < 0.01$. Through the pairwise comparison, results revealed that T1 ($p = 0.04$) and T2 ($p < 0.01$) showed a

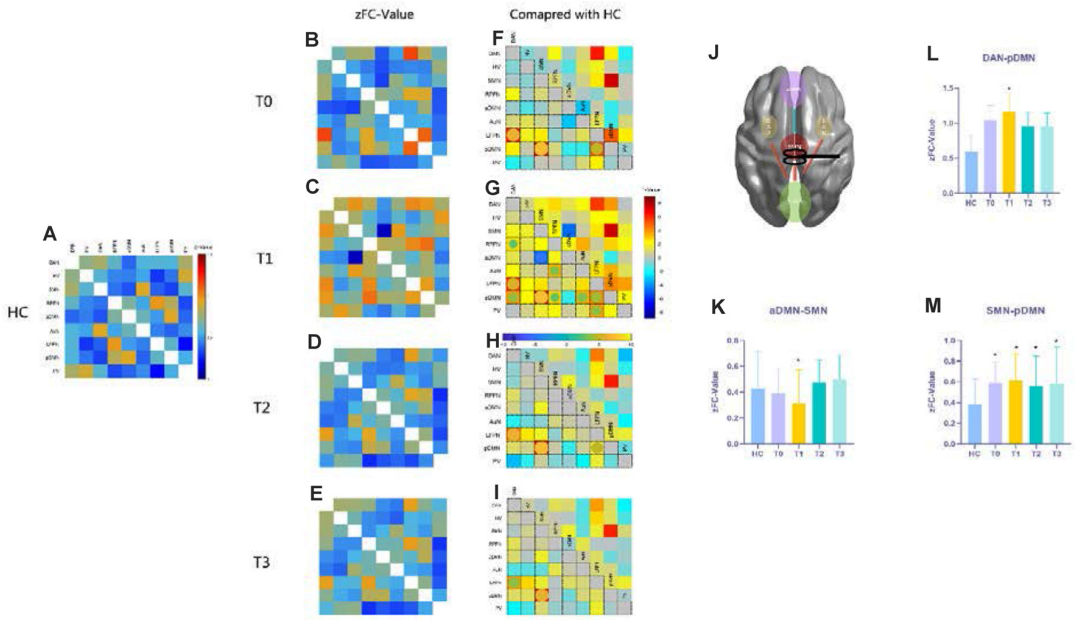

FIGURE 4 | Functional network connectivity (FNC) results compared with those of HCs. Panels **(A–E)** show the resting functional network results with FNC values that underwent Fisher's *r* to *z* transformation, referring to the color bar in **(A)**; **(F–I)** the *t*-maps give the information about the contrast of FC compared to HCs at each time point, the significant differences emphasized with spheres and their colors mean different *t*-values ($p < 0.05$, FDR corrected), referring to the horizontal bar in **(G)**; panels **(K–M)** show the FNC *z*-values for SMN-aDMN, SMN-pDMN, and pDMN-DAN connections in HCs and patients at each time point with the asterisks indicating a significant difference compared with HCs ($p < 0.05$, FDR correlated). **(J)** A conceptional diagram with red lines representing hyperconnectivity and the blue line meaning hypoconnectivity after rTMS treatment. The nine functional networks are abbreviated in **Supplementary Table 2**. Abbreviations: HCs, healthy controls; SMN, sensorimotor network; aDMN, anterior default-mode network; pDMN, posterior default-mode network; DAN, dorsal attention network.

significant decrease after rTMS intervention but no discrepant change was found in T3 ($p = 0.08$) in **Figure 3B**. In addition, there was a significant correlation between MWSF and IEDs ($r = 0.7494$, $p = 0.002$) at baseline in **Figure 3C**, which meant the consistency of the clinical indicators.

Through the repetitive measurement ANOVA, the result produced markable differences in HAM-D and HAM-A scores, $F_{(3,18)} = 5.216$, $p = 0.009$, and $F_{(3,18)} = 8.302$, $p = 0.001$. After the *post hoc* test, we found that patients' symptoms improved on the HAM-D at T1 compared to baseline ($p = 0.022$) in **Figure 3D**. Moreover, anxiety assessment found decreased symptoms in T1 ($p = 0.015$) in **Figure 3E**. And there was a significant correlation between depressive and anxious scores in T0 ($r = 0.6527$, $p = 0.0026$) in **Figure 3F**.

Functional Network Connectivity

Functional network connectivity in the epilepsy groups (T0, T1, T2, and T3) and healthy control group were produced as shown in **Figures 3A–E**. We made comparisons between healthy controls and patient groups at each time point (T0–T3) with the covariates of age, sex, and head movement. The FNC results showed significant differences at the first follow-up time point (T1) shown in **Figures 4G** and **4J** while the baseline T0 in **Figure 4F** and subsequent follow-ups (T2 in **Figure 4H** and T3 in **Figure 4I**) were almost the same as HCs, with the exception of the posterior default-mode network (pDMN)–SMN connectivity (T2 $t = 6.19$, $p_{FDR} < 0.001$; T3 $t = 6.10$, $p_{FDR} < 0.001$) shown in **Figure 4M**. Importantly, we found that SMN–anterior DMN (aDMN) connectivity decreased after rTMS intervention at T1 ($t = -4.85$, $p_{FDR} < 0.001$) shown in **Figure 4K**. With respect to the final follow-up, T3 returned back to the baseline level in T0.

After 10 days rTMS treatment for the patient group, the aDMN showed temporarily lower connectivity with the SMN ($t = -4.2446$, $p_{FDR} < 0.001$), and hyperconnectivity with the dorsal attention network (DAN; $t = 2.0828$, $p_{FDR} = 0.0472$) appeared in T1 (**Figures 5A** and **5B**), which could not be found in further follow-ups of T2 and T3. Moreover, T2 and T3 demonstrated no significant alteration in contrast with T0 ($p_{FDR} > 0.05$). Then, according to the improvement in clinical seizure frequency on T1, we divided the patients into two groups: bad and good response on rTMS. Patients who showed a better response to rTMS were statistically distinguishable from the *z*-value of aDMN-SMN by the two-sample *t*-test ($t = 2.980$, $p = 0.0115$). However, it was temporary because T2 and T3 were not found (**Figure 5C**). To test whether the *z*-value of aDMN-SMN in T1 was related to treatment response, we used Pearson's correlation to find that the *z*-value of aDMN-SMN was anticorrelated with depression scores of T1 in **Figure 5D** ($r = -0.67$, $p = 0.0022$), which meant an improvement in depressive symptoms. Other clinical measures showed no significance with the FNC *z*-value of aDMN-SMN.

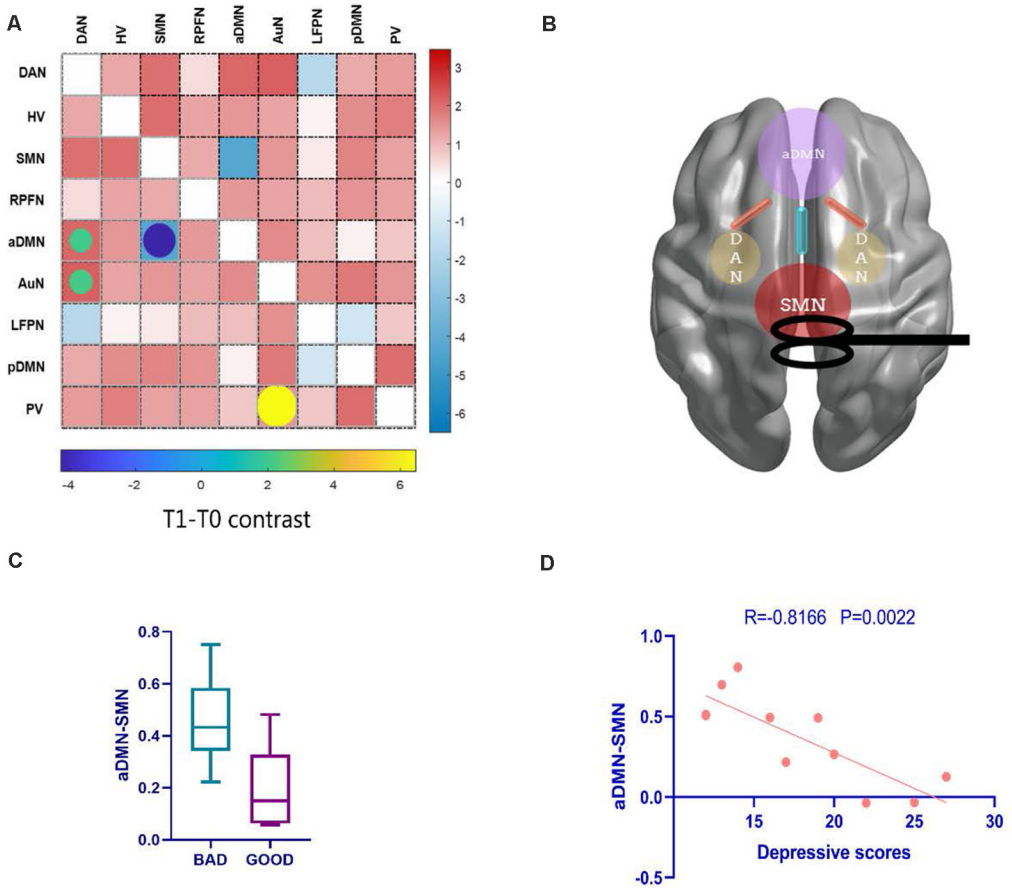

FIGURE 5 | The alteration of FNC and their clinical correlations after rTMS. **(A)** Posttreatment FNC in T1 shows a decreasing change in internetwork connectivity between the SMN and aDMN, while the DAN-aDMN, DAN-AuN, and PV-AuN pairs demonstrated hyperconnectivity after rTMS. **(B)** A conceptional graph of the important and temporary changes in T1. **(C)** Comparing bad and good response groups in T1, a two-sample *t*-test was used to test the significant difference in FNC *z*-value of aDMN-SMN ($p = 0.0115$). **(D)** With the correlation analysis of the FNC in the aDMN-SMN and depressive scores, the results showed a more than moderate correlation (Pearson's correlation $r = -0.67$, $p = 0.0022$). AuN, auditory network.

DISCUSSION

Epilepsy is an abnormal network disease and it is potential to use network modulation in order to an antiepileptic efficacy (Tecchio et al., 2018). Our study demonstrated the antiepileptic effect of low-frequency rTMS over the vertex (in SMN) in refractory epilepsy patients. Due to our strict work on patient filters, almost every patient had visible movement seizures during the ictal period and more than once a week. The positive outcome was achieved in the first follow-up but disappeared in the following observation periods. The results on the persistent period of rTMS after-effects are consistent with previous studies, which would prolong the antiepileptic efficacy for no more than 6–8 weeks posttreatment observation period (Theodore et al., 2002; Fregni et al., 2006; Sun et al., 2012), suggesting that a long-term after-effect are needed for sustainable treatment.

For FNC analysis, the present study investigated whether vertex-suppressive rTMS could modulate brain functional networks in patients with refractory epilepsy and whether modulated functional connectivity was associated with changes in clinical symptoms. To investigate RSN reorganization induced by the antiepileptic effect of rTMS on vertex suppression, we compared the changes in resting-state FNC before and after rTMS. Our findings suggest that a 10-session 0.5-Hz rTMS targeting the vertex may improve epileptic symptoms by modulating functional links connecting to the SMN, DMN, and DAN for patients with refractory epilepsy.

In contrast to healthy subjects, the SMN showed a higher FNC with the pDMN in patients with refractory epilepsy, and the posterior cingulate cortex (PCC) is a core region in the DMN that is associated with autobiographical, self, and social functions (Buckner et al., 2008). Previous studies proposed that the PCC was crucial for the motor circus, suggesting that the abnormal function of the PCC might impact the motor circus through projections from the PCC to the anterior thalamus (Yeterian and Pandya, 1988). And a recent study demonstrated that thalamic hyperexcitability contributed to the cortical maintenance of epileptic susceptibility in juvenile myoclonic epilepsy (Assenza et al., 2020a). Because there are direct projections from the thalamus to the PCC, abnormal

IEDs from the thalamus lead to precuneus/PCC abnormalities (Avoli et al., 2001; Gotman et al., 2005). The abnormal functional activity in the PCC was associated with impairment of awareness in the ictal period (Archer et al., 2003; Jia et al., 2018), which might partly explain consequent attention disorders during the interictal period (Brandt, 1984; Lui et al., 2008). As most patients in our study had generalized motor seizures accompanied by consciousness disorders, the enhanced coupling between the SMN and PCC (in the pDMN) might suggest an overexciting motor circus in refractory epilepsy. However, vertex-suppressive rTMS did not show changes in SMN-pDMN connectivity in the treatment groups.

Due to its special location in the distributed functional network, as in previous studies, we use the vertex (in SMN) as the stimulus point (Tergau et al., 2003; Cantello et al., 2007). The sensorimotor network, as demonstrated in a wealth of studies, is partially integrated into a multimodal network associated with motor systems and cognitive hubs (Sepulcre et al., 2012). After rTMS intervention, RSN temporary reorganization appeared among the aDMN, SMN, and DAN. We used inhibitive rTMS to lower neural activity in the SMN, while the aDMN showed lower synchrony with the SMN and higher synchrony with the pDMN. The DMN showed an active state in response to rTMS that was considered to be involved in a high degree of neuroplasticity (Raichle et al., 2001; Fjell et al., 2014). In the correlation analysis, we found that SMN-aDMN connectivity was anticorrelated with depressive scores and related to seizure improvement. Our results are consistent with previous fMRI studies, suggesting that medial prefrontal cortex (in the aDMN) disruption has been implicated in changes in emotional impairments (Satpute and Lindquist, 2019). For treat-resistant patients, a recent fMRI study of the DMN has found that internetwork connectivity of the DMN presented an anticorrelation with the duration of epilepsy, suggesting that DMN connectivity might be a predictor of the antiepileptic effect (Yang et al., 2021).

Several limitations should be acknowledged while interpreting our results. On the one hand, sham stimulation groups are omitted, as the stimulator's factors were overcome by our manipulations, such as choosing noiseless equipment and no extra physical contact with patients. Moreover, we included IEDs as objective outcome measures that could reflect a more impersonal evaluation. On the other hand, we hope to add subcortical nuclear analysis, such as analysis of the thalamus and its posterior movement circuit of the basal ganglia, in our further studies. As mentioned above, the thalamus plays a hub role related to the pathological manifestation in epilepsy (Bestmann et al., 2004; Jobst and Cascino, 2017; Assenza et al., 2020a,b). Basal ganglia involved in movement circus discussion may help to better explain our results with respect to the interaction between the pDMN and SMN.

DATA AVAILABILITY STATEMENT

The original contributions presented in the study are included in the article/**Supplementary Material**, further inquiries can be directed to the corresponding author/s.

ETHICS STATEMENT

The study protocol was approved by the Tianjin Medical University Institutional Review Board. The patients/participants provided their written informed consent to participate in this study.

AUTHOR CONTRIBUTIONS

JY and CF: conceptualization. CF: methodology and writing—original draft preparation. ZC, AA, and QY: validation. AA and QY: resources. AA and ZC: data curation. JY and WY: writing—review and editing. WY and JY: supervision. WY: funding acquisition. All authors contributed to the article and approved the submitted version.

FUNDING

This work was supported by the Natural Science Foundation of Tianjin City (grant number 12JCYBJC16900).

ACKNOWLEDGMENTS

We thank all the authors for their work on this study. We also thank the patients and healthy controls who contributed their time and effort to this study.

SUPPLEMENTARY MATERIAL

The Supplementary Material for this article can be found online at: https://www.frontiersin.org/articles/10.3389/fnhum.2021.667619/full#supplementary-material.

REFERENCES

Archer, J. S., Abbott, D. F., Waites, A. B., and Jackson, G. D. (2003). fMRI "deactivation" of the posterior cingulate during generalized spike and wave. *NeuroImage* 20, 1915–1922. doi: 10.1016/s1053-8119(03)00294-5

Assenza, G., Lanzone, J., Dubbioso, R., Coppola, A., Boscarino, M., Ricci, L., et al. (2020a). Thalamic and cortical hyperexcitability in juvenile myoclonic epilepsy. *Clin. Neurophysiol.* 131, 2041–2046. doi: 10.1016/j.clinph.2020.04.164

Assenza, G., Lanzone, J., Insola, A., Amatori, G., Ricci, L., Tombini, M., et al. (2020b). Thalamo-cortical network dysfunction in temporal lobe epilepsy. *Clin. Neurophysiol.* 131, 548–554. doi: 10.1016/j.clinph.2019.10.017

Avoli, M., Rogawski, M. A., and Avanzini, G. (2001). Generalized epileptic disorders: an update. *Epilepsia* 42, 445–457. doi: 10.1046/j.1528-1157.2001.39800.x

Badawy, R. A., Freestone, D. R., Lai, A., and Cook, M. J. (2012). Epilepsy: ever-changing states of cortical excitability. *Neuroscience* 222, 89–99. doi: 10.1016/j.neuroscience.2012.07.015

Barker, A. T. (1999). The history and basic principles of magnetic nerve stimulation. *Electroencephalogr. Clin. Neurophysiol. Suppl.* 51, 3–21.

Bestmann, S., Baudewig, J., Siebner, H. R., Rothwell, J. C., and Frahm, J. (2004). Functional MRI of the immediate impact of transcranial magnetic stimulation

on cortical and subcortical motor circuits. *Eur. J. Neurosci.* 19, 1950–1962. doi: 10.1111/j.1460-9568.2004.03277.x

Bonilha, L., Edwards, J. C., Kinsman, S. L., Morgan, P. S., Fridriksson, J., Rorden, C., et al. (2010). Extrahippocampal gray matter loss and hippocampal deafferentation in patients with temporal lobe epilepsy. *Epilepsia* 51, 519–528. doi: 10.1111/j.1528-1167.2009.02506.x

Brandt, J. (1984). Defective stimulus set attention in generalized epilepsy. *Brain Cogn.* 3, 140–151. doi: 10.1016/0278-2626(84)90013-7

Buckner, R. L., Andrews-Hanna, J. R., and Schacter, D. L. (2008). The brain's default network: anatomy, function, and relevance to disease. *Ann. N Y Acad. Sci.* 1124, 1–38. doi: 10.1196/annals.1440.011

Cantello, R., Civardi, C., Cavalli, A., Varrasi, C., Tarletti, R., Monaco, F., et al. (2000). Cortical excitability in cryptogenic localization-related epilepsy: interictal transcranial magnetic stimulation studies. *Epilepsia* 41, 694–704. doi: 10.1111/j.1528-1157.2000.tb00230.x

Cantello, R., Rossi, S., Varrasi, C., Ulivelli, M., Civardi, C., Bartalini, S., et al. (2007). Slow repetitive TMS for drug-resistant epilepsy: clinical and EEG findings of a placebo-controlled trial. *Epilepsia* 48, 366–374. doi: 10.1111/j.1528-1167.2006.00938.x

Chen, R., Classen, J., Gerloff, C., Celnik, P., Wassermann, E. M., Hallett, M., et al. (1997). Depression of motor cortex excitability by low-frequency transcranial magnetic stimulation. *Neurology* 48, 1398–1403. doi: 10.1212/wnl.48.5.1398

Chou, Y.-H., You, H., Wang, H., Zhao, Y.-P., Hou, B., Chen, N.-K., et al. (2015). Effect of repetitive transcranial magnetic stimulation on fMRI resting-state connectivity in multiple system atrophy. *Brain Connect.* 5, 451–459. doi: 10.1089/brain.2014.0325

Corbetta, M., and Shulman, G. L. (2002). Control of goal-directed and stimulus-driven attention in the brain. *Nat. Rev. Neurosci.* 3, 201–215. doi: 10.1038/nrn755

Fjell, A. M., McEvoy, L., Holland, D., Dale, A. M., and Walhovd, K. B. (2014). What is normal in normal aging? Effects of aging, amyloid and Alzheimer's disease on the cerebral cortex and the hippocampus. *Prog. Neurobiol.* 117, 20–40. doi: 10.1016/j.pneurobio.2014.02.004

Fox, M. D., Buckner, R. L., White, M. P., Greicius, M. D., and Pascual-Leone, A. (2012a). Efficacy of transcranial magnetic stimulation targets for depression is related to intrinsic functional connectivity with the subgenual cingulate. *Biol. Psychiatry* 72, 595–603. doi: 10.1016/j.biopsych.2012.04.028

Fox, M. D., Halko, M. A., Eldaief, M. C., and Pascual-Leone, A. (2012b). Measuring and manipulating brain connectivity with resting state functional connectivity magnetic resonance imaging (fcMRI) and transcranial magnetic stimulation (TMS). *NeuroImage* 62, 2232–2243. doi: 10.1016/j.neuroimage.2012.03.035

Fregni, F., Otachi, P. T. M., Valle, A. D., Boggio, P. S., and Valente, K. D. (2006). A randomized clinical trial of repetitive transcranial magnetic stimulation in patients with refractory epilepsy. *Ann. Neurol.* 60, 447–455. doi: 10.1002/ana.20950

Gotman, J., Grova, C., Bagshaw, A., Kobayashi, E., Aghakhani, Y., and Dubeau, F. (2005). Generalized epileptic discharges show thalamocortical activation and suspension of the default state of the brain. *Proc. Natl. Acad. Sci. U S A* 102, 15236–15240. doi: 10.1073/pnas.0504935102

ILAE. (1989). Proposal for revised classification of epilepsies and epileptic syndromes. Commission on classification and terminology of the international league against epilepsy. *Epilepsia* 30, 389–399. doi: 10.1111/j.1528-1157.1989.tb05316.x

Jia, X., Ma, S., Jiang, S., Sun, H., Dong, D., Chang, X., et al. (2018). Disrupted coupling between the spontaneous fluctuation and functional connectivity in idiopathic generalized epilepsy. *Front. Neurol.* 9:838. doi: 10.3389/fneur.2018.00838

Jobst, B. C., and Cascino, G. D. (2017). Thalamus as a "hub" to predict outcome after epilepsy surgery. *Neurology* 88, 2246–2247. doi: 10.1212/WNL.0000000000004043

Joo, E. Y., Han, S.-J., Chung, S. H., Cho, J.-W., Seo, D. W., and Hong, S. B. (2007). Antiepileptic effects of low-frequency repetitive transcranial magnetic stimulation by different stimulation durations and locations. *Clin. Neurophysiol.* 118, 702–708. doi: 10.1016/j.clinph.2006.11.008

Keel, J. C., Smith, M. J., and Wassermann, E. M. (2001). A safety screening questionnaire for transcranial magnetic stimulation. *Clin. Neurophysiol.* 112:720. doi: 10.1016/s1388-2457(00)00518-6

Kinoshita, M., Ikeda, A., Begum, T., Yamamoto, J., Hitomi, T., and Shibasaki, H. (2005). Low-frequency repetitive transcranial magnetic stimulation for seizure suppression in patients with extratemporal lobe epilepsy-a pilot study. *Seizure* 14, 387–392. doi: 10.1016/j.seizure.2005.05.002

Kramer, M. A., and Cash, S. S. (2012). Epilepsy as a disorder of cortical network organization. *Neuroscientist* 18, 360–372. doi: 10.1177/1073858411422754

Kwan, P., Arzimanoglou, A., Berg, A. T., Brodie, M. J., Allen Hauser, W., Mathern, G., et al. (2010). Definition of drug resistant epilepsy: consensus proposal by the *ad hoc* Task Force of the ILAE Commission on Therapeutic Strategies. *Epilepsia* 51, 1069–1077. doi: 10.1111/j.1528-1167.2009.02397.x

Lui, S., Ouyang, L., Chen, Q., Huang, X., Tang, H., Chen, H., et al. (2008). Differential interictal activity of the precuneus/posterior cingulate cortex revealed by resting state functional MRI at 3T in generalized vs. partial seizure. *J. Magn. Reson. Imaging* 27, 1214–1220. doi: 10.1002/jmri.21370

Pascual-Leone, A., Valls-Solé, J., Wassermann, E. M., and Hallett, M. (1994). Responses to rapid-rate transcranial magnetic stimulation of the human motor cortex. *Brain* 117, 847–858. doi: 10.1093/brain/117.4.847

Pereira, L. S., Muller, V. T., da Mota Gomes, M., Rotenberg, A., and Fregni, F. (2016). Safety of repetitive transcranial magnetic stimulation in patients with epilepsy: a systematic review. *Epilepsy Behav.* 57, 167–176. doi: 10.1016/j.yebeh.2016.01.015

Qin, Y., Zhang, N., Chen, Y., Zuo, X., Jiang, S., Zhao, X., et al. (2020). Rhythmic network modulation to thalamocortical couplings in epilepsy. *Int. J. Neural Syst.* 30:2050014. doi: 10.1142/S0129065720500148

Raichle, M. E., MacLeod, A. M., Snyder, A. Z., Powers, W. J., Gusnard, D. A., and Shulman, G. L. (2001). A default mode of brain function. *Proc. Natl. Acad. Sci. U S A* 98, 676–682. doi: 10.1073/pnas.98.2.676

Satpute, A. B., and Lindquist, K. A. (2019). The default mode network's role in discrete emotion. *Trends Cogn. Sci.* 23, 851–864. doi: 10.1016/j.tics.2019.07.003

Schmidt, D., and Löscher, W. (2005). Drug resistance in epilepsy: putative neurobiologic and clinical mechanisms. *Epilepsia* 46, 858–877. doi: 10.1111/j.1528-1167.2005.54904.x

Sepulcre, J., Sabuncu, M. R., Yeo, T. B., Liu, H., and Johnson, K. A. (2012). Stepwise connectivity of the modal cortex reveals the multimodal organization of the human brain. *J. Neurosci.* 32, 10649–10661. doi: 10.1523/JNEUROSCI.0759-12.2012

Song, X.-W., Dong, Z.-Y., Long, X.-Y., Li, S.-F., Zuo, X.-N., Zhu, C.-Z., et al. (2011). REST: a toolkit for resting-state functional magnetic resonance imaging data processing. *PLoS One* 6:e25031:e25031. doi: 10.1371/journal.pone.0025031

Sun, W., Mao, W., Meng, X., Wang, D., Qiao, L., Tao, W., et al. (2012). Low-frequency repetitive transcranial magnetic stimulation for the treatment of refractory partial epilepsy: a controlled clinical study. *Epilepsia* 53, 1782–1789. doi: 10.1111/j.1528-1167.2012.03626.x

Tecchio, F., Cottone, C., Porcaro, C., Cancelli, A., Di Lazzaro, V., and Assenza, G. (2018). Brain functional connectivity changes after transcranial direct current stimulation in epileptic patients. *Front. Neural Circuits* 12:44. doi: 10.3389/fncir.2018.00044

Tergau, F., Naumann, U., Paulus, W., and Steinhoff, B. J. (1999). Low-frequency repetitive transcranial magnetic stimulation improves intractable epilepsy. *Lancet* 353:2209. doi: 10.1016/S0140-6736(99)01301-X

Tergau, F., Neumann, D., Rosenow, F., Nitsche, M. A., Paulus, W., and Steinhoff, B. (2003). Can epilepsies be improved by repetitive transcranial magnetic stimulation?—interim analysis of a controlled study. *Suppl. Clin. Neurophysiol.* 56, 400–405. doi: 10.1016/s1567-424x(09)70244-2

Theodore, W. H., Hunter, K., Chen, R., Vega-Bermudez, F., Boroojerdi, B., Reeves-Tyer, P., et al. (2002). Transcranial magnetic stimulation for the treatment of seizures: a controlled study. *Neurology* 59, 560–562. doi: 10.1212/wnl.59.4.560

Tombini, M., Pellegrino, G., Pasqualetti, P., Assenza, G., Benvenga, A., Fabrizio, E., et al. (2013). Mobile phone emissions modulate brain excitability in patients with focal epilepsy. *Brain Stimul.* 6, 448–454. doi: 10.1016/j.brs.2012.07.006

Tsuboyama, M., Kaye, H. L., and Rotenberg, A. (2020). Review of transcranial magnetic stimulation in epilepsy. *Clin. Ther.* 42, 1155–1168. doi: 10.1016/j.clinthera.2020.05.016

Varrasi, C., Civardi, C., Boccagni, C., Cecchin, M., Vicentini, R., Monaco, F., et al. (2004). Cortical excitability in drug-naive patients with partial epilepsy: a cross-

sectional study. *Neurology* 63, 2051–2055. doi: 10.1212/01.wnl.0000145770.95990.82

Wang, J., Wang, X., Xia, M., Liao, X., Evans, A., and He, Y. (2015). GRETNA: a graph theoretical network analysis toolbox for imaging connectomics. *Front. Hum. Neurosci.* 9:386. doi: 10.3389/fnhum.2015.00386

Wiebe, S., Blume, W. T., Girvin, J. P., Eliasziw, M., and Effectiveness and Efficiency of Surgery for Temporal Lobe Epilepsy Study Group. (2001). A randomized, controlled trial of surgery for temporal-lobe epilepsy. *N. Engl. J. Med.* 345, 311–318. doi: 10.1056/NEJM200108023450501

Xia, M., Wang, J., Yong, H., and Peter, C. (2013). BrainNet viewer: a network visualization tool for human brain connectomics. *PLoS One* 8:e68910. doi: 10.1371/journal.pone.0068910

Yang, S., Zhang, Z., Chen, H., Meng, Y., Li, J., Li, Z., et al. (2021). Temporal variability profiling of the default mode across epilepsy subtypes. *Epilepsia* 62, 61–73. doi: 10.1111/epi.16759

Ye, H., and Kaszuba, S. (2019). Neuromodulation with electromagnetic stimulation for seizure suppression: from electrode to magnetic coil. *IBRO Rep.* 7, 26–33. doi: 10.1016/j.ibror.2019.06.001

Yeterian, E. H., and Pandya, D. N. (1988). Corticothalamic connections of paralimbic regions in the rhesus monkey. *J. Comp. Neurol.* 269, 130–146. doi: 10.1002/cne.902690111

Conflict of Interest: The authors declare that the research was conducted in the absence of any commercial or financial relationships that could be construed as a potential conflict of interest.

frontiers in Human Neuroscience

ORIGINAL RESEARCH
published: 12 August 2021
doi: 10.3389/fnhum.2021.679977

Intensity-Dependent Changes in Quantified Resting Cerebral Perfusion With Multiple Sessions of Transcranial DC Stimulation

Matthew S. Sherwood[1]*, *Lindsey McIntire*[2], *Aaron T. Madaris*[2,3], *Kamin Kim*[4], *Charan Ranganath*[4,5] and *R. Andy McKinley*[6]

[1] Science & Space, KBR Inc., Beavercreek, OH, United States, [2] Infoscitex, Inc., Beavercreek, OH, United States, [3] Department of Biomedical, Industrial and Human Factors Engineering, Wright State University, Dayton, OH, United States, [4] Department of Psychology, University of California, Davis, Davis, CA, United States, [5] Center for Neuroscience, University of California, Davis, Davis, CA, United States, [6] Air Force Research Laboratory, Wright-Patterson AFB, Dayton, OH, United States

OPEN ACCESS

Edited by:
Masaki Sekino,
The University of Tokyo, Japan

Reviewed by:
Umer Asgher,
National University of Sciences and Technology, Pakistan
Jovana Bjekic,
University of Belgrade, Serbia

***Correspondence:**
Matthew S. Sherwood
matt.sherwood@us.kbr.com

Specialty section:
This article was submitted to Brain Imaging and Stimulation, a section of the journal Frontiers in Human Neuroscience

Received: 12 March 2021
Accepted: 15 July 2021
Published: 12 August 2021

Citation:
Sherwood MS, McIntire L, Madaris AT, Kim K, Ranganath C and McKinley RA (2021) Intensity-Dependent Changes in Quantified Resting Cerebral Perfusion With Multiple Sessions of Transcranial DC Stimulation. Front. Hum. Neurosci. 15:679977. doi: 10.3389/fnhum.2021.679977

Transcranial direct current stimulation (tDCS) to the left prefrontal cortex has been shown to produce broad behavioral effects including enhanced learning and vigilance. Still, the neural mechanisms underlying such effects are not fully understood. Furthermore, the neural underpinnings of repeated stimulation remain understudied. In this work, we evaluated the effects of the repetition and intensity of tDCS on cerebral perfusion [cerebral blood flow (CBF)]. A cohort of 47 subjects was randomly assigned to one of the three groups. tDCS of 1- or 2-mA was applied to the left prefrontal cortex on three consecutive days, and resting CBF was quantified before and after stimulation using the arterial spin labeling MRI and then compared with a group that received sham stimulation. A widespread decreased CBF was found in a group receiving sham stimulation across the three post-stimulation measures when compared with baseline. In contrast, only slight decreases were observed in the group receiving 2-mA stimulation in the second and third post-stimulation measurements, but more prominent increased CBF was observed across several brain regions including the locus coeruleus (LC). The LC is an integral region in the production of norepinephrine and the noradrenergic system, and an increased norepinephrine/noradrenergic activity could explain the various behavioral findings from the anodal prefrontal tDCS. A decreased CBF was observed in the 1-mA group across the first two post-stimulation measurements, similar to the sham group. This decreased CBF was apparent in only a few small clusters in the third post-stimulation scan but was accompanied by an increased CBF, indicating that the neural effects of stimulation may persist for at least 24 h and that the repeated stimulation may produce cumulative effects.

Keywords: MRI, arterial spin labeling, cerebral perfusion, neuromodulation, transcranial DC stimulation, prefrontal cortex, locus coeruleus

INTRODUCTION

Transcranial electrical stimulation (TES) refers to a spectrum of techniques focused on delivering electrical currents non-invasively to the brain with the goal of modulating neural activity. TES has experienced an increased interest over the past 15 years in basic to applied clinical research (Fregni et al., 2015). TES that uses a weak, constant current delivered to the scalp is referred to as the transcranial direct current stimulation (tDCS) (Coffman et al., 2012). The specific application of tDCS with the anode placed on the frontal scalp sites ("anodal prefrontal tDCS") has been routinely applied in the literature with demonstrable behavioral effects in combatting performance decrements associated with vigilance (Nelson et al., 2014), decreasing the effect of fatigue on the cognitive performance (McIntire et al., 2014, 2017a,b), accelerating learning processes (Bullard et al., 2011; Clark et al., 2012; Coffman et al., 2012; McKinley et al., 2013), enhancing multitasking performance (Nelson et al., 2016), and improving procedural memory (McKinley et al., 2017b).

Despite the broad applications of tDCS and those specific to anodal prefrontal stimulation, the neural mechanisms underlying tDCS are not fully understood. It has been suggested that anodal tDCS increases excitability in the neocortex (Liebetanz, 2002) by altering neuronal membrane potentials (Bindman et al., 1962). This theory is supported by the evidence of enhanced glutamatergic activity, measured from proton magnetic resonance spectroscopy, following the application of anodal tDCS at rest (Clark et al., 2011). Synaptic plasticity, the ability of the brain to form and restructure synaptic connections (Pittenger and Duman, 2008), is thought to coincide with the increased glutamatergic activity (Hunter et al., 2013) and, thus, is theorized as a mechanism of action in tDCS, as evident in the lasting behavioral effects (e.g., McIntire et al., 2014, 2017b) and the acceleration of learning processes (Bullard et al., 2011; Clark et al., 2012; McKinley et al., 2013). Despite the expansive literature on the anodal prefrontal stimulation and neural mechanisms of tDCS, studies exploring the behavioral effects and neural underpinnings of multiple sessions of stimulation are limited. The goal of the present study was to further our understanding of the neural effects of repetitive stimulation to evaluate the potential dosage and tolerance effects.

Non-invasive Measurement of Cerebral Perfusion

The measurement of cerebral perfusion [volume of blood delivered to a volume of tissue per unit time, referred to as the cerebral blood flow (CBF)] is a growing method for studying neural processes. O^{15}-H_2O PET is the standard for quantifying CBF; however, this imaging requires the injection of a radioactive tracer. Alternatively, the *in vivo* quantification of CBF can be performed non-invasively using MRI through an arterial spin labeling (ASL) pulse sequence (Weber et al., 2013; Grade et al., 2015). ASL uses a simple modification to the standard MRI acquisitions to turn the blood in the neck into an MR tracer. This is completed by labeling blood in a slab inferior to the imaging field of view using magnetic inversion. This inversion will decrease the measured signal, and, thus, CBF can be extracted by comparing the labeled image with a control (unlabeled) image. ASL imaging is clinically used to identify the early pathophysiological changes in Alzheimer's disease (Du et al., 2006; Noguchi et al., 2008; Xu et al., 2010) and other disorders such as dementia (Xu et al., 2010; Borogovac and Asllani, 2012; Weber et al., 2013). In comparison to signals based on blood oxygen, CBF has better reliability and intersubject variability (Weber et al., 2013). Furthermore, CBF is directly responsible for the delivery of glucose and oxygen. Both oxygen and glucose are necessary to maintain ATP production and needs to be replenished to support the continued neural activity. Although CBF is not a direct measure of neural activity, it is a tightly coupled correlate: CBF changes with neural activity which occurs with a changing metabolism (i.e., resting activity) or during task activation (Borogovac and Asllani, 2012).

Rationale and Hypothesis

Behaviorally, our group has observed various effects from anodal prefrontal tDCS. Increased information throughput (Nelson et al., 2019) and multitasking throughput capacity (Nelson et al., 2016) during the multi-attribute task battery were observed in groups receiving 2-mA compared with those of sham stimulation. Improvements in the target detection were observed during an air traffic controller task in subjects receiving 2-mA compared to those in sham stimulation (Nelson et al., 2014). A similar improvement in the target detection was observed in a vigilance task from a group receiving a 2-mA stimulation compared to those receiving a lower-amplitude stimulation (0.5, 1, and 1.5 mA) as well as sham stimulation (McKinley et al., 2017a). McIntire et al. (2017a,b) observed attentional decrements due to sleep deprivation stress in a sham stimulation group; however, 6 h of improved attentional accuracy and reaction time following a single application of 2-mA stimulation was reported. In addition, self-reports from the 2-mA group revealed more vigor, less fatigue, and reduced boredom than those from the sham group. These effects were found to be reliable and repeated in a duplicated study on a new subject sample (McIntire et al., 2019). A final study observed a decreased sleep time without negative effects on mood or sleep quality following a single session of a 2-mA stimulation compared to the sham group (McIntire et al., 2020).

The study of the resting CBF in anodal prefrontal tDCS may provide critical, novel insights that could help elucidate the mechanisms of the anodal prefrontal tDCS resulting in these various behavioral effects. For instance, increased neural activity associated with anodal tDCS would increase the resting metabolism and, thus, would enhance CBF (Gsell et al., 2000; Nielsen and Lauritzen, 2001; Sheth et al., 2004). Few previous studies have used ASL to assess such neural effects of tDCS. In one study, increased regional CBF within and between subjects was found underneath the site of anodal tDCS, with transfer effects observed in brain regions functionally connected to the stimulation site following a single stimulation of 0.8- to 2-mA (Zheng et al., 2011). In another study where 1-mA anodal and cathodal stimulations were provided to the prefrontal cortex 1 week apart, immediate and lasting changes in CBF were found to

be associated with the anodal left prefrontal tDCS (Stagg et al., 2013). Despite observing increased CBF in regions anatomically close to the dorsolateral prefrontal cortex, a widespread CBF was observed after both anodal and cathodal tDCS. Through the comparison of multiple levels of stimulation across concurrent days with that of the sham stimulation, we sought to identify tolerance or cumulative effects of tDCS on the resting CBF.

MATERIALS AND METHODS

Participants

The previous research from our group, in between-subject experiments, has used Cohen's *d* in power analysis to help determine the sample size. Cohen's *d* of 0.8 or larger is considered a large effect. Using a two-sample *t*-test with a power of 0.8, an alpha error of 0.05, and a Cohen's *d* value of 0.8 results in 26 subjects per group. In the current study, there are three groups. Due to constraints of time and funding, and a plan to run follow-up studies, it was decided to use 20 subjects per group.

This study reports the findings from 47 healthy volunteers (mean age = 27.9 ± 4.85, 9 women). In total, we recruited 77 healthy, active-duty, Air Force military members aged 18–42 that did not meet our exclusion criteria (see **Supplementary Table 1** for a full list of exclusion criteria). Participants were recruited from Wright Patterson Air Force Base, Ohio, and were randomly assigned to one of our three experimental groups. Withdrawals and disqualifications (detailed below) during the experimental progress resulted in exceeding our planned recruitment of 60 subjects. Additional disqualifications were made during our data analysis due to data issues, resulting in 47 participants being included in this report.

Written informed consent was obtained from each participant prior to any experimental procedures. At the time of consent (∼1–2 days prior to the first experimental session), participants were randomly assigned to one of the three groups, received written instructions, and practiced tasks including 5-min of training on the Mackworth Clock test (McIntire et al., 2017b; McKinley, 2018). The experimental protocol was approved by the Air Force Research Laboratory Institutional Review Board at Wright-Patterson Air Force Base under Protocol # FWR20130126H. Participants eligible for compensation (i.e., if participation occurred in an off-duty status) received equal remuneration.

Of the 77 participants recruited and consented, the reported cohort was reduced due to medical disqualification ($n = 1$), withdrawal prior to MRI procedures ($n = 6$; e.g., family issues, being uncomfortable with MRI procedures once seen in person, or illness), self-withdrawal due to illness/family issues or being uncomfortable with MRI procedures (e.g., noise; $n = 6$), incomplete data collection due to MRI scheduling conflicts ($n = 1$), or being medically disqualified due to incidental findings during the initial MRI scan ($n = 1$). Additionally, participants were removed due to missing or corrupted data ($n = 13$) and bad registration between ASL and anatomical images ($n = 2$). Data from the remaining 47 participants were evaluated.

Experimental Design

This study was a parallel-group sham-controlled design with two active tDCS conditions (1- and 2-mA for 30 min) and one sham condition (30 s of 2-mA followed by 29.5 min of no stimulation). Each participant completed three experimental sessions, with each session separated by ∼24 h. The procedures at each session were identical – first, an initial MRI was performed followed by tDCS executed outside of the MRI, and finally, a second MRI with identical procedures similar to the first MRI (see **Figure 1**).

The sessions were conducted in the evenings to not only reduce the work-related conflicts but also conform to the availability of MRI. For most of the sessions, two participants were grouped on the same days with staggered start times (see **Table 1**). We attempted to hold start times consistent within the participants across the three sessions; however, the variability in MRI availability and participant delays could not be fully accounted.

Each of the three groups received the same instructions and performed the same tasks with the exception of stimulation. In the two experimental groups, 1-mA (ACT_{1mA}, $n = 15$, mean age = 26.93 ± 3.53, 2 women) or 2-mA (ACT_{2mA}, $n = 17$, mean age = 28.61 ± 5.79, 4 women), stimulation was provided for 30 min, while in the control group (CON, $n = 15$, mean age = 28.14 ± 5.08, 3 women), sham stimulation consisting of 2-mA was applied for 30 s followed by 29.5 min of no stimulation. The study was a single-blinded study – the participants, not the experimenters, were uninformed of the validity and intensity of the simulation. Since handedness was not controlled, self-reported handedness was queried. The CON group consisted of one left-handed participant, ACT_{1mA} had none, and ACT_{2mA} had seven.

Transcranial Direct Current Stimulation

On each of the three sessions, anodal stimulation was applied to the left prefrontal cortex (approximately F3) in a monopolar montage (i.e., extracephalic cathode). The DC stimulation (MagStim DC Stimulator, Magstim Company Limited, Whitland, UK) was delivered in a manner consistent with the previous reports (McIntire et al., 2017b, 2019; McKinley et al., 2017a; Sherwood et al., 2018). A constant current of 1- or 2-mA depending on the assigned condition was supplied through a ring of five custom Na/NaCl electrodes (Rio Grande Neurosciences, Inc., Sante Fe, NM). The electrodes were arranged in a 1.6-cm radius circle and separated by 0.1 cm (outer edge to outer edge), and the stimulation was distributed evenly among the five anode electrodes (see Petree et al., 2011 for further details on electrodes). Multistage current monitoring is used to ensure that constant current levels are delivered to the anode. The same ring configuration was used at the cathode location, which was placed on the contralateral upper bicep. The extracephalic reference was used to exclude any effects that may be due to the reference (i.e., cathode) electrodes (Nitsche et al., 2007; Priori et al., 2008). Each electrode was placed in a small plastic "cup" and secured to the participant using medical bandages. The electrode cups were filled with a highly conductive gel (SignaGel, Parker Laboratories, Fairfield, NJ) to ensure the current transfer to the scalp and bicep, and air bubbles were removed using a small

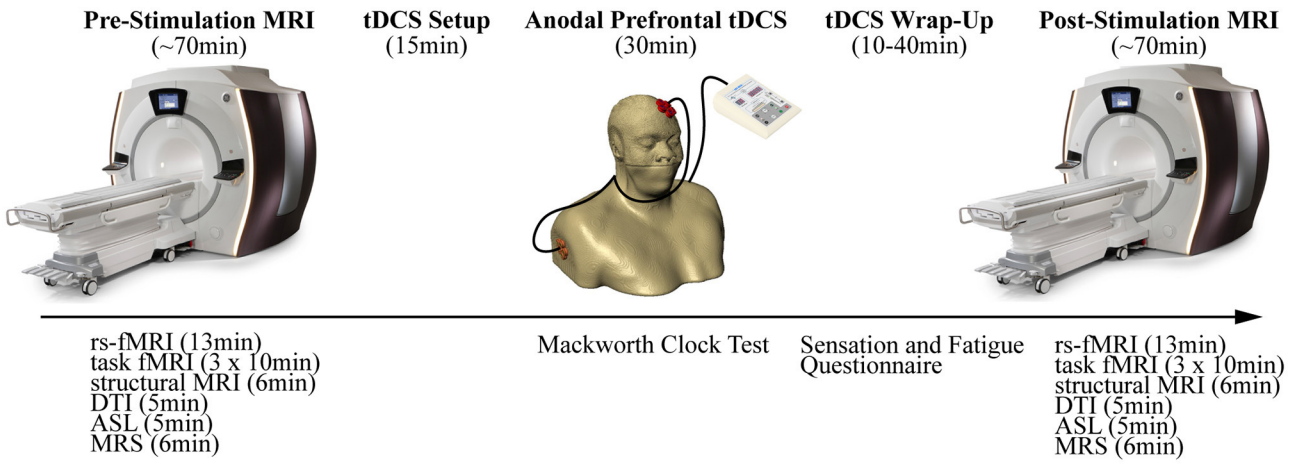

FIGURE 1 | Overview of the experimental design depicting the procedures. Each session began with a pre-stimulation MRI. Participants were then removed from the MRI and anodal prefrontal transcranial direct current stimulation (tDCS) was applied. Finally, a post-stimulation MRI repeated the procedures from the pre-stimulation MRI.

TABLE 1 | Starting times for the experimental procedures.

	Procedure	Start time	ASL scan time	End time
Participant 1	Pre-stimulation MRI	5:00 p.m.	6:10 p.m.	6:15 p.m.
	Transcranial DC stimulation	6:30 p.m.	n/a	7:00 p.m.
	Post-stimulation MRI	7:30 p.m.	8:40 p.m.	8:45 p.m.
Participant 2	Pre-stimulation MRI	6:15 p.m.	7:25 p.m.	7:30 p.m.
	Transcranial DC stimulation	7:45 p.m.	n/a	8:15 p.m.
	Post-stimulation MRI	8:45 p.m.	9:55 p.m.	10:00 p.m.

Participants completed the three sessions in groups of two with staggered start times.

wood dowel. Sham stimulation lasted 30 s and followed the same procedures but consisted of a 15-s ramp up to a 2-mA current and a 15-s ramp down to mimic the skin sensations during the active stimulation conditions that are due to the current ramp-up. During stimulation, the participants completed a 30-min laboratory vigilance task (Mackworth, 1948).

MRI Acquisition

MRI data were acquired at each session prior to and ∼30 min following the application of tDCS on a 3 Tesla (T) MRI (Discovery 750 W, GE Healthcare, Madison, WI) equipped with a 24-channel head coil. The MRI acquisition consisted of the following sequences: a 12-min resting-state functional MRI (fMRI) (Kim et al., 2021), three 10-min task fMRIs (Sherwood et al., 2018), T1-weighted MRI (6.5 min for session 1 pre-stimulation, 3.5 min for the remaining sessions), diffusion tensor imaging (DTI; 5 min), single-voxel magnetic resonance spectroscopy (MRS; 6 min), and resting ASL (5 min). As this work is part of a much larger study, we will only be presenting the resting ASL data herein.

Images of CBF were acquired ∼20 min prior to the application of tDCS and ∼1.5 h after the conclusion of stimulation using a pseudo-continuous arterial spin labeling (pcASL) technique (Silva and Kim, 1999). This sequence administers inversion (tagging) pulses immediately inferior to the imaging volume. All images were acquired with a true axial orientation (i.e., perpendicular to the scanner bore) using a post-label delay time (PLD) of 2,025 ms. Five background suppression pulses were applied to reduce the signal of stationary tissues (Dixon et al., 1991; Mani et al., 1997; Ye et al., 2000) and improve the signal-to-noise ratio (SNR) of arterial blood. A 3D fast spin echo (3D FSE) sequence was used for the acquisition of the imaging volume. To reduce motion sensitivity, to improve acquisition time, and to minimize susceptibility artifacts, a stack-of-spiral readout gradient starting at the center of k-space was used (Glover, 2012). A total of eight spiral arms were used for the k-space sampling. Echoes were re-binned to the Cartesian space in a 128 × 128 matrix, with TR = 4,640 ms, TE = 10.7 ms, voxel size = 1.875 × 1.875 mm^2, slice thickness = 4 mm, and flip angle = 111°. The sequence acquired a total of 3 tag/control pairs. The total acquisition time was 4 min 46 s. During the scan, the participants were instructed to remain awake and focus on a fixation dot presented on the display. This condition has demonstrated a significantly

greater reliability in the resting-state functional MRI across all within-network connections, as well as within default-mode, attention, and auditory networks when compared to eyes open (no specified fixation) and closed methods (Patriat et al., 2013).

Structural (T1-weighted) images were acquired using a 3D brain volume imaging (BRAVO) pulse sequence, which uses an inversion recovery prepared fast spoiled gradient-echo (FSPGR). The structural images were acquired using a 256 × 256 element matrix, 172 slices oriented to the anterior commissure (AC)–posterior commissure (PC) plane, 1 mm^3 isotropic voxels, 0.8 phase field of view factor, an inversion time (TI) of 450 ms, a TE of 3.224 ms, a flip angle of 13°, and an autocalibrated reconstruction for Cartesian sampling with a phase acceleration factor of 1.0 for the session 1 pre-stimulation session and 2.0 for all the remaining sessions. The longer scan (lower acceleration factor) was used to acquire one higher quality image for other portions of the project. The acceleration factor was increased for the remaining sessions to produce images that are of high enough quality for registration purposes but also to reduce the scan time as much as possible.

Data Processing and Analysis

Cerebral blood flow maps (see **Supplementary Figure 1**) were computed and quantified from the automated functions in the GE reconstruction software. First, the three tagged and three control volumes were averaged in place (without motion correction). Then, difference images were calculated for all participants by subtracting the average tagged volume from the average control volume. Finally, quantitative CBF maps (see **Supplementary Figure 1** for example of raw CBF maps) were generated from the difference images, the associated proton density (PD)-weighted volumes, and the standard single-compartment model (Alsop and Detre, 1996; Mutsaerts et al., 2014; Alsop et al., 2015) using the formula:

$$CBF = 6000 * \lambda \frac{\left(1-e^{-\frac{ST(s)}{T_{1t}(s)}}\right) e^{\frac{PLD(s)}{T_{1b}(s)}}}{2T_{1b}\,(s)\left(1-e^{-\frac{LT(s)}{T_{1b}(s)}}\right)\varepsilon * NEX_{PW}} \left(\frac{PW}{SF_{PW}PD}\right)$$

where CBF is calculated in ml/100g/min. In this equation, T_{1b} is the T1 of blood and is assumed to be 1.6 s at 3 T. The partial saturation of the reference image (PD) is corrected using a T_{1t} of 1.2 s (typical of gray matter). The saturation time, *ST*, is set to 2 s, and the partition coefficient λ is set to a whole brain average of 0.9. The efficiency, ε, is the overall efficiency (0.6), a combination of both inversion efficiency (0.8) and background suppression efficiency (0.75). The PLD used for the ASL protocol was 2,025 ms, and the labeling duration, *LT*, was set to 1.5 s in the current version. *PW* is the perfusion weighted or the raw difference, and SF_{PW} is the scaling factor of the PW sequence. The number of excitations for PW images, NEX_{PW}, was set to 3.

The CBF maps from each session were exported from the MRI scanner and processed using the FMRIB Software Library (FSL; Smith et al., 2004; Woolrich et al., 2009) on a 128-core Rocks Cluster Distribution (www.rocksclusters.org) high-performance computing system capable of running 256 threads in parallel. Then, the high-resolution structural image of an individual was registered to the MNI-152 T1-weighted 2 mm template provided in FSL (Collins et al., 1995; Mazziotta et al., 2001) using a 12-parameter model (Jenkinson and Smith, 2001; Jenkinson et al., 2002; see **Supplementary Figure 2A**). Next, the raw PW images were registered to the high-resolution structural image by estimating the motion from a boundary-based registration method, which includes a field-map-based distortion correction (Greve and Fischl, 2009) (see **Supplementary Figure 2B**). In order to co-register all volumes, the CBF maps were converted to the standard space using the transforms responsible for morphing the PD-weighted image of each data set to the structural image and the structural image to the template (see **Supplementary Figure 2C**).

Voxelwise non-parametric analyses were performed using the conditional Monte Carlo permutation testing based on the method of Freeman and Lane (1983) implemented in randomise of FSL (Anderson and Robinson, 2001; Winkler et al., 2014). Due to the mixed effect of our design and how the data would need to be permuted, we were not able to perform proper between-group repeated measures ANOVAs. However, we implemented the following steps to evaluate run x group interaction effects. First, we subtracted each post-stimulation CBF map (in the standard space) from the corresponding baseline (session 1 pre-stimulation). Next, unpaired *t*-tests were performed to evaluate the between-group differences in the change from baseline per post-stimulation measurement (sessions 1–3 post-stimulation). These tests were conducted to compare ACT_{1mA} and ACT_{2mA} groups with the CON group separately. This resulted in a total of six analyses, analogous to the *post-hoc* pairwise testing that would be conducted to interpret a significant interaction effect. Null *t* distributions for the contrast representative of the between-group difference were derived by performing 2,000,000 random permutations of the data. Each permutation was created by exchanging the assigned group (Nichols and Holmes, 2003). A final *t* statistic was computed for each voxel by testing the unshuffled, real arrangement against the permutation distribution.

Additionally, voxelwise non-parametric, within-group one-way ANOVAs were performed on the session 1 pre-stimulation, session 1 post-stimulation, session 2 post-stimulation, and session 3 post-stimulation co-registered resting CBF maps. This analysis was also conducted using randomise of FSL. Null distributions for contrasts representative of the main effect of session (sessions 1–3 post-stimulation subtracted from the baseline) were derived by performing 2,000,000 random permutations of the data. Each permutation was created by exchanging the assigned session while maintaining subject membership. Then, an *F* test compared the means from each session (sessions 1–3 post-stimulation subtracted from the baseline). Pairwise comparisons were executed during the completion of the one-way ANOVAs. The results of the pairwise comparisons were further corrected for multiple comparisons to account for false positives due to the multiple comparisons (Worsley, 2001). This method considered adjacent voxels with a

TABLE 2 | Results of the one-way ANOVAs comparing the initiation time of each scan between groups.

		p-value
Session 1	Pre-stimulation	0.158
	Post-stimulation	0.258
Session 2	Pre-stimulation	0.172
	Post-stimulation	0.231
Session 3	Pre-stimulation	0.132
	Post-stimulation	0.099

Family-wise error correction was not applied to be more sensitive toward differences in groups.

t statistic of 2.3 or greater to be a cluster. The significance of each cluster was estimated and compared to a threshold of $p < 0.05$ using the Gaussian random field theory-based maximum height thresholding and a one-tailed *t*-test. The significance of voxels that either did not pass the significance level threshold or do not belong to a cluster was set to zero.

RESULTS

Scanning Time

Concerns regarding the potential bias in the data due to the within-subject variability in scanning start time arose during the analysis (see **Supplementary Table 2** for a complete list of the scan initiation times). To address this concern and the potential impact of the session time on any one group in particular, we evaluated the scan initiation times between groups by the session and scan. First, we extracted the scan initiation times from the log files. Next, we performed between-group one-way ANOVAs separately for the pre- and post-stimulation scan initiation times for each session. We did not correct for the family-wise error to be more sensitive to timing differences between groups. Our analyses did not find any significant variability ($p > 0.05$; **Table 2**) between groups for the scan start time for any of the scan sessions (**Figure 2**). There was also concern raised regarding the variable durations between the stimulation and the post-stimulation ASL that may disproportionally affect the results. Unfortunately, the stimulation time was not recorded in reference to the scan time. Therefore, we used the end time for the pre-stimulation task scan as the best approximation since the setup time for tDCS and post-task scanning was fairly consistent and much less variable than the total scan times. The duration between the pre-stimulation task end time and the post-stimulation scan start time was computed, and one-way ANOVAs were conducted to compare the groups across each session. Again, we did not correct for a family-wise error. The results did not reveal any significant variability ($p > 0.05$) in duration between the pre- and post-stimulation scans (**Figure 3**).

Changes in CBF

Interaction effects between the run and stimulation were assessed *via* the unpaired *t*-tests following a subtraction of the post-stimulation measurement from the pre-stimulation measurement from session 1 (i.e., baseline). The comparison of resting CBF from baseline and post-stimulation between CON and ACT_{1mA} groups resulted in significant variations across the three sessions (**Figure 4**). A similar trend was observed between CON and ACT_{2mA} (**Figure 5**). Frontal areas in these analyses appeared with an increasing statistical significance and extent, with stronger effects observed in the comparison between CON and ACT_{2mA}. These consisted of the bilateral superior frontal gyrus (SFG) and the right middle frontal and inferior frontal gyri (MFG and IFG, respectively). Posterior regions such as the right superior parietal lobule, the inferior parietal lobule, the middle temporal gyrus, and the precuneus demonstrated a trend with a decreasing statistical significance and extent.

These results are difficult to interpret alone and could represent either a greater decrease from baseline or a smaller

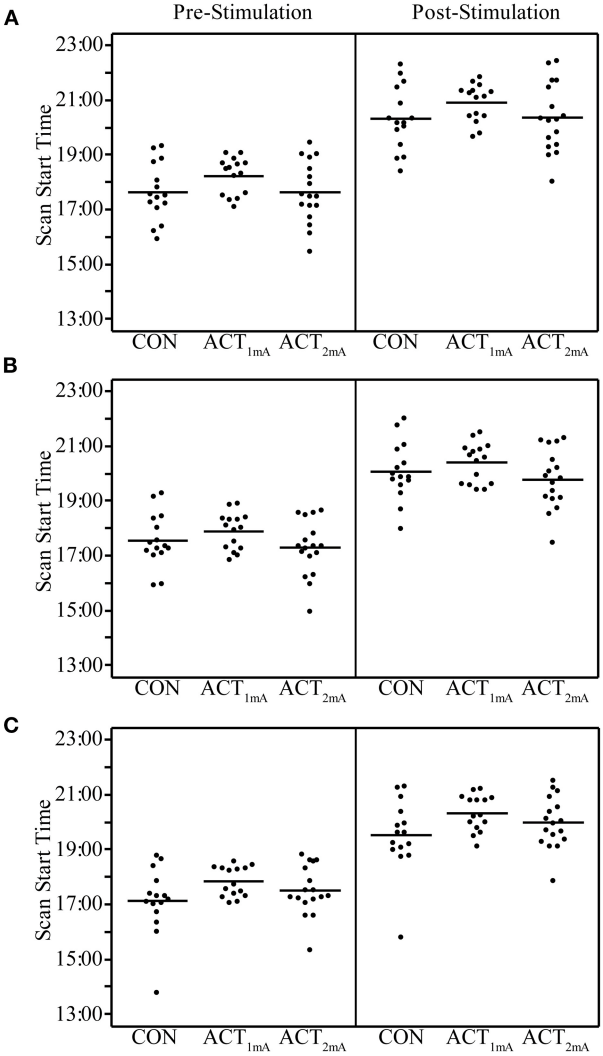

FIGURE 2 | Pre- and post-stimulation scan start times for session 1 **(A)**, session 2 **(B)**, and session 3 **(C)** separated by group. Group averages are indicated by the bar.

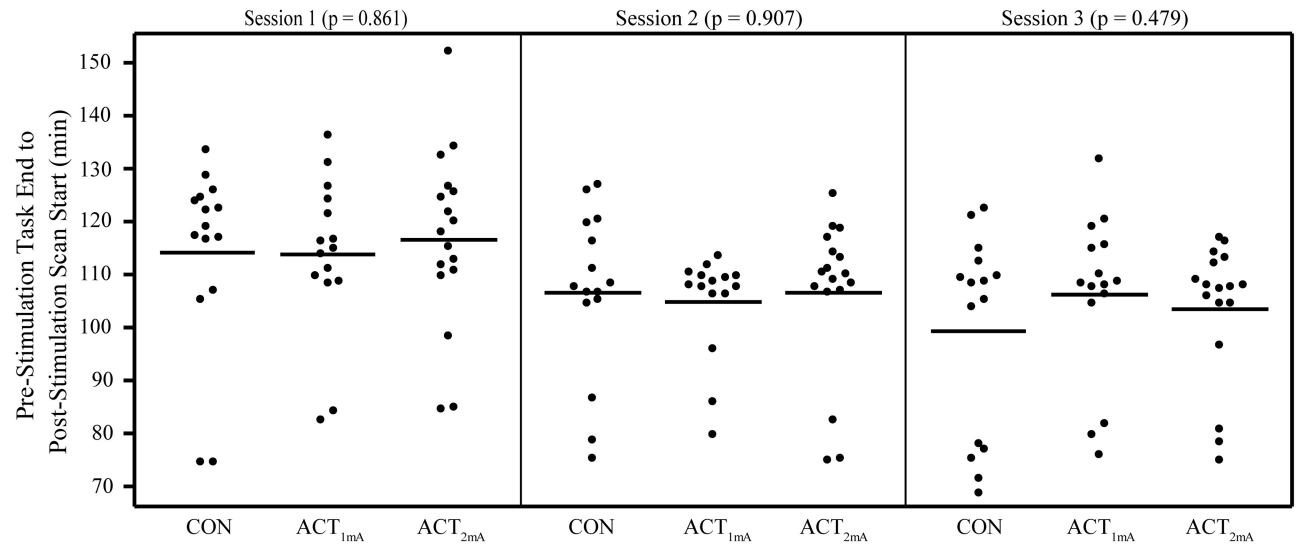

FIGURE 3 | Duration from pre-stimulation task end time to post-stimulation scan start time separated by groups and sessions. No significant differences were revealed in one-way ANOVAs comparing groups per session.

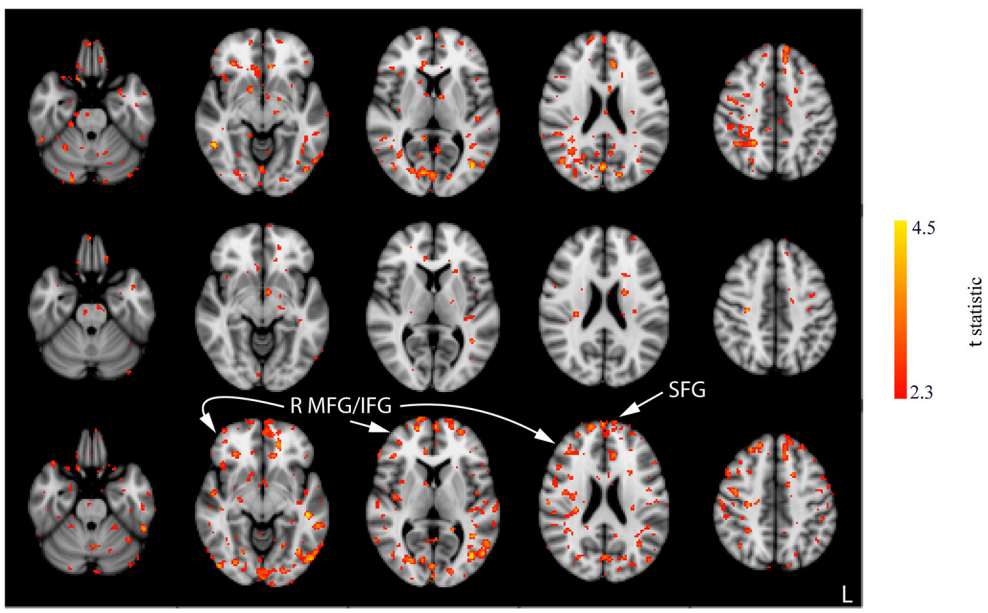

FIGURE 4 | Results of the unpaired *t*-tests between CON and ACT_{1mA} for the change between session 1 pre-stimulation and session 1 post-stimulation (top row), session 2 post-stimulation (middle row), and session 3 post-stimulation (bottom row). Axial slices are taken from MNI coordinates z = −26, −8, 6, 22, and 44 mm (left to right).

increase from baseline between the CON group and the active group. Therefore, the within-group analyses were conducted to provide a clearer understanding of these effects. For the CON and ACT_{1mA} groups, repeated-measure one-way ANOVAs revealed significant differences in CBF across four different measurements (baseline and sessions 1–3 post-stimulation; see **Figure 6**). Regions identified in these analyses include the LC, superior temporal gyrus (STG), inferior temporal gyrus (ITG), supramarginal gyrus (SMG), and SFG. There were no significant findings for the main effect of the session in the ACT_{2mA} group. However, pairwise comparisons were further conducted to evaluate CBF each post-stimulation measure in comparison to the baseline for each group. The results summarized from these analyses identifying a decreased CBF from baseline are shown in **Table 3** and the increased CBF from baseline are shown in **Table 4**.

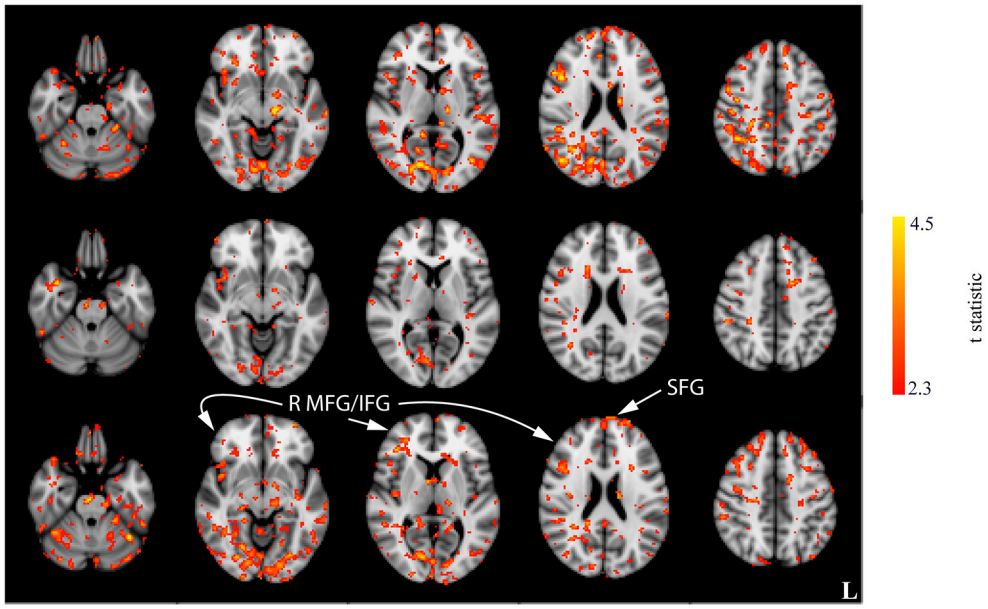

FIGURE 5 | Results of the unpaired *t*-tests between CON and ACT_{2mA} for the change between session 1 pre-stimulation and session 1 post-stimulation (top row), session 2 post-stimulation (middle row), and session 3 post-stimulation (bottom row). Axial slices are taken from MNI coordinates z = −26, −8, 6, 22, and 44 mm (left to right).

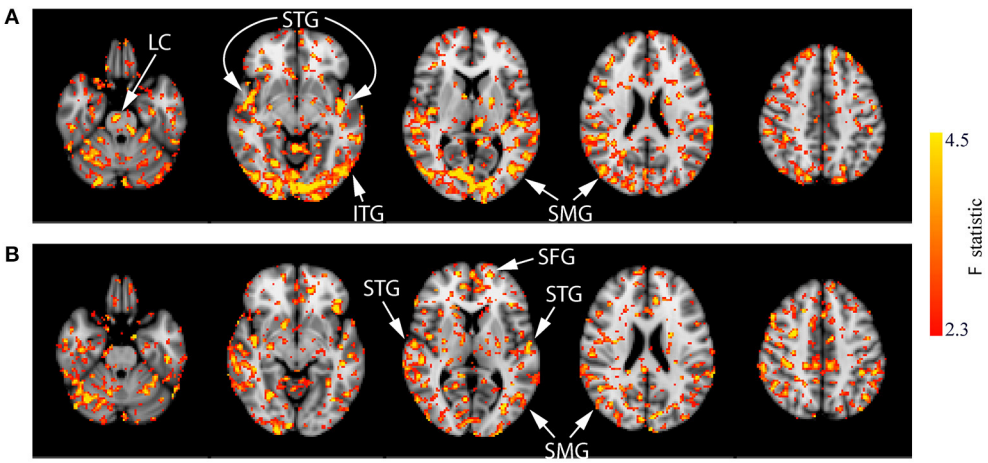

FIGURE 6 | Results of the one-way ANOVA demonstrating the main effect of session for the CON **(A)** and ACT_{1mA} **(B)** groups. Axial slices are taken from MNI coordinates z = −26, −8, 6, 22, and 44 mm (left to right).

Compared to the baseline, decreases in CBF were observed in all three post-stimulation sessions for the CON group (**Figure 7**; **Supplementary Figure 3**). The amount CBF was lowered in comparison to that of session 1 pre-stimulation increased in statistical reliability, extent, and magnitude by session 3 post-stimulation. Of note, decreased CBF was observed consistently in the bilateral STG and pre-central gyrus. Decreases in CBF in the ITG and SMG were observed in the post-stimulation measures for sessions 1 and 3. Additionally, decreased CBF in the LC was observed in the post-stimulation measures for sessions 2 and 3.

Few significant findings were present in the ACT_{1mA} group at session 1 post-stimulation but widespread decreases in CBF were observed at session 2 post-stimulation (**Figure 8**, top and middle rows; **Supplementary Figure 4**). These decreases share similarities with that observed in post-stimulation measures from sessions 1 and 3 in the sham group including the SMG and ITG. A decreased CBF diminished by session 3 with only a few small clusters remaining (**Figure 8**, bottom row). The diminished CBF at session 3 was accompanied by an increased CBF appearing bilaterally in the SFG and the anterior cingulate cortex (ACC).

TABLE 3 | Summarized findings highlighting regions with significantly decreased CBF resulting from the pairwise comparisons of each post-stimulation measurement with baseline.

	Session 1 post-stimulation	**Session 2 post-stimulation**	**Session 3 post-stimulation**
Sham	Several clusters including ITG, SMG, and pre-central gyrus	Several clusters including STG and LC	Widespread including ITG, SMG, LC, STG, and pre-central gyrus
ACT_{1mA}	Few small clusters	Widespread including STG, ITG, and SMG	Few small clusters
ACT_{2mA}	n.s.	Clusters in the pre-central gyrus and STG	Very few, small clusters

No significant findings are reported as n.s.

TABLE 4 | Summarized findings highlighting regions with significantly increased CBF resulting from the pairwise comparisons of each post-stimulation measurement with baseline.

	Baseline minus session 1 post-stimulation	**Baseline minus session 2 post-stimulation**	**Baseline minus session 3 post-stimulation**
Sham	Very few, small clusters	Very few, small clusters	Very few, small clusters
ACT_{1mA}	Few small clusters	Very few, small clusters	Few clusters including the ACC and SFG
ACT_{2mA}	n.s.	Few small clusters	Several clusters including the LC, IFG, insula, SFG, thalamus, hippocampus, and fusiform gyrus

No significant findings are reported as n.s.

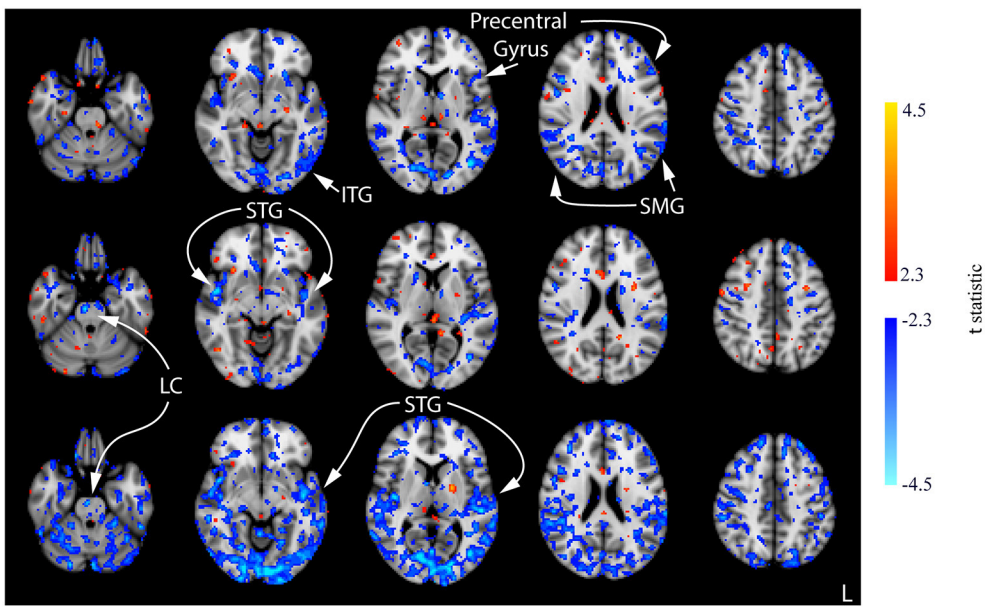

FIGURE 7 | Results of the one-way ANOVA for the CON group displayed through *post-hoc*, pairwise comparisons between session 1 pre-stimulation and session 1 post-stimulation (top row), session 2 post-stimulation (middle row), and session 3 post-stimulation (bottom row). Corresponding images demonstrating the magnitude of CBF changes are given in **Supplementary Figure 3**. Axial slices are taken from MNI coordinates z = −26, −8, 6, 22, and 44 mm (left to right).

In contrast with the CON and ACT_{1mA} groups, no significant changes in CBF were observed between baseline and the session 1 post-stimulation measurement for the ACT_{2mA} group. Less defined changes in CBF were observed in the session 2 post-stimulation scan (**Figure 9**, top row; **Supplementary Figure 5**). The largest clusters of decreased CBF were observed in the left STG and the left pre-central gyrus; these areas were also observed to have a decreased CBF in the CON group across all three comparisons. For the ACT_{2mA} group, more defined increases were observed by the third post-stimulation session (**Figure 9**, bottom row). Clusters were observed in the LC, the left hippocampus, the bilateral fusiform gyrus, the left thalamus, the right insula, the right IFG, and the left SFG.

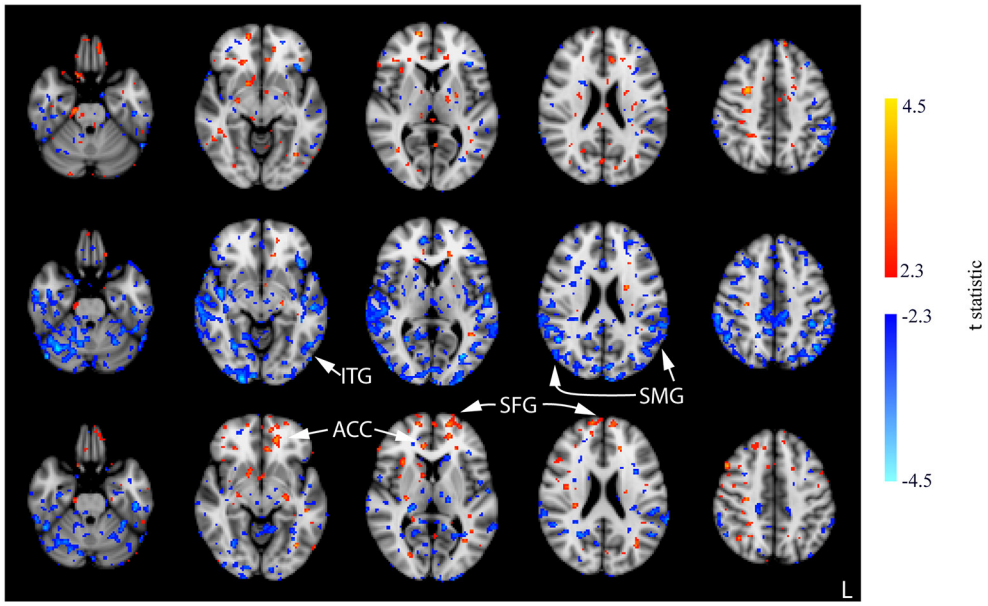

FIGURE 8 | Results of the one-way ANOVA for the ACT_{1mA} group displayed through *post-hoc*, pairwise comparisons between session 1 pre-stimulation and session 1 post-stimulation (top row), session 2 post-stimulation (middle row), and session 3 post-stimulation (bottom row). Corresponding images demonstrating the magnitude of CBF changes are given in **Supplementary Figure 4**. Axial slices are taken from MNI coordinates z = −26, −8, 6, 22, and 44 mm (left to right).

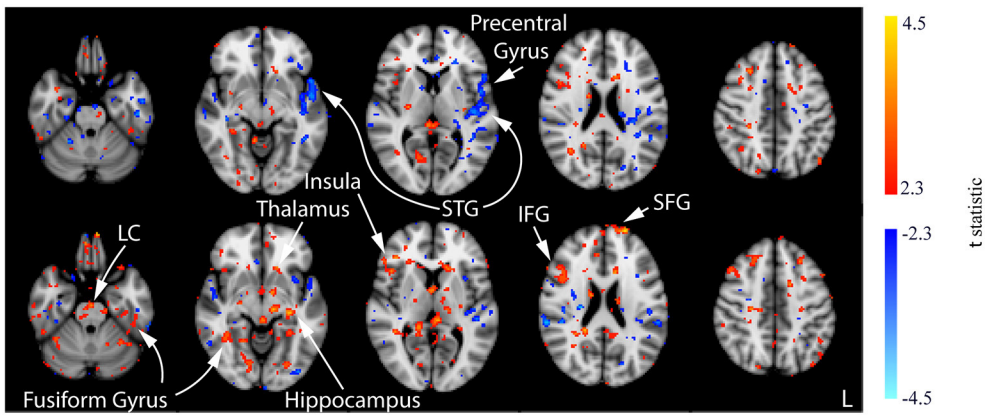

FIGURE 9 | Results of the one-way ANOVA for the ACT_{2mA} group displayed through *post-hoc*, pairwise comparisons between session 1 pre-stimulation and session 2 post-stimulation (top row) and session 3 post-stimulation (bottom row). Corresponding images demonstrating the magnitude of CBF changes are given in **Supplementary Figure 5**. Axial slices are taken from MNI coordinates z = −26, −8, 6, 22, and 44 mm (left to right).

DISCUSSION

This study examined the effect of tDCS on the resting CBF, quantified using 3D pcASL, at different stimulation intensity levels across three consecutive days. There was significant variability in the resting CBF from baseline (session 1 pre-stimulation) and post-stimulation measures between our sham group and both experimental groups receiving 1- or 2-mA anodal tDCS applied to the prefrontal cortex (**Figures 4**, **5**). In the sham group, significant, widespread decreases in CBF were revealed between the baseline scan (session 1 pre-stimulation) and all three post-stimulation scans. The magnitude, extent, and significance of these decreases rose across the sessions (**Figure 6**). One postulation for this observation is the cognitive demands of our experimental protocol. Decreased CBF has been associated with a sustained mental workload and an increased time on the task (Paus et al., 1997; Coull and Nobre, 1998; Lim et al., 2010). The time-on-task effect on behavioral performance, an effect of the sustained mental workload, is theorized to arise from the consumption of resources that cannot be immediately replenished and not likely an effect of boredom. Evidence supporting this theory has been observed in PET studies,

which have identified a decreased regional CBF as time-on-task increased (Paus et al., 1997; Coull and Nobre, 1998). Further support has been found using ASL, where better performance was associated with smaller decreases in CBF from pre- to post-task imaging (Lim et al., 2010).

It is also possible for the demands of home life, work, and completing the experimental protocol resulted in inadvertent effects on sleep, such as mild reductions in sleep time or quality. While this was not directly measured, either *via* actigraphs or sleep questionnaires, it could help explain our observations. Overt sleep restriction has also been associated with altered neural patterns. Poudel et al. (2012) observed a decreased CBF measured from ASL following acute sleep loss (4 h of restricted sleep) in comparison to the "rested" scans in the same subjects. Shenfield et al. (2020) discovered that changes in the alpha and delta power in electroencephalography (EEG) were related to the subjective sleepiness and performance on the psychomotor vigilance task. EEG signals are summed excitatory and inhibitory postsynaptic potentials, which require metabolic energy and have been found to be positively correlated with the cerebral oxygen uptake and blood flow (Ingvar et al., 1976; Kuschinsky, 1993), suggesting that lower CBF would accompany the decreased EEG power. Decreased delta power has been observed during non-REM sleep in groups restricted to 4 h and 6 h of sleep over 14 continuous days, with effects equivalent to 48 h of sleep deprivation (Van Dongen et al., 2003).

On the contrary to the sham group, the decreased CBF for our group receiving a 2-mA prefrontal tDCS was mostly absent across the post-stimulation comparisons with baseline over the three sessions. Decreased CBF was minimal in the 2-mA group but was observed in its largest magnitude, significance, and extent in the session 2 post-stimulation scan, mainly localized to the left STG and the pre-central gyrus. Recent evidence from our group has shown that sleep time on the night following a 2-mA anodal prefrontal stimulation was decreased compared with that of the sham and stimulation over the primary motor cortex without any significant effects on subjective measures of mood or sleep quality (McIntire et al., 2020). This suggests that the anodal prefrontal stimulation may provide more efficient sleep leading to a lower impact of the potential effects from sleep restriction, which would be present in the form of a decreased CBF. Alternatively, an increased CBF was revealed in post-stimulation measures from sessions 2 and 3, increasing in significance, extent, and magnitude from session 2 to 3. This observation may be explained by an increased CBF in the LC in our ACT_{2mA} group (see **Figure 9**) compared with the decreased CBF in the CON group (see **Figure 7**). LC cells of the pons are responsible for triggering the production of norepinephrine and are projected *via* the bilateral ascending pathways to target numerous subcortical and cortical regions (Jenkins et al., 2016). This noradrenergic system allows the LC to modulate multiple distant brain regions simultaneously and can exert its effect by binding to receptors on both pre- and postsynaptic cells (Arnsten, 2000). The lack of decreased CBF, which appeared in the sham group potentially due to time-on-task and/or sleep restriction effects, may be a direct result of stimulation or an effect produced by higher arousal states from an increase in the noradrenergic system. However, the altered noradrenergic system between sham and 2-mA anodal prefrontal tDCS may explain the various behavioral findings from our group (Nelson et al., 2014, 2015, 2016, 2019; McIntire et al., 2017b, 2019; McKinley et al., 2017a).

Results from our 1-mA stimulation group were intriguing. Decreases in CBF were observed at sessions 1 and 2 post-stimulation when compared to baseline, a trend similar to sham and dissimilar to the 2-mA group. These decreases were most prominent by session 2 post-stimulation. However, the magnitude, extent, and statistical significance of these prominent session 2 decreases were lowered at the end of session 3, and a higher CBF was observed in some areas common with the 2-mA stimulation group including the SFG (see **Figures 8**, **9**). This shift in polarity, from decreasing CBF to increasing CBF between sessions 2 and 3, suggests that there may be cumulative effects from tDCS when applied within 24 h. tDCS is believed to modulate the excitability of neural populations by depolarizing neurons below the cathode, increasing the resting membrane potential and neuronal excitability (Nitsche et al., 2008; Nitsche and Paulus, 2011; Brunoni et al., 2012; McKinley et al., 2012; Romero Lauro et al., 2014; Adachi et al., 2015); however, it is currently not known how long these neural changes may persist. Our findings suggest that neural effects of stimulation may persist for at least 24 h allowing consecutive stimulation protocols to compound. This finding adds to previous behavioral findings, which indicated improved arousal appearing for up to 24 h post-stimulation (McIntire et al., 2017a) and improved behavior for at least 6 h post-stimulation (McIntire et al., 2014). More recent evidence suggests that repetitive stimulation may not produce additive benefits (McIntire et al., 2020); however, our findings indicate that stimulation may produce neural effects lasting at least 24 h, and these effects may compound with repeated stimulation.

In conclusion, we observed that the resting CBF decreased from baseline in all three post-stimulation measures from our sham group. In the group receiving 2-mA anodal prefrontal tDCS, little to no decreases in CBF were observed but increases were observed in the post-stimulation measures from sessions 2 and 3. These increases were localized to a few areas. Notably, the LC had a significant increased resting CBF at session 3 post-stimulation compared to baseline, which could indicate increased norepinephrine production and enhanced activity of the noradrenergic system. If found to be true, this could help explain the broad range of behavioral changes observed following anodal prefrontal tDCS. Our group receiving 1-mA tDCS appeared similar to the sham group through session 2 post-stimulation, with observations of decreased resting CBF with little to no increases. By session 3, however, decreases in CBF were minimal and increased resting CBF trends were observed, indicating the potential for the neural effects of tDCS to persist for up to 24 h following stimulation.

DATA AVAILABILITY STATEMENT

The datasets presented in this article are not readily available because it has not been approved for public release and,

therefore, may not be available upon request. The decision to release the data cannot be made by the authors. Requests to access the datasets should be directed to Matthew S. Sherwood, matt.sherwood@us.kbr.com.

ETHICS STATEMENT

The studies involving human participants were reviewed and approved by Air Force Research Laboratory Institutional Review Board, Air Force Research Laboratory, Wright-Patterson Air Force Base. The patients/participants provided their written informed consent to participate in this study.

AUTHOR CONTRIBUTIONS

MS, LM, and RM contributed to the design and provided the conception of and overall guidance to the project. MS, LM, and AM contributed to the data collection. MS and AM contributed to the data analysis. MS, LM, AM, KK, CR, and RM contributed to the interpretation of the data. MS contributed to the initial drafting of the manuscript and produced the final artwork. All authors contributed to the writing, revising, approving of the manuscript, and are equally accountable for all aspects of the work.

FUNDING

This study was supported by the Air Force Research Laboratory (AFRL) under the Human Interface and Research Technology program (contract FA8650-14-D-6500).

ACKNOWLEDGMENTS

The authors thank Casserly R. Mullenger for her assistance in data collection. The authors also thank Charles Goodyear for his assistance in analyzing the scan time data. The authors also extend their final gratitude to Dayton Children's Hospital who graciously allowed them to use their facility to perform this research. This study would not have been completed without these people and resources.

SUPPLEMENTARY MATERIAL

The Supplementary Material for this article can be found online at: https://www.frontiersin.org/articles/10.3389/fnhum.2021.679977/full#supplementary-material

REFERENCES

Adachi, L. N. S., Quevedo, A. S., de Souza, A., Scarabelot, V. L., Rozisky, J. R., de Oliveira, C., et al. (2015). Exogenously induced brain activation regulates neuronal activity by top-down modulation: conceptualized model for electrical brain stimulation. *Exp. brain Res.* 233, 1377–1389. doi: 10.1007/s00221-015-4212-1

Alsop, D. C., and Detre, J. A. (1996). Reduced transit-time sensitivity in noninvasive magnetic resonance imaging of human cerebral blood flow. *J. Cereb. Blood Flow Metab.* 16, 1236–1249. doi: 10.1097/00004647-199611000-00019

Alsop, D. C., Detre, J. A., Golay, X., Günther, M., Hendrikse, J., Hernandez-Garcia, L., et al. (2015). Recommended implementation of arterial spin-labeled perfusion MRI for clinical applications: a consensus of the ISMRM perfusion study group and the European consortium for ASL in dementia. *Magn. Reson. Med.* 73, 102–116. doi: 10.1002/mrm.25197

Anderson, M. J., and Robinson, J. (2001). Permutation tests for linear models. *Aust. N. Z. J. Stat.* 43, 75–88. doi: 10.1111/1467-842X.00156

Arnsten, A. F. (2000). Through the looking glass: differential noradrenergic modulation of prefrontal cortical function. *Neural Plast.* 7, 133–146. doi: 10.1155/NP.2000.133

Bindman, L. J., Lippold, O. C. J., and Redfearn, J. W. T. (1962). Long-lasting changes in the level of the electrical activity of the cerebral cortex produced by polarizing currents. *Nature* 196, 584–585. doi: 10.1038/196584a0

Borogovac, A., and Asllani, I. (2012). Arterial spin labeling (ASL) fMRI: advantages, theoretical constrains and experimental challenges in neurosciences. *Int. J. Biomed. Imaging* 2012, 1–13. doi: 10.1155/2012/658101

Brunoni, A. R., Nitsche, M. A., Bolognini, N., Bikson, M., Wagner, T., Merabet, L., et al. (2012). Clinical research with transcranial direct current stimulation (tDCS): challenges and future directions. *Brain Stimul.* 5, 175–195. doi: 10.1016/j.brs.2011.03.002

Bullard, L. M., Browning, E. S., Clark, V. P., Coffman, B. A., Garcia, C. M., Jung, R. E., et al. (2011). Transcranial direct current stimulation's effect on novice versus experienced learning. *Exp. Brain Res.* 213, 9–14. doi: 10.1007/s00221-011-2764-2

Clark, V. P., Coffman, B. A., Mayer, A. R., Weisend, M. P., Lane, T. D. R., Calhoun, V. D., et al. (2012). TDCS guided using fMRI significantly accelerates learning to identify concealed objects. *Neuroergonom. Hum. Brain Act. Work* 59, 117–128. doi: 10.1016/j.neuroimage.2010.11.036

Clark, V. P., Coffman, B. A., Trumbo, M. C., and Gasparovic, C. (2011). Transcranial direct current stimulation (tDCS) produces localized and specific alterations in neurochemistry: a 1H magnetic resonance spectroscopy study. *Neurosci. Lett.* 500, 67–71. doi: 10.1016/j.neulet.2011.05.244

Coffman, B. A., Trumbo, M. C., Flores, R. A., Garcia, C. M., van der Merwe, A. J., Wassermann, E. M., et al. (2012). Impact of tDCS on performance and learning of target detection: interaction with stimulus characteristics and experimental design. *Neuropsychologia* 50, 1594–1602. doi: 10.1016/j.neuropsychologia.2012.03.012

Collins, D. L., Holmes, C. J., Peters, T. M., and Evans, A. C. (1995). Automatic 3-D model-based neuroanatomical segmentation. *Hum. Brain Mapp.* 3, 190–208. doi: 10.1002/hbm.460030304

Coull, J. T., and Nobre, A. C. (1998). Where and when to pay attention: the neural systems for directing attention to spatial locations and to time intervals as revealed by both PET and fMRI. *J. Neurosci.* 18, 7426–7435. doi: 10.1523/JNEUROSCI.18-18-07426.1998

Dixon, W. T., Sardashti, M., Castillo, M., and Stomp, G. P. (1991). Multiple inversion recovery reduces static tissue signal in angiograms. *Magn. Reson. Med.* 18, 257–268. doi: 10.1002/mrm.1910180202

Du, A. T., Jahng, G. H., Hayasaka, S., Kramer, J. H., Rosen, H. J., Gorno-Tempini, M. L., et al. (2006). Hypoperfusion in frontotemporal dementia and Alzheimer disease by arterial spin labeling MRI. *Neurology* 67, 1215–1220. doi: 10.1212/01.wnl.0000238163.71349.78

Freeman, D., and Lane, D. (1983). A nonstochastic interpretation of reported significance level. *J. Bus. Econ. Stat.* 1, 292–298. doi: 10.1080/07350015.1983.10509354

Fregni, F., Nitsche, M. A., Loo, C. K., Brunoni, A. R., Marangolo, P., Leite, J., et al. (2015). Regulatory considerations for the clinical and research use of transcranial direct current stimulation (tDCS): review and recommendations from an expert panel. *Clin. Res. Regul. Aff.* 32, 22–35. doi: 10.3109/10601333.2015.980944

Glover, G. H. (2012). Spiral imaging in fMRI. *Neuroimage* 62, 706–712. doi: 10.1016/j.neuroimage.2011.10.039

Grade, M., Hernandez Tamames, J. A., Pizzini, F. B., Achten, E., Golay, X., and Smits, M. (2015). A neuroradiologist's guide to arterial spin labeling MRI in clinical practice. *Neuroradiology* 57, 1181–1202. doi: 10.1007/s00234-015-1571-z

Greve, D. N., and Fischl, B. (2009). Accurate and robust brain image alignment using boundary-based registration. *Neuroimage* 48, 63–72. doi: 10.1016/j.neuroimage.2009.06.060

Gsell, W., De Sadeleer, C., Marchalant, Y., MacKenzie, E. T., Schumann, P., and Dauphin, F. (2000). The use of cerebral blood flow as an index of neuronal activity in functional neuroimaging: experimental and pathophysiological considerations. *J. Chem. Neuroanat.* 20, 215–224. doi: 10.1016/S0891-0618(00)00095-8

Hunter, M., Coffman, B., Trumbo, M., and Clark, V. (2013). Tracking the neuroplastic changes associated with transcranial direct current stimulation: a push for multimodal imaging. *Front. Hum. Neurosci.* 7:495. doi: 10.3389/fnhum.2013.00495

Ingvar, D. H., Sjölund, B., and Ard,ö, A. (1976). Correlation between dominant EEG frequency, cerebral oxygen uptake and blood flow. *Electroencephalogr. Clin. Neurophysiol.* 41, 268–276. doi: 10.1016/0013-4694(76)90119-X

Jenkins, P. O., Mehta, M. A., and Sharp, D. J. (2016). Catecholamines and cognition after traumatic brain injury. *Brain* 139, 2345–2371. doi: 10.1093/brain/aww128

Jenkinson, M., Bannister, P., Brady, M., and Smith, S. (2002). Improved Optimization for the robust and accurate linear registration and motion correction of brain images. *Neuroimage* 17, 825–841. doi: 10.1006/nimg.2002.1132

Jenkinson, M., and Smith, S. (2001). A global optimisation method for robust affine registration of brain images. *Med. Image Anal.* 5, 143–156. doi: 10.1016/S1361-8415(01)00036-6

Kim, K., Sherwood, M. S., McIntire, L. K., McKinley, R. A., and Ranganath, C. (2021). Transcranial direct current stimulation modulates connectivity of left dorsolateral prefrontal cortex with distributed cortical networks. *J. Cogn. Neurosci.* 33, 1381–1395. doi: 10.1162/jocn_a_01725

Kuschinsky, W. (1993). "Is the EEG correlated with the brain metabolism and cerebral blood flow?," in *BT - Basic Mechanisms of the EEG*, eds. S. Zschocke and E.-J. Speckmann (Boston, MA: Birkhäuser Boston), 109–119.

Liebetanz, D. (2002). Pharmacological approach to the mechanisms of transcranial DC-stimulation-induced after-effects of human motor cortex excitability. *Brain* 125, 2238–2247. doi: 10.1093/brain/awf238

Lim, J., Wu, W., chau, Wang, J., Detre, J. A., Dinges, D. F., and Rao, H. (2010). Imaging brain fatigue from sustained mental workload: an ASL perfusion study of the time-on-task effect. *Neuroimage* 49, 3426–3435. doi: 10.1016/j.neuroimage.2009.11.020

Mackworth, N. H. (1948). The breakdown of vigilance during prolonged visual search. *Q. J. Exp. Psychol.* 1, 6–21. doi: 10.1080/17470214808416738

Mani, S., Pauly, J., Conolly, S., Meyer, C., and Nishimura, D. (1997). Background suppression with multiple inversion recovery nulling: applications to projective angiography. *Magn. Reson. Med.* 37, 898–905. doi: 10.1002/mrm.1910370615

Mazziotta, J., Toga, A., Evans, A., Fox, P., Lancaster, J., Zilles, K., et al. (2001). A probabilistic atlas and reference system for the human brain: International Consortium for Brain Mapping (ICBM). *Philos. Trans. R. Soc. Lond. Series B Biol. Sci.* 356, 1293–1322. doi: 10.1098/rstb.2001.0915

McIntire, L., McKinley, A., and Goodyear, C. (2019). The positive effects of tDCS on sustained attention performance under sleep deprivation conditions are consistent and repeatable. *Brain Stimul. Basic Transl. Clin. Res. Neuromodul.* 12:402. doi: 10.1016/j.brs.2018.12.297

McIntire, L., McKinley, R. A., Nelson, J., and Goodyear, C. (2017a). "Transcranial direct current stimulation (tDCS) versus caffeine to sustain wakefulness at night when dosing at start-of-shift," in *Advances in Neuroergonomics and Cognitive Engineering: Proceedings of the AHFE 2016 International Conference on Neuroergonomics and Cognitive Engineering, July 27-31, 2016, Walt Disney World®, Florida, USA*, eds. K. S. Hale and K. M. Stanney (Cham: Springer International Publishing), 157–172.

McIntire, L. K., Andy McKinley, R., Goodyear, C., McIntire, J. P., and Nelson, J. M. (2020). "Cognitive performance after repeated exposure to transcranial direct current stimulation (tDCS) during sleep deprivation," in *BT - Advances in Safety Management and Human Performance*, eds. P. M. Arezes and R. L. Boring (Cham: Springer International Publishing), 302–313.

McIntire, L. K., McKinley, R. A., Goodyear, C., and Nelson, J. (2014). A comparison of the effects of transcranial direct current stimulation and caffeine on vigilance and cognitive performance during extended wakefulness. *Brain Stimul.* 7, 499–507. doi: 10.1016/j.brs.2014.04.008

McIntire, L. K., McKinley, R. A., Nelson, J. M., and Goodyear, C. (2017b). Transcranial direct current stimulation versus caffeine as a fatigue countermeasure. *Brain Stimul.* 7, 499–507.

McKinley, R., McIntire, L., Tabares, B., Nelson, J., Geier, B., Harshman, S., et al. (2017a). P174 Effects of transcranial direct current stimulation (tDCS) intensity on vigilance performance. *Clin. Neurophysiol.* 128:e102. doi: 10.1016/j.clinph.2016.10.295

McKinley, R. A. (2018). "Chapter 139 – Transcranial direct current stimulation for fatigue and attentional disorders." in *Neuromodulation*. 2nd Edn, eds, E. S. Krames, P. H. Peckham, and A. R. Rezai (San Diego: Academic Press), 1637–48.

McKinley, R. A., Bridges, N., Walters, C. M., and Nelson, J. (2012). Modulating the brain at work using noninvasive transcranial stimulation. *Neuroergonom. Hum. Brain Act. Work* 59, 129–137. doi: 10.1016/j.neuroimage.2011.07.075

McKinley, R. A., McIntire, L., Bridges, N., Goodyear, C., and Weisend, M. P. (2013). Acceleration of image analyst training with transcranial direct current stimulation. *Behav. Neurosci.* 127, 936–946. doi: 10.1037/a0034975

McKinley, R. A., McIntire, L., Nelson, J., Nelson, J., and Goodyear, C. (2017b). "The effects of transcranial direct current stimulation (tDCS) on training during a complex procedural task," in *Advances in Neuroergonomics and Cognitive Engineering*, eds. K. S. Hale and K. M. Stanney (Cham: Springer International Publishing).

Mutsaerts, H. J. M. M., Steketee, R. M. E., Heijtel, D. F. R., Kuijer, J. P. A., van Osch, M. J. P., Majoie, C. B. L. M., et al. (2014). Inter-vendor reproducibility of pseudo-continuous arterial spin labeling at 3 tesla. *PLoS ONE* 9:e104108. doi: 10.1371/journal.pone.0104108

Nelson, J., Mckinley, R., McIntire, L., Goodyear, C., and Walters, C. (2015). Augmenting visual search performance with transcranial direct current stimulation (tDCS). *Mil. Psychol.* 27, 335–347. doi: 10.1037/mil0000085

Nelson, J., Mckinley, R. A., Phillips, C., McIntire, L., Goodyear, C., Camden, A. K., et al. (2016). The effects of transcranial direct current stimulation (tDCS) on multitasking throughput capacity. *Front. Hum. Neurosci.* 10:589. doi: 10.3389/fnhum.2016.00589

Nelson, J., Phillips, C., McKinley, R., McIntire, L., Goodyear, C., and Monforton, L. (2019). The effects of transcranial direct current stimulation (tDCS) on multitasking performance and oculometrics. *Mil. Psychol.* 31, 1–15. doi: 10.1080/08995605.2019.1598217

Nelson, J. T., McKinley, R. A., Golob, E. J., Warm, J. S., and Parasuraman, R. (2014). Enhancing vigilance in operators with prefrontal cortex transcranial direct current stimulation (tDCS). *Neuroimage* 85, 909–917. doi: 10.1016/j.neuroimage.2012.11.061

Nichols, T., and Holmes, A. (2003). Nonparametric permutation tests for functional neuroimaging. *Hum. Brain Funct.* 15, 887–910. doi: 10.1016/B978-012264841-0/50048-2

Nielsen, A. N., and Lauritzen, M. (2001). Coupling and uncoupling of activity-dependent increases of neuronal activity and blood flow in rat somatosensory cortex. *J. Physiol.* 533, 773–785. doi: 10.1111/j.1469-7793.2001.00773.x

Nitsche, M. A., Cohen, L. G., Wassermann, E. M., Priori, A., Lang, N., Antal, A., et al. (2008). Transcranial direct current stimulation: state of the art 2008. *Brain Stimul.* 1, 206–223. doi: 10.1016/j.brs.2008.06.004

Nitsche, M. A., Doemkes, S., Karaköse, T., Antal, A., Liebetanz, D., Lang, N., et al. (2007). Shaping the effects of transcranial direct current stimulation of the human motor cortex. *J. Neurophysiol.* 97, 3109–3117. doi: 10.1152/jn.01312.2006

Nitsche, M. A., and Paulus, W. (2011). Transcranial direct current stimulation – update 2011. *Restor. Neurol. Neurosci.* 29, 463–492. doi: 10.3233/RNN-2011-0618

Noguchi, T., Yoshiura, T., Hiwatashi, A., Togao, O., Yamashita, K., Nagao, E., et al. (2008). Perfusion imaging of brain tumors using arterial spin-labeling: correlation with histopathologic vascular density. *Am. J. Neuroradiol.* 29, 688–693. doi: 10.3174/ajnr.A0903

Patriat, R., Molloy, E. K., Meier, T. B., Kirk, G. R., Nair, V. A., Meyerand, M. E., et al. (2013). The effect of resting condition on resting-state fMRI reliability and

consistency: a comparison between resting with eyes open, closed, and fixated. *Neuroimage* 78, 463–473. doi: 10.1016/j.neuroimage.2013.04.013

Paus, T., Zatorre, R. J., Hofle, N., Caramanos, Z., Gotman, J., Petrides, M., et al. (1997). Time-related changes in neural systems underlying attention and arousal during the performance of an auditory vigilance task. *J. Cogn. Neurosci.* 9, 392–408. doi: 10.1162/jocn.1997.9.3.392

Petree, L. E., Bullard, L. M., Jung, R. E., Shoemaker, J. M., Vakhtin, A. A., van der Merwe, A. J., et al. (2011). "Alternative electrode methodology for the administration of transcranial direct current stimulation," in *Society for Neuroscience Annual Meeting, Washington, DC*.

Pittenger, C., and Duman, R. S. (2008). Stress, depression, and neuroplasticity: a convergence of mechanisms. *Neuropsychopharmacology* 33, 88–109. doi: 10.1038/sj.npp.1301574

Poudel, G. R., Innes, C. R. H., and Jones, R. D. (2012). Cerebral perfusion differences between drowsy and nondrowsy individuals after acute sleep restriction. *Sleep* 35, 1085–1096. doi: 10.5665/sleep.1994

Priori, A., Mameli, F., Cogiamanian, F., Marceglia, S., Tiriticco, M., Mrakic-Sposta, S., et al. (2008). Lie-specific involvement of dorsolateral prefrontal cortex in deception. *Cereb. Cortex* 18, 451–455. doi: 10.1093/cercor/bhm088

Romero Lauro, L. J., Rosanova, M., Mattavelli, G., Convento, S., Pisoni, A., Opitz, A., et al. (2014). TDCS increases cortical excitability: direct evidence from TMS–EEG. *Cortex* 58, 99–111. doi: 10.1016/j.cortex.2014.05.003

Shenfield, L., Beanland, V., Filtness, A., and Apthorp, D. (2020). The impact of sleep loss on sustained and transient attention: an EEG study. *PeerJ* 8:e8960. doi: 10.7717/peerj.8960

Sherwood, M. S., Madaris, A. T., Mullenger, C. R., and McKinley, R. A. (2018). Repetitive transcranial electrical stimulation induces quantified changes in resting cerebral perfusion measured from arterial spin labeling. *Neural Plast.* 2018, 1–12. doi: 10.1155/2018/5769861

Sheth, S. A., Nemoto, M., Guiou, M., Walker, M., Pouratian, N., and Toga, A. W. (2004). Linear and nonlinear relationships between neuronal activity, oxygen metabolism, and hemodynamic responses. *Neuron* 42, 347–355. doi: 10.1016/S0896-6273(04)00221-1

Silva, A. C., and Kim, S.-G. (1999). Pseudo-continuous arterial spin labeling technique for measuring CBF dynamics with high temporal resolution. *Magn. Reson. Med.* 42, 425–429. doi: 10.1002/(SICI)1522-2594(199909)42:3<425::AID-MRM3>3.0.CO;2-S

Smith, S. M., Jenkinson, M., Woolrich, M. W., Beckmann, C. F., Behrens, T. E. J., Johansen-Berg, H., et al. (2004). Advances in functional and structural MR image analysis and implementation as FSL. *Math. Brain Imaging* 23, S208–S219. doi: 10.1016/j.neuroimage.2004.07.051

Stagg, C. J., Lin, R. L., Mezue, M., Segerdahl, A., Kong, Y., Xie, J., et al. (2013). Widespread modulation of cerebral perfusion induced during and after transcranial direct current stimulation applied to the left dorsolateral prefrontal cortex. *J. Neurosci.* 33, 11425–11431. doi: 10.1523/JNEUROSCI.3887-12.2013

Van Dongen, H. P. A., Maislin, G., Mullington, J. M., and Dinges, D. F. (2003). The cumulative cost of additional wakefulness: dose-response effects on neurobehavioral functions and sleep physiology from chronic sleep restriction and total sleep deprivation. *Sleep* 26, 117–126. doi: 10.1093/sleep/26.2.117

Weber, M. J., Detre, J. A., Thompson-Schill, S. L., and Avants, B. B. (2013). Reproducibility of functional network metrics and network structure: a comparison of task-related BOLD, resting ASL with BOLD contrast, and resting cerebral blood flow. *Cogn. Affect. Behav. Neurosci.* 13, 627–640. doi: 10.3758/s13415-013-0181-7

Winkler, A. M., Ridgway, G. R., Webster, M. A., Smith, S. M., and Nichols, T. E. (2014). Full-text. *Neuroimage* 92, 381–397. doi: 10.1016/j.neuroimage.2014.01.060

Woolrich, M. W., Jbabdi, S., Patenaude, B., Chappell, M., Makni, S., Behrens, T., et al. (2009). Bayesian analysis of neuroimaging data in FSL. *Math. Brain Imaging* 45, S173–S186. doi: 10.1016/j.neuroimage.2008.10.055

Worsley, K. J. (2001). "Statistical analysis of activation images," in *Functional MRI: An Introduction to Methods*, eds. P. M. Matthews, P. Jezzard, and S. M. Smith (London: Oxford UP) 251–270.

Xu, G., Rowley, H. A., Wu, G., Alsop, D. C., Shankaranarayanan, A., Dowling, M., et al. (2010). Reliability and precision of pseudo-continuous arterial spin labeling perfusion MRI on 3.0 T and comparison with 15 O-water PET in elderly subjects at risk for Alzheimer's disease. *NMR Biomed.* 23, 286–293. doi: 10.1002/nbm.1462

Ye, F. Q., Frank, J. A., Weinberger, D. R., and McLaughlin, A. C. (2000). Noise reduction in 3D perfusion imaging by attenuating the static signal in arterial spin tagging (ASSIST). *Magn. Reson. Med.* 44, 92–100. doi: 10.1002/1522-2594(200007)44:1<92::AID-MRM14>3.0.CO;2-M

Zheng, X., Alsop, D. C., and Schlaug, G. (2011). Effects of transcranial direct current stimulation (tDCS) on human regional cerebral blood flow. *Neuroimage* 58, 26–33. doi: 10.1016/j.neuroimage.2011.06.018

Author Disclaimer: The opinions expressed herein belong solely to the authors. They do not represent and should not be interpreted as being those of or endorsed by the Department of Defense or any other branch of the federal government. The U.S. Government is authorized to reproduce and distribute reprints for governmental purposes notwithstanding any copyright notation thereon. The voluntary, fully informed consent of the subjects used in this research was obtained as required by 32 CFR 210 and DODI 3216.02_AFI 40-402.

Conflict of Interest: MS is employed by the company KBR Inc. MS serves in an unpaid role as a member of Aaron Madaris's Dissertation Committee at Wright State University. AM received compensation for this work as an intern through Infoscitex, Inc. and is also a student at Wright State University. LM is employed by Infoscitex, Inc.

The remaining authors declare that the research was conducted in the absence of any commercial or financial relationships that could be construed as a potential conflict of interest.

Publisher's Note: All claims expressed in this article are solely those of the authors and do not necessarily represent those of their affiliated organizations, or those of the publisher, the editors and the reviewers. Any product that may be evaluated in this article, or claim that may be made by its manufacturer, is not guaranteed or endorsed by the publisher.

frontiers in Human Neuroscience

ORIGINAL RESEARCH
published: 26 August 2021
doi: 10.3389/fnhum.2021.707816

Prevention and Treatment of Hardware-Related Infections in Deep Brain Stimulation Surgeries: A Retrospective and Historical Controlled Study

Jiping Li[1†], Wenjie Zhang[1†], Shanshan Mei[2], Liang Qiao[1], Yunpeng Wang[1], Xiaohua Zhang[1], Jianyu Li[1], Yongsheng Hu[1], Xiaofei Jia[1] and Yuqing Zhang[1]*

[1] Department of Functional Neurosurgery, Beijing Institute of Functional Neurosurgery, Xuanwu Hospital, Capital Medical University, Beijing, China, [2] Department of Neurology, Xuanwu Hospital, Capital Medical University, Beijing, China

OPEN ACCESS

Edited by:
Masaki Sekino,
The University of Tokyo, Japan

Reviewed by:
Yasushi Shimo,
Juntendo University Nerima Hospital, Japan
Francesco Motolese,
Campus Bio-Medico University, Italy

***Correspondence:**
Yuqing Zhang
yuqzhang@vip.163.com

[†] These authors have contributed equally to this work and share first authorship

Specialty section:
This article was submitted to Brain Imaging and Stimulation, a section of the journal Frontiers in Human Neuroscience

Received: 10 May 2021
Accepted: 02 August 2021
Published: 26 August 2021

Citation:
Li J, Zhang W, Mei S, Qiao L, Wang Y, Zhang X, Li J, Hu Y, Jia X and Zhang Y (2021) Prevention and Treatment of Hardware-Related Infections in Deep Brain Stimulation Surgeries: A Retrospective and Historical Controlled Study. Front. Hum. Neurosci. 15:707816. doi: 10.3389/fnhum.2021.707816

Background: Hardware-related infection in deep brain stimulation (DBS) is one of the most commonly reported complications frequently resulting in the removal of implantable pulse generator (IPG).

Objective: The aim of this study was to establish a useful strategy to better prevent and treat those infections and to improve the preservation rates of IPG.

Methods: We conducted a retrospective and historical controlled study of all adult patients (≥18 years old) who had undergone initial DBS implantation at a single center. All participants were enrolled in the control group (between June 2005 and June 2014) or intervention group (between July 2014 and May 2019) based on their surgery dates. We used the intraoperative irrigation with hydrogen dioxide solution in the intervention group. Based on the dates of diagnosis, patients with hardware-related infection after DBS were enrolled in group A (between June 2005 and June 2014) or group B (between July 2014 and May 2019). IPG-sparing algorithm (Isa) was applied for group B. The early-onset IPG infections of the control and intervention groups were evaluated. The IPG preservation rates in both groups A and B were statistically analyzed.

Results: Six cases of early IPG infection and subsequent IPG removal occurred in the control group, while none occurred after intraoperative usage of the hydrogen dioxide in the intervention group. IPG preservation rate of infected cases in group B was significantly higher than that in group A (70% vs.16%, $p = 0.004$).

Conclusion: The combined application of hydrogen dioxide solution and Isa seems to be an effective strategy to prevent IPG infection.

Keywords: deep brain stimulation, implantable pulse generator, infection, hardware-related complication, treatment of infection

INTRODUCTION

Deep brain stimulation (DBS) has been widely accepted as an effective treatment for a variety of movement disorders such as Parkinson's disease (PD), essential tremor (ET), and dystonia. The applications of DBS continue to expand as it is also employed in a range of other refractory neurological or psychiatric conditions (Awan et al., 2009). DBS-related infection has been identified as one of the most serious complications, with the reported incidence ranging widely between 1.2 and 23% (Hamani and Lozano, 2006; Sillay et al., 2008; Miller et al., 2009; Bhatia et al., 2010; Hardaway et al., 2018). Management of hardware-related infections can be challenging and it often involves prolonged hospital stays, further surgery, and partial or even complete hardware removal. However, effective prevention and treatment strategies for hardware-related infection of DBS remain under-investigated.

The most common sites involved in infection after DBS included frontal, postauricular area, and infraclavicular region with related DBS hardware of intracranial lead, connection cable, and implantable pulse generator (IPG), respectively. The IPG-related infection was of particular concern to our patients given that the rechargeable IPG was widely used since the second half of 2014. The cost of this new IPG type accounted for about 80% of the cost of the whole DBS system and it was higher than that of earlier non-rechargeable models, which was not covered by our national healthcare insurance system. Some reported that complete removal of the whole DBS device was performed in most cases with infections around any part of the DBS system, despite initial attempts of localized treatment (Oh et al., 2002; Umemura et al., 2003; Constantoyannis et al., 2005; Bhatia et al., 2010; Chen et al., 2017). The IPG salvage attempts frequently failed due to recurrent infections, except for one study group suggesting reuse of IPG following sterilization with ethylene oxide (Gocmen et al., 2014). According to the National Health Industry Standard, hospitals have not been allowed to reuse IPG after sterilization on their own since 2014. Furthermore, usage of rechargeable IPG (15-year warranty) implies a sustained risk of IPG infection. Those practices highlight the need for regular assessment for any suspected infections, better before the IPG is contaminated.

To establish a better strategy to prevent and manage those hardware-related infections following initial DBS surgery and to improve the preservation rates of IPG, we conducted a retrospective and historical controlled study in our DBS population.

MATERIALS AND METHODS

Study Design

We analyzed all adult patients (≥18 years old) who had undergone primary DBS implantation procedures performed in the period from June 2005 to May 2019 at a single center. As a historical controlled study, we reviewed their data retrospectively (**Figure 1**). Patients who underwent initial DBS implantation before June 2014 (control group) were compared with those who underwent DBS implantation after July 2014 (intervention group). Cases of hardware-related infection diagnosed before June 2014 (group A) were compared with those diagnosed after July 2014 (group B). We included only those patients who had received DBS implantation for the first time and excluded patients who had isolated IPG replacements. All infection rates were calculated based on the dates of diagnosis of infection. This study was approved by the Ethics Committee of Hospital and all patients signed consent documents.

DBS Procedure

A multidisciplinary team selected the appropriate target nucleus: typically subthalamic nucleus (STN) or globus pallidus internus (GPi) for PD, ventralis intermedius (VIM) for ET, and GPi for dystonia and tics. Standard stereotactic techniques were used for all lead placements. MRI-CT fusion targeting was used for all patients, and intraoperative electrophysiology (microelectrode recording and macrostimulation) was used to help determine the final intracranial lead position. Lead implantations were performed under local anesthesia with monitored anesthesia care. For bilateral lead placements, the left lead was tunneled subgaleally to the right side to facilitate the placement of a single–dual channel IPG. Under general anesthesia, the IPG was placed in the infraclavicular region and connected to each intracranial lead by an extension cable in the same surgical setting. All procedures were performed by two neurosurgeons, namely, Zhang and Li.

Definition and Classification of Infections

Only deep infections were considered in this study. Deep infections were defined as infections that extended into the subcutaneous layer and were in contact with at least one part of the DBS system (Piacentino et al., 2011).

Hardware infections of any part of the system were classified into early onset (<3 months) and late onset (>3 months). IPG infections were classified into primary and secondary infections based on their original sites. An infection presented initially in the subcutaneous pocket created for the IPG was classified as primary IPG infection. Secondary IPG infection was defined as an infection arising initially from frontal or postauricular and occurring at IPG pocket subsequently. The cellulites or purulent drainage could be seen and tracked in surgery, along the subcutaneous tunnel from the IPG pocket toward postauricular and frontal areas.

General Antibiotic Regimen for Patients in the Control and Intervention Groups

All patients received prophylactic antibiotics intravenously 30 min before surgery, and postoperative antibiotic administration for 5 days following procedures. Ceftriaxone was administered as the prophylactic antibiotic for most patients (1 g intravenously 30 min before incision and 2 g intravenously per day postoperatively). Clindamycin was administered in cases of ceftriaxone allergy. Since July 2014, for all patients of DBS implantation, an additional 3% solution of hydrogen peroxide

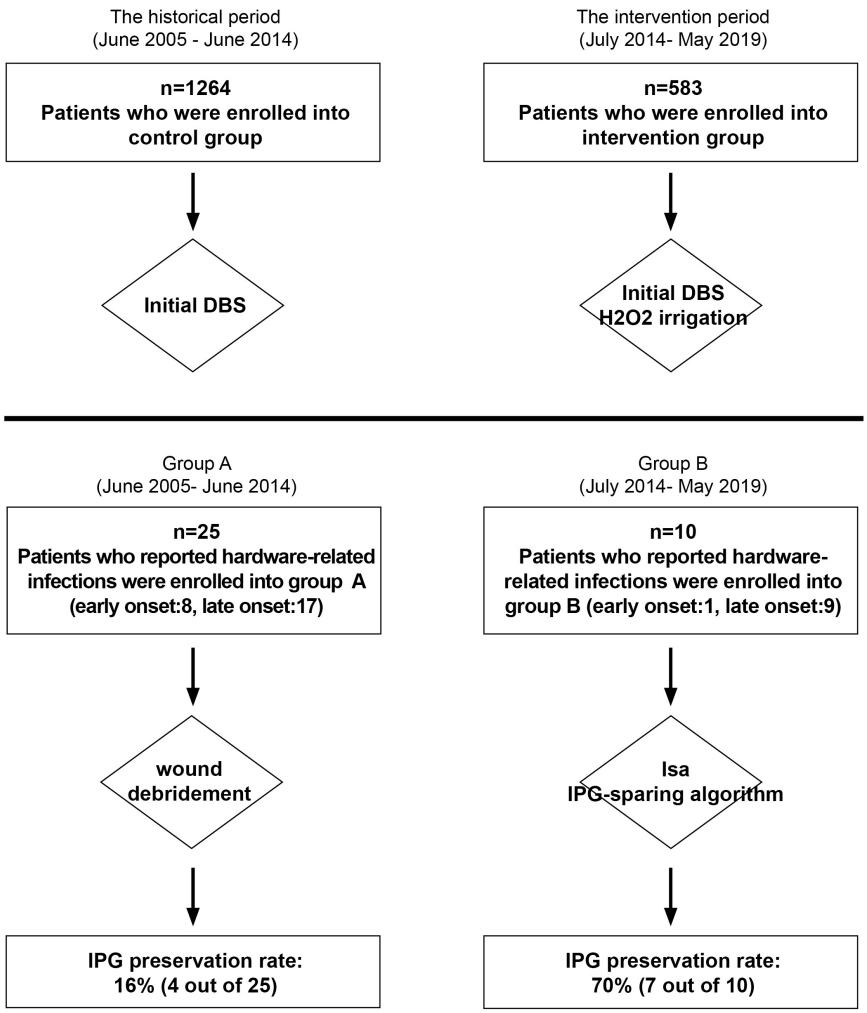

FIGURE 1 | Enrollment of patients and flow diagram. DBS, deep brain stimulation; IPG, implantable pulse generator; H_2O_2, 3% solution of hydrogen peroxide, which was used at the IPG pocket to prevent the early and primary IPG infection.

was used at the IPG pocket to prevent the early and primary IPG infection (**Figure 1**).

Treatment of Hardware-Related Infections in Group A

We first attempted conservative treatments consisting of antibiotic treatment, wound debridement, and occasional scalp rotational flap. Decisions to remove hardware partially or completely were made for those patients following failure in conservative treatments. With or without hardware removal, patients were all managed with 2–4 weeks of intravenously administered antibiotics based on bacterial culture and sensitivity results.

Treatment of Hardware-Related Infections in Group B

If infection presented originally from IPG pocket, antibiotic treatment, wound debridement, and IPG removal were performed. If infection occurred in the frontal or postauricular area, an IPG-sparing algorithm (Isa) was performed. Isa included the following three steps: (1) skin of the whole chest was prepped, and the IPG (with no signs of infection presented) was prophylactic ex-planted and reimplanted instantly into a new made pocket at contralateral infraclavicular region; (2) after prepping and draping again, hardware (intracranial leads and extensions) in the contaminated area was totally removed; and (3) 3 months later, if no clinical infection signs presented at the new IPG pocket, new DBS leads and extensions were implanted stereotactically and connected to the saved IPG through a new made tunnel at contralateral postauricular site. Patients were managed with the intravenous administration of antibiotics for 7 consecutive days following each of step (2) and step (3).

Statistical Analysis

The gender, age at surgery, disease duration, disease categories, overall infection rate, and the number of early IPG infections of

patients were compared between the control and intervention groups. IPG preservation rates, infection-related procedures, and accumulative hospital stay in group A and group B were statistically analyzed. The paired sample *t*-test, two-sample *t*-test, chi-square test, or Fisher's exact test was used as appropriate for variables examined. $P < 0.05$ was considered statistically significant. Statistical analyses were performed by using SPSS 20.0 (SPSS Inc., Chicago, IL, United States).

RESULTS

Patient Demographic of Control Group and Intervention Group

In total, 1,264 patients underwent DBS between June 2005 and June 2014 (control group), and 583 patients who underwent DBS between July 2014 and May 2019 (intervention group) were included in this study. Their demographics and diagnosis are reported in **Table 1**. There was no statistical difference in gender, age at surgery, disease duration, disease categories, or overall infection rate between the control and intervention groups. Six cases of early primary IPG infection and subsequent IPG removal occurred in the control group, while none occurred after intraoperative usage of the hydrogen dioxide in the intervention group. No intracranial abscesses were observed in both groups. The minimum follow-up of patients was 70 months (range: 70–178 months) in the control group and 12 months (range: 12–70 months) in the intervention group.

Statistical Analysis of Infection in Both Group A and Group B

After the application of Isa (**Table 2**), the IPG preservation rate in group B was significantly higher than that in group A (70% vs. 16%, $p = 0.004$). The infection-related procedures in group B were significantly reduced than that in group A (2.2 vs. 3.6, $p = 0.002$). The accumulative hospital stay in group B was significantly shortened than that in group A (26.0 vs. 33.7 days, $p = 0.008$).

Clinical Characteristics of Infection in Group A

Twenty-five hardware-related infections were diagnosed in group A and the characteristics of that group were described as early onset and late onset (**Figure 2**). Most (seven out of eight) of the early infective patients developed primary IPG infection. Of those seven patients, six presented recurrence of IPG infection after conservative treatment and finally resulted in IPG removal. The only one early primary infection with successful salvage of IPG was reported with sterilization of IPG using ethylene oxide (**Figure 2**).

The late infections appeared to be more common than early infections in this group (17 vs. 8). Of those 17 late infections, 15 were aroused from frontal and/or postauricular areas. Three frontal infections occurring at 5, 29, and 90 months postimplantation, respectively, were managed by intracranial lead removal and reimplanted 3 months later without infection recurrence (**Figure 2**). The other 12 infections spread and resulted in secondary IPG infection and IPG removal.

In total, there were 22 IPG infections (9 primary and 13 secondary) resulting in 21 cases of IPG removal (**Figure 3**), and 4 out of 25 cases (16%) resulted in successful IPG preservation. An average of 3.6 infection-related procedures was performed and the accumulative hospital stay of patients was 33.7 days.

The Acceleration in the Process of Infection Spreading in Group A

We found that the infection spreading presented an accelerating process for patients in group A (**Figure 4**). It took about 3–73 months for the pathogen to spread from head to postauricular. While it took as quickly as 2–184 days for the pathogen to spread from postauricular to infraclavicular region (IPG pocket). Significant difference in spreading duration was reported between two sections (Wilcoxon signed-rank test, $p = 0.025$).

Clinical Characteristics of Infection in Group B

Ten hardware-related infections were diagnosed in group B (**Figure 5**). After Isa strategy was applied, seven infective cases were succeeded in preventing the infection from spreading down to IPG pocket and succeeded in IPG preservation. An average of 2.2 infection-related procedures was performed and the accumulative hospital stay of patients was 26 days.

Safe Time Window for Application of Isa in Group B

As in group A, the interval for an infection spreading from frontal to postauricular area was 3–73 months. However, the interval for an infection spreading from postauricular to IPG pocket was 8–33 weeks (**Figure 3**). The safe time window was calculated based on the abovementioned minimal time interval. Therefore, for all seven patients with infection arouse from frontal and/or postauricular in group B, the IPGs were transimplanted to the contralateral chest subcutaneously within the safe time window (**Figure 4**), if only the infection was timely diagnosed.

Adverse Effects

No operative complications related to reimplantation of intracranial lead occurred. No side effects of the application of intraoperative hydrogen dioxide solution, such as air embolism, were recorded.

DISCUSSION

The initial motivation for this study started in 2014 when there was a significant push to offer rechargeable IPG due to its advantage of a longer lifetime and less-frequent battery replacement (Waln and Jimenez-Shahed, 2014). However, the cost of this new IPG type is much higher than that of earlier non-rechargeable models and cannot be covered by our national healthcare insurance system. Many literatures have focused on the hardware salvage after infection (Sillay et al., 2008;

TABLE 1 | Demographics of control group and intervention group.

	Control group	Intervention group
No. of DBS patients	1264	583
Male:female	740:524	358:225
Age at surgery (mean ± SD, years)	56.7 ± 13.4	58.8 ± 12.7
Disease duration (mean ± SD, years)	9.3 ± 7.6	8.4 ± 6.1
Diagnosis		
Parkinson's disease	1119	534
Dystonia	72	23
Essential tremor	41	20
Tic	28	5
Others*	4	1
No. of rechargeable IPG patients (%)	49 (3.9%)	476 (81.6%)
Preventive measures against infection	antibiotic	antibiotic and H_2O_2 irrigation at IPG pocket
No. of overall infection (%)	25 (2.0%)	10 (1.7%)
No. of early primary IPG infection and IPG removal	6	0
Follow-up (range, months)	70–178	12–70

DBS, deep brain stimulation; IPG, implantable pulse generator; H_2O_2, 3% solution of hydrogen peroxide; others, vegetative state, chorea, hemiballis, and cerebral palsy.*

TABLE 2 | Statistical analysis of infection in group A and group B.

	Group A	Group B	*P*
No. of hardware-related infection	25	10	
Early onset, <3 months (%)	8 (32%)	1 (10%)	0.235
Late onset, >3 months (%)	17 (68%)	9 (90%)	
Arising from IPG pocket (%)	9 (36%)	1 (10%)	0.218
Arising from frontal or postauricular area (%)	16 (64%)	9 (90%)	
IPG infection, *n* (%)	22 (88%)	3 (30%)	0.002
IPG removal, *n* (%)	21 (84%)	3 (30%)	0.004
IPG preservation, *n* (%)	4 (16%)	7 (70%)	0.004
Infection related surgery (per patient)	3.6	2.2	0.002
Infection related hospital stay (days per patient)	33.7	26	0.008

Miller et al., 2009; Bhatia et al., 2010; Dlouhy et al., 2012; Atchley et al., 2019). However, the detailed description of effective preventive procedures for IPG infections in DBS surgery remains quite limited.

The increased surgical experience may reduce the incidence of infection; however, this viewpoint was not applied in our study. First, our surgical team had years of experience before data collection. In addition, in our long-term follow-up research, the more common infections were of late onset, which were attributable to patient-related factors rather than procedure-related factors. Therefore, our results showed that there was no significant difference in the overall hardware infection rate between the control and intervention groups.

The Preventive Strategy for Primary IPG Infections

Primary IPG infections would probably arise early within 2 months, resulting in IPG removal despite multiple salvage attempts (Oh et al., 2002; Sillay et al., 2008; Miller et al., 2009). We observed the same in our study. Most early infections were associated with the procedure itself rather than the characteristics of patients. Sterilization of contaminated IPG with ethylene oxide fuming was suggested by a study group and succeeded in one of our patients of group A (Gocmen et al., 2014). However, this approach carried out by hospital rather than by manufacturer was not allowed according to the National Health Industry Standard (Regulation of Disinfection Technique in Healthcare Settings) since 2014. Moreover, there was no recommendation by the manufacturer regarding the approach to the problem. We did not employ junctive vancomycin powder intraoperatively because its beneficial was uncertain in literature (Waln and Jimenez-Shahed, 2014; Atchley et al., 2019; Bernstein et al., 2019).

Hydrogen peroxide has a broad spectrum of activity against gram-positive and gram-negative bacteria, bacterial spores, viruses, and yeast (Urban et al., 2019; Welman et al., 2019). There have been documented cases of hydrogen peroxide, resulting in air embolism from the formation of oxygen gas when used in closed cavities (Linley et al., 2012; Lu and Hansen, 2017). We would therefore advise that hydrogen peroxide should not be used with pressure or *via* intracranial. After junctive usage of hydrogen peroxide intraoperatively in the intervention group, no early primary IPG infection was observed with a minimum follow-up of 12 months. Although no statistically significant presented, the intraoperative usage of hydrogen peroxide did result in decreased cases of early primary IPG infection and subsequent IPG removal.

The Preventive Strategy for Secondary IPG Infections

Secondary IPG infections resulted mostly from late infections, which were more common than early infections in our study. Analysis has concluded that most of the late infections are attributable to patient-related factors rather than procedure-related factors (Owens and Stoessel, 2008). Indeed, the risk of hardware-related infection can persist for up to several

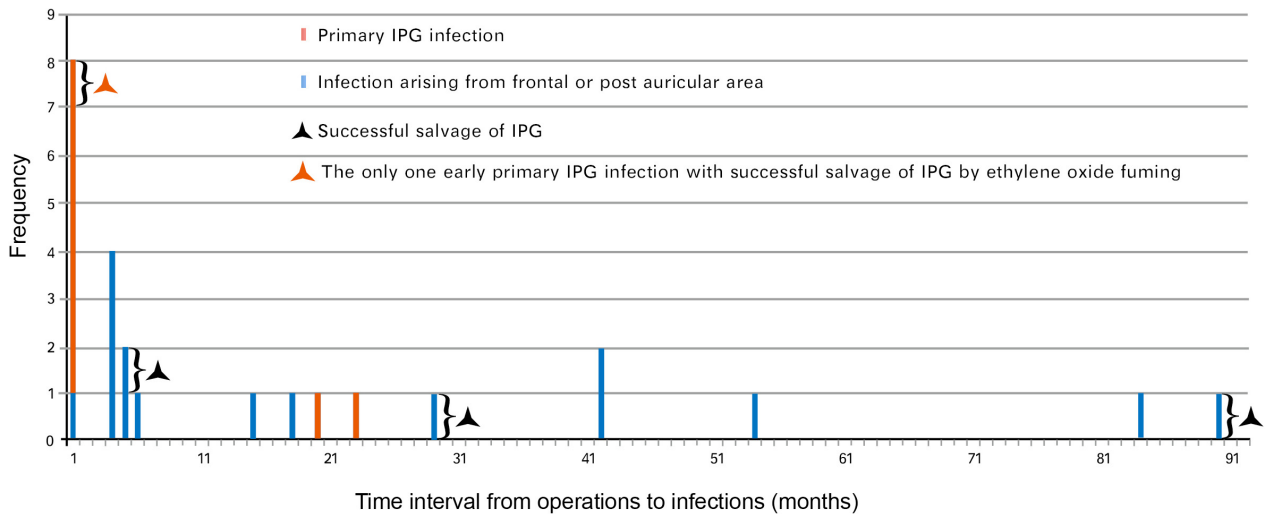

FIGURE 2 | Hardware-related infections in group A (time interval to diagnosis of infection). Twenty-five cases of hardware-related infections were enrolled in group A (between June 2005 and June 2014) based on the date of diagnosis. Eight cases presented early-onset infection while 17 cases presented late-onset infection. IPG, implantable pulse generator.

years after the patient was given an implant. There was a constant risk of IPG infection as long as the foreign materials remained *in situ* over the lifetime of patients (Barrett et al., 2018). Studies show that the infection risk was increasing as health conditions, such as hygiene habits, poor personal hygiene, and low cultural background, would have been worse particularly in advanced PD patients (Fischer et al., 2001; Bachmann and Trenkwalder, 2006; Owens and Stoessel, 2008; Sixel-Döring et al., 2010). This may also be the reason why the late infection was more likely to involve incision of frontal and postauricular areas. Compared with chest skin, the scalp hygiene was supposed to be more difficult to manage. And the skin around postauricular incision is more vulnerable to repeated friction. All those stress the necessity of a long-term follow-up and continued patient/caregiver education, particularly for patients implanted with a rechargeable and 15-year lifetime IPG.

Before Isa was applied, late infections would probably result in secondary IPG infection and IPG removal. Therapeutic strategy of initial infection was essential for preventing secondary IPG infection. There were usually several treatment options of initial infection as follows: (a) antibiotic treatment alone; (b) antibiotic therapy with wound incision and debridement; and (c) partial or complete removal of implanted DBS hardware. It was often surgeon dependent about which option should be initially conducted and the successful rates of hardware salvage differed widely among centers.

Based on our follow-up evaluation in group A, we found that most lead and/or connection infections would finally involve an IPG pocket (**Figure 3**). One possibility is that latent colonized bacteria of residual hardware may inoculate the newly implanted system, or translocate along the punctured tunnel, such that the infection showed in the least vascular IPG pocket. These results implied that the colonized bacteria in frontal or postauricular area would in great chance reach the IPG pocket and resulted in IPG removal if IPG-sparing management were not conducted promptly. While waiting for the therapeutic response of treatment in the traditional way, we would probably pass a valuable time window to protect the IPG in advance.

We considered altering our IPG salvage strategy by application of Isa in group B to (a) transimplant IPG before it was contaminated; (b) make a new tunnel to connect the new implanted lead and saved IPG to avoid the suspected organisms colonized in the old tunnel when reopening old incision. Isa strategy could significantly reduce secondary (late the majority) IPG infection if conducted within the safe time window (**Figure 4**). Those practices highlight the need for regular assessment for any suspected infections. Timely and effective communication among the neurosurgeon, patient, caregiver, and nurse practitioner is essential for the successful salvage of IPG.

Limitations

As a retrospective and historical controlled study, this investigation did not involve all potential risk factors related to IPG infection. Thus, we did not have enough collection of variables to explore whether there were other factors contributing to IPG infection. The data might suggest to some degree that early IPG infection is frequently related to the surgical procedure itself while late IPG infection is commonly associated with the relevant factors of patients. Therefore, different potential prevention and treatment strategies are needed according to various characteristics of early and late infection.

Combined application of hydrogen peroxide solution and Isa could not reduce overall hardware infection since late infection accounted for the majority, which was assumed to be related

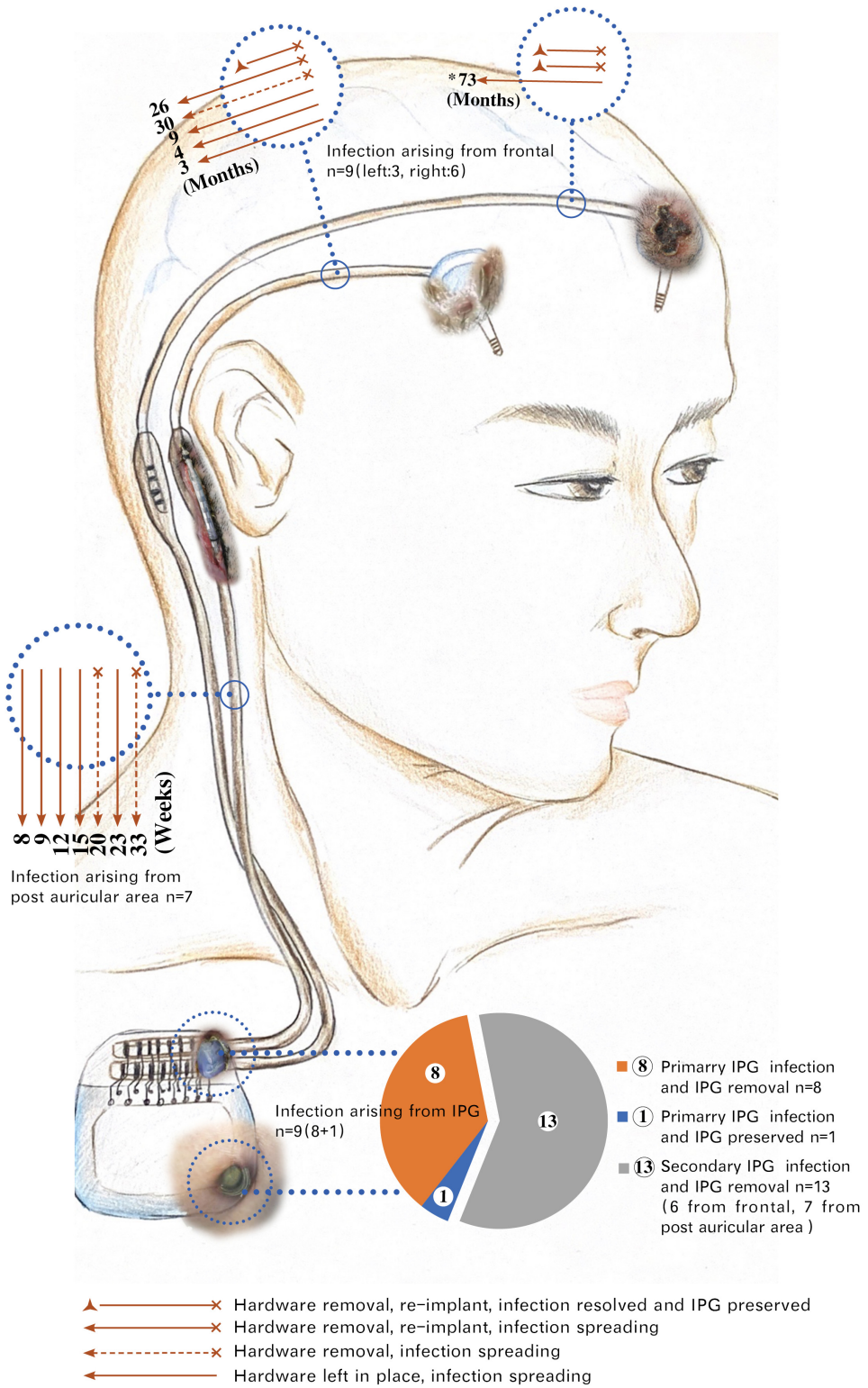

FIGURE 3 | Spreading of hardware-related infections in group A. *73: The infection arising from the left head spread to the right postauricular area 73 months post-diagnosis of infection. This patient underwent five times of local incision debridement (including two times of rotational flap) before intracranial lead removal. Months: Time interval of infections spreading from frontal to postauricular area counted by months. Weeks: Time interval of infections spreading from postauricular area to infraclavicular region (IPG pocket) counted by weeks. Six infections of frontal origin and seven infections of postauricular origin finally spread to IPG. Among a total of 22 IPG infections, 21 were removed, with only 1 IPG remaining at a place after being sterilized with ethylene oxide. The exposed parts of the hardware in the picture were taken from real photos. IPG, implantable pulse generator.

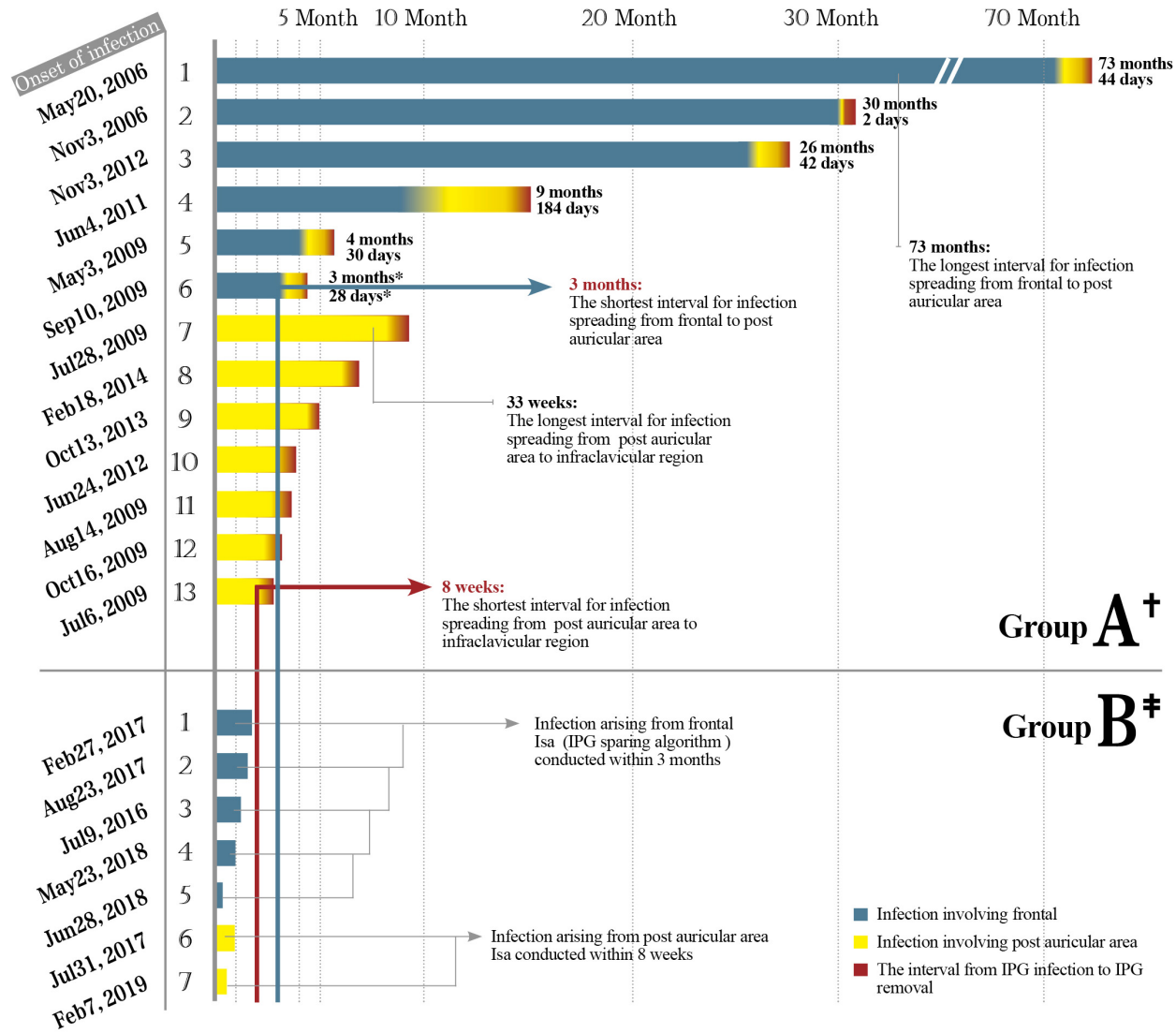

FIGURE 4 | The safe time window for the application of Isa. Thirteen cases of infection spread to IPG in group A including six originating from frontal while seven originating from postauricular area. Seven cases of infection in group B underwent Isa within the safe time window. Months and days: The interval of infection spreading from frontal to postauricular area counted in months and subsequently to infraclavicular region (IPG pocket) counted in days. Significant difference in the interval duration was reported between two sections (Wilcoxon signed-rank test, $p = 0.025$). IPG, implantable pulse generator.

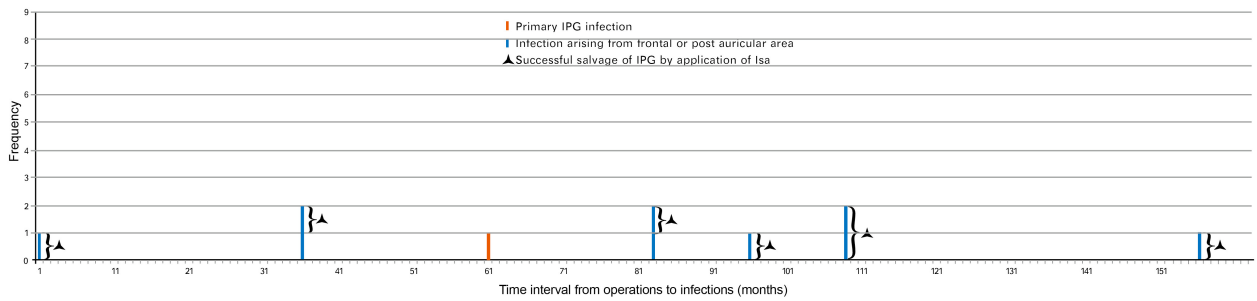

FIGURE 5 | Hardware-related infections in group B (time interval to diagnosis of infection). Ten cases of hardware-related infections were enrolled in group B (between July 2014 and May 2019) based on the date of diagnosis. One case presented early-onset infection while nine cases presented late-onset infection. IPG, implantable pulse generator.

to poor hygienic conditions and advanced age. Moreover, Isa may not be suitable for the elderly patients (>80) and those who cannot tolerate even a brief absence of stimulation delivered by the DBS device.

Early infections of our DBS patients were all documented, as their first follow-up for DBS programming was performed 3 months postoperatively in our hospital. However, there were chances of some cases of late-onset infection diagnosed and managed at other hospitals.

CONCLUSION

The use of hydrogen peroxide can lower the incidence of primary IPG infection, and the Isa strategy can help prevent the occurrence of secondary IPG infection. Therefore, the combined use of the above two can effectively prevent and treat IPG infection, increase the preservation rate of IPG, and reduce infection-related procedures and hospital stays.

DATA AVAILABILITY STATEMENT

The original contributions presented in the study are included in the article/supplementary material, further inquiries can be directed to the corresponding author/s.

ETHICS STATEMENT

The studies involving human participants were reviewed and approved by Ethics Committee of Xuan Wu Hospital. The patients/participants provided their written informed consent to participate in this study. Written informed consent was obtained from the individual(s) for the publication of any potentially identifiable images or data included in this article.

AUTHOR CONTRIBUTIONS

JPL, WZ, and YZ were the major contributors in writing the manuscript. SM, LQ, YW, XZ, JYL, and YH contributed to the diagnosis and treatment of the patients. JPL, WZ, SM, and XJ contributed to the data acquisition. JPL, WZ, and XJ contributed to the data analysis. LQ contributed to editing the manuscript. YZ reviewed the manuscript thoroughly and was accountable for all aspects of the work in ensuring that questions related to the accuracy or integrity of any part of the work. All authors read and approved the final manuscript.

ACKNOWLEDGMENTS

We would like to acknowledge Yunxia Wang for her hand-painted draft support of **Figure 3**.

REFERENCES

Atchley, T. J., Laskay, N. M. B., Sherrod, B. A., Rahman, A. K. M. F., Walker, H. C., and Guthrie, B. L. (2019). Reoperation for device infection and erosion following deep brain stimulation implantable pulse generator placement. *J. Neurosurg.* doi: 10.3171/2019.3.JNS183023 Online ahead of print.

Awan, N. R., Lozano, A., and Hamani, C. (2009). Deep brain stimulation: current and future perspectives. *Neurosurg. Focus* 7:E2.

Bachmann, C. G., and Trenkwalder, C. (2006). Body weight in patients with Parkinson's disease. *Mov. Disord.* 21, 1824–1830. doi: 10.1002/mds.21068

Barrett, T. F., Rasouli, J. J., Taub, P., and Kopell, B. H. (2018). Technical note: preemptive surgical revision of impending deep brain stimulation hardware erosion. *World Neurosurg.* 111, 41–46. doi: 10.1016/j.wneu.2017.12.045

Bernstein, J. E., Kashyap, S., Ray, K., and Ananda, A. (2019). Infections in Deep Brain stimulator surgery. *Cureus* 11:e5440.

Bhatia, S., Zhang, K., Oh, M., Angle, C., and Whiting, D. (2010). Infections and hardware salvage after deep brain stimulation surgery: a single-center study and review of the literature. *Stereotact. Funct. Neurosurg.* 88, 147–155. doi: 10.1159/000303528

Chen, T., Mirzadeh, Z., Lambert, M., Gonzalez, O., Moran, A., Shetter, A. G., et al. (2017). Cost of deep brain stimulation infection resulting in explantation. *Stereotact. Funct. Neurosurg.* 95, 117–124. doi: 10.1159/000457964

Constantoyannis, C., Berk, C., Honey, C. R., Mendez, I., and Brownstone, R. M. (2005). Reducing hardware-related complications of deep brain stimulation. *Can. J. Neurol. Sci.* 32, 194–200.

Dlouhy, B. J., Reddy, A., Dahdaleh, N. S., and Greenlee, J. D. (2012). Antibiotic impregnated catheter coverage of deep brain stimulation leads facilitates lead preservation after hardware infection. *J. Clin. Neurosci.* 19, 1369–1375. doi: 10.1016/j.jocn.2012.02.008

Fischer, M., Gemende, I., Marsch, W. C., and Fischer, P. A. (2001). Skin function and skin disorders in Parkinson's disease. *J. Neural. Transm.* 108, 205–213. doi: 10.1007/s007020170088

Gocmen, S., Celiker, O., Topcu, A., Panteli, A., Acar, G., and Acar, F. (2014). Reuse of internal pulse generator in cases of infection after deep brain stimulation surgery. *Stereotact. Funct. Neurosurg.* 92, 140–144. doi: 10.1159/000360585

Hamani, C., and Lozano, A. M. (2006). Hardware-related complications of deep brain stimulation: a review of the published literature. *Stereotact. Funct. Neurosurg.* 84, 248–251. doi: 10.1159/000096499

Hardaway, F. A., Raslan, A. M., and Burchiel, K. J. (2018). Deep brain stimulation-related infections: analysis of rates. timing, and seasonality. *Neurosurgery* 83, 540–547. doi: 10.1093/neuros/nyx505

Linley, E., Denyer, S. P., McDonnell, G., Simons, C., and Maillard, J. Y. (2012). Use of hydrogen peroxide as a biocide: new consideration of its mechanisms of biocidal action. *J. Antimicrob. Chemother.* 67, 1589–1596. doi: 10.1093/jac/dks129

Lu, M., and Hansen, E. N. (2017). Hydrogen peroxide wound irrigation in orthopaedic surgery. *J. Bone Jt. Infect.* 2, 3–9. doi: 10.7150/jbji.16690

Miller, J. P., Acar, F., and Burchiel, K. J. (2009). Significant reduction in stereotactic and functional neurosurgical hardware infection after local neomycin/polymyxin application. *J. Neurosurg.* 110, 247–250. doi: 10.3171/2008.6.17605

Oh, M. Y., Abosch, A., Kim, S. H., Lang, A. E., and Lozano, A. M. (2002). Long-term hardware-related complications of deep brain stimulation. *Neurosurgery* 50, 1268–1274. doi: 10.1227/00006123-200206000-00017

Owens, C. D., and Stoessel, K. (2008). Surgical site infections: epidemiology, microbiology and prevention. *J. Hosp. Infect.* 70, 3–10. doi: 10.1016/s0195-6701(08)60017-1

Piacentino, M., Pilleri, M., and Bartolomei, L. (2011). Hardware-related infections after deep brain stimulation surgery: review of incidence, severity and management in 212 single-center procedures in the first year after implantation. *Acta Neurochir.* 153, 2337–2341. doi: 10.1007/s00701-011-1130-2

Sillay, K. A., Larson, P. S., and Starr, P. A. (2008). Deep brain stimulator hardware-related infections: incidence and management in a large series. *Neurosurgery* 62, 360–366. doi: 10.1227/01.neu.0000316002.03765.33

Sixel-Döring, F., Trenkwalder, C., Kappus, C., and Hellwig, D. (2010). Skin complications in deep brain stimulation for Parkinson's disease: frequency, time course, and risk factors. *Acta Neurochir.* 152, 195–200. doi: 10.1007/s00701-009-0490-3

Umemura, A., Jaggi, J. L., Hurtig, H. I., Siderowf, A. D., Colcher, A., Stern, M. B., et al. (2003). Deep brain stimulation for movement disorders: morbidity and mortality in 109 patients. *J. Neurosurg.* 98, 779–784. doi: 10.3171/jns.2003.98.4.0779

Urban, M. V., Rath, T., and Radtke, C. (2019). Hydrogen peroxide (H(2)O(2)): a review of its use in surgery. *Wien. Med. Wochenschr.* 169, 222–225. doi: 10.1007/s10354-017-0610-2

Waln, O., and Jimenez-Shahed, J. (2014). Rechargeable deep brain stimulation implantable pulse generators in movement disorders: patient satisfaction and conversion parameters. *Neuromodulation* 17, 425–430. doi: 10.1111/ner.12115

Welman, T., McKean, A. R., Torres-Grau, J., Tickunas, T., and McArthur, G. (2019). Hydrogen peroxide in the operating theatre: too dilute to dilute? *Injury* 50, 369–370. doi: 10.1016/j.injury.2018.12.010

Conflict of Interest: The authors declare that the research was conducted in the absence of any commercial or financial relationships that could be construed as a potential conflict of interest.

Publisher's Note: All claims expressed in this article are solely those of the authors and do not necessarily represent those of their affiliated organizations, or those of the publisher, the editors and the reviewers. Any product that may be evaluated in this article, or claim that may be made by its manufacturer, is not guaranteed or endorsed by the publisher.

frontiers in Human Neuroscience

ORIGINAL RESEARCH
published: 13 September 2021
doi: 10.3389/fnhum.2021.726604

Effects of Slow Oscillatory Transcranial Alternating Current Stimulation on Motor Cortical Excitability Assessed by Transcranial Magnetic Stimulation

Asher Geffen[1†], Nicholas Bland[1,2,3†] and Martin V. Sale[1,2†]*

[1] School of Health and Rehabilitation Sciences, The University of Queensland, St Lucia, QLD, Australia, [2] Queensland Brain Institute, The University of Queensland, St Lucia, QLD, Australia, [3] School of Human Movement and Nutrition Sciences, The University of Queensland, St Lucia, QLD, Australia

OPEN ACCESS

Edited by:
Masaki Sekino,
The University of Tokyo, Japan

Reviewed by:
Joaquim Pereira Brasil-Neto,
Unieuro, Brazil
Till R. Schneider,
University of Hamburg, Germany

***Correspondence:**
Asher Geffen
a.geffen@uq.net.au

†ORCID:
Asher Geffen
orcid.org/0000-0002-9982-9534
Nicholas Bland
orcid.org/0000-0001-9610-9972
Martin V. Sale
orcid.org/0000-0002-2913-9212

Specialty section:
This article was submitted to Brain Imaging and Stimulation, a section of the journal Frontiers in Human Neuroscience

Received: 17 June 2021
Accepted: 24 August 2021
Published: 13 September 2021

Citation:
Geffen A, Bland N and Sale MV (2021) Effects of Slow Oscillatory Transcranial Alternating Current Stimulation on Motor Cortical Excitability Assessed by Transcranial Magnetic Stimulation. Front. Hum. Neurosci. 15:726604. doi: 10.3389/fnhum.2021.726604

Converging evidence suggests that transcranial alternating current stimulation (tACS) may entrain endogenous neural oscillations to match the frequency and phase of the exogenously applied current and this entrainment may outlast the stimulation (although only for a few oscillatory cycles following the cessation of stimulation). However, observing entrainment in the electroencephalograph (EEG) during stimulation is extremely difficult due to the presence of complex tACS artifacts. The present study assessed entrainment to slow oscillatory (SO) tACS by measuring motor cortical excitability across different oscillatory phases during (i.e., online) and outlasting (i.e., offline) stimulation. 30 healthy participants received 60 trials of intermittent SO tACS (0.75 Hz; 16 s on/off interleaved) at an intensity of 2 mA peak-to-peak. Motor cortical excitability was assessed using transcranial magnetic stimulation (TMS) of the hand region of the primary motor cortex ($M1_{HAND}$) to induce motor evoked potentials (MEPs) in the contralateral thumb. MEPs were acquired at four time-points within each trial – early online, late online, early offline, and late offline – as well as at the start and end of the overall stimulation period (to probe longer-lasting aftereffects of tACS). A significant increase in MEP amplitude was observed from pre- to post-tACS (paired-sample *t*-test; $t_{29} = 2.64$, $P = 0.013$, $d = 0.48$) and from the first to the last tACS block ($t_{29} = -2.93$, $P = 0.02$, $d = 0.54$). However, no phase-dependent modulation of excitability was observed. Therefore, although SO tACS had a facilitatory effect on motor cortical excitability that outlasted stimulation, there was no evidence supporting entrainment of endogenous oscillations as the underlying mechanism.

Keywords: transcranial alternating current stimulation, transcranial magnetic stimulation, entrainment, plasticity, neural oscillations

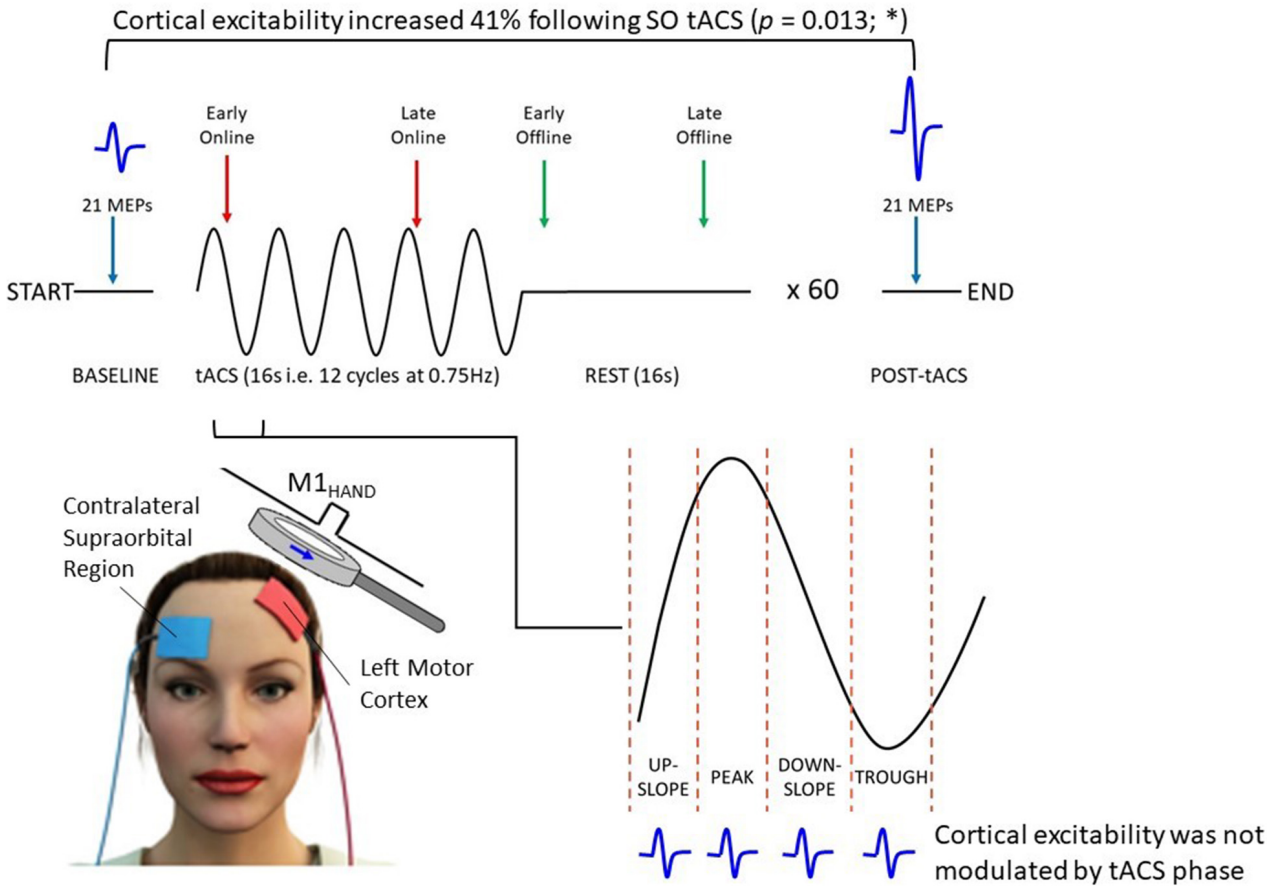

GRAPHICAL ABSTRACT | Thirty healthy participants received 60 trials of intermittent SO (0.75 Hz) tACS (1 trial = 16 s on + 16 s off) at an intensity of 2 mA. Motor cortical excitability was assessed using TMS-induced MEPs (blue waveforms) acquired across different oscillatory phases during (i.e., online; red arrows) and outlasting (i.e., offline; green arrows) tACS, as well as at the start and end of the stimulation session (blue arrows). Mean MEP amplitude increased by ∼41% from pre- to post-tACS (P = 0.013); however, MEP amplitudes were not modulated with respect to the tACS phase.

INTRODUCTION

Neural oscillations (i.e., cyclic fluctuations in neuronal excitability) are proposed to provide phase-dependent temporal regulation of neural information processing (Buzsáki, 2006). In order to explore the functional relationships between neural oscillations and behavior in normal brain function, rhythmic subtypes of transcranial electrical stimulation (tES) have been used to attempt to modulate endogenous neural oscillatory activity experimentally. tES has already been shown to influence various aspects of behavior and cognition by modulating the power of specific neural oscillations known to be associated with such tasks (for reviews see, Antal and Paulus, 2013; Herrmann et al., 2016; Vosskuhl et al., 2018; Bland and Sale, 2019). However, despite promising findings of behavioral effects induced by transcranial alternating current stimulation (tACS), the neurophysiological mechanisms behind these effects are still not well understood.

Converging evidence from animal (e.g., Krause et al., 2019; see also review by Reato et al., 2013), computational (Reato et al., 2010; Ali et al., 2013; Huang et al., 2021), and human studies (Helfrich et al., 2014a,b; Witkowski et al., 2016) suggests that during stimulation, tES may be able to entrain (i.e., synchronize) endogenous neural oscillations with respect to the frequency and phase of the exogenously applied current. However, unlike the well-documented immediate (online) effects of tES, there is less agreement regarding the magnitude and duration of post-stimulus (offline) effects (for review see, Veniero et al., 2015). These offline effects cannot be fully explained by a direct continuation of online entrainment (referred to as entrainment "echoes"), since these "echoes" only persist for a few oscillatory cycles following cessation of stimulation (Marshall et al., 2006; Thut et al., 2011; Hanslmayr et al., 2014; van Bree et al., 2021). Therefore, longer-lasting offline effects (referred to as aftereffects) lasting up to 70 min are likely to reflect mechanisms other than

Abbreviations: tES, transcranial electrical stimulation; tACS, transcranial alternating current stimulation; tDCS, transcranial direct current stimulation; SO, slow oscillatory; TMS, transcranial magnetic stimulation; EEG, electroencephalography; EMG, electromyography; MEP, motor evoked potential; $M1_{HAND}$, hand area of the primary motor cortex; APB, *abductor pollicis brevis;* FISSFO, fade-in, short stimulation, fade-out; STDP, spike-timing dependent plasticity.

entrainment *per se* (e.g., synaptic plasticity) (Neuling et al., 2013; Veniero et al., 2015; Vossen et al., 2015; Kasten et al., 2016).

The effects of tES on endogenous oscillatory activity have traditionally been quantified in humans using electroencephalography (EEG; Marshall et al., 2006; Kirov et al., 2009; Jones et al., 2018; Ketz et al., 2018). However, observing entrainment in the EEG concurrently with tES is extremely difficult due to the presence of complex artifacts (Noury et al., 2016; Noury and Siegel, 2017; Kasten and Herrmann, 2019) and we have therefore used an alternative method to assess entrainment of endogenous neural oscillations by tES. Single-pulse transcranial magnetic stimulation (TMS) is a form of non-invasive brain stimulation that can be used to indirectly probe the excitability of neocortical networks with high spatiotemporal precision of the order of millimeters and milliseconds (Hallett, 2007). When applied to the hand area of the primary motor cortex ($M1_{HAND}$), each TMS pulse induces a motor evoked potential (MEP) in the contralateral target muscle, the amplitude of which can then be measured using electromyography (EMG; Barker et al., 1985). These MEP amplitudes provide an indirect measure of motor cortical excitability with good topographical specificity (Di Lazzaro et al., 2004; Hallett, 2007; Ilmoniemi and Kicić, 2010; Bergmann et al., 2012). By applying TMS pulses within a particular oscillatory phase of tES (referred to as phase-dependent stimulation), TMS can be used to assess entrainment of endogenous neural oscillations by tES (i.e., whether motor cortical excitability is modulated with respect to the phase of tES; Raco et al., 2016; Zrenner et al., 2018; Schaworonkow et al., 2019). Importantly, the artifact issues of EEG are not present with TMS–EMG measures, thus allowing for an unambiguous investigation of the phasic effects of tES on motor cortical excitability.

Because we wanted to probe the phase-specific effects of tES, we chose to apply tES at a low frequency to allow MEP sampling across the different phases of stimulation. In this manner, the phase-cycle of low-frequency tACS could be conceptualized as representing alternating periods of classic "anodal" and "cathodal" transcranial direct current stimulation (tDCS), on which much earlier work has focused (Antal and Paulus, 2013; Reato et al., 2013; Liu et al., 2018; Bland and Sale, 2019). Therefore, in the present investigation, we chose to examine the online and offline effects of slow oscillatory (SO; 0.75 Hz) tACS on motor cortical excitability using TMS.

Slow oscillations are typically prevalent during slow-wave sleep and play an important role in sleep-dependent consolidation of motor learning (Marshall and Binder, 2013). Despite the lack of endogenous SO activity during wakefulness, anodal SO tDCS during wakefulness has been shown to increase endogenous SO EEG power with relatively short-lasting offline effects (<1 min) (Kirov et al., 2009), though the exact duration of these offline effects was not thoroughly assessed. However, it is important to note that these increases in SO power were more restricted topographically to the prefrontal cortex (the predominant source of endogenous slow oscillations during sleep) and were less pronounced than those observed following SO tDCS applied *during* sleep (Marshall et al., 2006). Furthermore, due to the previously mentioned complexity of tES artifacts in the EEG, the authors could not determine whether these localized increases in EEG SO power were in fact due to the entrainment of slow oscillations by SO tDCS. Therefore, it remains unclear whether slow oscillations can be reliably entrained in the awake brain at intensities typical of tES (i.e., 1–2 mA).

Anodal SO tDCS during wakefulness has also been shown to induce lasting increases in motor cortical excitability that persist beyond stimulation (Bergmann et al., 2009; Groppa et al., 2010). However, due to the anodal component (i.e., positive current offset) of this stimulation—which in itself can cause an increase in cortical excitability (Nitsche and Paulus, 2000; Nitsche et al., 2007; Bergmann et al., 2009)—it cannot be concluded that these effects are a direct result of the influence of the applied slow oscillations. tACS has a significant technical advantage over tDCS in this regard, since it has no DC offset (i.e., an average current of 0 mA). Despite this, the effects of SO tACS on motor cortical excitability have not been thoroughly examined in previous literature. Antal et al. (2008) found no significant changes in motor cortical excitability following SO (1 Hz) tACS; however, their stimulation protocol was suboptimal for inducing changes in endogenous oscillatory activity due to the low stimulation intensity (0.4 mA; Reato et al., 2010; Huang et al., 2017) and constant rather than intermittent application of tACS (Jones et al., 2018; Ketz et al., 2018).

The aims of this study were: (1) to investigate the online effects of SO tACS applied intermittently at high intensity on motor cortical excitability; (2) to determine if tACS-induced changes in motor cortical excitability persist beyond each trial of stimulation (i.e., entrainment echoes) as well as beyond the total stimulation period (i.e., offline aftereffects).

It was hypothesized that SO tACS will induce SO-like sinusoidal changes in motor cortical excitability that correspond with the tACS phase, with high MEP amplitudes at oscillatory peaks and low amplitudes at oscillatory troughs, supporting online entrainment. Secondly, that sinusoidal changes in motor cortical excitability will persist for a few oscillatory cycles immediately following each trial of stimulation, thus demonstrating entrainment echoes. Thirdly, that motor cortical excitability will increase over the total duration of stimulation (although this relationship may not necessarily be linear), and this increase will be sustained beyond the total stimulation period (i.e., offline aftereffects).

MATERIALS AND METHODS

Subjects

Forty-one neurologically healthy, right-handed participants (17 male, aged 24 ± 4 years) were recruited by advertisement, although 11 participants were excluded from the final analysis (see "MEP screening" below) leaving a sample size of 30 participants. All participants completed a safety screening questionnaire (Keel et al., 2001) and provided a written statement of informed consent prior to commencing the experiment. The exclusion criteria for participants included: personal or family history of epilepsy/seizures, medication that could affect

seizure threshold, history of brain injury/condition (e.g., stroke, concussion, etc.), implanted devices or metal in the head, frequent or severe headaches, or current pregnancy. Approval was granted by The University of Queensland Human Research Ethics Committee.

Quantification of Motor Cortical Excitability Using TMS

Motor cortical excitability was assessed by measuring TMS-induced MEP amplitudes that were recorded from the target muscle using surface EMG. The target site for the TMS was the left $M1_{HAND}$ region, specifically the region associated with the *abductor pollicis brevis* (APB), a large thumb muscle.

Experimental Setup

EMG

Participants were seated comfortably in a chair and their right forearm placed on a foam mat with their forearm supinated. EMG activity of the APB muscle was recorded using disposable surface electrodes (H124SG 30 mm × 24 mm). The active electrode was placed over the APB muscle belly, the reference electrode was placed over the first metacarpophalangeal joint, and the ground electrode was placed on the anterior surface of the wrist.

TMS

Transcranial magnetic stimulation pulses were applied to the left $M1_{HAND}$ region using a Magstim Double 70 mm Remote Control Coil charged by a Magstim 200^2 stimulator (Magstim, United Kingdom). The individual location of the left $M1_{HAND}$ region as well as the TMS intensity were determined for each participant using manual TMS "hot-spotting" (Rossini et al., 1994). This involves systematically adjusting the position of the TMS coil on the participant's head whilst also adjusting the stimulation intensity until MEPs are consistently induced (i.e., in at least five out of ten successive trials) with amplitudes within a desired range (in our case, 0.5–1.5 mV; see Cuypers et al., 2014; Thies et al., 2018; Ogata et al., 2019). The location of the left $M1_{HAND}$ region was then marked on the participant's scalp using an erasable marker.

tACS

Transcranial alternating current stimulation was applied using a NeuroConn DC Stimulator Plus. The 42 × 45 mm tACS pad electrodes were applied to the scalp using a classical M1-contralateral supraorbital region electrode montage (see Heise et al., 2016), with the target electrode placed over the left M1 (which roughly corresponds with the EEG coordinate C3) and the return electrode placed over the contralateral supraorbital region. However, the electrode targeting the left M1 was not placed directly over the TMS hotspot itself, but rather ∼2 cm posterolateral to the hotspot (which roughly corresponds with Cp3). This slight increase in inter-electrode distance is thought to reduce current shunting through the scalp and cerebrospinal fluid, thus, maximizing current density at the target site and increasing the effectiveness of the tACS (Faria et al., 2011). Before attaching the electrodes, the scalp was rubbed with ethanol (70%) and Ten20 conductive paste was applied to the electrodes to minimize resistance between the electrodes and scalp.

Recording tACS Output

The tACS output was recorded using disposable surface electrodes (H124SG 30 mm × 24 mm). These electrodes were placed over the tACS pad targeting the supraorbital region and on the left side of the forehead, and referenced to the nose tip. The tACS artifact was used to synchronize stimulation with the computer used for MEP acquisition (i.e., such that each probe by TMS was timed with respect to the phase of tACS).

Data Collection

All surface electrode measurements (i.e., APB EMG and tACS output electrodes) were acquired (1 KHz sampling rate; 20–1000 Hz band pass filtering) via an electrode adaptor (Model CED1902-1 1/2), before being amplified by a CED1902, and finally recorded by a CED1401 MICRO3 (Cambridge Electronic Designs, Cambridge, United Kingdom). TMS triggers were directly recorded by the CED1401 MICRO3. All data were then transferred from the CED1401 MICRO3 to a PC and saved via Signal (Ver. 6.04) software (Cambridge Electronic Designs, Cambridge, United Kingdom), before being exported to MATLAB (Ver. R2019a) and subsequently JASP (Ver. 0.14.1.0) for analysis.

Experimental Procedure

tACS Paradigm

Participants received 60 trials of tACS, with each trial consisting of 16 s (12 cycles at 0.75 Hz) of tACS at an intensity of 2 mA ("Online"), followed by 16 s of no tACS ("Offline"), for a total of 16 min of tACS and 16 min of no tACS (**Figure 1A**). The entire stimulation period was divided into 3 blocks (∼10 min comprising 20 trials each), with 5-min rest periods (no tACS or TMS delivered) between blocks.

TMS Paradigm

To examine the online and offline effects of SO tACS on motor cortical excitability, MEPs were acquired at 4 time-points within each trial (1 MEP per time-point): early online (0.1–1.43 s after tACS starts), late online (8.1–9.43 s after tACS starts), early offline (0.1–1.43 s after tACS ends), and late offline (8.1–9.43 s after tACS ends) (**Figure 1B**). Therefore, 60 MEPs were acquired for each time-point (i.e., once each per trial).

To examine if the effects of SO tACS on motor cortical excitability are specific to the tACS phase (both online and offline), sufficient MEPs need to be acquired across the different phases of the tACS (Zoefel et al., 2019). This was achieved by implementing a "jitter" (i.e., a randomized time delay that covers the length of a single tACS cycle) to the delivery of TMS so that the delivery was not locked to a specific phase of the tACS (i.e., the timing of TMS delivery was random across the tACS cycle), and thus, TMS pulses were approximately uniformly delivered across the different phases across the entire stimulation block (**Figure 1C**).

To examine the cumulative effects of the entire tACS paradigm on motor cortical excitability, 21 TMS-induced MEPs were

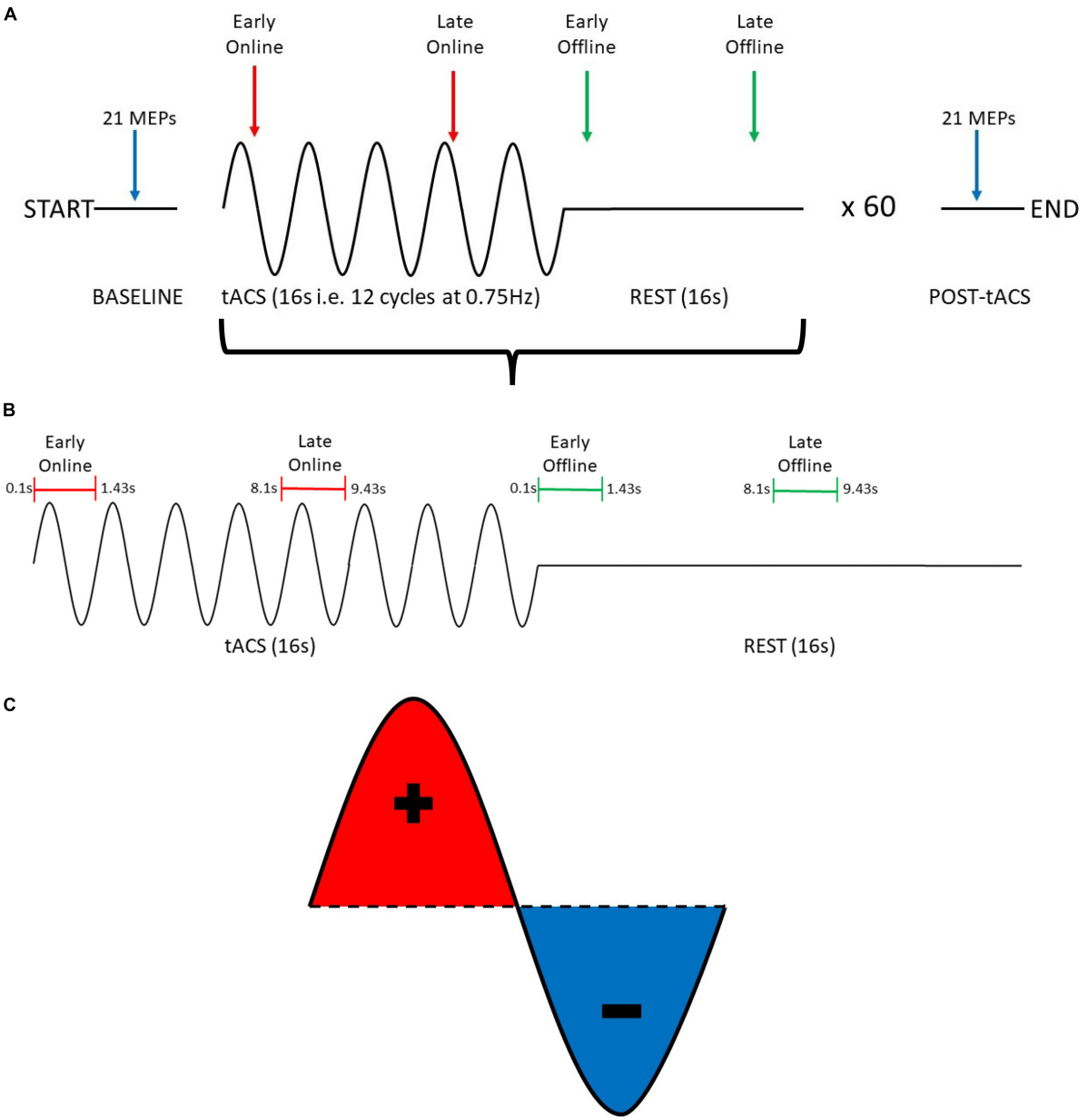

FIGURE 1 | Summary of experimental procedure for probing changes in motor cortical excitability induced by SO tACS. **(A)** The experimental session consisted of a 16-s tACS period (represented as sine waves) followed by a 16-s rest period (represented as flat lines), repeated 60 times for a total of ∼32 min. To probe how tACS-induced changes in motor cortical excitability evolve over time, 21 TMS-induced MEPs were acquired at the start and the end of the experimental session (blue arrows), 2 MEPs were acquired at each tACS period (red arrows), and 2 MEPs were acquired at each rest period (green arrows). **(B)** Within each tACS trial (i.e., tACS + rest period), MEPs were acquired at 4 distinct time-points (1 MEP per time-point): early online, late online, early offline, and late offline. **(C)** tACS alternates polarity between the anode and cathode to produce a sinusoidal current with both positive (red) and negative (blue) peaks.

acquired both at baseline and at the end of the entire period of tACS delivery (**Figure 1A**). TMS was delivered at ∼0.2 Hz.

Statistical Analysis

Data Transformation

The first MEP for each data set (as well as the first MEP after each of the rest periods) was always excluded, since initial MEP amplitudes may be larger (Brasil-Neto et al., 1994) and more variable (Schmidt et al., 2009) than subsequent MEPs, which can impact the reliability of TMS measures of cortical excitability. Further, individual MEPs were excluded if voluntary pre-MEP EMG activity was detected in the 500 ms prior to TMS delivery (2.72% of MEPs excluded). Finally, participants with mean pre-tACS amplitudes less than 0.5 or greater than 1.5 mV were excluded from the final analysis (11 participants excluded). This is because excessively small or large pre-tACS

MEPs may have introduced floor and ceiling effects, respectively (Cuypers et al., 2014).

The TMS triggers were then automatically categorized into their respective time-points (i.e., early online, late online, early offline, and late offline–see **Figure 1B**) and the "late online" triggers were used to calculate the tACS phase, since these triggers are the only ones where tACS was present both before and after TMS was applied, thus, providing the most reliable estimate of tACS phase. If tACS-induced phase entrainment persists beyond stimulation, we would expect the tACS phase to continue into the offline period. To assess this, the computed phase for the late online triggers was extrapolated (both forward and backward) and its values computed at each of the other time-points (**Figure 2**).

Data Analysis

To determine if the effects of SO tACS on motor cortical excitability are specific to the tACS phase a permutation analysis was performed (Zoefel et al., 2019). This analysis was performed separately for each of the four time-points (∼60 MEPs per time-point per participant) as well as for all online and offline MEPs (∼120 MEPs online/offline per participant).

For the permutation analysis, an ideal (i.e., best-fitting, 0.75 Hz) sinusoidal model was fitted to each participant's observed MEP amplitudes based on their phase for each of the four time-points (Bland and Sale, 2019), and the amplitudes of these models were summed. Because these models were fitted with bias (baseline), amplitude, and phase all free to vary across participants, there was no need for alignment of individual "preferred" phase. The MEP amplitudes were then shuffled with respect to their phases to form a surrogate distribution of expected amplitudes under the null hypothesis (which assumes that the MEP amplitudes are not modulated with respect to phase). Next, ideal sinusoidal models were fitted to the shuffled data, and the amplitudes of these shuffled models were summed. This process was repeated for a total of 1000 permutations per participant. The true and shuffled summed amplitudes were then compared. In this analysis, the *P*-value is the proportion of shuffled summed amplitudes exceeding the true sum of amplitudes, remembering that under the null hypothesis the amplitude of these sinusoidal models should be small (i.e., closer to zero). Because the permutation procedure disrupts any phasic effects that may be present, the shuffled MEPs act as a negative control for the true MEPs, and thus, the permutation analysis does not require a sham stimulation condition as a negative control.

To determine if there was a significant difference in mean MEP amplitudes between the pre- and post-tACS measurements, a paired sample *t*-test was performed. To determine if there was a significant difference in mean MEP amplitudes between the online and offline measurements or between the three tACS blocks, a two-way repeated measures ANOVA was performed with *stimulation* (online, offline) and *block* (1, 2, 3) as the two repeated measures factors. *Post hoc t*-tests (corrected for multiple comparisons using Holm's method) were then performed to compare the individual groups against each other. To examine how offline changes in MEP amplitudes evolve throughout the tACS period, mean MEP amplitudes for the pre- and post-tACS MEPs and the offline MEPs of each tACS block were compared using a one-way repeated measures ANOVA with *time* as the repeated measures factor (5 levels). Again, *post hoc t*-tests were then performed to compare the individual groups against each other. For the repeated measures ANOVAs, standardized effect sizes for any significant differences were calculated as η^2 values. For the *post hoc t*-tests, standardized effect sizes for any significant differences were calculated as Cohen's *d* values.

RESULTS

Phase-Specificity of tACS Effects

The phase-specificity of acute changes in motor cortical excitability induced by SO tACS was assessed by a permutation analysis. Ideal sinusoidal models were fitted to each participant's

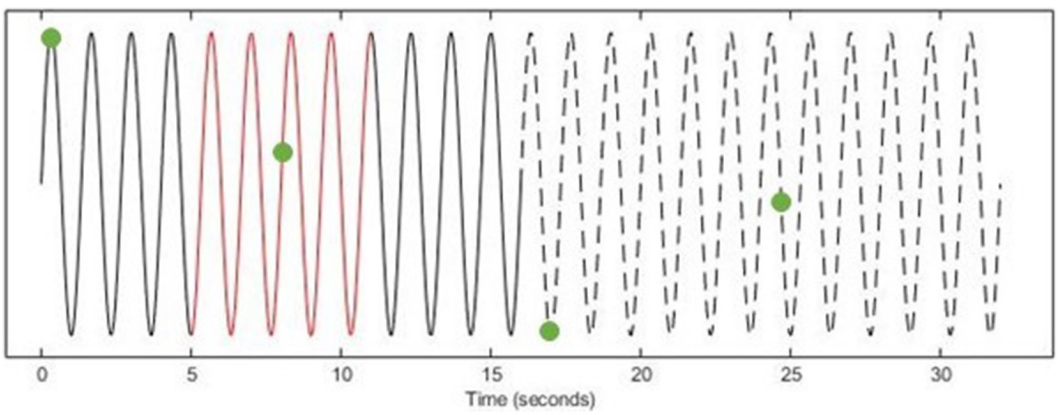

FIGURE 2 | Determining tACS phase at TMS triggers (EXAMPLE ONLY). Using the tACS-output recording (Solid Line), a 6-s window (Red) of the instantaneous phase (*centered* on each late online trigger) was computed. The computed phase was then extrapolated both forward into the offline period (Dashed Line) and backward to the early online triggers (Solid Line) and the phase was computed at each of the other time-points (Green Dots).

observed MEP amplitudes based on their phase for each TMS time-point (∼60 MEPs per time-point per participant, see **Supplementary Figure S1**) and the amplitudes of these models (see **Supplementary Figure S2**) were summed. An example of one of these fitted sinusoidal models is shown in **Figure 3**. The true sum of amplitudes was then compared against the summed amplitudes of 1000 permutations of the MEP amplitudes, with *P*-values representing the proportion of shuffled summed amplitudes exceeding the true sum of amplitudes. The permutation analysis did not reveal significant phase-specific modulation of motor cortical excitability at any of the four TMS time-points (P = 0.86, 0.81, 0.21, and 0.70 for early online, late online, early offline, and late offline, respectively). Combining the early and late online/offline MEPs (∼120 MEPs online/offline per participant) also failed to reveal any significant phase-specific modulation of motor cortical excitability online or offline to tACS (P = 0.89 and 0.90, respectively).

Cumulative Effects of SO tACS on Motor Cortical Excitability

The cumulative effects of the tACS paradigm on motor cortical excitability was assessed by comparing mean MEP amplitudes pre- and post-tACS. As shown in **Figure 4**, MEP amplitudes were found to be significantly greater post-tACS (mean = 1.19 mV ± 0.84) compared to pre-tACS (mean = 0.82 mV ± 0.26) (t_{29} = 2.64, P = 0.013, d = 0.48).

Because there was a significant increase in mean MEP amplitude from pre- to post-tACS, the question arose of whether this overall change in MEP amplitude occurred gradually over time within the stimulation period. We therefore compared online and offline mean MEP amplitudes across each of the three tACS blocks. A two-way repeated measures ANOVA revealed a significant main effect of *block* ($F_{2,58}$ = 3.77, P = 0.03, η^2 = 0.1) but no main effect of *stimulation* ($F_{1,29}$ = 0.65, P = 0.43) and no significant *block* × *stimulation* interaction ($F_{2,58}$ = 1.29, P = 0.28). As shown in **Figure 5**, subsequent *post hoc* *t*-tests confirmed a significant increase in MEP amplitudes between the 1st (mean = 1.19 mV ± 0.72) and 3rd (mean = 1.46 mV ± 0.94) blocks (t_{29} = −2.93, P = 0.02, d = 0.54), whereas there were no significant differences between the 1st and 2nd (mean = 1.33 mV ± 0.79) blocks or between the 2nd and 3rd blocks (t_{29} = −1.6 and −1.04, respectively, P = 0.24 and 0.31, respectively). This suggests a gradual build-up of cortical excitability from tACS.

We also wished to compare mean MEP amplitudes from the offline periods of each block against each other as well as against the pre- and post-tACS mean amplitudes. A one-way repeated measures ANOVA revealed a significant main effect of *time* ($F_{4,116}$ = 7.84, P < 0.001, η^2 = 0.21). As shown in **Figure 5**, subsequent *post hoc* *t*-tests revealed that offline mean MEP amplitudes for all 3 blocks were significantly greater than pre-tACS mean amplitudes (t_{29} = −3.24, −4.02, and −4.56; P = 0.024, 0.003, and <0.001; d = 0.59, 0.73, and 0.83 for blocks 1, 2, and 3, respectively). However, no other significant differences in offline mean amplitude were reported when comparing the blocks against each other or against the post-tACS amplitudes, although the difference between the 1st and 3rd blocks was only marginally insignificant (t_{29} = −2.81, P = 0.06).

It is worth mentioning that widening the exclusion criteria for participants based on their pre-tACS mean MEP amplitudes (0.5–1.5 mV to 0.4–2 mV) did not affect the significance of

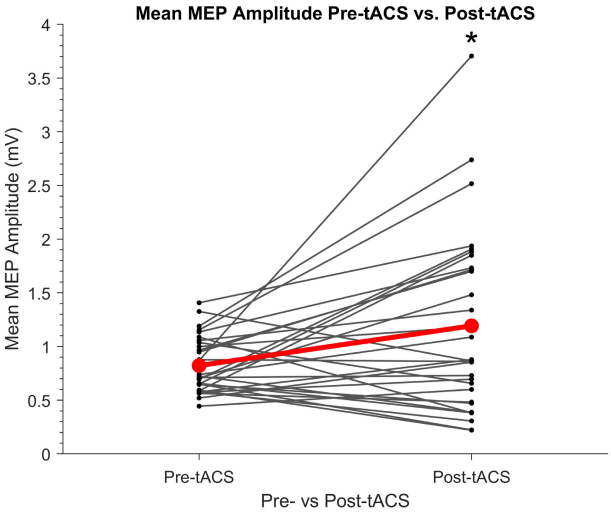

FIGURE 4 | Individual mean amplitudes of TMS-induced MEPs before and after SO tACS. Points represent each participant's mean MEP amplitude from 20 TMS-induced MEPs (per participant) acquired before (pre-tACS) and after (post-tACS) receiving 60 "trials" (∼32 min) of SO tACS, with each trial consisting of 16 s of tACS (12 cycles at 0.75 Hz) followed by 16 s of rest. Individual differences in mean MEP amplitude are represented by the solid lines. The global mean MEP amplitude for each group is represented by a red point, with the global mean difference from pre- to post-tACS represented by a red line connecting the two red points. A significant increase in MEP amplitude from pre-tACS to post-tACS was reported (paired sample *t*-test t_{29} = 2.64, P = 0.013, d = 0.48; indicated by *); n = 30.

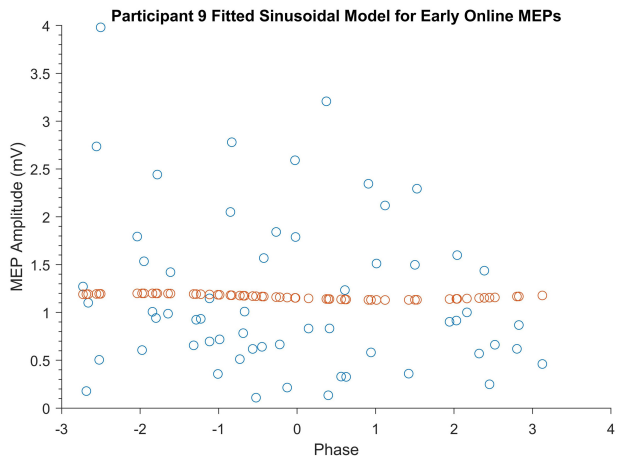

FIGURE 3 | Example of a participant's fitted sinusoidal model for early online MEPs. Blue dots represent Participant 9's early online MEPs sorted according to tACS phase. Orange dots represent the fitted sinusoidal model for these MEPs.

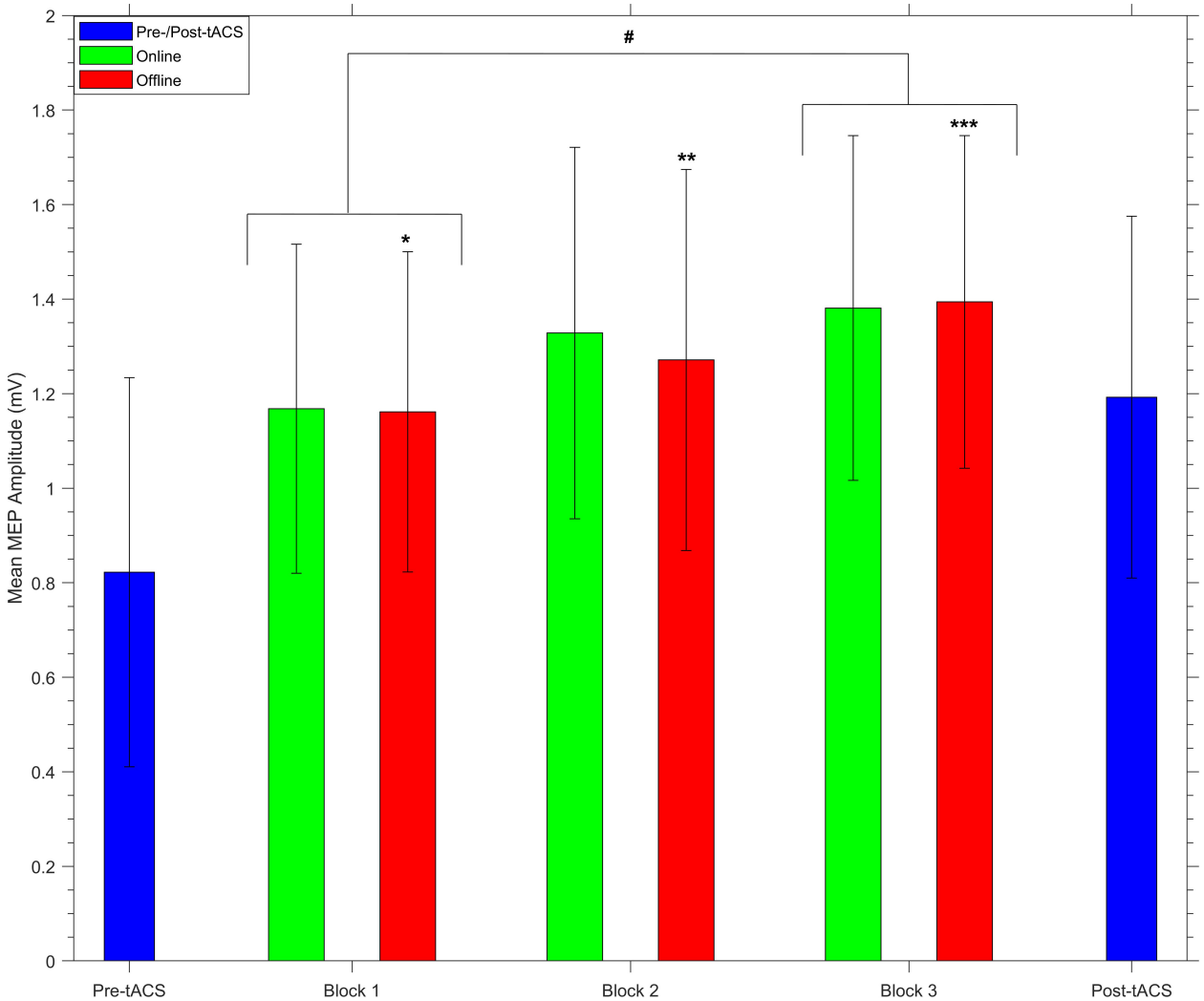

FIGURE 5 | Group mean MEP amplitudes before, during, and after receiving SO tACS. Blue bars represent mean MEP amplitudes (with within-subjects error bars) from 20 TMS-induced MEPs (per participant) acquired before (pre-tACS) and after (post-tACS) receiving 60 "trials" (∼32 min, split into 3 20-trial "blocks") of SO tACS, with each trial consisting of 16 s of tACS (online, 12 cycles at 0.75 Hz) followed by 16 s of rest (offline). Mean MEP amplitudes from 40 MEPs acquired during the online and offline periods of each block are represented by green and red bars, respectively. There was a significant increase in mean amplitude from the 1st to the 3rd block ($t_{29} = -2.93$, $P = 0.02$, $d = 0.54$; indicated by #). Furthermore, offline mean amplitudes were significantly greater than pre-tACS mean amplitudes for all three blocks ($t_{29} = -3.24$, -4.02, and -4.56; $P = 0.024$, 0.003, and <0.001; $d = 0.59$, 0.73, and 0.83 for blocks 1, 2, and 3, respectively; indicated by *, **, and ***, respectively); $n = 30$.

the cumulative or phase-specific effects of SO tACS in the present study, despite increasing the sample size from 30 to 36 participants.

DISCUSSION

Although there has been a plethora of studies in the last decade reporting behavioral, perceptual, and electrophysiological effects induced by tACS (for reviews see, Antal and Paulus, 2013; Herrmann et al., 2016; Vosskuhl et al., 2018; Bland and Sale, 2019), the mechanisms underlying these effects remain only rudimentarily understood. In the present study, we aimed to probe SO tACS-induced entrainment of endogenous slow oscillations both online and offline by assessing motor cortical excitability across different oscillatory phases using TMS-induced MEP amplitudes. We also assessed the cumulative effects of SO tACS on motor cortical excitability by comparing mean excitability pre- and post-stimulation as well as comparing mean excitability across stimulation blocks.

Regarding the cumulative effects of SO tACS, we present the first evidence of enhanced motor cortical excitability induced by SO tACS in the awake brain, with a significant increase in TMS-induced MEP amplitudes from pre- to post-tACS as well as from

the 1st to the 3rd tACS block. Excitability increases induced by anodal SO tDCS have been reported previously (Bergmann et al., 2009; Groppa et al., 2010). However, compared to the SO tDCS study by Bergmann et al. (2009), the present study using SO tACS demonstrated a greater MEP amplitude increase (45.05% vs. 22%) despite shorter stimulation periods (16 s vs. 30 s), shorter total duration of stimulation (16 min vs. 17.5 min), longer rest periods between trials (16 s vs. 5 s) and two additional 5-min rest periods. Critically, due to the lack of an anodal component for tACS, this excitatory effect cannot be attributed to a general depolarization of cortical motor neurons and is thus driven by some other factor.

It is theoretically possible that the cumulative increase in motor cortical excitability was associated with an entrainment of endogenous slow oscillations (Marshall et al., 2006; Kirov et al., 2009; Jones et al., 2018; Ketz et al., 2018). However, the acute effects of stimulation did not appear to be dependent on the tACS phase, with the permutation analysis providing no evidence for phase-specific modulation of motor cortical excitability at any of the four TMS time-points (i.e., early/late online/offline) or for the combined online/offline MEPs.

The most likely explanation for the lack of an entrainment effect in the present results is that endogenous slow oscillations are not prevalent enough in the wake brain to be effectively entrained by SO tACS. This conclusion is in line with previous SO tDCS/tACS studies (Marshall et al., 2006; Bergmann et al., 2009; Kirov et al., 2009; Groppa et al., 2010; Jones et al., 2018; Ketz et al., 2018) as well as tACS studies using different stimulation frequencies (Antal et al., 2008; Kanai et al., 2008; Ali et al., 2013) that found stimulation to be most effective when the frequency of the exogenously applied oscillations closely matches the frequency of the predominant endogenous oscillations. These findings suggest that network resonance is a key underlying mechanism by which tACS modulates large-scale cortical network activity. These resonance dynamics are characterized by a phenomenon called an "Arnold Tongue," where the current intensity required to induce a particular oscillation increases the more the frequency of that oscillation deviates from the resonant (eigen) frequency of the network (Ali et al., 2013; Thut et al., 2017; Liu et al., 2018).

If slow oscillations were in fact entrained by SO tACS, these entrained slow oscillations would likely be of a smaller magnitude than those that naturally occur during sleep (Marshall et al., 2006; Kirov et al., 2009; Jones et al., 2018; Ketz et al., 2018). Therefore, it is possible that the sensitivity of the current permutation analysis was insufficient to detect such a subtle entrainment effect. The sensitivity of our permutation analysis may have been impacted by the relatively low number of MEPs (60 MEPs per time-point per participant), which we know from simulation studies impacts detectability (Zoefel et al., 2019). However, it is important to note that the number of MEPs we could acquire was limited by a number of practical considerations, including coil recharge time, coil heating, and session length, whereas simulation MEP numbers are unencumbered by practical limitations. Because the number of MEPs we can acquire in a single stimulation session is limited by these practical considerations, an alternative option to increase the number of MEPs would be to increase the number of sessions per participant and then pool the MEPs across sessions.

In future experiments, tACS will instead be applied at a frequency that is naturally present in the motor cortex during wakefulness, such as the sensorimotor mu (μ) rhythm (8–13 Hz; Antal et al., 2008; Wach et al., 2013; Gundlach et al., 2017; Thies et al., 2018; Feurra et al., 2019; Madsen et al., 2019). This will also allow us to determine if the excitatory effect observed in the present experiment is specific to SO tACS or if similar effects are observed for other stimulation frequencies.

Alternatively, because the present experiment did not include a negative control stimulation condition for SO tACS (e.g., sham stimulation), it is theoretically possible that the observed increase in motor cortical excitability is simply a time-dependent effect and not mediated by tACS and this is a limitation of the experiment. However, this seems highly unlikely given that a recent meta-analysis by Dissanayaka et al. (2018) reported no significant effects of sham tES on cortical excitability compared to baseline, even up to 90 min following sham tES (Moliadze et al., 2010, 2012; Chaieb et al., 2011). Although only some of the assessed tES studies specifically investigated tACS, all of the studies used a comparable fade-in, short stimulation, fade-out (FISSFO) sham condition, and thus, they can all be used to make inferences about the likely tACS-free changes in MEP amplitude (i.e., solely due to time). This provides a compelling null comparator for the significant increase in MEP amplitude by SO tACS.

Although the underlying cause of the observed increase in MEP amplitude cannot be concluded from the present results, the lack of phase-specific entrainment suggests that this excitatory effect may instead be driven by plasticity-related mechanisms, such as spike-timing dependent plasticity (STDP; Veniero et al., 2015; Vossen et al., 2015). In the STDP model, even a slight mismatch between the stimulation frequency and an individual's spontaneous peak frequency could influence the direction of any induced changes, which may explain the heterogeneity of tACS aftereffects across studies (Veniero et al., 2015). Tests of this model should therefore tailor stimulation frequency to each participant's individual peak frequency rather than use a standard frequency such as was used in the present study.

It is important to note that entrainment and plastic-like effects induced by tACS are not mutually exclusive (Vosskuhl et al., 2018). In fact, Helfrich et al. (2014a,b) found the magnitude of induced aftereffects to be positively correlated with the magnitude of online entrainment and also demonstrated that online effects occurred within a narrow frequency range whilst offline effects occurred across a broader band around the frequency of tACS. This suggests that whilst online effects may be explained by entrainment, sustained aftereffects may be better explained by entrainment-mediated changes to network strength, which then oscillates close (but not necessarily equal) to the frequency of stimulation.

Elucidation of the mechanisms underlying the online and offline effects of tACS will better its therapeutic applications. For example, the ability to induce lasting plastic changes in the motor cortex using tACS may improve the effectiveness of existing rehabilitation for neurological conditions where motor function is compromised.

CONCLUSION

In summary, the significant increase in TMS-induced MEP amplitudes from pre- to post-SO tACS as well as from the 1st to the 3rd SO tACS block suggests that, similar to previously reported excitability increases induced by anodal SO tDCS, SO tACS had a facilitatory effect on motor cortical excitability that outlasted the stimulation period. Importantly, the present findings suggest that these motor cortical excitability increases are not simply due to anodal stimulation. However, given the acute effects of SO tACS were independent of phase, this study does not support entrainment of endogenous slow oscillations as an underlying mechanism for this excitatory effect.

DATA AVAILABILITY STATEMENT

The datasets presented in this study can be found in online repositories. The names of the repository/repositories and accession number(s) can be found below: https://doi.org/10.17605/OSF.IO/DAV4T, Open Science Framework, Reference "SO tACS 2019."

ETHICS STATEMENT

The studies involving human participants were reviewed and approved by The University of Queensland Human Research Ethics Committee. The patients/participants provided their written informed consent to participate in this study.

AUTHOR CONTRIBUTIONS

AG: conceptualization, methodology, software, formal analysis, investigation, data curation, writing–original draft, and visualization. NB: conceptualization, methodology, software, data curation, writing–review and editing, visualization, and supervision. MS: conceptualization, methodology, validation, resources, writing–review and editing, project administration, funding acquisition, and supervision. All authors contributed to the article and approved the submitted version.

FUNDING

This work was supported by the U.S. Office of Naval Research Global (grant number N62909-17-1-2139) awarded to MS. The funding body had no involvement in the study design; the collection, analysis, and interpretation of data; the writing of the report; or the decision to submit the article for publication.

ACKNOWLEDGMENTS

We would like to thank Kylie Tucker for her role as co-supervisor during AG's honors research program. We would also like to thank Laurie and Gina Geffen for their help in proofreading the manuscript.

SUPPLEMENTARY MATERIAL

The Supplementary Material for this article can be found online at: https://www.frontiersin.org/articles/10.3389/fnhum.2021.726604/full#supplementary-material

Supplementary Figure S1 | Fitted sinusoidal models for each participant's late online MEPs. Each scatter plot represents one participant (n = 30), with blue dots (n = 60) representing individual MEP amplitudes (y-axis) sorted according to tACS phase (x-axis). Orange dots represent the sinusoidal model fitted to each scatter plot. A permutation analysis across all participants revealed no significant modulation of late online MEP amplitudes with respect to tACS phase (p = 0.81). Note there was a "gap" in phase values for the first 3 participants due to an error in the MATLAB script that determined the timing of TMS delivery, but this error was addressed after the 3rd participant and the phase gap is not present in any of the other participants.

Supplementary Figure S2 | Histograms of fitted sinusoidal model amplitudes for each position. Bars represent the number of participants with fitted sinusoidal model amplitudes within the range specified on the x-axis for **(A)** early online, **(B)** late online, **(C)** early offline, and **(D)** late offline MEPs.

REFERENCES

Ali, M. M., Sellers, K. K., and Frohlich, F. (2013). Transcranial alternating current stimulation modulates large-scale cortical network activity by network resonance. *J. Neurosci.* 33, 11262–11275. doi: 10.1523/jneurosci.5867-12.2013

Antal, A., Boros, K., Poreisz, C., Chaieb, L., Terney, D., and Paulus, W. (2008). Comparatively weak after-effects of transcranial alternating current stimulation (tACS) on cortical excitability in humans. *Brain Stimul.* 1, 97–105. doi: 10.1016/j.brs.2007.10.001

Antal, A., and Paulus, W. (2013). Transcranial alternating current stimulation (tACS). *Front. Hum. Neurosci.* 7:317. doi: 10.3389/fnhum.2013.00317

Barker, A. T., Jalinous, R., and Freeston, I. L. (1985). Non-invasive magnetic stimulation of human motor cortex. *Lancet* 325, 1106–1107. doi: 10.1016/S0140-6736(85)92413-4

Bergmann, T. O., Groppa, S., Seeger, M., Mölle, M., Marshall, L., and Siebner, H. R. (2009). Acute changes in motor cortical excitability during slow oscillatory and constant anodal transcranial direct current stimulation. *J. Neurophysiol.* 102, 2303–2311. doi: 10.1152/jn.00437.2009

Bergmann, T. O., Mölle, M., Schmidt, M. A., Lindner, C., Marshall, L., Born, J., et al. (2012). EEG-guided transcranial magnetic stimulation reveals rapid shifts in motor cortical excitability during the human sleep slow oscillation. *J. Neurosci.* 32, 243–253. doi: 10.1523/JNEUROSCI.4792-11.2012

Bland, N. S., and Sale, M. V. (2019). Current challenges: the ups and downs of tACS. *Exp. Brain Res.* 237, 3071–3088. doi: 10.1007/s00221-019-05666-0

Brasil—Neto, J. P., Cohen, L. G., and Hallett, M. (1994). Central fatigue as revealed by postexercise decrement of motor evoked potentials. *Muscle Nerve* 17, 713–719. doi: 10.1002/mus.880170702

Buzsáki, G. (2006). *Rhythms of the Brain*. Oxford: Oxford University Press.

Chaieb, L., Antal, A., and Paulus, W. (2011). Transcranial alternating current stimulation in the low kHz range increases motor cortex excitability. *Restorat. Neurol. Neurosci.* 29, 167–175. doi: 10.3233/RNN-2011-0589

Cuypers, K., Thijs, H., and Meesen, R. L. J. (2014). Optimization of the transcranial magnetic stimulation protocol by defining a reliable estimate for corticospinal excitability. *PLoS One* 9:e86380. doi: 10.1371/journal.pone.0086380

Di Lazzaro, V., Oliviero, A., Pilato, F., Saturno, E., Dileone, M., Mazzone, P., et al. (2004). The physiological basis of transcranial motor cortex stimulation

in conscious humans. *Clin. Neurophysiol.* 115, 255–266. doi: 10.1016/j.clinph.2003.10.009

Dissanayaka, T., Zoghi, M., Farrell, M., Egan, G. F., and Jaberzadeh, S. (2018). Sham transcranial electrical stimulation and its effects on corticospinal excitability: a systematic review and meta-analysis. *Rev. Neurosci.* 29, 223–232. doi: 10.1515/revneuro-2017-0026

Faria, P., Hallett, M., and Miranda, P. C. (2011). A finite element analysis of the effect of electrode area and inter-electrode distance on the spatial distribution of the current density in tDCS. *J. Neural Eng.* 8:066017. doi: 10.1088/1741-2560/8/6/066017

Feurra, M., Blagovechtchenski, E., Nikulin, V. V., Nazarova, M., Lebedeva, A., Pozdeeva, D., et al. (2019). State-dependent effects of transcranial oscillatory currents on the motor system during action observation. *Sci. Rep.* 9:12858. doi: 10.1038/s41598-019-49166-1

Groppa, S., Bergmann, T. O., Siems, C., Mölle, M., Marshall, L., and Siebner, H. R. (2010). Slow-oscillatory transcranial direct current stimulation can induce bidirectional shifts in motor cortical excitability in awake humans. *Neuroscience* 166, 1219–1225. doi: 10.1016/j.neuroscience.2010.01.019

Gundlach, C., Müller, M. M., Nierhaus, T., Villringer, A., and Sehm, B. (2017). Modulation of somatosensory alpha rhythm by transcranial alternating current stimulation at mu-frequency. *Front. Hum. Neurosci.* 11:432. doi: 10.3389/fnhum.2017.00432

Hallett, M. (2007). Transcranial magnetic stimulation: a primer. *Neuron* 55, 187–199. doi: 10.1016/j.neuron.2007.06.026

Hanslmayr, S., Matuschek, J., and Fellner, M.-C. (2014). Entrainment of prefrontal beta oscillations induces an endogenous echo and impairs memory formation. *Curr. Biol.* 24, 904–909. doi: 10.1016/j.cub.2014.03.007

Heise, K.-F., Kortzorg, N., Saturnino, G. B., Fujiyama, H., Cuypers, K., Thielscher, A., et al. (2016). Evaluation of a modified high-definition electrode montage for transcranial alternating current stimulation (tACS) of pre-central areas. *Brain Stimul.* 9, 700–704. doi: 10.1016/j.brs.2016.04.009

Helfrich, R. F., Knepper, H., Nolte, G., Strüber, D., Rach, S., Herrmann, C. S., et al. (2014a). Selective modulation of interhemispheric functional connectivity by HD-tACS shapes perception. *PLoS Biol.* 12:e1002031. doi: 10.1371/journal.pbio.1002031

Helfrich, R. F., Schneider, T. R., Rach, S., Trautmann-Lengsfeld, S. A., Engel, A. K., and Herrmann, C. S. (2014b). Entrainment of brain oscillations by transcranial alternating current stimulation. *Curr. Biol.* 24, 333–339. doi: 10.1016/j.cub.2013.12.041

Herrmann, C. S., Strüber, D., Helfrich, R. F., and Engel, A. K. (2016). EEG oscillations: from correlation to causality. *Int. J. Psychophysiol.* 103, 12–21. doi: 10.1016/j.ijpsycho.2015.02.003

Huang, W. A., Stitt, I. M., Negahbani, E., Passey, D. J., Ahn, S., Davey, M., et al. (2021). Transcranial alternating current stimulation entrains alpha oscillations by preferential phase synchronization of fast-spiking cortical neurons to stimulation waveform. *Nat. Commun.* 12:3151. doi: 10.1038/s41467-021-23021-2

Huang, Y., Liu, A. A., Lafon, B., Friedman, D., Dayan, M., Wang, X., et al. (2017). Measurements and models of electric fields in the in vivo human brain during transcranial electric stimulation. *eLife* 6:e18834. doi: 10.7554/eLife.18834

Ilmoniemi, R. J., and Kicić, D. (2010). Methodology for combined TMS and EEG. *Brain Topog.* 22, 233–248. doi: 10.1007/s10548-009-0123-4

Jones, A. P., Choe, J., Bryant, N. B., Robinson, C. S. H., Ketz, N. A., Skorheim, S. W., et al. (2018). Dose-dependent effects of closed-loop tACS delivered during slow-wave oscillations on memory consolidation. *Front. Neurosci.* 12:867. doi: 10.3389/fnins.2018.00867

Kanai, R., Chaieb, L., Antal, A., Walsh, V., and Paulus, W. (2008). Frequency-dependent electrical stimulation of the visual cortex. *Curr. Biol.* 18, 1839–1843. doi: 10.1016/j.cub.2008.10.027

Kasten, F. H., Dowsett, J., and Herrmann, C. S. (2016). Sustained aftereffect of α-tACS lasts up to 70 min after stimulation. *Front. Hum. Neurosci.* 10:245. doi: 10.3389/fnhum.2016.00245

Kasten, F. H., and Herrmann, C. S. (2019). Recovering brain dynamics during concurrent tACS-M/EEG: an overview of analysis approaches and their methodological and interpretational pitfalls. *Brain Topography* 32, 1013–1019. doi: 10.1007/s10548-019-00727-7

Keel, J. C., Smith, M. J., and Wassermann, E. M. (2001). A safety screening questionnaire for transcranial magnetic stimulation. *Clin. Neurophysiol.* 112:720. doi: 10.1016/s1388-2457(00)00518-6

Ketz, N. A., Jones, A. P., Bryant, N. B., Clark, V. P., and Pilly, P. K. (2018). Closed-loop slow-wave tACS improves sleep-dependent long-term memory generalization by modulating endogenous oscillations. *J. Neurosci.* 38, 7314–7326. doi: 10.1523/jneurosci.0273-18.2018

Kirov, R., Weiss, C., Siebner, H. R., Born, J., and Marshall, L. (2009). Slow oscillation electrical brain stimulation during waking promotes EEG theta activity and memory encoding. *PNAS* 106, 15460–15465. doi: 10.1073/pnas.0904438106

Krause, M. R., Vieira, P. G., Csorba, B. A., Pilly, P. K., and Pack, C. C. (2019). Transcranial alternating current stimulation entrains single-neuron activity in the primate brain. *PNAS* 116, 5747–5755. doi: 10.1073/pnas.1815958116

Liu, A. A., Vöröslakos, M., Kronberg, G., Henin, S., Krause, M. R., Huang, Y., et al. (2018). Immediate neurophysiological effects of transcranial electrical stimulation. *Nat. Commun.* 9, 5092–5092. doi: 10.1038/s41467-018-07233-7

Madsen, M., Takemi, M., Kesselheim, J., Tashiro, S., and Siebner, H. R. (2019). Focal TACS of the primary motor hand area at individual mu and beta rhythm–effects on cortical excitability. *Brain Stimul.* 12:572. doi: 10.1016/j.brs.2018.12.896

Marshall, L., and Binder, S. (2013). Contribution of transcranial oscillatory stimulation to research on neural networks: an emphasis on hippocampo-neocortical rhythms. *Front. Hum. Neurosci.* 7:614. doi: 10.3389/fnhum.2013.00614

Marshall, L., Helgadóttir, H., Mölle, M., and Born, J. (2006). Boosting slow oscillations during sleep potentiates memory. *Nature* 444:610. doi: 10.1038/nature05278

Moliadze, V., Antal, A., and Paulus, W. (2010). Boosting brain excitability by transcranial high frequency stimulation in the ripple range. *J. Physiol.* 588, 4891–4904. doi: 10.1113/jphysiol.2010.196998

Moliadze, V., Atalay, D., Antal, A., and Paulus, W. (2012). Close to threshold transcranial electrical stimulation preferentially activates inhibitory networks before switching to excitation with higher intensities. *Brain Stimul.* 5, 505–511. doi: 10.1016/j.brs.2011.11.004

Neuling, T., Rach, S., and Herrmann, C. S. (2013). Orchestrating neuronal networks: sustained after-effects of transcranial alternating current stimulation depend upon brain states. *Front. Hum. Neurosci.* 7:161. doi: 10.3389/fnhum.2013.00161

Nitsche, M. A., Doemkes, S., Karaköse, T., Antal, A., Liebetanz, D., Lang, N., et al. (2007). Shaping the effects of transcranial direct current stimulation of the human motor cortex. *J. Neurophysiol.* 97, 3109–3117. doi: 10.1152/jn.01312.2006

Nitsche, M. A., and Paulus, W. (2000). Excitability changes induced in the human motor cortex by weak transcranial direct current stimulation. *J. Physiol.* 527, 633–639. doi: 10.1111/j.1469-7793.2000.t01-1-00633.x

Noury, N., Hipp, J. F., and Siegel, M. (2016). Physiological processes non-linearly affect electrophysiological recordings during transcranial electric stimulation. *NeuroImage* 140, 99–109. doi: 10.1016/j.neuroimage.2016.03.065

Noury, N., and Siegel, M. (2017). Phase properties of transcranial electrical stimulation artifacts in electrophysiological recordings. *NeuroImage* 158, 406–416. doi: 10.1016/j.neuroimage.2017.07.010

Ogata, K., Nakazono, H., Uehara, T., and Tobimatsu, S. (2019). Prestimulus cortical EEG oscillations can predict the excitability of the primary motor cortex. *Brain Stimul.* 12, 1508–1516. doi: 10.1016/j.brs.2019.06.013

Raco, V., Bauer, R., Tharsan, S., and Gharabaghi, A. (2016). Combining TMS and tACS for closed-loop phase-dependent modulation of corticospinal excitability: a feasibility study. *Front. Cell. Neurosci.* 10:143. doi: 10.3389/fncel.2016.00143

Reato, D., Rahman, A., Bikson, M., and Parra, L. C. (2010). Low-intensity electrical stimulation affects network dynamics by modulating population rate and spike timing. *J. Neurosci.* 30, 15067–15079. doi: 10.1523/JNEUROSCI.2059-10.2010

Reato, D., Rahman, A., Bikson, M., and Parra, L. C. (2013). Effects of weak transcranial alternating current stimulation on brain activity—a review of known mechanisms from animal studies. *Front. Hum. Neurosci.* 7:687. doi: 10.3389/fnhum.2013.00687

Rossini, P. M., Barker, A. T., Berardelli, A., Caramia, M. D., Caruso, G., Cracco, R. Q., et al. (1994). Non-invasive electrical and magnetic stimulation of the brain, spinal cord and roots: basic principles and procedures for routine clinical application. Report of an IFCN committee. *Electroencephalogr. Clin. Neurophysiol.* 91, 79–92. doi: 10.1016/0013-4694(94)90029-9

Schaworonkow, N., Triesch, J., Ziemann, U., and Zrenner, C. (2019). EEG-triggered TMS reveals stronger brain state-dependent modulation of motor evoked potentials at weaker stimulation intensities. *Brain Stimul.* 12, 110–118. doi: 10.1016/j.brs.2018.09.009

Schmidt, S., Cichy, R. M., Kraft, A., Brocke, J., Irlbacher, K., and Brandt, S. A. (2009). An initial transient-state and reliable measures of corticospinal excitability in TMS studies. *Clin. Neurophysiol.* 120, 987–993. doi: 10.1016/j.clinph.2009.02.164

Thies, M., Zrenner, C., Ziemann, U., and Bergmann, T. O. (2018). Sensorimotor mu-alpha power is positively related to corticospinal excitability. *Brain Stimul.* 11, 1119–1122. doi: 10.1016/j.brs.2018.06.006

Thut, G., Bergmann, T. O., Fröhlich, F., Soekadar, S. R., Brittain, J.-S., Valero-Cabré, A., et al. (2017). Guiding transcranial brain stimulation by EEG/MEG to interact with ongoing brain activity and associated functions: a position paper. *Clin. Neurophysiol.* 128, 843–857. doi: 10.1016/j.clinph.2017.01.003

Thut, G., Veniero, D., Romei, V., Miniussi, C., Schyns, P., and Gross, J. (2011). Rhythmic TMS causes local entrainment of natural oscillatory signatures. *Curr. Biol.* 21, 1176–1185. doi: 10.1016/j.cub.2011.05.049

van Bree, S., Sohoglu, E., Davis, M. H., and Zoefel, B. (2021). Sustained neural rhythms reveal endogenous oscillations supporting speech perception. *PLoS Biol.* 19:e3001142. doi: 10.1371/journal.pbio.3001142

Veniero, D., Vossen, A., Gross, J., and Thut, G. (2015). Lasting EEG/MEG aftereffects of rhythmic transcranial brain stimulation: level of control over oscillatory network activity. *Front. Cell. Neurosci.* 9:477. doi: 10.3389/fncel.2015.00477

Vossen, A., Gross, J., and Thut, G. (2015). Alpha power increase after transcranial alternating current stimulation at alpha frequency (α-tACS) reflects plastic changes rather than entrainment. *Brain Stimul.* 8, 499–508. doi: 10.1016/j.brs.2014.12.004

Vosskuhl, J., Strüber, D., and Herrmann, C. S. (2018). Non-invasive brain stimulation: a paradigm shift in understanding brain oscillations. *Front. Hum. Neurosci.* 12:211. doi: 10.3389/fnhum.2018.00211

Wach, C., Krause, V., Moliadze, V., Paulus, W., Schnitzler, A., and Pollok, B. (2013). Effects of 10Hz and 20Hz transcranial alternating current stimulation (tACS) on motor functions and motor cortical excitability. *Behav. Brain Res.* 241, 1–6. doi: 10.1016/j.bbr.2012.11.038

Witkowski, M., Garcia-Cossio, E., Chander, B. S., Braun, C., Birbaumer, N., Robinson, S. E., et al. (2016). Mapping entrained brain oscillations during transcranial alternating current stimulation (tACS). *NeuroImage* 140, 89–98. doi: 10.1016/j.neuroimage.2015.10.024

Zoefel, B., Davis, M. H., Valente, G., and Riecke, L. (2019). How to test for phasic modulation of neural and behavioural responses. *NeuroImage* 202:116175. doi: 10.1101/517243

Zrenner, C., Desideri, D., Belardinelli, P., and Ziemann, U. (2018). Real-time EEG-defined excitability states determine efficacy of TMS-induced plasticity in human motor cortex. *Brain Stimul.* 11, 374–389. doi: 10.1016/j.brs.2017.11.016

Conflict of Interest: The authors declare that the research was conducted in the absence of any commercial or financial relationships that could be construed as a potential conflict of interest.

frontiers in Human Neuroscience

ORIGINAL RESEARCH
published: 12 October 2021
doi: 10.3389/fnhum.2021.738200

A Method to Experimentally Estimate the Conductivity of Chronic Stroke Lesions: A Tool to Individualize Transcranial Electric Stimulation

Joris van der Cruijsen[1,2], Maria Carla Piastra[3], Ruud W. Selles[1,4] and Thom F. Oostendorp[3]*

[1] Department of Rehabilitation Medicine, Erasmus MC, University Medical Center Rotterdam, Rotterdam, Netherlands, [2] Department of Biomechanical Engineering, Delft University of Technology, Delft, Netherlands, [3] Donders Institute for Brain, Cognition and Behavior, Radboud University Medical Center, Nijmegen, Netherlands, [4] Department of Plastic and Reconstructive Surgery and Hand Surgery, Erasmus MC, University Medical Center Rotterdam, Rotterdam, Netherlands

OPEN ACCESS

Edited by:
Masaki Sekino, The University of Tokyo, Japan

Reviewed by:
Brenton Hordacre, University of South Australia, Australia
Gregory Noetscher, Combat Capabilities Development Command United States Army, United States

***Correspondence:**
Joris van der Cruijsen
j.vandercruijsen@erasmusmc.nl

Specialty section:
This article was submitted to Brain Imaging and Stimulation, a section of the journal Frontiers in Human Neuroscience

Received: *08 July 2021*
Accepted: *20 September 2021*
Published: *12 October 2021*

Citation:
van der Cruijsen J, Piastra MC, Selles RW and Oostendorp TF (2021) A Method to Experimentally Estimate the Conductivity of Chronic Stroke Lesions: A Tool to Individualize Transcranial Electric Stimulation. Front. Hum. Neurosci. 15:738200. doi: 10.3389/fnhum.2021.738200

The inconsistent response to transcranial electric stimulation in the stroke population is attributed to, among other factors, unknown effects of stroke lesion conductivity on stimulation strength at the targeted brain areas. Volume conduction models are promising tools to determine optimal stimulation settings. However, stroke lesion conductivity is often not considered in these models as a source of inter-subject variability. The goal of this study is to propose a method that combines MRI, EEG, and transcranial stimulation to estimate the conductivity of cortical stroke lesions experimentally. In this simulation study, lesion conductivity was estimated from scalp potentials during transcranial electric stimulation in 12 chronic stroke patients. To do so, first, we determined the stimulation configuration where scalp potentials are maximally affected by the lesion. Then, we calculated scalp potentials in a model with a fixed lesion conductivity and a model with a randomly assigned conductivity. To estimate the lesion conductivity, we minimized the error between the two models by varying the conductivity in the second model. Finally, to reflect realistic experimental conditions, we test the effect rotation of measurement electrode orientation and the effect of the number of electrodes used. We found that the algorithm converged to the correct lesion conductivity value when noise on the electrode positions was absent for all lesions. Conductivity estimation error was below 5% with realistic electrode coregistration errors of 0.1° for lesions larger than 50 ml. Higher lesion conductivities and lesion volumes were associated with smaller estimation errors. In conclusion, this method can experimentally estimate stroke lesion conductivity, improving the accuracy of volume conductor models of stroke patients and potentially leading to more effective transcranial electric stimulation configurations for this population.

Keywords: bioimpedance, conductivity measurement, electroencephalography, tDCS, stroke lesion

INTRODUCTION

Non-invasive electric brain stimulation techniques, such as transcranial direct current, alternating current, and random noise stimulation (tDCS, tACS, and tRNS), have been proposed to increase the effectiveness of stroke rehabilitation by passing a small current through the cortical regions related to impaired physiological systems (Schlaug et al., 2008). Although favorable results of non-invasive brain stimulation on stroke survivors have been reported (Kim et al., 2010), systematic reviews indicate that the effectiveness of brain stimulation is not consistent in, among others, motor recovery (Lefebvre and Liew, 2017) and aphasia (Elsner et al., 2019).

A possible cause for the lack of consistent effects is that the electrode configurations used may not lead to stimulation reaching the targeted region as intended (Vöröslakos et al., 2018; Laakso et al., 2019). This effect is even more accentuated in stroke subjects due to the influence of brain lesions on the electric field distribution (Minjoli et al., 2017; Piastra et al., 2021a). Simulation of brain stimulation using MRI-based volume conduction models is a means to quantify and optimize stimulation strength at targeted brain regions and has been applied in both healthy subjects (Wagner et al., 2007) and many patient populations, including stroke subjects (Wagner et al., 2007; Datta et al., 2011).

A challenge of MRI-based volume conduction models in stroke patients is that (1) there is a large intersubject variability in lesion location and size (Wagner et al., 2007; Minjoli et al., 2017) and (2) the electric conductivity of the lesion is likely a commonly overlooked source of variability. Currently, most models with stroke lesions assume that the lesion consists only of cerebrospinal fluid (CSF) (Wagner et al., 2007; Datta et al., 2011; Minjoli et al., 2017), primarily based on 1-week post-stroke histology experiments in rodents (Jacobs et al., 2001; Soltanian-Zadeh et al., 2003). However, by visual inspection of MRI of chronic stroke patients, the composition of stroke lesions does not always appear as solely CSF (for examples from our patient sample, see **Figure 1**). Furthermore, a recent review showed that non-invasive measurements of lesion conductivity were highly variable, ranging from 0.1 to 1.77 S/m (McCann et al., 2019). Since simulation studies showed that the lesion conductivity could strongly affect the electric field generated by tDCS (Johnstone et al., 2021; Piastra et al., 2021a), knowing the lesion conductivity is vital in order to apply tDCS as intended.

Several methods have been proposed to estimate individualized head tissue conductivity (see McCann et al., 2019 for an overview). Among others, combined transcranial stimulation and scalp potentials have been used to estimate head tissue conductivity *in vivo* (Oostendorp et al., 2000; Gutiérrez et al., 2004; Dannhauer et al., 2011). A transcranial current is applied in these methods, and the induced scalp potentials are recorded using electroencephalography (EEG) electrodes. At the same time, a volume conductor model of the head is used to compute the scalp potentials assuming specific tissue conductivity. With the volume conductor model, the conductivity of one or more tissues can be estimated by varying the assumed tissue conductivity and minimizing the difference between the recorded and simulated potentials.

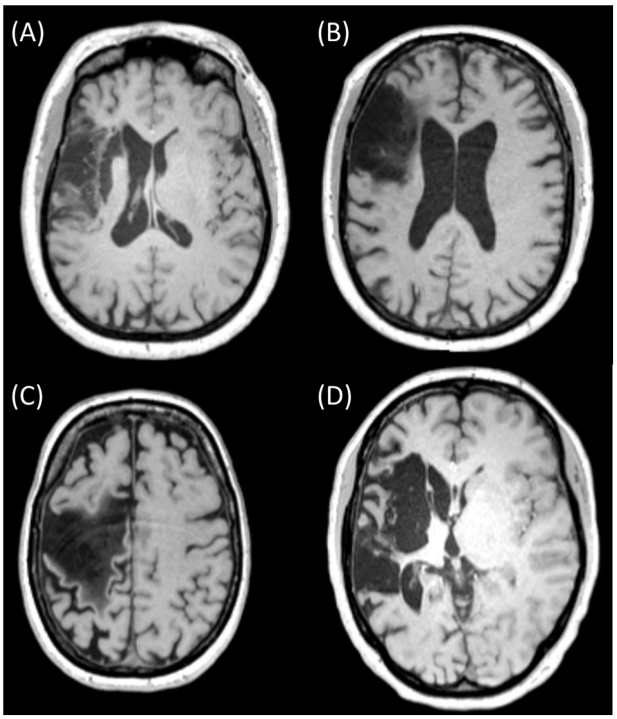

FIGURE 1 | MRI slices of four different chronic stroke subjects showing lesions of various sizes and mixed composition [**(A)** (subject 042), **(B)** (subject 034), and **(C)** (subject 051)] and with primarily CSF [**(D)** (subject 055)]. Ethical approval was acquired to record and publish the MRI slices with consent from the participants (see NL58437.091.17).

A combined transcranial stimulation-EEG-modeling approach has not yet been used for estimating stroke lesion conductivity. The goal of this simulation study is to demonstrate that simultaneous transcranial stimulation and EEG are suitable to estimate chronic stroke lesion conductivity in realistic experimental conditions.

MATERIALS AND METHODS

Data Acquisition

T1-weighted MRI recordings were acquired from 12 chronic stroke subjects (all > 1 year post-stroke, see **Table 1**). All MRIs were recorded using a 3T MAGNETOM Prisma or 3T MAGNETOM PrismaFit scanner. The anonymized MRI scans are available online through the Donders Data Sharing Collection (Piastra et al., 2021b). All MRI data were acquired under the approval of the Ethics Committee "CMO regio Arnhem-Nijmegen" (NL58437.091.17) (Piastra et al., 2021b) with the written informed consent of all patients.

Volume Conductor Model

A four-compartment boundary element model was created from the MRI scan of 12 chronic stroke subjects, using the FieldTrip toolbox (Oostenveld et al., 2011). The models consisted of scalp, skull, CSF, and brain compartments, all modeled with 3,200 mesh

TABLE 1 | Stroke lesion volume and optimal stimulation pairs to estimate the lesion conductivity for each subject.

Subject	Lesion volume (ml)	Lesion depth (mm)	Anode	Cathode
034	37.3	38.5	I2	FTT9h
035	11.9	35.0	TPP10h	Fp1
041	0.2	24.9	P9	FT10
042	13.1	40.5	T7	FTT10h
046	58.9	40.8	P10	F7
048	11.2	38.5	P10	TP7
050	0.1	38.2	P9	F8
051	48.9	37.7	P9	Fp2
053	0.3	25.2	I1	FT10
054	53.3	39.4	FTT10h	FTT9h
055	53.5	36.6	FT9	F8
056	85.2	35.8	TPP10h	TTP7h

elements. The lesion of each stroke patient was segmented using the LINDA algorithm (Pustina et al., 2016). The lesion volumes ranged from 0.1 to 85 ml. In order to assess the effects of lesion depth on the conductivity estimation, we calculated the depth of each lesion as the distance from the lesion centroid to the nearest node of the scalp compartment. For each patient, we created a model without and with the lesion.

MR images of subjects in our sample indicated that the lesion contained mainly CSF (1.71 S/m; McCann et al., 2019; **Figure 1D**), whereas other patients had clear signs of the presence of brain tissue (0.37 S/m) in the lesion (**Figures 1A–C**). Given this variation and the range described in the literature (0.1–1.77 S/m, McCann et al., 2019), we modeled the lesion consecutively with three conductivities: 0.74, 1.23, and 1.71 S/m. The conductivities assigned to scalp, skull, CSF, and brain were, respectively, 0.414, 0.016, 1.71, and 0.37 S/m.

The transcranial stimulation was simulated as described by Oostendorp et al. (2000): the stimulation electrodes were modeled as current monopoles and located 3 mm inside the scalp compartment. The scalp and skull surface meshes were refined near the stimulation electrodes to account for the large gradient of the electric potentials in that region, resulting in—for each patient—approximately 4,000 elements for the scalp and skull compartments. We used the boundary element method to compute the electric potential at the surface of the tissue compartments (Barnard et al., 1967; Oostendorp et al., 2000; Fuchs et al., 2002; Oostenveld and Oostendorp, 2002; Akalin-Acar and Gençer, 2004; Kybic et al., 2006; Stenroos and Sarvas, 2012; Makarov et al., 2020), as the result of a 0.1 mA stimulation current.

Stimulation Configurations

To estimate the lesion conductivity from recorded potentials, the recorded potentials needed to be affected substantially by the presence of a lesion. Therefore, we identified the optimal stimulation electrode pair for each lesion model as the pair with the highest root-mean-square difference (RMSD) in scalp potentials between the same head model with and without a lesion. We performed this step for all patients separately to control for any between-subject differences in the lesion location and size, which cannot be achieved with fixed electrode montages. We considered from the 128 EEG electrodes in the international 10/5 system (Oostenveld and Praamstra, 2001) the subset of electrodes on the outer edge (Fp1/Fp2, F7/F8, FT9/FT10, FTT9h/FTT10h, T7/T8, TTP7h/TTP8h, TP7/TP8, TPP9h/TPP10h, P9/P10, and I1/I2) as potential stimulation electrodes. For each possible pair of these stimulation electrodes, the resulting scalp potentials were calculated at the remaining 126 electrodes not used for stimulation. These scalp potentials were then used to identify the optimal electrode pair based on the RMSD between the model with the lesion and the model without the lesion.

Construction of Recorded Potentials

We simulated scalp potentials for the optimal stimulation pair and extracted data from either 8, 16, 32, 64, and 128 electrodes to investigate the quality of the conductivity estimation with an increasing number of electrodes. For the subset of eight electrodes, we used the eight electrodes closest to the Cz electrode (i.e., Cz, FCz, CPz, C1, C2, FFC1h, Fz, and AFF1). We included an additional electrode at the nasion as the reference electrode for the EEG recordings.

To reflect realistic experimental scenarios, we simulated electrode position errors by imposing a rotation of 0°–5° (corresponding to mean displacements of 0–9 mm, respectively) of the electrode positions around the coronal and sagittal head axes.

Conductivity Estimation

The computed electrode potentials for the optimal stimulation pair were regarded as the measured potentials in an experimental setting, and we will refer to it as the "recorded" potential ψ .

The lesion conductivity was then estimated by the non-linear parameter estimation procedure described in Oostendorp et al. (2000). In this procedure, first, 10 random initial estimates $\widehat{\sigma}_0$ for the lesion conductivity are chosen in an interval between 0.033 and 2 S/m, and the simulated electrode potentials $\varphi(\widehat{\sigma}_0)$ for every conductivity value are computed. Based on the difference between the "recorded" potentials ψ and the simulated model potentials $\varphi(\widehat{\sigma}_0)$, an improved estimate of the lesion conductivity $\widehat{\sigma}_1$ is determined. This process is re-iterated until convergence is reached, defined as <0.1% change in the value of $\widehat{\sigma}_{k-1}$ and $\widehat{\sigma}_k$ at iteration k. We repeated this procedure for each combination of electrode numbers and position errors on the electrodes. Finally, we used the absolute error between the estimated conductivity $\widehat{\sigma}_k$ and the actual conductivity used for the "recorded" potentials as a measure for the quality of the conductivity estimation.

RESULTS

Figure 2 shows the differences in scalp potentials between the models with and without the lesion for subject 035 (small lesion) and subject 055 (large lesion) for the optimal stimulation pair (for an overview of all subjects, see **Table 1**). For most subjects, the anodes of the optimal electrode pairs were primarily located

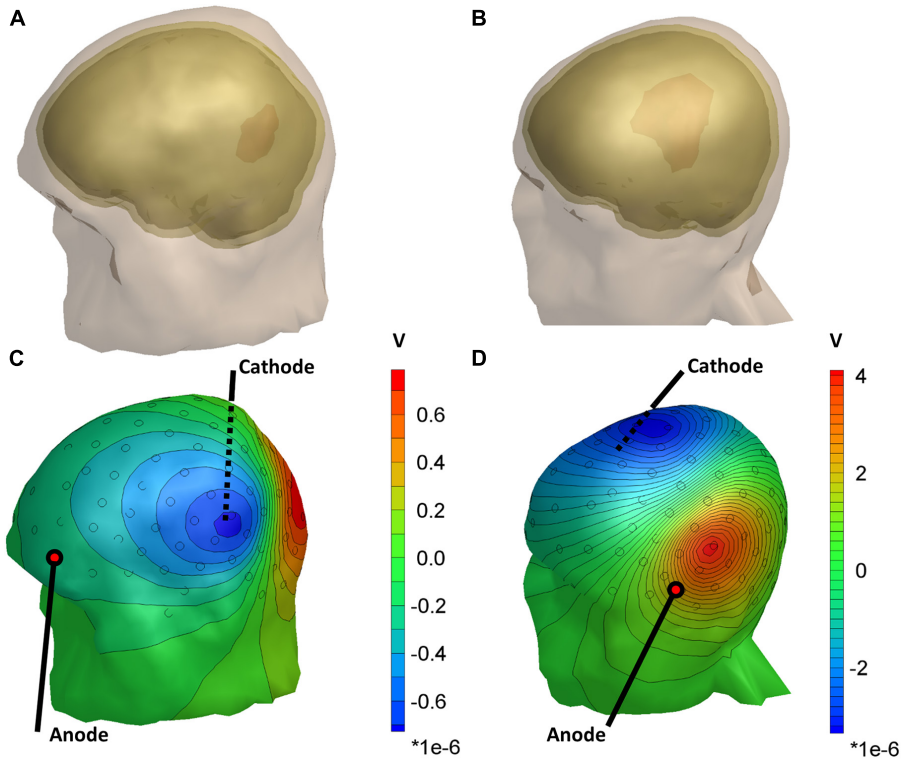

FIGURE 2 | Head models of subject 035 **(A)** and subject 055 **(B)**, showing the lesion volume in red. **(C,D)** The distribution of the difference in scalp potentials between the models with and without the lesion and isopotential lines for the optimal stimulation pair. Black circles represent the 128 measurement electrodes. Note that the magnitude of the color bar varies between the two subjects.

around the left temporal area of the head and the cathodes around the right temporal area (see **Supplementary Figure 1**). However, subjects 034, 035, 051, and 053 had an electrode pair that consisted of frontal (Fp1/Fp2) or occipital (I1/I2) electrodes combined with a temporal electrode. The electric potential difference between the models with and without the lesion showed similar patterns for both subjects: positive potential differences in the vicinity of the anode and negative difference near the cathode. However, the effect of the larger lesion (subject 055, 53.5 ml) on the scalp potentials was about four times larger than for the smaller lesion (subject 035, 11.9 ml).

We found that the conductivity of all lesions was estimated correctly in the absence of electrode rotation (**Figure 3**). For the lesions with the lowest conductivity (0.74 S/m), rotation in coronal direction resulted in mean absolute errors of 0.12 ± 0.18 (mean $\pm$ sd) S/m for 0.1° and 0.24 ± 0.18 for 0.5° rotation. In the sagittal direction, absolute errors of 0.12 ± 0.15 and 0.43 ± 0.28 S/m were found for 0.1° and 0.5° rotation, respectively. **Figure 3** also shows that the estimation errors were highly dependent on lesion size. However, lesion size alone could not fully explain the estimation errors. Lesions larger than 60 ml could be estimated with relative errors near 5%. Interestingly, the 48.9 and 58.9 ml lesions had lower estimation errors than the 53.2 and 85.2 ml lesions. These differences also did not seem to be related to lesion depth, as the smaller lesions were located deeper inside the brain (40.8 and 37.7 mm compared to 35.8–39.4 mm).

For both coronal and sagittal electrode rotation, the estimation error increased with increasing rotation angles, regardless of the lesion size. However, the estimation error did not appear to be consistently related to the number of electrodes used for the conductivity estimation. For instance, for 0.72 S/m lesions and 0.1° coronal rotation, the 11.2 ml lesion (subject 048) was estimated with an error of 0.01 S/m using 16 electrodes. However, the absolute error ranged from 0.06 to 0.17 S/m for the other electrode subsets. Furthermore, for 0.1° coronal rotation, the 37 ml lesion was estimated with an absolute error of at least 0.06 S/m. However, when rotated 0.1° in the sagittal direction, the 37 ml lesion was estimated with absolute errors below 0.05 S/m. For rotation up to 0.5° in coronal direction, the conductivity of lesions larger than 48 ml was estimated with errors below 0.05 S/m for 64 and 128 electrode subsets. In contrast, an opposite pattern was observed for rotation in the sagittal direction: increasing the rotation to 0.5° resulted in estimation errors ranging up as high as the lesion conductivity itself, indicating high sensitivity for coronal rotation.

The effect of modeled lesion conductivity was also tested for all models and electrode rotations. The robustness to 0.5° rotation improved for higher lesion conductivity, with similar mean absolute errors but relative errors reducing from 0.32 ± 0.24 for 0.74 S/m lesions to 0.21 ± 0.17 for 1.72 S/m lesions. For rotations above 1° in either coronal or sagittal direction, the optimization algorithm never converged to the correct lesion

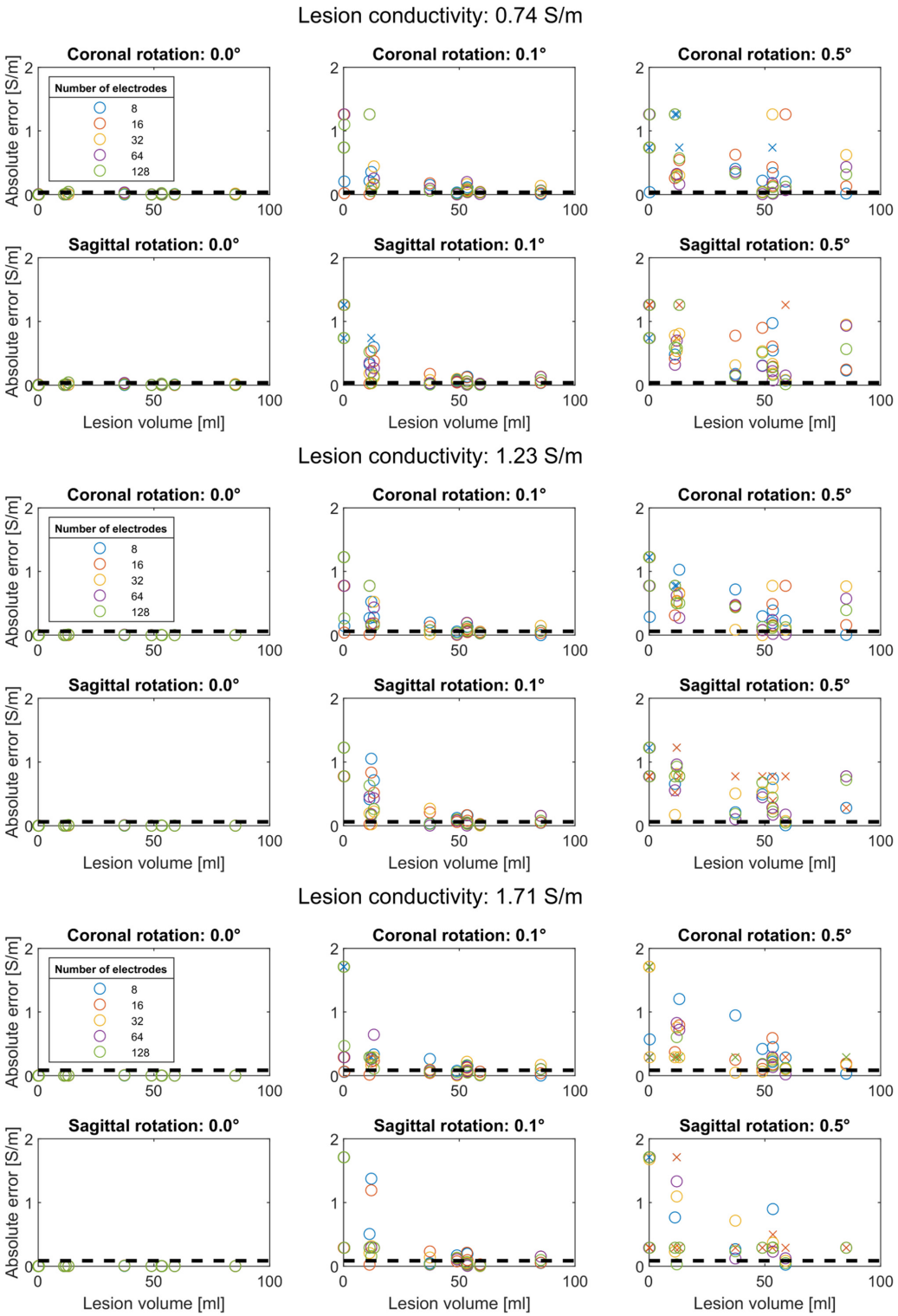

FIGURE 3 | Conductivity estimation accuracy for coronal rotation (first row) and sagittal rotation (second row) for a lesion conductivity of 0.74, 1.23, and 1.71 S/m. Each color represents a different subset of electrodes. The black dashed lines indicate a 5% relative error to the modeled conductivity. Conductivity estimations that did not converge are marked with an "x". Each panel shows that the absolute conductivity estimation error (*y*-axis) reduces with increasing lesion volume (*x*-axis) for rotations up to 0.5°. Without electrode rotation (left column), the conductivity is correctly estimated regardless of lesion size. At the lowest lesion conductivity (0.74 S/m), the estimation procedure is more sensitive to coronal and sagittal electrode rotation, as reflected by larger absolute errors, compared to higher lesion conductivity (1.23 and 1.71 S/m).

conductivity for any combination of electrode subset, lesion volume, or lesion conductivity.

DISCUSSION

We propose a method that combines MRI, EEG, and transcranial stimulation to estimate the conductivity of cortical stroke lesions experimentally. We simulated this method in head models of 12 chronic stroke patients with lesion volumes within the ranges reported in the literature (Chen et al., 2000) and evaluated the effect of the number of EEG recording electrodes and errors in EEG electrode placement. We found that the optimization algorithm converged to the correct lesion conductivity value when noise on the electrode positions was absent. In the case of electrode rotations, estimation error depended on lesion size. However, the conductivity of lesions larger than 50 ml could be estimated with low relative errors when coronal and sagittal rotations remained at 0.1°.

The method we propose requires only a single post-stroke MRI to estimate the lesion conductivity. In the first step of our method, we identified the optimal stimulation pair to estimate the lesion conductivity by evaluating the RMSD between a model with and without the lesion. We found optimal electrode pairs that were localized mainly around the left and right temporal areas. Likely, this is a consequence of the used patient sample, which consisted of stroke patients with lesions in approximately the same regions. Therefore, the optimal stimulation electrode pair is expected to be more variable for lesions at different locations.

The accuracy of the conductivity estimation method depends on several factors. For instance, the accuracy depended on lesion volume; larger lesions more strongly affect scalp potentials than smaller lesions. However, we observed some inconsistency in this pattern, which could not be explained by our measure for the lesion's depth. Nonetheless, more superficial lesions are expected to have a more profound effect on scalp potentials than lesions located deeper inside the brain. However, the measure we used for lesion depth—the distance between the lesion's centroid and the nearest scalp node—might not have been able to take this effect into account when calculated independently of the lesion's size.

Another explanation for the observed differences in estimation accuracy could be that the effects of small lesions were not sufficiently captured by the subsets of electrodes we used. For instance, **Figures 2C,D** show that the lesion introduces only local electric potential differences at the scalp. At the same time, the subsets of 16–128 electrodes we used were distributed uniformly over the scalp. Likewise, the subset of eight electrodes around Cz could be suboptimal if it does not record the largest potential differences due to the lesion. Therefore, selecting a subset of electrodes including only the most affected electrodes—which would vary per subject—could improve our proposed method for small lesions.

An additional factor influencing the accuracy of our results is the lesion conductivity we assumed in the models. We modeled the lesion with three different conductivity values, in-between two times the modeled brain conductivity and CSF conductivity. Like lesion volume, higher lesion conductivity increases the effect the lesion has on the scalp potentials. This is confirmed by the lower absolute errors we found for increased conductivity. Furthermore, the method proved more robust to electrode rotations for lesions with higher conductivity.

Although the conductivity of larger lesions (>50 ml) could successfully be estimated, we found that the conductivity estimation procedure is sensitive to incorrect electrode positions. Especially, rotation in the sagittal direction was detrimental to the conductivity estimation accuracy, which may be explained by the orientation of the isopotential lines near the electrodes that record the strongest effect of the presence of the lesion (**Figures 2C,D**). For coronal rotation, the electrodes rotate more tangent to the isopotential lines, resulting in lower relative differences between the recorded and modeled scalp potentials. This hypothesis is in line with the relatively high robustness to the sagittal rotation of the 37.2 ml lesion of subject 034, for whom an optimal stimulation pair consisting of I2 and FTT9h was found.

For electrode rotations above 1°, the optimization algorithm did not correctly estimate the lesion conductivity. In this situation, scalp potential differences due to electrode position errors surpass those introduced by the lesion. As a consequence, the optimization algorithm can only minimize these errors with unrealistic lesion conductivities, resulting in high relative errors. However, it should be noted that systematic rotations represent a worst-case scenario: in experimental conditions, electrode placement errors may be distributed randomly. Nonetheless, the estimation method results suggest that mean recording electrode position errors should remain below 0.1° (1 mm mean displacement) to keep estimation errors below 5%. These accuracies can only be realized with 3D scanning techniques (Dalal et al., 2014). When applying this method in practice, the patients should ideally wear an MRI-compatible EEG cap during the MRI acquisition to minimize the co-registration error and maximize the conductivity estimation accuracy.

Future work comprises the estimation of the range of lesion conductivities in stroke patients. Furthermore, the effect of more realistic volume conductor models with a more realistic description of the brain, i.e., a separate gray matter and white matter volume, remains to be explored.

Limitations

We did not add random noise reflecting background EEG activity to the scalp potentials. The effect of random noise can be compensated for by either averaging over a prolonged stimulation time or increasing the stimulation intensity. At this point, we simulated stimulation at an intensity of 0.1 mA, which ensures that the method can be applied with low discomfort to the patient. Also, we did not fully control for the depth of the lesions. The conductivity of lesions distant from the scalp, i.e., subcortical lesions, will be more challenging to estimate and potentially explain the inconsistency in the relation between lesion size and conductivity estimation error we observed. However, considering lesion size and depth as independent measures may be an oversimplification that did not explain the inconsistency between lesion size and the observed conductivity estimation error.

We used a four-compartment model without a separate representation of gray and white matter. This simplification was made to reduce the computational load that the segmentation of the complex structure of the brain would introduce. As an alternative, the finite element method would be a more suitable approach to model the human head more efficiently and realistically. The modeled conductivities for the scalp, skull CSF, and brain were based on the literature (McCann et al., 2019) and assumed known. However, skull conductivity varies significantly between individuals (McCann et al., 2019), and an inaccurate assumption would translate to low accuracy of the lesion conductivity estimation. One potential solution is to estimate the skull conductivity based on the scalp potentials in electrodes whose potentials are affected minimally by the lesion.

CONCLUSION

In conclusion, estimating the lesion conductivity can easily be incorporated in experimental procedures that combine tDCS, EEG, and MRI for individualized head models. The achievable estimation accuracy depends on the balance between lesion volume, lesion depth, lesion conductivity, and the measurement electrodes' co-registration error. The accuracy of MRI-based volume conductor models can be improved by including an individualized estimate of the stroke lesion conductivity with our proposed method. As a result, this can lead to the improved application of transcranial electric stimulation in stroke patients.

DATA AVAILABILITY STATEMENT

Publicly available datasets were analyzed in this study. These data can be found here: https://data.donders.ru.nl/collections/di/dcmn/DSC_4020000.14_955?0.

ETHICS STATEMENT

The studies involving human participants were reviewed and approved by the CMO Regio Arnhem-Nijmegen. The patients/participants provided their written informed consent to participate in this study.

AUTHOR CONTRIBUTIONS

JC performed the data analysis. All authors were involved in the design of the study, interpretation of the results, drafted and revised the manuscript, and read and approved the final manuscript.

FUNDING

This work was supported by the Netherlands Organisation of Scientific Research (NWO), domain Applied and Engineering Science (TTW) (i-tDCS: Grant No. 14902).

ACKNOWLEDGMENTS

We would like to thank Vitoria Piai for making the MRI data set available for this study.

SUPPLEMENTARY MATERIAL

The Supplementary Material for this article can be found online at: https://www.frontiersin.org/articles/10.3389/fnhum.2021.738200/full#supplementary-material

REFERENCES

Akalin-Acar, Z., and Gençer, N. G. (2004). An advanced boundary element method (BEM) implementation for the forward problem of electromagnetic source imaging. *Phys. Med. Biol.* 49, 5011–5028. doi: 10.1088/0031-9155/49/21/012

Barnard, A. C. L., Duck, I. M., Lynn, M. S., and Timlake, W. P. (1967). The application of electromagnetic theory to electrocardiology: II. Numerical solution of the integral equations. *Biophys. J.* 7, 463–491. doi: 10.1016/S0006-3495(67)86599-8

Chen, C. L., Tang, F. T., Chen, H. C., Chung, C. Y., and Wong, M. K. (2000). Brain lesion size and location: effects on motor recovery and functional outcome in stroke patients. *Arch. Phys. Med. Rehabil.* 81, 447–452. doi: 10.1053/mr.2000.3837

Dalal, S. S., Rampp, S., Willomitzer, F., and Ettl, S. (2014). Consequences of EEG electrode position error on ultimate beamformer source reconstruction performance. *Front. Neurosci.* 8:42. doi: 10.3389/fnins.2014.00042

Dannhauer, M., Lanfer, B., Wolters, C. H., and Knösche, T. R. (2011). Modeling of the human skull in EEG source analysis. *Hum. Brain Mapp.* 32, 1383–1399. doi: 10.1002/hbm.21114

Datta, A., Baker, J. M., Bikson, M., and Fridriksson, J. (2011). Individualized model predicts brain current flow during transcranial direct-current stimulation treatment in responsive stroke patient. *Brain Stimul.* 4, 169–174. doi: 10.1016/j.brs.2010.11.001

Elsner, B., Kugler, J., Pohl, M., and Mehrholz, J. (2019). Transcranial direct current stimulation (tDCS) for improving aphasia in adults with aphasia after stroke. *Cochrane Database Syst. Rev.* 5:CD009760. doi: 10.1002/14651858.CD009760.pub4

Fuchs, M., Kastner, J., Wagner, M., Hawes, S., and Ebersole, J. S. (2002). A standardized boundary element method volume conductor model. *Clin. Neurophysiol.* 113, 702–712. doi: 10.1016/S1388-2457(02)00030-5

Gutiérrez, D., Nehorai, A., and Muravchik, C. H. (2004). Estimating brain conductivities and dipole source signals with EEG arrays. *IEEE Trans. Biomed. Eng.* 51, 2113–2122. doi: 10.1109/TBME.2004.836507

Jacobs, M. A., Zhang, Z. G., Knight, R. A., Soltanian-Zadeh, H., Goussev, A. V., Peck, D. J., et al. (2001). A model for multiparametric MRI tissue characterization in experimental cerebral ischemia with histological validation in rat: part 1. *Stroke* 32, 943–949. doi: 10.1161/01.STR.32.4.943

Johnstone, A., Zich, C., Evans, C., Lee, J., and Ward, N. (2021). The impact of brain lesions on tDCS-induced electric field magnitude 2 3. *bioRxiv* [Preprint] doi: 10.1101/2021.03.19.436124 bioRxiv 2021.03.19.436124,

Kim, D. Y., Lim, J. Y., Kang, E. K., You, D. S., Oh, M. K., Oh, B. M., et al. (2010). Effect of transcranial direct current stimulation on motor recovery in patients with subacute stroke. *Am. J. Phys. Med. Rehabil.* 89, 879–886. doi: 10.1097/PHM.0b013e3181f70aa7

Kybic, J., Clerc, M., Faugeras, O., Keriven, R., and Papadopoulo, T. (2006). Generalized head models for MEG/EEG: boundary element method beyond

nested volumes. *Phys. Med. Biol.* 51, 1333–1346. doi: 10.1088/0031-9155/51/5/021

Laakso, I., Mikkonen, M., Koyama, S., Hirata, A., and Tanaka, S. (2019). Can electric fields explain inter-individual variability in transcranial direct current stimulation of the motor cortex? *Sci. Rep.* 9:626. doi: 10.1038/s41598-018-37226-x

Lefebvre, S., and Liew, S. L. (2017). Anatomical parameters of tDCS to modulate the motor system after stroke: a review. *Front. Neurol.* 8:1. doi: 10.3389/fneur.2017.00029

Makarov, S., Hamalainen, M., Okada, Y., Noetscher, G. M., Ahveninen, J., and Nummenmaa, A. (2020). Boundary element fast multipole method for enhanced modeling of neurophysiological recordings. *IEEE Trans. Biomed. Eng.* 68, 308–318. doi: 10.1109/tbme.2020.2999271

McCann, H., Pisano, G., and Beltrachini, L. (2019). Variation in reported human head tissue electrical conductivity values. *Brain Topogr.* 32, 825–858. doi: 10.1007/s10548-019-00710-2

Minjoli, S., Saturnino, G. B., Blicher, J. U., Stagg, C. J., Siebner, H. R., Antunes, A., et al. (2017). The impact of large structural brain changes in chronic stroke patients on the electric field caused by transcranial brain stimulation. *NeuroImage Clin.* 15, 106–117. doi: 10.1016/j.nicl.2017.04.014

Oostendorp, T. F., Delbeke, J., and Stegeman, D. F. (2000). The conductivity of the human skull: results of in vivo and in vitro measurements. *IEEE Trans. Biomed. Eng.* 47, 1487–1492. doi: 10.1109/TBME.2000.880100

Oostenveld, R., Fries, P., Maris, E., and Schoffelen, J. M. (2011). FieldTrip: Open source software for advanced analysis of MEG, EEG, and invasive electrophysiological data. *Comp. Intell. Neurosci.* 2011, 1–9. doi: 10.1155/2011/156869

Oostenveld, R., and Oostendorp, T. F. (2002). Validating the boundary element method for forward and inverse EEG computations in the presence of a hole in the skull. *Hum. Brain Mapp.* 17, 179–192. doi: 10.1002/hbm.10061

Oostenveld, R., and Praamstra, P. (2001). The five percent electrode system for high-resolution EEG and ERP measurements. *Clin. Neurophysiol.* 112, 713–719. doi: 10.1016/S1388-2457(00)00527-7

Piastra, M. C., van der Cruijsen, J., Piai, V., Jeukens, F. E. M., Manoochehri, M., Schouten, A., et al. (2021a). ASH: an automatic pipeline to generate realistic and individualized chronic stroke volume conduction head models. *J. Neural Eng.* 18:044001. doi: 10.1088/1741-2552/abf00b

Piastra, M. C., van der Cruijsen, J., Piai, V., Jeukens, F. E. M., Manoochehri, M., Schouten, A., et al. (2021b). Donders Repository. ASH: an Automatic pipeline to generate realistic and individualized chronic Stroke volume conduction Head models. *J. Neural Eng.* doi: 10.34973/5752-rf24

Pustina, D., Coslett, H. B., Turkeltaub, P. E., Tustison, N., Schwartz, M. F., and Avants, B. (2016). Automated segmentation of chronic stroke lesions using LINDA: Lesion identification with neighborhood data analysis. *Hum. Brain Mapp.* 37, 1405–1421. doi: 10.1002/hbm.23110

Schlaug, G., Renga, V., and Nair, D. (2008). Transcranial direct current stimulation in stroke recovery. *Arch. Neurol.* 65, 1571–1576. doi: 10.1001/archneur.65.12.1571

Soltanian-Zadeh, H., Pasnoor, M., Hammoud, R., Jacobs, M. A., Patel, S. C., Mitsias, P. D., et al. (2003). MRI tissue characterization of experimental cerebral ischemia in rat. *J. Magnetic Resonance Imaging* 17, 398–409. doi: 10.1002/jmri.10256

Stenroos, M., and Sarvas, J. (2012). Bioelectromagnetic forward problem: isolated source approach revis(it)ed. *Phys. Med. Biol.* 57, 3517–3535. doi: 10.1088/0031-9155/57/11/3517

Vöröslakos, M., Takeuchi, Y., Brinyiczki, K., Zombori, T., Oliva, A., Fernández-Ruiz, A., et al. (2018). Direct effects of transcranial electric stimulation on brain circuits in rats and humans. *Nat. Commun.* 9:483. doi: 10.1038/s41467-018-02928-3

Wagner, T., Fregni, F., Fecteau, S., Grodzinsky, A., Zahn, M., and Pascual-Leone, A. (2007). Transcranial direct current stimulation: a computer-based human model study. *NeuroImage* 35, 1113–1124. doi: 10.1016/j.neuroimage.2007.01.027

Conflict of Interest: The authors declare that the research was conducted in the absence of any commercial or financial relationships that could be construed as a potential conflict of interest.

Publisher's Note: All claims expressed in this article are solely those of the authors and do not necessarily represent those of their affiliated organizations, or those of the publisher, the editors and the reviewers. Any product that may be evaluated in this article, or claim that may be made by its manufacturer, is not guaranteed or endorsed by the publisher.

frontiers in Human Neuroscience

SYSTEMATIC REVIEW
published: 27 October 2021
doi: 10.3389/fnhum.2021.730134

New Methods, Old Brains—A Systematic Review on the Effects of tDCS on the Cognition of Elderly People

Anna Siegert, Lukas Diedrich and Andrea Antal*

Department of Neurology, University Medical Center Göttingen, Göttingen, Germany

The world's population is aging. With this comes an increase in the prevalence of age-associated diseases, which amplifies the need for novel treatments to counteract cognitive decline in the elderly. One of the recently discussed non-pharmacological approaches is transcranial direct current stimulation (tDCS). TDCS delivers weak electric currents to the brain, thereby modulating cortical excitability and activity. Recent evidence suggests that tDCS, mainly with anodal currents, can be a powerful means to non-invasively enhance cognitive functions in elderly people with age-related cognitive decline. Here, we screened a recently developed tDCS database (http://tdcsdatabase.com) that is an open access source of published tDCS papers and reviewed 16 studies that applied tDCS to healthy older subjects or patients suffering from Alzheimer's Disease or pre-stages. Evaluating potential changes in cognitive abilities we focus on declarative and working memory. Aiming for more standardized protocols, repeated tDCS applications (2 mA, 30 min) over the left dorso-lateral prefrontal cortex (LDLPFC) of elderly people seem to be one of the most efficient non-invasive brain stimulation (NIBS) approaches to slow progressive cognitive deterioration. However, inter-subject variability and brain state differences in health and disease restrict the possibility to generalize stimulation methodology and increase the necessity of personalized protocol adjustment by means of improved neuroimaging techniques and electrical field modeling.

Keywords: transcranial direct current stimulation (tDCS), cognition, episodic memory, declarative memory, aging, elderly

OPEN ACCESS

Edited by:
Masaki Sekino,
The University of Tokyo, Japan

Reviewed by:
Maxciel Zortea,
Hospital de Clínicas de Porto Alegre, Brazil
Anirban Dutta,
University at Buffalo, United States

****Correspondence:***
Anna Siegert
anna.siegert@stud.uni-goettingen.de

Specialty section:
This article was submitted to Brain Imaging and Stimulation, a section of the journal Frontiers in Human Neuroscience

Received: *24 June 2021*
Accepted: *28 September 2021*
Published: *27 October 2021*

Citation:
Siegert A, Diedrich L and Antal A (2021) New Methods, Old Brains—A Systematic Review on the Effects of tDCS on the Cognition of Elderly People. Front. Hum. Neurosci. 15:730134. doi: 10.3389/fnhum.2021.730134

INTRODUCTION

The prognoses are alarming: by 2050 about 16% of the world's population will be aged over 65 (United Nations, 2019). With this comes a dramatic increase in the prevalence of age-related cognitive deterioration: in 30 years ∼152 million people will be suffering from dementia, 60–70% of which with Alzheimer's Disease (AD) (World Health Organization, 2020). Although the body of research on neurodegenerative diseases is extensive, there is no intervention available to cure or to stop the progression of neurodegeneration and thus cognitive decline. This makes clear the necessity for novel treatment.

One of the recently discussed interventions among the novel treatment options is non-invasive brain stimulation (NIBS). The most common electrical stimulation method in the NIBS family used on humans is transcranial direct current stimulation (tDCS). Therefore, in this review we will focus on tDCS and its potential to interfere with age-related cognitive decline.

During tDCS constant weak electric currents (usually 1–2 mA) are applied to the cerebral cortex via external non-invasive electrodes to modulate neuronal excitability, firing rates and thus overall cortical activity (Priori et al., 1998; Nitsche and Paulus, 2000, 2001). Excitability changes are based on altered neuronal membrane potentials resulting in higher probabilities for de- or hyperpolarization (Purpura and McMurtry, 1965; Nitsche et al., 2003a; Lefaucheur et al., 2017). Depending on the direction of current flow (relative to orientations of neuronal axes) membrane potentials increase or decrease–with anodal tDCS being more likely to potentiate depolarization by increasing excitability, whereas cathodal tDCS tends to shift potentials toward hyperpolarization (Bindman et al., 1962; Purpura and McMurtry, 1965; Gorman, 1966; Nitsche and Paulus, 2000, 2001). However, these polarity-dependent predispositions cannot be generalized. Variations in several factors such as stimulation intensity (Batsikadze et al., 2013), duration (Nitsche et al., 2008; Batsikadze et al., 2013) or neuron orientation (more precisely somato-dendritic axis orientation) with respect to current flow (Kabakov et al., 2012; Rahman et al., 2013) may reverse excitatory into inhibitory effects and vice versa (Lefaucheur et al., 2017). Effects of tDCS have not only been observed online (during stimulation) but also offline (after stimulation) (Nitsche and Paulus, 2000, 2001; Nitsche et al., 2003c). Evidence from pharmacological studies suggests that tDCS impacts neuronal plasticity by modulating synaptic transmission via NMDA receptors (Liebetanz et al., 2002; Nitsche et al., 2003a, 2004) and GABA levels (Stagg et al., 2009). On a larger scale tDCS seems to affect functional network connectivity and the synchronization of neuronal populations across the cerebral cortex and within subcortical areas (Keeser et al., 2011; Polanía et al., 2011a,b, 2012).

In the past few years, based on the potential of tDCS to impact neuronal plasticity as well as network connectivity, tDCS studies have been extended to precisely investigate cognitive effects [for review see Shin et al. (2015)]. Evidence has been found that tDCS can modulate memory functions and enhance cognition in physiological (Berryhill and Jones, 2012; Hsu et al., 2015; Prehn and Flöel, 2015) as well as pathological aging (Flöel, 2014). Functional neuroplastic network modifications (Nitsche et al., 2003b) may compensate for age- and neurodegeneration-related cognitive impairments. Further, on the molecular level, tDCS may modulate or induce synaptic plasticity, which potentially results in longer-lasting altered learning and memory capabilities as long-term potentiation (LTP) and –depression (LTD) are thought to be the physiological basis of learning and memory (Bear and Malenka, 1994; Baudry, 2001; Braunewell and Manahan-Vaughan, 2001). Consequently, applying tDCS in the context of age-related cognitive decline [for review see Coffman et al. (2014)] seems promising to restore memory and prevent further deterioration.

TDCS treatment approaches, mainly using anodal stimulation, that can interfere with cognitive decline in early disease-stages appear particularly promising to prevent or slow disease progression such as in mild cognitive impairment (MCI) (Petersen and Negash, 2008). However, since re-discovery of tDCS ∼20 years ago, scientists have applied electrical stimulation in multiple fashions varying montage, current intensity and polarization, and duration as well as the context of application (Lefaucheur et al., 2017). Therefore, tDCS experiments have revealed promising albeit highly variable effects on cognition (Elder and Taylor, 2014). Reining in the high variance through method standardization would be a necessary next step toward developing efficient treatment approaches.

Here we review the potential of tDCS to modulate cognitive functions in the elderly using the tDCS database (http://tdcsdatabase.com). The tDCS database is an open-access community-driven database that has been introduced to the scientific community by prestigious scientists of the field in 2018 (Grossman et al., 2018) and comprises 4.747 entries as of the writing of this review. It compiles mainly human tDCS studies that have been peer-reviewed and include all essential details on the application procedure as well as stimulation parameters (Grossman et al., 2018). Grossman et al. thereby aim to transparently provide scientists with all necessary information to develop efficient tDCS protocols and promote or improve clinical applications, facilitate meta-analysis across studies, and finally reduce variability of tDCS outcomes by optimizing experimental parameters based on previous evidence. For further details of inclusion criteria and maintenance of the database see Grossman et al. (2018).

We aimed to provide a comprehensive overview and further propose suitable tDCS procedures and parameters for future studies aiming to counteract cognitive age-associated deterioration. We focused on studies that investigated modulatory effects of tDCS to intervene with declarative and working memory deterioration as this is one of the major features of age-related cognitive decline (Rönnlund et al., 2005) and is accelerated in dementia (Reitz and Mayeux, 2014).

METHODS

TDCS Database Research

Literature database research was carried out in the tDCS database (http://tdcsdatabase.com) in February 2021. To ensure an efficient database screening several inclusion and exclusion criteria were determined. Inclusion criteria comprised: original paper on tDCS application(s) (previously unpublished data); subject age range starting ≥50 years (studies with old and young subjects were included if the old subject's age range started ≥50 years); focus on cognitive outcome measures of declarative or working memory and a double-blinded, randomized, and sham/placebo-controlled study design (unless it was a pilot or preliminary study). Aging is considered the strongest risk factor for MCI and AD. The prevalence of MCI is increasing dramatically wit age starting from 6.7% for individuals in the range of 60-64 years up to 25.2% for people in the range of 80–84 years (Petersen et al., 2018). A similar situation applies for AD with the first symptoms usually occurring after the age of 60 years (Ballard et al., 2011). With our age range starting ≥50 years we include all potential patients in early and later stages of disease. In this analysis we excluded reviews as well as meta-analyses, single-blinded or uncontrolled studies, case reports, and studies in which the blinding procedure was not mentioned or

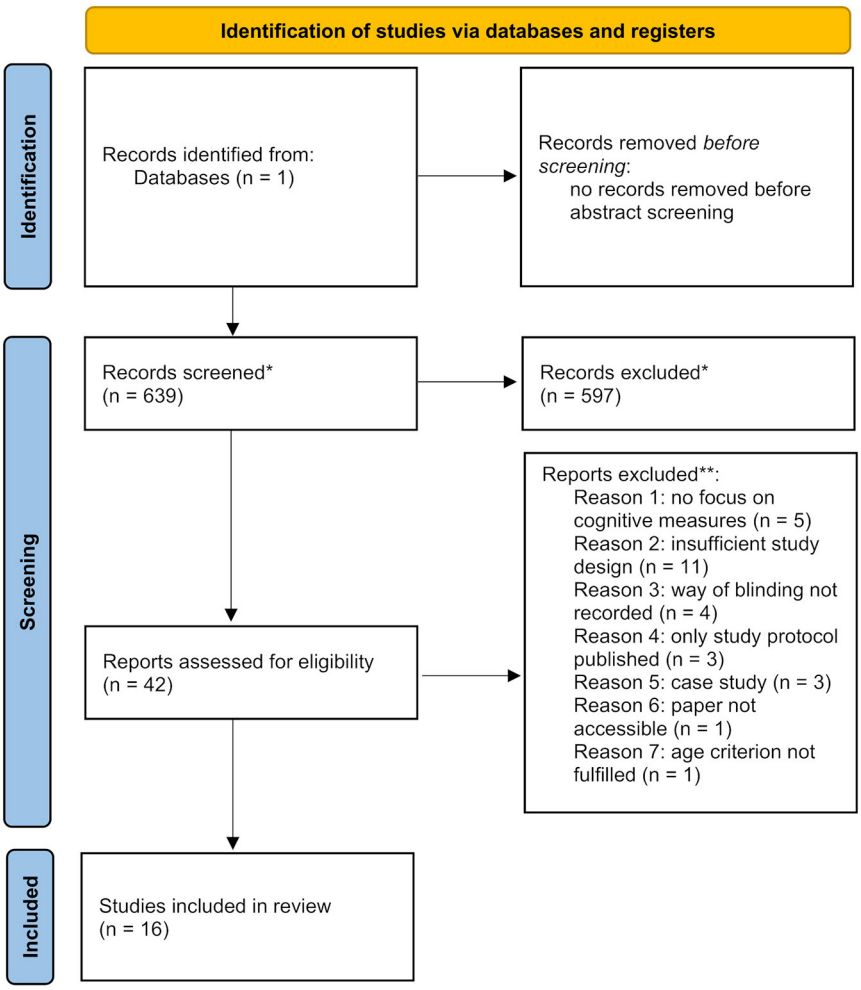

FIGURE 1 | PRISMA flow diagram depicting identification, screening, and inclusion strategies for the selection of the reviewed studies [modified from Page et al. (2021)].

insufficiently described so that it could not clearly be extracted whether double-blinding was assured. The whole process of study identification, screening, eligibility assessment and inclusion was summarized in a PRISMA flow diagram (**Figure 1**).

Keyword Search

Several keyword combinations were used to collect studies (that were further filtered according to above listed inclusion and exclusion criteria). Before precise filtering, abstracts were screened and all preliminary screening results were listed (**Table 1**). The following documentation of keyword search corresponds to the screening order whereby already included publications were not mentioned or listed again if repeatedly returned for other keyword combinations. To begin with, the keywords "transcranial direct current stimulation" or "tDCS" and "elderly" returned two studies that were directly excluded. Next, the search for "transcranial direct current stimulation" and "aging" revealed 186 studies. Abstract screening resulted in 12 studies considered relevant. Furthermore, "tDCS" and "aging" returned 24 additional studies of which two were selected. The keywords "transcranial direct current stimulation" or "tDCS" and "older" or "old" filtered out five studies of which 1 passed the abstract screening. Subsequently, the screening process was further specified. A combination of "transcranial direct current stimulation," "cognition" and "aging" returned 19 studies with 1 relevant publication. Keyword filtering for "transcranial direct current stimulation" or "tDCS," "memory" and "aging" added 1 more relevant publication out of 25 results, while "tDCS" and "memory" returned 34 studies of which five were considered relevant according to their abstracts. Another more focused

TABLE 1 | List of all studies that passed the keyword and abstract screening in the tDCS database.

Keywords (or other search key)	# Studies	Selected studies (PMID)	Title	References	Country	Consideration for review*
Transcranial direct current stimulation, aging	186	31196835	Effects of 6-month at-home transcranial direct current stimulation on cognition and cerebral glucose metabolism in Alzheimer's disease	Im et al., 2019	South Korea	included
		33160420	Cognitive training and brain stimulation in prodromal Alzheimer's disease (AD-Stim)-study protocol for a double-blind randomized controlled phase IIb (monocenter) trial	Thams et al., 2020	Germany	included
		26923418	Older adults get episodic memory boosting from non-invasive stimulation of prefrontal cortex during learning	Sandrini et al., 2016	Italy	included
		26200716	Better together: Left and right hemisphere engagement to reduce age-related memory loss	Brambilla et al., 2015	Italy	excluded, (1) and (2)
		25449530	Transcranial direct current stimulation in mild cognitive impairment: Behavioral effects and neural mechanisms	Meinzer et al., 2015	Germany	included
		29050849	Neuronal and behavioral effects of multi-day brain stimulation and memory training	Antonenko et al., 2018	Germany	excluded, (3)
		28946572	Anodal transcranial direct current stimulation over the right hemisphere improves auditory comprehension in a case of dementia	Costa et al., 2017	Italy	excluded, (5)
		28707568	Effects of transcranial direct current stimulation on neural networks in young and older adults	Martin et al., 2017	Germany	excluded, (1) and (3)
		28314813	tDCS-induced modulation of GABA levels and resting-state functional connectivity in older adults	Antonenko et al., 2017	Germany	excluded, (1)
		27903289	Changes in cerebral glucose metabolism after 3 weeks of non-invasive electrical stimulation of mild cognitive impairment patients	Yun et al., 2016	South Korea	included
		27381076	Brain stimulation during an afternoon nap boosts slow oscillatory activity and memory consolidation in older adults	Ladenbauer et al., 2016	Germany	excluded, (2)
		27178247	Older adults improve on everyday tasks after working memory training and neurostimulation	Stephens and Berryhill, 2016	USA	excluded, (2)
tDCS, aging	24	24062685	Enhancing verbal episodic memory in older and young subjects after non-invasive brain stimulation	Manenti et al., 2013	Italy	excluded, (2)
		26696882	No significant effect of prefrontal tDCS on working memory performance in older adults	Nilsson et al., 2015	Sweden	excluded, (2)
Transcranial direct current stimulation (or tDCS), older	5	27247261	Boosting slow oscillatory activity using tDCS during early nocturnal slow wave sleep does not improve memory consolidation in healthy older adults	Paßmann et al., 2016	Germany	excluded, (2)
Transcranial direct current stimulation, cognition, aging	19	28062255	Differential effects of bihemispheric and unihemispheric transcranial direct current stimulation in young and elderly adults in verbal learning	Fiori et al., 2017	Italy	included
Transcranial direct current stimulation (or tDCS), memory, aging	25	26116933	Memory improvement via slow-oscillatory stimulation during sleep in older adults	Westerberg et al., 2015	USA	included

(Continued)

TABLE 1 | Continued

Keywords (or other search key)	# Studies	Selected studies (PMID)	Title	References	Country	Consideration for review*
tDCS, memory	34	24678298	Anodal tDCS during face-name associations memory training in Alzheimer's patients	Cotelli et al., 2014	Italy	excluded, (4)
		22016735	Improved proper name recall in aging after electrical stimulation of the anterior temporal lobes	Ross et al., 2011	USA	excluded, (3)
		28485663	Can 8 months of daily tDCS application slow the cognitive decline in Alzheimer's disease? A case study	Bystad et al., 2017	Norway	excluded, (5)
		28509625	Direct-current stimulation does little to improve the outcome of working memory training in older adults	Nilsson et al., 2017	Sweden	excluded, (3)
		26250473	Effects of transcranial direct current stimulation upon attention and visuoperceptual function in Lewy body dementia: A preliminary study	Elder et al., 2016	UK	excluded, (1)
Transcranial direct current stimulation (or tDCS), memory, aged	44	28934620	Clinical utility and tolerability of transcranial direct current stimulation in mild cognitive impairment	Murugaraja et al., 2017	India	excluded, (2)
		28637840	Promoting sleep oscillations and their functional coupling by transcranial stimulation enhances memory consolidation in mild cognitive impairment	Ladenbauer et al., 2017	Germany	excluded, (2)
		27653887	At-home tDCS of the left dorsolateral prefrontal cortex improves visual short-term memory in mild vascular dementia	André et al., 2016	Germany	excluded, (1)
		27005937	Transcranial direct current stimulation as a memory enhancer in patients with Alzheimer's disease: A randomized, placebo-controlled trial	Bystad et al., 2016	Norway	included
		31529691	Randomized controlled trial of tDCS on cognition in 201 seniors with mild neurocognitive disorder	Lu et al., 2019	Hong Kong	included
		26499250	Would transcranial direct current stimulation (tDCS) enhance the effects of working memory training in older adults with mild neurocognitive disorder due to Alzheimer's disease: Study protocol for a randomized controlled trial	Cheng et al., 2015	Hong Kong	excluded, (4); actual study: PMID 31529691
		28390970	Transcranial direct current stimulation can enhance working memory in Huntington's disease	Eddy et al., 2017	UK	excluded, (7)
Transcranial direct current stimulation, cognition, aged	48	25379604	Transcranial direct current stimulation and cognitive training in the rehabilitation of Alzheimer's disease: A case study	Penolazzi et al., 2015	Italy	excluded, (5)
Found in a review	1	23884951	Anodal transcranial direct current stimulation temporarily reverses age-associated cognitive decline and functional brain activity changes	Meinzer et al., 2013	Germany	included
Found in a previously listed paper	1	25346688	A double-blind randomized clinical trial on the efficacy of cortical direct current stimulation for the treatment of Alzheimer's disease	Khedr et al., 2014	Egypt	included
Transcranial direct current stimulation, memory	194	27555381	Effects of anodal transcranial direct current stimulation and serotonergic enhancement on memory performance in young and older adults	Prehn et al., 2017	Germany	included

(Continued)

TABLE 1 | Continued

Keywords (or other search key)	# Studies	Selected studies (PMID)	Title	References	Country	Consideration for review*
Manenti, Sandrini	4	29259554	Strengthening of existing episodic memories through non-invasive stimulation of prefrontal cortex in older adults with subjective memory complaints	Manenti et al., 2017	Italy	included
Ferrucci	41	18525028	Transcranial direct current stimulation improves recognition memory in Alzheimer's disease	Ferrucci et al., 2008	Italy	included
		16843494	Effects of transcranial direct current stimulation on working memory in patients with Parkinson's disease	Boggio et al., 2006	Brazil	excluded, (2)
		21840288	Prolonged visual memory enhancement after direct current stimulation in Alzheimer's disease	Boggio et al., 2012	Italy, Brazil	included
Berryhill, Jones	9	22684095	tDCS selectively improves working memory in older adults with more education	Berryhill and Jones, 2012	USA	excluded, (2)
PubMed studies (that will be added to tDCS database)	4	29736192	The effects of transcranial direct current stimulation on the cognitive functions in older adults with mild cognitive impairment: A pilot study	Cruz Gonzalez et al., 2018	Hong Kong	included
		30395314	Effects of transcranial direct current stimulation on episodic memory in amnestic mild cognitive impairment: A pilot study	Manenti et al., 2020	Italy or UK	excluded, (6)
		29313802	Augmenting cognitive training in older adults (The ACT Study): Design and Methods of a Phase III tDCS and cognitive training trial	Woods et al., 2018	USA	excluded, (4)
		30783198	tDCS-induced episodic memory enhancement and its association with functional network coupling in older adults	Antonenko et al., 2019	Germany	excluded, (2)

**Results tabulated include studies prior to application of inclusion/exclusion criteria with indication whether the study was included or excluded as well as reasons for exclusion. *Reasons for exclusion: (1) cognitive (declarative or working memory) outcome measures of tDCS effects are not a focus of the study, (2) study design insufficient (single-blinded, not sham/placebo controlled), (3) blinding procedure not recorded, (4) publication only contains study protocol, (5) case study, (6) restricted access to the paper until submission of this review, (7) age criterion not fulfilled.*

search for "transcranial direct current stimulation" or "tDCS," "memory" and "aged" resulted in 44 and for "transcranial direct current stimulation," "cognition" and "aged" in 48 studies of which a total number of eight studies remained after abstract selection. Two more studies were found and included as they were cited in a review or one of the previously included papers. Finally, the keywords "transcranial direct current stimulation" and "memory" only returned 1 more relevant study out of 194 results as other appropriate papers were already included. Based on further evidence for relevant studies extracted from previous inclusions an author search for "Manenti" and "Sandrini" (four results), "Ferrucci" (41 results) and "Berryhill" and "Jones" (nine results) returned five other relevant studies. These were not found previously as they did not contain the keywords "transcranial direct current stimulation." Four more recently published studies that seemed relevant were only available on PubMed but will subsequently be added to the tDCS database upon approval. The abstract screening eventually resulted in a list of 42 publications (**Table 1**) that were precisely filtered according to exclusion and inclusion criteria so that 16 studies remained to be reviewed (**Table 2**).

RESULTS

Overview

The 16 studies that met all inclusion criteria were performed between 2008 and 2019 (more recent publications had to be excluded, see **Table 1**) and included 543 subjects comprising 60.8% females and 39.2% males. Thirty-eight subjects dropped out during the course of the respective study making a total drop-out rate of 7.1%. All older participants were aged between 50 and 90 years (only 2 studies included younger control groups). Five out of 16 studies included only healthy elderlies (Meinzer et al., 2013; Westerberg et al., 2015; Sandrini et al., 2016; Fiori et al., 2017; Prehn et al., 2017), while the remaining studies applied tDCS to patients suffering from MCI, subjective memory decline (SMC), neurocognitive disorder due to AD (NCD-AD) or probable as well as mild to moderate AD (Ferrucci et al., 2008; Boggio et al., 2012; Cotelli et al., 2014; Khedr et al., 2014; Meinzer et al., 2015; Bystad et al., 2016; Yun et al., 2016; Manenti et al., 2017; Cruz Gonzalez et al., 2018; Im et al., 2019; Lu et al., 2019). In order to evaluate the effectiveness of tDCS protocols applied to patients suffering from different age-associated diseases, the results section considers outcomes in healthy subjects and patients with the above listed cognitive diseases separately. Thereby, we aim to provide an overview of limitations and successes of tDCS in patients in comparison to healthy individuals. We think that efficient stimulation methodologies to treat age-related cognitive decline can only be proposed when considering disease-related variability in tDCS efficiency. Variability may exist when comparing applications in healthy vs. diseased brains but also in the different age-associated diseases as well as different disease states due to varying degrees of progression of neurodegeneration or different brain areas affected.

TDCS in Healthy Elderly People

To begin with, assuming that tDCS has the potential to modulate cognitive functions in healthy aging, Meinzer et al. combined anodal tDCS during an overt semantic learning task with functional magnetic resonance imaging (fMRI) to investigate effects on task performance as well as local brain activity. The main outcome of this study was enhanced word retrieval and restoring of "youth-like" network connectivity in old subjects after receiving unihemispheric anodal tDCS to the left ventral inferior frontal gyrus in comparison to the old and young sham groups (Meinzer et al., 2013). Based on this, Fiori et al. tried to assess whether bihemispheric tDCS over temporo-parietal areas (with the anode on the left and the cathode on the right contralateral hemisphere) differently impacts the performance in a verbal learning task in old vs. young subjects in comparison to unihemispheric tDCS. Here, stimulation did not affect the performance in young participants while older subjects seemed to profit from bihemispheric tDCS manifested in significantly higher numbers of correctly retrieved words (Fiori et al., 2017). Both studies referred to evidence on age-related altered network connectivity and aimed to compensate for "bihemispehric hyperactivities." Another study investigated combined effects of tDCS and selective serotonin reuptake inhibitors (SSRIs) on healthy cognition in elderly people (Prehn et al., 2017). Prehn et al. assumed that this combination of two potential cognition-enhancing methodologies might lead to synergistic effects and thus ameliorate memory performance. The assessment of object-location learning indicated that a combination of SSRIs and tDCS but not single-modality treatment improved immediate memory but surprisingly worsened learning performance in comparison to other conditions. However, this was one of the only studies placing the anode on the right (temporal) cortex (Prehn et al., 2017). Sandrini et al. showed that anodal tDCS over the left dorso-lateral prefrontal cortex (LDLPFC) improved delayed recall in comparison to sham tDCS in old subjects after a verbal episodic memory task when applied during the learning phase (Sandrini et al., 2016). Finally, Westerberg et al. applied bilateral anodal sinusoidal slow-oscillatory tDCS (so-tDCS) with a frequency of 0.75 Hz to the mid-lateral frontal cortex of healthy elderlies during sleep, hypothesizing that age-related memory decline could be a consequence of decreased memory consolidation during altered sleep upon aging. So-tDCS enhanced verbal recall in old participants in comparison to sham so-tDCS and slow-oscillatory activity in the frontal lobe (Westerberg et al., 2015).

TDCS in Age-Associated Diseases

Mild Cognitive Impairment and Subjective Memory Complaints

Expanding their examinations on the potential of tDCS to counteract cognitive decline, Meinzer et al. performed another study applying a similar tDCS and fMRI methodologies as in Meinzer et al. (2013) to patients with MCI (Meinzer et al., 2015). In baseline conditions patients performed significantly worse in a word retrieval task compared to elderly healthy controls. However, word-retrieval performance was significantly ameliorated up to the level of controls after anodal tDCS over

TABLE 2 | Summary of all studies reviewed including most important features and tDCS parameters.

References (PMID)	Study design	Participants (N, female/male, age [mean ± SD and/or range], condition*)	Drop-outs	Stimulation parameters					Behavioral (cognitive) effects
				Montage	Intensity	Duration	# Active tDCS sessions	Timepoint of tDCS	
Im et al. (2019) (31196835)	Sham-controlled, double-blinded, randomized	*N* = 18, 15/3, 73.4, 60–85, early AD	2	Anode F3, cathode F4	2 mA	30 min	Every day for 6 months	Baseline	+
Sandrini et al. (2016) (26923418)	Sham-controlled, double-blinded, randomized	*N* = 28, 17/11, 68.9, healthy	None	Anode F3, cathode right supraorbital region	1.5 mA	15 min	Up to 5	During learning phase	+
Meinzer et al. (2015) (25449530)	Sham-controlled, double-blinded, randomized, counterbalanced	*N* = 36, 14/22, 69.56 ± 5.56 (healthy group), 67.44 ± 7.27 (MCI group), healthy and MCI	None	Anode left ventral IFG, cathode right supraorbital area	1 mA	20 min	1	During rs- and task-related fMRI (semantic word retrieval)	+
Yun et al. (2016) (27903289)	Sham-controlled, double-blinded, randomized	*N* = 16, 11/5, 73.9, 65–86, MCI	None	Anode F3, cathode F4	2 mA	30 min	9 (in 3 weeks)	Baseline	+
Fiori et al. (2017) (28062255)	Sham-controlled, double-blinded, randomized, counterbalanced	*N* = 30, 29 ± 6 20–40 (young group), 72 ± 6 60–80 (old group), healthy	None	Unihemispheric: anode CP5, cathode right orbito-frontal cortex; bihemispheric: anode CP5 cathode CP4	2 mA	20 min	2 (uni- and bi-hemispheric)	During retrieval phase	+
Westerberg et al. (2015) (26116933)	Sham-controlled, double-blinded, randomized	*N* = 18, 16/3, 73.4 65–85, healthy	None	Anodes F7 and F8, references to ipsilateral mastoids	so-tDCS: 0.75 Hz, 0-260 μA	5 times 5 min	1	During sleep	+
Cotelli et al. (2014) (24678298)	Sham-controlled, double-blinded, randomized	*N* = 36, 29/7, 76.5, probable mild to moderate AD	2 before 3-months, 4 before 6-months follow-up	Anode left DLPFC (8 cm frontally, 6 cm laterally), cathode right deltoid muscle	2 mA	25 min	10 (in 2 weeks)	During memory or motor training	−
Bystad et al. (2016) (27005937)	Sham-controlled, double-blinded, randomized	*N* = 25, 14/11, 72.5 (AD group); *N* = 22, 18/4, 68.8 ± 6.8, 59–83 (healthy group), AD and healthy	None	Anode T3, cathode FP2	2 mA	30 min	6 (in 10 days)	Baseline	−
Lu et al. (2019) (31529691)	Sham-controlled, double-blinded, randomized	*N* = 173, 108/65, 74, 60–90, NCD-AD	28	Anode T3, cathode contralateral upper limb	2 mA	20 min	12 (in 3 weeks)	During WM training	+
Meinzer et al. (2013) (23884951)	Sham-controlled, double-blinded, within-subject	*N* = 20, 10/10, 26.4 ± 3.4 19–31 (young group), 68 ± 5.7 60–76 (old group), healthy	None	Anode left ventral IFG, cathode right supraorbital area	1 mA	20 min	1	During rs- and task-related fMRI (semantic word retrieval)	+

(Continued)

TABLE 2 | Continued

References (PMID)	Study design	Participants (N, female/male, age [mean ± SD and/or range], condition*)	Drop-outs	Stimulation parameters					Behavioral (cognitive) effects
				Montage	Intensity	Duration	# Active tDCS sessions	Timepoint of tDCS	
Khedr et al. (2014) (25346688)	Sham-controlled, double-blinded, randomized	*N* = 34, 15/19, 69.7 ± 4.8 62–79, mild to moderate AD	None	atDCS: anode LDLPFC, cathode contralateral supraorbital region; ctDCS: vice versa	2 mA	25 min	10 consecutive days	Baseline	+
Prehn et al. (2017) (27555381)	Sham-controlled, double-blinded, randomized	*N* = 39, 23/17, 24 ± 4 18–35 (young group), 66 ± 7 50–80 (old group), healthy	1	Anode T6, cathode contralateral frontopolar cortex	1 mA	20 min	2	During learning phase	+
Manenti et al. (2017) (2925955)	Sham-controlled, double-blinded, randomized	*N* = 22, 14/8, 74.5 ± 5.9, SMC	None	Anode F3, cathode right supraorbital area	1.5 mA	15 min	1	After learning phase but before recall	+
Ferrucci et al. (2008) (18525028)	Sham-controlled, double-blinded, randomized, cross-balanced	*N* = 10, 7/3, 75.2 ± 7.3 64–84, probable AD	None	Anode P3-T5 left and P6-T4 right, cathode contralateral deltoid muscle	1.5 mA	15 min	2 (anodal and cathodal)	Between tasks	+
Boggio et al. (2012) (21840288)	Sham-controlled, double-blinded, randomized, counterbalanced	*N* = 15, 7/8, 77.5 ± 6.9 (Italian group), 80.6 ± 9.5 (Brazilian group), AD	None	Anodes bilaterally T3 and T4, cathode right deltoid muscle	2 mA	30 min	5 consecutive days	Baseline	+
Cruz Gonzalez et al. (2018) (29736192)	Sham-controlled, single-subject study A-B-C-A design	*N* = 5, 2/3, 72.8 ± 6.6, 67–81, MCI	1 before last baseline session	Anode F3, cathode contralateral deltoid muscle	2 mA	30 min	1–5 (in 1 week)	During cognitive training	+

*Disease conditions: *AD, Alzheimer's Disease; SCD, subjective cognitive decline; MCI, mild cognitive impairment; NCD-AD, neurocognitive disorder due to Alzheimer's Disease; SMC, subjective memory complaints.*

the left ventral IFG (Meinzer et al., 2015). Yun et al. found that repeated application of anodal tDCS over the DLPFC (nine times 30 min in 3 weeks) significantly increased brain metabolism in MCI patients (measured by FDG-PET) and enhanced memory performance compared to sham tDCS (Yun et al., 2016). Anodal tDCS applied over the left lateral PFC after learning and before recall of an episodic memory task in patients with subjective memory complaints (SMC) significantly increased word recognition performance up 30 days after learning in comparison to the sham group (Manenti et al., 2017). Moreover, in a pilot study of Cruz Gonzalez et al. anodal or cathodal tDCS over the DLPFC was combined with cognitive training during stimulation to synergistically enhance declined cognition in MCI. Tendencies of increased processing speed, selective attention, working memory activities, and the completion time in planning ability and divided attention tasks were observed for both anodal and cathodal stimulation in comparison to sham tDCS. However, due to the small sample size and the lack of randomization, results were highly variable and need further investigation and confirmation (Cruz Gonzalez et al., 2018). The biggest study (including 201 participants) has been performed by Lu et al. who also combined tDCS over left temporal areas and (working) memory training in patients with neurocognitive disorder due to AD (NCD-AD). Participants underwent 12 sessions of anodal tDCS in 3 weeks and performed working memory tasks during stimulation. Performance significantly increased up to 8 or even 12 weeks post-intervention in secondary outcome measures (delayed recall, working memory tests, logical memory) for subjects receiving tDCS and working memory training compared to control groups. However, primary outcomes (global cognition measured by ADAS-Cog and the working memory training performance) improved throughout all groups without stimulation-dependent differences (Lu et al., 2019).

Alzheimer's Disease

Two of the first small studies to investigate tDCS in patients with AD were performed by Ferrucci et al. in 2008 and Boggio et al. in 2012. Ferrucci et al. applied anodal and cathodal tDCS to the temporo-parietal cortex and were able to show that a single session of anodal tDCS significantly increased accuracy in a word recognition task while cathodal tDCS had contrary effects. However, no stimulation-type-dependent changes in reaction times were found based on the assessment of a visual attention task (Ferrucci et al., 2008). Subsequently, Boggio et al. used bilateral anodal tDCS applied for five consecutive days over the temporal cortex, which significantly ameliorated performance of AD patients in a visual recognition task but not in a visual attention task compared to sham tDCS (Boggio et al., 2012). Examining longer-term effects of 10 sessions of anodal tDCS over the LDLPFC on cognitive abilities in AD, Khedr et al. found that MMSE scores significantly improved for both anodal and cathodal stimulation compared to sham tDCS even 2 months post-intervention (Khedr et al., 2014). Cotelli et al. also applied 10 sessions of tDCS over the LDLPFC in AD patients but combined with individualized memory training during stimulation. This study failed to show a significant effect of anodal tDCS on memory performance in AD (Cotelli et al., 2014). Similarly, Bystad et al. could not reveal significant effects of anodal tDCS applied over the left temporal cortex in subjects suffering from AD. Verbal memory test scores did not differ significantly after active stimulation in comparison to sham. However, a tendency of increased delayed recall was observed for the group receiving active tDCS (Bystad et al., 2016). Finally, the findings of Im et al., who studied the effects of 6-months daily at home tDCS in AD patients, were in line with Khedr et al. (2014). The main outcomes were significant benefits of anodal tDCS on global cognition assessed via MMSE and improved language function based on ameliorated performance in the Boston Naming Test (BNT), stabilization of some executive functions in AD patients compared to patients receiving sham stimulation as well as increased cerebral glucose metabolism (Im et al., 2019).

DISCUSSION

Methodological Considerations

In the 16 reviewed studies tDCS intensity varied between 1 and 2 mA [except for the study of Westerberg et al. (2015) who applied so-tDCS with a frequency of 0.75 Hz and 0–260 μA intensity], one session lasted between 15 and 30 min and for most studies the number of sessions varied between 1 and 10 (**Figure 2**). Exceptions in session number were the study of Lu et al. (2019) who applied 12 sessions of tDCS and Im et al. (2019) who chose to use daily at home tDCS over 6 months to treat patients with AD (**Figure 2**).

In the majority of applications stimulation intensity was rather high (2 mA) and most of the sessions lasted 25–30 min. Importantly, none of the studies reported severe adverse effects resulting from tDCS or so-tDCS. In 3 studies (Khedr et al., 2014; Sandrini et al., 2016; Lu et al., 2019) rarely occurring mild side effects were skin irritation, itching, and redness under the area of the electrodes. In only 2 studies (Prehn et al., 2017; Cruz Gonzalez et al., 2018) a few subjects reported a mild headache and dizziness after the stimulation, which only lasted for several hours. However, the occurrence of mild adverse effects did not seem to correlate with the magnitude of stimulation intensity, session duration or session number.

A more precise investigation of electrode montage revealed that 12 out of 16 studies stimulated the left cortical hemisphere, mostly targeting the (pre-)frontal cortex (**Figure 3**). However, several studies also stimulated temporal or temporo-parietal areas (**Figure 3**). The difference in stimulation location may be traced back to deviating hypotheses and different aims in modulating cognitive functions. All but 1 study, that targeted the temporal or temporo-parietal cortex, aimed to ameliorate or slow AD progression, as the medial temporal lobe (MTL), including the hippocampus, is one of the major and earliest affected brain regions in disease (Smith, 2002; Dickerson et al., 2004). The reason for targeting the temporal cortices might be to reach areas that are mainly affected by decline of neuroplasticity due to neurodegeneration and thereby potentially counteract the loss of neuronal connections. Although episodic memory is thought to mainly depend on intact functioning of MTL and hippocampus

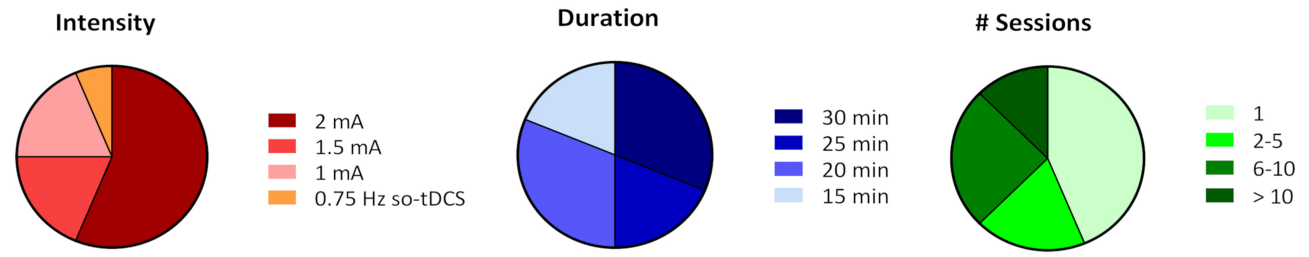

FIGURE 2 | Relative comparison of tDCS parameters intensity, session duration, and session number (# session) chosen in the 16 reviewed studies. Percentages were calculated based on the number of studies that chose a certain parameter out of the total number of 16 studies and do not resemble relative frequencies based on the number of subjects.

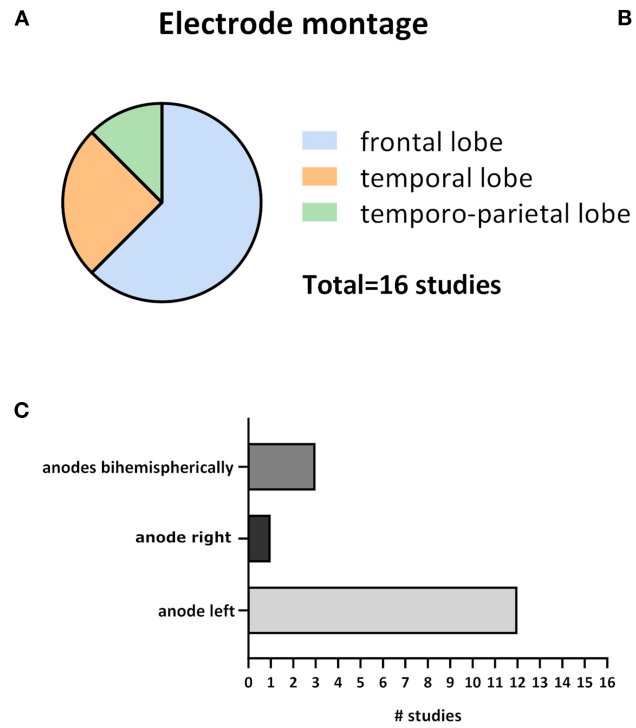

B

	Anode	cathode	# studies
Frontal lobe	F3	right supraorbital area	3
	right supraorbital area	F3	
	F3	contralateral deltoid muscle	2
	F3	F4	2
	left ventral IFG	right supraorbital area	2
	F7 and F8	ipsilateral mastoids	1
Temporal lobe	T3	FP2	1
	T3	contralateral upper limb	1
	T3 and T4	right deltoid muscle	1
	T6	contralateral frontopolar cortex	1
Temporo-parietal lobe	CP5	CP4 or right orbital area	1
	P3-T5 left and P4-T6 right	contralateral deltoid muscle	1

FIGURE 3 | Variations in electrode montages extracted from the 16 reviewed studies. **(A)** Shows the relative numbers of studies out of all 16 studies that chose frontal, temporal or temporo-parietal cortical targets for tDSC. **(B)** Depicts exact anode and cathode positions as well as the number of studies that applied respective montage. **(C)** Compares the frequency of anodal left, right, and bihemispheric cortical stimulation (the anode is usually considered as the active electrode).

(Dickerson and Eichenbaum, 2010), the PFC and non-disturbed communication between all these areas seem crucial in cognitive processes relying on episodic memory (Fletcher and Henson, 2001; Brem et al., 2013).

Scientists targeting the frontal lobe (mainly the DLPFC) mostly aimed to modify cognitive processes by directly impacting underlying neuronal networks and indirectly subcortical areas (Frith and Dolan, 1996). Of the two studies that failed to show significant effects of tDCS on cognitive functions Cotelli et al. (2014) targeted the LDLPFC, while Bystad et al. (2016) stimulated the left temporal cortex. In both studies the subjects were suffering from AD. Because neuronal network connectivity and synchrony seem to change upon aging (Goh, 2011; Meinzer et al., 2013), further or increased alterations might occur in disease, which should be considered when developing new tDCS protocols to treat patients with cognitive impairment or advanced dementia. It might be beneficial to include individual computational modeling of current distribution to account for structural brain alterations happening upon aging such as atrophy along with raising volumes of the ventricular system (Fjell and Walhovd, 2010). Indeed, increased cerebrospinal fluid (CSF) volume and reduced tissue density significantly impact current distribution throughout the brain (Opitz et al., 2015) as conductivity is higher in more aqueous media and tissues. This

was further confirmed in a recent study by Antonenko et al. who used computational modeling to show that the cerebral electric field induced by transcranial electrical stimulation is higher for young compared to older people (Antonenko et al., 2021). In the studies reviewed here, mean age of participants differs up to 13 years (Prehn et al., 2017: 66 years; Boggio et al., 2012: 79.1 years) (**Table 2**) which exemplifies that age differences also occur in studies of the elderly. Age-related electrical field variations may cause controversial results, even when comparing studies performed within similar age groups but with significant mean age deviations. In addition to age-related increase of brain atrophy, individual head anatomy seems to impact the induced electric field strengths (Antonenko et al., 2021). Computational models have shown that large electrodes which are most frequently used in tDCS studies produce large diffuse electric fields in the brain. Not only strengths but also the distributions of these fields are highly dependent on individual head and brain anatomy. Lately, smaller electrodes as well as novel montages, including high-definition tDCS (HD-tDCS) arrangements have been introduced to improve the focality of the stimulation. However, a recent study just reported that better electric field focality was achieved only at the cost of increased interindividual variability (Mikkonen et al., 2020). Nevertheless, another recent study using HD-tDCS and current modeling demonstrated that focal current delivery to the DLPFC with sufficient magnitude of the induced current, modulated the neural activity in older adults (Gbadeyan et al., 2019). However, it remains to be elucidated whether more precise stimulation localization is beneficial in patients suffering from cognitive decline that is mostly caused by neurodegeneration in multiple brain areas affecting widespread cortical networks rather than precisely localized brain regions. Altogether, this highlights the importance of individually predicting the electric field distribution by means of structural brain imaging combined with computational modeling as this may be a crucial factor when applying tDCS to aging brains and lead to decreased effect variability as well as ameliorated spatial accuracy.

The outcomes of the reviewed studies show a high degree of variability—in the results themselves but also in their respective measures (**Table 3**). Consequently, to reduce variability, the application of multiple and precise cognitive outcome measures that assess a representative range of cognitive functions, is essential when performing tDCS experiments that aim to modulate cognition in the elderly. It seems like the effect of tDCS can sometimes be rather specific for single aspects of human cognition. This might correlate with the part of the cortex that has been stimulated, however, it needs to be pointed out that the spatial resolution of tDCS is rather low. The use of screening tools such as widely applied MMSE or MoCA to evaluate effects on global cognition may be insufficient as these tests resemble a very limited spectrum of cognitive functions and have been developed for quick clinical diagnoses and screenings. Moreover, only few of the reviewed studies included both physiological and cognitive measures. The combination of extensive standardized cognitive assessments with physiological methods such as EEG or fMRI may reveal origins of variability and facilitate the evaluation of tDCS effects.

Out of all studies only three combined tDCS with cognitive training (Cotelli et al., 2014; Cruz Gonzalez et al., 2018; Lu et al., 2019). Even though results depicted here are not very consistent, the idea of synergistic amelioration and intervention of cognitive decline, by combining methods that positively impact cognitive functions in the elderly, seems promising. However, when assessing the effects as well as comparing active to sham stimulation conditions it needs to be considered that cognitive training itself might already improve cognition in both groups. Consequently, effects of tDCS may result in only slight differences that might be hard to detect using semi-sensitive cognitive outcome measures. Further some participants might not respond to the stimulation. A relatively high number of participants is important to properly assess the effects of tDCS on cognition of elderly people. Therefore, future studies may be designed in a multicentric fashion to increase participant numbers and thus reliability of experimental outcomes.

When treating diseases such as MCI or AD, it is crucial to consider long-term (LT) effects of tDCS. We define LT effects as those measured at least 1 week after the end of the intervention. Among the studies reviewed here, only seven examined LT effects (Boggio et al., 2012; Cotelli et al., 2014; Khedr et al., 2014; Sandrini et al., 2016; Manenti et al., 2017; Prehn et al., 2017; Lu et al., 2019) (**Table 3**), of which only 5 revealed significant results (Boggio et al., 2012; Cotelli et al., 2014; Khedr et al., 2014; Manenti et al., 2017; Lu et al., 2019) meaning that at least one cognitive test score was significantly better at LT timepoints (after stimulation) compared to either baseline (before stimulation) or to the respective control condition (e.g., sham stimulation). When comparing active vs. sham stimulation, only three out of these five studies revealed significant improvement of the active group over the sham group at LT timepoints (Boggio et al., 2012; Khedr et al., 2014; Manenti et al., 2017). Interestingly, the two studies that did not find significant LT effects when comparing active to sham stimulation used a combination therapy of tDCS and cognitive training (Cotelli et al., 2014; Lu et al., 2019). In both studies the tDCS sham group received cognitive training. Taken together, this indicates that, as suggested above, both methods—tDCS and cognitive training—can positively impact cognition in the elderly and both potentially result in LT effects. Whether a combination of both methods enhances LT effects remains to be elucidated. A possible explanation for the absence of LT effects in the remaining two studies (Sandrini et al., 2016; Prehn et al., 2017) is that the total time of stimulation (duration of one session multiplied by the number of sessions) applied by Sandrini et al. (15–75 min; stimulation time varied between subjects as stimulation was repeated until a certain test score was achieved) and Prehn et al. (40 min) deviates strongly from the mean time of stimulation (181 min) of all studies that showed significant LT effects.

Future Perspectives

In conclusion, based on recently available data (http://tdcsdatabase.com) to counteract age-associated cognitive decline, anodal tDCS should be applied repeatedly to the left cortical hemisphere. In adulthood, several cognitive processes

TABLE 3 | Summary of all studies reviewed, listing respective cognitive assessments including the timepoints of the assessment, exact measures, and main outcomes.

References	Cognitive assessment (to evaluate tDCS effects on cognition)		
	Timepoints	**Measures***	**Outcomes**
Im et al. (2019)	Baseline and after 6 months of treatment	MMSE, CDR, neurological test battery (digit span test, BNT, RCFT with immediate and delayed recall and recognition, clock drawing test, SVLT with immediate and delayed recall and recognition, contrasting program, Go-no go test, COWAT, Stroop word and color reading)	• MMSE and BNT scores significantly improved after active tDCS compared to sham • Active tDCS resulted in consistent performance (at lower score levels) in contrasting program and Stroop word reading while scores decreased for sham
Sandrini et al. (2016)	Learning performance, recall after 48 h and recall after 1 month	Learning and recall of a list of 20 words	• Significant effect for recall after 48 h: Active tDCS group recalled significantly more words compared to sham • No significant differences after 1 month
Meinzer et al. (2015)	During stimulation (and fMRI)	Semantic word retrieval task	• tDCS significantly improved semantic word-retrieval performance in the patients to the level of controls
Yun et al. (2016)	Baseline and after 3-weeks of treatment	MMQ (MMQ-C, MMQ-A, MMQ-S)	• MMQ-C significantly increased after active tDCS compared to sham • Results for MMQ-A were similar to MMQ-C results but not significant between the active and sham groups • No significant difference for MMQ-S between active tDCS and sham
Fiori et al. (2017)	During word retrieval: 1–10 presentations for each picture-word pair (T1-T10)	Training, verification, and word retrieval of 20 pseudoword-picture associations (bisyllabic pseudowords)	• Bihemispheric: higher number of correct responses in the old group during T10 compared to T1 compared to unihemispheric and sham condition • No differences between the three conditions in the young age group • During T10 the young group was significantly more accurate than the old group for unihemispheric and sham; no significant difference in the bihemispehric condition • Same results for vocal reaction times
Westerberg et al. (2015)	Before a 90-min nap and 30 min after	Two declarative memory tests (word-pair recall, fast recognition test), 1 non-declarative test (object-priming test)	• Recall improvement from pre-nap to post-nap was significantly larger for active so-tDCS compared to sham • No significant fast recognition or object priming performance difference between active and sham so-tDCS after the nap (both increased significantly)
Cotelli et al. (2014)	Baseline (T0), after 2 weeks of treatment (T1), after 3 months (T2), after 6 months (T3)	Face-name association task (FNAT), neuropsychological tests (picture naming task, BADA, Rivermead behavioral memory test, Rey auditory verbal learning test, Rey-Osterrieth test, complex figure copy, TMT A and B)	• FNAT: active or sham tDCS + memory training group showed significantly improved performances compared to active tDCS + motor training group at T1 and similar for T2, at T3 sham + memory training was still significant compared to the other two groups • No differences in neuropsychological tests (except an improvement for both tDCS and sham + memory training at T3 in the TMT A score)
Bystad et al. (2016)	Before and after stimulation	Primary: immediate and delayed recall and recognition of CVLT-II Secondary: MMSE, clock drawing test, TMT A and B	• CVLT-II: no significant differences between active and sham tDCS but a tendency toward higher improvement in CVLT-II recall after active tDCS • No significant differences for secondary outcome measures
Lu et al. (2019)	Baseline (T0), after 4 weeks of treatment (T1), 4 weeks after post-intervention (T2), 8 weeks after post-intervention (T3)	Primary: WM test (RT), ADAS-Cog Secondary: CVFT, TMT, Chinese neuropsychiatric inventory (CNIP)	• ADAS-Cog: significant improvement for all groups at T1, but no difference between groups, tendency of falling back to baseline at T2 and T3 for all groups • WM test: significant improvement for all groups until T3, tDCS+WMT showed highest WM capacity at T1 compared to other groups • CVFT: tDCS-WMT showed a greater improvement in delayed recall compared to single-modality interventions; at T3 only the tDCS+WMT group showed significant enhancement on delayed recall performance over baseline • tDCS-WMT group showed better performance of logical memory at 12th week
Meinzer et al. (2013)	During stimulation (and fMRI)	Overt semantic word generation task	• During sham younger adults produced significantly less errors than elderly • Older subjects produced significantly less errors during active tDCS in comparison to sham

(Continued)

TABLE 3 | Continued

References	Cognitive assessment (to evaluate tDCS effects on cognition)		
	Timepoints	**Measures***	**Outcomes**
			• Response times (RTs) were comparable between young and old subjects during sham; no difference in RTs for elderly during active tDCS compared to sham
Khedr et al. (2014)	Baseline (T0), after 10 days of treatment (T1), after 1 month (T2), after 2 months (T3)	MMSE, WAIS-III (verbal comprehension, arithmetic and digit span, perceptual organization, processing speed)	• MMSE: significant improvement in anodal and cathodal tDCS compared to sham (increase of nearly 2 points at T1 and further increase of 2 points at T2 and T3); anodal tDCS group showed better improvement in orientation, registration, attention, and naming object compared to cathodal tDCS • WAIS-III: only cathodal and not anodal tDCS showed improved performance IQ compared to sham
Prehn et al. (2017)	Immediate recall, delayed recall after 6 h, 1 day later and 1 week later	Object-location learning task (LOCATO), primary outcome: immediate recall, secondary outcome: delayed recall	• Significant effect of SSRI but not of stimulation on immediate recall scores • Young and old group profited most from atDCS+SSRI • No significant effects on delayed recall
Manenti et al. (2017)	Baseline (after learning), free recall and recognition 48 h and 30 days after learning (and tDCS)	Learning, recall, and recognition of a list of 20 words	• Significant difference on hit-false alarms score between atDCS and sham at day 30, anodal tDCS significantly improved memory recognition on day 30 • atDCS and sham group showed similar free recall performance at day 30
Ferrucci et al. (2008)	Baseline and 30 min after stimulation	Word recognition task (WRT), visual attention task	• atDCS improved WRT accuracy, while ctDCS significantly worsened it, sham left it unchanged; same results for DI (derived by subtracting false positive from true positive responses) • No significant differences in RTs in the visual attention task for atDCS or ctDCS compared to sham
Boggio et al. (2012)	Baseline (T0), at the end of treatment day 5 (T1), 1 week later (T2), 4 weeks later (T3)	MMSE, ADAS-Cog, visual recognition task (VRT), visual attention task (VAT)	• No significant effects for MMSE, ADAS-Cog, and VAT scores between active and sham tDCS • VRT: significant main effect for tDCS performance changes from baseline: 8.99% after anodal and 2.62% after sham tDCS (for T1, T2 and T3)
Cruz Gonzalez et al. (2018)	Screening, baseline (after CS training), after sham+CS, after tDCS+CS, post assessment (after CS)	Cognitive stimulation (planning ability and divided attention, processing speed and selective attention, short-term memory, calculation and WM), CDR, MoCA	• Enhanced cognitive performance in processing speed, selective attention, WM activities, completion time in planning ability and divided attention tasks for active tDCS compared to sham • Variable CS outcomes but subjects did not show significantly better outcomes in sham intervention compared to baseline CS

*The only two studies that did not reveal significant effects are highlighted in gray. Cognitive measures: *MMSE, Minimal Mental State Examination; CDR, Clinical Dementia Rating (Morris, 1993); BNT, Boston Naming Test; RCFT, Rey Complex Figure Test; SVLT, Seoul Verbal Learning Test; COWAT, Controlled Oral Word Association Test; MMQ, Multifactorial Memory Questionnaire; BADA, Battery for the Analysis of the Aphasic Deficit; TMT, Trail Making Test; CVLT-II, California verbal learning test second edition; WM, Working Memory; ADAS-Cog, Alzheimer's Disease assessment scale-cognition subscale; CVFT, Category Verbal Fluency Test; WAIS-III, Wechsler Adult Intelligence Subscales; MoCA, Montreal Cognitive Assessment; CS, Cognitive Stimulation.*

show dominant activity in the left cortex, while cognitive decline upon aging seems to correlate with network alterations and "bihemispheric hyperactivity" (Goh, 2011; Antonenko et al., 2012; Meinzer et al., 2013). Targeting the LDLPFC may be one of the most effective possibilities as human cognition highly depends on cortical as well as subcortical networks involving the PFC (Frith and Dolan, 1996). Further, tDCS has very little mild adverse effects, which seem to depend on subjective sensation rather than stimulation parameters, so that a stimulation intensity of 2 mA may be chosen and sessions could last up to 30 min without risking significant side effects. Moreover, LT effects should be considered in future studies as they are advantageous for therapy considering the following aspects. Even though stimulators are now small and mobile, and the stimulations could be performed regularly by patients themselves after being trained by a specialist, at home tDCS is time consuming and requires certain skills as well as mobility. Independent application is particularly difficult for patients with cognitive disorders such as MCI or AD and a trained assistant such as a relative or a family doctor would be required to perform the stimulations properly. Additionally, in some cases repetitive stimulation may cause minor side effects as described above. Considering these limitations, treatment effects should outlast the time during stimulation, especially for application of tDCS in elderly people with cognitive impairment, and likewise persist in LT measurements.

In the field of NIBS research, stimulation interventions have so far mostly focused on group-based, general protocols. While standardization of study protocols may increase comparability which potentially facilitates translation of experimental studies into clinical applications, it can also be a major limitation

of this methodology. Generalized stimulation practices might miss to fully consider the underlying mechanisms in the individual brain that guide the effective response to a given intervention. Therefore, NIBS protocols leveraging on the combination of stimulation approaches with electrical field modeling, neuroimaging and electrophysiology (Esmaeilpour et al., 2020) could advance the characterization of personalized response and prognostic biomarker discovery. This will result in a better understanding and reduction of variability of the response to stimulation. However, simulations of individual brains cannot be perfect due to uncertainties of the model parameters (e.g., conductivity) and EEG as well as fMRI methods both suffer from electric field artifacts. A recent study suggests the functional near-infrared spectroscopy (fNIRS) may be a better neuroimaging technique in order to study the hemodynamics response evoked by tDCS and consequently better dosing the stimulation (Arora et al., 2021). Indeed, a recent study investigated the feasibility of portable neuroimaging of cerebellar tDCS in conjunction with electroencephalography (EEG) to measure changes in the brain activation at the PFC and the sensorimotor cortex (SMC) in hemiparetic chronic stroke survivors. It was observed that there is a clear relationship between mean lobular electric field strength and oxy-hemoglobin concentrations/log10-transformed EEG band power. Nevertheless, future studies are needed to investigate and replicate these effects in a larger cohort and to clearly discriminate non-responders from responders. Afterall, an extended meta-analysis of the here reviewed studies and respective results could contribute to further specification and suggestions for future tDCS studies aiming to introduce novel treatment approaches to intervene with age-related cognitive deterioration as well as neurodegeneration.

DATA AVAILABILITY STATEMENT

The original contributions presented in the study are included in the article/supplementary material, further inquiries can be directed to the corresponding author.

AUTHOR CONTRIBUTIONS

AS performed database research and analysis, prepared figures and tables, and wrote the manuscript. LD reviewed and contributed to the manuscript. AA supervised the database research and analysis and reviewed the manuscript. All authors contributed to the article and approved the submitted version.

FUNDING

This study was supported by the Ministry of Lower Saxony for Science and Culture (76251-12-7/19; ZN 3456). We acknowledge support by the German Research Foundation and the Open Access Publication Funds of the Georg–August University Göttingen, Germany.

REFERENCES

André, S., Heinrich, S., Kayser, F., Menzler, K., Kesselring, J., Khader, P. H., et al. (2016). At-home tDCS of the left dorsolateral prefrontal cortex improves visual short-term memory in mild vascular dementia. *J. Neurol. Sci.* 369, 185–190. doi: 10.1016/j.jns.2016.07.065

Antonenko, D., Grittner, U., Saturnino, G., Nierhaus, T., Thielscher, A., and Flöel, A. (2021). Inter-individual and age-dependent variability in simulated electric fields induced by conventional transcranial electrical stimulation. *NeuroImage* 224:117413. doi: 10.1016/j.neuroimage.2020.117413

Antonenko, D., Hayek, D., Netzband, J., Grittner, U., and Flöel, A. (2019). tDCS-induced episodic memory enhancement and its association with functional network coupling in older adults. *Sci. Rep.* 9:2273. doi: 10.1038/s41598-019-38630-7

Antonenko, D., Külzow, N., Sousa, A., Prehn, K., Grittner, U., and Flöel, A. (2018). Neuronal and behavioral effects of multi-day brain stimulation and memory training. *Neurobiol. Aging* 61, 245–254. doi: 10.1016/j.neurobiolaging.2017.09.017

Antonenko, D., Meinzer, M., Lindenberg, R., Witte, A. V., and Flöel, A. (2012). Grammar learning in older adults is linked to white matter microstructure and functional connectivity. *NeuroImage.* 62:1667–1674. doi: 10.1016/j.neuroimage.2012.05.074

Antonenko, D., Schubert, F., Bohm, F., Ittermann, B., Aydin, S., Hayek, D., et al. (2017). tDCS-induced modulation of GABA levels and resting-state functional connectivity in older adults. *J. Neurosci.* 37, 4065–4073. doi: 10.1523/JNEUROSCI.0079-17.2017

Arora, Y., Walia, P., Hayashibe, M., Muthalib, M., Chowdhury, S. R., Perrey, S., et al. (2021). Grey-box modeling and hypothesis testing of functional near-infrared spectroscopy-based cerebrovascular reactivity to anodal high-definition tDCS in healthy humans. *In Review*. 17:e1009386. doi: 10.1371/journal.pcbi.1009386

Ballard, C., Gauthier, S., Corbett, A., Brayne, C., Aarsland, D., and Jones, E. (2011). Alzheimer's disease. *Lancet* 377, 1019–1031. doi: 10.1016/S0140-6736(10)61349-9

Batsikadze, G., Moliadze, V., Paulus, W., Kuo, M.-F., and Nitsche, M. A. (2013). Partially non-linear stimulation intensity-dependent effects of direct current stimulation on motor cortex excitability in humans. *J. Physiol.* 591, 1987–2000. doi: 10.1113/jphysiol.2012.249730

Baudry, M. (2001). "Long-term potentiation (Hippocampus)," in *International Encyclopedia of the Social and Behavioral Sciences*, eds N. J. Smelser and B. Baltes (Amsterdam: Elsevier), 9081–9083,

Bear, M. F., and Malenka, R. C. (1994). Synaptic plasticity: LTP and LTD. *Curr. Opin. Neurobiol.* 4, 389–399. doi: 10.1016/0959-4388(94)90101-5

Berryhill, M. E., and Jones, K. T. (2012). tDCS selectively improves working memory in older adults with more education. *Neurosci. Lett.* 521, 148–151. doi: 10.1016/j.neulet.2012.05.074

Bindman, L. J., Lippold, O. C. J., and Redfearn, J. W. T. (1962). Long-lasting changes in the level of the electrical activity of the cerebral cortex produced by polarizing currents. *Nature* 196, 584–585. doi: 10.1038/196584a0

Boggio, P. S., Ferrucci, R., Mameli, F., Martins, D., Martins, O., Vergari, M., et al. (2012). Prolonged visual memory enhancement after direct current stimulation in Alzheimer's disease. *Brain Stimul.* 5, 223–230. doi: 10.1016/j.brs.2011.06.006

Boggio, P. S., Ferrucci, R., Rigonatti, S. P., Covre, P., Nitsche, M., Pascual-Leone, A., et al. (2006). Effects of transcranial direct current stimulation on working memory in patients with Parkinson's disease. *J. Neurol. Sci.* 249, 31–38. doi: 10.1016/j.jns.2006.05.062

Brambilla, M., Manenti, R., Ferrari, C., and Cotelli, M. (2015). Better together: left and right hemisphere engagement to reduce age-related memory loss. *Behav. Brain Res.* 293, 125–133. doi: 10.1016/j.bbr.2015.07.037

Braunewell, K.-H., and Manahan-Vaughan, D. (2001). Long-term depression: a cellular basis for learning? *Rev. Neurosci.* 12, 121–40. doi: 10.1515/REVNEURO.2001.12.2.121

Brem, A.-K., Ran, K., and Pascual-Leone, A. (2013). Learning and memory. *Handb. Clin. Neurol.* 116, 693–737. doi: 10.1016/B978-0-444-53497-2.00055-3

Bystad, M., Grønli, O., Rasmussen, I. D., Gundersen, N., Nordvang, L., Wang-Iversen, H., et al. (2016). Transcranial direct current stimulation as a memory enhancer in patients with Alzheimer's disease: a randomized, placebo-controlled trial. *Alzheimers Res. Ther.* 8:13. doi: 10.1186/s13195-016-0180-3

Bystad, M., Rasmussen, I. D., Grønli, O., and Aslaksen, P. M. (2017). Can 8 months of daily tDCS application slow the cognitive decline in Alzheimer's disease? a case study. *Neurocase* 23, 146–148. doi: 10.1080/13554794.2017.1325911

Cheng, C. P. W., Chan, S. S. M., Mak, A. D. P., Chan, W. C., Cheng, S. T., Shi, L., et al. (2015). Would transcranial direct current stimulation (tDCS) enhance the effects of working memory training in older adults with mild neurocognitive disorder due to Alzheimer's disease: study protocol for a randomized controlled trial. *Trials* 16:479. doi: 10.1186/s13063-015-0999-0

Coffman, B. A., Clark, V. P., and Parasuraman, R. (2014). Battery powered thought: Enhancement of attention, learning, and memory in healthy adults using transcranial direct current stimulation. *NeuroImage* 85, 895–908. doi: 10.1016/j.neuroimage.2013.07.083

Costa, V., Brighina, F., Piccoli, T., Realmuto, S., and Fierro, B. (2017). Anodal transcranial direct current stimulation over the right hemisphere improves auditory comprehension in a case of dementia. *NeuroRehabilitation* 41, 567–575. doi: 10.3233/NRE-162062

Cotelli, M., Manenti, R., Brambilla, M., Petesi, M., Rosini, S., Ferrari, C., et al. (2014). Anodal tDCS during face-name associations memory training in Alzheimer's patients. *Front. Aging Neurosci.* 6:38. doi: 10.3389/fnagi.2014.00038

Cruz Gonzalez, P., Fong, K. N. K., and Brown, T. (2018). The effects of transcranial direct current stimulation on the cognitive functions in older adults with mild cognitive impairment: a pilot study. *Behav. Neurol.* 2018, 1–14. doi: 10.1155/2018/5971385

Dickerson, B. C., and Eichenbaum, H. (2010). The episodic memory system: neurocircuitry and disorders. *Neuropsychopharmacol. Off. Publ. Am. Coll. Neuropsychopharmacol.* 35, 86–104. doi: 10.1038/npp.2009.126

Dickerson, B. C., Salat, D. H., Bates, J. F., Atiya, M., Killiany, R. J., Greve, D. N., et al. (2004). Medial temporal lobe function and structure in mild cognitive impairment. *Ann. Neurol.* 56, 27–35. doi: 10.1002/ana.20163

Eddy, C. M., Shapiro, K., Clouter, A., Hansen, P. C., and Rickards, H. E. (2017). Transcranial direct current stimulation can enhance working memory in Huntington's disease. *Prog. Neuropsychopharmacol. Biol. Psychiatry* 77, 75–82. doi: 10.1016/j.pnpbp.2017.04.002

Elder, G. J., Firbank, M. J., Kumar, H., Chatterjee, P., Chakraborty, T., Dutt, A., et al. (2016). Effects of transcranial direct current stimulation upon attention and visuoperceptual function in Lewy body dementia: a preliminary study. *Int. Psychogeriatr.* 28, 341–347. doi: 10.1017/S1041610215001180

Elder, G. J., and Taylor, J.-P. (2014). Transcranial magnetic stimulation and transcranial direct current stimulation: treatments for cognitive and neuropsychiatric symptoms in the neurodegenerative dementias? *Alzheimers Res. Ther.* 6:74. doi: 10.1186/s13195-014-0074-1

Esmaeilpour, Z., Shereen, A. D., Ghobadi-Azbari, P., Datta, A., Woods, A. J., Ironside, M., et al. (2020). Methodology for tDCS integration with fMRI. *Hum. Brain Mapp.* 41, 1950–1967. doi: 10.1002/hbm.24908

Ferrucci, R., Mameli, F., Guidi, I., Mrakic-Sposta, S., Vergari, M., Marceglia, S., et al. (2008). Transcranial direct current stimulation improves recognition memory in Alzheimer disease. *Neurology* 71, 493–498. doi: 10.1212/01.wnl.0000317060.43722.a3

Fiori, V., Nitsche, M., Iasevoli, L., Cucuzza, G., Caltagirone, C., and Marangolo, P. (2017). Differential effects of bihemispheric and unihemispheric transcranial direct current stimulation in young and elderly adults in verbal learning. *Behav. Brain Res.* 321, 170–175. doi: 10.1016/j.bbr.2016.12.044

Fjell, A. M., and Walhovd, K. B. (2010). Structural brain changes in aging: courses, causes and cognitive consequences. *Rev. Neurosci.* 21, 187–221. doi: 10.1515/revneuro.2010.21.3.187

Fletcher, P. C., and Henson, R. N. (2001). Frontal lobes and human memory: insights from functional neuroimaging. *Brain J. Neurol.* 124, 849–881. doi: 10.1093/brain/124.5.849

Flöel, A. (2014). tDCS-enhanced motor and cognitive function in neurological diseases. *NeuroImage* 85 (Pt 3), 934–947. doi: 10.1016/j.neuroimage.2013.05.098

Frith, C., and Dolan, R. (1996). The role of the prefrontal cortex in higher cognitive functions. *Brain Res. Cogn. Brain Res.* 5, 175–181. doi: 10.1016/s0926-6410(96)00054-7

Gbadeyan, O., Steinhauser, M., Hunold, A., Martin, A. K., Haueisen, J., and Meinzer, M. (2019). Modulation of adaptive cognitive control by prefrontal high-definition transcranial direct current stimulation in older adults. *J. Gerontol. Ser. B* 74, 1174–1183. doi: 10.1093/geronb/gbz048

Goh, J. O. S. (2011). Functional dedifferentiation and altered connectivity in older adults: neural accounts of cognitive aging. *Aging Dis.* 2, 30–48.

Gorman, A. L. (1966). Differential patterns of activation of the pyramidal system elicited by surface anodal and cathodal cortical stimulation. *J. Neurophysiol.* 29, 547–564. doi: 10.1152/jn.1966.29.4.547

Grossman, P., Alekseichuk, I., de Lara, G., Paneri, K., Kunz, P., Turi, Z., et al. (2018). transcranial Direct Current Stimulation Studies Open Database (tDCS-OD). bioRxiv [Preprint]. doi: 10.1101/369215

Hsu, W.-Y., Ku, Y., Zanto, T. P., and Gazzaley, A. (2015). Effects of noninvasive brain stimulation on cognitive function in healthy aging and Alzheimer's disease: a systematic review and meta-analysis. *Neurobiol. Aging* 36, 2348–2359. doi: 10.1016/j.neurobiolaging.2015.04.016

Im, J. J., Jeong, H., Bikson, M., Woods, A. J., Unal, G., Oh, J. K., et al. (2019). Effects of 6-month at-home transcranial direct current stimulation on cognition and cerebral glucose metabolism in Alzheimer's disease. *Brain Stimul.* 12, 1222–1228. doi: 10.1016/j.brs.2019.06.003

Kabakov, A. Y., Muller, P. A., Pascual-Leone, A., Jensen, F. E., and Rotenberg, A. (2012). Contribution of axonal orientation to pathway-dependent modulation of excitatory transmission by direct current stimulation in isolated rat hippocampus. *J. Neurophysiol.* 107, 1881–1889. doi: 10.1152/jn.00715.2011

Keeser, D., Meindl, T., Bor, J., Palm, U., Pogarell, O., Mulert, C., et al. (2011). Prefrontal transcranial direct current stimulation changes connectivity of resting-state networks during fMRI. *J. Neurosci. Off. J. Soc. Neurosci.* 31, 15284–15293. doi: 10.1523/JNEUROSCI.0542-11.2011

Khedr, E. M., Gamal, N. F. E., El-Fetoh, N. A., Khalifa, H., Ahmed, E. M., Ali, A. M., et al. (2014). A double-blind randomized clinical trial on the efficacy of cortical direct current stimulation for the treatment of Alzheimer's disease. *Front. Aging Neurosci.* 6:275. doi: 10.3389/fnagi.2014.00275

Ladenbauer, J., Külzow, N., Passmann, S., Antonenko, D., Grittner, U., Tamm, S., et al. (2016). Brain stimulation during an afternoon nap boosts slow oscillatory activity and memory consolidation in older adults. *NeuroImage* 142, 311–323. doi: 10.1016/j.neuroimage.2016.06.057

Ladenbauer, J., Ladenbauer, J., Külzow, N., de Boor, R., Avramova, E., Grittner, U., et al. (2017). Promoting sleep oscillations and their functional coupling by transcranial stimulation enhances memory consolidation in mild cognitive impairment. *J. Neurosci.* 37, 7111–7124. doi: 10.1523/JNEUROSCI.0260-17.2017

Lefaucheur, J.-P., Antal, A., Ayache, S. S., Benninger, D. H., Brunelin, J., Cogiamanian, F., et al. (2017). Evidence-based guidelines on the therapeutic use of transcranial direct current stimulation (tDCS). *Clin. Neurophysiol.* 128, 56–92. doi: 10.1016/j.clinph.2016.10.087

Liebetanz, D., Nitsche, M. A., Tergau, F., and Paulus, W. (2002). Pharmacological approach to the mechanisms of transcranial DC-stimulation-induced after-effects of human motor cortex excitability. *Brain J. Neurol.* 125, 2238–2247. doi: 10.1093/brain/awf238

Lu, H., Chan, S. S. M., Chan, W. C., Lin, C., Cheng, C. P. W., and Linda Chiu Wa, L. (2019). Randomized controlled trial of TDCS on cognition in 201 seniors with mild neurocognitive disorder. *Ann. Clin. Transl. Neurol.* 6, 1938–1948. doi: 10.1002/acn3.50823

Manenti, R., Brambilla, M., Petesi, M., Ferrari, C., and Cotelli, M. (2013). Enhancing verbal episodic memory in older and young subjects after non-invasive brain stimulation. *Front. Aging Neurosci.* 5:49. doi: 10.3389/fnagi.2013.00049

Manenti, R., Sandrini, M., Gobbi, E., Binetti, G., and Cotelli, M. (2020). Effects of transcranial direct current stimulation on episodic memory in amnestic mild cognitive impairment: a pilot study. *J. Gerontol. B. Psychol. Sci. Soc. Sci.* 75, 1403–1413. doi: 10.1093/geronb/gby134

Manenti, R., Sandrini, M., Gobbi, E., Cobelli, C., Brambilla, M., Binetti, G., et al. (2017). Strengthening of existing episodic memories through non-invasive stimulation of prefrontal cortex in older adults with subjective memory complaints. *Front. Aging Neurosci.* 9:401. doi: 10.3389/fnagi.2017.00401

Martin, A. K., Meinzer, M., Lindenberg, R., Sieg, M. M., Nachtigall, L., and Flöel, A. (2017). Effects of transcranial direct current stimulation on neural networks in young and older adults. *J. Cogn. Neurosci.* 29, 1817–1828. doi: 10.1162/jocn_a_01166

Meinzer, M., Lindenberg, R., Antonenko, D., Flaisch, T., and Floel, A. (2013). Anodal transcranial direct current stimulation temporarily reverses age-associated cognitive decline and functional brain activity changes. *J. Neurosci.* 33, 12470–12478. doi: 10.1523/JNEUROSCI.5743-12.2013

Meinzer, M., Lindenberg, R., Phan, M. T., Ulm, L., Volk, C., and Flöel, A. (2015). Transcranial direct current stimulation in mild cognitive impairment: behavioral effects and neural mechanisms. *Alzheimers Dement.* 11, 1032–1040. doi: 10.1016/j.jalz.2014.07.159

Mikkonen, M., Laakso, I., Tanaka, S., and Hirata, A. (2020). Cost of focality in TDCS: interindividual variability in electric fields. *Brain Stimul.* 13, 117–124. doi: 10.1016/j.brs.2019.09.017

Morris, J. C. (1993). The Clinical Dementia Rating (CDR): Current version and scoring rules. *Neuro.* 43:2412.2–2412-a. doi: 10.1212/WNL.43.11.2412-a

Murugaraja, V., Shivakumar, V., Sivakumar, P. T., Sinha, P., and Venkatasubramanian, G. (2017). Clinical utility and tolerability of transcranial direct current stimulation in mild cognitive impairment. *Asian J. Psychiatry* 30, 135–140. doi: 10.1016/j.ajp.2017.09.001

Nilsson, J., Lebedev, A. V., and Lövdén, M. (2015). No significant effect of prefrontal tDCS on working memory performance in older adults. *Front. Aging Neurosci.* 7:230. doi: 10.3389/fnagi.2015.00230

Nilsson, J., Lebedev, A. V., Rydström, A., and Lövdén, M. (2017). Direct-current stimulation does little to improve the outcome of working memory training in older adults. *Psychol. Sci.* 28, 907–920. doi: 10.1177/0956797617698139

Nitsche, M. A., Cohen, L. G., Wassermann, E. M., Priori, A., Lang, N., Antal, A., et al. (2008). Transcranial direct current stimulation: state of the art 2008. *Brain Stimul.* 1, 206–223. doi: 10.1016/j.brs.2008.06.004

Nitsche, M. A., Fricke, K., Henschke, U., Schlitterlau, A., Liebetanz, D., Lang, N., et al. (2003a). Pharmacological modulation of cortical excitability shifts induced by transcranial direct current stimulation in humans. *J. Physiol.* 553, 293–301. doi: 10.1113/jphysiol.2003.049916

Nitsche, M. A., Jaussi, W., Liebetanz, D., Lang, N., Tergau, F., and Paulus, W. (2004). Consolidation of human motor cortical neuroplasticity by D-cycloserine. *Neuropsychopharmacol. Off. Publ. Am. Coll. Neuropsychopharmacol.* 29, 1573–1578. doi: 10.1038/sj.npp.1300517

Nitsche, M. A., Liebetanz, D., Antal, A., Lang, N., Tergau, F., and Paulus, W. (2003b). Modulation of cortical excitability by weak direct current stimulation–technical, safety and functional aspects. *Suppl. Clin. Neurophysiol.* 56, 255–276. doi: 10.1016/s1567-424x(09)70230-2

Nitsche, M. A., Nitsche, M. S., Klein, C. C., Tergau, F., Rothwell, J. C., and Paulus, W. (2003c). Level of action of cathodal DC polarisation induced inhibition of the human motor cortex. *Clin. Neurophysiol. Off. J. Int. Fed. Clin. Neurophysiol.* 114, 600–604. doi: 10.1016/s1388-2457(02)00412-1

Nitsche, M. A., and Paulus, W. (2000). Excitability changes induced in the human motor cortex by weak transcranial direct current stimulation. *J. Physiol.* 527, 633–639. doi: 10.1111/j.1469-7793.2000.t01-1-00633.x

Nitsche, M. A., and Paulus, W. (2001). Sustained excitability elefations induced by transcranial DC motor cortex stimulation in humans. *Neurology* 57, 1899–1901. doi: 10.1212/WNL.57.10.1899

Opitz, A., Paulus, W., Will, S., Antunes, A., and Thielscher, A. (2015). Determinants of the electric field during transcranial direct current stimulation. *NeuroImage* 109, 140–150. doi: 10.1016/j.neuroimage.2015.01.033

Page, M. J., McKenzie, J. E., Bossuyt, P. M., Boutron, I., Hoffmann, T. C., Mulrow, C. D., et al. (2021). The PRISMA 2020 statement: an updated guideline for reporting systematic reviews. *BMJ* 372:n71. doi: 10.1136/bmj.n71

Paßmann, S., Külzow, N., Ladenbauer, J., Antonenko, D., Grittner, U., Tamm, S., et al. (2016). Boosting Slow Oscillatory Activity Using tDCS during Early Nocturnal Slow Wave Sleep Does Not Improve Memory Consolidation in Healthy Older Adults. *Brain Stimulat.* 9, 730–739. doi: 10.1016/j.brs.2016.04.016

Penolazzi, B., Bergamaschi, S., Pastore, M., Villani, D., Sartori, G., and Mondini, S. (2015). Transcranial direct current stimulation and cognitive training in the rehabilitation of Alzheimer disease: A case study. *Neuropsychol. Rehabil.* 25, 799–817. doi: 10.1080/09602011.2014.977301

Petersen, R. C., Lopez, O., Armstrong, M. J., Getchius, T. S. D., Ganguli, M., Gloss, D., et al. (2018). Practice guideline update summary: Mild cognitive impairment: Report of the Guideline Development, Dissemination, and Implementation Subcommittee of the American Academy of Neurology. *Neurology* 90, 126–135. doi: 10.1212/WNL.0000000000004826

Petersen, R. C., and Negash, S. (2008). Mild cognitive impairment: an overview. *CNS Spectr.* 13, 45–53. doi: 10.1017/s1092852900016151

Polanía, R., Nitsche, M. A., and Paulus, W. (2011a). Modulating functional connectivity patterns and topological functional organization of the human brain with transcranial direct current stimulation. *Hum. Brain Mapp.* 32, 1236–1249. doi: 10.1002/hbm.21104

Polanía, R., Paulus, W., Antal, A., and Nitsche, M. A. (2011b). Introducing graph theory to track for neuroplastic alterations in the resting human brain: a transcranial direct current stimulation study. *NeuroImage* 54, 2287–2296. doi: 10.1016/j.neuroimage.2010.09.085

Polanía, R., Paulus, W., and Nitsche, M. A. (2012). Modulating cortico-striatal and thalamo-cortical functional connectivity with transcranial direct current stimulation. *Hum. Brain Mapp.* 33, 2499–2508. doi: 10.1002/hbm.21380

Prehn, K., and Flöel, A. (2015). Potentials and limits to enhance cognitive functions in healthy and pathological aging by tDCS. *Front. Cell. Neurosci.* 9. doi: 10.3389/fncel.2015.00355

Prehn, K., Stengl, H., Grittner, U., Kosiolek, R., Ölschläger, A., Weidemann, A., et al. (2017). Effects of anodal transcranial direct current stimulation and serotonergic enhancement on memory performance in young and older adults. *Neuropsychopharmacology* 42, 551–561. doi: 10.1038/npp.2016.170

Priori, A., Berardelli, A., Rona, S., Accornero, N., and Manfredi, M. (1998). Polarization of the human motor cortex through the scalp. *Neuroreport* 9, 2257–2260. doi: 10.1097/00001756-199807130-00020

Purpura, D. P., and McMurtry, J. G. (1965). Intracellular activities and evoked potential changes during polarization of motor cortex. *J. Neurophysiol.* 28, 166–185. doi: 10.1152/jn.1965.28.1.166

Rahman, A., Reato, D., Arlotti, M., Gasca, F., Datta, A., Parra, L. C., et al. (2013). Cellular effects of acute direct current stimulation: somatic and synaptic terminal effects. *J. Physiol.* 591, 2563–2578. doi: 10.1113/jphysiol.2012.247171

Reitz, C., and Mayeux, R. (2014). Alzheimer disease: epidemiology, diagnostic criteria, risk factors and biomarkers. *Biochem. Pharmacol.* 88, 640–651. doi: 10.1016/j.bcp.2013.12.024

Rönnlund, M., Nyberg, L., Bäckman, L., and Nilsson, L.-G. (2005). Stability, growth, and decline in adult life span development of declarative memory: cross-sectional and longitudinal data from a population-based study. *Psychol. Aging* 20, 3–18. doi: 10.1037/0882-7974.20.1.3

Ross, L. A., McCoy, D., Coslett, H. B., Olson, I. R., and Wolk, D. A. (2011). Improved proper name recall in aging after electrical stimulation of the anterior temporal lobes. *Front. Aging Neurosci.* 3:16. doi: 10.3389/fnagi.2011.00016

Sandrini, M., Manenti, R., Brambilla, M., Cobelli, C., Cohen, L. G., and Cotelli, M. (2016). Older adults get episodic memory boosting from noninvasive stimulation of prefrontal cortex during learning. *Neurobiol. Aging* 39, 210–216. doi: 10.1016/j.neurobiolaging.2015.12.010

Shin, Y.-I., Foerster, Á., and Nitsche, M. A. (2015). Transcranial direct current stimulation (tDCS)—application in neuropsychology. *Neuropsychologia* 69, 154–175. doi: 10.1016/j.neuropsychologia.2015.02.002

Smith, A. D. (2002). Imaging the progression of Alzheimer pathology through the brain. *Proc. Natl. Acad. Sci. U.S.A.* 99, 4135–4137. doi: 10.1073/pnas.082107399

Stagg, C. J., Best, J. G., Stephenson, M. C., O'Shea, J., Wylezinska, M., Kincses, Z. T., et al. (2009). Polarity-sensitive modulation of cortical neurotransmitters by transcranial stimulation. *J. Neurosci.* 29, 5202–5206. doi: 10.1523/JNEUROSCI.4432-08.2009

Stephens, J. A., and Berryhill, M. E. (2016). Older adults improve on everyday tasks after working memory training and neurostimulation. *Brain Stimulat.* 9, 553–559. doi: 10.1016/j.brs.2016.04.001

Thams, F., Kuzmina, A., Backhaus, M., Li, S.-C., Grittner, U., Antonenko, D., et al. (2020). Cognitive training and brain stimulation in prodromal Alzheimer's disease (AD-Stim)—study protocol for a double-blind randomized controlled phase IIb (monocenter) trial. *Alzheimers Res. Ther.* 12:142. doi: 10.1186/s13195-020-00692-5

United Nations (2019). *Growing at a Slower Pace, World Population Is Expected to Reach 9.7 Billion in 2050 and Could Peak at Nearly 11 Billion Around 2100 | UN DESA | United Nations Department of Economic and Social Affairs*. Available online at: https://www.un.org/development/desa/en/news/population/world-population-prospects-2019.html (accessed March 2, 2021).

Westerberg, C. E., Florczak, S. M., Weintraub, S., Mesulam, M.-M., Marshall, L., Zee, P. C., et al. (2015). Memory improvement via slow-oscillatory stimulation during sleep in older adults. *Neurobiol. Aging* 36, 2577–2586. doi: 10.1016/j.neurobiolaging.2015.05.014

Woods, A. J., Cohen, R., Marsiske, M., Alexander, G. E., Czaja, S. J., and Wu, S. (2018). Augmenting cognitive training in older adults (The ACT Study): design and Methods of a Phase III tDCS and cognitive training trial. *Contemp. Clin. Trials* 65, 19–32. doi: 10.1016/j.cct.2017.11.017

World Health Organization (2020). Dementi*a*. Available online at: https://www.who.int/news-room/fact-sheets/detail/dementia (accessed March 2, 2021).

Yun, K., Song, I.-U., and Chung, Y.-A. (2016). Changes in cerebral glucose metabolism after 3 weeks of noninvasive electrical stimulation of mild cognitive impairment patients. *Alzheimers Res. Ther.* 8:49. doi: 10.1186/s13195-016-0218-6

Conflict of Interest: The authors declare that the research was conducted in the absence of any commercial or financial relationships that could be construed as a potential conflict of interest.

frontiers in Human Neuroscience

ORIGINAL RESEARCH
published: 12 November 2021
doi: 10.3389/fnhum.2021.748241

The Immediate Effects of Intermittent Theta Burst Stimulation of the Cerebellar Vermis on Cerebral Cortical Excitability During a Balance Task in Healthy Individuals: A Pilot Study

Hui-Xin Tan[1,2†], Qing-Chuan Wei[1,2†], Yi Chen[1,2], Yun-Juan Xie[1,2], Qi-Fan Guo[1,2], Lin He[1,2] and Qiang Gao[1,2]*

[1] West China Hospital, Sichuan University, Chengdu, China, [2] Department of Rehabilitation Medicine, West China Hospital, Sichuan University, Chengdu, China

OPEN ACCESS

Edited by:
Masaki Sekino,
The University of Tokyo, Japan

Reviewed by:
Jack Jiaqi Zhang,
Hong Kong Polytechnic University, Hong Kong SAR, China
Kenneth N. K. Fong,
Hong Kong Polytechnic University, Hong Kong SAR, China

***Correspondence:**
Qiang Gao
gaoqiang_hxkf@163.com

[†] These authors have contributed equally to this work

Specialty section:
This article was submitted to Brain Imaging and Stimulation, a section of the journal Frontiers in Human Neuroscience

Received: 27 July 2021
Accepted: 25 October 2021
Published: 12 November 2021

Citation:
Tan H-X, Wei Q-C, Chen Y, Xie Y-J, Guo Q-F, He L and Gao Q (2021) The Immediate Effects of Intermittent Theta Burst Stimulation of the Cerebellar Vermis on Cerebral Cortical Excitability During a Balance Task in Healthy Individuals: A Pilot Study. Front. Hum. Neurosci. 15:748241. doi: 10.3389/fnhum.2021.748241

Objective: This pilot study aimed to investigate the immediate effects of single-session intermittent theta-burst stimulation (iTBS) on the cerebellar vermis during a balance task, which could unveil the changes of cerebral cortical excitability in healthy individuals.

Subjects: A total of seven right-handed healthy subjects (26.86 ± 5.30 years) were included in this study.

Interventions: Each subject received single-session iTBS on cerebellar vermis in a sitting position.

Main Measures: Before and after the intervention, all subjects were asked to repeat the balance task of standing on the left leg three times. Each task consisted of 15 s of standing and 20 s of resting. Real-time changes in cerebral cortex oxygen concentrations were monitored with functional near-infrared spectroscopy (fNIRS). During the task, changes in blood oxygen concentration were recorded and converted into the mean HbO_2 for statistical analysis.

Results: After stimulation, the mean HbO_2 in the left SMA ($P = 0.029$) and right SMA ($P = 0.043$) significantly increased compared with baseline. However, no significant changes of mean HbO_2 were found in the bilateral dorsolateral prefrontal lobe ($P > 0.05$).

Conclusion: Single-session iTBS on the cerebellar vermis in healthy adults can increase the excitability of the cerebral cortex in the bilateral supplementary motor areas during balance tasks.

Clinical Trial Registration: [www.ClinicalTrials.gov], identifier [ChiCTR2100048915].

Keywords: intermittent theta-burst stimulation, cerebellar vermis, balance, functional near-infrared spectroscopy, transcrancial magnetic stimulation (TMS)

INTRODUCTION

Balance is one of the most a critical function that supports the normal activities of daily life in humans. Maintaining balance requires a complex integration and coordination of multiple systems (such as the vestibular system, visual system and auditory system) in the body (Ataullah and Naqvi, 2021). The cerebellum is strongly involved in the integration process associated with balance in the central nervous system (CNS) (Nashef et al., 2019), as demonstrated by previous functional magnetic resonance imaging studies and clinical trials (Maurer et al., 2016; Esterman et al., 2017). According to the functional divisions of the cerebellum, the three functional areas include the cerebrocerebellum, the spinocerebellum and the vestibulocerebellum. These three functional areas all play a vital role in the process of maintaining balance and motor control. In the spinocerebellum, the cerebellar vermis plays a key role in balance and motor control. Recent evidence suggests that the cerebellar vermis is critical for maintaining equilibrium and coordinating speech, eye and body movement because the vermis provides information regarding sensations along the extremities, as well as the different stimuli that pertain to balance, visual and auditory processes (Fujita et al., 2020). In addition, the cerebellar vermis participates in anticipatory postural adjustment and compensatory postural adjustment to maintain balance during functional activities (Richard et al., 2017). Study has displayed patients with lesions in the vermis mainly exhibit balance dysfunction (Harris et al., 2018), while patients with lesions in the cerebellar hemispheres mainly exhibit global coordination dysfunction (Carass et al., 2018; Maas et al., 2020).

Except for the important role of cerebellum in balance, cerebral cortex is also involved. Previous studies illustrated that the supplementary motor area (SMA) and the dorsal lateral prefrontal cortex (DLPFC) are crucial during balance tasks (Richard et al., 2017; Harris et al., 2018; Fernandez et al., 2020). Richard et al. (2017) pointed out that the SMA plays an important role in the initiation of gait and the initiation of standing on one leg, which is related to maintaining stability during change of posture. Other studies have also confirmed the results obtained by Richard et al. (Mihara et al., 2012; Dale et al., 2019). Moreover, the increase in HbO_2 related to postural disturbance in the contralesional SMA is significantly correlated with the increase in balance function measured by the Berg balance scale, and the postural disturbance-related changes in HbO_2 signals in the bilateral SMA in stroke patients are positively correlated (Fujimoto et al., 2014). Studies also demonstrated that increased HbO_2 was positively correlated with cortical excitability and functional improvement (Liu et al., 2018; Kinoshita et al., 2019). In addition, studies have demonstrated that intercortical connections exist between the DLPFC and primary motor cortex (M1). The connections from the DLPFC to the M1 transfer crucial information for the execution of motor output (Cao et al., 2018). The results from Teo et al. (2018) highlighted the involvement of the DLPFC in maintaining postural control. Study also demonstrated that the prefrontal cortex (PFC) and temporal-parietal regions were engaged during active balancing process, which was thought to be involved with allocation of attentional demands in standing postural control (Mihara et al., 2008). The non-invasive brain stimulation (NIBS) was applied to the DLPFC in patients with Parkinson's disease and balance dysfunction, and balance function improved after intervention (Lattari et al., 2017). The results of a fNIRS study demonstrate that after external disturbances in healthy subjects, the bilateral DLPFC undergoes significant activation, which also indicates that the DLPFC also participates in maintaining balance (Mihara et al., 2012).

In current understandings, the process of maintaining balance involves the close cooperation between cerebellum and the cerebral. Some studies have established a strong anatomical and functional connections between cerebellum and M1 cortex through cerebellar-thalamus-M1 circuit (Coffman et al., 2011; Maurer et al., 2016). It is well worthy noted that previous study showed that the cerebellar vermis is a target of extensive projections from motor areas of cerebral cortex, which are involved in the regulation of whole-body posture and locomotion (Coffman et al., 2011). Additionally, anatomical experiment on monkey brains have shown that some cortical regions, especially the prefrontal cortex, receive projections from the cerebellum (Dale et al., 2019). Furthermore, Cho et al. (2012) pointed that the cerebellum connects not only to the M1 area and SMA but also to the DLPFC.

In recent years, NIBS of the cerebellum has also been a research hotspot (Benussi et al., 2020). There are a number of NIBS studies on the cerebellar hemisphere; however, studies of cerebellar vermis are relatively rare. Intermittent theta burst stimulation (iTBS), a type of repetitive transcranial magnetic stimulation (rTMS), which serves as a NIBS method, has been proved to have the positive effects on neuroplasticity and central nervous system excitability (Cotoi et al., 2019; Katagiri et al., 2020). It exhibits long lasting effects compared with traditional TMS with shorter stimulation period than traditional TMS (Kim et al., 2015; Hurtado-Puerto et al., 2020). Studies also demonstrated that iTBS can also modulate corticospinal excitability (Li et al., 2020). It is well known that regional hemodynamic responses are associated with cortical brain activation (Kinoshita et al., 2019). Recently, the use of fNIRS has become more widespread because the fNIRS system provides cortical brain activation information by measuring hemodynamic changes non-invasively (Kinoshita et al., 2019). Moreover, the cortical neural activity results obtained from fNIRS were similar to that from functional MRI (fMRI). The fNIRS is a useful tool that has been applied to record brain activation during balance tasks in previous study (Hoppes et al., 2020). Previous works by our research group have demonstrated that iTBS of the cerebellar hemisphere could improve balance and gait in patients with cerebral stroke. However, no significant changes in cortical excitability were observed (Liao et al., 2021).

Based on the extensive studies examining the relationship between cerebellum and cortex during balance tasks with the help of fNIRS, herein this study aimed to use fNIRS to explore the changes in cortical activation in the cerebral cortex (SMA and DLPFC) after iTBS of the cerebellar vermis during balance tasks.

We hypothesized that activation of the SMA and DLPFC regions may increase after iTBS stimulation compared to baseline.

MATERIALS AND METHODS

Subjects

A total of seven healthy volunteers were included in this study. The inclusion criteria were as follows: (1) age 18 to 35 years old (Aloraini et al., 2019), (2) free from neurological and psychiatric disorders, (3) right-handed dominance, (4) body mass index from 18.5 to 23.9 (Corp et al., 2018), and (5) signed informed consents. The exclusion criteria were as follows: (1) having suffered from neuropsychological diseases (depression, anxiety, schizophrenia and so on) in the past, (2) having a history of drug abuse (drugs that are potential hazards for rTMS, especially drugs that can lower seizure threshold) (Rossi et al., 2009), (3) individuals with musculoskeletal disorders, especially disorders in the lower limb and trunk, (4) subjects with vestibular deficits and (5) participated in other TMS experiments without reporting TMS exclusion criteria.

Intermittent Theta Burst Stimulation

A CCY-I rapid magnetic stimulator, which was connected to a double-cone coil (YIRUIDE Medical, China) was used to stimulate the cerebellar vermis for single-session iTBS. The coil type was a V1320T double-cone coil. The parameters of the coil were listed as follow: (1) outside diameter: Φ130 mm; (2) inside diameter: Φ70 mm; (3) distance between the two highest points at the top of the coil: 200 mm; (4) angle formed by the two conical coils: 120°. The targeted point was located 1 cm below the "inion" (the highest point of the external occipital protuberance) i.e., midline cerebellum (Cattaneo et al., 2014; Garg et al., 2016), and the coil was positioned tangentially to the scalp. When applying iTBS, the stimulator output intensity was set to the level of individual's maximum tolerated intensity (MTI) (Spampinato et al., 2020). The iTBS protocol began with a two-second burst train (totally 30 pulses), which repeats every 10 s. Each burst train consisted of ten triplet pulses with an inter-burst interval of 0.16s, thus the triplets fire at a rate of 5 Hz (**Figure 1**). Overall, each subject received 600 stimuli during a single-session iTBS (Huang et al., 2005). The total duration of the iTBS protocol was 3′20″ (Cao et al., 2018).

fNIRS Measurement

A multichannel fNIRS system (NirScan, HuiChuang, China) was used to record changes of HbO_2 in the cortex of the SMA and DLPFC. The wavelengths were set to 730 and 850 nm. Data were sampled at a frequency of 10 Hz (Lu et al., 2019). Fifty five channels (defined as the midpoint of the corresponding light source-detector pair) were established, with 20 light sources and 20 detectors for measurement. These channels were symmetrically distributed in the left and right cerebral hemispheres of the participants. The center of the middle probe set row was placed at approximately FPz, according to the 10/20 international system (Hu et al., 2019). The optodes were positioned over the left and right DLPFC (L-DLPFC: S10-D4, S10-D9, S11-D23 and S14-D23; R-DLPFC: S8-D2, S8-D8, S13-D17 and S13-D20) and the left and right SMA (L-SMA: S14-D15 and S15-D15; R-SMA: S12-D14 and S12-D20) (**Figure 2**).

Experimental Procedure

There were three phases of this experimental procedure (**Figure 3A**). During the trial, the humidity and temperature of the environment were kept stable, and the personnel present remained quiet. The three phases comprised a session of iTBS (while sitting) and balance tasks (while standing), which were identical before and after the stimulus (T1 and T2 phases). For the balance tasks, we set the process and the prompt sound at the corresponding time point in NirScan. During the balance task, participants were asked to stand with their left leg raised three times separate (**Figure 3B**). To minimize the error of the fNIRS recording process, which is usually due to postural changes, we allowed 10 s for sit-stand postural changes before and after stimulation (Liu et al., 2018; Koch et al., 2019). Throughout the three phases, real-time HbO_2 data was collected using fNIRS. In addition, we ensured that the temperature and humidity in the test process were basically unchanged, and everyone in the room (subject and assessor) remained silent throughout the entire test period (Bu et al., 2019).

Data Processing

The NirSpark (HuiChuang, China) software package was used to analyze the fNIRS data. First, light intensity was converted to optical density (OD). Then, motion artifacts were corrected the moving standard deviation and cubic spline interpolation method. A bandpass filter with cutoff frequencies of 0.01–0.1 Hz was then applied to remove physiological noise (respiration, cardiac activity and low-frequency signal drift). Finally, the filtered OD signal was converted to Delta-HbO2 and Delta-HHB according to the modified Beer-Lambert law. After that, we averaged the HbO_2 data of the three periods standing on one leg during T1 and T2. The mean value in the range of 10–15 s (relative to condition onset) was used for further statistical analysis.

Statistical Analysis

The mean HbO_2 values of each channel for 7 subjects before and after stimulation were imported into SPSS version 24.0 (IBM Corp) for analysis. The normality of the data was assessed using the Kolmogorov–Smirnov test. Except for channels S12-D14, the data from all channels passed the Kolmogorov–Smirnov test, which presented as the means (± standard deviations, SDs). The rank sum test was used for data from channels S12-D14, the data are presented as the medians (interquartile ranges, IQRs). For the DLPFC, the data from all channels passed the Kolmogorov–Smirnov test. A paired *t*-test was used for the data of the remaining channels, and presented as the means (± standard deviations, SDs). A difference with $P < 0.05$ was considered statistically significant.

Ethics Committee

Ethical approval was obtained from the biomedical ethics committee of West China Hospital at Sichuan University. The

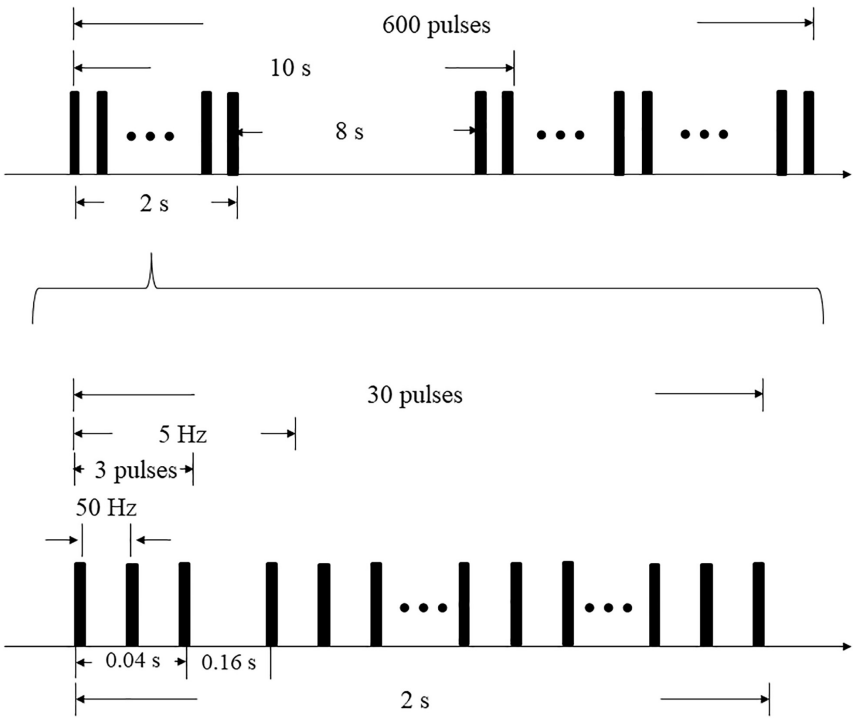

FIGURE 1 | iTBS protocol.

protocol of this study was registered with the Chinese Clinical Trial Registry (registration number: ChiCTR2100048915).

RESULTS

All subjects tolerated the trial, with no adverse events (**Table 1**). Mean HbO_2 significantly increased in channels S12-D14 ($P = 0.043$, $Z = 2.028$) and S15-D15 ($P = 0.029$, $t = 2.849$) at T2 compared with T1 (**Table 2** and **Figure 4**). There was no difference in any channel in the DLPFC ($P > 0.05$) (**Table 2** and **Figure 4**). In addition, we also found that the mean changes in HbO_2 in the bilateral brain region before and after stimulation were obvious through the distribution map of mean HbO_2 (**Figure 5**).

DISCUSSION

In this study, we found that single-session iTBS of the cerebellar vermis could increase the concentration of HbO_2 in the SMA region during the balance task, but no significant increase was found in the DLPFC.

After a single-session of iTBS on cerebellar vermis, the increments of HbO2 in the SMA region indicated an excitability increase in the SMA cortex. This result indicates a potential connection between the cerebellar vermis and the SMA, which is consistent with previous studies (Coffman et al., 2011; Franca et al., 2018). Animal study has demonstrated that cortical motor areas are a source of input to the cerebellar vermis, especially lobules VB–VIIIB (Coffman et al., 2011). One of these areas is the SMA. In our study, it was interesting that the excitability of the bilateral SMA increased during the balance task after iTBS on cerebellar vermis, which may indicate that the cerebellar vermis and bilateral SMA are involved in neuromotor control and balance processes. A study conducted by Fujimoto et al. (2014) showed that increased cortical excitability in the bilateral SMA regions was positively correlated with improved balance function (Fujimoto et al., 2014), some other studies obtained the same results (Kinoshita et al., 2019). Therefore, the cerebellar vermis may be a new target for iTBS stimulation to influence balance function and postural control in humans, but more formal studies are needed to prove this hypothesis.

In this study, we found no significant changes in HbO_2 in the DLPFC. However, previous studies have demonstrated that the DLPFC is also involved in postural control (Taube et al., 2015), coordinating with the cerebellar vermis (Farzan et al., 2016). Furthermore, the DLPFC participates in planning actions by providing flexibility among already acquired solutions (Torriero et al., 2007). Early results indicated that, in addition to the long-established role of the cerebellum in motor coordination, the cerebellum appears to be involved in the central integration of cognition and emotion (Demirtas-Tatlidede et al., 2011; Cho et al., 2012). The connection between the cerebellum and the contralateral motor cortex is close and important. In addition to the M1 area, the cerebellum also projects to the DLPFC (Maas et al., 2020). Our study result is inconsistent with the results of previous studies (Mihara et al., 2012). A possible explanation for this result might derived from the small sample

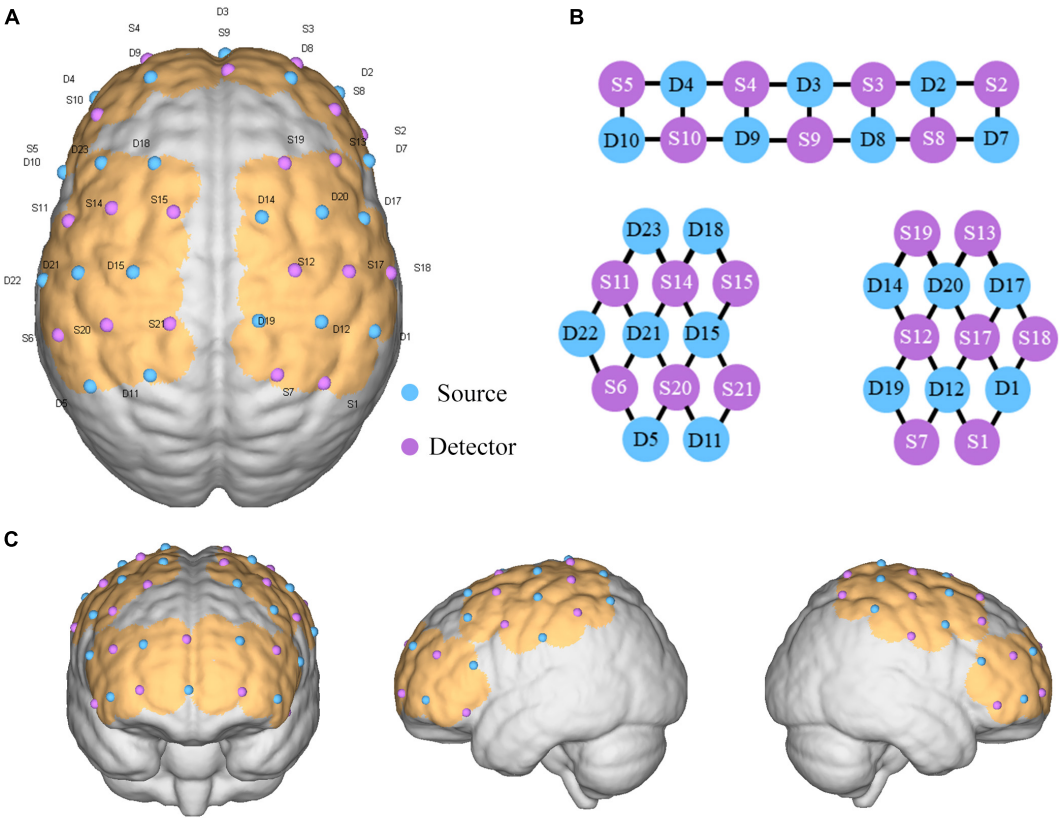

FIGURE 2 | Placement of optode. **(A)** Optode set arrangement with numbers displayed on a three-dimensional model of the brain (ICBM 152 Non-linear Atlases, version 2009). **(B)** Two-dimensional distribution of the light source and detection point. **(C)** Cerebral cortex where channels are covered.

FIGURE 3 | The experimental procedure **(A)** includes three phases; "T1" and "T2" indicate balance tasks, **(B)** balance task in T1 and T2: "a" means standing on the right leg for 15 s, "b" means resting for 20 s while standing.

TABLE 1 | Characteristics of the subjects ($N = 7$).

Subjects	Gender	Hand dominance	Age (year)	Height (cm)	Weight (kg)
1	M	Right	20	170	67
2	M	Right	34	169	60
3	M	Right	26	182	65
4	M	Right	27	165	78
5	M	Right	24	187	85
6	M	Right	22	172	64
7	M	Right	35	160	55
All	M	Right	26.86 ± 5.30[a]	172.14 ± 8.71[a]	67.71 ± 9.62[a]

[a]*Mean ± standard deviation.*

size. The balance task is very simple, which does not involve much cognitive function or motor integration, may be another possible explanation (Torriero et al., 2007). Moreover, the DLPFC, along with its association connections, constitutes a potential cortical network for visual reaching (Johnson et al., 1996). However, in our study, subjects were required to open their eyes while standing on a single leg to maintain balance, which may account for the lack of significant differences in the data.

We already know that these inter-connections between cerebellum and cerebral tissue are mainly bundles of white matter fibers with the following connective pathways: the cortico-ponto-cerebellar pathway and cerebello-thalamo-cortical (CTC) pathway (Iwata and Ugawa, 2005; Opie and Semmler, 2020). These neural pathways are functionally involved in motor coordination and cognitive functions (Bonnì et al., 2014). Moreover, previous studies have demonstrated that fibers from the cerebellar hemispheres could project to the contralateral cerebral cortex (Tramontano et al., 2020; Solanki et al., 2021). In addition, in right-handed individuals, the connection between the right cerebellum and the left M1 is usually stronger than that of the contralateral network (Schlerf et al., 2015). This implicates that we can explore the differences in cortical excitatory activation on both sides in future studies.

In the studies we reviewed, NIBS of the cerebellar vermis could be traced back to 1995. Hashimoto et al. used TMS on cerebellar vermis of humans to explore the relationship between the cerebellar vermis and eye saccades (Hashimoto and Ohtsuka, 1995). The results of their study

TABLE 2 | Mean HbO_2 for each channel at T1 and T2.

Brain area	Channel	T1	T2
SMA			
R-SMA	S12-D14	0.09 (0.2)	0.1 (0.21)*
	S12-D20	0.01 ± 0.09	0.07 ± 0.03
L-SMA	S14-D15	0.05 ± 0.11	0.13 ± 0.07
	S15-D15	0.11 ± 0.11	0.21 ± 0.10*
DLPFC			
R-DLPFC	S8-D2	0.039 ± 0.1	0.05 ± 0.07
	S8-D8	0.11 ± 0.07	0.12 ± 0.64
	S13-D17	0.07 ± 0.04	0.10 ± 0.07
	S13-D20	0.04 ± 0.07	0.08 ± 0.08
L-DLPFC	S10-D4	0.09 ± 0.1	0.07 ± 0.08
	S10-D9	0.11 ± 0.07	0.10 ± 0.06
	S11-D23	0.03 ± 0.08	0.85 ± 0.06
	S14-D23	0.04 ± 0.07	0.09 ± 0.06

*$P < 0.05$.

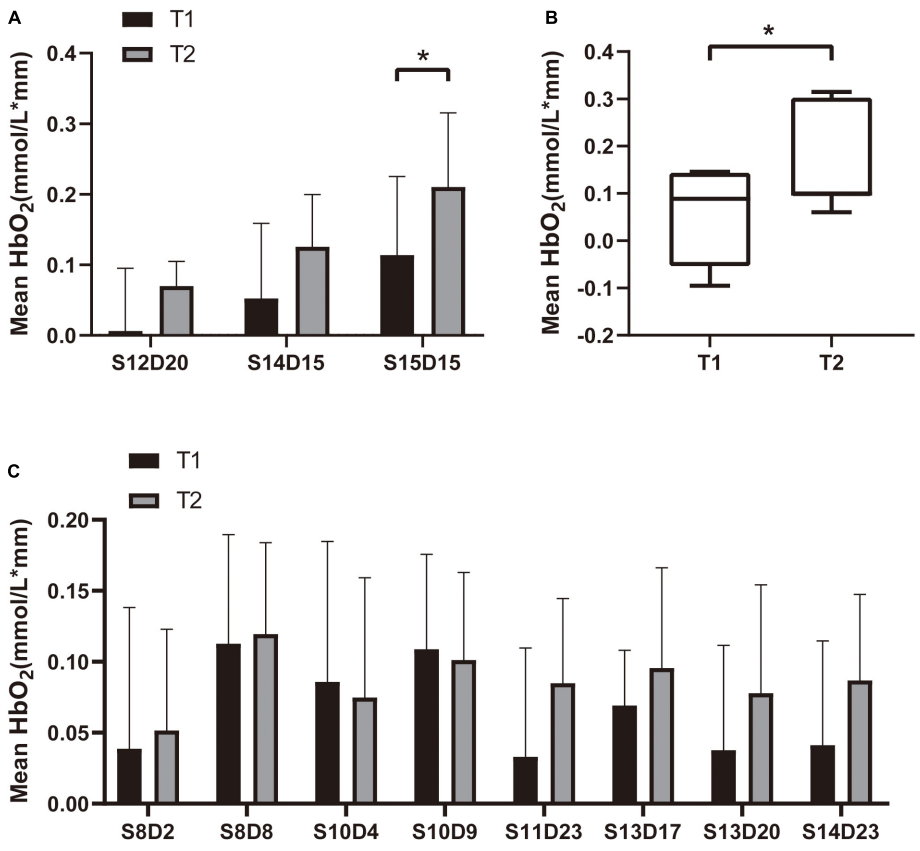

FIGURE 4 | Mean HbO_2 for each channel in the **(A)** SMA (S12D20, S14D15 and S15D15), **(B)** SMA (S12D14), and **(C)** DLPFC. We plot the mean with SD in panels **(A,C)**, and median with min to max in panel **(B)**. *$P < 0.05$.

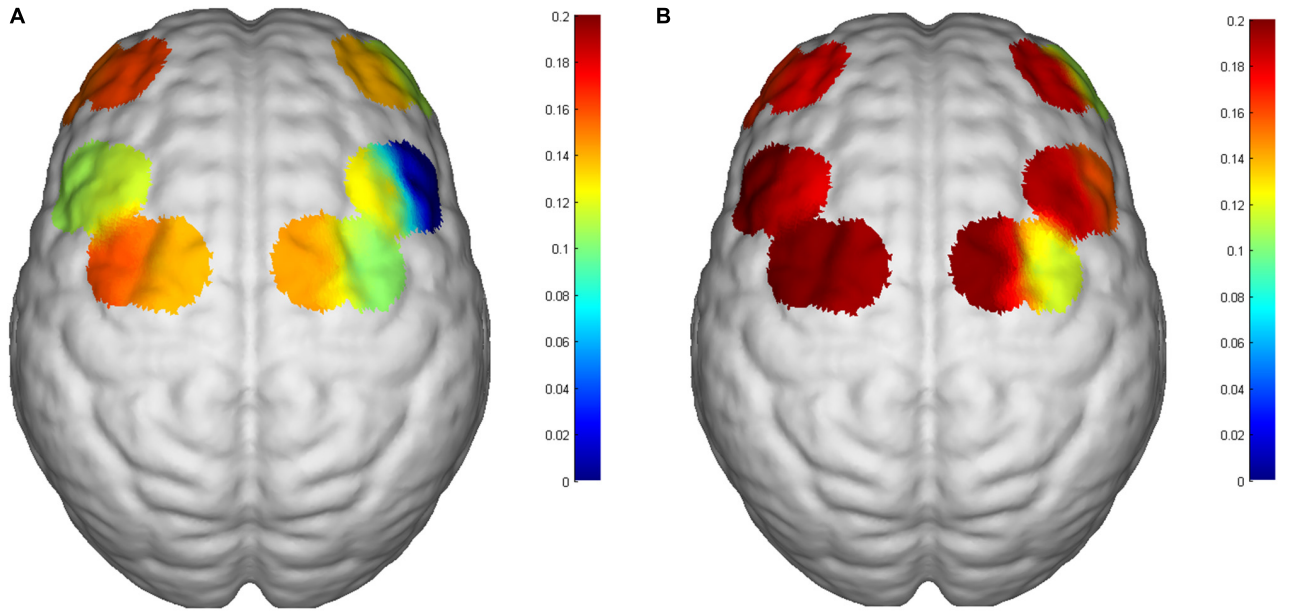

FIGURE 5 | Changes in mean HbO2 of the 6th subject. **(A)** Before iTBS and **(B)** post iTBS. Significant activation in the SMA in the post-iTBS phase relative to baseline. The number on the left of the color bar stands for mean HbO2, which means that the larger the mean HbO2 value of a channel, the closer the color is to red; otherwise, the closer it is to blue.

demonstrated that the posterior medial cerebellum in humans is involved in controlling the accuracy of visually guided saccades. Since then, due to neurophysiology of the connections between the cerebellum and different cortical layers of the cerebral cortex drew much attention, studies of NIBS of the cerebellum have gradually increased in different fields. For balance function and postural control in males, Cha YH indicated that cTBS on occipital cortex or the cerebellar vermis could effectively reduce the wobbling vertigo of Mal de Debarquement syndrome and may yield long-term benefits for patients (Cha et al., 2019). In 2020, a feasibility study found an association between cerebellar lobular mean electric field strength and changes in quantitative gait parameters after a single cerebellar transcranial direct-current stimulation (tDCS) session in chronic stroke patients (Kumari et al., 2020). In addition, the cerebellar vermis is involved in directing the postural response to a vestibular perturbation, which supports our hypothesis that the cerebellar vermis could be a target of NIBS to affect balance function and walking. Additionally, a study demonstrated that cTBS stimulating cerebellar vermis could lead to a significant influence on balance function as body sway increases (Colnaghi et al., 2017). For other effects on humans, Sasegbon et al. (2021) found that TMS on cerebellar vermis has an inhibitory effect on pharyngeal cortical activity and swallowing. Moreover, Argyropoulos et al. (2011) demonstrated that TBS of the right neocerebellar vermis can selectively disrupt the practice-induced acceleration of lexical decisions. As pointed out in neurophysiological research, the cerebellar vermis may be involved in the regulation of a series of non-physical functions (Van Overwalle et al., 2020). iTBS of the cerebellar vermis could result in the negative symptoms of schizophrenia patients. Similarly, non-invasive brain stimulation of the cerebellar vermis can also relieve symptoms of depression (Escelsior et al., 2019).

Regarding the coils we used, previous studies presented mostly used a figure-8 coil for iTBS (Franca et al., 2018). However, the latest research recommends a double-cone coil (Spampinato et al., 2020) because the use of a double-cone coil can achieve deeper stimulation effects in the cerebellar vermis. The safety of the double-cone coil in iTBS is guaranteed (Spampinato et al., 2020). In summary, stimulation of the cerebellar vermis with iTBS can increase the cortical excitability of the bilateral SMA, but the changes in the DLPFC are not significant and still need further exploration in formal studies.

LIMITATIONS

There are some limitations of our pilot study. Firstly, the major limitation of our study is that we did not used behavioral assessments to prove whether iTBS could improve balance function. However, more behavioral assessments will be performed in our future formal studies to determine whether iTBS of the cerebellar vermis could improve balance function. Second, the study had a small sample size and was limited to healthy volunteers, and a larger sample size is needed in future studies. The focus of future trials should be the inclusion of more patients. Third, our trial did not use navigational equipment, which may have reduced the accuracy of iTBS processes. In future studies, we will include navigational devices in experiments to improve the accuracy of iTBS on cerebellar vermis. Besides, the statistical tests in our study were not Bonferroni-corrected, which

may increase the probability of type I error. Furthermore, we used only a single-session of iTBS of the cerebellar vermis in this study, and the long-term effects of iTBS of the cerebellar vermis will be explored in formal experiments in the future.

CONCLUSION

In this study, we found that a single-session iTBS of the cerebellar vermis in healthy adults can increase the excitability of the cerebral cortex in the bilateral SMA during the balance tasks. Therefore, the iTBS on the cerebellar vermis may be a potentially effective intervention for improving balance function for the stroke patients with balance disorders.

DATA AVAILABILITY STATEMENT

The original contributions presented in the study are included in the article/supplementary material, further inquiries can be directed to the corresponding author/s.

ETHICS STATEMENT

The studies involving human participants were reviewed and approved by Institutional Review Board of West China Hospital, Sichuan University. The patients/participants provided their written informed consent to participate in this study.

AUTHOR CONTRIBUTIONS

H-XT and Q-CW devised the project under the supervision of QG and drafted the manuscript. YC, Y-JX, Q-FG, and LH conducted the data collection and data analysis. All authors provided critical feedback and helped shape the research, analysis, and manuscript.

FUNDING

The author(s) disclosed receipt of the following financial support for the research, authorship, and/or publication of this article: (1) This study was funded by the 1·3·5 Project for Disciplines of Excellence–Clinical Research Incubation Project, West China Hospital, Sichuan University (Grant Number: 2020HXFH051) and (2) the Department of Science and Technology of Sichuan Province (Grant Number: 2021YFS0069).

ACKNOWLEDGMENTS

We would like to thank the healthy subjects who participated in the project and to the researchers involved in this study who work at the Department of Rehabilitation Medicine of West China Hospital at Sichuan University.

REFERENCES

Aloraini, S. M., Glazebrook, C. M., Sibley, K. M., Singer, J., and Passmore, S. (2019). Anticipatory postural adjustments during a Fitts' task: Comparing young versus older adults and the effects of different foci of attention. *Hum. Mov. Sci.* 64, 366–377. doi: 10.1016/j.humov.2019.02.019

Argyropoulos, G. P., Kimiskidis, V. K., and Papagiannopoulos, S. (2011). θ-burst stimulation of the right neocerebellar vermis selectively disrupts the practice-induced acceleration of lexical decisions. *Behav. Neurosci.* 125, 724–734. doi: 10.1037/a0025134

Ataullah, A., and Naqvi, I. A. (2021). "Cerebellar dysfunction," in *StatPearls* (Treasure Island, FL: StatPearls Publishing).

Benussi, A., Pascual-Leone, A., and Borroni, B. (2020). Non-Invasive Cerebellar Stimulation in Neurodegenerative Ataxia: A Literature Review. *Int. J. Mol. Sci.* 21:1948. doi: 10.3390/ijms21061948

Bonnì, S., Ponzo, V., Caltagirone, C., and Koch, G. (2014). Cerebellar theta burst stimulation in stroke patients with ataxia. *Funct. Neurol.* 29, 41–45. doi: 10.11138/FNeur/2014.29.1.041

Bu, L., Huo, C., Qin, Y., Xu, G., Wang, Y., and Li, Z. (2019). Effective Connectivity in Subjects With Mild Cognitive Impairment as Assessed Using Functional Near-Infrared Spectroscopy. *Am. J. Phys. Med. Rehabil.* 98, 438–445. doi: 10.1097/PHM.0000000000001118

Cao, N., Pi, Y., Liu, K., Meng, H., Wang, Y., Zhang, J., et al. (2018). Inhibitory and facilitatory connections from dorsolateral prefrontal to primary motor cortex in healthy humans at rest-An rTMS study. *Neurosci. Lett.* 687, 82–87. doi: 10.1016/j.neulet.2018.09.032

Carass, A., Cuzzocreo, J. L., Han, S., Hernandez-Castillo, C. R., Rasser, P. E., Ganz, M., et al. (2018). Comparing fully automated state-of-the-art cerebellum parcellation from magnetic resonance images. *Neuroimage* 183, 150–172. doi: 10.1016/j.neuroimage.2018.08.003

Cattaneo, Z., Renzi, C., Casali, S., Silvanto, J., Vecchi, T., Papagno, C., et al. (2014). Cerebellar vermis plays a causal role in visual motion discrimination. *Cortex* 58, 272–280. doi: 10.1016/j.cortex.2014.01.012

Cha, Y. H., Gleghorn, D., and Doudican, B. (2019). Occipital and Cerebellar Theta Burst Stimulation for Mal De Debarquement Syndrome. *Otol. Neurotol.* 1, e928–e937. doi: 10.1097/MAO.0000000000002341

Cho, S. S., Yoon, E. J., Bang, S. A., Park, H. S., Kim, Y. K., Strafella, A. P., et al. (2012). Metabolic changes of cerebrum by repetitive transcranial magnetic stimulation over lateral cerebellum: a study with FDG PET. *Cerebellum* 1, 739–748. doi: 10.1007/s12311-011-0333-7

Coffman, K. A., Dum, R. P., and Strick, P. L. (2011). Cerebellar vermis is a target of projections from the motor areas in the cerebral cortex. *Proc. Natl. Acad. Sci. U S A.* 108, 16068–16073. doi: 10.1073/pnas.1107904108

Colnaghi, S., Honeine, J. L., Sozzi, S., and Schieppati, M. (2017). Body Sway Increases After Functional Inactivation of the Cerebellar Vermis by cTBS. *Cerebellum* 16, 1–14. doi: 10.1007/s12311-015-0758-5

Corp, D. T., Youssef, G. J., Clark, R. A., Gomes-Osman, J., Yücel, M. A., Oldham, S. J., et al. (2018). Reduced motor cortex inhibition and a 'cognitive-first' prioritisation strategy for older adults during dual-tasking. *Exp. Gerontol.* 113, 95–105. doi: 10.1016/j.exger.2018.09.018

Cotoi, A., Mirkowski, M., Iruthayarajah, J., Anderson, R., and Teasell, R. (2019). The effect of theta-burst stimulation on unilateral spatial neglect following stroke: a systematic review. *Clin. Rehabil.* 33, 183–194. doi: 10.1177/0269215518804018

Dale, M. L., DeVries, W. H., Mancini, M., and George, M. S. (2019). Cerebellar rTMS for motor control in progressive supranuclear palsy. *Brain Stimul.* 1, 1588–1591. doi: 10.1016/j.brs.2019.07.017

Demirtas-Tatlidede, A., Freitas, C., Pascual-Leone, A., and Schmahmann, J. D. (2011). Modulatory effects of theta burst stimulation on cerebellar nonsomatic functions. *Cerebellum* 1, 495–503. doi: 10.1007/s12311-010-0230-5

Escelsior, A., Belvederi Murri, M., Calcagno, P., Cervetti, A., Caruso, R., Croce, E., et al. (2019). Effectiveness of Cerebellar Circuitry Modulation in Schizophrenia: A Systematic Review. *J. Nerv. Ment. Dis.* 1, 977–986. doi: 10.1097/NMD.0000000000001064

Esterman, M., Thai, M., Okabe, H., DeGutis, J., Saad, E., Laganiere, S. E., et al. (2017). Network-targeted cerebellar transcranial magnetic stimulation

improves attentional control. *Neuroimage* 156, 190–198. doi: 10.1016/j.neuroimage.2017.05.011

Farzan, F., Pascual-Leone, A., Schmahmann, J. D., and Halko, M. (2016). Enhancing the Temporal Complexity of Distributed Brain Networks with Patterned Cerebellar Stimulation. *Sci. Rep.* 6:23599. doi: 10.1038/srep23599

Fernandez, L., Rogasch, N. C., Do, M., Clark, G., Major, B. P., Teo, W. P., et al. (2020). Cerebral Cortical Activity Following Non-invasive Cerebellar Stimulation-a Systematic Review of Combined TMS and EEG Studies. *Cerebellum* 19, 309–335. doi: 10.1007/s12311-019-01093-7

Franca, C., de Andrade, D. C., Teixeira, M. J., Galhardoni, R., Silva, V., Barbosa, E. R., et al. (2018). Effects of cerebellar neuromodulation in movement disorders: A systematic review. *Brain Stimul.* 1, 249–260. doi: 10.1016/j.brs.2017.11.015

Fujimoto, H., Mihara, M., Hattori, N., Hatakenaka, M., Kawano, T., Yagura, H., et al. (2014). Cortical changes underlying balance recovery in patients with hemiplegic stroke. *Neuroimage* 85, 547–554. doi: 10.1016/j.neuroimage.2013.05.014

Fujita, H., Kodama, T., and du Lac, S. (2020). Modular output circuits of the fastigial nucleus for diverse motor and nonmotor functions of the cerebellar vermis. *Elife* 9:2209. doi: 10.7554/eLife.58613

Garg, S., Sinha, V. K., Tikka, S. K., Mishra, P., and Goyal, N. (2016). The efficacy of cerebellar vermal deep high frequency (theta range) repetitive transcranial magnetic stimulation (rTMS) in schizophrenia: A randomized rater blind-sham controlled study. *Psychiatry Res.* 243, 413–420. doi: 10.1016/j.psychres.2016.07.023

Harris, D. M., Rantalainen, T., Muthalib, M., Johnson, L., Duckham, R. L., Smith, S. T., et al. (2018). Concurrent exergaming and transcranial direct current stimulation to improve balance in people with Parkinson's disease: study protocol for a randomised controlled trial. *Trials* 19:387. doi: 10.1186/s13063-018-2773-6

Hashimoto, M., and Ohtsuka, K. (1995). Transcranial magnetic stimulation over the posterior cerebellum during visually guided saccades in man. *Brain* 118, 1185–1193. doi: 10.1093/brain/118.5.1185

Hoppes, C. W., Huppert, T. J., Whitney, S. L., Dunlap, P. M., DiSalvio, N. L., Alshebber, K. M., et al. (2020). Changes in Cortical Activation During Dual-Task Walking in Individuals With and Without Visual Vertigo. *J. Neurol. Phys. Ther.* 44, 156–163. doi: 10.1097/NPT.0000000000000310

Hu, X., Zhuang, C., Wang, F., Liu, Y. J., Im, C. H., and Zhang, D. (2019). fNIRS Evidence for Recognizably Different Positive Emotions. *Front. Hum. Neurosci.* 13:120. doi: 10.3389/fnhum.2019.00120

Huang, Y. Z., Edwards, M. J., Rounis, E., Bhatia, K. P., and Rothwell, J. C. (2005). Theta burst stimulation of the human motor cortex. *Neuron* 45, 201–206. doi: 10.1016/j.neuron.2004.12.033

Hurtado-Puerto, A. M., Nestor, K., Eldaief, M., and Camprodon, J. A. (2020). Safety Considerations for Cerebellar Theta Burst Stimulation. . *Clin. Therapeut.* 42, 1169–1190. doi: 10.1016/j.clinthera.2020.06.001

Iwata, N. K., and Ugawa, Y. (2005). The effects of cerebellar stimulation on the motor cortical excitability in neurological disorders: a review. *Cerebellum* 1, 218–223. doi: 10.1080/14734220500277007

Johnson, P. B., Ferraina, S., Bianchi, L., and Caminiti, R. (1996). Cortical networks for visual reaching: physiological and anatomical organization of frontal and parietal lobe arm regions. *Cereb. Cortex* 6, 102–119. doi: 10.1093/cercor/6.2.102

Katagiri, N., Yoshida, S., Koseki, T., Kudo, D., Namba, S., Tanabe, S., et al. (2020). Interindividual Variability of Lower-Limb Motor Cortical Plasticity Induced by Theta Burst Stimulation. *Front. Neurosci.* 14:563293. doi: 10.3389/fnins.2020.563293

Kim, D. H., Shin, J. C., Jung, S., Jung, T. M., and Kim, D. Y. (2015). Effects of intermittent theta burst stimulation on spasticity after stroke. *Neuroreport* 26, 561–566. doi: 10.1097/wnr.0000000000000388

Kinoshita, S., Tamashiro, H., Okamoto, T., Urushidani, N., and Abo, M. (2019). Association between imbalance of cortical brain activity and successful motor recovery in sub-acute stroke patients with upper limb hemiparesis: a functional near-infrared spectroscopy study. *Neuroreport* 30, 822–827. doi: 10.1097/WNR.0000000000001283

Koch, G., Bonni, S., Casula, E. P., Iosa, M., Paolucci, S., Pellicciari, M. C., et al. (2019). Effect of Cerebellar Stimulation on Gait and Balance Recovery in Patients With Hemiparetic Stroke: A Randomized Clinical Trial. *JAMA Neurol.* 1, 170–178. doi: 10.1001/jamaneurol.2018.3639

Kumari, N., Taylor, D., Olsen, S., Rashid, U., and Signal, N. (2020). Cerebellar transcranial direct current stimulation for motor learning in people with chronic stroke: a pilot randomized controlled trial. *Brain sci.* 10:982. doi: 10.3390/brainsci10120982

Lattari, E., Costa, S. S., Campos, C., de Oliveira, A. J., Machado, S., and Maranhao Neto, G. A. (2017). Can transcranial direct current stimulation on the dorsolateral prefrontal cortex improves balance and functional mobility in Parkinson's disease? *Neurosci. Lett.* 636, 165–169. doi: 10.1016/j.neulet.2016.11.019

Li, J., Ren, M., Wang, W., Xu, S., Zhang, S., Li, Y., et al. (2020). Human Theta Burst Stimulation Combined with Subsequent Electroacupuncture Increases Corticospinal Excitability. *Evid. Based Complement Alternat. Med.* 9, 1–8. doi: 10.1155/2020/8824530

Liao, L. Y., Xie, Y. J., Chen, Y., and Gao, Q. (2021). Cerebellar Theta-Burst Stimulation Combined With Physiotherapy in Subacute and Chronic Stroke Patients: A Pilot Randomized Controlled Trial. *Neurorehabil. Neural Repair.* 35, 23–32. doi: 10.1177/1545968320971735

Liu, Y. C., Yang, Y. R., Tsai, Y. A., Wang, R. Y., and Lu, C. F. (2018). Brain Activation and Gait Alteration During Cognitive and Motor Dual Task Walking in Stroke-A Functional Near-Infrared Spectroscopy Study. *IEEE Trans. Neural Syst. Rehabil. Eng.* 26, 2416–2423. doi: 10.1109/TNSRE.2018.2878045

Lu, K., Xu, G., Li, W., Huo, C., Liu, Q., Lv, Z., et al. (2019). Frequency-specific functional connectivity related to the rehabilitation task of stroke patients. *Med. Phys.* 46, 1545–1560. doi: 10.1002/mp.13398

Maas, R., Helmich, R. C. G., and van de Warrenburg, B. P. C. (2020). The role of the cerebellum in degenerative ataxias and essential tremor: Insights from noninvasive modulation of cerebellar activity. *Mov. Disord.* 35, 215–227. doi: 10.1002/mds.27919

Maurer, C. W., LaFaver, K., Ameli, R., Epstein, S. A., Hallett, M., and Horovitz, S. G. (2016). Impaired self-agency in functional movement disorders: A resting-state fMRI study. *Neurology* 87, 564–570.

Mihara, M., Miyai, I., Hatakenaka, M., Kubota, K., and Sakoda, S. (2008). Role of the prefrontal cortex in human balance control. *Neuroimage* 43, 329–336. doi: 10.1016/j.neuroimage.2008.07.029

Mihara, M., Miyai, I., Hattori, N., Hatakenaka, M., Yagura, H., Kawano, T., et al. (2012). Cortical control of postural balance in patients with hemiplegic stroke. *Neuroreport* 23, 314–319. doi: 10.1097/WNR.0b013e328351757b

Nashef, A., Cohen, O., Harel, R., Israel, Z., and Prut, Y. (2019). Reversible Block of Cerebellar Outflow Reveals Cortical Circuitry for Motor Coordination. *Cell Rep.* 27, 2608–2619.

Opie, G. M., and Semmler, J. G. (2020). Characterising the influence of cerebellum on the neuroplastic modulation of intracortical motor circuits. *PLoS One* 1:e0236005. doi: 10.1371/journal.pone.0236005

Richard, A., Van Hamme, A., Drevelle, X., Golmard, J. L., Meunier, S., and Welter, M. L. (2017). Contribution of the supplementary motor area and the cerebellum to the anticipatory postural adjustments and execution phases of human gait initiation. *Neuroscience* 358, 181–189. doi: 10.1016/j.neuroscience.2017.06.047

Rossi, S., Hallett, M., Rossini, P. M., and Pascual-Leone, A. (2009). Safety, ethical considerations, and application guidelines for the use of transcranial magnetic stimulation in clinical practice and research. *Clin. Neurophysiol.* 12, 2008–2039. doi: 10.1016/j.clinph.2009.08.016

Sasegbon, A., Niziolek, N., Zhang, M., Smith, C. J., Bath, P. M., Rothwell, J., et al. (2021). The Effects of Midline Cerebellar rTMS on Human Pharyngeal Cortical Activity in the Intact Swallowing Motor System. *Cerebellum* 20, 101–115. doi: 10.1007/s12311-020-01191-x

Schlerf, J. E., Galea, J. M., Spampinato, D., and Celnik, P. A. (2015). Laterality Differences in Cerebellar-Motor Cortex Connectivity. *Cereb. Cortex* 7, 1827–1834. doi: 10.1093/cercor/bht422

Solanki, D., Rezaee, Z., Dutta, A., and Lahiri, U. (2021). Investigating the feasibility of cerebellar transcranial direct current stimulation to facilitate post-stroke overground gait performance in chronic stroke: a partial least-squares regression approach. *J. Neuroeng. Rehabil.* 18:18. doi: 10.1186/s12984-021-00817-3

Spampinato, D., Ibanez, J., Spanoudakis, M., Hammond, P., and Rothwell, J. C. (2020). Cerebellar transcranial magnetic stimulation: The role of coil type

from distinct manufacturers. *Brain Stimul.* 1, 153–156. doi: 10.1016/j.brs.2019.09.005

Taube, W., Mouthon, M., Leukel, C., Hoogewoud, H. M., Annoni, J. M., and Keller, M. (2015). Brain activity during observation and motor imagery of different balance tasks: an fMRI study. *Cortex* 64, 102–114. doi: 10.1016/j.cortex.2014.09.022

Teo, W. P., Goodwill, A. M., Hendy, A. M., Muthalib, M., and Macpherson, H. (2018). Sensory manipulation results in increased dorsolateral prefrontal cortex activation during static postural balance in sedentary older adults: An fNIRS study. *Brain Behav.* 8:e01109. doi: 10.1002/brb3.1109

Torriero, S., Oliveri, M., Koch, G., Caltagirone, C., and Petrosini, L. (2007). The what and how of observational learning. *J. Cogn. Neurosci.* 10, 1656–1663. doi: 10.1162/jocn.2007.19.10.1656

Tramontano, M., Grasso, M. G., Soldi, S., Casula, E. P., Bonnì, S., Mastrogiacomo, S., et al. (2020). Cerebellar Intermittent Theta-Burst Stimulation Combined with Vestibular Rehabilitation Improves Gait and Balance in Patients with Multiple Sclerosis: a Preliminary Double-Blind Randomized Controlled Trial. *Cerebellum* 19, 897–901. doi: 10.1007/s12311-020-01166-y

Van Overwalle, F., Manto, M., Cattaneo, Z., Clausi, S., Ferrari, C., Gabrieli, J. D. E., et al. (2020). Consensus Paper: Cerebellum and Social Cognition. *Cerebellum* 19, 833–868. doi: 10.1007/s12311-020-01155-1

Conflict of Interest: The authors declare that the research was conducted in the absence of any commercial or financial relationships that could be construed as a potential conflict of interest.

Publisher's Note: All claims expressed in this article are solely those of the authors and do not necessarily represent those of their affiliated organizations, or those of the publisher, the editors and the reviewers. Any product that may be evaluated in this article, or claim that may be made by its manufacturer, is not guaranteed or endorsed by the publisher.

frontiers in Human Neuroscience

REVIEW
published: 23 November 2021
doi: 10.3389/fnhum.2021.735561

Using Transcranial Electrical Stimulation in Audiological Practice: The Gaps to Be Filled

Mujda Nooristani[1,2], Thomas Augereau[1,2], Karina Moïn-Darbari[1,2], Benoit-Antoine Bacon[3] and François Champoux[1,2]*

[1] École d'Orthophonie et d'Audiologie, Université de Montréal, Montréal, QC, Canada, [2] Centre de Recherche de l'Institut Universitaire de Gériatrie de Montréal, Montréal, QC, Canada, [3] Department of Psychology, Carleton University, Ottawa, ON, Canada

The effects of transcranial electrical stimulation (tES) approaches have been widely studied for many decades in the motor field, and are well known to have a significant and consistent impact on the rehabilitation of people with motor deficits. Consequently, it can be asked whether tES could also be an effective tool for targeting and modulating plasticity in the sensory field for therapeutic purposes. Specifically, could potentiating sensitivity at the central level with tES help to compensate for sensory loss? The present review examines evidence of the impact of tES on cortical auditory excitability and its corresponding influence on auditory processing, and in particular on hearing rehabilitation. Overall, data strongly suggest that tES approaches can be an effective tool for modulating auditory plasticity. However, its specific impact on auditory processing requires further investigation before it can be considered for therapeutic purposes. Indeed, while it is clear that electrical stimulation has an effect on cortical excitability and overall auditory abilities, the directionality of these effects is puzzling. The knowledge gaps that will need to be filled are discussed.

Keywords: transcranial electrical stimulation, transcranial direct current stimulation, transcranial alternating current stimulation, transcranial random noise stimulation, auditory processing, auditory abilities, audiology

OPEN ACCESS

Edited by:
Ken-Ichiro Tsutsui, Tohoku University, Japan

Reviewed by:
Luca Sebastianelli, Hospital of Vipiteno, Italy
Anita D'Anselmo, University of Bologna, Italy

****Correspondence:***
Mujda Nooristani
mujda.nooristani@umontreal.ca

Specialty section:
This article was submitted to Brain Imaging and Stimulation, a section of the journal Frontiers in Human Neuroscience

Received: *02 July 2021*
Accepted: *01 November 2021*
Published: *23 November 2021*

Citation:
Nooristani M, Augereau T, Moïn-Darbari K, Bacon B-A and Champoux F (2021) Using Transcranial Electrical Stimulation in Audiological Practice: The Gaps to Be Filled. Front. Hum. Neurosci. 15:735561. doi: 10.3389/fnhum.2021.735561

INTRODUCTION

Transcranial Electrical Stimulation (tES) is a Non-Invasive Brain Stimulation (NIBS) approach, in use for several decades, that involves applying a low electrical current on the human head and assessing its effects. tES has been shown to modulate spontaneous cortical activity and excitability, leading to alterations of behavior, cognition and sensory perception (for a review: Yavari et al., 2018). tES can be generated by applying either *direct* current or *alternating* current.

Transcranial Direct Current Stimulation (tDCS) is the most frequently used type of tES in both clinical and research domains. tDCS has been reported to modulate resting membrane potentials by depolarizing or hyperpolarizing cortical neurons, thereby altering their firing rate (Creutzfeldt et al., 1962; Bindman et al., 1964; Purpura and McMurtry, 1965; Radman et al., 2009). This technique consists of applying a weak direct electrical current through two or more electrodes (Priori et al., 1998). The polarity of the active electrode can be positive (anode) or negative (cathode), and the effects induced by tDCS notably depend on the polarity of the current applied. Anodal tDCS (a-tDCS) at 1 mA has been shown to typically have an excitatory effect as it induces a depolarization of

the resting membrane potential and consequently an increase of the firing rate of neurons (Nitsche and Paulus, 2000). On the contrary, cathodal tDCS (c-tDCS) at 1 mA induces a hyperpolarization of the resting membrane potential, which thereby decreases the firing rate of neurons. These effects were demonstrated in the motor cortex by means of Motor Evoked Potentials (MEPs); a-tDCS increased MEPs amplitude and c-tDCS decreased it (Paulus, 2011). However, a reverse effect of a-tDCS and c-tDCS can be observed depending on many factors, such as the direction of current flow relative to neuronal orientation or duration of stimulation (Jefferys, 1981; Bikson et al., 2004; Kabakov et al., 2012; Paulus et al., 2013). tDCS effects have been observed during stimulation (online effect), but also after a sufficient stimulation (offline effect). Previous studies demonstrated that the after-effect of tDCS can last for several minutes and even hours following the end of stimulation. However, to induce an offline effect, the intensity and duration of stimulation have to be adjusted. This effect is mediated by mechanisms similar to Long-Term Potentiation (LTP) and Long-Term Depression (LTD) (Bindman et al., 1964; Nitsche and Paulus, 2000; Fritsch et al., 2010; Paulus et al., 2012).

Transcranial Alternating Current Stimulation (tACS) consists of a sinusoidal current applied at a specific frequency that alternates between electrodes (Reed and Kadosh, 2018). This neuromodulation technique modulates neuronal firing to the external frequency applied with tACS and thereby synchronizes cortical oscillation (Antal and Paulus, 2013; Herrmann et al., 2013). tACS therefore enables to assess the influence of cortical oscillation on perception and cognition. It has been demonstrated to have an after-effect similar to tDCS, which is linked to induced neuroplastic changes (Vossen et al., 2015).

Multiple alternating currents can also be applied simultaneously in an approach known as *transcranial Random Noise Stimulation* (tRNS). tRNS induces noise by means of multiple alternating currents varying in amplitude and frequency. The bandwidth can vary from 0.1 to 640 Hz, and it can also be divided into lower (0.1–100 Hz) or higher (100–640 Hz) frequency bands. The mechanism behind the effect of tRNS is Stochastic Resonance (SR) which enables the enhancement of information processing and detection of subthreshold signals by adding noise in a non-linear system, such as the human brain (McDonnell and Ward, 2011). A previous study has demonstrated that tRNS applied on the motor cortex induces an enhancement of cortical excitability and effect lasting up to 1-h post-stimulation (Terney et al., 2008). The putative mechanism of tRNS action has been linked to the potentiation of voltage-gated sodium channels (Terney et al., 2008).

tES has been primarily shown to have an influence on motor cortical excitability by increasing and decreasing MEPs (Nitsche and Paulus, 2000), however, the application of tES on the motor cortex can also modulate a number of motor functions. Indeed, a-tDCS has been shown to improve performance of different motor tasks (e.g., Boggio et al., 2006; Vines et al., 2008; Sohn et al., 2012). Recently, there has been increasing evidence of the therapeutic effects of tES, notably an enhancement of motor functions and cognitive performances in older adults and in individuals with various neurological disorders. A recent meta-analysis reported robust beneficial evidences of a-tDCS for an array of motor functions, but also for some cognitive functions, such as working memory and language production (Summers et al., 2016).

Another clinical population that seems to benefit from tES approaches is stroke patients. Specifically, multiple studies reported that electrical stimulation, and more particularly tDCS, enhanced the upper and lower limb recovery of stroke patients showing motor dysfunctions (for review see Bai et al., 2019). Interestingly, other studies reported improvement on motor tasks as well as an enhancement of the acquisition of motor tasks in stroke patients with tDCS, and the effect lasted minutes to hours post-stimulation (Hummel et al., 2005; Zimerman et al., 2012). Stroke patients can also benefit from a-tDCS for language recovery, as such stimulation has been shown to improve naming performance and naming reaction time (Baker et al., 2010; Fridriksson et al., 2011). Furthermore, tES techniques seem to have therapeutic effects for several other neurological disorders, notably Parkinson's disease (Broeder et al., 2015; Chen and Chen, 2019) and Alzheimer's disease (Hsu et al., 2015; Chang et al., 2018). However, it is still unclear whether these therapeutic effects would extend to the sensory field.

Here, we review the evidence that supports the use of tES as a tool for targeting and modulating plasticity in the sensory field. Indeed, if tES is recognized as a potentiator of sensitivity at the central level, it could help to alleviate sensory loss. We more specifically sought to examine the evidence revealing the impact of tES on cortical auditory excitability and its corresponding effect on auditory processing, and in particular on hearing rehabilitation.

The Effects of Transcranial Electrical Stimulation on Auditory Cortical Excitability

Emerging literature suggests that tES techniques can have an effect on the excitability of the auditory cortex. Indeed it was repeatedly demonstrated, as summarized in **Table 1**, that electrophysiological responses are modulated by electrical stimulation. Two different paradigms are generally employed to investigate the effects of tES on auditory electrophysiological responses, namely (*i*) Auditory Evoked Potentials (AEPs) and (*ii*) auditory event-related potentials (AERPs).

Zaehle et al. (2011) reported the effect of tDCS on AEPs amplitude, with a-tDCS increasing P50 amplitude and c-tDCS increasing N1 amplitude. These effects were dependent on the position of the active electrode: a-tDCS had an effect when the TP7 region was stimulated and c-tDCS had an effect when applied on CP5. Heimrath et al. (2016) demonstrated similar AEPs results in response to voiced and voiceless natural CV syllables. However, Kunzelmann et al. (2018) did not find an effect of a-tDCS on AEPs. These discrepancies can be attributed to the positioning of the active electrode and to the specificities of stimulation parameters. Indeed, Kunzelmann et al. (2018) placed the active electrode at a temporo-parietal location (over TP7 and P7), while Zaehle et al. (2011) placed the active electrode slightly higher (CP5) in the temporo-parietal area, or at a temporal

TABLE 1 | Auditory electrophysiological responses.

References	Population	Paradigm	Stimulation type	Active electrode	References electrode	Stimulation parameters	Acquisition	Results
Zaehle et al. (2011)	Adults (M_{age} = 26) n = 14	Auditory evoked potentials (AEPs)	a-tDCS c-tDCS Sham	35 cm^2 TP7 CP5	35 cm^2 Contralateral supraorbital region	1.25 mA 0.04 mA/cm^2 11 min	Offline	a-tDCS (TP7) increased P50 amplitude; c-tDCS (CP5) increased N1 amplitude and a-tDCS reduced N1 latency
Chen et al. (2014)	Adults (M_{age} = 32) n = 10	Auditory ERPs: MMN	a-tDCS c-tDCS Sham	35 cm^2 F4	35 cm^2 Left supraorbital region	2.0 mA 0.06 mA/cm^2 25 min	Offline	a-tDCS reduced MMN amplitude
Heimrath et al. (2015)	Adults (M_{age} = 25.9) n = 12	Auditory ERPs: MMN	a-tDCS (HD) c-tDCS (HD) Sham (HD)	3.4 cm^2 C5 C6	3.4 cm^2 FC5/FC6, C3/C4, CP5/CP6, T7/T8	0.5 mA 0.1 mA/cm^2 21 min	Online	a-tDCS on left AC increased MMN amplitude in the temporal condition
Dunn et al. (2016)	Schizophrenia patients n = 36	AEPs ERPs: MMN, P3	a-tDCS c-tDCS Sham	35 cm^2 Fp1 and Fp2	35 cm^2 Right upper arm	1 mA 0.03 mA/cm^2 40 min	Offline	a-tDCS reduced MMN amplitude
Impey et al. (2016)	Adults (age: 18–35) n = 12	Auditory ERPs: MMN	a-tDCS c-tDCS Sham	19.4 cm^2 C5-T7	50 cm^2 Contralateral supraorbital region	2 mA mA/cm^2 20 min	Offline	a-tDCS increased MMN amplitude and c-tDCS reduced MMN amplitude in baseline-stratified groups
Heimrath et al. (2016)	Adults (M_{age} = 25.9) n = 13	AEPs	a-tDCS c-tDCS Sham	25 cm^2 T7 and T8	50 cm^2 Cz	1.5 mA 0.06 mA/cm^2 22 min	Offline	a-tDCS increased P50 amplitude in response to natural CV syllables
Rufener et al. (2017)	Adults (age: 20–35) n = 18	AEPs	tRNS Sham	35 cm^2 T7 and T8		1.5 mA 0.04 mA/cm^2 20 min	Online	tRNS diminished P50 and N1 latency
Royal et al. (2018)	Adults (M_{age} = 22.6) n = 13	Auditory ERPs: MMN, P3	c-tDCS Sham	35 cm^2 AF8-F8 T8-TP8	35 cm^2 FP1-AF3-AF7	2 mA 0.1 mA/cm^2 20 min	Offline	c-tDCS reduced P3 amplitude
Kunzelmann et al. (2018)	Adults (M_{age} = 26.4) n = 24	AEPs	a-tDCS Sham	35 cm^2 TP7-P7	25 cm^2 Fp2-AF4-AF8	1 mA 0.03 mA/cm^2 20 min	Online and Offline	No effect of a-tDCS on auditory evoked potentials during and after stimulation
Boroda et al. (2020)	Adults (M_{age} = 24.9) n = 22	ERP-based plasticity	a-tDCS Sham	3.14 cm^2 T7 and T8	3.14 cm^2 Fp1 and Fp2	1 mA 0.318 mA/cm^2 5 min	Offline	a-tDCS enhanced N100 amplitude for the target tone, thereby it enhanced plasticity
Jones et al. (2020)	Adults (M_{age} = 20.9) n = 45	EEG during auditory click trains	40 Hz tACS a-tDCS Sham	25 cm^2 T7	25 cm^2 Contralateral cheek	1 mA 0.04 mA/cm^2 10 min	Offline	tACS increased gamma power and phase locking; tDCS enhanced the coupling of gamma activity to alpha oscillations
Hanenberg et al. (2019)	Adults (M_{age} = 24.3) Older adults (M_{age} = 70.4) n = 20; n = 19	ERP	a-tDCS c-tDCS Sham	35 cm^2 C6-T8	98 cm^2 Contralateral shoulder	1 mA 0.03 mA/cm^2 16 min	Offline	a-tDCS increased N2 amplitude in young and older adults

level (TP7). A temporal area (T7 and T8) was also chosen by Heimrath et al. (2016), and the results were similar to Zaehle et al. (2011), as an increase of P50 was observed with a-tDCS. These results underline the importance of electrode positioning in the assessment of tES effects on electrophysiological responses. The different stimulation parameters used also contributed to the discrepancies of results; notably, current intensity, current density, the duration of stimulation and the size of electrodes were different in all three studies.

Only one study examined the effect of tRNS on AEPs. Rufener et al. (2017) revealed that such stimulation reduced P50 and N1 latency. These results are in line with the improved performance observed on the Gap Detection Task (GDT) assessed in the second part of their study (see section on "Temporal Processing"). Therefore, they suggest that tRNS can improve neural conduction time by reducing responses latencies.

Several studies also used the auditory event-related potentials paradigm to study the influence of tES on electrophysiological responses, and there are once again large discrepancies between studies. Indeed, some studies demonstrated a decrease of the mismatch negativity (MMN) amplitude with a-tDCS when stimulating frontal regions (Chen et al., 2014; Dunn et al., 2016), while others showed that a-tDCS over auditory cortices increased MMN amplitude (Heimrath et al., 2015;

TABLE 2 | Temporal processing.

References	Population	Paradigm	Stimulation types	Active electrode	References electrode	Stimulation parameters	Acquisition	Results
Ladeira et al. (2011)	Adults (M_{age} = 21.4) *n* = 11	Random gap detection task (RGDT)	a-tDCS c-tDCS Sham	35 cm^2 T3 and T4	35 cm^2 Right deltoid muscle	2 mA 0.06 mA/cm^2 10 min	Online	a-tDCS enhanced temporal resolution with 4 kHz and clicks subtests; c-tDCS reduced temporal resolution with 4 kHz subtest
Heimrath et al. (2014)	Adults (M_{age} = 24.4) *n* = 15	Gap detection task	a-tDCS Sham	25 cm^2 T7 T8	50 cm^2 C3/C4	1.5 mA 0.06 mA/cm^2	Online	a-tDCS over left AC decreased temporal resolution
Heimrath et al. (2016)	Adults (M_{age} = 25.9) *n* = 13	Voice onset time (VOT) categorization	a-tDCS c-tDCS Sham	25 cm^2 T7 and T8	50 cm^2 Cz	1.5 mA 0.06 mA/cm^2 22 min	Online	c-tDCS over AC bilaterally improved categorization of CV-syllables in a VOT continuum
Rufener et al. (2016a)	Adults (M_{age} = 24.1) *n* = 25 Elderly (M_{age} = 69.8) *n* = 20	VOT categorization	tACS 6 Hz 40 Hz	35 cm^2 T7 and T8		1.5–1.6 mA** (6 Hz) 1.3–1.4 mA ** (40 Hz) 0.04–0.05 mA/cm^2 8 min	Online	40 Hz tACS decreased precision of VOT categorization in adults. 40 Hz tACS enhanced precision of VOT categorization in older adults
Rufener et al. (2016b)	Adults (M_{age} = 25.9) *n* = 38	VOT categorization	tACS 6 Hz 40 Hz	35 cm^2 T7 and T8		1 mA (6 Hz)** mA (40 Hz)** 0.03 mA/cm^2 18 min	Offline	40 Hz tACS reduced the repetition-induced improvement in phoneme categorization (reduced learning effect)
Rufener et al. (2017)	Adults (age: 20–35) *n* = 18	Gap detection task (GDT) Pitch discrimination threshold (PDT)	tRNS Sham	35 cm^2 T7 and T8		1.5 mA 0.04 mA/cm^2 20 min	Online	tRNS increased detection rate for near-threshold stimuli on GDT only
Baltus et al. (2018)	Adults (M_{age} = 24.0) *n* = 26	GDT	tACS Individual gamma frequency (IGF) + 4 Hz IGF–4 Hz	4.9 cm^2 FC5 and TP7/P7 FC6 and TP8/P8		1 mA 0.12 mA/cm^2 7 min	Online	IGF + 4 Hz tACS enhanced temporal resolution

***Intensity was adjusted to the optimal level for each participant.*

Impey et al., 2016). No study found effects of c-tDCS on MMN, but one reported a reduction of P3 amplitude (Royal et al., 2018). Stimulation locations and electrode montage differed between the various studies. It is expected that a variety of effects that can be obtained through different stimulation parameters, considering that MMN can originate from multiple generators.

Interestingly, Heimrath et al. (2015) used a novel type of electrode montage, namely High-Definition (HD) tDCS. This stimulation montage consists of 4 reference electrodes, making a ring around the active electrode on the target region. This electrode montage has been reported to improve spatial definition, to induce a higher electrical field and to reduce the risk of unwanted effect from a single reference electrode (Datta et al., 2009, 2012). They revealed an increase of MMN amplitude with HD a-tDCS, lateralized to the left auditory cortex.

Using an ERP-based paradigm, Boroda et al. (2020) demonstrated that a-tDCS applied bilaterally to the auditory cortex enhanced cortical plasticity. The application of a-tDCS during the repetitive presentation of the target tone induced an additional enhancement of the N100 amplitude, as compared to sham stimulation.

Another electrophysiological indication of the potential of tES approaches in rehabilitation was shown by Jones et al. (2020) who revealed that tACS and tDCS can modulate different components of auditory gamma responses. Indeed, tACS increased gamma evoked power and phase locking to the auditory stimulus, while tDCS strengthened the alpha-gamma phase-amplitude coupling in the absence of auditory stimuli. This finding is particularly interesting considering that multiple neurological disorders, such as autism spectrum disorder (Khan et al., 2013; Rojas and Wilson, 2014), schizophrenia (Edgar et al., 2014; Hirano et al., 2018) and bipolar disorder (Maharajh et al., 2007), present a disrupted auditory gamma responses and a disrupted cross-frequency coupling to gamma activity. Therefore, such tES techniques could potentially be used as a therapeutic approach on populations with these neurological disorders.

The Effects of Transcranial Electrical Stimulation on Auditory Processing

Considering the impact of tES on auditory cortical excitability, behavioral effects would be expected to follow. Behavioral studies have focused on tES effects on temporal processing, spectral

TABLE 3 | Spectral processing.

References	Population	Paradigm	Stimulation type	Active electrode	Reference electrode	Stimulation parameters	Acquisition	Results
Mathys et al. (2010)	Adults (M_{age} = 25.9) n = 26	Pitch direction discrimination task	a-tDCS c-tDCS	16.3 cm^2 C3–T3 C4–T4 O1–O2 (control)	30 cm^2 Contralateral supraorbital region	2 mA 0.1 mA/cm^2 25 min	Offline	c-tDCS over the left and right AC reduced pitch discrimination
Tang and Hammond (2013) Experiment 1	Adults (age: 18–27) n = 15	Frequency discrimination	a-tDCS Sham	24 cm^2 C4–T4	24 cm^2 Contralateral supraorbital region	1 mA 0.04 mA/cm^2 20 min	Online	a-tDCS over right AC temporarily impaired frequency discrimination (< 24 h)
Tang and Hammond (2013) Experiment 2A	Adults (age: 18–27) n = 7	Frequency selectivity	a-tDCS Sham	24 cm^2 C4–T4	24 cm^2 Contralateral supraorbital region	1 mA 0.04 mA/cm^2 20 min	Online	a-tDCS reduced frequency selectivity
Tang and Hammond (2013) Experiment 2B	Adults (age: 18–27) n = 6	Frequency discrimination; Temporal fine structure (TFS)	a-tDCS Sham	24 cm^2 C4–T4	24 cm^2 Contralateral supraorbital region	1 mA 0.04 mA/cm^2 20 min	Online	a-tDCS decreased frequency discrimination by disrupting temporal coding
Matsushita et al. (2015)	Adults (M_{age} = 22.2) n = 42	Pitch discrimination task	a-tDCS c-tDCS Sham	35 cm^2 Right Heschl's gyri (HG)	35 cm^2 Above left eyebrow	1 mA 0.03 mA/cm^2 20 min	Online and Offline	a-tDCS impaired auditory pitch learning
Loui et al. (2010)	Adults (M_{age} = 25.3) n = 9	Pitch perception Pitch matching Pitch production	c-tDCS Sham	16 cm^2 TP7–C5 (STG) TP8–C6 (STG) F7–C5 (IFG) F8–C6 (IFG)	16 cm^2 Contralateral supraorbital region	2 mA mA/cm^2 20 min	Offline	c-tDCS over right STG and left IFG reduced accuracy in pitch matching

STG, Superior temporal gyrus; IFG, Inferior frontal gyrus.

processing, binaural integration, auditory scene analysis and speech comprehension.

Temporal Processing

Results of different studies investigating the effect of tES approaches on temporal processing are summarized in **Table 2**. Using a random GDT to examine temporal resolution performance, Ladeira et al. (2011) have been the first to suggest (*i*) an enhancement of performance with a-tDCS and (*ii*) a decrease of performance with c-tDCS. Studies have also examined the effect of tES in GDT: Baltus et al. (2018) demonstrated that applying tACS at 4 Hz above the individual's gamma frequency enabled subjects to detect significantly smaller gap sizes. On the other hand, Rufener et al. (2017) studied the effect of tRNS on the GDT, showing an enhancement of temporal processing. Conversely, Heimrath et al. (2014) showed a decrease of temporal resolution on the GDT induced by a-tDCS.

The different methodologies used in these studies might explain the disparities in the effect of a-tDCS on temporal processing. First, the different results could be explained partially by the electrode montage used as Ladeira et al. (2011) used a bilateral montage that stimulated both temporal cortices simultaneously, whereas only one temporal cortex was stimulated by Heimrath et al. (2014). Furthermore, the intensity of the current applied differed between those two experiments, as well as the size of the active electrode and the position of the active and reference electrodes (extracephalic vs. cephalic). The importance of these parameters has been shown previously in the motor domain (Dissanayaka et al., 2017). For example, an extracephalic reference electrode can reduce electrical field due to the greater distance between the active and reference electrodes (Moliadze et al., 2010). However, this type of electrode montage reduces the stimulation of unsolicited cortical areas (Im et al., 2012).

To further examine the effects of tES on temporal processing, a few studies investigated the influence of tDCS and tACS on a voice onset time categorization task, with similarly conflicting outcomes. Indeed, while the results of Heimrath et al. (2016) suggest an improvement in temporal processing induced by c-tDCS, other results using 40 Hz tACS appear to be dependent of the age of the participant, indicating an improvement of performance in older subjects, and reduced performance in younger adults (Rufener et al., 2016a,b).

Spectral Processing

The effects of tDCS on spectral processing are summarized in **Table 3**. The first evidence of the impact of tDCS on spectral processing was reported by Mathys et al. (2010), as they examined the effect of a-tDCS and c-tDCS on a pitch direction discrimination task. Results showed that c-tDCS over the left and the right auditory cortex lead to reduced performance in pitch discrimination. However, a-tDCS did not have any effect on performance in this task. Other researchers also studied pitch discrimination, but with a specific focus on pitch learning (Matsushita et al., 2015). The results showed that a-tDCS blocked pitch discrimination learning, as compared to c-tDCS and sham, as the only group showing no significant improvement of threshold over the 3 days of training was the one stimulated with a-tDCS.

Tang and Hammond (2013) reported similar effects of tDCS on learning processes. Indeed, they showed through a series of

TABLE 4 | Binaural integration.

References	Population	Paradigm	Stimulation type	Active electrode	References electrode	Stimulation parameters	Acquisition	Results
D'Anselmo et al. (2015)	Adults (M_{age} = 21) n = 47	Dichotic listening task	a-tDCS c-tDCS Sham	16.3 cm^2 C3–T3 C4–T4	35 cm^2 Contralateral shoulder	2 mA 0.1 mA/cm^2 25 min	Online	No effect of a-tDCS nor c-tDCS on dichotic listening task performance
Prete et al. (2018) Experiment 1	Adults (M_{age} = 22.8) n = 41	Dichotic listening task	Bilateral hf-tRNS Sham	25 cm^2 47.5 cm^2 T3 and T4		1.5 mA 0.03–0.06 mA/cm^2 20 min	Online	Bilateral hf-tRNS enhanced the right ear advantage
Prete et al. (2018) Experiment 2	Adults (M_{age} = 24.4) n = 20	Dichotic listening task	Unilateral hf-tRNS Sham	25 cm^2 T3 T4	47.5 cm^2 Contralateral shoulder	1.5 mA 0.06 mA/cm^2 20 min	Online	No effect of unilateral hf-tRNS on the right ear advantage

hf-tRNS, high frequency tRNS.

experiments that a-tDCS had detrimental effects on frequency discrimination and learning processes, as well as on frequency selectivity. Interestingly, in their first experiment they showed that both the a-tDCS and sham groups presented a similarly rapid perceptual learning, as they both improved over the experimental blocks. Although no significant difference for rate of learning was found, subjects in the a-tDCS group were not performing as well as the sham group, suggesting a decreased frequency discrimination without affecting learning process. Nevertheless, when assessed on the second day (without stimulation), the performance of participants in the a-tDCS group nearly returned to baseline levels, while performance of the sham group remained stable. This finding suggested that a-tDCS blocked the learning and consolidation process. Furthermore, this study also suggests that tDCS had a sustained effect on frequency discrimination, as subjects in the tDCS group still performed more poorly compared to the sham group on the second day. In their second experiment, Tang and Hammond (2013) demonstrated that tDCS decreased frequency selectivity, as a-tDCS caused psychophysical tuning curves to be broader.

Pitch processing was further examined by Loui et al. (2010), using pitch perception, pitch matching and pitch production tasks. This study revealed that c-tDCS only influences pitch matching by decreasing task accuracy.

Taken together, these results suggest that a-tDCS and c-tDCS both seem to have similar effects on various spectral processing tasks, leading to a decrease in performance. However, it is noteworthy to mention that all experiments conducted so far involved healthy young adults, which were arguably already performing at an optimal level. It should be noted, also, that all experiments used a similar stimulation duration (20–25 min) and an electrode montage with an active electrode on the temporal cortex (right/left) and an extracephalic reference electrode, which may explain the homogeneous results obtained. The varying current intensity (1–2 mA), density (0.03–0.1 mA/cm^2) and electrode sizes (16–35 cm^2) between studies did not induce different task performance patterns.

Binaural Integration

The influence of tES techniques on binaural integration have only been investigated in a few experiments, as can be seen in **Table 4**. Using a unilateral montage, D'Anselmo et al. (2015) reported no effects of a-tDCS and c-tDCS on performance at a dichotic listening task. More recently, Prete et al. (2018) observed a similar result with unilateral high frequency tRNS (hf-tRNS). However, in a second experiment, Prete et al. (2018) demonstrated that a bilateral montage of hf-tRNS enhanced the right ear advantage. These results on the effect of tES on binaural integration suggest that only a bilateral montage can modulate this auditory ability, presumably by more efficiently inducing stochastic resonance, as compared to unilateral tRNS where only one active electrode induces noise in the system. Similarly, it was also shown in language rehabilitation and sound perception that a bilateral montage is more effective than a unilateral montage (Galletta et al., 2015; Prete et al., 2017). Differences in the parameters used might also had an impact on the results. Indeed, both studies using a unilateral montage used an extracephalic reference electrode, therefore increasing the distance between the electrodes. According to Moliadze et al. (2010) such a montage may explain the absence of a stimulation effect.

Auditory Scene Analysis

Auditory scene analysis has been studied to a lesser extent in the tES domain, as can be seen in **Table 5**. Lewald (2016) reported no effect of tDCS on sound localization, but a significant effect on spatial sound separation. Indeed, a-tDCS placed on the left Superior Temporal Gyrus (STG) and c-tDCS placed over the right STG improved the accuracy of target localization in the left hemispace. The author suggested that bipolar tDCS with c-tDCS over the right STG increased the suppression of the activity of neuronal populations coding for locations of concurrent sounds, thus facilitating the segregation of target sound vs. concurrent sounds. This result shows the efficiency of bipolar tDCS in improving auditory segregation by decreasing concurrent neural activity. Deike et al. (2016) also revealed an effect of tDCS on auditory segregation. They used a segregation task where subjects had to listen to harmonic tone complexes and to indicate if only one stream or two separate streams were perceived. They revealed a reduction in performance following a-tDCS, which is contrary to the results of Lewald (2016). Such discrepancy can be partially related to different tasks and montage, as Lewald (2016) applied a bilateral bipolar montage and stimulated both STGs simultaneously with different current polarities, while Deike et al. (2016) used a unilateral montage

TABLE 5 | Auditory scene analysis.

References	Population	Paradigm	Stimulation type	Active electrode	References electrode	Stimulation parameters	Acquisition	Results
Lewald (2016)	Adults (M_{age} = 23.7) *n* = 74	Sound localization	a-tDCS c-tDCS	3.5 cm^2 STG IPL SMC		0.4 mA 0.01 mA/cm^2 12 min	Online and Offline	No effect of bipolar tDCS on sound localization Left a-tDCS and right c-tDCS over STG improved spatial sound separation
Deike et al. (2016)	Adults (age: 21–41) *n* = 22	Auditory stream segregation	a-tDCS c-tDCS Sham	35 cm^2 T7	35 cm^2 Contralateral supraorbital region	1 mA 0.03 mA/cm^2 15 min	Offline	a-tDCS reduced auditory segregation
Hanenberg et al. (2019)	Young adults (M_{age} = 24.3) *n* = 20 Older adults (M_{age} = 70.4) *n* = 19	Sound localization (cocktail-party situation)	a-tDCS c-tDCS Sham	35 cm^2 C6-T8	98 cm^2 Contralateral shoulder	1 mA 0.03 mA/cm^2 16 min	Offline	a-tDCS improved localization error in young adults
Lewald (2019)	Adults (M_{age} = 22.6) *n* = 22.6	Sound localization (cocktail-party situation)	a-tDCS Sham	35 cm^2 C6-T8 and C5-T7	98 cm^2 Shoulders	1 mA 0.03 mA/cm^2 30 min	Offline	a-tDCS improved localization of a target speaker in a simulated cocktail-party situation

STG, Superior temporal gyrus; IPL, Inferior parietal lobule; SMC, Somatosensory motor cortex.

with one current polarity. Different use of current intensity and density applied could also explain such differences in the results. Indeed, both stimulation parameters were higher in Deike et al. (2016). Furthermore, previous studies in the motor domain have demonstrated that increasing current intensity can invert the direction of excitability. This suggests that a-tDCS could lead to a decrease in cortical excitability, whereas c-tDCS could generate the opposite (Batsikadze et al., 2013).

Hanenberg et al. (2019) investigated the effects of tDCS on the electrophysiological correlates of auditory selective spatial attention, with a focus on the N2 component of the ERP, in young and older adults. Their data demonstrated behavioral and electrophysiological effects of a-tDCS, more specifically an increased N2 amplitude, and improved localization performances. However, no effects of c-tDCS were revealed, in opposition to previous results (Lewald, 2016). The demonstrated impact of a-tDCS on sound localization in a cocktail-party situation in young adults was confirmed by Lewald (2019). Based on the theory that during a complex task, neuronal patterns encoding concurrent distractors are activated in addition to the patterns encoding the target stimulus, it was proposed that a-tDCS specifically increased the excitability of inhibitory interneurons that suppress irrelevant sound sources, thereby facilitating effects of selective attention.

Speech Comprehension

Research on the impact of tES on speech comprehension are summarized in **Table 6**. Giustolisi et al. (2018) demonstrated that a-tDCS over the left inferior frontal gyrus in healthy adults can improve the language comprehension of syntactically simple and complex sentences. Indeed, participants stimulated with a-tDCS for 30 min showed improved accuracy compared to participants in the sham group. Lum et al. (2019) showed that a-tDCS can have an impact on sentence comprehension, as they reported that applying electrical stimulation on the left inferior frontal gyrus improved reaction time as compared to baseline performance. Therefore, their results suggest that a-tDCS can improve the speed of sentence comprehension. On the other hand, Kadir et al. (2020) aimed at investigating whether tACS with a speech envelope could modulate speech in noise comprehension, and showed that electrical stimulation mostly worsened the speech comprehension of normal hearing adults in a background of babble noise.

DISCUSSION

The present review summarizes how transcranial electrical stimulation (tES) techniques can have a significant impact on the excitability of auditory cortical regions and its behavioral effects. Overall, research suggests that these techniques can be used to modulate nearly all auditory functions and abilities. However, there are tremendous discrepancies between studies, making it difficult to predict the directionality of the various effects.

Experimental reports on temporal and spectral processing are the only ones reporting constant outcomes. Indeed, all studies suggest that a-tDCS and c-tDCS have a positive effect on temporal processing, but a negative effect on spectral processing. Other results are scarce or often conflicting.

The results on the effect of tES techniques, notably bilateral tRNS, on binaural integration seem promising. However, more research is needed to determine whether tES could present a potential enhancing effect on binaural integration. Likewise, the potential improvement of auditory scene analysis with tDCS needs to be confirmed, as data are still preliminary. Finally,

TABLE 6 | Speech comprehension.

References	Population	Paradigm	Stimulation type	Active electrode	References electrode	Stimulation parameters	Acquisition	Results
Giustolisi et al. (2018)	Adults (M_{age} = 22) n = 44	Sentence comprehension	a-tDCS Sham	9 cm^2 F5	35 cm^2 Contralateral supraorbital	0.75 mA 0.08 mA/cm^2 30 min	Online	a-tDCS over left IFG improved language comprehension of both syntactically simple and complex sentences
Lum et al. (2019)	Adults (M_{age} = 22.9) n = 36	Sentence comprehension Word comprehension	a-tDCS Sham	25 cm^2 Between T3-Fz and F7-Cz	35 cm^2	1 mA 0.04 mA/cm^2 15 min	Online	a-tDCS improved reaction time for sentence comprehension task compared to baseline performance No effect of a-tDCS on word comprehension task
Kadir et al. (2020)	Adults (M_{age} = 23.4) n = 17	Speech in noise comprehension	env-tACS Sham a-tDCS c-tDCS	35 cm^2 T7 and T8	35 cm^2 Cz	0.2–1.5 mA (M = 0.9) 0.006–0.04 mA/cm^2 (M = 0.03)	Online	env-tACS modulated the comprehension of speech in noise by mostly worsening speech comprehension compared to sham

Env-tACS, tACS with a speech envelope.

current knowledge does not allow the drawing of a clear conclusion on the impact of tES on speech comprehension, considering the very limited number of studies and the significant discrepancies between the results of these studies.

Since it is not possible to predict a constant improvement for one auditory process without affecting other aspects of auditory function, it is not possible to make any recommendation at this time. Indeed, from an audiological point of view, the use of this technique could even be harmful, and studies on spectral processing suggest that the potential applicability of tES techniques in auditory rehabilitation could be particularly damaging.

Stimulation parameters and electrode montage differ largely across studies, which could partially account for the discrepancies in the results. The importance of stimulation parameters on the induced effect has already been reported in the motor domain (e.g., Dissanayaka et al., 2017). Indeed, previous studies in the motor as well as in sensory domains demonstrate that an increase of current intensity, stimulation duration and electrode montage can invert the direction of the effect of tDCS (Paulus et al., 2013; Parkin et al., 2019). Indeed, Parkin et al. (2019) notably demonstrated that the classic effects of unilateral tDCS reported by Nitsche and Paulus (2000), as a-tDCS induces excitation and c-tDCS induces inhibition, are not extended to every stimulation protocols. No significant effect was obtained on MEP amplitude when bilateral 1 mA tDCS was applied or when the intensity was increased to 2 mA. The impact of changes in stimulation parameters are less known for tACS and tRNS, but some studies suggest that these techniques are frequency-dependent (Moreno-Duarte et al., 2014). The type of acquisition (i.e., online; offline) might also have an influence on the effect induced. Indeed, undergoing a task during stimulation could reverse the effect expected since there is ongoing brain activity due to the task (see Batsikadze et al., 2013). As such, until a concerted effort is made to use the same parameters and montage and to establish proper stimulation guidelines, there is no doubt that these observed discrepancies will persist.

Another possible explanation for the significant variations of tES results in the auditory domain could be the anatomical location of the auditory cortex, which is located deep in the superior temporal gyrus (STG) and extends to the lateral sulcus and Heschl's Gyrus (HG). It was previously suggested that tES has a larger effect on superficial neurons (Paulus et al., 2013). This may therefore suggest that higher stimulation intensity and/or bilateral stimulation would be more likely to induce an effect on auditory functions, as it was demonstrated to stimulate deeper region in the motor cortex (Paulus et al., 2013).

Furthermore, the auditory cortex has different tonotopic gradients and neurons have different characteristic frequencies. As such, neuronal orientation may vary throughout the cortex (Talavage et al., 2004; Humphries et al., 2010; Costa et al., 2011; Langers and van Dijk, 2012; Tang and Hammond, 2013). Some studies demonstrated that the effect of tES, and more specifically tDCS, depends on the direction of the current relative to neuronal orientation. Indeed, a current applied parallel to a neuron can induce hyperpolarization while a current applied perpendicularly can induce depolarization or no effect at all (Jefferys, 1981; Bikson et al., 2004; Kabakov et al., 2012). The latter results may suggest that in the auditory cortex, where neuron orientation is not uniform, part of the neuronal population may be hyperpolarized, and another part depolarized depending on the direction of the current applied.

In the same vein, the variability of neuronal orientations in the auditory cortex underlines the importance of the active electrode position, since a small difference in position might change the effects due to a different alignment with neuronal orientation (Talavage et al., 2004; Humphries et al., 2010; Costa et al., 2011; Langers and van Dijk, 2012). This is indeed the hypothesis proposed by Ladeira et al. (2011) who showed that tDCS only had an effect at 4,000 Hz, but no effect at 500, 1,000, and 2,000 Hz. Indeed, lower frequencies are coded in the anterolateral portion of the HG, whereas higher frequencies are coded in the postero-medial part of the HG (Bhatgnagar, 2002; Langers et al., 2007).

The stimulation electrodes used by Ladeira et al. (2011) were placed in the posterior portion of the temporal cortex, which may explain the specific improvement of random GDT at 4,000 Hz.

One could also suggest that it might be more appropriate to use tRNS on the auditory cortex to avoid effects of neuronal orientation, since tRNS stimulate neurons irrespective of their spatial orientation (Terney et al., 2008). As suggested by the present review, all the studies using tRNS reported an improvement in performance. However, the number of studies is too limited to conclude with certainty that tRNS is more efficient. In addition, there is no clear evidence as to which tES technique is optimal in the auditory domain. As such, the data do not support the use of this technique in audiological practice.

Another obvious shortcoming is the lack of data in populations with impaired hearing function or impaired auditory processing, notably older adults. Indeed, it is well known that a decrease in temporal processing occurs with age (Fitzgibbons and Gordon-Salant, 1996; Pichora-Fuller and Souza, 2003) and that the improvements induced by tDCS have been hypothesized to be greater in non-proficient systems (Reis et al., 2014). For example, some effects discussed earlier appear to be age-dependent—with an improved performance being observed in older subjects and conversely a reduced performance being seen in younger adults (Rufener et al., 2016a,b). These results suggest that the effects of tES on voice onset time categorization might depend on the efficiency of the auditory system. These elements alone could explain the improvements in temporal processing induced in older adults. Indeed, it is possible that tACS perturbs a normal, well-functioning system and leads to a processing deterioration in younger adults, because the neuronal reactivity level is already optimal in this group (Krause et al., 2013; Schaal et al., 2013). Future studies should therefore investigate the effect of tES techniques in older adults with hearing loss and/or impaired auditory processing, to determine if such techniques could have a clinical relevance in audiology.

Another important variable might also explain the divergence found between younger and older participants, namely, the homeostatic control of cortical excitability (Schaal et al., 2017). Unfortunately, the studies included in the present review were only conducted with normal-hearing individuals. One may therefore wonder if such variability in results would have been present in people with a suboptimal auditory system. For example, all studies using tDCS on spectral processing reported a decreased performance in the different tasks studied. However, it is important to note that all the studies reviewed studied young adults with no apparent spectral processing difficulties. Furthermore, a few studies even recruited participants with musical experience. Therefore, it can be hypothesized that the participants not only had no spectral processing impairment, but also had great auditory skills. As such, adding electrical stimulation could only disrupt that optimal level and decrease their performance. It would be important to assess the impact of tES on populations with impaired spectral processing, and then draw conclusion on the rehabilitation potential of this method.

In conclusion, the present review demonstrated that tES can have an influence on several auditory abilities. While the results are still inconclusive, the impact of the stimulation of other cortical structures on auditory perception would also deserve attention, particularly in relation to auditory scene analysis and speech comprehension, which depend on multisensory processes. Indeed, results of preliminary studies on the effect of tDCS on multisensory integration are promising. Marques et al. (2014) examined the influence of a-tDCS and c-tDCS on the McGurk illusion, a multisensory integration task. They reported that c-tDCS appears to reduce the McGurk illusion when active electrodes are placed on temporal cortices, but that applying a-tDCS to the same regions has no effect. However, a-tDCS applied on parietal cortices increased the McGurk illusion. It is therefore likely that further studies of the effect of tES on multisensory cortical structures could provide interesting avenues for audiological practice. Furthermore, this review underlined important methodological discrepancies between studies, therefore, future studies should determine the optimal stimulation parameters to apply.

AUTHOR CONTRIBUTIONS

MN, TA, KM-D, B-AB, and FC wrote the article. All authors discussed the results and commented on the manuscript at all stages.

FUNDING

This work was supported by the Natural Sciences and Engineering Research Council of Canada (NSERC) (Grant No. RGPIN-2016-05211).

REFERENCES

Antal, A., and Paulus, W. (2013). Transcranial alternating current stimulation (tACS). *Front. Hum. Neurosci.* 7:317.

Bai, X., Guo, Z., He, L., Ren, L., McClure, M. A., and Mu, Q. (2019). Different therapeutic effects of transcranial direct current stimulation on upper and lower limb recovery of stroke patients with motor dysfunction: a meta-analysis. *Neural Plast.* 2019:e1372138. doi: 10.1155/2019/1372138

Baker, J. M., Rorden, C., and Fridriksson, J. (2010). Using transcranial direct-current stimulation to treat stroke patients with aphasia. *Stroke* 41, 1229–1236.

Baltus, A., Wagner, S., Wolters, C. H., and Herrmann, C. S. (2018). Optimized auditory transcranial alternating current stimulation improves individual auditory temporal resolution. *Brain Stimul.* 11, 118–124. doi: 10.1016/j.brs.2017.10.008

Batsikadze, G., Moliadze, V., Paulus, W., Kuo, M.-F., and Nitsche, M. A. (2013). Partially non-linear stimulation intensity-dependent effects of direct current stimulation on motor cortex excitability in humans. *J. Physiol.* 591, 1987–2000. doi: 10.1113/jphysiol.2012.249730

Bhatgnagar, S. (2002). *Neurociências para o Estudo dos Distúrbios da Comunicação.* Rio de Janeiro: Guanabara Koogan.

Bikson, M., Inoue, M., Akiyama, H., Deans, J. K., Fox, J. E., Miyakawa, H., et al. (2004). Effects of uniform extracellular DC electric fields on excitability in rat hippocampal slices *in vitro*. *J. Physiol.* 557, 175–190. doi: 10.1113/jphysiol.2003.055772

Bindman, L. J., Lippold, O. C. J., and Redfearn, J. W. T. (1964). The action of brief polarizing currents on the cerebral cortex of the rat (1) during current flow and (2) in the production of long-lasting after-effects. *J. Physiol.* 172, 369–382. doi: 10.1113/jphysiol.1964.sp007425

Boggio, P. S., Castro, L. O., Savagim, E. A., Braite, R., Cruz, V. C., Rocha, R. R., et al. (2006). Enhancement of non-dominant hand motor function by anodal transcranial direct current stimulation. *Neurosci. Lett.* 404, 232–236.

Boroda, E., Sponheim, S. R., Fiecas, M., and Lim, K. O. (2020). Transcranial direct current stimulation (tDCS) elicits stimulus-specific enhancement of cortical plasticity. *NeuroImage* 211:116598. doi: 10.1016/j.neuroimage.2020.116598

Broeder, S., Nackaerts, E., Heremans, E., Vervoort, G., Meesen, R., Verheyden, G., et al. (2015). Transcranial direct current stimulation in Parkinson's disease: neurophysiological mechanisms and behavioral effects. *Neurosci. Biobehav. Rev.* 57, 105–117. doi: 10.1016/j.neubiorev.2015.08.010

Chang, C.-H., Lane, H.-Y., and Lin, C.-H. (2018). Brain stimulation in Alzheimer's disease. *Front. Psychiatry* 9:201.

Chen, J. C., Hämmerer, D., Strigaro, G., Liou, L. M., Tsai, C. H., Rothwell, J. C., et al. (2014). Domain-specific suppression of auditory mismatch negativity with transcranial direct current stimulation. *Clin. Neurophysiol.* 125, 585–592. doi: 10.1016/j.clinph.2013.08.007

Chen, K.-H. S., and Chen, R. (2019). Invasive and noninvasive brain stimulation in Parkinson's disease: clinical effects and future perspectives. *Clin. Pharmacol. Ther.* 106, 763–775. doi: 10.1002/cpt.1542

Costa, S. D., Zwaag, W., Marques, J. P., Frackowiak, R. S. J., Clarke, S., and Saenz, M. (2011). Human primary auditory cortex follows the shape of Heschl's Gyrus. *J. Neurosci.* 31, 14067–14075. doi: 10.1523/jneurosci.2000-11.2011

Creutzfeldt, O. D., Fromm, G. H., and Kapp, H. (1962). Influence of transcortical d-c currents on cortical neuronal activity. *Exp. Neurol.* 5, 436–452. doi: 10.1016/0014-4886(62)90056-0

D'Anselmo, A., Prete, G., Tommasi, L., and Brancucci, A. (2015). The dichotic right ear advantage does not change with Transcranial Direct Current Stimulation (tDCS). *Brain Stimul. Basic Transl. Clin. Res. Neuromodulation* 8, 1238–1240. doi: 10.1016/j.brs.2015.09.007

Datta, A., Bansal, V., Diaz, J., Patel, J., Reato, D., and Bikson, M. (2009). Gyri-precise head model of transcranial DC stimulation: improved spatial focality using a ring electrode versus conventional rectangular pad. *Brain Stimul.* 2, 201–207. doi: 10.1016/j.brs.2009.03.005

Datta, A., Truong, D., Minhas, P., Parra, L. C., and Bikson, M. (2012). Inter-individual variation during transcranial direct current stimulation and normalization of dose using MRI-Derived computational models. *Front. Psychiatry* 3:91. doi: 10.3389/fpsyt.2012.00091

Deike, S., Deliano, M., and Brechmann, A. (2016). Probing neural mechanisms underlying auditory stream segregation in humans by transcranial direct current stimulation (tDCS). *Neuropsychologia* 91, 262–267. doi: 10.1016/j.neuropsychologia.2016.08.017

Dissanayaka, T., Zoghi, M., Farrell, M., Egan, G. F., and Jaberzadeh, S. (2017). Does transcranial electrical stimulation enhance corticospinal excitability of the motor cortex in healthy individuals? a systematic review and meta-analysis. *Eur. J. Neurosci.* 46, 1968–1990. doi: 10.1111/ejn.13640

Dunn, W., Rassovsky, Y., Wynn, J. K., Wu, A. D., Iacoboni, M., Hellemann, G., et al. (2016). Modulation of neurophysiological auditory processing measures by bilateral transcranial direct current stimulation in schizophrenia. *Schizophr. Res.* 174, 189–191. doi: 10.1016/j.schres.2016.04.021

Edgar, J. C., Chen, Y.-H., Lanza, M., Howell, B., Chow, V. Y., Heiken, K., et al. (2014). Cortical thickness as a contributor to abnormal oscillations in schizophrenia? *NeuroImage Clin.* 4, 122–129. doi: 10.1016/j.nicl.2013.11.004

Fitzgibbons, P. J., and Gordon-Salant, S. (1996). Auditory temporal processing in elderly listeners. *J. Am. Acad. Audiol.* 7, 183–189.

Fridriksson, J., Richardson, J. D., Baker, J. M., and Rorden, C. (2011). Transcranial direct current stimulation improves naming reaction time in fluent aphasia. *Stroke* 42, 819–821. doi: 10.1161/strokeaha.110.600288

Fritsch, B., Reis, J., Martinowich, K., Schambra, H. M., Ji, Y., Cohen, L. G., et al. (2010). Direct current stimulation promotes BDNF-dependent synaptic plasticity: potential implications for motor learning. *Neuron* 66, 198–204. doi: 10.1016/j.neuron.2010.03.035

Galletta, E. E., Cancelli, A., Cottone, C., Simonelli, I., Tecchio, F., Bikson, M., et al. (2015). Use of computational modeling to Inform tDCS electrode montages for the promotion of language recovery in post-stroke Aphasia. *Brain Stimul.* 8, 1108–1115. doi: 10.1016/j.brs.2015.06.018

Giustolisi, B., Vergallito, A., Cecchetto, C., Varoli, E., and Romero Lauro, L. J. (2018). Anodal transcranial direct current stimulation over left inferior frontal gyrus enhances sentence comprehension. *Brain Lang.* 176, 36–41. doi: 10.1016/j.bandl.2017.11.001

Hanenberg, C., Getzmann, S., and Lewald, J. (2019). Transcranial direct current stimulation of posterior temporal cortex modulates electrophysiological correlates of auditory selective spatial attention in posterior parietal cortex. *Neuropsychologia* 131, 160–170. doi: 10.1016/j.neuropsychologia.2019.05.023

Heimrath, K., Breitling, C., Krauel, K., Heinze, H.-J., and Zaehle, T. (2015). Modulation of pre-attentive spectro-temporal feature processing in the human auditory system by HD-tDCS. *Eur. J. Neurosci.* 7, 1580–1586. doi: 10.1111/ejn.12908

Heimrath, K., Fischer, A., Heinze, H.-J., and Zaehle, T. (2016). Changed categorical perception of consonant–vowel syllables induced by transcranial direct current stimulation (tDCS). *BMC Neurosci.* 17:8. doi: 10.1186/s12868-016-0241-3

Heimrath, K., Kuehne, M., Heinze, H.-J., and Zaehle, T. (2014). Transcranial direct current stimulation (tDCS) traces the predominance of the left auditory cortex for processing of rapidly changing acoustic information. *Neuroscience* 261, 68–73. doi: 10.1016/j.neuroscience.2013.12.031

Herrmann, C. S., Rach, S., Neuling, T., and Strüber, D. (2013). Transcranial alternating current stimulation: a review of the underlying mechanisms and modulation of cognitive processes. *Front. Hum. Neurosci.* 7:279.

Hirano, S., Nakhnikian, A., Hirano, Y., Oribe, N., Kanba, S., Onitsuka, T., et al. (2018). Phase-amplitude coupling of the electroencephalogram in the auditory cortex in schizophrenia. *Biol. Psychiatry Cogn. Neurosci. Neuroimaging* 3, 69–76. doi: 10.1016/j.bpsc.2017.09.001

Hsu, W.-Y., Ku, Y., Zanto, T. P., and Gazzaley, A. (2015). Effects of noninvasive brain stimulation on cognitive function in healthy aging and Alzheimer's disease: a systematic review and meta-analysis. *Neurobiol. Aging* 36, 2348–2359. doi: 10.1016/j.neurobiolaging.2015.04.016

Hummel, F., Celnik, P., Giraux, P., Floel, A., Wu, W.-H., Gerloff, C., et al. (2005). Effects of non-invasive cortical stimulation on skilled motor function in chronic stroke. *Brain* 128, 490–499. doi: 10.1093/brain/awh369

Humphries, C., Liebenthal, E., and Binder, J. R. (2010). Tonotopic organization of human auditory cortex. *Neuroimage* 50, 1202–1211. doi: 10.1016/j.neuroimage.2010.01.046

Im, C.-H., Park, J.-H., Shim, M., Chang, W. H., and Kim, Y.-H. (2012). Evaluation of local electric fields generated by transcranial direct current stimulation with an extracephalic reference electrode based on realistic 3D body modeling. *Phys. Med. Biol.* 57, 2137–2150. doi: 10.1088/0031-9155/57/8/2137

Impey, D., de la Salle, S., and Knott, V. (2016). Assessment of anodal and cathodal transcranial direct current stimulation (tDCS) on MMN-indexed auditory sensory processing. *Brain Cogn.* 105, 46–54. doi: 10.1016/j.bandc.2016.03.006

Jefferys, J. G. (1981). Influence of electric fields on the excitability of granule cells in guinea-pig hippocampal slices. *J. Physiol.* 319, 143–152. doi: 10.1113/jphysiol.1981.sp013897

Jones, K. T., Johnson, E. L., Tauxe, Z. S., and Rojas, D. C. (2020). Modulation of auditory gamma-band responses using transcranial electrical stimulation. *J. Neurophysiol.* 123, 2504–2514. doi: 10.1152/jn.00003.2020

Kabakov, A. Y., Muller, P. A., Pascual-Leone, A., Jensen, F. E., and Rotenberg, A. (2012). Contribution of axonal orientation to pathway-dependent modulation of excitatory transmission by direct current stimulation in isolated rat hippocampus. *J. Neurophysiol.* 107, 1881–1889. doi: 10.1152/jn.00715.2011

Kadir, S., Kaza, C., Weissbart, H., and Reichenbach, T. (2020). Modulation of speech-in-noise comprehension through transcranial current stimulation with the phase-shifted speech envelope. *IEEE Trans. Neural Syst. Rehabil. Eng.* 28, 23–31. doi: 10.1109/TNSRE.2019.2939671

Khan, S., Gramfort, A., Shetty, N. R., Kitzbichler, M. G., Ganesan, S., Moran, J. M., et al. (2013). Local and long-range functional connectivity is reduced in concert in autism spectrum disorders. *PNAS* 110, 3107–3112. doi: 10.1073/pnas.1214533110

Krause, B., Márquez-Ruiz, J., and Cohen Kadosh, R. (2013). The effect of transcranial direct current stimulation: a role for cortical excitation/inhibition balance? *Front. Hum. Neurosci.* 7:602.

Kunzelmann, K., Meier, L., Grieder, M., Morishima, Y., and Dierks, T. (2018). No effect of transcranial direct current stimulation of the auditory cortex on auditory-evoked potentials. *Front. Neurosci.* 12:880.

Ladeira, A., Fregni, F., Campanhã, C., Valasek, C. A., Ridder, D. D., Brunoni, A. R., et al. (2011). Polarity-dependent transcranial direct current stimulation effects on central auditory processing. *PLoS One* 6:e25399. doi: 10.1371/journal.pone.0025399

Langers, D. R. M., and van Dijk, P. (2012). Mapping the tonotopic organization in human auditory cortex with minimally salient acoustic stimulation. *Cereb. Cortex* 22, 2024–2038. doi: 10.1093/cercor/bhr282

Langers, D. R., Backes, W. H., and van Dijk, P. (2007). Representation of lateralization and tonotopy in primary versus secondary human auditory cortex. *Neuroimage* 34, 264–273. doi: 10.1016/j.neuroimage.2006.09.002

Lewald, J. (2016). Modulation of human auditory spatial scene analysis by transcranial direct current stimulation. *Neuropsychologia* 84, 282–293. doi: 10.1016/j.neuropsychologia.2016.01.030

Lewald, J. (2019). Bihemispheric anodal transcranial direct-current stimulation over temporal cortex enhances auditory selective spatial attention. *Exp. Brain Res.* 237, 1539–1549. doi: 10.1007/s00221-019-05525-y

Loui, P., Hohmann, A., and Schlaug, G. (2010). Inducing disorders in pitch perception and production: a reverse-engineering approach. *Proc. Mtgs. Acoust.* 9:050002. doi: 10.1121/1.3431713

Lum, J. A. G., Clark, G. M., Rogers, C. M., Skalkos, J. D., Fuelscher, I., Hyde, C., et al. (2019). Effects of Anodal Transcranial Direct Current Stimulation (atDCS) on sentence comprehension. *J. Int. Neuropsychol. Soc.* 25, 331–335. doi: 10.1017/s1355617718001121

Maharajh, K., Abrams, D., Rojas, D. C., Teale, P., and Reite, M. L. (2007). Auditory steady state and transient gamma band activity in bipolar disorder. *Int. Congress Ser.* 1300, 707–710. doi: 10.1016/j.ics.2006.12.073

Marques, L. M., Lapenta, O. M., Merabet, L. B., Bolognini, N., and Boggio, P. S. (2014). Tuning and disrupting the brain—modulating the McGurk illusion with electrical stimulation. *Front. Hum. Neurosci.* 8:533. doi: 10.3389/fnhum.2014.00533

Mathys, C., Loui, P., Zheng, X., and Schlaug, G. (2010). Non-invasive brain stimulation applied to Heschl's Gyrus modulates pitch discrimination. *Front. Psychol.* 1:193. doi: 10.3389/fpsyg.2010.00193

Matsushita, R., Andoh, J., and Zatorre, R. J. (2015). Polarity-specific transcranial direct current stimulation disrupts auditory pitch learning. *Front. Neurosci.* 9:174. doi: 10.3389/fnins.2015.00174

McDonnell, M. D., and Ward, L. M. (2011). The benefits of noise in neural systems: bridging theory and experiment. *Nat. Rev. Neurosci.* 12, 415–425. doi: 10.1038/nrn3061

Moliadze, V., Antal, A., and Paulus, W. (2010). Electrode-distance dependent after-effects of transcranial direct and random noise stimulation with extracephalic reference electrodes. *Clin. Neurophysiol.* 121, 2165–2171. doi: 10.1016/j.clinph.2010.04.033

Moreno-Duarte, I., Nigel, G., Schestatsky, P., Guleyupoglu, B., Reato, D., Bikson, M., et al. (2014). "Transcranial electrical stimulation: Transcranial direct current stimulation (tDCS), Trascranial Alternating current stimulation (tACS), Transcranial Pulsed current stimulation (tPCS), and Transcranial random noise stimulation (tRNS)," in *The Stimulated Brain: Cognitive Enhancement Using Non-Invasive Brain Stimulation*, ed. R. C. Kodosh (London: Elsevier), 35–39.

Nitsche, M. A., and Paulus, W. (2000). Excitability changes induced in the human motor cortex by weak transcranial direct current stimulation. *J. Physiol.* 527, 633–639. doi: 10.1111/j.1469-7793.2000.t01-1-00633.x

Parkin, B. L., Bhandari, M., Glen, J. C., and Walsh, V. (2019). The physiological effects of transcranial electrical stimulation do not apply to parameters commonly used in studies of cognitive neuromodulation. *Neuropsychologia* 128, 332–339. doi: 10.1016/j.neuropsychologia.2018.03.030

Paulus, W. (2011). Transcranial electrical stimulation (tES – tDCS; tRNS, tACS) methods. *Neuropsychol. Rehabil.* 21, 602–617.

Paulus, W., Antai, A., and Nitsche, M. (2012). "Physiological basis and methodological aspects of transcranial electric stimulation (tDCS, tACS and tRNS)," in *Transcranial Brain Stimulation*, eds C. Miniussi, W. Paulus, and M. Rossini (Milton Park: Taylor and Francis Group). doi: 10.1080/09602011.2011.557292

Paulus, W., Peterchev, A. V., and Ridding, M. (2013). "Transcranial electric and magnetic stimulation: technique and paradigms," in *Handbook of Clinical Neurology Brain Stimulation*, eds A. M. Lozano and M. Hallett (Amsterdam: Elsevier), 329–342.

Pichora-Fuller, M. K., and Souza, P. E. (2003). Effects of aging on auditory processing of speech. *Int. J. Audiol.* 42, 11–16.

Prete, G., D'Anselmo, A., Tommasi, L., and Brancucci, A. (2017). Modulation of illusory auditory perception by transcranial electrical stimulation. *Front. Neurosci.* 11:351.

Prete, G., D'Anselmo, A., Tommasi, L., and Brancucci, A. (2018). Modulation of the dichotic right ear advantage during bilateral but not unilateral transcranial random noise stimulation. *Brain Cogn.* 123, 81–88. doi: 10.1016/j.bandc.2018.03.003

Priori, A., Berardelli, A., Rona, S., Accornero, N., and Manfredi, M. (1998). Polarization of the human motor cortex through the scalp. *NeuroReport* 9, 2257–2260.

Purpura, D. P., and McMurtry, J. G. (1965). Intracellular activities and evoked potential changes during polarization of motor cortex. *J. Neurophysiol.* 28, 166–185. doi: 10.1152/jn.1965.28.1.166

Radman, T., Ramos, R. L., Brumberg, J. C., and Bikson, M. (2009). Role of cortical cell type and morphology in subthreshold and suprathreshold uniform electric field stimulation *in vitro*. *Brain Stimul.* 2, 215–228.e3. doi: 10.1016/j.brs.2009.03.007

Reed, T., and Kadosh, R. C. (2018). Transcranial electrical stimulation (tES) mechanisms and its effects on cortical excitability and connectivity. *J. Inherit. Metab. Dis.* 41, 1123–1130.

Reis, J., Prichard, G., and Fritsch, B. (2014). "Chapter 8 - motor system," in *The Stimulated Brain*, ed. R. Cohen Kadosh (San Diego: Academic Press).

Rojas, D. C., and Wilson, L. B. (2014). γ-band abnormalities as markers of autism spectrum disorders. *Biomark. Med.* 8, 353–368. doi: 10.2217/bmm.14.15

Royal, I., Zendel, B. R., Desjardins, M. -È, Robitaille, N., and Peretz, I. (2018). Modulation of electric brain responses evoked by pitch deviants through transcranial direct current stimulation. *Neuropsychologia* 109, 63–74. doi: 10.1016/j.neuropsychologia.2017.11.028

Rufener, K. S., Oechslin, M. S., Zaehle, T., and Meyer, M. (2016a). Transcranial Alternating Current Stimulation (tACS) differentially modulates speech perception in young and older adults. *Brain Stimul.* 9, 560–565. doi: 10.1016/j.brs.2016.04.002

Rufener, K. S., Zaehle, T., Oechslin, M. S., and Meyer, M. (2016b). 40Hz-Transcranial alternating current stimulation (tACS) selectively modulates speech perception. *Int. J. Psychophysiol.* 101, 18–24. doi: 10.1016/j.ijpsycho.2016.01.002

Rufener, K. S., Ruhnau, P., Heinze, H.-J., and Zaehle, T. (2017). Transcranial Random Noise Stimulation (tRNS) shapes the processing of rapidly changing auditory information. *Front. Cell. Neurosci.* 11:162. doi: 10.3389/fncel.2017.00162

Schaal, N. K., Pollok, B., and Banissy, M. J. (2017). Hemispheric differences between left and right supramarginal gyrus for pitch and rhythm memory. *Sci. Rep.* 7:42456. doi: 10.1038/srep42456

Schaal, N. K., Williamson, V. J., and Banissy, M. J. (2013). Anodal transcranial direct current stimulation over the supramarginal gyrus facilitates pitch memory. *Eur. J. Neurosci.* 38, 3513–3518. doi: 10.1111/ejn.12344

Sohn, M. K., Kim, B. O., and Song, H. T. (2012). Effect of stimulation polarity of transcranial direct current stimulation on non-dominant hand function. *Ann. Rehabil. Med.* 36, 1–7. doi: 10.5535/arm.2012.36.1.1

Summers, J. J., Kang, N., and Cauraugh, J. H. (2016). Does transcranial direct current stimulation enhance cognitive and motor functions in the ageing brain? a systematic review and meta- analysis. *Ageing Res. Rev.* 25, 42–54. doi: 10.1016/j.arr.2015.11.004

Talavage, T. M., Sereno, M. I., Melcher, J. R., Ledden, P. J., Rosen, B. R., and Dale, A. M. (2004). Tonotopic organization in human auditory cortex revealed by progressions of frequency sensitivity. *J. Neurophysiol.* 91, 1282–1296. doi: 10.1152/jn.01125.2002

Tang, M. F., and Hammond, G. R. (2013). Anodal transcranial direct current stimulation over auditory cortex degrades frequency discrimination by affecting temporal, but not place, coding. *Eur. J. Neurosci.* 38, 2802–2811. doi: 10.1111/ejn.12280

Terney, D., Chaieb, L., Moliadze, V., Antal, A., and Paulus, W. (2008). Increasing human brain excitability by transcranial high-frequency random noise stimulation. *J. Neurosci.* 28, 14147–14155. doi: 10.1523/jneurosci.4248-08.2008

Vines, B. W., Nair, D., and Schlaug, G. (2008). Modulating activity in the motor cortex affects performance for the two hands differently depending upon which hemisphere is stimulated. *Eur. J. Neurosci.* 28, 1667–1673. doi: 10.1111/j.1460-9568.2008.06459.x

Vossen, A., Gross, J., and Thut, G. (2015). Alpha power increase after transcranial alternating current stimulation at alpha frequency (α-tACS) reflects plastic changes rather than entrainment. *Brain Stimul.* 8, 499–508. doi: 10.1016/j.brs.2014.12.004

Yavari, F., Jamil, A., Mosayebi Samani, M., Vidor, L. P., and Nitsche, M. A. (2018). Basic and functional effects of transcranial electrical stimulation (tES)—an introduction. *Neurosci. Biobehav. Rev.* 85, 81–92. doi: 10.1016/j.neubiorev.2017.06.015

Zaehle, T., Beretta, M., Jäncke, L., Herrmann, C. S., and Sandmann, P. (2011). Excitability changes induced in the human auditory cortex by transcranial direct current stimulation: direct electrophysiological evidence. *Exp. Brain Res.* 215, 135–140.

Zimerman, M., Heise, K. F., Hoppe, J., Cohen, L. G., Gerloff, C., and Hummel, F. C. (2012). Modulation of training by single-session transcranial direct current stimulation to the intact motor cortex enhances motor skill acquisition of the paretic hand. *Stroke* 43, 2185–2191. doi: 10.1161/STROKEAHA.111.645382

Conflict of Interest: The authors declare that the research was conducted in the absence of any commercial or financial relationships that could be construed as a potential conflict of interest.

Publisher's Note: All claims expressed in this article are solely those of the authors and do not necessarily represent those of their affiliated organizations, or those of the publisher, the editors and the reviewers. Any product that may be evaluated in this article, or claim that may be made by its manufacturer, is not guaranteed or endorsed by the publisher.

frontiers in Human Neuroscience

ORIGINAL RESEARCH
published: 26 November 2021
doi: 10.3389/fnhum.2021.786225

Difference in Analgesic Effects of Repetitive Transcranial Magnetic Stimulation According to the Site of Pain

Nobuhiko Mori[1], Koichi Hosomi[1], Asaya Nishi[1], Dong Dong[2], Takufumi Yanagisawa[1,3], Hui Ming Khoo[1], Naoki Tani[1], Satoru Oshino[1], Youichi Saitoh[2,4] and Haruhiko Kishima[1]*

[1] Department of Neurosurgery, Osaka University Graduate School of Medicine, Suita, Japan, [2] Department of Mechanical Science and Bioengineering, Osaka University Graduate School of Engineering Science, Toyonaka, Japan, [3] Osaka University Institute for Advanced Co-Creation Studies, Suita, Japan, [4] Tokuyukai Rehabilitation Clinic, Toyonaka, Japan

High-frequency repetitive transcranial magnetic stimulation (rTMS) of the primary motor cortex for neuropathic pain has been shown to be effective, according to systematic reviews and therapeutic guidelines. However, our large, rigorous, investigator-initiated, registration-directed clinical trial failed to show a positive primary outcome, and its subgroup analysis suggested that the analgesic effect varied according to the site of pain. The aim of this study was to investigate the differences in analgesic effects of rTMS for neuropathic pain between different pain sites by reviewing our previous clinical trials. We included three clinical trials in this mini meta-analysis: a multicenter randomized controlled trial at seven hospitals (N = 64), an investigator-initiated registration-directed clinical trial at three hospitals (N = 142), and an exploratory clinical trial examining different stimulation parameters (N = 22). The primary efficacy endpoint (change in pain scale) was extracted for each patient group with pain in the face, upper limb, or lower limb, and a meta-analysis of the efficacy of active rTMS against sham stimulation was performed. Standardized mean difference (SMD) with 95% confidence interval (CI) was calculated for pain change using a random-effects model. The analgesic effect of rTMS for upper limb pain was favorable (SMD = −0.45, 95% CI: −0.77 to −0.13). In contrast, rTMS did not produce significant pain relief on lower limb pain (SMD = 0.04, 95% CI: −0.33 to 0.41) or face (SMD = −0.24, 95% CI: −1.59 to 1.12). In conclusion, these findings suggest that rTMS provides analgesic effects in patients with neuropathic pain in the upper limb, but not in the lower limb or face, under the conditions of previous clinical trials. Owing to the main limitation of small number of studies included, many aspects should be clarified by further research and high-quality studies in these patients.

Keywords: repetitive transcranial magnetic stimulation (rTMS), motor cortex stimulation, neuropathic pain, meta-analysis, pain sites, upper limb, lower limb

OPEN ACCESS

Edited by:
Masaki Sekino,
The University of Tokyo, Japan

Reviewed by:
Carmen Terranova,
University of Messina, Italy
Enrica Laura Santarcangelo,
University of Pisa, Italy

****Correspondence:***
Koichi Hosomi
k-hosomi@nsurg.med.osaka-u.ac.jp

Specialty section:
This article was submitted to Brain Imaging and Stimulation, a section of the journal Frontiers in Human Neuroscience

Received: *29 September 2021*
Accepted: *29 October 2021*
Published: *26 November 2021*

Citation:
Mori N, Hosomi K, Nishi A, Dong D, Yanagisawa T, Khoo HM, Tani N, Oshino S, Saitoh Y and Kishima H (2021) Difference in Analgesic Effects of Repetitive Transcranial Magnetic Stimulation According to the Site of Pain. Front. Hum. Neurosci. 15:786225. doi: 10.3389/fnhum.2021.786225

INTRODUCTION

Migita et al. (1995) reported the pain-relieving effects of repetitive transcranial magnetic stimulation (rTMS) in two patients with central neuropathic pain. Since then, rTMS has been developed as a promising, safe, and non-invasive brain stimulation treatment tool with fewer side effects for chronic pain that may benefit patients who do not respond to conventional

pharmacological therapies. In the early 2000s, 10-Hz rTMS to the primary motor cortex (M1) was shown to be effective in patients with neuropathic pain (Lefaucheur et al., 2001a,b). Since then, many studies have been conducted to investigate the optimal parameters. M1 of the hand area contralateral to the painful side was stimulated regardless of the pain site in some previous studies (Lefaucheur et al., 2001a,b, 2008; Khedr et al., 2005, 2015; André-Obadia et al., 2006, 2008, 2011, 2021; Sun et al., 2019; Quesada et al., 2020). Lefaucheur et al. included patients with unilateral pain predominating at the hands because anatomically, the M1 of the hand area can be identified more reliably as the stimulation site than the face and lower limbs areas (Lefaucheur et al., 2001a, 2006a). Some other study groups restricted their inclusion criteria to predominantly upper limb pain patients with central post-stroke pain or complex regional pain syndrome, and they also showed that active TMS relieved pain more effectively compared with sham stimulation (Pleger et al., 2004; Picarelli et al., 2010; Ojala et al., 2021). In contrast, some studies have examined the effectiveness of rTMS in alleviating pain at different stimulation sites (Hirayama et al., 2006; Lefaucheur et al., 2006b; Jette et al., 2013; de Oliveira et al., 2014; Lindholm et al., 2015; Ayache et al., 2016; Nurmikko et al., 2016; André-Obadia et al., 2018; Galhardoni et al., 2019; Attal et al., 2021; Freigang et al., 2021; Ojala et al., 2021). We have reported that 5 Hz-rTMS to M1 relieved neuropathic pain, but that to the primary somatosensory cortex, premotor area, and supplementary motor area did not (Hirayama et al., 2006). Based on earlier promising results, we subsequently conducted a large, rigorous, multicenter, randomized, blinded, controlled, parallel trial involving 144 patients with neuropathic pain. The results showed that five daily sessions of rTMS over M1 with 500 pulses/session at 5 Hz did not achieve better pain relief than sham stimulation. However, the subgroup analysis suggested that the analgesic effect of rTMS for upper limb pain was superior to that of rTMS for lower limb pain (Hosomi et al., 2020). Similarly, another study reported that the efficacy of rTMS for upper limb pain tended to be higher than that for lower limb pain (Hosomi et al., 2013). Considering our previous studies, we hypothesized that the pain relief effects of rTMS might differ, depending on the pain site.

In some systematic reviews and therapeutic guidelines, high-frequency rTMS of the M1 for neuropathic pain has been shown to be effective (Jin et al., 2015; Cruccu et al., 2016; Singer et al., 2017; O'Connell et al., 2018; Aamir et al., 2020; Lefaucheur et al., 2020; Leung et al., 2020; Moisset et al., 2020; Shen et al., 2020; Yang and Chang, 2020; Attia et al., 2021; Knotkova et al., 2021; Zhang et al., 2021). Moreover, the effectiveness of high-frequency rTMS has also been reported in some types of painful conditions, such as various non-neuropathic pain (Galhardoni et al., 2015; Lan et al., 2017; Cardinal et al., 2019; Ferreira et al., 2019). In addition to reports on the efficacy of rTMS for a variety of pain-causing conditions, differences in the pain-relieving effects of rTMS have been investigated for a variety of factors, including stimulation location and frequency, number of stimulation pulses per session, and number of sessions. Although various factors that influence the pain-relieving effects of rTMS treatment have been investigated, evidence of the pain-relieving effects of rTMS by pain site is lacking. Therefore, the primary purpose of this study was to investigate the differences in analgesic effects of rTMS over M1 for neuropathic pain between different pain sites by reviewing our previous clinical trials.

MATERIALS AND METHODS

Study Design, Studies Selection, and Data Source

This study was a meta-analysis based on the results of our previous studies, which aimed to investigate the pain-relieving effects of rTMS treatment by pain site. Meta-analyses must generally be performed according to a predetermined procedure, which is the preferred reporting item for systematic reviews and meta-analyses statements (Liberati et al., 2009; Rethlefsen et al., 2021). However, to the best of our knowledge, only two studies have examined the differences in the pain relief effects of high-frequency rTMS by pain site (Lefaucheur et al., 2004; Ayache et al., 2016). In these studies, the level of significance (*P*-value) is clearly provided, but the amount or rate of the decrease in pain intensity is not, and there is a lack of data available for meta-analysis by pain site. Therefore, we defined this study as a mini meta-analysis, because only our previous trials were extracted and analyzed. We extracted randomized controlled trials (RCTs) of rTMS using the figure-of-8 coil for neuropathic pain, conducted at Osaka University Hospital as the main study institution, because this was the first attempt to review the analgesic effects at different pain sites. We included three of our previous clinical trials in this meta-analysis (Hosomi et al., 2013, 2020; Mori et al., 2021b). Hosomi et al. (2013) conducted a randomized, double-blind, sham-controlled trial, from 2009 to 2011, at seven centers in Japan, to assess the efficacy and safety of 10 daily doses of rTMS in patients with neuropathic pain. A series of 10 daily 5-Hz rTMS (500 pulses/session) of M1 or sham stimulation was applied to each patient with a follow-up of 17 days. This study was divided into two groups: group A had an active rTMS period followed by a sham period, and group B had a sham period followed by an active rTMS period. Therefore, the two groups were analyzed separately in this analysis. From the data from Hosomi et al. (2013), we used the mean visual analog scale (VAS) decrease over 10 sessions for this analysis. This was calculated by subtracting the VAS value immediately before the intervention from the VAS value immediately after the intervention for each session and then averaging them. Second, in a trial by Hosomi et al. (2020), a randomized, patient- and assessor-blinded, sham-controlled, parallel trial was conducted from 2016 to 2017 at three centers to obtain regulatory approval in Japan. A series of five daily 5-Hz rTMS (500 pulses/session) of M1 or sham stimulation was applied to each patient with a follow-up of 4 weeks. We used the mean VAS decrease over five sessions for this analysis from the data of Hosomi et al. (2020). The mean decrease in VAS score was calculated using the procedure described by Hosomi et al. (2013). Finally, in a trial by Mori et al. (2021b), a randomized, single-blind, sham-controlled, crossover exploratory study was conducted from 2017 to 2018 at Osaka University Hospital to explore the optimal stimulus conditions for treating neuropathic pain. Four single sessions

of M1-rTMS at different parameters (1, 5-Hz with 500 pulses per session; 2, 10-Hz with 500 pulses per session; 3, 10-Hz with 2000 pulses per session; and 4, sham stimulation) were conducted in random order. From the data of Mori et al. (2021b), we used VAS decrease, which was calculated by subtracting the VAS score immediately after the intervention from that immediately before the intervention for this analysis. Since Mori et al. (2021b) conducted a crossover study examining four different stimulation conditions, the results of the rTMS condition (10 Hz over M1 hand, 2000 pulses/session) that produced significantly more effective pain relief compared with the sham stimulation were extracted and integrated into the present study. These studies were approved by the institutional review boards, and written informed consent was obtained from all participants.

Data Synthesis and Analysis

Changes in pain scale (VAS scale: 0 = no pain to 100 = maximal pain) were extracted as a primary efficacy endpoint from each trial, and a mini meta-analysis of the efficacy of active rTMS against sham stimulation was performed. Next, the efficacy of rTMS was analyzed for each patient group with pain in the face and upper or lower limbs. The chi-squared test and I^2 statistic were used to quantify the heterogeneity between the trials. Heterogeneity was considered significant when chi-squared $P < 0.10$, and the I^2 statistic was used to evaluate the degree of heterogeneity. Substantial heterogeneity was considered to be present when I^2 was >50%. In this analysis, a random-effects model was used regardless of heterogeneity, considering the small sample size (Cochrane Handbook for Systematic Reviews of Interventions, Version 6.1, 2020; Chapter 10. Analyzing data and undertaking meta-analyses[1]). Standardized mean difference (SMD) with 95% confidence interval (CI) was calculated for pain change using a random-effects model. This analysis was performed using the Cochrane Collaboration's software program Review Manager (RevMan) version 5.4.1. software (Cochrane Collaboration, Oxford, United Kingdom).

Assessment of Resting Motor Threshold

The relationship between resting motor threshold (RMT) and pain site was examined in an investigator-initiated registration-directed clinical trial (Hosomi et al., 2020), in which RMT was recorded at M1 corresponding to the painful body part. The multicenter RCT (Hosomi et al., 2013) and the exploratory clinical trial (Mori et al., 2021b) were excluded from the RMT analysis because RMT was only partially recorded in the former, and RMT at M1 of the hand was recorded regardless of the pain site in the latter. The difference in RMT by pain site was analyzed using a one-way analysis of variance (ANOVA).

RESULTS

A total of 228 patients from three clinical trials were included in the analysis (**Table 1**). In group A of Hosomi et al. (2013), a total of 28 patients were included (upper limb pain, $n = 15$; lower limb pain, $n = 8$; facial pain, $n = 5$). The etiologies of neuropathic pain were as follows: cerebral lesion in 21 patients, spinal lesion in 4, peripheral nerve injury in 1, phantom limb in 1, and root avulsion in 1 patient. In group B of Hosomi et al. (2013), a total of 35 patients were included (upper limb pain, $n = 20$; lower limb pain, $n = 14$; facial pain, $n = 1$). The etiologies of neuropathic pain were as follows: cerebral lesion, 30 patients; spinal lesion, 3 patients; and phantom limb, 2 patients. In Hosomi et al. (2020), 142 patients were included (upper limb pain, $n = 67$; lower limb pain, $n = 59$; facial pain, $n = 16$). The etiologies of neuropathic pain were as follows: cerebral lesion, 54 patients; postherpetic neuralgia, 12 patients; spinal lesion, 9 patients; root avulsion, 9 patients; complex regional pain syndrome, 4 patients; phantom limb, 2 patients; and other lesions, 52 patients. In Mori et al. (2021b), a total 22 patients were included (upper limb pain, $n = 10$; lower limb pain, $n = 10$; facial pain, $n = 2$). The etiologies of neuropathic pain were as follows: cerebral lesion in 15 patients, complex regional pain syndrome in 3, peripheral nerve injury in 2, spinal lesion in 1, and root avulsion in 1 patient.

Figure 1 shows the results of the mini meta-analysis for the entire population. Heterogeneity was moderate (Chi-squared = 7.30, $P = 0.06$, $I^2 = 59\%$), and the analysis of the pooled analgesic outcome showed that the effect size was not statistically significant −0.33 (95% CI, −0.70 to 0.04; $P = 0.08$). In the analysis of the group of upper limb pain, heterogeneity was low (Chi-squared = 0.50, $P = 0.92$, $I^2 = 0\%$), and the analysis of the pooled analgesic outcome showed a significant effect size of −0.45 (95% CI, −0.77 − −0.13; $P < 0.01$) (**Figure 2**). This suggests that rTMS for neuropathic pain in the upper limbs was effective in decreasing pain intensity. In the analysis of the groups of lower limb pain and facial pain, heterogeneity was low (Chi-squared = 3.12, $P = 0.37$, $I^2 = 4\%$) and moderate (Chi-squared = 3.67, $P = 0.16$, $I^2 = 46\%$), respectively. The effect size for pain change was 0.04 (95% CI, −0.33 to 0.41; $P = 0.82$) for lower limb pain and −0.24 (95% CI, −1.59 to 1.12; $P = 0.73$) for facial pain (**Figures 3**, **4**). rTMS was unlikely to be effective for neuropathic pain in the lower limbs or faces. The funnel plots were symmetrical, suggesting that the publication bias was low.

According to Hosomi et al. (2020), the mean RMTs (SD) at M1 face, hand, and foot were 60.3% of the maximum stimulator output (19.0), 60.1% (19.1), and 81.2% (13.1), respectively. There was a significant difference in RMT by pain site ($P < 0.01$) (**Figure 5**).

DISCUSSION

This study investigated the differences in analgesic effects of rTMS over the M1 using a figure-of-8 coil for neuropathic pain between pain sites. The findings from the three extracted clinical trials showed that rTMS for patients with neuropathic pain in the upper limb was particularly effective. Meanwhile, rTMS for patients with neuropathic pain in the lower limb and face was not confirmed to be effective.

Our main finding showed that high-frequency rTMS treatment using a figure-of-8 coil for neuropathic pain ($N = 226$) had a different effect on pain relief at the pain site. There

[1]https://training.cochrane.org/handbook/archive/v6.1/chapter-10

TABLE 1 | Characteristics of our previous rTMS studies using the figure-of-eight coil.

Study	N	Pain origin (N)	Target of stimulation	Parameters and Dosage	Design/Study center	Stimulator/Coil	Sham condition
Hosomi et al., 2013	29	Stroke (22), Spinal lesion (4), Phantom limb (1), Root avulsion (1), Peripheral nerve injury (1)	M1 contralateral to painful side	5-Hz, 90%RMT, total 500 pulses/session (50 pulses × 10 train/session, 10 sessions, ITI = 50 s)	Cross-over RCT/7 centers	Magstim Rapid, Magstim Company, or AAA- 81077, Nihon Kohden Corp./figure-of-8	Sham coil + simultaneous electrical stimulation to the scalp
Hosomi et al., 2013	35	Stroke (30), Spinal lesion (3), Phantom limb (2), Root avulsion (0), Peripheral nerve injury (0)					
Hosomi et al., 2020	Active: 72	Stroke (31), Spinal lesion (2), Postherpetic neuralgia (6), Root avulsion (4), Phantom limb (2), CRPS (2), Other (25)	M1 contralateral to painful side	5-Hz, 90%RMT, total 500 pulses/session (50 pulses × 10 train/session, 5 sessions, ITI = 50 s)	Parallel RCT/3 centers	TEN-P11, Teijin Pharma Limited/eccentric figure-of-8	
	Sham: 70	Stroke (23), Spinal lesion (7), Postherpetic neuralgia (6), Root avulsion (5), Phantom limb (0), CRPS (2), Other (27)					Sham coil + simultaneous electrical stimulation to the scalp
Mori et al., 2021b	22	Stroke (15), CRPS (3), Spinal lesion (1), Root avulsion (1), Peripheral nerve injury (2)	the M1 hand area contralateral to the painful side	10-Hz, 90%RMT, total 2000 pulses/session (50 pulses × 40 train/session, 1 session, ITI = 25 s)	Cross-over RCT/single center	MagPro X100, MagVenture/figure-of-8	Sham coil

N, Numbers of subjects; RMT, Resting Motor Threshold; M1, Primary motor cortex; CRPS, Complex Regional Painful Syndrome; RCT, Randomized Controlled Trial; ITI, Inter-train Interval; sec, second.

The Hosomi et al. (2013) (treatment group A) study includes participants with an active rTMS period followed by a sham period, and the Hosomi et al. (2013) (treatment group B) study includes participants with a sham period followed by an active rTMS period.

have been many studies on the pain relief effects of rTMS for neuropathic pain, but to the best of our knowledge, there are few reports on the differences in pain relief effects by pain site (Lefaucheur et al., 2004; Ayache et al., 2016). Ayache et al. showed that pain intensity was significantly reduced after rTMS for both upper and lower limb pain (N = 20 and 16, respectively) (Ayache et al., 2016). Lefaucheur et al. showed that rTMS was more effective over the M1 hand area in facial pain (N = 14) than in upper and lower limb pain (N = 27 and 19, respectively) (Lefaucheur et al., 2004). The participants in these studies experienced a mixed condition of neuropathic pain, that is, central or peripheral neuropathic pain, similar to the participants in our three clinical trials. The stimulation condition set by Hosomi et al. (2013, 2020) was relatively low compared to those set by Lefaucheur et al. (2004) and Ayache et al. (2016) (5 Hz with 500 pulses/session vs. 10 Hz with 1,000 to 3,000 pulses/session). Mori et al. (2021b) adopted a high-dose (10 Hz with 2,000 pulses/session), but the results were not favorable for lower limb pain (SMD −0.04, 95% CI −0.91 to 0.84). The other difference was the manner of sham stimulation. In our previous trials, realistic sham stimulation, which produces scalp sensations and sounds similar to active stimulation without cortical stimulation, was performed by electrical stimulation and kept the conditions as similar as possible between active and sham stimulation. Consequently, realistic sham stimulation may have produced a large placebo effect. Although the manner of sham stimulation has differed between clinical trials, we do not think it is related to the difference in pain relief effect by pain site. Thus, the following comparison assessed the differences between the meta-analysis of the Cochrane review in single-session studies of high-frequency rTMS of M1 and this study. The SMD (95% CI) of pain score change in the Cochrane review (N = 249) was −0.38 (−0.49 to −0.27), and that for the whole population in this study was −0.33 (−0.70 to 0.04). Furthermore, the SMD (95% CI) for upper limbs pain in this study was −0.45 (−0.77 to −0.13). The SMDs (95% CI) of the two meta-analyses did not seem to be significantly different. Therefore, the results of the current study suggest that rTMS is clearly effective for upper limb pain and less effective for lower limb pain, as far as our previous studies are concerned.

We need to consider the factors that contribute to the difference in pain relief effects of rTMS for upper and lower limb pain. First, we showed that the RMT of the hand was clearly lower than that of the lower limb (Hosomi et al., 2013, 2020; Shimizu et al., 2017). Previous studies have demonstrated the correlation between RMT and the distance from the coil to the superficial layer of the brain (Stokes et al., 2005; Shimizu et al., 2017). Furthermore, previous studies in healthy subjects have reported that RMT was higher in the lower limb muscle (tibialis anterior) than that in the upper limb muscle (first dorsal interosseous), and it was higher in the figure-of-8 coil than that in the double-cone

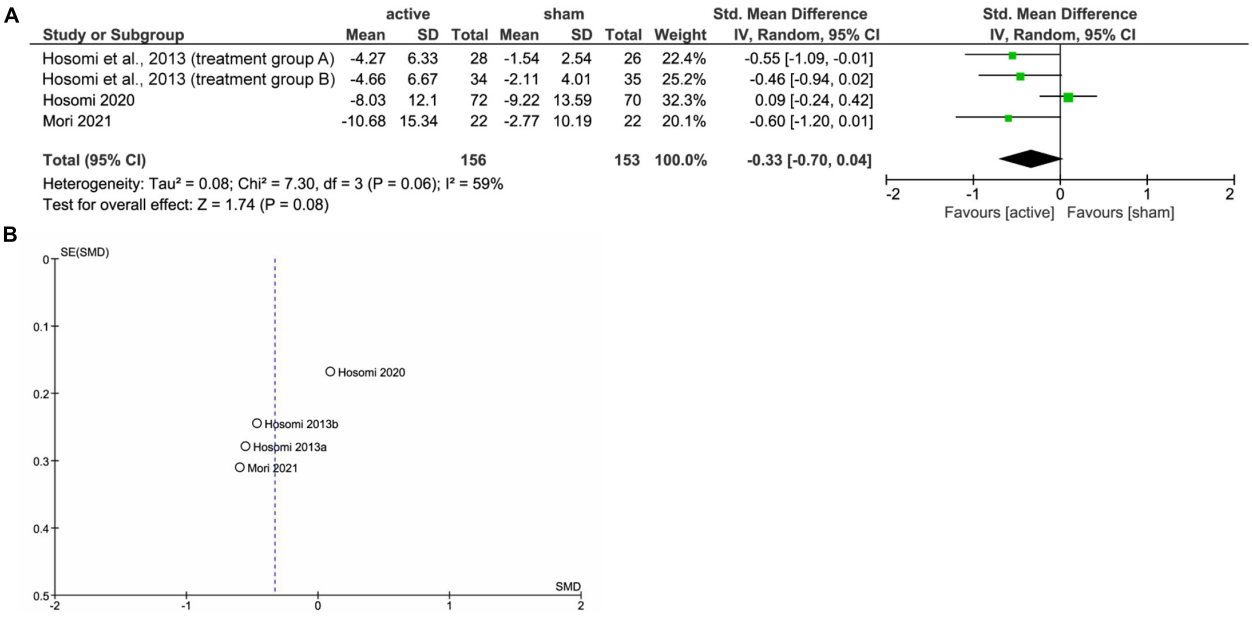

FIGURE 1 | The forest plot **(A)** and funnel plot **(B)** of the analysis for the whole population.

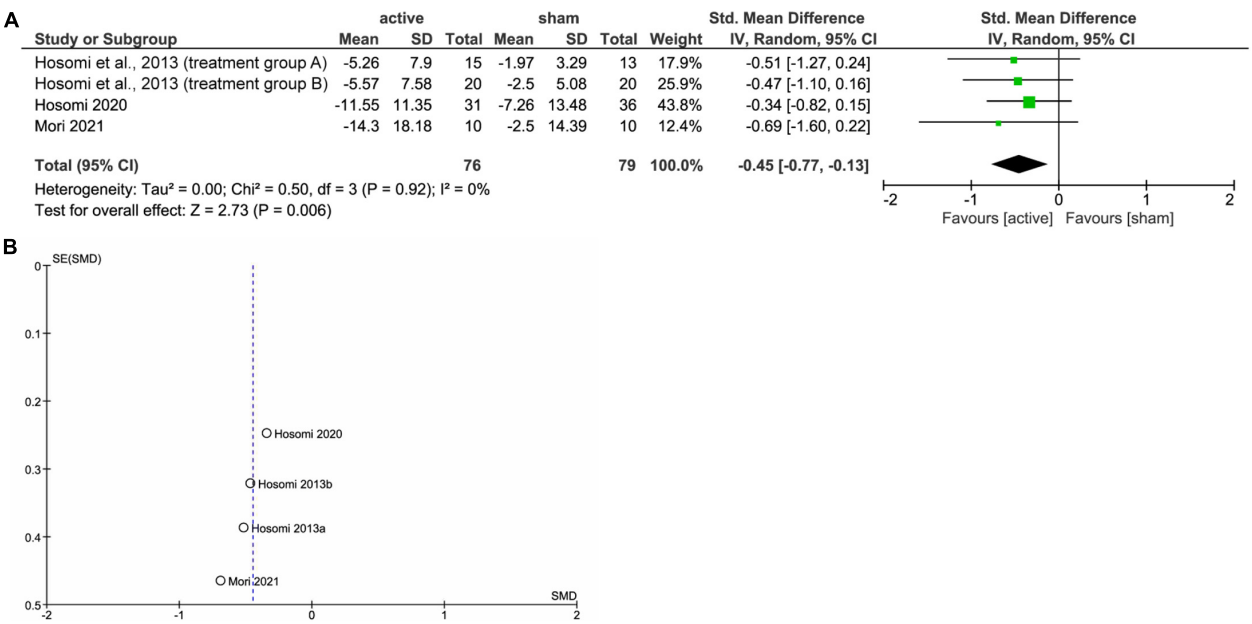

FIGURE 2 | The forest plot **(A)** and funnel plot **(B)** of the analysis for the upper limb pain.

coil. The magnetic field strength produced by the double-cone coil is higher than that of the figure-of-8 coil (Schecklmann et al., 2020). This is due to the fact that the electric field generated by the figure-of-8 coil attenuates in relation to the depth of the target. Therefore, it is difficult to sufficiently stimulate the deep part of the brain with the figure-of-8 coil, especially the M1 foot area. To solve this problem of insufficient stimulation of the M1 foot area, rTMS with 3,000 pulses per session was performed under different stimulation conditions, such as stimulation intensity (90 or 110% RMT), coil position (M1 hand or foot area), and coil direction (anteroposterior or mediolateral) (Mori et al., 2021a). The results indicated that the analgesic effect was obtained in all conditions except sham stimulation, but simply increasing the intensity of the stimulation was not enough to eliminate pain. Second, the H-coil and double-cone coil, which can generate electric fields in the deep brain, have been used to stimulate the deep brain more effective than the figure-of-8 coil. One study investigated the analgesic effects of rTMS over the anterior

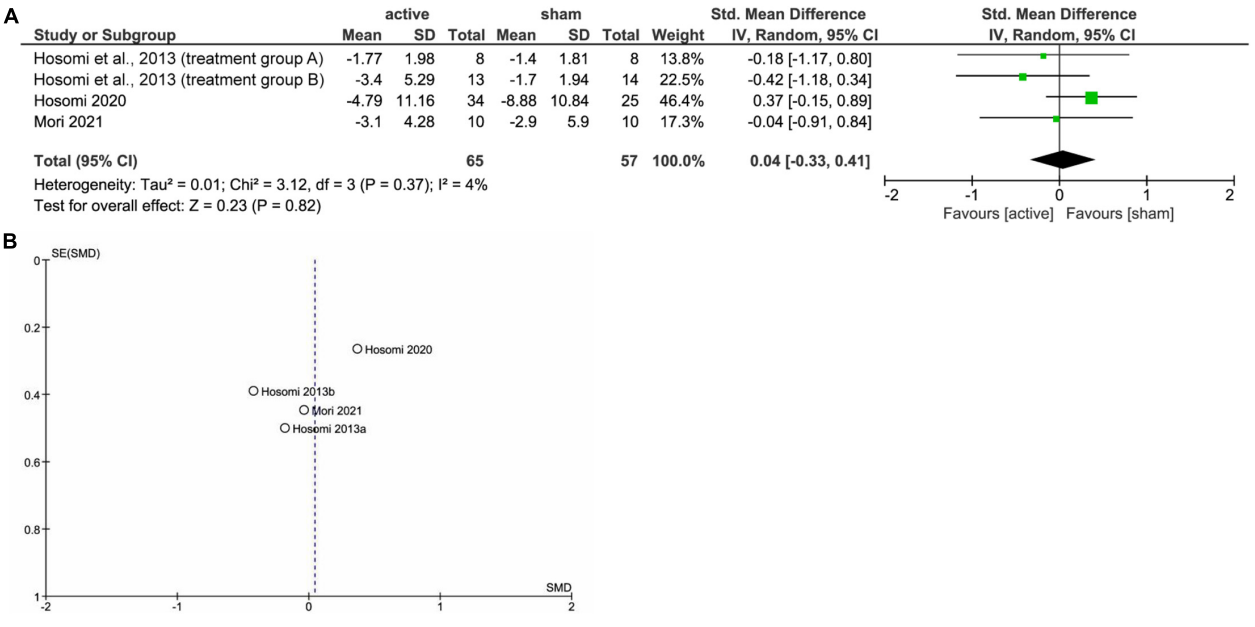

FIGURE 3 | The forest plot **(A)** and funnel plot **(B)** of the analysis for the lower limb pain.

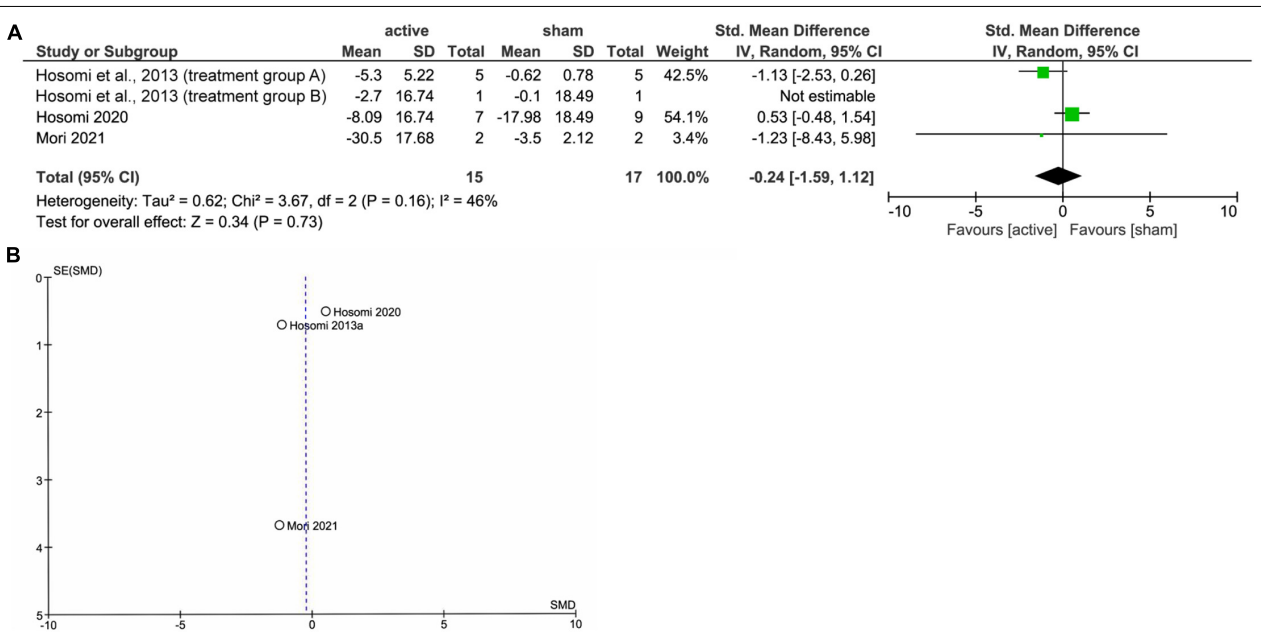

FIGURE 4 | The forest plot **(A)** and funnel plot **(B)** of the analysis for the facial pain.

cingulate cortex using an H-coil (Galhardoni et al., 2019). In addition, there are also reports that investigated the analgesic effect on foot pain with rTMS targeting the M1 foot using the H-coil (Onesti et al., 2013; Shimizu et al., 2017). In contrast, a pilot study of rTMS using a double-cone coil for chronic lower limb pain and a circular coil for upper limb pain failed to show significantly more effective pain relief compared with sham stimulation (Rollnik et al., 2002). According to a case report of invasive motor cortical stimulation, electrodes were implanted in the epidural area of the cortical regions corresponding to the painful area in patients with pain in the upper and lower limbs (Pommier et al., 2020). The stimulation of lower limb pain was inadvertently turned off and did not produce sufficient analgesic effect, but a turned-on stimulation reproduced sufficient pain relief. In addition, we implanted the subdural electrode over M1 corresponding to the painful site (Saitoh et al., 2000; Hosomi et al., 2008). Electrodes were implanted in the midline of the brain surface or in the interhemispheric fissure for lower limb pain

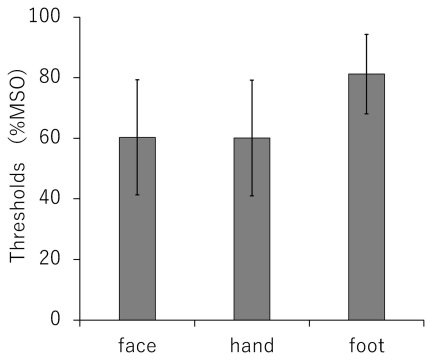

FIGURE 5 | Comparison of resting motor thresholds for each stimulation site (primary motor cortex face, hand, and foot area). MSO, maximum stimulus output.

(Hosomi et al., 2008). Presumably, another group used a similar technique to implant electrodes (Nguyen et al., 2011). These findings indicate the somatotopically driven analgesic efficacy of neuromodulation for lower limb pain. To alleviate pain with rTMS, it may be necessary to properly stimulate the target region. In the future, the efficacy of rTMS using an H-coil or double-cone coil for chronic pain needs to be further investigated.

In this meta-analysis, we focused on differences in the analgesic effects of rTMS over M1 at different pain sites. To date, some RCTs have been conducted in many centers to investigate various conditions. For example, trials have examined the pain-relieving effects of rTMS at different frequencies, different stimulation sites, and in single or multiple sessions, as well as trials examining the efficacy of rTMS for various neuropathic pain conditions, such as spinal cord injury (Yilmaz et al., 2014; Nardone et al., 2017; Sun et al., 2019), phantom limb pain (Ahmed et al., 2011; Malavera et al., 2016), traumatic brain injury (Choi et al., 2018), and radiculopathy (Attal et al., 2016). In recent years, some systematic reviews and meta-analyses have shown the efficacy and stimulation parameters of high-frequency rTMS for neuropathic pain (Baptista et al., 2019; Lefaucheur et al., 2020; Leung et al., 2020), and a practical algorithm for rTMS in the treatment of chronic pain in daily clinical practice has been proposed (Lefaucheur et al., 2020). In this algorithm, the stimulation site is not set to one specific area but to the M1 of the hand contralateral to the painful side or to the M1 corresponding to the painful area. If no improvement in pain is obtained, flexible parameters are proposed to change to a different stimulation site. Although this algorithm is a good clinically adapted setting, we consider that the optimal stimulation site to produce the analgesic effects of rTMS is controversial. Therefore, we reviewed RCTs of high-frequency rTMS in more than 10 patients with neuropathic pain (duration of more than 3 months) (**Supplementary Table 1**). We found that the M1 lower limb region was stimulated for lower limb pain in two studies using an H-coil (Onesti et al., 2013; Shimizu et al., 2017) and nine studies (Hirayama et al., 2006; Defrin et al., 2007; Saitoh et al., 2007; Kang et al., 2009; Hosomi et al., 2013, 2020; Jette et al., 2013; Ayache et al., 2016; Nurmikko et al., 2016) using a figure-of-8 coil. In contrast, the stimulation site in more than 10 studies targeted the M1 hand area, regardless of the pain site. A recent large RCT reported that rTMS over the M1 hand area was effective in patients with peripheral neuropathic pain. Approximately 60% of the participants were patients with lower limb pain (Attal et al., 2021). Previous studies have reported the efficacy of rTMS for peripheral neuropathic pain (Lefaucheur et al., 2004; Attal et al., 2016; Pei et al., 2019), and rTMS may be effective for peripheral neuropathic pain regardless of the pain site. However, considering the findings of previous studies, it is not clear whether targeting the somatotopic organization of M1 corresponding to painful areas can enhance pain relief. In the future, it will be necessary to investigate the optimal stimulation site according to the pain site and to select the optimal target population according to the stimulation site.

Our study has a few limitations. First, the main limitation of this study is the small sample size and the small number of studies included, which made the sensitivity analyses difficult. Second, as a methodological consideration of this analysis, the procedure of meta-analysis must be considered. Although a meta-analysis should be conducted according to a predetermined procedure (Liberati et al., 2009; Rethlefsen et al., 2021), we extracted and analyzed only three RCTs mainly conducted by Osaka University Hospital because there was little data to incorporate. Therefore, there was an obvious selection bias. The findings of this study suggest that a rigorous meta-analysis of the efficacy of rTMS by pain sites needs to be performed, and these findings need to be validated in the future. To achieve this, future prospective clinical trials should also provide site-specific pain results. Third, heterogeneity should be considered when interpreting the results of the meta-analysis. According to the Cochrane Handbook Version 6.2 see text footnote 1, caution should be taken when interpreting heterogeneity due to the poor power of the chi-squared test when the number of studies incorporated in the analysis is small. To compensate for the lack of power, the significance level of heterogeneity for the chi-squared test was set at 0.10 rather than the conventional level of 0.05. In this study, no heterogeneity was identified in the results for upper and lower limb pain, which was the main focus of this study. However, we found moderate heterogeneity in the results of the entire population and facial pain. As far as we could check, through visual inspection of the funnel plots of our previous studies incorporated in these analyses, it does not seem to be a non-specific asymmetry. We believe that the heterogeneity was significant for facial pain (N = 16) because the number of patients was too small compared to the analysis of upper limb pain (N = 76) and lower limb pain (N = 65). Because this study has been analyzed with a small number of patients, with only our previously generated results, it is necessary to take sufficient care while interpreting these results.

CONCLUSION

In conclusion, this study suggests differences in the analgesic effects of high-frequency rTMS over the M1 using the figure-of-8 coil for neuropathic pain between pain sites. More importantly, rTMS for upper limb pain was clearly effective in relieving pain.

Meanwhile, rTMS for lower limb pain and facial pain did not produce an analgesic effect under the conditions of previous clinical trials. However, considering the small number of included studies, our findings should be considered tentative.

DATA AVAILABILITY STATEMENT

The raw data supporting the conclusions of this article will be made available by the authors, without undue reservation.

ETHICS STATEMENT

The studies involving human participants were reviewed and approved by the Ethics Committee of Osaka University Hospital. Written informed consent to participate in this study was provided by the participants' legal guardian/next of kin.

AUTHOR CONTRIBUTIONS

KH and NM contributed to trial design and conducted experiments and data collection. YS, SO, and HK supervised the study. All authors contributed to the data interpretation. NM drafted the manuscript. KH edited the manuscript. NM and KH conducted statistical analyses. All authors reviewed and approved the final manuscript.

FUNDING

This study was partly supported by the Japan Agency for Medical Research and Development (AMED) under grant nos. JP17hk0102029, JP19ek0610016, JP19dm0307007, and JP19dm0307008, and the Japan Society for the Promotion of Science (JSPS) KAKENHI under grant nos. JP17K10893, JP18K08993, and JP19K19867.

SUPPLEMENTARY MATERIAL

The Supplementary Material for this article can be found online at: https://www.frontiersin.org/articles/10.3389/fnhum.2021.786225/full#supplementary-material

REFERENCES

Aamir, A., Girach, A., Sarrigiannis, P. G., Hadjivassiliou, M., Paladini, A., Varrassi, G., et al. (2020). Repetitive magnetic stimulation for the management of peripheral neuropathic pain: a systematic review. *Adv. Ther.* 37, 998–1012. doi: 10.1007/s12325-020-01231-2

Ahmed, M. A., Mohamed, S. A., and Sayed, D. (2011). Long-term antalgic effects of repetitive transcranial magnetic stimulation of motor cortex and serum beta-endorphin in patients with phantom pain. *Neurol. Res.* 33, 953–958. doi: 10.1179/1743132811Y.0000000045

André-Obadia, N., Magnin, M., and Garcia-Larrea, L. (2011). On the importance of placebo timing in rTMS studies for pain relief. *Pain* 152, 1233–1237. doi: 10.1016/j.pain.2010.12.027

André-Obadia, N., Magnin, M., and Garcia-Larrea, L. (2021). Theta-burst versus 20 Hz repetitive transcranial magnetic stimulation in neuropathic pain: a head-to-head comparison. *Clin. Neurophysiol.* 132, 2702–2710. doi: 10.1016/j.clinph.2021.05.022

André-Obadia, N., Magnin, M., Simon, E., and Garcia-Larrea, L. (2018). Somatotopic effects of rTMS in neuropathic pain? A comparison between stimulation over hand and face motor areas. *Eur. J. Pain* 22, 707–715. doi: 10.1002/ejp.1156

André-Obadia, N., Mertens, P., Gueguen, A., Peyron, R., and Garcia-Larrea, L. (2008). Pain relief by rTMS: differential effect of current flow but no specific action on pain subtypes. *Neurology* 71, 833–840. doi: 10.1212/01.wnl.0000325481.61471.f0

André-Obadia, N., Peyron, R., Mertens, P., Mauguiere, F., Laurent, B., and Garcia-Larrea, L. (2006). Transcranial magnetic stimulation for pain control. Double-blind study of different frequencies against placebo, and correlation with motor cortex stimulation efficacy. *Clin. Neurophysiol.* 117, 1536–1544. doi: 10.1016/j.clinph.2006.03.025

Attal, N., Ayache, S. S., Ciampi De Andrade, D., Mhalla, A., Baudic, S., Jazat, F., et al. (2016). Repetitive transcranial magnetic stimulation and transcranial direct-current stimulation in neuropathic pain due to radiculopathy: a randomized sham-controlled comparative study. *Pain* 157, 1224–1231. doi: 10.1097/j.pain.0000000000000510

Attal, N., Poindessous-Jazat, F., De Chauvigny, E., Quesada, C., Mhalla, A., Ayache, S. S., et al. (2021). Repetitive transcranial magnetic stimulation for neuropathic pain: a randomized multicentre sham-controlled trial. *Brain* doi: 10.1093/brain/awab208 [Epub Online ahead of print].

Attia, M., McCarthy, D., and Abdelghani, M. (2021). Repetitive transcranial magnetic stimulation for treating chronic neuropathic pain: a systematic review. *Curr. Pain Headache Rep.* 25:48. doi: 10.1007/s11916-021-00960-5

Ayache, S. S., Ahdab, R., Chalah, M. A., Farhat, W. H., Mylius, V., Goujon, C., et al. (2016). Analgesic effects of navigated motor cortex rTMS in patients with chronic neuropathic pain. *Eur. J. Pain* 20, 1413–1422. doi: 10.1002/ejp.864

Baptista, A. F., Fernandes, A., Sa, K. N., Okano, A. H., Brunoni, A. R., Lara-Solares, A., et al. (2019). Latin American and Caribbean consensus on noninvasive central nervous system neuromodulation for chronic pain management (LAC2-NIN-CP). *Pain Rep.* 4:e692. doi: 10.1097/PR9.0000000000000692

Cardinal, T. M., Antunes, L. C., Brietzke, A. P., Parizotti, C. S., Carvalho, F., De Souza, A., et al. (2019). Differential neuroplastic changes in fibromyalgia and depression indexed by up-regulation of motor cortex inhibition and disinhibition of the descending pain system: an exploratory study. *Front. Hum. Neurosci.* 13:138. doi: 10.3389/fnhum.2019.00138

Choi, G. S., Kwak, S. G., Lee, H. D., and Chang, M. C. (2018). Effect of high-frequency repetitive transcranial magnetic stimulation on chronic central pain after mild traumatic brain injury: a pilot study. *J. Rehabil. Med.* 50, 246–252. doi: 10.2340/16501977-2321

Cruccu, G., Garcia-Larrea, L., Hansson, P., Keindl, M., Lefaucheur, J. P., Paulus, W., et al. (2016). EAN guidelines on central neurostimulation therapy in chronic pain conditions. *Eur. J. Neurol.* 23, 1489–1499. doi: 10.1111/ene.13103

de Oliveira, R. A., de Andrade, D. C., Mendonca, M., Barros, R., Luvisoto, T., Myczkowski, M. L., et al. (2014). Repetitive transcranial magnetic stimulation of the left premotor/dorsolateral prefrontal cortex does not have analgesic effect on central poststroke pain. *J. Pain* 15, 1271–1281. doi: 10.1016/j.jpain.2014.09.009

Defrin, R., Grunhaus, L., Zamir, D., and Zeilig, G. (2007). The effect of a series of repetitive transcranial magnetic stimulations of the motor cortex on central pain after spinal cord injury. *Arch. Phys. Med. Rehabil.* 88, 1574–1580. doi: 10.1016/j.apmr.2007.07.025

Ferreira, N. R., Junqueira, Y. N., Correa, N. B., Fonseca, E. O., Brito, N. B. M., Menezes, T. A., et al. (2019). The efficacy of transcranial direct current stimulation and transcranial magnetic stimulation for chronic orofacial pain: a systematic review. *PLoS One* 14:e0221110. doi: 10.1371/journal.pone.0221110

Freigang, S., Lehner, C., Fresnoza, S. M., Mahdy Ali, K., Hlavka, E., Eitler, A., et al. (2021). Comparing the impact of multi-session left dorsolateral prefrontal

and primary motor cortex neuronavigated repetitive transcranial magnetic stimulation (nrTMS) on chronic pain patients. *Brain Sci.* 11:961. doi: 10.3390/brainsci11080961

Galhardoni, R., Aparecida da Silva, V., Garcia-Larrea, L., Dale, C., Baptista, A. F., Barbosa, L. M., et al. (2019). Insular and anterior cingulate cortex deep stimulation for central neuropathic pain: disassembling the percept of pain. *Neurology* 92, e2165–e2175. doi: 10.1212/WNL.0000000000007396

Galhardoni, R., Correia, G. S., Araujo, H., Yeng, L. T., Fernandes, D. T., Kaziyama, H. H., et al. (2015). Repetitive transcranial magnetic stimulation in chronic pain: a review of the literature. *Arch. Phys. Med. Rehabil.* 96, S156–S172. doi: 10.1016/j.apmr.2014.11.010

Hirayama, A., Saitoh, Y., Kishima, H., Shimokawa, T., Oshino, S., Hirata, M., et al. (2006). Reduction of intractable deafferentation pain by navigation-guided repetitive transcranial magnetic stimulation of the primary motor cortex. *Pain* 122, 22–27. doi: 10.1016/j.pain.2005.12.001

Hosomi, K., Saitoh, Y., Kishima, H., Oshino, S., Hirata, M., Tani, N., et al. (2008). Electrical stimulation of primary motor cortex within the central sulcus for intractable neuropathic pain. *Clin. Neurophysiol.* 119, 993–1001. doi: 10.1016/j.clinph.2007.12.022

Hosomi, K., Shimokawa, T., Ikoma, K., Nakamura, Y., Sugiyama, K., Ugawa, Y., et al. (2013). Daily repetitive transcranial magnetic stimulation of primary motor cortex for neuropathic pain: a randomized, multicenter, double-blind, crossover, sham-controlled trial. *Pain* 154, 1065–1072. doi: 10.1016/j.pain.2013.03.016

Hosomi, K., Sugiyama, K., Nakamura, Y., Shimokawa, T., Oshino, S., Goto, Y., et al. (2020). A randomized controlled trial of 5 daily sessions and continuous trial of 4 weekly sessions of repetitive transcranial magnetic stimulation for neuropathic pain. *Pain* 161, 351–360. doi: 10.1097/j.pain.0000000000001712

Jette, F., Cote, I., Meziane, H. B., and Mercier, C. (2013). Effect of single-session repetitive transcranial magnetic stimulation applied over the hand versus leg motor area on pain after spinal cord injury. *Neurorehabil. Neural. Repair* 27, 636–643. doi: 10.1177/1545968313484810

Jin, Y., Xing, G., Li, G., Wang, A., Feng, S., Tang, Q., et al. (2015). High frequency repetitive transcranial magnetic stimulation therapy for chronic neuropathic pain: a Meta-analysis. *Pain. Physician.* 18, E1029–E1046.

Kang, B. S., Shin, H. I., and Bang, M. S. (2009). Effect of repetitive transcranial magnetic stimulation over the hand motor cortical area on central pain after spinal cord injury. *Arch. Phys. Med. Rehabil.* 90, 1766–1771. doi: 10.1016/j.apmr.2009.04.008

Khedr, E. M., Kotb, H., Kamel, N. F., Ahmed, M. A., Sadek, R., and Rothwell, J. C. (2005). Longlasting antalgic effects of daily sessions of repetitive transcranial magnetic stimulation in central and peripheral neuropathic pain. *J. Neurol. Neurosurg. Psychiatry* 76, 833–838. doi: 10.1136/jnnp.2004.055806

Khedr, E. M., Kotb, H. I., Mostafa, M. G., Mohamad, M. F., Amr, S. A., Ahmed, M. A., et al. (2015). Repetitive transcranial magnetic stimulation in neuropathic pain secondary to malignancy: a randomized clinical trial. *Eur. J. Pain* 19, 519–527. doi: 10.1002/ejp.576

Knotkova, H., Hamani, C., Sivanesan, E., Le Beuffe, M. F. E., Moon, J. Y., Cohen, S. P., et al. (2021). Neuromodulation for chronic pain. *Lancet* 397, 2111–2124. doi: 10.1016/S0140-6736(21)00794-7

Lan, L., Zhang, X., Li, X., Rong, X., and Peng, Y. (2017). The efficacy of transcranial magnetic stimulation on migraine: a meta-analysis of randomized controlled trails. *J. Headache Pain* 18:86. doi: 10.1186/s10194-017-0792-4

Lefaucheur, J. P., Aleman, A., Baeken, C., Benninger, D. H., Brunelin, J., Di Lazzaro, V., et al. (2020). Evidence-based guidelines on the therapeutic use of repetitive transcranial magnetic stimulation (rTMS): an update (2014-2018). *Clin. Neurophysiol.* 131, 474–528. doi: 10.1016/j.clinph.2019.11.002

Lefaucheur, J. P., Drouot, X., Keravel, Y., and Nguyen, J. P. (2001a). Pain relief induced by repetitive transcranial magnetic stimulation of precentral cortex. *Neuroreport* 12, 2963–2965. doi: 10.1097/00001756-200109170-00041

Lefaucheur, J. P., Drouot, X., and Nguyen, J. P. (2001b). Interventional neurophysiology for pain control: duration of pain relief following repetitive transcranial magnetic stimulation of the motor cortex. *Neurophysiol. Clin.* 31, 247–252. doi: 10.1016/s0987-7053(01)00260-x

Lefaucheur, J. P., Drouot, X., Menard-Lefaucheur, I., Keravel, Y., and Nguyen, J. P. (2006a). Motor cortex rTMS restores defective intracortical inhibition in chronic neuropathic pain. *Neurology* 67, 1568–1574. doi: 10.1212/01.wnl.0000242731.10074.3c

Lefaucheur, J. P., Hatem, S., Nineb, A., Menard-Lefaucheur, I., Wendling, S., Keravel, Y., et al. (2006b). Somatotopic organization of the analgesic effects of motor cortex rTMS in neuropathic pain. *Neurology* 67, 1998–2004. doi: 10.1212/01.wnl.0000247138.85330.88

Lefaucheur, J. P., Drouot, X., Menard-Lefaucheur, I., Keravel, Y., and Nguyen, J. P. (2008). Motor cortex rTMS in chronic neuropathic pain: pain relief is associated with thermal sensory perception improvement. *J. Neurol. Neurosurg. Psychiatry* 79, 1044–1049. doi: 10.1136/jnnp.2007.135327

Lefaucheur, J. P., Drouot, X., Menard-Lefaucheur, I., Zerah, F., Bendib, B., Cesaro, P., et al. (2004). Neurogenic pain relief by repetitive transcranial magnetic cortical stimulation depends on the origin and the site of pain. *J. Neurol. Neurosurg. Psychiatry* 75, 612–616. doi: 10.1136/jnnp.2003.022236

Leung, A., Shirvalkar, P., Chen, R., Kuluva, J., Vaninetti, M., Bermudes, R., et al. (2020). Transcranial magnetic stimulation for pain, headache, and comorbid depression: INS-NANS expert consensus panel review and recommendation. *Neuromodulation* 23, 267–290. doi: 10.1111/ner.13094

Liberati, A., Altman, D. G., Tetzlaff, J., Mulrow, C., Gotzsche, P. C., Ioannidis, J. P., et al. (2009). The PRISMA statement for reporting systematic reviews and meta-analyses of studies that evaluate health care interventions: explanation and elaboration. *PLoS Med.* 6:e1000100. doi: 10.1371/journal.pmed.1000100

Lindholm, P., Lamusuo, S., Taiminen, T., Pesonen, U., Lahti, A., Virtanen, A., et al. (2015). Right secondary somatosensory cortex-a promising novel target for the treatment of drug-resistant neuropathic orofacial pain with repetitive transcranial magnetic stimulation. *Pain* 156, 1276–1283. doi: 10.1097/j.pain.0000000000000175

Malavera, A., Silva, F. A., Fregni, F., Carrillo, S., and Garcia, R. G. (2016). Repetitive Transcranial magnetic stimulation for phantom limb pain in land mine victims: a double-blinded, randomized, sham-controlled trial. *J. Pain* 17, 911–918. doi: 10.1016/j.jpain.2016.05.003

Migita, K., Uozumi, T., Arita, K., and Monden, S. (1995). Transcranial magnetic coil stimulation of motor cortex in patients with central pain. *Neurosurgery* 36, 1037–1039. doi: 10.1227/00006123-199505000-00025

Moisset, X., Bouhassira, D., Avez Couturier, J., Alchaar, H., Conradi, S., Delmotte, M. H., et al. (2020). Pharmacological and non-pharmacological treatments for neuropathic pain: systematic review and French recommendations. *Rev. Neurol. (Paris)* 176, 325–352. doi: 10.1016/j.neurol.2020.01.361

Mori, N., Hosomi, K., Nishi, A., Oshino, S., Kishima, H., and Saitoh, Y. (2021b). Analgesic effects of repetitive transcranial magnetic stimulation at different stimulus parameters for neuropathic pain: a randomized study. *Neuromodulation* doi: 10.1111/ner.13328 [Epub Online ahead of print].

Mori, N., Hosomi, K., Nishi, A., Matsugi, A., Dong, D., Oshino, S., et al. (2021a). An exploratory study of optimal parameters of repetitive transcranial magnetic stimulation for neuropathic pain in the lower extremities. *Pain Rep.* 6:e964.

Nardone, R., Holler, Y., Langthaler, P. B., Lochner, P., Golaszewski, S., Schwenker, K., et al. (2017). rTMS of the prefrontal cortex has analgesic effects on neuropathic pain in subjects with spinal cord injury. *Spinal Cord.* 55, 20–25. doi: 10.1038/sc.2016.87

Nguyen, J. P., Nizard, J., Keravel, Y., and Lefaucheur, J. P. (2011). Invasive brain stimulation for the treatment of neuropathic pain. *Nat. Rev. Neurol.* 7, 699–709. doi: 10.1038/nrneurol.2011.138

Nurmikko, T., MacIver, K., Bresnahan, R., Hird, E., Nelson, A., and Sacco, P. (2016). Motor cortex reorganization and repetitive transcranial magnetic stimulation for pain-a methodological study. *Neuromodulation* 19, 669–678. doi: 10.1111/ner.12444

O'Connell, N. E., Marston, L., Spencer, S., DeSouza, L. H., and Wand, B. M. (2018). Non-invasive brain stimulation techniques for chronic pain. *Cochrane Database. Syst. Rev.* 4:CD008208. doi: 10.1002/14651858.CD008208.pub5

Ojala, J., Vanhanen, J., Harno, H., Lioumis, P., Vaalto, S., Kaunisto, M. A., et al. (2021). A randomized, sham-controlled trial of repetitive transcranial magnetic stimulation targeting m1 and s2 in central poststroke pain: a pilot trial. *Neuromodulation* doi: 10.1111/ner.13496 [Epub Online ahead of print].

Onesti, E., Gabriele, M., Cambieri, C., Ceccanti, M., Raccah, R., Di Stefano, G., et al. (2013). H-coil repetitive transcranial magnetic stimulation for pain relief in patients with diabetic neuropathy. *Eur. J. Pain* 17, 1347–1356. doi: 10.1002/j.1532-2149.2013.00320.x

Pei, Q., Wu, B., Tang, Y., Yang, X., Song, L., Wang, N., et al. (2019). Repetitive Transcranial magnetic stimulation at different frequencies for postherpetic

neuralgia: a double-blind, sham-controlled, randomized trial. *Pain Physician* 22, E303–E313.

Picarelli, H., Teixeira, M. J., de Andrade, D. C., Myczkowski, M. L., Luvisotto, T. B., Yeng, L. T., et al. (2010). Repetitive transcranial magnetic stimulation is efficacious as an add-on to pharmacological therapy in complex regional pain syndrome (CRPS) type I. *J. Pain* 11, 1203–1210. doi: 10.1016/j.jpain.2010.02.006

Pleger, B., Janssen, F., Schwenkreis, P., Volker, B., Maier, C., and Tegenthoff, M. (2004). Repetitive transcranial magnetic stimulation of the motor cortex attenuates pain perception in complex regional pain syndrome type I. *Neurosci. Lett.* 356, 87–90. doi: 10.1016/j.neulet.2003.11.037

Pommier, B., Quesada, C., Nuti, C., Peyron, R., and Vassal, F. (2020). Is the analgesic effect of motor cortex stimulation somatotopically driven or not? *Neurophysiol. Clin.* 50, 195–203. doi: 10.1016/j.neucli.2020.04.002

Quesada, C., Pommier, B., Fauchon, C., Bradley, C., Creac'h, C., Murat, M., et al. (2020). New procedure of high-frequency repetitive transcranial magnetic stimulation for central neuropathic pain: a placebo-controlled randomized crossover study. *Pain* 161, 718–728. doi: 10.1097/j.pain.0000000000001760

Rethlefsen, M. L., Kirtley, S., Waffenschmidt, S., Ayala, A. P., Moher, D., Page, M. J., et al. (2021). PRISMA-S: an extension to the PRISMA Statement for Reporting Literature Searches in Systematic Reviews. *Syst. Rev.* 10:39. doi: 10.1186/s13643-020-01542-z

Rollnik, J. D., Wustefeld, S., Dauper, J., Karst, M., Fink, M., Kossev, A., et al. (2002). Repetitive transcranial magnetic stimulation for the treatment of chronic pain - a pilot study. *Eur. Neurol.* 48, 6–10. doi: 10.1159/000064950

Saitoh, Y., Hirayama, A., Kishima, H., Shimokawa, T., Oshino, S., Hirata, M., et al. (2007). Reduction of intractable deafferentation pain due to spinal cord or peripheral lesion by high-frequency repetitive transcranial magnetic stimulation of the primary motor cortex. *J. Neurosurg.* 107, 555–559. doi: 10.3171/JNS-07/09/0555

Saitoh, Y., Shibata, M., Hirano, S., Hirata, M., Mashimo, T., and Yoshimine, T. (2000). Motor cortex stimulation for central and peripheral deafferentation pain. Report of eight cases. *J. Neurosurg.* 92, 150–155. doi: 10.3171/jns.2000.92.1.0150

Schecklmann, M., Schmausser, M., Klinger, F., Kreuzer, P. M., Krenkel, L., and Langguth, B. (2020). Resting motor threshold and magnetic field output of the figure-of-8 and the double-cone coil. *Sci. Rep.* 10:1644. doi: 10.1038/s41598-020-58034-2

Shen, Z., Li, Z., Ke, J., He, C., Liu, Z., Zhang, D., et al. (2020). Effect of non-invasive brain stimulation on neuropathic pain following spinal cord injury: a systematic review and meta-analysis. *Medicine (Baltimore)* 99:e21507. doi: 10.1097/MD.0000000000021507

Shimizu, T., Hosomi, K., Maruo, T., Goto, Y., Yokoe, M., Kageyama, Y., et al. (2017). Efficacy of deep rTMS for neuropathic pain in the lower limb: a randomized, double-blind crossover trial of an H-coil and figure-8 coil. *J. Neurosurg.* 127, 1172–1180. doi: 10.3171/2016.9.JNS16815

Singer, J., Conigliaro, A., Spina, E., Law, S. W., and Levine, S. R. (2017). Central poststroke pain: a systematic review. *Int. J. Stroke* 12, 343–355. doi: 10.1177/1747493017701149

Stokes, M. G., Chambers, C. D., Gould, I. C., Henderson, T. R., Janko, N. E., Allen, N. B., et al. (2005). Simple metric for scaling motor threshold based on scalp-cortex distance: application to studies using transcranial magnetic stimulation. *J. Neurophysiol.* 94, 4520–4527. doi: 10.1152/jn.00067.2005

Sun, X., Long, H., Zhao, C., Duan, Q., Zhu, H., Chen, C., et al. (2019). Analgesia-enhancing effects of repetitive transcranial magnetic stimulation on neuropathic pain after spinal cord injury:An fNIRS study. *Restor. Neurol. Neurosci.* 37, 497–507. doi: 10.3233/RNN-190934

Yang, S., and Chang, M. C. (2020). Effect of repetitive transcranial magnetic stimulation on pain management: a systematic narrative review. *Front. Neurol.* 11:114. doi: 10.3389/fneur.2020.00114

Yilmaz, B., Kesikburun, S., Yasar, E., and Tan, A. K. (2014). The effect of repetitive transcranial magnetic stimulation on refractory neuropathic pain in spinal cord injury. *J. Spinal Cord Med.* 37, 397–400. doi: 10.1179/2045772313Y.0000000172

Zhang, K. L., Yuan, H., Wu, F. F., Pu, X. Y., Liu, B. Z., Li, Z., et al. (2021). Analgesic effect of noninvasive brain stimulation for neuropathic pain patients: a systematic review. *Pain Ther.* 10, 315–332. doi: 10.1007/s40122-021-00252-1

Conflict of Interest: The authors declare that the research was conducted in the absence of any commercial or financial relationships that could be construed as a potential conflict of interest.

Publisher's Note: All claims expressed in this article are solely those of the authors and do not necessarily represent those of their affiliated organizations, or those of the publisher, the editors and the reviewers. Any product that may be evaluated in this article, or claim that may be made by its manufacturer, is not guaranteed or endorsed by the publisher.

frontiers in Human Neuroscience

SYSTEMATIC REVIEW
published: 10 December 2021
doi: 10.3389/fnhum.2021.782305

Effects of Combining Online Anodal Transcranial Direct Current Stimulation and Gait Training in Stroke Patients: A Systematic Review and Meta-Analysis

Tsubasa Mitsutake[1], Takeshi Imura[2], Tomonari Hori[3], Maiko Sakamoto[4] and Ryo Tanaka[5]*

[1] Department of Physical Therapy, Fukuoka International University of Health and Welfare, Fukuoka, Japan, [2] Department of Rehabilitation, Faculty of Health Sciences, Hiroshima Cosmopolitan University, Hiroshima, Japan, [3] Department of Rehabilitation, Fukuyama Rehabilitation Hospital, Hiroshima, Japan, [4] Education and Research Centre for Community Medicine, Faculty of Medicine, Saga University, Saga, Japan, [5] Graduate School of Humanities and Social Sciences, Hiroshima University, Hiroshima, Japan

OPEN ACCESS

Edited by:
Ken-Ichiro Tsutsui, Tohoku University, Japan

Reviewed by:
Camila Bonin Pinto, Northwestern University, United States
Faddi Ghassan Saleh Velez, Spaulding Rehabilitation Hospital, United States

***Correspondence:**
Tsubasa Mitsutake
mitutuba1012@gmail.com

Specialty section:
This article was submitted to Brain Imaging and Stimulation, a section of the journal Frontiers in Human Neuroscience

Received: *24 September 2021*
Accepted: *25 November 2021*
Published: *10 December 2021*

Citation:
Mitsutake T, Imura T, Hori T, Sakamoto M and Tanaka R (2021) Effects of Combining Online Anodal Transcranial Direct Current Stimulation and Gait Training in Stroke Patients: A Systematic Review and Meta-Analysis. Front. Hum. Neurosci. 15:782305. doi: 10.3389/fnhum.2021.782305

Objective: Combining transcranial direct current stimulation (tDCS) and repetitive gait training may be effective for gait performance recovery after stroke; however, the timing of stimulation to obtain the best outcomes remains unclear. We performed a systematic review and meta-analysis to establish evidence for changes in gait performance between online stimulation (tDCS and repetitive gait training simultaneously) and offline stimulation (gait training after tDCS).

Methods: We comprehensively searched the electronic databases Medline, Cochrane Central Register of Controlled Trials, Physiotherapy Evidence Database, and Cumulative Index to Nursing and Allied Health Literature, and included studies that combined cases of anodal tDCS with motor-related areas of the lower limbs and gait training. Nine studies fulfilled the inclusion criteria and were included in the systematic review, of which six were included in the meta-analysis.

Result: The pooled effect estimate showed that anodal tDCS significantly improved the 10-m walking test ($p = 0.04$; $I^2 = 0\%$) and 6-min walking test ($p = 0.001$; $I^2 = 0\%$) in online stimulation compared to sham tDCS.

Conclusion: Our findings suggested that simultaneous interventions may effectively improve walking ability. However, we cannot draw definitive conclusions because of the small sample size. More high-quality studies are needed on the effects of online stimulation, including various stimulation parameters.

Keywords: transcranial direct current stimulation, gait training, combination, online stimulation, stroke

INTRODUCTION

Stroke often causes walking problems due to sensorimotor dysfunction, such as motor paresis, decreased muscle strength, and impaired proprioceptive capabilities. Patients with stroke may experience a decreased quality of life (QOL) and limited activities of daily living because of disease-related walking dysfunction. Walking speed is the most common measure of walking ability and is one of the predictors of independence, mortality, functional status at home and in the community, and QOL (Wonsetler and Bowden, 2017). Therefore, improving mobility, including the walking speed, is an important goal for patients with stroke.

Regarding gait rehabilitation methods, repetitive gait training has presented beneficial effects in improving mobility. Body weight-supported treadmill training (BWSTT) has the potential to facilitate symmetrical gait training and promote cortical activities after stroke (Oh et al., 2021). In addition, robot-assisted gait training (RAGT) is effective for improving neuroplastic and clinical outcomes in individuals with hemiparetic stroke (Kim et al., 2020). A systematic review of the current guidelines showed that RAGT is generally recommended to improve lower limb motor function, including gait and strength (Calabró et al., 2021). These repetitive walking exercises are expected to induce cortical motor plasticity and improve mobility.

Transcranial direct current stimulation (tDCS) is another intervention that has the potential to greatly assist stroke rehabilitation (Hordacre et al., 2018; Klamroth-Marganska, 2018). TDCS is a non-invasive brain stimulation (NIBS) method that may promote motor function in patients with stroke by modulating cortical excitability (Nitsche and Paulus, 2001; Liew et al., 2014). Previous studies have reported that applying anodal tDCS over the lower extremity area of the primary motor cortex significantly improves force steadiness (Montenegro et al., 2016) as well as motor cortex excitability and function (Chang et al., 2015). The safety and effectiveness of tDCS technology have been proven in the treatment of various conditions (Lefaucheur et al., 2017).

Given the independent effectiveness of tDCS and repetitive gait training, the combination of these methods may be more effective than using them separately for gait performance recovery. Previous studies on brain function have showed that brain activity during walking increased bilaterally in the medial primary sensory and supplementary motor cortices (Miyai et al., 2001). Moreover, anodal stimulation of the primary motor cortex with tDCS increased cortical excitability (Nitsche and Paulus, 2001). Thus, gait training with simultaneous tDCS may improve gait performance *via* the re-enforced learning of neural networks, including the primary motor cortex.

Previous systematic reviews have showed that NIBS combined with other treatments improved various symptoms (Volz et al., 2012; Salazar et al., 2018; Cardenas-Rojas et al., 2020). Among them, the combination of tDCS and other therapies significantly improved gait performance in patients post-stroke (Vaz et al., 2019; Navarro-López et al., 2021). However, another review reported that there were no conclusive results supporting the role of tDCS in enhancing the effect of gait rehabilitation among patients with neurological disorders (de Paz et al., 2019). Improving balance performance by tDCS may limit the effects of tDCS on walking speed and/or walking endurance (Tien et al., 2020). The main limitation of previous tDCS reviews is the lack of uniformity in parameters, application patterns, and evaluation variables (de Paz et al., 2019; Santos et al., 2020). A potentially important aspect of the intervention method of combining tDCS with gait training is whether the treatments are applied simultaneously or after the stimulation. Previous studies have demonstrated an increase in corticospinal tract excitability by adapting robotic training after tDCS (Giacobbe et al., 2013; Powell et al., 2016). In contrast, another study showed that tDCS to bilateral primary motor areas while performing RAGT was more effective for the recovery of lower limb function in patients with stroke (Naro et al., 2021). Thus, it remains unclear which application timing of tDCS is optimal. Such detailed analysis of stimulus timing is novel in tDCS studies and may contribute to the establishment of effective intervention methods.

The objectives of this systematic review were to investigate the effects of the combination of anodal tDCS on motor-related areas and repetitive gait training, including BWSTT and RAGT on walking ability, and examine the differences between online stimulation, in which tDCS and repetitive gait training are performed simultaneously, and offline stimulation, in which tDCS is followed by gait training.

MATERIALS AND METHODS

A systematic review of the literature was performed according to the Preferred Reporting Items for Systematic reviews and Meta-Analysis Protocol (PRISMA) guidelines (Page et al., 2021). This review was registered with PROSPERO (ID: CRD42021247018).

Eligibility Criteria

Studies were included in this systematic review if they met the following criteria: (1) the patients were diagnosed with hemorrhagic or ischemic stroke with unilateral hemiplegia; (2) the patients could walk without support and maintain their own body weight or balance; (3) a combination of anodal tDCS on the motor-related areas and repetitive gait training was performed; (4) gait performance outcomes were assessed; (5) the study was a randomized controlled trial (RCT), crossover RCT, or high-quality comparative studies; (6) the study was a clinical trial with at least seven sessions per week; and (7) the article was written in English.

Studies that met the following criteria were excluded: (1) the study included patients with subarachnoid hemorrhages; (2) the study included patients with a higher brain dysfunction, such as unilateral spatial neglect, that may affect gait performance; (3) the study was a meta-analysis, review, or case study; or (4) the study had insufficient data to calculate the effect size for quantitative analysis.

Information Sources

The electronic databases Medline, Cochrane Central Register of Controlled Trials, Physiotherapy Evidence Database (PEDro),

and Cumulative Index to Nursing and Allied Health Literature were comprehensively searched. The searches were performed on March 19, 2021.

Search Strategy

The search terms of "patient," "intervention," and "outcome" were combined with the "AND" operator. "Patient" was defined as patients with stroke. "Intervention" was defined as a combination of tDCS and gait training. "Outcome" was defined as gait performance. For each concept, we combined synonyms and Medical Subject Headings terms with the "OR" operator. There were no limits on the dates. An example of the search strategy used in the Medline database is provided in **Supplementary Table 1**.

Study Selection

The articles identified through database searching were summarized into spreadsheets that were created using Microsoft Excel 2019. After duplicates were removed, two authors (TM and TI) independently screened each article based on the titles and abstracts using predetermined eligibility criteria in order to determine relevant manuscripts for full-text review. Subsequently, full-text copies of articles that were not excluded based on the titles or abstracts were retrieved, and the inclusion and exclusion criteria were reapplied to these studies to determine their suitability for the final inclusion. Any disagreements at the article screening and selection stages were resolved through discussion, and decisions were made by a third party (RT) to reach a consensus.

Data Collection Process

We prepared and used simple predesigned spreadsheets that were created using Microsoft Excel 2019 to extract data on participants, interventions, outcome measurements, and results. Two authors (TM and TI) discussed and decided whether the outcomes reported in the extracted studies corresponded to kinetic or kinematic measurements.

Data Items

The following outcome measures were chosen for our meta-analysis: (1) 10-m walking test (10 MWT), which examines the walking speed; (2) 6-min walking test (6 MWT), which examines the walking endurance; (3) Functional Ambulatory Category (FAC), which examines the walking independence and functional ambulation; (4) walking cadence (the number of steps per minute), which examines the quality of walking ability; and (5) timed up and go test (TUGT), which examines functional mobility.

Risk of Bias Evaluation in Individual Studies

To evaluate the risk of bias in each trial (de Morton, 2009), two researchers (TM and HT) independently applied the PEDro scale (Verhagen et al., 1998). Any differences in items were resolved through a discussion and decided by the agreement of a third party (TI). Studies were considered to be of high and moderate quality when the PEDro score was $\geq$6 and 4 or 5, respectively (Maher et al., 2003; Wallis and Taylor, 2011). Studies with scores $<$4 were excluded from further analysis (Van Peppen et al., 2004; Veerbeek et al., 2014; Kwakkel et al., 2015).

Effect Measures

Regarding continuous outcomes, if the unit of measurements was consistent across trials, the results were presented as the weighted mean difference (MD) with 95% confidence intervals (95% CIs). If the outcome did not use the same units across studies, we used the standardized mean difference (SMD) instead of the MD.

Synthesis Methods

All statistical comparisons were performed using Review Manager, version 5.4 (Cochrane Collaboration, London, United Kingdom). The included studies were selected to perform anodal tDCS to the motor-related areas of the lower limbs, as well as repetitive gait training and sham stimulation in the intervention and control groups, respectively. In addition, we included intervention studies with two or more of the same assessment methods. This meta-analysis used the mean and standard deviation of the difference in the values obtained pre- and post-intervention. When the means and standard deviations were not provided in the manuscript, we used the post-intervention values. Moreover, the 10 MWT evaluated in time (s) was transformed into a negative value to be consistent with the values evaluated in speed (m/s). This meta-analysis excluded those studies that measured walking speed by means other than the 10 MWT to quantitatively assess walking ability.

We analyzed the effect of anodal tDCS on gait performance, followed by a subgroup analysis with online or offline stimuli. Subgroup meta-analysis was possible when at least two studies with a similar design were available for each stimulus group. A random-effects model was used to account for differences in effect sizes between the studies (Borenstein et al., 2010). Statistical heterogeneity was assessed using the I^2 statistic. I^2 values $>$25 and 50% were considered indicative of moderate and high heterogeneity, respectively. Statistical significance was set at $p < 0.05$.

Certainty Assessment

The quality of evidence for each evaluation parameter was assessed using the Grading of Recommendations Assessment, Development and Evaluation (GRADE) system (Guyatt et al., 2011). The GRADE system was implemented when there were at least two applicable outcomes. The quality of evidence was assessed as "very low," "low," "moderate," or "high" based on certain criteria. Factors downgrading the quality (risk of bias, inconsistency, indirectness, impression, and publication bias) or upgrading the quality (large effect, plausible confounding, and dose-response) were evaluated (Yamakawa et al., 2015).

RESULTS

Search Selection

The combined database search identified 785 trials (**Figure 1**). After adjusting for duplicates, 554 trials were included in the analyses, of which 518 did not meet the selection criteria on

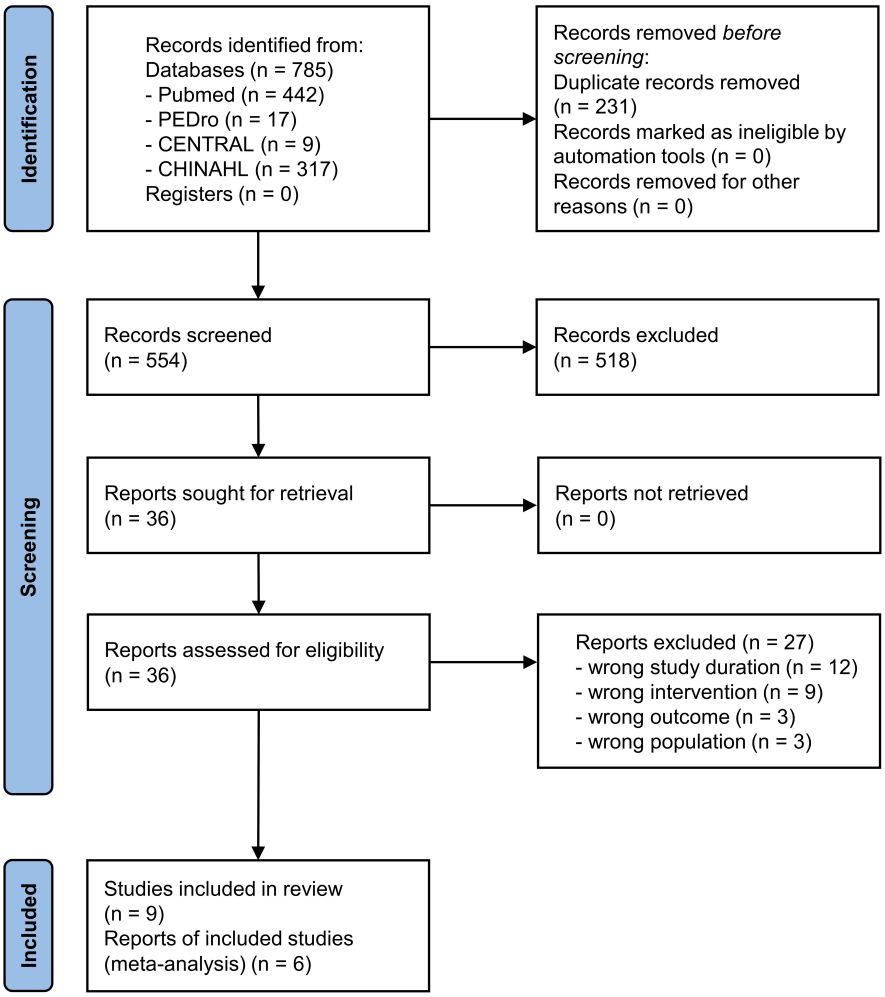

FIGURE 1 | Flow diagram of the study selection process.

reviewing the article titles and abstracts. The complete text of the remaining 36 studies were examined in detail. Twenty-seven studies did not meet the inclusion criteria. Finally, nine studies fulfilled the inclusion criteria and were included in the systematic review (Geroin et al., 2011; Picelli et al., 2015, 2018; Leon et al., 2017; Seo et al., 2017; Manji et al., 2018; Madhavan et al., 2020; Mitsutake et al., 2021; Naro et al., 2021). Then, six of these studies were included in the meta-analysis (Geroin et al., 2011; Picelli et al., 2015; Seo et al., 2017; Manji et al., 2018; Madhavan et al., 2020; Mitsutake et al., 2021). The critical information of the six studies are summarized in **Table 1**, including the study population, tDCS parameters, intervention methods, and main outcomes.

Study Characteristics

Six RCTs (Geroin et al., 2011; Picelli et al., 2015, 2018; Seo et al., 2017; Madhavan et al., 2020; Mitsutake et al., 2021), one crossover trial (Manji et al., 2018), one active-control article (Leon et al., 2017), and one retrospective clinical trial (Naro et al., 2021) were included in this study. The sample sizes ranged from 20 (Picelli et al., 2015, 2018) to 41 (Madhavan et al., 2020), and the participants were divided into the intervention and control groups. The average age of the participants of nine studies ranged from 49 (Leon et al., 2017) to 74.9 years (Mitsutake et al., 2021). In addition, the stroke phase at baseline ranged from 37.1 days (Mitsutake et al., 2021) to 152.5 months (Seo et al., 2017) after onset. Seven studies that reported results from the 10 MWT (Geroin et al., 2011; Leon et al., 2017; Seo et al., 2017; Manji et al., 2018; Madhavan et al., 2020; Mitsutake et al., 2021; Naro et al., 2021), six studies reported results from the 6 MWT (Geroin et al., 2011; Picelli et al., 2015, 2018; Seo et al., 2017; Madhavan et al., 2020; Naro et al., 2021), six studies reported FAC (Geroin et al., 2011; Picelli et al., 2015, 2018; Leon et al., 2017; Seo et al., 2017; Naro et al., 2021), three studies reported walking cadence (Geroin et al., 2011; Picelli et al., 2015, 2018), and two studies reported results from the TUGT (Manji et al., 2018; Madhavan et al., 2020).

The tDCS intensity was tested at 1.0, 1.5, or 2.0 mA (two, one, and six studies, respectively). The electrode size was 12.5, 25, or 35 cm^2 (two, one, and six studies, respectively). Regarding the electrode placement locations, seven studies applied the anodal

TABLE 1 | Summary of included studies.

Study (Author, Journal, Year)	Study design	Size N (IG/CG)	Age Mean ± SD (IG/CG)	Sex M/F	Time since stroke	Intervention	Area of stimulation	Current density	Sessions; intervals	Stimulation timing	Order of application	Outcome measures
Naro et al., 2021	Retrospective	IG: 9 OG1: 15 OG2: 13	IG: 68 ± 4 OG1: 66 ± 5 OG2: 72 ± 4	IG: 4/5 OG1: 6/9 OG2: 5/8	IG: 10 ± 2 m OG1: 11 ± 3 m OG2: 8 ± 2 m	IG: dstDCS + RAGT (on-RAGT) OG1: dstDCS + RAGT (post-RAGT) OG2: dstDCS + RAGT (pre-RAGT)	A; PMA-affected side (C3/4) C; PMA-non affected side (C3/4)	2.0 mA 35 cm^2 0.057 mA/cm^2	48 s; 8 weeks	ONLINE	dstDCS (first 10 min) + RAGT (50 min)	10 MWT; 6 MWT; FAC; MI; Tinetti scale; FIM; MEP
Picelli et al., 2018	RCT	IG: 10 OG: 10	IG: 62.6 ± 8.3 OG: 62.8 ± 11.8	IG: 7/3 OG: 6/4	IG: 67.1 ± 46.8 m OG: 51.9 ± 41.2 m	IG: Anodal tDCS + tsDCS + RAGT OG: Cathodal tcDCS + tsDCS + RAGT	IG: A; PMA-affected LE (Cz), C; OA-CL CG: A; cerebellar hemisphere (O1/2), C; buccinator muscle-IL	2.0 mA 12.56 cm^2 0.159 mA/cm^2	10 s; 2 weeks	ONLINE	tDCS (20 min) + RAGT (20 min)	6 MWT; FAC; MI; Gait analysis (cadence); ashworth scale
Picelli et al., 2015	RCT	IG: 10 CG: 10 OG: 10	IG: 62.8 ± 11.8 CG: 61.0 ± 7.2 OG: 64.8 ± 6.0	IG: 7/3 CG: 8/2 OG: 7/3	IG: 51.9 ± 41.1 m CG: 54.8 ± 32.9 m OG: 61.3 ± 29.3 m	IG: Anodal tDCS + tsDCS + RAGT CG: Sham tDCS + tsDCS + RAGT OG: Anodal tDCS + sham tsDCS + RAGT	A; PMA-affected side (C3/4) C; OA-CL	2.0 mA 35 cm^2 0.057 mA/cm^2	10 s; 2 weeks	ONLINE	tDCS (20min) + RAGT (20 min)	6 MWT; FAC; MI; Gait analysis (cadence); ashworth scale
Geroin et al., 2011	RCT	IG: 10 CG: 10 OG: 10	IG: 63.6 ± 6.7 CG: 63.3 ± 6.4 OG: 61.1 ± 6.3	IG: 8/2 CG: 6/4 OG: 9/1	IG: 25.7 ± 6.0 m CG: 26.7 ± 5.1 m OG: 26.9 ± 5.8 m	IG: Anodal tDCS + RAGT CG: Sham tDCS + RAGT OG: Walking exercises	A; PMA-affected LE C; SOA-CL	1.5 mA 35 cm^2 0.043 mA/cm^2	10 s; 2 weeks	ONLINE	tDCS (7 min) + RAGT (20 min)	10 MWT; 6MWT; FAC; MI; Gait analysis (cadence); RMI
Madhavan et al., 2020	RCT	IG: 21 CG: 20 OG1: 20 OG2: 20	IG: 58 ± 11 CG: 58 ± 10 OG1: 60 ± 9 OG2: 59 ± 9	IG: 14/7 CG: 11/9 OG1: 15/5 OG2: 15/5	IG: 4.3 ± 3.6 y CG: 6.1 ± 4.2 y OG1: 5.6 ± 3.6 y OG2: 5.9 ± 5.6 y	IG: Anodal tDCS + HISTT CG: Sham tDCS + HISTT OG1: AMT + HISTT OG2: tDCS + AMT + HISTT	A; PMA-affected LE C; SOA-CL	1.0 mA 12.5 cm^2 0.080 mA/cm^2	12 s; 4 weeks	OFFLINE	tDCS (15 min) → HISTT (40 min)	10 MWT; 6 MWT; BBS; TUGT; mini-BESTest; ABC; FMA; SIS; MEP
Manji et al., 2018	Crossover	IG: 15 CG: 15	IG: 62.2 ± 10.1 CG: 63.7 ± 11.0	IG: 10/5 CG: 11/4	IG: 134.5 ± 55.7 d CG: 149.7 ± 24.2 d	IG: Anodal tDCS + BWSTT CG: Sham tDCS + BWSTT	A; SMA (3.5 cm anterior to Cz) C; EOC	1.0 mA 25 cm^2 0.040 mA/cm^2	7 s; 1 week	ONLINE	tDCS (20 min) + BWSTT (20 min)	10 MWT; TUGT; FMA; POMA; TCT
Seo et al., 2017	RCT	IG: 11 CG: 10	IG: 61.1 ± 8.9 CG: 62.9 ± 8.9	IG: 9/2 CG: 7/3	IG: 75.5 ± 83.4 m CG: 152.5 ± 122.8 m	IG: Anodal tDCS + RAGT CG: Sham tDCS + RAGT	A; PMA-affected LE C; SOA-CL	2.0 mA 35 cm^2 0.057 mA/cm^2	10 s; 2 weeks	OFFLINE	tDCS (20 min) → RAGT (45 min)	10 MWT; 6 MWT; FAC; BBS; FMA; MRCS; MEP

(Continued)

TABLE 1 | (Continued)

Study (Author, Journal, Year)	Study design	Size N (IG/CG)	Age Mean ± SD (IG/CG)	Sex M/F	Time since stroke	Intervention	Area of stimulation	Current density	Sessions; intervals	Stimulation timing	Order of application	Outcome measures
Leon et al., 2017	Active control	IG: 10 CG: 23 OG: 17	IG: 49 ± 9 CG: 49 ± 11 OG: 47 ± 11	IG: 6/4 CG: 17/6 OG: 12/5	IG: 53 ± 25 d CG: 64 ± 33 d OG: 56 ± 38 d	IG: Anodal tDCS + RAGT CG: Sham tDCS + RAGT OG: Anodal tDCS (C3/4) + RAGT	A; Cz C; SOA-Rt	2.0 mA 35 cm^2 0.057 mA/cm^2	20 s; 4 weeks	ONLINE	tDCS (first 20 min) + RAGT (30 – 45 min)	10 MWT; FAC
Mitsutake et al., 2021	RCT	IG: 11 CG: 12 OG: 11	IG: 74.9 ± 9.2 CG: 67.3 ± 12.1 OG: 75.6 ± 11.0	IG: 6/5 CG: 9/3 OG: 4/7	IG: 44.6 ± 31.7 d CG: 37.1 ± 27.3 d OG: 34.6 ± 17.8 d	IG: Anodal tDCS + FES CG: Sham tDCS + FES OG: Anodal tDCS	A; PMA-affected LE C; SOA-CL	2.0 mA 35 cm^2 0.057 mA/cm^2	7 s; 1 week	ONLINE	tDCS (20 min) + FES (20 min)	10 MWT; Gait analysis (acceleration parameters)

RCT, randomized controlled trial; IG, intervention group; CG, control group; OG, other group; tDCS, transcranial direct current stimulation; dstDCS, dual-site transcranial direct current stimulation; tcDCS, transcranial cerebellar direct current stimulation; tsDCS transcutaneous spinal direct current stimulation; RAGT, robot-assisted gait training; HISTT, high-intensity speed-based treadmill training; AMT, ankle motor tracking; BWSTT, body weight-supported treadmill training; FES, functional electrical stimulation; A, anode; C, cathode; PMA, primary motor area; LE, lower extremity; OA, orbital area; CL, contralateral side; iL, ipsilateral side; SOA, supra-orbital area; SMA, supplementary motor area; EOC, exterior occipital crest; 10 MWT, 10-m walking test; 6 MWT, 6-min walking test; FAC, functional ambulatory category; MI, mobility index; FIM, functional independence measure; MEP, motor evoked potential; RMI, rivermead mobility index; BBS, berg balance scale; TUG, timed up and go test; mini-BESTest, mini-balance evaluation systems test; FMA, fugl-meyer assessment; ABC, activities-specific balance confidence scale; SIS, stroke impact scale; POMA, performance-oriented mobility assessment; TIS, trunk controltest; MRCS, medical research council scale.

and cathodal electrodes in the motor-related area, including the primary motor area, and the orbital area, respectively (Geroin et al., 2011; Picelli et al., 2015, 2018; Leon et al., 2017; Seo et al., 2017; Madhavan et al., 2020; Mitsutake et al., 2021), while one study applied the anodal electrodes in the supplementary motor area and the cathodal electrodes in the exterior occipital crest (Manji et al., 2018). Another study performed dual-site tDCS with electrodes placed in the bilateral primary motor areas (Naro et al., 2021). Regarding the tDCS intervention methods in the control group, seven studies tested the combined effects of sham stimulation and repetitive walking training (Geroin et al., 2011; Picelli et al., 2015; Leon et al., 2017; Seo et al., 2017; Manji et al., 2018; Madhavan et al., 2020; Mitsutake et al., 2021), and one study compared anodal tDCS performed in the primary motor area with cathodal tDCS performed in the cerebellar hemispheres (tcDCS; Picelli et al., 2018). Moreover, one study compared the tDCS while performing walking training to that followed by walking training. The results showed that simultaneous intervention significantly improved walking endurance compared to gait training after tDCS (Picelli et al., 2018). Regarding the non-cortical tDCS intervention, two studies performed the tDCS combined with cathodal transcutaneous spinal direct current stimulation (tsDCS; Picelli et al., 2015, 2018). The combination of cathodal tcDCS and cathodal tsDCS during RAGT significantly improved walking endurance compared to the combination of anodal tDCS and cathodal tsDCS during RAGT (Picelli et al., 2018).

Concerning the repetitive walking training methods, six, one, one, and one studies performed RAGT (Geroin et al., 2011; Picelli et al., 2015, 2018; Leon et al., 2017; Seo et al., 2017; Naro et al., 2021), BWSTT (Manji et al., 2018), high-intensity speed-based treadmill training (HISTT; Madhavan et al., 2020), and functional electrical stimulation (FES; Mitsutake et al., 2021), respectively.

Risk of Bias in Studies

The application of the PEDro scale revealed that all studies (Geroin et al., 2011; Picelli et al., 2015, 2018; Leon et al., 2017; Seo et al., 2017; Manji et al., 2018; Madhavan et al., 2020; Mitsutake et al., 2021; Naro et al., 2021) had good methodological quality and met the evaluation criteria with scores $\geq$6 deemed to contain good scientific evidence (**Table 2**).

Results of Individual Studies and Syntheses

Six studies were divided broadly into two research categories: (1) online stimulation, in which anodal tDCS and repetitive gait training were performed simultaneously; and (2) offline stimulation, in which anodal tDCS was followed by gait training. Four and two studies used online (Geroin et al., 2011; Picelli et al., 2015; Manji et al., 2018; Mitsutake et al., 2021) and offline stimulation (Seo et al., 2017; Madhavan et al., 2020), respectively.

Five studies involving 135 patients were included in the meta-analysis of 10 MWT, of which three and two involved online and offline stimulation, respectively. The test for subgroup differences showed no statistically significant subgroup effect (p = 0.26), suggesting that stimulation timing did not modify the effect of

TABLE 2 | Methodological quality of included studies in accordance with the PEDro scores.

Study	1*	2	3	4	5	6	7	8	9	10	11	Total
Naro et al., 2021	✓			✓			✓	✓	✓	✓	✓	6/10
Picelli et al., 2018	✓	✓	✓	✓	✓		✓	✓	✓	✓	✓	9/10
Picelli et al., 2015	✓	✓	✓	✓	✓		✓	✓	✓	✓	✓	9/10
Geroin et al., 2011	✓	✓		✓	✓		✓	✓	✓	✓	✓	8/10
Madhavan et al., 2020	✓	✓	✓	✓	✓		✓	✓	✓	✓	✓	9/10
Manji et al., 2018	✓	✓		✓	✓	✓		✓	✓	✓	✓	8/10
Seo et al., 2017	✓	✓	✓	✓	✓	✓	✓		✓	✓	✓	9/10
Leon et al., 2017	✓			✓	✓			✓	✓	✓	✓	6/10
Mitsutake et al., 2021	✓	✓	✓	✓	✓		✓	✓		✓	✓	8/10

**Not included in the total score. PEDro scores: 1, eligibility criteria specified; 2, participants randomly allocated to groups; 3, allocation concealed; 4, groups similar at baseline; 5, participants were blinded; 6, therapists were blinded; 7, assessors were blinded; 8, data available for more than 85% of participants; 9, participants received the treatment as allocated or intention-to-treat analysis was used; 10, statistical analyses were reported; 11, point measures and variability measures of data reported.*

anodal tDCS in comparison to sham tDCS. The pooled effect estimate favored anodal tDCS in online stimulation: anodal tDCS (n = 36) significantly increased the walking speed compared to sham tDCS (n = 37) (SMD: 0.48; 95% CI: 0.01–0.94; p = 0.04; I^2 = 0%, **Figure 2A**). In the offline stimulation, the effect of anodal tDCS (n = 32) was not significantly different from that of sham tDCS (n = 30) (SMD: 0.08; 95% CI: −0.41, 0.58; p = 0.74; I^2 = 0%, **Figure 2A**). After combining data from both online and offline stimulations, anodal tDCS (n = 68) did not significantly increase the walking speed compared to sham tDCS (n = 67) (SMD: 0.29; 95% CI: −0.05, 0.64; p = 0.09; I^2 = 0%).

Four studies involving 102 patients were included in the meta-analysis of the 6 MWT, of which two tested online stimulation and two tested offline stimulation. The test for subgroup differences showed a statistically significant subgroup effect (p = 0.002). The pooled effect estimate showed that anodal tDCS (n = 20) significantly increased walking distance in online stimulation compared to sham tDCS (n = 20) (SMD: 1.09; 95% CI: 0.42–1.77; p = 0.001; I^2 = 0%, **Figure 2B**). In the offline stimulation, the effect of anodal tDCS (n = 32) was not significantly different from that of sham tDCS (n = 30) (SMD: −0.25; 95% CI: −0.76–0.25; p = 0.32; I^2 = 0%, **Figure 2B**). On combining data from both online and offline stimulations, anodal tDCS (n = 52) did not significantly increase walking distance compared to the sham tDCS (n = 50), and the studies presented high heterogeneity (SMD: 0.40; 95% CI: −0.38–1.18; p = 0.32; I^2 = 72%).

Subgroup analysis was not performed for FAC, walking cadence, or TUGT because of the small number of included studies. Two studies involving 41 patients were included in the meta-analysis and showed no significant difference in FAC in the anodal tDCS compared to the sham tDCS (SMD: 0.00; 95% CI: −1.82–1.81; p = 1.00; I^2 = 87%, **Figure 3A**).

Two studies involving 40 patients were included in the meta-analysis and showed no significant difference in walking cadence in the anodal tDCS compared to the sham tDCS (SMD: 0.67; 95% CI: −0.60–1.93; p = 0.30; I^2 = 73%, **Figure 3B**).

Two studies involving 71 patients were included in the meta-analysis and showed no significant difference in TUGT in anodal tDCS compared to that in sham tDCS (SMD: 0.26; 95% CI: −0.20–0.73; p = 0.27; I^2 = 0%, **Figure 3C**).

Certainty of Evidence

When the quality of evidence was evaluated using the GRADE system, all parameters were rated from very low to moderate, with a risk of bias, inconsistency, and impression as factors that reduced quality. The 6 MWT was rated as "very low" for the combined online and offline data, but was rated as "moderate" for each item with inconsistencies indicated as "not serious" (**Table 3**).

DISCUSSION

This systematic review aimed to investigate the effects of the combination of anodal tDCS on motor-related areas and repetitive gait training, including BWSTT and RAGT, on walking ability. Moreover, it aimed to examine the differences between online stimulation, in which tDCS and repetitive gait training are performed simultaneously, and offline stimulation, in which tDCS is followed by gait training.

Of the six studies that met the inclusion criteria for meta-analysis, four and two were classified as online and offline stimulation studies, respectively. The quality of the evidence, including the risk of bias described in these studies, was generally high, as assessed by the PEDro scale and GRADE criteria.

The results of the subgroup analysis showed that online stimulation significantly increased the distance in the 6 MWT compared to offline stimulation. Moreover, anodal tDCS significantly improved the results of the 10 MWT and 6 MWT compared to sham tDCS. The 10 MWT and 6 MWT are general indices of walking ability. Decreased cardiovascular fitness in stroke survivors may negatively impact their social life and QOL (Mayo et al., 1999). The walking speed of patients post-stroke is significantly related to walking performance, QOL, social participation, and even the ability to return to work (Suttiwong et al., 2018; Grau-Pellicer et al., 2019; Jarvis et al., 2019). The current meta-analysis showed that online stimulation may have greater effects on walking performance than offline stimulation. Interestingly, Naro et al. (2021) investigated the efficacy and safety of dual-site tDCS in the bilateral primary motor area timed with RAGT in patients with stroke. They showed that simultaneous intervention of tDCS and RAGT

TABLE 3 | Summary of GRADE findings.

		Certainty assessment							No. of patients		Certainty	Importance
Outcomes	**Stimulation timing**	**No. of studies**	**Study design**	**Risk of bias**	**Inconsistency**	**Indirectness**	**Imprecision**	**Other considerations**	**Intervention group**	**Control group**		
10 MWT	Online	3	RCT	Serious[a]	Not serious	Not serious	Not serious	None	36	37	⊕⊕⊕○ Moderate	Important
	Offline	2	RCT	Not serious	Not serious	Not serious	Serious[f]	None	32	30	⊕⊕⊕○ Moderate	Important
	Total	5	RCT	Serious[a]	Not serious	Not serious	Serious[f]	None	68	67	⊕⊕○○ Low	Important
6 MWT	Online	2	RCT	Serious[b]	Not serious	Not serious	Not serious	None	20	20	⊕⊕⊕○ Moderate	Important
	Offline	2	RCT	Not serious	Not serious	Not serious	Serious[f]	None	32	30	⊕⊕⊕○ Moderate	Important
	Total	4	RCT	Serious[b]	Serious[c]	Not serious	Serious[f]	None	52	50	⊕○○○ Very low	Important
FAC	Online	1	RCT	Serious[b]	N.A.	Not serious	Not serious	None	10	10	N.A.	Important
	Offline	1	RCT	Not serious	N.A.	Not serious	Not serisous	None	11	10	N.A.	Important
	Total	2	RCT	Serious[b]	Serious[d]	Not serious	Serious[f]	None	21	20	⊕○○○ Very low	Important
Gait analysis (cadence)	Online	2	RCT	Serious[b]	Serious[e]	Not serious	Serious[f]	None	20	20	⊕○○○ Very low	Important
	Offline	–	–	–	–	–	–	–	–	–	–	–
	Total	2	RCT	Serious[b]	Serious[e]	Not serious	Serious[f]	None	20	20	⊕○○○ Very low	Important
TUGT	Online	1	RCT	Serious[b]	N.A.	Not serious	Serious[f]	None	15	15	N.A.	Important
	Offline	1	RCT	Not serious	N.A.	Not serious	Serious[f]	None	21	20	N.A.	Important
	Total	2	RCT	Serious[b]	Not serious	Not serious	Serious[f]	None	36	35	⊕⊕○○ Low	Important

N.A.: Not applicable, 10 MWT: 10-m walking test, 6 MWT: 6-min walking test, FAC: Functional ambulation category, TUGT: Timed up and go test, RCT: Randomized controlled trial.
[a]Indicating three studies with moderate risk of bias, [b]Indicating one study with moderate risk of bias, [c]I^2 = 72%, [d]I^2 = 87%, [e]I^2 = 73%, and [f]Wide 95% confidence interval.

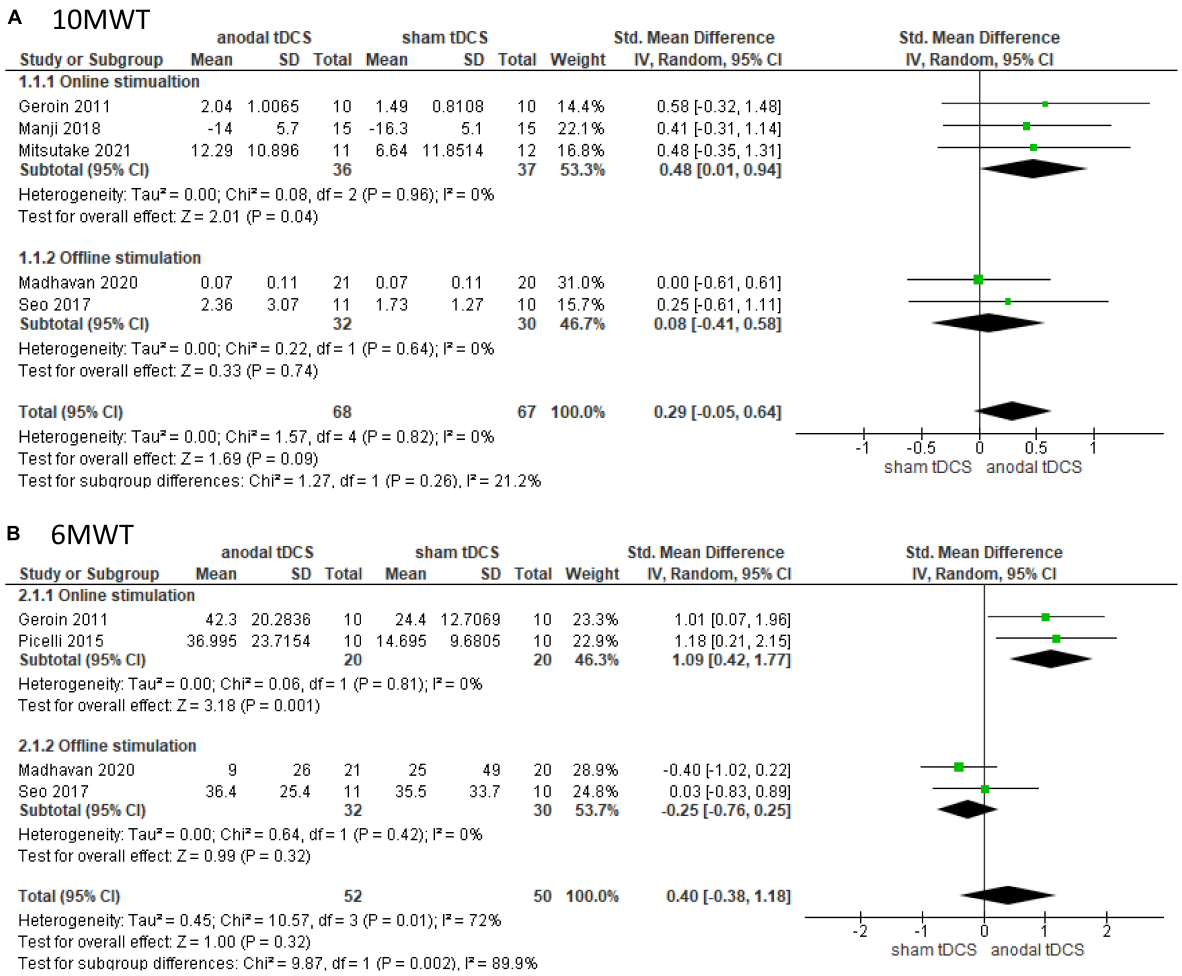

FIGURE 2 | Forrest plot displaying the standardized mean differences (SMD) between anodal and sham tDCSs. **(A)** Subgroup analysis based on stimulus timing for the 10-m walking test (10 MWT). **(B)** Subgroup analysis based on stimulus timing for the 6-min walking test (6 MWT).

significantly improved gait endurance compared to RAGT after tDCS (Naro et al., 2021). Given that the combination of tDCS and repetitive gait training facilitates neuroplasticity in patients post-stroke through aerobic effort (Mellow et al., 2020), walking training with simultaneous tDCS may improve gait performance *via* the re-enforced learning of neural networks, including the primary motor area.

The test for the overall effect showed no significant difference in all parameters, including the 10 MWT, 6 MWT, FAC, walking cadence, or TUGT. Madhavan et al. (Madhavan et al., 2020) reported that combining HISTT and tDCS to the primary motor cortex at a current intensity of 1.0 mA did not improve walking speed or secondary behavioral outcome measures. Geroin et al. (2011) also showed that tDCS to the primary motor cortex at a current intensity of 1.5 mA had no additional effect on RAGT. Interestingly, these studies (Geroin et al., 2011; Madhavan et al., 2020) tended to have shorter tDCS intervention times compared to those of the other studies (Picelli et al., 2015, 2018; Leon et al., 2017; Seo et al., 2017; Manji et al., 2018; Mitsutake et al., 2021). The motor cortex of the lower limb is located deep between both hemispheres and requires higher intensity stimulation compared to the upper limb (Jeffery et al., 2007). Applying anodal tDCS to the ipsilateral hemisphere may not help recovery in all individuals, and neuromodulation interventions should be individually tailored (Liew et al., 2014; Plow et al., 2016). These findings suggested that tDCS may decrease cortical excitability and limit the effects of priming (Wiethoff et al., 2014; Madhavan et al., 2016), indicating that the tDCS intervention should be carefully observed for stimulus timing, intensity, and duration.

Regarding tDCS to the cerebellum and spinal cord, Picelli et al. (2018) reported that the combination of cathodal tDCS and cathodal tsDCS during RAGT significantly improved walking endurance compared to the combination of anodal tDCS and cathodal tsDCS during RAGT. The cerebellum plays an important role in the coordinated movements of the limbs and posture. Cerebellar stimulation may increase inhibition of the cerebellar nuclei and decrease abnormal excitation of the cerebral cortex (Naro et al., 2017). Cathodal tsDCS has the potential to improve motor unit recruitment (Bocci et al., 2014).

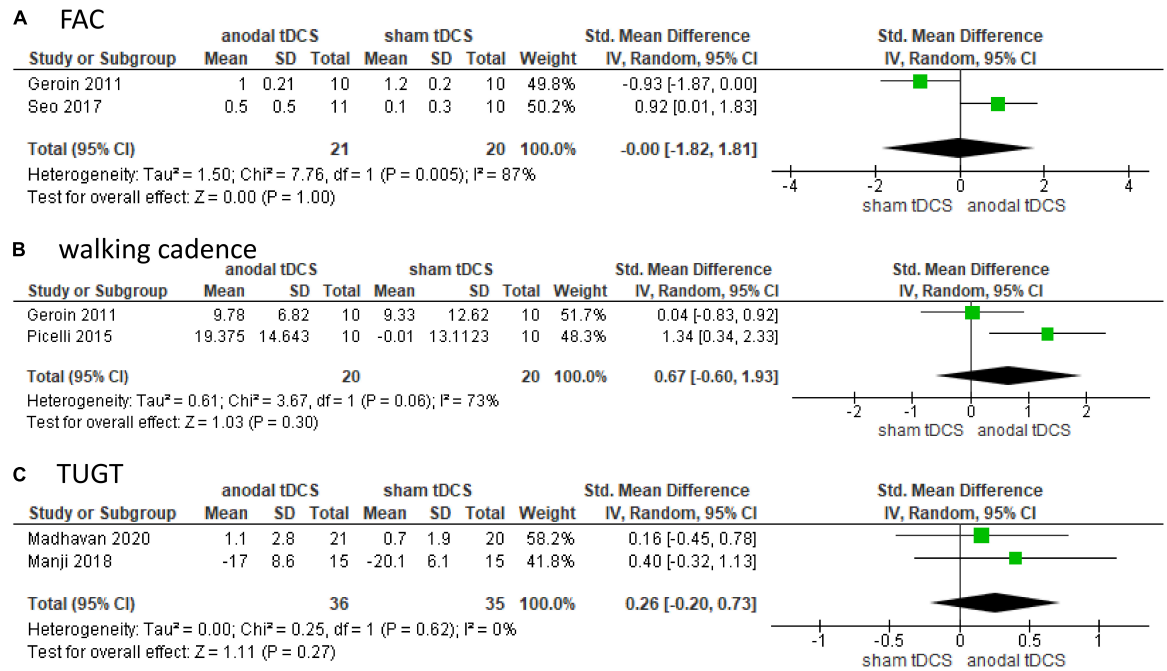

FIGURE 3 | Forrest plot displaying the standardized mean differences (SMD) between anodal and sham tDCSs. **(A)** Functional Ambulatory Category (FAC). **(B)** Walking cadence. **(C)** Timed up and go test (TUGT).

We applied the PEDro scale to evaluate the risks of bias and the GRADE system to evaluate the quality of evidence. The GRADE system is currently the most widely accepted approach for grading the quality of evidence in systematic reviews and clinical practice guidelines, and for grading the strength of recommendations in clinical practice guidelines. A major strength of this study was that online and offline stimulations were assessed separately, resulting in a relatively high quality of evidence. However, given the small number of included studies, further studies are required to establish a strong evidence base.

However, this review had several limitations. First, we might not have identified all the relevant studies, as our inclusion criteria consisted of selected keywords and databases. Second, we only included studies published in English; therefore, it was unavoidable to have certain language biases and limited generalizability of these studies. Third, this meta-analysis was limited to a small number of studies to rigorously compare anodal tDCS with sham tDCS on motor-related areas of the lower limbs. Therefore, this systematic review could not draw definitive conclusions because of the limited sample size. Future studies should increase the sample size and investigate whether the combination of online tDCS and gait training could improve the walking ability. Fourth, given that the included studies differed in time since stroke onset, intervention method, stimulation site, stimulation intensity, and repetitive gait training method, drawing conclusions from the present results requires careful interpretation.

Despite these limitations, to our knowledge, this is the first report that summarizes the evidence comparing and validating online and offline stimulations for patients post-stroke. Future studies with a larger sample size and a longer follow-up period should reproduce the results to establish appropriate stimulation parameters and gait interventions to improve gait performance in patients post-stroke.

In conclusion, this systematic review and meta-analysis suggests that simultaneous application of anodal tDCS to motor-related areas of the lower limbs while repetitive gait training appears to improve walking ability more effectively. We could demonstrate important factors in tDCS intervention methods; however, we could not make definitive conclusions regarding the effects of simultaneous tDCS and gait training intervention because of the small sample size. Therefore, more high-quality studies are needed on the effects of online stimulation, including various stimulation parameters.

DATA AVAILABILITY STATEMENT

The original contributions presented in the study are included in the article/**Supplementary Material**, further inquiries can be directed to the corresponding author.

AUTHOR CONTRIBUTIONS

TM: conceptualization and writing–original draft. TM and RT: supervision. TM, TI, and TH: literature search and acquisition of data. TM, TI, TH, and RT: literature collection and writing–review and editing. TM, TI, and RT: methodology and interpretation of data. All authors contributed to the article and approved the submitted version.

FUNDING

This work was supported by the Takeda Science Foundation and the Japan Society for the Promotion of Sciences (JSPS) KAKENHI grant number 20H04059.

SUPPLEMENTARY MATERIAL

The Supplementary Material for this article can be found online at: https://www.frontiersin.org/articles/10.3389/fnhum.2021.782305/full#supplementary-material

REFERENCES

Bocci, T., Vannini, B., Torzini, A., Mazzatenta, A., Vergari, M., Cogiamanian, F., et al. (2014). Cathodal transcutaneous spinal direct current stimulation (tsDCS) improves motor unit recruitment in healthy subjects. *Neurosci. Lett.* 578, 75–79. doi: 10.1016/j.neulet.2014.06.037

Borenstein, M., Hedges, L., Higgins, J., and Rothstein, H. (2010). A basic introduction to fixed-effect and random-effects models for meta-analysis. *Res. Synth. Methods* 1, 97–111. doi: 10.1002/jrsm.12

Calabró, R. S., Sorrentino, G., Cassio, A., Mazzoli, D., Andrenelli, E., Bizzarini, E., et al. (2021). Robotic-assisted gait rehabilitation following stroke: a systematic review of current guidelines and practical clinical recommendations. *Eur. J. Phys. Rehabil. Med.* 57, 460–471. doi: 10.23736/S1973-9087.21.06887-8

Cardenas-Rojas, A., Pacheco-Barrios, K., Giannoni-Luza, S., Rivera-Torrejon, O., and Fregni, F. (2020). Noninvasive brain stimulation combined with exercise in chronic pain: a systematic review and meta-analysis. *Expert. Rev. Neurother.* 20, 401–412. doi: 10.1080/14737175.2020.1738927

Chang, M. C., Kim, D. Y., and Park, D. H. (2015). Enhancement of cortical excitability and lower limb motor function in patients with stroke by transcranial direct current stimulation. *Brain Stimul.* 8, 561–566. doi: 10.1016/j.brs.2015.01.411

de Morton, N. A. (2009). The PEDro scale is a valid measure of the methodological quality of clinical trials: a demographic study. *Aust. J. Physiother.* 55, 129–133. doi: 10.1016/s0004-9514(09)70043-1

de Paz, R. H., Serrano-Muñoz, D., Pérez-Nombela, S., Bravo-Esteban, E., Avendaño-Coy, J., and Gómez-Soriano, J. (2019). Combining transcranial direct-current stimulation with gait training in patients with neurological disorders: a systematic review. *J. Neuroeng. Rehabil.* 16:114. doi: 10.1186/s12984-019-0591-z

Geroin, C., Picelli, A., Munari, D., Waldner, A., Tomelleri, C., and Smania, N. (2011). Combined transcranial direct current stimulation and robot-assisted gait training in patients with chronic stroke: a preliminary comparison. *Clin. Rehabil.* 25, 537–548. doi: 10.1177/0269215510389497

Giacobbe, V., Krebs, H. I., Volpe, B. T., Pascual-Leone, A., Rykman, A., Zeiarati, G., et al. (2013). Transcranial direct current stimulation (tDCS) and robotic practice in chronic stroke: the dimension of timing. *NeuroRehabilitation* 33, 49–56. doi: 10.3233/NRE-130927

Grau-Pellicer, M., Chamarro-Lusar, A., Medina-Casanovas, J., and Serdà Ferrer, B. C. (2019). Walking speed as a predictor of community mobility and quality of life after stroke. *Top. Stroke Rehabil.* 26, 349–358. doi: 10.1080/10749357.2019.1605751

Guyatt, G., Oxman, A. D., Akl, E. A., Kunz, R., Vist, G., Brozek, J., et al. (2011). GRADE guideline. *J. Clin. Epidemiol.* 64, 383–394. doi: 10.1016/j.jclinepi.2010.04.026

Hordacre, B., Moezzi, B., and Ridding, M. C. (2018). Neuroplasticity and network connectivity of the motor cortex following stroke: a transcranial direct current stimulation study. *Hum. Brain Mapp.* 39, 3326–3339. doi: 10.1002/hbm.24079

Jarvis, H. L., Brown, S. J., Price, M., Butterworth, C., Groenevelt, R., Jackson, K., et al. (2019). Return to employment after stroke in young adults: how important is the speed and energy cost of walking? *Stroke* 50, 3198–3204. doi: 10.1161/STROKEAHA.119.025614

Jeffery, D. T., Norton, J. A., Roy, F. D., and Gorassini, M. A. (2007). Effects of transcranial direct current stimulation on the excitability of the leg motor cortex. *Exp. Brain Res.* 182, 281–287. doi: 10.1007/s00221-007-1093-y

Kim, H., Park, G., Shin, J. H., and You, J. H. (2020). Neuroplastic effects of end-effector robotic gait training for hemiparetic stroke: a randomised controlled trial. *Sci. Rep.* 10:12461. doi: 10.1038/s41598-020-69367-3

Klamroth-Marganska, V. (2018). Stroke rehabilitation: therapy robots and assistive devices. *Adv. Exp. Med. Biol.* 1065, 579–587. doi: 10.1007/978-3-319-77932-4_35

Kwakkel, G., Veerbeek, J. M., van Wegen, E. E., and Wolf, S. L. (2015). Constraint-induced movement therapy after stroke. *Lancet Neurol.* 14, 224–234. doi: 10.1016/S1474-4422(14)70160-7

Lefaucheur, J. P., Antal, A., Ayache, S. S., Benninger, D. H., Brunelin, J., Cogiamanian, F., et al. (2017). Evidence-based guidelines on the therapeutic use of transcranial direct current stimulation (tDCS). *Clin. Neurophysiol.* 128, 56–92. doi: 10.1016/j.clinph.2016.10.087

Leon, D., Cortes, M., Elder, J., Kumru, H., Laxe, S., Edwards, D. J., et al. (2017). tDCS does not enhance the effects of robot-assisted gait training in patients with subacute stroke. *Restor. Neurol. Neurosci.* 35, 377–384. doi: 10.3233/RNN-170734

Liew, S. L., Santarnecchi, E., Buch, E. R., and Cohen, L. G. (2014). Non-invasive brain stimulation in neurorehabilitation: local and distant effects for motor recovery. *Front. Hum. Neurosci.* 8:378. doi: 10.3389/fnhum.2014.00378

Madhavan, S., Cleland, B. T., Sivaramakrishnan, A., Freels, S., Lim, H., Testai, F. D., et al. (2020). Cortical priming strategies for gait training after stroke: a controlled, stratified trial. *J. Neuroeng. Rehabil.* 17:111. doi: 10.1186/s12984-020-00744-9

Madhavan, S., Sriraman, A., and Freels, S. (2016). Reliability and variability of tDCS induced changes in the lower limb motor cortex. *Brain Sci.* 6:26. doi: 10.3390/brainsci6030026

Maher, C. G., Sherrington, C., Herbert, R. D., Moseley, A. M., and Elkins, M. (2003). Reliability of the PEDro scale for rating quality of randomized controlled trials. *Phys Ther.* 83, 713–721.

Manji, A., Amimoto, K., Matsuda, T., Wada, Y., Inaba, A., and Ko, S. (2018). Effects of transcranial direct current stimulation over the supplementary motor area body weight-supported treadmill gait training in hemiparetic patients after stroke. *Neurosci. Lett.* 662, 302–305. doi: 10.1016/j.neulet.2017.10.049

Mayo, N. E., Wood-Dauphinee, S., Ahmed, S., Gordon, C., Higgins, J., McEwen, S., et al. (1999). Disablement following stroke. *Disabil. Rehabil.* 21, 258–268. doi: 10.1080/096382899297684

Mellow, M. L., Goldsworthy, M. R., Coussens, S., and Smith, A. E. (2020). Acute aerobic exercise and neuroplasticity of the motor cortex: a systematic review. *J. Sci. Med. Sport.* 23, 408–414. doi: 10.1016/j.jsams.2019.10.015

Mitsutake, T., Sakamoto, M., Nakazono, H., and Horikawa, E. (2021). The effects of combining transcranial direct current stimulation and gait training with functional electrical stimulation on trunk acceleration during walking in patients with subacute stroke. *J. Stroke Cerebrovasc. Dis.* 30:105635. doi: 10.1016/j.jstrokecerebrovasdis.2021.105635

Miyai, I., Tanabe, H. C., Sase, I., Eda, H., Oda, I., Konishi, I., et al. (2001). Cortical mapping of gait in humans: a near-infrared spectroscopic topography study. *Neuroimage* 14, 1186–1192. doi: 10.1006/nimg.2001.0905

Montenegro, R. A., Midgley, A., Massaferri, R., Bernardes, W., Okano, A. H., and Farinatti, P. (2016). Bihemispheric motor cortex transcranial direct current stimulation improves force steadiness in post-stroke hemiparetic patients: a randomized crossover controlled trial. *Front. Hum. Neurosci.* 10:426. doi: 10.3389/fnhum.2016.00426

Naro, A., Billeri, L., Manuli, A., Balletta, T., Cannavò, A., Portaro, S., et al. (2021). Breaking the ice to improve motor outcomes in patients with chronic stroke: a retrospective clinical study on neuromodulation plus robotics. *Neurol. Sci.* 42, 2785–2793. doi: 10.1007/s10072-020-04875-8

Naro, A., Bramanti, A., Leo, A., Manuli, A., Sciarrone, F., Russo, M., et al. (2017). Effects of cerebellar transcranial alternating current stimulation on motor cortex excitability and motor function. *Brain Struct. Funct.* 222, 2891–2906. doi: 10.1007/s00429-016-1355-1

Navarro-López, V., Molina-Rueda, F., Jiménez-Jiménez, S., Alguacil-Diego, I. M., and Carratalá-Tejada, M. (2021). Effects of transcranial direct current stimulation combined with physiotherapy on gait pattern, balance, and functionality in stroke patients. A systematic review. *Diagnostics (Basel)* 11:656. doi: 10.3390/diagnostics11040656

Nitsche, M. A., and Paulus, W. (2001). Sustained excitability elevations induced by transcranial DC motor cortex stimulation in humans. *Neurology* 57, 1899–1901. doi: 10.1212/wnl.57.10.1899

Oh, K., Park, J., Jo, S. H., Hong, S. J., Kim, W. S., Paik, N. J., et al. (2021). Improved cortical activity and reduced gait asymmetry during poststroke self-paced walking rehabilitation. *J. Neuroeng. Rehabil.* 18:60. doi: 10.1186/s12984-021-00859-7

Page, M. J., McKenzie, J. E., Bossuyt, P. M., Boutron, I., Hoffmann, T. C., Mulrow, C. D., et al. (2021). The PRISMA 2020 statement: an updated guideline for reporting systematic reviews. *BMJ* 372:n71. doi: 10.1136/bmj.n71

Picelli, A., Chemello, E., Castellazzi, P., Filippetti, M., Brugnera, A., Gandolfi, M., et al. (2018). Combined effects of cerebellar transcranial direct current stimulation and transcutaneous spinal direct current stimulation on robot-assisted gait training in patients with chronic brain stroke: a pilot, single blind, randomized controlled trial. *Restor. Neurol. Neurosci.* 36, 161–171. doi: 10.3233/RNN-170784

Picelli, A., Chemello, E., Castellazzi, P., Roncari, L., Waldner, A., Saltuari, L., et al. (2015). Combined effects of transcranial direct current stimulation (tDCS) and transcutaneous spinal direct current stimulation (tsDCS) on robot-assisted gait training in patients with chronic stroke: a pilot, double blind, randomized controlled trial. *Restor. Neurol. Neurosci.* 33, 357–368. doi: 10.3233/RNN-140474

Plow, E. B., Sankarasubramanian, V., Cunningham, D. A., Potter-Baker, K., Varnerin, N., Cohen, L. G., et al. (2016). Models to tailor brain stimulation therapies in stroke. *Neural. Plast.* 2016:4071620. doi: 10.1155/2016/4071620

Powell, E. S., Carrico, C., Westgate, P. M., Chelette, K. C., Nichols, L., Reddy, L., et al. (2016). Time configuration of combined neuromodulation and motor training after stroke: a proof-of-concept study. *NeuroRehabilitation* 39, 439–449. doi: 10.3233/NRE-161375

Salazar, A. P. S., Vaz, P. G., Marchese, R. R., Stein, C., Pinto, C., and Pagnussat, A. S. (2018). Noninvasive brain stimulation improves hemispatial neglect after stroke: a systematic review and meta-analysis. *Arch. Phys. Med. Rehabil.* 99, 355–366. doi: 10.1016/j.apmr.2017.07.009

Santos, L. V., Lopes, J. B. P., Duarte, N. A. C., Castro, C. R. A. P., Grecco, L. A. C., and Oliveira, C. S. (2020). tDCS and motor training in individuals with central nervous system disease: a systematic review. *J. Bodyw. Mov. Ther.* 24, 442–451. doi: 10.1016/j.jbmt.2020.07.010

Seo, H. G., Lee, W. H., Lee, S. H., Yi, Y., Kim, K. D., and Oh, B. M. (2017). Robotic-assisted gait training combined with transcranial direct current stimulation in chronic stroke patients: a pilot double-blind, randomized controlled trial. *Restor. Neurol. Neurosci.* 35, 527–536. doi: 10.3233/RNN-170745

Suttiwong, J., Vongsirinavarat, M., and Hiengkaew, V. (2018). Predictors of community participation among individuals with first stroke: a thailand study. *Ann. Rehabil. Med.* 42, 660–669. doi: 10.5535/arm.2018.42.5.660

Tien, H. H., Liu, W. Y., Chen, Y. L., Wu, Y. C., and Lien, H. Y. (2020). Transcranial direct current stimulation for improving ambulation after stroke: a systematic review and meta-analysis. *Int. J. Rehabil. Res.* 43, 299–309. doi: 10.1097/MRR.0000000000000427

Van Peppen, R. P., Kwakkel, G., Wood-Dauphinee, S., Hendriks, H. J., Van der Wees, P. J., and Dekker, J. (2004). The impact of physical therapy on functional outcomes after stroke: what's the evidence? *Clin. Rehabil.* 18, 833–862. doi: 10.1191/0269215504cr843oa

Vaz, P. G., Salazar, A. P. D. S., Stein, C., Marchese, R. R., Lukrafka, J. L., Plentz, R. D. M., et al. (2019). Noninvasive brain stimulation combined with other therapies improves gait speed after stroke: a systematic review and meta-analysis. *Top. Stroke Rehabil.* 26, 201–213. doi: 10.1080/10749357.2019.1565696

Veerbeek, J. M., van Wegen, E., van Peppen, R., van der Wees, P. J., Hendriks, E., Rietberg, M., et al. (2014). What is the evidence for physical therapy poststroke? A systematic review and meta-analysis. *PLoS One* 9:e87987. doi: 10.1371/journal.pone.0087987

Verhagen, A. P., de Vet, H. C., de Bie, R. A., Kessels, A. G., Boers, M., Bouter, L. M., et al. (1998). The Delphi list: a criteria list for quality assessment of randomized clinical trials for conducting systematic reviews developed by Delphi consensus. *J. Clin. Epidemiol.* 51, 1235–1241. doi: 10.1016/s0895-4356(98)00131-0

Volz, M. S., Volz, T. S., Brunoni, A. R., de Oliveira, J. P., and Fregni, F. (2012). Analgesic effects of noninvasive brain stimulation in rodent animal models: a systematic review of translational findings. *Neuromodulation* 15, 283–295. doi: 10.1111/j.1525-1403.2012.00478.x

Wallis, J. A., and Taylor, N. F. (2011). Pre-operative interventions (non-surgical and non-pharmacological) for patients with hip or knee osteoarthritis awaiting joint replacement surgery–a systematic review and meta-analysis. *Osteoarthritis Cartilage* 19, 1381–1395. doi: 10.1016/j.joca.2011.09.001

Wiethoff, S., Hamada, M., and Rothwell, J. C. (2014). Variability in response to transcranial direct current stimulation of the motor cortex. *Brain Stimul.* 7, 468–475. doi: 10.1016/j.brs.2014.02.003

Wonsetler, E. C., and Bowden, M. G. (2017). A systematic review of mechanisms of gait speed change post-stroke. Part 1: spatiotemporal parameters and asymmetry ratios. *Top. Stroke Rehabil.* 24, 435–446. doi: 10.1080/10749357.2017.1285746

Yamakawa, K., Aihara, M., Ogura, H., Yuhara, H., Hamasaki, T., and Shimazu, T. (2015). Recombinant human soluble thrombomodulin in severe sepsis: a systematic review and meta-analysis. *J. Thromb. Haemost.* 13, 508–519. doi: 10.1111/jth.12841

Conflict of Interest: The authors declare that the research was conducted in the absence of any commercial or financial relationships that could be construed as a potential conflict of interest.

Publisher's Note: All claims expressed in this article are solely those of the authors and do not necessarily represent those of their affiliated organizations, or those of the publisher, the editors and the reviewers. Any product that may be evaluated in this article, or claim that may be made by its manufacturer, is not guaranteed or endorsed by the publisher.

frontiers in Human Neuroscience

MINI REVIEW
published: 16 December 2021
doi: 10.3389/fnhum.2021.805971

Figure-Eight Coils for Magnetic Stimulation: From Focal Stimulation to Deep Stimulation

Shoogo Ueno[1] and Masaki Sekino[2]**

[1] Department of Biomedical Engineering, Graduate School of Medicine, The University of Tokyo, Tokyo, Japan, [2] Department of Bioengineering, Graduate School of Engineering, The University of Tokyo, Tokyo, Japan

This article reviews the evolution and recent developments of transcranial magnetic brain stimulation using figure-eight coils to stimulate localized areas in the human brain. Geometric variations of figure-eight coils and their characteristics are reviewed and discussed for applications in neuroscience and medicine. Recent topics of figure-eight coils, such as focality of figure-eight coils, tradeoff between depth and focality, and approaches for extending depth, are discussed.

Keywords: transcranial magnetic stimulation, figure-eight coil, brain stimulation, brain mapping, depth-focality tradeoff

OPEN ACCESS

Edited by:
Shinichiro Nakajima,
Keio University, Japan

Reviewed by:
Aron T. Hill,
Deakin University, Australia

****Correspondence:***
Shoogo Ueno
ushoogo@yahoo.co.jp
Masaki Sekino
sekino@g.ecc.u-tokyo.ac.jp

Specialty section:
This article was submitted to Brain Imaging and Stimulation, a section of the journal Frontiers in Human Neuroscience

Received: *31 October 2021*
Accepted: *22 November 2021*
Published: *16 December 2021*

Citation:
Ueno S and Sekino M (2021) Figure-Eight Coils for Magnetic Stimulation: From Focal Stimulation to Deep Stimulation. Front. Hum. Neurosci. 15:805971. doi: 10.3389/fnhum.2021.805971

INTRODUCTION

Transcranial magnetic stimulation (TMS) is a technique employed for the transcranial stimulation of the human brain using a coil positioned on the surface of the head. The coil is driven by pulsed electric currents of several hundred amperes for approximately 50–150 μs to produce transient magnetic fields of approximately 1 T. This induces electric fields in the brain in accordance with Faraday's law. The induced electric fields influence neurons in the brain when the neurons receive some level of electric excitation. TMS was first reported over three decades ago in a study using a circular coil (Barker et al., 1985), in which a recordable electromyography response was elicited from the stimulation to the motor cortex (MC). This successful demonstration greatly impacted the scientific community. However, it was difficult to locally stimulate the targeted areas in the brain using a circular coil. Subsequently, a method of localized brain stimulation with a figure-eight coil was proposed (Ueno et al., 1988), and the stimulation of the human MC within a 5-mm resolution was achieved (Ueno et al., 1990).

Implementing TMS using a figure-eight coil is advantageous in the localized stimulation of the brain. This has led to a rapid expansion in the study of functional brain research; studies concerning the functional organization of the human brain, neuronal dynamic connectivity, and neuronal plasticity in the cortex have been successfully conducted using figure-eight coils. In view of its excellent performance in localized brain stimulation, TMS with a figure-eight coil is now widely used in basic and clinical medicine (Ueno, 2021).

Building on the success of TMS, repetitive TMS (rTMS) with repetitive pulsed stimulation was introduced in clinical medicine as a potential treatment for pain, depression, Parkinson's disease, and neurorehabilitation. To treat these ailments, specific areas in the deeper parts of the brain need

to be stimulated. To achieve this type of deep brain stimulation, several coil configurations were developed (Roth et al., 2002; Zangen et al., 2005; Crowther et al., 2011; Lu and Ueno, 2015, 2017).

In this article, we introduce TMS using a figure-eight coil and structural variations of figure-eight coil, as well as other coil configurations for surface and deep brain stimulation. We discuss the advantages and limitations of these coil configurations, focusing on the focality, tradeoff between depth and focality, and approaches for extending depth.

FOCALITY OF FIGURE-EIGHT COILS

When we use a round coil, induced electric fields in the brain flow in a concentric manner as shown in **Figure 1A**. The intensity of the electric fields increases in proportion to the radius; the intensity is zero at the center of the coil, and the maximum at the edge of the coil. In contrast, when we use a figure-eight coil, induced electric fields flow in the brain, making two vortices, as shown in **Figure 1B**. The two vortices merge at the center of the figure-eight. Thereby we can deliver localized and focal brain stimulation (Ueno et al., 1988, 1990). Our computer simulation showed that the electric fields at the target is three times higher than those at non-target areas (Ueno et al., 1988; Sekino and Ueno, 2004a,b).

Since the induced electric fields, or, induced electric currents, flow in the direction of the tangent of coils, the direction of stimulating currents is controlled by rotating the coil. The direction-controlled magnetic stimulation, or, so-called vectorial magnetic stimulation is carried out by changing the amplitude and direction of stimulating currents.

The localized and direction-controlled stimulation of neurons in the brain is useful in studying both anatomical and functional organizations of the brain. The pyramidal neurons in the cortex are more easily excited when the stimulating electric fields, or, stimulating electric currents, flow in parallel to the axons of the pyramidal neurons, compared with the stimulation by currents which flow in the direction perpendicular to the axons. The neuronal excitation is caused by transmembrane potentials across the cell membrane. The transmembrane potential is caused by the outward currents out of the neurons, which results in the depolarization of the membrane. When the depolarization exceeds a threshold of the excitable tissue, the neuron is excited. The outward currents are driven by the activating function, or, the negative value of spatial gradient of induced electric fields (Basser et al., 1992).

Therefore, TMS with a figure-eight coil has the advantages in targeted and vectorial stimulation of the brain, compared with those with round coil configurations.

STRUCTURAL VARIATION OF FIGURE-EIGHT COILS

Since the invention of the figure-eight coil, researchers have constantly attempted to improve its performance. The focus of these attempts has been the geometry of the coil windings, since it greatly affects the performance of the coil. Over the years, various modifications of the coil geometry and their resulting advantages have been reported. **Figure 1** summarizes the major variations in the design of the figure-eight coils. **Figure 1B** shows a simple planar coil consisting of a pair of circles, which is the most basic form among the variants. The induced electric field converges directly below the center of the coil, which exhibits a locally high electric field intensity. Butterfly coils or double cone coils, shown in **Figure 1C**, are now widely used in clinical applications. The coil is bent at an acute angle at the center between the left and right wings. The bending forces the coil to conform to the shape of the human head. Moreover, it results in an increased depth of the induced electric fields in the brain. The quadruple butterfly coils illustrated in **Figure 1D** are also bent at the center of the coil, but at an obtuse angle (Rastogi et al., 2017). This coil achieves a high electric-field intensity at the intersection of the wings. Additionally, the bent shape leads to a reduction in the current density in the surrounding areas. Thus, this coil enhances the focality of the induced electric field. Slinky coils, illustrated in **Figure 1E**, are another variation of figure-eight coils (Krasteva et al., 2002). Because of the contributions of coil elements having obtuse angles, the coil provides electric field distributions with an enhanced focality. Eccentric figure-eight coils, shown in **Figure 1F**, can achieve an enhanced electric field intensity owing to their modified in-plane winding geometry (Sekino et al., 2015). The winding centers of the left and right coils are shifted toward the middle, forming a dense coil conductor in the middle. Its high efficiency in inducing electric fields, leads to downsizing of the driving circuit. Moreover, the dense conductors in the middle enhances the focality of stimulation. Double-D coils, shown in **Figure 1G**, are intended for the stimulation of wider areas of the brain (Sekino et al., 2017). This coil has a deformation in the direction opposite to that of the eccentric figure-eight coils. The double-D coils have straight conductors in the middle, with gaps between the conductors. Because of the extended area of stimulation, the stimulating effect is more stable despite the small displacements of the coil that naturally occur during repeated stimulations. H-coils offer a series of coil geometries designed for generating electric fields being deeper than those of typical TMS coils which only stimulate more superficial layers of the cortex (Tendler et al., 2016). As shown in **Figure 1H**, several coil geometries in the H-coil series are based on figure-eight coils. These H-coils have characteristics similar to those of butterfly coils, and are now widely applied in the treatment of depression. **Figure 1I** presents a combination of two figure-eight coils that generate electric fields in orthogonal directions (Rotem et al., 2014). When biphasic pulse currents are applied to the two coils with a phase shift of a quarter cycle, the resulting electric field rotates in the coil plane. The excitability of cortical tissues depends on the direction of the electric field. Thus, the rotating electric fields provide stable stimulating effects regardless of the coil orientation. The electric power efficiency of figure-eight coils can be improved by using an iron core, as illustrated in **Figure 1J**. This enables the generation of strong magnetic fields with smaller driving currents (Yamamoto et al., 2016). The improvement of power efficiency is beneficial for

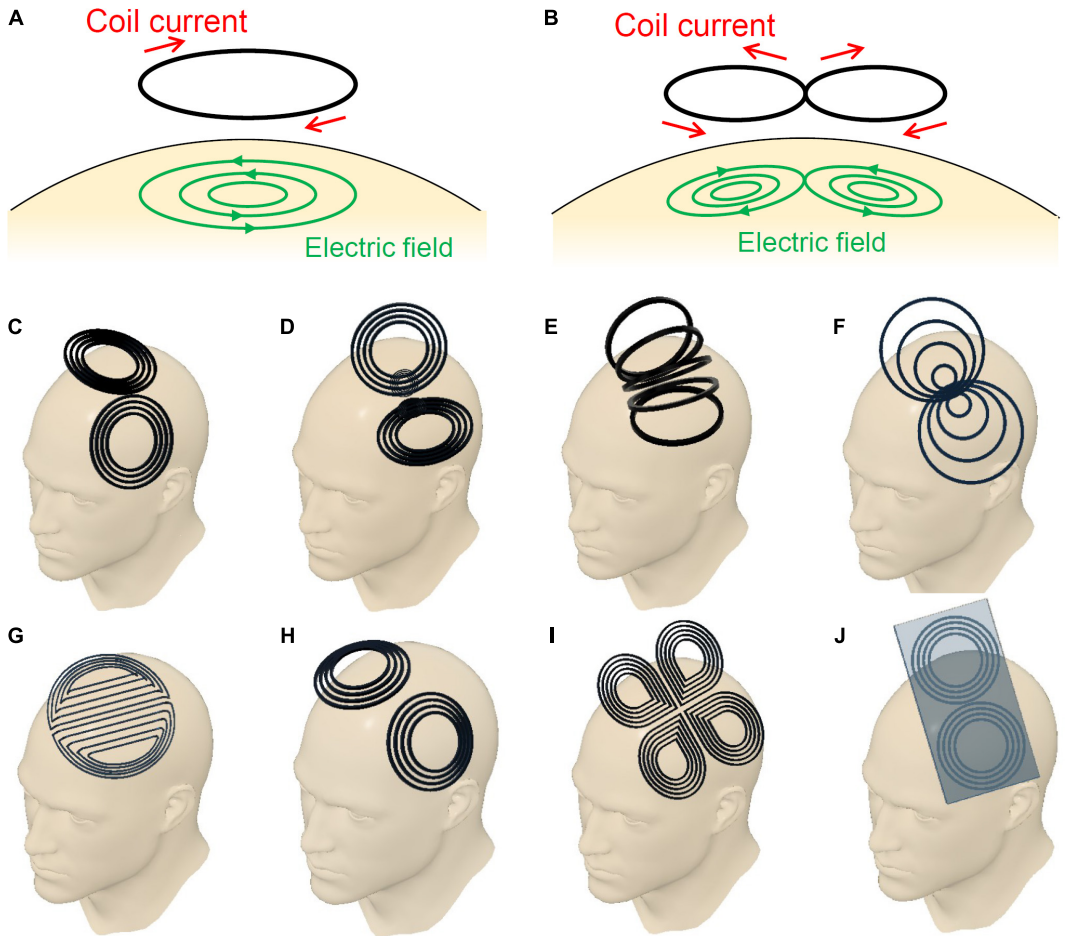

FIGURE 1 | (A) Circular coil, **(B)** planar figure-eight coil, **(C)** butterfly coil, **(D)** quadruple butterfly coil, **(E)** slinky coil, **(F)** eccentric figure-eight coil, **(G)** double-D coil, **(H)** H6-coil, **(I)** cloverleaf coil, and **(J)** figure-eight coil with iron core.

therapeutic applications that require repeated stimulations with frequencies over 5 Hz. However, the iron core should be designed to minimize eddy currents in the core.

TRADEOFF BETWEEN DEPTH AND FOCALITY

As electromagnetic fields generated from a coil attenuate with increasing distance from the coil, superficial areas in the brain, such as the cerebral cortex, are more strongly stimulated by TMS. This leads to excitation or inhibition of deeper regions in the brain depending on the functional connectivity in the brain. Such neuromodulation of the deeper regions is considered to be the key to obtaining therapeutic effects. Extensive research and development has been conducted to increase the depth of electric fields. Several clinical studies on TMS treatment have conclusively demonstrated that deeper stimulations achieve better therapeutic effects (Shimizu et al., 2017). However, direct stimulation of deeper regions of the brain continues to be one of the biggest technical challenges in TMS.

Figure 2 shows a numerical simulation of electric currents induced by figure-eight coils with four different diameters ranging from 40 to 100 mm. The increase in the coil diameter leads to an increased depth of the induced electric fields, suggesting that larger coils are suitable for achieving deeper stimulations. However, larger coils exhibit an extended area of stimulation, which leads to stimulation outside the target area, increasing the potential risk of side effects. To provide effective and safe TMS, coils with both depth and focality are preferred. This simulation shows that there is a trade-off between depth and focality in induced electric fields.

A comparison of the electric fields in the human brain induced by a butterfly coil, H-coil, Halo coil, and planar figure-eight coil was conducted in a study (Lu and Ueno, 2017). The butterfly, H-, and Halo coils have significantly deep field penetrations compared to the planar figure-eight coil, at the expense of focality. The intensities of electric fields in the thalamus were 86.2, 28.7, 47.7, and 21.7 V/m for the butterfly, H-, Halo, and planar figure-eight coils, respectively. Interestingly, the butterfly and Halo coils are more adept at stimulating deep brain subregions

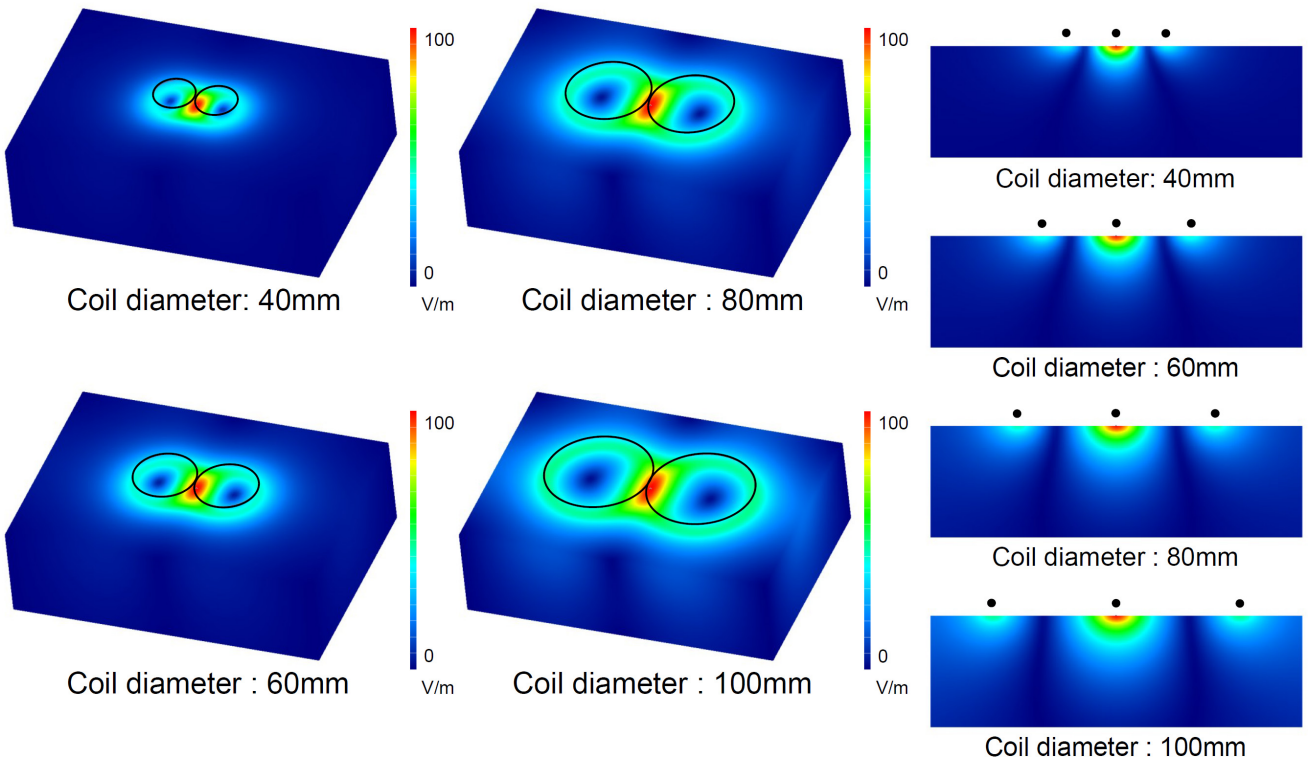

FIGURE 2 | Numerical simulation of electric fields induced by figure-eight coils with four different diameters. The electric current in the coil was 1 kA for the four diameters.

compared to the H-coil. Therefore, the butterfly coil has an appropriate balance of depth and focality.

A systematic benchmarking of TMS coils was conducted by comparing the electric field distributions of 50 different coils (Deng et al., 2013). The results showed that there is a clear tradeoff between depth and focality, and coils with deeper penetrations exhibited wider stimulated areas. The figure-eight and H-coils are most suitable for focused and wide stimulations, respectively. The butterfly coil exhibited both moderate depth and focality. A significant observation of this study was that the bending angle between the two wings of the butterfly coil affected the balance between depth and focality. In the study, the maximum field depth was obtained at a bending angle of 110°.

RECENT APPROACHES TO EXTENDING DEPTH

Realizing the importance of deeper penetration of the induced electric field in TMS, recent studies have proposed novel approaches to this problem.

Mathematical methodologies for solving inverse problems play an important role in biomagnetics, specifically magnetoencephalography. These methodologies have recently been applied to the coil design of TMS. In the history of TMS, researchers have invented various coils. The characteristics of these coils can be compared to determine which of them is best suited to specific applications. Inverse analysis provides a framework for optimizing the geometry and size of coil windings for a given target electric field distribution in the brain (Peeren, 2003; Liu et al., 2020). A hypothetical potential is defined on a two-dimensional curved surface on which the coil windings are formed. Partial derivatives of the potential provide current distributions in the coil. Biot–Savart's law and Faraday's law of induction describe a linear relationship between the potential on the coil surface and the electric field distribution inside the plane. A cost function is defined as the spatially integrated difference between the given target electric field and the electric field generated from the coil potential. Then, the optimum coil potential for the target electric field can be obtained by minimizing the cost function. Notably, a focused target electric field led to a solution of figure-eight coils, although the algorithm did not have prior knowledge of figure-eight coils (Liu et al., 2020). This result provides evidence from a mathematical viewpoint that a figure-eight coil is feasible for providing focal stimulation. This framework will be used in the future to systematically study coil designs to realize deeper brain stimulations.

A recent study showed the concept of temporally interfering electric stimulation, which uses a pair of electric fields with slightly different frequencies (Grossman et al., 2017). Simultaneous application of the two electric fields generates an envelope of waveforms that vary with the frequency difference between the two carrier frequencies. When the carrier frequencies

exceeded 10^3 Hz, the neurons were unresponsive. However, the envelope frequency is approximately 10 Hz, which induces neuron excitation. Interestingly, the maximum magnitude of the envelope may appear in the deep regions of the brain. This technique enables the local stimulation of deep regions from electrodes attached to the surface of the head. The concept of temporal interference can also be introduced into TMS. An inductive temporal interference stimulation from figure-eight coils achieves deeper and more focused stimulation than that achieved in the aforementioned tradeoff (Xin et al., 2021).

NEUROSCIENTIFIC APPLICATION

Transcranial magnetic stimulation with a figure-eight coil stimulates the human brain within a high spatial resolution. For example, we stimulated the human motor cortex related to the hand and foot areas with a 5 mm resolution. We put electrodes at five hand muscles, such as, abductor pollicis brevis (APB), first dorsal interosseous (FDI), abductor digiti minimi (ADM), brachioradial (BR), biceps brachii (BB), and tibialis anterior (TA) muscles, and we observed motor evoked potentials (MEPs) from these muscles responded to the brain stimulation. We obtained the functional map in this motor cortex (Ueno et al., 1990). The distance between grid points in the functional map is 5 mm. Each functional area has its optimal direction for brain stimulation. When we stimulate the point related to the thumb with the opposite direction with respect to the optimal direction, the thumb does not respond. In the functional map obtained by the TMS with a figure-eight coil, the regional and directional dependences of excitability reflect gyri and sulci of the brain.

Therefore, TMS with a figure-eight coil enables us to study the dynamic spatiotemporal neuronal network in the human brain non-invasively. We can produce so-called virtual lesion transiently. In other words, TMS with a figure-eight coil can cause a transient disturbance locally in the brain for a short period of time. The virtual lesion approach using TMS is a powerful tool for the studies of dynamic mechanisms of the human brain, since the spatiotemporal information processing in the brain has not yet been well clarified.

Epstein conducted an interesting study on episodic memory using the virtual lesion approach when he visited our laboratory (Epstein et al., 2002). Ten Japanese subjects underwent sequential visual stimuli, which contained 18 sets of simple Kanji words and unfamiliar abstract patterns, and the brain was disturbed by TMS with a figure-eight coil between the visual stimulations. The TMS coil was placed at the left dorsolateral prefrontal cortex (DLPFC), right DLPFC, the central vertex, and off the head as a control. After the set of stimuli, subjects took a test to check the memory correctness of the pair of Kanji and abstract patterns. The results indicate that the right DLPFC has an important role in generating the episodic memory. As in this example, TMS with a figure-eight coil can elucidate the dynamic mechanisms of the human higher brain function.

APPLICATIONS TO MEDICINE

Clinical studies have shown that rTMS is effective for various psychiatric and neurological diseases. The use of figure-eight coils has enabled us to efficiently induce electric fields in the target area while minimizing the potential risk of side effects caused by the stimulation of surrounding areas. Magnetic stimulators equipped with figure-eight coils have obtained regulatory approval in many countries and are now commercially available. A guideline for the therapeutic use of rTMS was published, based on a review of clinical studies of rTMS (Lefaucheur et al., 2020). In this guideline, the efficacy of rTMS for various psychiatric and neurological diseases was evaluated, and its efficacy in treating depression, motor stroke, and neuropathic pain were categorized as Level A, indicating definite efficacy.

The United States Food and Drug Administration approved the treatment of depression in 2008. The DLPFC is the primary target in the treatment of depression. rTMS treatment is effective in drug-resistant cases.

The successful treatment of neuropathic pain has also been reported in several clinical studies. Stimulation of the primary motor cortex showed positive effects on treatment. The eccentric figure-eight coil shown in **Figure 1F** was developed and applied for the treatment of neuropathic pain (Hosomi et al., 2020). Clinical studies have shown that the therapeutic effect strongly depends on the conditions and protocol of stimulation.

CONCLUDING REMARKS

Figure-eight coils were originally invented for achieving non-invasive and focal stimulation of the brain. Additionally, its ability of functional mapping of the brain made a significant contribution to neuroscience. In tandem with neuroscientific applications, the therapeutic application of rTMS has also expanded in recent years. Systematic studies of coils have demonstrated the figure-eight coil's ability to balance the focality and depth of induced fields. In conclusion, it can be surmised that figure-eight coils will continue to play important roles in both neuroscience and medicine, incorporating further technological updates.

AUTHOR CONTRIBUTIONS

SU wrote introduction, focality of figure-eight coils, and neuroscience application. MS wrote structural variation of figure-eight coils, tradeoff between depth and focality, recent approaches to extending depth, and applications to medicine. Both authors contributed to the article and approved the submitted version.

FUNDING

This work was supported by the JSPS KAKENHI Grant Number 20H05759.

REFERENCES

Barker, A. T., Jalinous, R., and Freeston, I. L. (1985). Non-invasive magnetic stimulation of the human motor cortex. *Lancet* 1, 1106–1107. doi: 10.1016/s0140-6736(85)92413-4

Basser, P. J., Wijesinghe, R. S., and Roth, B. J. (1992). The activating function for magnetic stimulation derived from a three-dimensional volume conductor model. *IEEE Trans. Biomed. Eng.* 39, 1207–1210. doi: 10.1109/10.168686

Crowther, L. J., Marketos, P., Williams, P. I., Melikhov, Y., and Jiles, D. C. (2011). Transcranial magnetic stimulation: Improved coil design for deep brain investigation. *J. Appl. Phys.* 109:07B314. doi: 10.1063/1.3563076

Deng, Z. D., Lisanby, S. H., and Peterchev, A. V. (2013). Electric field depth-focality tradeoff in transcranial magnetic stimulation: simulation comparison of 50 coil designs. *Brain Stimul.* 6, 1–13. doi: 10.1016/j.brs.2012.02.005

Epstein, C. M., Sekino, M., Yamaguchi, K., Kamiya, S., and Ueno, S. (2002). Asymmetries of prefrontal cortex in human episodic memory: Effects of transcranial magnetic stimulation on learning abstract patterns. *Neurosci. Lett.* 320, 5–8. doi: 10.1016/s0304-3940(01)02573-3

Grossman, N., Bono, D., Dedic, N., Kodandaramaiah, S. B., Rudenko, A., Suk, H. J., et al. (2017). Noninvasive deep brain stimulation via temporally interfering electric fields. *Cell* 169, 1029–1041. doi: 10.1016/j.cell.2017.05.024

Hosomi, K., Sugiyama, K., Nakamura, Y., Shimokawa, T., Oshino, S., Goto, Y., et al. (2020). A randomized controlled trial of 5 daily sessions and continuous trial of 4 weekly sessions of repetitive transcranial magnetic stimulation for neuropathic pain. *Pain* 161, 351–360. doi: 10.1097/j.pain.0000000000001712

Krasteva, V. T., Papazov, S. P., and Daskalov, I. K. (2002). Magnetic stimulation for non-homogeneous biological structures. *Biomed. Eng. Online* 1:3. doi: 10.1186/1475-925X-1-3

Lefaucheur, J. P., Aleman, A., Baeken, C., Benninger, D. H., Brunelin, J., Di Lazzaro, V., et al. (2020). Evidence-based guidelines on the therapeutic use of repetitive transcranial magnetic stimulation (rTMS): An update (2014–2018). *Clin. Neurophysiol.* 131, 474–528. doi: 10.1016/j.clinph.2019.11.002

Liu, S., Kuwahata, A., and Sekino, M. (2020). Design of a multi-locus transcranial magnetic stimulation coil with a single driver. *URSI Radio Sci. Lett.* 2, 1–5. doi: 10.46620/20-0057

Lu, M., and Ueno, S. (2015). Computational study toward deep transcranial magnetic stimulation using coaxial circular coils. *IEEE Trans. Biomed. Eng.* 62, 2911–2919. doi: 10.1109/tbme.2015.2452261

Lu, M., and Ueno, S. (2017). Comparison of the induced fields using different coil configurations during deep transcranial magnetic stimulation. *PLoS One* 12:e0178422. doi: 10.1371/journal.pone.0178422

Peeren, G. N. (2003). Stream function approach for determining optimal surface currents. *J. Comput. Phys.* 191, 305–321. doi: 10.1016/S0021-9991(03)00320-6

Rastogi, P., Lee, E. G., Hadimani, R. L., and Jiles, D. C. (2017). Transcranial magnetic stimulation-coil design with improved focality. *AIP Adv.* 7:056705. doi: 10.1063/1.4973604

Rotem, A., Neef, A., Neef, N. E., Agudelo-Toro, A., Rakhmilevitch, D., Paulus, W., et al. (2014). Solving the orientation specific constraints in transcranial magnetic stimulation by rotating fields. *PLoS One* 9:e86794. doi: 10.1371/journal.pone.0086794

Roth, Y., Zangen, A., and Hallett, M. (2002). A coil design for transcranial magnetic stimulation of deep brain regions. *J. Clin. Neurophysiol.* 19, 361–370. doi: 10.1097/0000469-200208000-00008

Sekino, M., and Ueno, S. (2004a). FEM-based determination of optimum current distribution in transcranial magnetic stimulation as an alternative to electroconvulsive therapy. *IEEE Trans. Magn.* 40, 2167–2169. doi: 10.1109/TMAG.2004.828982

Sekino, M., and Ueno, S. (2004b). Numerical calculation of eddy currents in transcranial magnetic stimulation for psychiatric treatment. *Neurol. Clin. Neurophysiol.* 88, 1–5.

Sekino, M., Ohsaki, H., Takiyama, Y., Yamamoto, K., Matsuzaki, T., Yasumuro, Y., et al. (2015). Eccentric figure-eight coils for transcranial magnetic stimulation. *Bioelectromagnetics* 36, 55–65. doi: 10.1002/bem.21886

Sekino, M., Yamamoto, K., and Kawasaki, Y. (2017). *Coil and magnetic stimulator using same*. International patent publication number: WO2017/150490. Geneva: WIPO.

Shimizu, T., Hosomi, K., Maruo, T., Goto, Y., Yokoe, M., Kageyama, Y., et al. (2017). Efficacy of deep rTMS for neuropathic pain in the lower limb: a randomized, double-blind crossover trial of an H-coil and figure-8 coil. *J. Neurosurg.* 127, 1172–1180. doi: 10.3171/2016.9.JNS16815

Tendler, A., Ygael, N. B., Roth, Y., and Zangen, A. (2016). Deep transcranial magnetic stimulation (dTMS) - beyond depression. *Expert Rev. Med. Devices* 13, 987–1000. doi: 10.1080/17434440.2016.1233812

Ueno, S. (2021). New horizons in electromagnetics in medicine and biology. *Radio Sci.* 56, 1–17. doi: 10.1029/2020RS007152

Ueno, S., Matsuda, T., and Fujiki, M. (1990). Functional mapping of the human motor cortex obtained by focal and vectorial magnetic stimulation of the brain. *IEEE Trans. Magn.* 26, 1539–1544. doi: 10.1109/20.104438

Ueno, S., Tashiro, T., and Harada, K. (1988). Localized stimulation of neural tissues in the brain by means of a paired configuration of time-varying magnetic fields. *J. Appl. Phys.* 64, 5862–5864. doi: 10.1063/1.342181

Xin, Z., Kuwahata, A., Liu, S., and Sekino, M. (2021). Magnetically induced temporal interference for focal and deep-brain stimulation. *Front. Hum. Neurosci.* 15:693207. doi: 10.3389/fnhum.2021.693207

Yamamoto, K., Miyawaki, Y., Saitoh, Y., and Sekino, M. (2016). Improvement in efficiency of transcranial magnetic stimulator coil by combination of iron core plates laminated in different directions. *IEEE Trans. Magn.* 52:5100504. doi: 10.1109/TMAG.2016.2514321

Zangen, A., Roth, Y., Voller, B., and Hallett, M. (2005). Transcranial magnetic stimulation of deep brain regions: Evidence for efficacy of the H-coil. *Clin. Neurophysiol.* 116, 775–779. doi: 10.1016/j.clinph.2004.11.008

Conflict of Interest: The authors declare that the research was conducted in the absence of any commercial or financial relationships that could be construed as a potential conflict of interest.

frontiers in Human Neuroscience

PERSPECTIVE
published: 04 January 2022
doi: 10.3389/fnhum.2021.785620

Closed-Loop Transcutaneous Auricular Vagal Nerve Stimulation: Current Situation and Future Possibilities

Yutian Yu[1,2*†], *Jing Ling*[3†], *Lingling Yu*[4], *Pengfei Liu*[2,5] *and Min Jiang*[1,2*]

[1]Acupuncture Department, Beijing Shijitan Hospital, Capital Medical University, Beijing, China, [2]Ninth School of Clinical Medicine, Peking University, Beijing, China, [3]Department of Gynecology, Shenzhen Traditional Chinese Medicine Hospital, Shenzhen, China, [4]Department of Chinese and Western Medicine, Tongji Hospital, Tongji Medical College, Huazhong University of Science and Technology, Wuhan, China, [5]Department of Anesthesiology, Beijing Shijitan Hospital, Capital Medical University, Beijing, China

OPEN ACCESS

Edited by:
Ken-Ichiro Tsutsui, Tohoku University, Japan

Reviewed by:
Ricardo Nuno Braço Forte Salvador, Neuroelectrics (Spain), Spain
Francesco Motolese, Campus Bio-Medico University, Italy

***Correspondence:**
Yutian Yu
yutianyu@bjsjth.cn
Min Jiang
jiangmin545@bjsjth.cn

[†]*These authors share first authorship*

Specialty section:
This article was submitted to Brain Imaging and Stimulation, a section of the journal Frontiers in Human Neuroscience

Received: *29 September 2021*
Accepted: *11 November 2021*
Published: *04 January 2022*

Citation:
Yu Y, Ling J, Yu L, Liu P and Jiang M (2022) Closed-Loop Transcutaneous Auricular Vagal Nerve Stimulation: Current Situation and Future Possibilities. Front. Hum. Neurosci. 15:785620. doi: 10.3389/fnhum.2021.785620

Closed-loop (CL) transcutaneous auricular vagal nerve stimulation (taVNS) was officially proposed in 2020. This work firstly reviewed two existing CL-taVNS forms: motor-activated auricular vagus nerve stimulation (MAAVNS) and respiratory-gated auricular vagal afferent nerve stimulation (RAVANS), and then proposed three future CL-taVNS systems: electroencephalography (EEG)-gated CL-taVNS, electrocardiography (ECG)-gated CL-taVNS, and subcutaneous humoral signals (SHS)-gated CL-taVNS. We also highlighted the mechanisms, targets, technical issues, and patterns of CL-taVNS. By reviewing, proposing, and highlighting, this work might draw a preliminary blueprint for the development of CL-taVNS.

Keywords: closed-loop (CL), transcutaneous auricular vagal nerve stimulation (taVNS), electromyography (EMG), electroencephalography (EEG), electrocardiography (ECG), subcutaneous humoral signals (SHS), non-invasive brain stimulation (NIBS)

INTRODUCTION

Timing: From VNS to CL-taVNS

Vagal nerve stimulation (VNS) was initially a non-invasive neuromodulation technique with a history that can be traced back to the 1880s (Lanska, 2002). However, throughout the 20th century, studies on stimulation of the vagal nerve were almost inseparable from the characteristic of invasiveness (Thompson et al., 2021). Intriguingly, by the end of the second millennium, transcutaneous auricular vagal nerve stimulation (taVNS), an authentic non-invasive brain stimulation (NIBS), had emerged (Ventureyra, 2000). Inspired by neuroanatomy [the distribution of the auricular branch of the vagal nerve (ABVN) in the auricular concha], auricular acupuncture (AA), and invasive VNS (iVNS), the concept of taVNS opened a new era in the field of neuromodulation (Wang et al., 2021), particularly having a similar pattern of activation with the iVNS (Badran et al., 2018). In 2020, further progress was made based on taVNS, with researchers officially proposing the closed-loop taVNS (CL-taVNS; Badran et al., 2020; Cook et al., 2020).

Anatomical Basis, Mechanisms, and Indications of taVNS

The ABVN is directly connected to the nucleus tractus solitarii (NTS) in the medulla, which is the endpoint of the afferent fibers of the vagal nerve and is recognized as a relay station for visceral sensation, plays a relay role in receiving signals from the ear, and adjusts the function of the body (Schachter and Saper, 1998). The NTS makes forward projections directly or indirectly to locus ceruleus, hypothalamus, thalamus, amygdala, hippocampus, and prefrontal cortex (Ricardo and Koh, 1978; Ter Horst et al., 1989; Van Eden and Buijs, 2000; Castle et al., 2005), with the release of neurotransmitters including norepinephrine (NE), serotonin (5-HT) and dopamine (DA; Badran et al., 2018). Efferent fibers in the vagal nerve can control multiple peripheral organs (Wang et al., 2021), including the heart, lungs, liver, stomach, pancreas, and kidneys (Moini and Piran, 2020). Therefore, taVNS has confirmed and potential applications for various diseases related to the central and peripheral nervous systems.

Principally by balancing the autonomic nervous system (increasing parasympathetic activity and reducing sympathetic activity; Deuchars et al., 2018), taVNS has several indications in the brain, cardiovascular, and digestive system diseases (Wang et al., 2021). In addition, taVNS has potential benefits for type 2 diabetes (T2D; Wang et al., 2015), obesity (Yu et al., 2021), and rheumatoid arthritis (RA; Addorisio et al., 2019). Due to the anatomical properties of the vagal nerve and the major mechanism of taVNS, more indications of taVNS may emerge in the future.

From Open-Loop to Closed-Loop taVNS

Some of these taVNS indications are associated with clinically detectable, altered dynamics, and the aberrant activity, in principle, can be restored through taVNS. Moreover, these abnormal patterns occur intermittently and sometimes unpredictably. Thus, it is necessary to modify the original taVNS from open-loop to closed-loop to correct the anomaly at an early stage.

The CL-taVNS systems adapt rapidly to changing conditions and thus offer a personalized taVNS for individualized control with increased therapeutic efficiency, improved quality of life, and reduced severity of side effects (Kaniusas et al., 2019a). A brief definition of CL-taVNS might be an automatic control taVNS system in which its process is regulated by biofeedback signal(s). As a result, a CL-taVNS system should primarily include a biosignal(s) sensor (identifier) and a taVNS stimulator integrated with remote-control solutions (Kaniusas et al., 2019a). For instance, in the existing CL-taVNS systems, behavioral changes are the biomarkers for switching the stimulation process (Napadow et al., 2012; Garcia et al., 2017; Badran et al., 2020; Cook et al., 2020). It can be inferred that other biomarkers may also be available for developing new CL-taVNS systems and multiple types of CL-taVNS systems triggered by specific biomarkers and leaving other functions unaffected are therefore desirable.

Disease-Oriented Development of CL-taVNS

The development of CL-taVNS systems may be diverse, but we consider that they should be disease-oriented. Thus, in addition to a short review of the known CL-taVNS systems, three future putative applications of the technique are suggested in this article (**Figure 1**) which aims to inform the development of CL-taVNS from a clinical perspective.

EXISTING CL-taVNS SYSTEMS

Motor-Activated Auricular Vagus Nerve Stimulation (MAAVNS)

The field of CL-taVNS was pioneered by Badran et al. (2019), with an abstract in which the authors described their method as electromyography (EMG)-gated CL-taVNS. They followed up the study and formally proposed the CL-taVNS in 2020 (Cook et al., 2020) and named it motor-activated auricular vagus nerve stimulation (MAAVNS). MAAVNS pairs taVNS with motor activity, delivering taVNS during targeted motor activity (Cook et al., 2020). Their studies demonstrated that MAAVNS is a promising neurorehabilitation tool in neonates (Badran et al., 2020; Cook et al., 2020). MAAVNS has been translated to adult upper limb rehabilitation, and this application is being investigated in a small randomized trial (ClinicalTrials.gov Identifier: NCT04129242).

Respiratory-Gated Auricular Vagal Afferent Nerve Stimulation (RAVANS)

Another form of CL-taVNS proposed much earlier than MAAVNS is respiratory-gated auricular vagal afferent nerve stimulation (RAVANS). RAVANS works on the principle that inhalation induces transient inhibition of vagal nerve activity (Thompson et al., 2021). Positive results were recorded when RAVANS was applied in pain subjects, including pelvic pain (Napadow et al., 2012) and migraine (Garcia et al., 2017). Furthermore, although no firm conclusions have been drawn, it seemed that RAVANS might also lower blood pressure in hypertensive patients (Fisher et al., 2018; Stowell et al., 2019). Significantly, in healthy subjects, expiratory-gated and non-respiratory-gated taVNS exert apparent cardioinhibitory effects with high pre-stimulatory heart rate, whereas inspiratory-gated taVNS does not affect heart rate (Paleczny et al., 2021).

FUTURE CL-taVNS SYSTEMS

MAAVNS uses EMG to trigger the taVNS procedure, while RAVANS applies mechanical signals with subjects outfitted with a thoracic belt to measure respiratory excursions (**Figure 1**). However, electroencephalographic (EEG) and electrocardiographic (ECG) signals should not be ignored. Moreover, since taVNS is a potential treatment option for T2D and RA, subcutaneous humoral signals (SHS) may be an option to trigger taVNS in specific patients. Therefore, in the following sections, we propose three potential CL-taVNS systems.

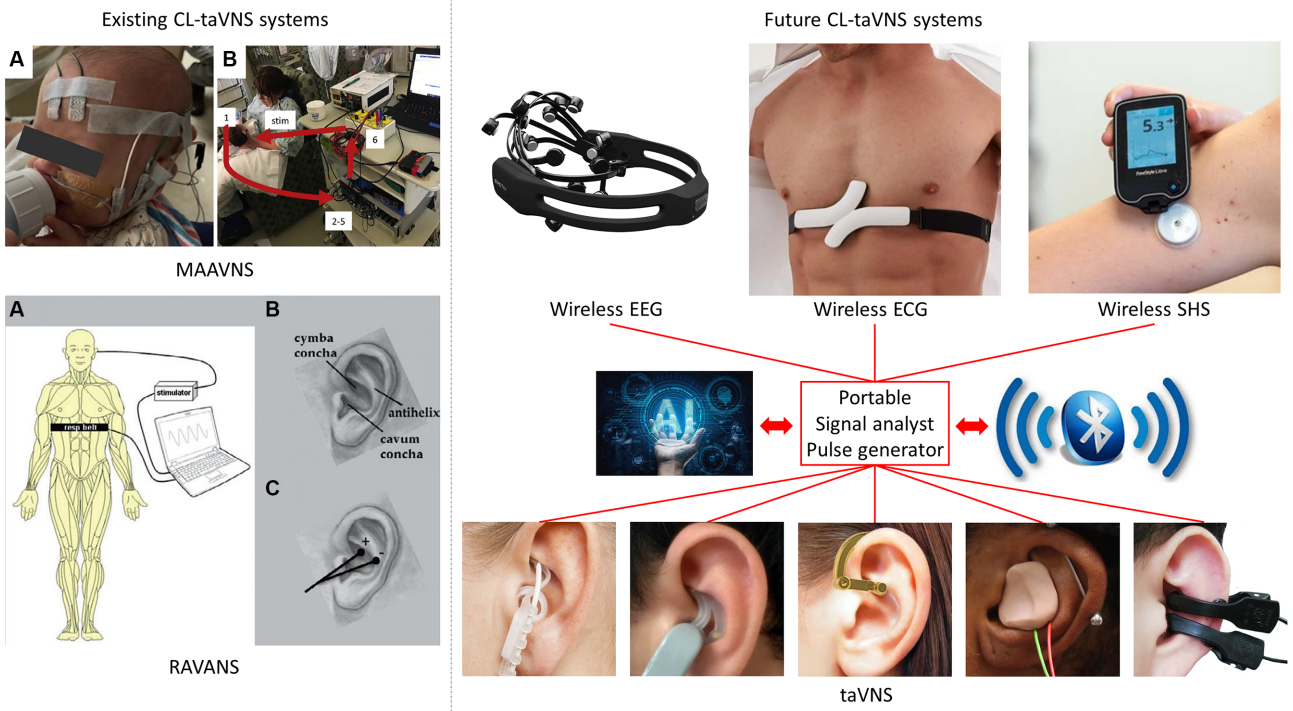

FIGURE 1 | Illustration of two known and three future CL-taVNS systems. MAAVNS (image from https://doi.org/10.1016/j.brs.2020.02.028): motor-activated auricular vagus nerve stimulation. **(A)** EMG lead placement: active lead on buccinator, reference lead on the frontal eminence, ground lead in the center of the forehead. **(B)** Overview of MAAVNS setup: EMG signals from facial muscles (1) were processed (2–5) and used to trigger stimulation (6, stim). RAVANS (image from https://doi.org/10.1111/j.1526-4637.2012.01385.x): respiratory-gated auricular vagal afferent nerve stimulation. **(A)** Subjects were outfitted with a thoracic belt to measure respiratory excursions. This signal was transduced and fed into a laptop controller, allowing for left transcutaneous auricular vagal nerve stimulation to occur only during the expiratory phase of respiration. **(B)** Auricular anatomy includes essential regions, including the cymba and cavum conchae, as well as the antihelix. **(C)** Auricular electrodes were placed within the cymba concha and antihelix, the two regions found to be most consistently innervated by the auricular branch of the vagal nerve. EEG-gated taVNS, EEG: electroencephalography, including the use of artificial intelligence (AI) and Bluetooth. ECG-gated taVNS, ECG: electrocardiography, including the use of artificial intelligence (AI) and Bluetooth. SHS-gated taVNS, SHS: subcutaneous humoral signals, including the use of artificial intelligence (AI) and Bluetooth. taVNS: transcutaneous auricular vagal nerve stimulation.

EEG-Gated CL-taVNS

Clinical evidence indicates that taVNS is an effective treatment for epilepsy (Rong et al., 2014) and major depressive disorder (MDD; Fang et al., 2016; Rong et al., 2016). EEG is the most specific method to define the epileptogenic cortex (Noachtar and Rémi, 2009). Meanwhile, the EEG-based computer-aided technique may be a suitable clinical diagnostic tool for MDD (Mumtaz et al., 2017). Therefore, we speculate that it is possible to develop an EEG-gated CL-taVNS system. In such a system, detection of an abnormal EEG signal would immediately activate ABVN stimulation to alleviate symptoms. For example, spike-and-wave patterns, typically arising from complex interactions between thalamic and neocortical neurons, are the hallmark of generalized absence seizure (Berényi et al., 2012), and may be an apposite EEG biomarker for epilepsy and could provide a trigger for EEG-gated CL-taVNS as a treatment for epilepsy. A recent replication study supports the diagnostic value of EEG-vigilance regulation and its usefulness as a biomarker for treatment choice in MDD (Ip et al., 2021), which can also be a candidate for switching EEG-gated CL-taVNS in treating MDD.

In addition to epilepsy and MDD, a myriad of neurological and psychiatric disorders have event-related EEG biomarkers. Therefore, EEG-gated CL-taVNS may be extended to more brain diseases in the future, including but not limited to Alzheimer's disease (AD; Chang et al., 2018; Gaubert et al., 2019), and ischaemic stroke (Ajčević et al., 2021; Dawson et al., 2021). A more in-depth systematic review should focus primarily on the EEG biomarkers of the taVNS-ameliorable brain diseases to explore potential therapeutic applications.

Previously, ear-EEG-gated CL-taVNS has been proposed to modulate attention (Ruhnau and Zaehle, 2021); however, its apparent limitations and challenges make it seem not practical. Hence, we suggest that EEG-gated CL-taVNS optimized from the original EEG headset is a more promising form (**Figure 1**).

ECG-Gated CL-taVNS

Cardiovascular diseases are often treated on the basis of inhibiting the over-excitation of the sympathetic system by pharmacological interventions, while vagal modulation has been largely ignored (Liu et al., 2019). The vagal nerve provides

the primary parasympathetic innervation to the heart. Due to the critical VNS mechanism (reducing sympathetic activity and increasing parasympathetic activity), VNS may be a therapeutic approach for chronic heart failure (De Ferrari et al., 2010). Preclinical studies applying taVNS [low-level tragus stimulation (LLTS)] in canines and rodents have shown promising results in suppressing atrial fibrillation, alleviating post-myocardial infarction, ventricular arrhythmias, and ischemia-reperfusion injury along with improving diastolic parameters in heart failure with preserved left ventricular ejection fraction (Jiang et al., 2020). Preliminary pilot clinical studies using taVNS with low-level tragus stimulation in patients with the above heart conditions have demonstrated promising results (Jiang et al., 2020). These include suppression of atrial fibrillation (Stavrakis et al., 2015, 2020), reduction of myocardial ischemia-reperfusion injury in patients with ST-segment elevation myocardial infarction (STEMI; Yu et al., 2017), antianginal effect (Zamotrinsky et al., 1997), amelioration of left ventricular strain (Tran et al., 2019), and improved endothelial function in patients with heart failure with reduced ejection fraction (Dasari et al., 2018).

ECG is a reliable tool for monitoring heart diseases. Thus, the development of an ECG-gated CL-taVNS is important and imminent. Such a system might work as follows: when an irregular ECG signal is detected, immediate taVNS may help to reduce or terminate the anomaly. The current wearable ECG device might be heavy and uncomfortable (**Figure 1**), but it is clear that a more lightweight device can be designed.

We speculate that ECG-gated CL-taVNS might be available for only a portion of patients with cardiovascular problems. Therefore, like EEG-gated CL-taVNS, a more in-depth systematic review of ECG biomarkers in cardiovascular problems amenable or otherwise to taVNS is urgently needed to inform the development of the ECG-gated CL-taVNS.

SHS-Gated CL-taVNS

SHS-gated CL-taVNS can be developed for the treatment of T2D and RA, with the capacity to detect abnormally elevated blood glucose or cytokine levels (**Figure 1**).

VNS or taVNS has potential applications in treating T2D (Johnson and Wilson, 2018). However, preclinical results are controversial. VNS has been shown to increase blood glucose levels in non-diabetic rats (Meyers et al., 2016; Stauss et al., 2018), but VNS or taVNS reduced levels in diabetic rats (Wang et al., 2015; Yin et al., 2019). These results suggest that the beneficial effects of VNS or taVNS on blood glucose levels are only apparent in the context of diabetes. Thus, it is essential to develop a blood-glucose-gated CL-taVNS which on detecting hyperglycemia would activate taVNS to reduce and stabilize the levels.

Clinical evidence shows that taVNS attenuates systemic inflammatory responses in RA patients (Addorisio et al., 2019). Thus, it is also possible to develop a cytokine-gated CL-taVNS system which would inhibit inflammatory responses on detection of abnormal cytokine levels. This system might also be applicable to other autoimmune disorders, such as systemic lupus erythematosus (Aranow et al., 2021) and Sjögren syndrome.

To our knowledge, SHS-gated CL-taVNS may also extend to other diseases, so other SHS-altered-associated internal conditions, which are reversible by taVNS, also merit a systematic review.

DISCUSSION

The Electroceuticals Through the Vagal Nerve

The vagal nerve offers an alternative means to modify brain and other organ functions *via* artificial stimulation (Moore, 2015). In recent years, electrical stimulation of the vagal nerve has progressively come into focus as a non-pharmaceutical or electroceutical treatment option for various diseases (Kaniusas et al., 2019b). Therefore, both invasive and non-invasive VNS have gained particular interest worldwide (Kaniusas et al., 2019a).

The Potential of CL-taVNS

Since its clinical applications began in the 1990s, iVNS has become a pioneering tool of vagal modulation (Moore, 2015), and 20 years of development of taVNS has refined this remarkable tool (Ventureyra, 2000). Given that other closed-loop neuromodulation studies, such as closed-loop transcranial electrical stimulation (CL-TES; Berényi et al., 2012) and closed-loop transcranial alternating current stimulation (CL-tACS; Brittain et al., 2013), show exciting results, the potential of CL-taVNS is clear, even in its infancy.

Artifacts of the Proposed CL-taVNS Systems

It is worth noting that due to the electrical peculiarities of tACS, the artifacts of tACS make it difficult (although technically possible) to parse EEG signals during stimulation (Wu et al., 2021) but viable only in intermittent closed-loop stimulation protocol, in which EEG recordings are performed before and after stimulation (Stecher et al., 2021). However, EEG-gated CL-taVNS is unaffected by these artifacts, so it will not have such a technical limitation. Also, it can be inferred that ECG-gated CL-taVNS and SHS-gated CL-taVNS will not have the same problem due to their technical properties.

Artificial Intelligence (AI) and Bluetooth in CL-taVNS and the Wearable Devices

The known CL-taVNS systems, RAVANS (Napadow et al., 2012; Garcia et al., 2017) and MAAVNS (Badran et al., 2020; Cook et al., 2020), majorly pair with behaviors, while the future CL-taVNS systems we propose rely predominantly on objective indices, such as EEG, ECG, blood glucose levels, and cytokine levels. Therefore, artificial intelligence (AI) with specific algorithms might be needed for these CL-taVNS systems. Furthermore, wireless EEG, ECG, SHS, and taVNS devices are becoming popular, and Bluetooth or similar technologies should be used for communication among these wearable devices (**Figure 1**).

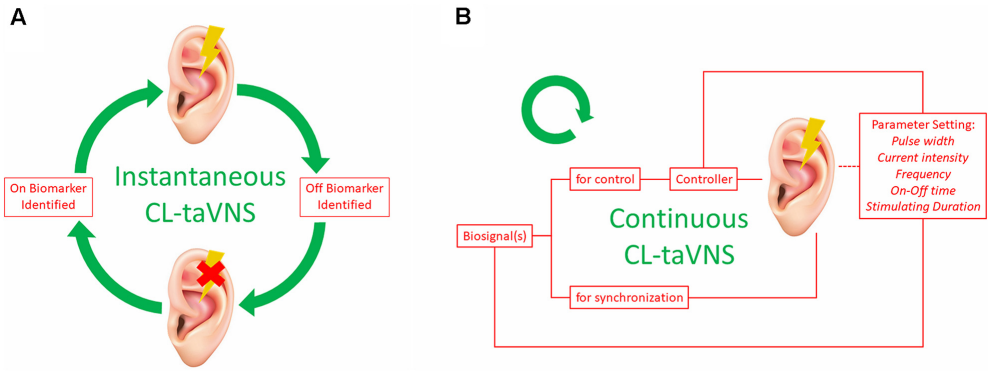

FIGURE 2 | Two Patterns of CL-taVNS. **(A)** workflow of instantaneous CL-taVNS. The system will be activated as soon as the On Biomarker is identified and deactivated when the Off Biomarker is determined by the identifier simultaneously. **(B)** Workflow of continuous CL-taVNS. The biofeedback is used to control stimulation parameters of taVNS (pulse width, current intensity, frequency, On-Off time, and stimulating duration) to adhere to momentary therapeutic needs. The biofeedback can also be used for temporal synchronization of the applied stimuli with inner body rhythms to interfere constructively with the dynamics of the body. CL-taVNS: Closed-loop transcutaneous auricular vagal nerve stimulation.

The future CL-taVNS systems we have proposed should primarily target some ongoing EEG/ECG/SHS activity biomarkers, such as the spike-and-wave patterns of epilepsy (EEG; Berényi et al., 2012) and the ST-segment elevation of myocardial infarction (ECG; Jiang et al., 2020). These biomarkers, which are condition-specific, should be identified automatically by AI, which would then immediately trigger the taVNS process to relieve the symptoms.

On-Off Biomarkers of CL-taVNS

The easiest way to close the loop is to provide a simple on-demand activation of taVNS *via* subjective biofeedback or via a biomarker from the patient (Kaniusas et al., 2019a). In all the above CL-taVNS systems, motor changes (RAVANS and MAAVNS) and abnormal EEG/ECG/SHS features are or will be employed as the biomarkers (On Biomarkers) which trigger the CL-taVNS systems. However, there is still a lack of confirmed biomarkers (Off Biomarkers) to turn off the CL-taVNS systems. End or reversal of the motor changes and normalized EEG/ECG/SHS features themselves might be possible Off Biomarkers. In addition to these, five potential neurophysiological biomarkers of taVNS include heart rate variability (which can be extracted from ECG data), vagal sensory evoked potentials, pupil diameter, event related potentials (ERP, especially P300), and salivary alpha-amylase secretion, which have been proposed in a narrative review (Burger et al., 2020). While the efficacy of taVNS biomarkers is controversial, pupil size in scotopic illumination with taVNS at 2 mA may be a reliable and non-invasive biomarker of vagal activation and could be used as a user-friendly online indicator of the stimulation's effectiveness (Capone et al., 2021) and as an Off Biomarker of CL-taVNS.

Instantaneous CL-taVNS

For some instant conditions, such as generalized absence seizure, instantaneous stimulation of the ABVN may suffice to eliminate the problem. The required stimulation may be short-term, and with the use of On-Off biomarkers, CL-taVNS may form a loop (**Figure 2A**). Briefly speaking, the system is activated and deactivated immediately with On and Off biomarkers, respectively. The existing CL-taVNS systems (RAVANS and MAAVNS) have already achieved the pattern successfully. However, additional studies are required to validate the feasibility of this workflow in the future CL-taVNS systems we proposed.

Continuous CL-taVNS

Continuous CL-taVNS has advantages for some sustained conditions such as hyperglycemia. Recording and analysis of biosignal(s) in response to taVNS may close the loop and thus allow optimization and personalization of taVNS therapy (Kaniusas et al., 2019a). The biosignal(s) should signal the controller to adjust the stimulus pattern and synchronize the stimulus. According to the biosignal changes, the controller cyclically modifies the parameter settings of taVNS (**Figure 2B**), including pulse width, current intensity, frequency, On-Off time, and stimulating duration (Thompson et al., 2021). Since the individual human body as the system to be controlled is never sufficiently known and is subjected to continuous changes over time, adaptive methods (such as AI and machine learning) might be used to define the controller (Kaniusas et al., 2019a).

SUMMARY

Optimizing from taVNS, CL-taVNS, which was formally proposed in 2020, has become a novel direction of neuromodulation. This work reviewed two known forms of CL-taVNS and proposed three future approaches. Significantly, the mechanisms, targets, technical issues, patterns of CL-taVNS, and motivations to move the method from open-loop to closed-loop were introduced and discussed. There is much

room for improvement as CL-taVNS continues to emerge as a promising neuromodulation modality.

DATA AVAILABILITY STATEMENT

The original contributions presented in the study are included in the article, further inquiries can be directed to the corresponding author/s.

AUTHOR CONTRIBUTIONS

All authors contributed to the content of this work, edited the manuscript, and approved the submission.

FUNDING

This work was supported by National Administration of Traditional Chinese Medicine (2019XZZX-JB004), Youth Project of Beijing Shijitan Hospital (2019-q04), National Natural Science Foundation of China (82104980, 82174500), and Beijing Municipal Administration of Hospitals Incubating Program (PZ2022005).

ACKNOWLEDGMENTS

Dr. YY cordially thanks Dr. Bashar W. Badran for his inspiring work.

REFERENCES

Addorisio, M. E., Imperato, G. H., de Vos, A. F., Forti, S., Goldstein, R. S., Pavlov, V. A., et al. (2019). Investigational treatment of rheumatoid arthritis with a vibrotactile device applied to the external ear. *Bioelectron. Med.* 5:4. doi: 10.1186/s42234-019-0020-4

Ajčević, M., Furlanis, G., Miladinović, A., Buoite Stella, A., Caruso, P., Ukmar, M., et al. (2021). Early EEG alterations correlate with CTP hypoperfused volumes and neurological deficit: a wireless EEG study in hyper-acute ischemic stroke. *Ann. Biomed. Eng.* 49, 2150–2158. doi: 10.1007/s10439-021-02735-w

Aranow, C., Atish-Fregoso, Y., Lesser, M., Mackay, M., Anderson, E., Chavan, S., et al. (2021). Transcutaneous auricular vagus nerve stimulation reduces pain and fatigue in patients with systemic lupus erythematosus: a randomised, double-blind, sham-controlled pilot trial. *Ann. Rheum. Dis.* 80, 203–208. doi: 10.1136/annrheumdis-2020-217872

Badran, B. W., Dowdle, L. T., Mithoefer, O. J., LaBate, N. T., Coatsworth, J., Brown, J. C., et al. (2018). Neurophysiologic effects of transcutaneous auricular vagus nerve stimulation (taVNS) *via* electrical stimulation of the tragus: a concurrent taVNS/fMRI study and review. *Brain Stimul.* 11, 492–500. doi: 10.1016/j.brs.2017.12.009

Badran, B. W., Jenkins, D. D., Cook, D., Thompson, S., Dancy, M., DeVries, W. H., et al. (2020). Transcutaneous auricular vagus nerve stimulation-paired rehabilitation for oromotor feeding problems in newborns: an open-label pilot study. *Front. Hum. Neurosci.* 14:77. doi: 10.3389/fnhum.2020.00077

Badran, B., Jenkins, D., DeVries, W., Dancy, M., Cook, D., Mappin, G., et al. (2019). Development of closed-loop transcutaneous auricular vagus nerve stimulation (taVNS) as a neurorehabilitation tool. *Brain Stimul.* 12:523. doi: 10.1016/j.brs.2018.12.721

Berényi, A., Belluscio, M., Mao, D., and Buzsáki, G. (2012). Closed-loop control of epilepsy by transcranial electrical stimulation. *Science* 337, 735–737. doi: 10.1126/science.1223154

Brittain, J.-S., Probert-Smith, P., Aziz, T. Z., and Brown, P. (2013). Tremor suppression by rhythmic transcranial current stimulation. *Curr. Biol.* 23, 436–440. doi: 10.1016/j.cub.2013.01.068

Burger, A. M., D'Agostini, M., Verkuil, B., and Van Diest, I. (2020). Moving beyond belief: a narrative review of potential biomarkers for transcutaneous vagus nerve stimulation. *Psychophysiology* 57:e13571. doi: 10.1111/psyp.13571

Capone, F., Motolese, F., Di Zazzo, A., Antonini, M., Magliozzi, A., Rossi, M., et al. (2021). The effects of transcutaneous auricular vagal nerve stimulation on pupil size. *Clin. Neurophysiol.* 132, 1859–1865. doi: 10.1016/j.clinph.2021.05.014

Castle, M., Comoli, E., and Loewy, A. (2005). Autonomic brainstem nuclei are linked to the hippocampus. *Neuroscience* 134, 657–669. doi: 10.1016/j.neuroscience.2005.04.031

Chang, C.-H., Lane, H.-Y., and Lin, C.-H. (2018). Brain stimulation in Alzheimer's disease. *Front. Psychiatry* 9:201. doi: 10.3389/fpsyt.2018.00201

Cook, D. N., Thompson, S., Stomberg-Firestein, S., Bikson, M., George, M. S., Jenkins, D. D., et al. (2020). Design and validation of a closed-loop, motor-activated auricular vagus nerve stimulation (MAAVNS) system for neurorehabilitation. *Brain Stimul.* 13, 800–803. doi: 10.1016/j.brs.2020.02.028

Dasari, T. W., Gabor, F., Csipo, T., Palacios, F. S., Yabluchanskiy, A., Samannan, R., et al. (2018). Non-invasive neuromodulation of vagus activity improves endothelial function in patients with heart failure with reduced ejection fraction: a randomized study. *J. Cardiac Failure* 24, S59–S60. doi: 10.1016/j.cardfail.2018.07.266

Dawson, J., Liu, C. Y., Francisco, G. E., Cramer, S. C., Wolf, S. L., Dixit, A., et al. (2021). Vagus nerve stimulation paired with rehabilitation for upper limb motor function after ischaemic stroke (VNS-REHAB): a randomised, blinded, pivotal, device trial. *Lancet* 397, 1545–1553. doi: 10.1016/S0140-6736(21)00475-X

De Ferrari, G. M., Crijns, H. J. G. M., Borggrefe, M., Milasinovic, G., Smid, J., Zabel, M., et al. (2010). Chronic vagus nerve stimulation: a new and promising therapeutic approach for chronic heart failure. *Eur. Heart J.* 32, 847–855. doi: 10.1093/eurheartj/ehq391

Deuchars, S. A., Lall, V. K., Clancy, J., Mahadi, M., Murray, A., Peers, L., et al. (2018). Mechanisms underpinning sympathetic nervous activity and its modulation using transcutaneous vagus nerve stimulation. *Exp. Physiol.* 103, 326–331. doi: 10.1113/EP086433

Fang, J., Rong, P., Hong, Y., Fan, Y., Liu, J., Wang, H., et al. (2016). Transcutaneous vagus nerve stimulation modulates default mode network in major depressive disorder. *Biol. Psychiatry* 79, 266–273. doi: 10.1016/j.biopsych.2015.03.025

Fisher, H., Stowell, J., Garcia, R., Sclocco, R., Goldstein, J., Napadow, V., et al. (2018). "Acute effects of respiratory-gated auricular vagal afferent nerve stimulation (RAVANS) in the modulation of blood pressure in hypertensive patients," in *2018 Computing in Cardiology Conference (CinC)*, Vol. 45, 1–4. doi: 10.22489/CinC.2018.346

Garcia, R. G., Lin, R. L., Lee, J., Kim, J., Barbieri, R., Sclocco, R., et al. (2017). Modulation of brainstem activity and connectivity by respiratory-gated auricular vagal afferent nerve stimulation (RAVANS) in migraine patients. *Pain* 158, 1461–1472. doi: 10.1097/j.pain.0000000000000930

Gaubert, S., Raimondo, F., Houot, M., Corsi, M.-C., Naccache, L., Diego Sitt, J., et al. (2019). EEG evidence of compensatory mechanisms in preclinical Alzheimer's disease. *Brain* 142, 2096–2112. doi: 10.1093/brain/awz150

Ip, C.-T., Ganz, M., Dam, V. H., Ozenne, B., Rüesch, A., Köhler-Forsberg, K., et al. (2021). NeuroPharm study: EEG wakefulness regulation as a biomarker in MDD. *J. Psychiatr. Res.* 141, 57–65. doi: 10.1016/j.jpsychires.2021.06.021

Jiang, Y., Po, S. S., Amil, F., and Dasari, T. W. (2020). Non-invasive low-level tragus stimulation in cardiovascular diseases. *Arrhythm. Electrophysiol. Rev.* 9, 40–46. doi: 10.15420/aer.2020.01

Johnson, R. L., and Wilson, C. G. (2018). A review of vagus nerve stimulation as a therapeutic intervention. *J. Inflamm. Res.* 11, 203–213. doi: 10.2147/JIR.S163248

Kaniusas, E., Kampusch, S., Tittgemeyer, M., Panetsos, F., Gines, R. F., Papa, M., et al. (2019a). Current directions in the auricular vagus nerve stimulation II - an engineering perspective. *Front. Neurosci.* 13:772. doi: 10.3389/fnins.2019.00772

Kaniusas, E., Kampusch, S., Tittgemeyer, M., Panetsos, F., Gines, R. F., Papa, M., et al. (2019b). Current directions in the auricular vagus nerve stimulation I - a physiological perspective. *Front. Neurosci.* 13:854. doi: 10.3389/fnins.2019.00854

Lanska, D. J. (2002). JL Corning and vagal nerve stimulation for seizures in the 1880s. *Neurology* 58, 452–459. doi: 10.1212/wnl.58.3.452

Liu, L., Zhao, M., Yu, X., and Zang, W. (2019). Pharmacological modulation of vagal nerve activity in cardiovascular diseases. *Neurosci. Bull.* 35, 156–166. doi: 10.1007/s12264-018-0286-7

Meyers, E. E., Kronemberger, A., Lira, V., Rahmouni, K., and Stauss, H. M. (2016). Contrasting effects of afferent and efferent vagal nerve stimulation on insulin secretion and blood glucose regulation. *Physiol. Rep.* 4:e12718. doi: 10.14814/phy2.12718

Moini, J., and Piran, P. (2020). "Chapter 10 - Cranial nerves," in *Functional and Clinical Neuroanatomy*, eds J. Moini and P. Piran (Academic Press), 319–344. doi: 10.1016/B978-0-12-817424-1.00010-0

Moore, S. (2015). *The Vagus Nerve: A Back Door for Brain Hacking.* New York, NY: IEEE Spectrum.

Mumtaz, W., Xia, L., Ali, S. S. A., Yasin, M. A. M., Hussain, M., and Malik, A. S. (2017). Electroencephalogram (EEG)-based computer-aided technique to diagnose major depressive disorder (MDD). *Biomed. Signal Process. Control* 31, 108–115. doi: 10.1016/j.bspc.2016.07.006

Napadow, V., Edwards, R. R., Cahalan, C. M., Mensing, G., Greenbaum, S., Valovska, A., et al. (2012). Evoked pain analgesia in chronic pelvic pain patients using respiratory-gated auricular vagal afferent nerve stimulation. *Pain Med.* 13, 777–789. doi: 10.1111/j.1526-4637.2012.01385.x

Noachtar, S., and Rémi, J. (2009). The role of EEG in epilepsy: a critical review. *Epilepsy Behav.* 15, 22–33. doi: 10.1016/j.yebeh.2009.02.035

Paleczny, B., Seredyński, R., and Ponikowska, B. (2021). Inspiratory-and expiratory-gated transcutaneous vagus nerve stimulation have different effects on heart rate in healthy subjects: preliminary results. *Clin. Auton. Res.* 31, 205–214. doi: 10.1007/s10286-019-00604-0

Ricardo, J. A., and Koh, E. T. (1978). Anatomical evidence of direct projections from the nucleus of the solitary tract to the hypothalamus, amygdala and other forebrain structures in the rat. *Brain Res.* 153, 1–26. doi: 10.1016/0006-8993(78)91125-3

Rong, P., Liu, J., Wang, L., Liu, R., Fang, J., Zhao, J., et al. (2016). Effect of transcutaneous auricular vagus nerve stimulation on major depressive disorder: a nonrandomized controlled pilot study. *J. Affect. Dis.* 195, 172–179. doi: 10.1016/j.jad.2016.02.031

Rong, P., Liu, A., Zhang, J., Wang, Y., He, W., Yang, A., et al. (2014). Transcutaneous vagus nerve stimulation for refractory epilepsy: a randomized controlled trial. *Clin. Sci. (Lond)* doi: 10.1042/CS20130518. [Online ahead of print].

Ruhnau, P., and Zaehle, T. (2021). Transcranial auricular vagus nerve stimulation (taVNS) and ear-EEG: potential for closed-loop portable non-invasive brain stimulation. *Front. Hum. Neurosci.* 15:699473. doi: 10.3389/fnhum.2021.699473

Schachter, S. C., and Saper, C. B. (1998). Vagus nerve stimulation. *Epilepsia* 39, 677–686. doi: 10.1111/j.1528-1157.1998.tb01151.x

Stauss, H. M., Stangl, H., Clark, K. C., Kwitek, A. E., and Lira, V. A. (2018). Cervical vagal nerve stimulation impairs glucose tolerance and suppresses insulin release in conscious rats. *Physiol. Rep.* 6:e13953. doi: 10.14814/phy2.13953

Stavrakis, S., Humphrey, M. B., Scherlag, B. J., Hu, Y., Jackman, W. M., Nakagawa, H., et al. (2015). Low-level transcutaneous electrical vagus nerve stimulation suppresses atrial fibrillation. *J. Am. Coll. Cardiol.* 65, 867–875. doi: 10.1016/j.jacc.2014.12.026

Stavrakis, S., Stoner, J. A., Humphrey, M. B., Morris, L., Filiberti, A., Reynolds, J. C., et al. (2020). TREAT AF (transcutaneous electrical vagus nerve stimulation to suppress atrial fibrillation): a randomized clinical trial. *JACC Clin. Electrophysiol.* 6, 282–291. doi: 10.1016/j.jacep.2019.11.008

Stecher, H. I., Notbohm, A., Kasten, F. H., and Herrmann, C. S. (2021). A comparison of closed loop vs. fixed frequency tACS on modulating brain oscillations and visual detection. *Front. Hum. Neurosci.* 15:661432. doi: 10.3389/fnhum.2021.661432

Stowell, J., Garcia, R. G., Staley, R., Sclocco, R., Fisher, H., Napadow, V., et al. (2019). "Dose-optimization of respiratory-gated auricular vagal afferent nerve stimulation (RAVANS) for blood pressure modulation in hypertensive patients," in *2019 Computing in Cardiology Conference (CinC)*, (IEEE), Vol. 46, 1–4. doi: 10.22489/CinC.2019.098

Ter Horst, G., De Boer, P., Luiten, P., and Van Willigen, J. (1989). Ascending projections from the solitary tract nucleus to the hypothalamus. A phaseolus vulgaris lectin tracing study in the rat. *Neuroscience* 31, 785–797. doi: 10.1016/0306-4522(89)90441-7

Thompson, S. L., O'Leary, G. H., Austelle, C. W., Gruber, E., Kahn, A. T., Manett, A. J., et al. (2021). A Review of parameter settings for invasive and non-invasive Vagus Nerve Stimulation (VNS) applied in neurological and psychiatric disorders. *Front. Neurosci.* 15:709436. doi: 10.3389/fnins.2021.709436

Tran, N., Asad, Z., Elkholey, K., Scherlag, B. J., Po, S. S., and Stavrakis, S. (2019). Autonomic neuromodulation acutely ameliorates left ventricular strain in humans. *J. Cardiovasc. Transl. Res.* 12, 221–230. doi: 10.1007/s12265-018-9853-6

Van Eden, C. G., and Buijs, R. M. (2000). "Functional neuroanatomy of the prefrontal cortex: autonomic interactions," in *Progress in Brain Research*, (Elsevier), 49–62. doi: 10.1016/S0079-6123(00)26006-8

Ventureyra, E. C. (2000). Transcutaneous vagus nerve stimulation for partial onset seizure therapy. *Childs Nerv. Syst.* 16, 101–102. doi: 10.1007/s003810050021

Wang, Y., Li, S.-Y., Wang, D., Wu, M.-Z., He, J.-K., Zhang, J.-L., et al. (2021). Transcutaneous auricular vagus nerve stimulation: from concept to application. *Neurosci. Bull.* 37, 853–862. doi: 10.1007/s12264-020-00619-y

Wang, S., Zhai, X., Li, S., McCabe, M. F., Wang, X., and Rong, P. (2015). Transcutaneous vagus nerve stimulation induces tidal melatonin secretion and has an antidiabetic effect in zucker fatty rats. *PLoS One* 10:e0124195. doi: 10.1371/journal.pone.0124195

Wu, L., Liu, T., and Wang, J. (2021). Improving the effect of transcranial alternating current stimulation (tACS): a systematic review. *Front. Hum. Neurosci.* 15:652393. doi: 10.3389/fnhum.2021.652393

Yin, J., Ji, F., Gharibani, P., and Chen, J. D. (2019). Vagal nerve stimulation for glycemic control in a rodent model of type 2 diabetes. *Obes. Surg.* 29, 2869–2877. doi: 10.1007/s11695-019-03901-9

Yu, Y., He, X., Zhang, J., Tang, C., and Rong, P. (2021). Transcutaneous auricular vagal nerve stimulation inhibits hypothalamic P2Y1R expression and attenuates weight gain without decreasing food intake in Zucker diabetic fatty rats. *Sci. Prog.* 104:00368504211009669. doi: 10.1177/00368504211009669

Yu, L., Huang, B., Po, S. S., Tan, T., Wang, M., Zhou, L., et al. (2017). Low-level tragus stimulation for the treatment of ischemia and reperfusion injury in patients with ST-segment elevation myocardial infarction: a proof-of-concept study. *JACC Cardiovasc. Interv.* 10, 1511–1520. doi: 10.1016/j.jcin.2017.04.036

Zamotrinsky, A., Afanasiev, S., Karpov, R. S., and Cherniavsky, A. (1997). Effects of electrostimulation of the vagus afferent endings in patients with coronary artery disease. *Coron. Artery Dis.* 8, 551–557.

Conflict of Interest: The authors declare that the research was conducted in the absence of any commercial or financial relationships that could be construed as a potential conflict of interest.

Publisher's Note: All claims expressed in this article are solely those of the authors and do not necessarily represent those of their affiliated organizations, or those of the publisher, the editors and the reviewers. Any product that may be evaluated in this article, or claim that may be made by its manufacturer, is not guaranteed or endorsed by the publisher.

frontiers in Human Neuroscience

ORIGINAL RESEARCH
published: 06 January 2022
doi: 10.3389/fnhum.2021.738605

Local and Transient Changes of Sleep Spindle Density During Series of Prefrontal Repetitive Transcranial Magnetic Stimulation in Patients With a Major Depressive Episode

*Takuji Izuno[1,2], Takashi Saeki[1,3], Nobuhide Hirai[4], Takuya Yoshiike[1,5], Masataka Sunagawa[2] and Motoaki Nakamura[1,6]**

[1] Laboratory of Neuromodulation, Kanagawa Psychiatric Center, Yokohama, Japan, [2] Department of Physiology, Showa University School of Medicine, Showa University, Tokyo, Japan, [3] Department of Psychiatry, Yokohama City University School of Medicine, Yokohama, Japan, [4] Department of Neuropsychiatry, Graduate School of Medicine, Tokyo Medical and Dental University, Tokyo, Japan, [5] Department of Sleep-Wake Disorders, National Institute of Mental Health, National Center of Neurology and Psychiatry, Tokyo, Japan, [6] Medical Institute of Developmental Disabilities Research, Showa University, Tokyo, Japan

OPEN ACCESS

Edited by:
Alia Benali,
Hertie Institute for Clinical Brain Research, Germany

Reviewed by:
Vishnudev Ramachandra, Computational Sensomotorics, Germany
Klaus Funke, Ruhr University Bochum, Germany

***Correspondence:**
Motoaki Nakamura
motoaki@motoaki.com

Specialty section:
This article was submitted to Brain Imaging and Stimulation, a section of the journal Frontiers in Human Neuroscience

Received: *09 July 2021*
Accepted: *13 December 2021*
Published: *06 January 2022*

Citation:
Izuno T, Saeki T, Hirai N, Yoshiike T, Sunagawa M and Nakamura M (2022) Local and Transient Changes of Sleep Spindle Density During Series of Prefrontal Repetitive Transcranial Magnetic Stimulation in Patients With a Major Depressive Episode. Front. Hum. Neurosci. 15:738605. doi: 10.3389/fnhum.2021.738605

The neuromodulatory effects of brain stimulation therapies notably involving repetitive transcranial magnetic stimulation (rTMS) on nocturnal sleep, which is critically disturbed in major depression and other neuropsychiatric disorders, remain largely undetermined. We have previously reported in major depression patients that prefrontal rTMS sessions enhanced their slow wave activity (SWA) power, but not their sigma power which is related to sleep spindle activity, for electrodes located nearby the stimulation site. In the present study, we focused on measuring the spindle density to investigate cumulative effects of prefrontal rTMS sessions on the sleep spindle activity. Fourteen male inpatients diagnosed with medication-resistant unipolar or bipolar depression were recruited and subjected to 10 daily rTMS sessions targeting the left dorsolateral prefrontal cortex (DLPFC). All-night polysomnography (PSG) data was acquired at four time points: Adaptation, Baseline, Post-1 (follow-up after the fifth rTMS session), and Post-2 (follow-up after the tenth rTMS session). Clinical and cognitive evaluations were longitudinally performed at Baseline, Post-1, and Post-2 time points to explore associations with the spindle density changes. The PSG data from 12 of 14 patients was analyzed to identify sleep spindles across the sleep stages II–IV at four electrode sites: F3 (frontal spindle near the stimulation site), F4 (contralateral homologous frontal region), P3 (parietal spindle in the hemisphere ipsilateral to the stimulation site), and P4 (contralateral parietal region). Statistical analysis by two-way ANOVA revealed that spindle density at F3 increased at Post-1 but decreased at Post-2 time points. Moreover, the local and transient increase of spindle density at F3 was associated with the previously reported SWA power increase at F3, possibly reflecting a shared mechanism of thalamocortical synchronization locally enhanced by diurnal prefrontal rTMS sessions.

Clinical and cognitive correlations were not observed in this dataset. These findings suggest that diurnal rTMS sessions transiently modulate nocturnal sleep spindle activity at the stimulation site, although clinical and cognitive effects of the local changes warrant further investigation.

Keywords: repetitive transcranial magnetic stimulation, sleep spindle, slow wave sleep, neuroplasticity, sleep disturbance, major depression

INTRODUCTION

Sleep-related complaints that are most frequently accompanied by a depressive episode are not only symptoms but also risk factors for mood disorders (Baglioni et al., 2011). During a major depressive episode, insomnia and hypersomnia are, respectively, reported in approximately 80% and 15–35% of patients (Steiger and Pawlowski, 2019). Even in partial or complete remission phase, 43% of patients suffer from insomnia, while residual insomnia is a risk factor for non-remission (Yoshiike et al., 2017, 2020). Sleep abnormalities observed in major depression are characterized by sleep fragmentation, disinhibition of rapid eye movement (REM) sleep, and inhibition of non-REM (NREM) sleep (Benca et al., 1997; Armitage, 2007). More specifically, sleep fragmentation comprises prolonged sleep latency, frequently interrupted sleep, and early-morning awakening. The disinhibition of REM sleep involves shortening of REM latency, increased REM density during the first REM period, and prolonged REM periods. Finally, inhibition of NREM sleep implicates decreased stage II and slow wave sleep (stages III and IV), which can result in excessive daytime sleepiness.

Most antidepressants inhibit the abnormally enhanced REM sleep in depressive patients (Dunleavy et al., 1972; Kluge et al., 2007) but also normal REM sleep in healthy volunteers (von Bardeleben et al., 1989). This pharmacological effect on REM sleep suppression may underlie the therapeutic actions of antidepressants, considering the reported antidepressant effects of selective REM sleep deprivation (Vogel et al., 1975). Meanwhile, it was also shown that some antidepressants increase the delta band power during NREM sleep (Chen, 1979; Kluge et al., 2007).

Unlike medication, brain stimulation therapies for depression such as electroconvulsive therapy (ECT) and repetitive transcranial magnetic stimulation (rTMS) do not affect the sleeping brain directly. To date, little attention has been paid about the neuromodulatory effects of diurnal brain stimulation therapies on nocturnal sleep. It has been reported that ECT administration in medicated patients with major depression suppressed REM density, especially for the first REM period, and increased NREM sleep, especially slow wave sleep (Hoffmann et al., 1985; Goder et al., 2016). Although these findings are intriguing, it remains unclear whether these changes of sleep characteristics are due to primary or secondary effects of a series of ECT sessions. It should be underscored here that any localized changes of NREM or REM sleep were not reported in previous sleep studies evaluating the effects of antidepressants or ECT.

As compared with ECT, rTMS performed with a figure 8-shaped coil achieves a focal neurostimulation with a spatial resolution of 5–10 mm over superficial cerebral cortices (Jalinous, 1991). Since the TMS-induced action potentials spread *via* commissural, association, and projection fibers, rTMS is highly selective to their corresponding neuronal circuitries (Pascual-Leone et al., 2011). Considering this selectivity, the reciprocal thalamocortical circuitry, underlying the synchronized nature of NREM sleep, may be locally affected by rTMS. A seminal work by Huber et al. (2007) demonstrated in healthy volunteers that high-frequency rTMS over the motor cortex induced cortical potentiation in the ipsilateral premotor cortex as an immediate after effect, resulting in local enhancement of slow wave activity (SWA) in the same region during subsequent sleep.

Inspired by their work, we have previously reported that high-frequency rTMS sessions over the left dorsolateral prefrontal cortex (DLPFC) in patients with major depression locally enhanced SWA power around the stimulation site during nocturnal sleep (Saeki et al., 2013). However, the sigma (11–15 Hz) power indicative of sleep spindle activity during NREM sleep did not change significantly over time. We postulated that not only SWA power but also sigma power may increase following the rTMS sessions, because the thalamocortical synchronization during NREM sleep involves thalamocortical neurons as well as thalamic reticular neurons serving as a spindle oscillator (Steriade et al., 1993). In the present study, we focused on the spindle density, the occurrence rate of sleep spindles, rather than the sigma power, to provide further insights into a different aspect of the sleep spindle activity.

To our knowledge, no study has reported yet the rTMS induced alteration of sleep spindle activity in patients with major depression. All-night natural sleep EEG recordings were carried out four times throughout the present study protocol, including 10 sequential rTMS sessions over the left DLPFC across 2 weeks, allowing to evaluate their cumulative effects on the sleep spindle activity. We hypothesized that the prefrontal sleep spindle density can be locally enhanced by rTMS sessions, as it shares an underlying mechanism with the previously reported enhancement of prefrontal SWA power.

MATERIALS AND METHODS

Study Participants

Inpatients with a DSM-IV-TR (APA, 2000) diagnostic of monopolar or bipolar depression were recruited for this open-label study. It should be noted here that participants and their entire dataset are completely identical to our previous study (Saeki et al., 2013). Participants with major sleep disorders (AASM, 2005) such as sleep apnea, circadian

rhythm disorder, parasomnia, narcolepsy, or other primary sleep disorders were excluded from this study. Participants with a history of neurological disorders, epilepsy, head trauma, or substance abuse were similarly excluded. Those meeting contraindications for TMS such as intracranial ferromagnetic implants and a cardiac pacemaker were also excluded. According to these criteria, fourteen male inpatients were recruited at the Kanagawa Psychiatric Center, Yokohama, Japan. Only male patients were recruited considering that only male staff was available to monitor the patients during all-night PSG recordings, performed in an EEG room within a different building from their inpatients ward. All participants suffered from insomnia related to major depressive episodes as defined by the DSM-IV-TR. The participants underwent 10 daily rTMS sessions, clinical and neuropsychological evaluation, and all-night polysomnography (PSG) recordings for four nights including an adaptation night.

This study was approved by the ethics committee of the Kanagawa Psychiatric Center (KPC201107, UMIN000001185). Prior to study participation, every participant provided a written informed consent based on the Declaration of Helsinki.

Due to significant recording artifacts caused by electrode instability and oversensing of electromyographic activity, PSG data from two participants was excluded from the analysis. Consequently, data from 12 out of the 14 patients (mean age of 47.5 ± 6.3 years) was analyzed, including seven patients with unipolar depression and five patients with bipolar depression. Also, one patient could not complete the fourth night of PSG recording for personal reasons. For this patient, data for the first three nights of PSG recording are included in the present analyses.

Experimental Design

Methodological details of the present study are described elsewhere (Saeki et al., 2013). Briefly, in the present open-label study, participants underwent 10 daily rTMS sessions and four all-night PSG recordings, as well as longitudinal clinical and cognitive evaluations during hospitalization. An outline of the experimental protocol is illustrated in **Figure 1A**. Of note, medication protocols were kept unchanged throughout the study period in order to minimize potential effects of medication changes on PSG and clinical symptoms.

Repetitive Transcranial Magnetic Stimulation Procedure

In a daily rTMS session, 1,000 pulses were delivered as 25 trains of 40 pulses at 20 Hz with an intertrain interval of 28 s. According to the participants' tolerability, the intensity of rTMS was adjusted to represent between 80 and 110% of the individual resting motor threshold. During a 2-week period of hospitalization, 10 daily rTMS sessions were administered corresponding to 10,000 pulses in total received for each participant. Of note, every rTMS session was performed between 9 am and noon, allowing to evaluate the cumulative effects rather than the acute after effect of rTMS sessions on the PSG recording performed later during the same day.

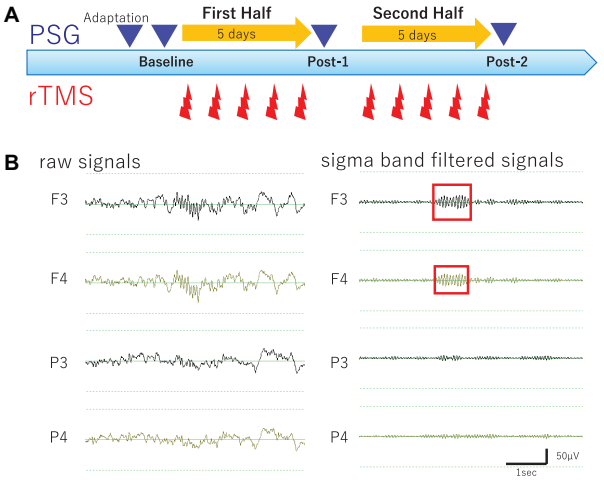

FIGURE 1 | Study Protocol and Raw EEG data. **(A)** Experimental protocol. Diagram illustrates the experimental protocol of the present study. To evaluate cumulative effects of diurnal rTMS sessions on the nocturnal sleep, PSG recordings were performed over four nights: Adaptation, Baseline, Post-1 (after the fifth rTMS session), and Post-2 (after the tenth rTMS session). In each rTMS session over left DLPFC, 1,000 pulses were delivered as 25 trains of 2 s at 20 Hz with an intertrain interval of 28 s. **(B)** Raw EEG data of all night polysomnography recordings. An example of raw EEG data was illustrated from four monopolar derivations of F3, F4, P3, and P4 during NREM Stage II sleep. Sigma band filtered signals were illustrated at the right.

The above-described high-frequency rTMS was delivered to the left DLPFC, using a Magstim Rapid system (Magstim Company Ltd., United Kingdom) with an air-cooled figure 8-shaped coil (70 mm; Magstim). To deliver precise and consistent stimulation, the TMS coil center location, where is at the middle third of the middle frontal gyrus, was determined by a real-time ultrasound-based navigation system (zebris Medical GmbH, Germany; BrainVoyager TMS Neuronavigator, Brain Innovation, Netherlands), combined with a 3D reconstruction image from the individual brain magnetic resonance imaging (MRI) data. During a rTMS session, the TMS coil was held by hand with an appropriate pitch and roll angle tangentially to the scalp and with a yaw angle parallel to the sagittal plane.

Polysomnography, Clinical, and Cognitive Data Acquisition

Each participant underwent PSG recordings during natural sleep from 9 pm to 6 am to acquire the following four PSG data; PSG data of adaptation night (Adaptation), baseline PSG data before the rTMS session (Baseline), follow-up PSG data after the fifth rTMS session (Post-1), and follow-up PSG data after the tenth rTMS session (Post-2). All-night PSG recordings were performed using a digital amplifier (Grass Technologies, West Warwick, RI), an elastic cap of 19 electrodes of the international 10–20 system for electroencephalography (EEG) measurement, and additional electrodes for electromyography (EMG) as well as electrooculography (EOG) measurements. During recording, skin-electrode impedance was kept below

10 kΩ. Band-pass filter (0.3–70 Hz) was applied to raw EEG signals with sampling rate of 400 Hz.

For clinical/cognitive evaluation, the 24-item Hamilton Depression Rating Scale (HAM-D 24) (Hamilton, 1960; Mazure et al., 1986), Beck Depression Inventory (BDI) (Beck et al., 1961), Wisconsin Card Sorting Test (WCST) (Grant and Berg, 1948), and word fluency test (Benton and Hamsher, 1976) were longitudinally assessed to explore possible changes following rTMS sessions and their correlations with PSG changes. Also, the five principal sleep disturbance components of the HAM-D (Milak et al., 2005) and the Kwansei Gakuin Sleepiness Scale (KSS) (Ishihara et al., 1982) were longitudinally evaluated to assess subjective sleep-related complaints of patients with major depressive episodes.

All-Night Sleep Electroencephalography Data Analysis

Electroencephalography signals of the 19 monopolar derivations, chin EMG, and EOG were displayed on a computer screen using the sleep EEG browser/analyzer software (AWA) originally developed by one of the authors (NH). Every 30-s epoch with prominent artifacts was visually removed from the analysis. Firstly, sleep stage scoring was visually conducted for every 30-s epoch according to the standard Rechtschaffen-Kales criteria (Rechtschaffen and Kales, 1968). Secondly, spectral power values (μV^2) of the delta (0.5–5 Hz) and sigma band (11–15 Hz) were calculated as power spectrum density for every 30-s epoch using Discrete Fourier Transform implemented in AWA (see Saeki et al., 2013 for detail). Thirdly, sleep spindles were visually identified by a single rater (TI) to investigate the sleep spindle density in NREM Sleep Stages II–IV. Finally, the amplitude, which is an average potential based on root-mean-square values, and the duration of each bandpass filtered (11–15 Hz) spindle waveform were measured using AWA to investigate morphological changes of spindle waveform over time. Of particular note, the rater was completely blinded to the data profiles such as identification of participants and time points of the PSG recordings. To this end, all PSG data files were completely renamed using a random number table exclusively for this analysis by a database manager (SO) and their header information including the subject profiles were totally excluded. The correspondence table of the PSG data file name linked to subject profile was password-protected by the database manager and thus inaccessible to everyone else until the analysis completion.

Sleep spindles were defined as waxing and waning waveform of sigma band oscillations lasting for 0.5–2.0 s during Stages II–IV, including two kinds of parietal and frontal spindles (Nakamura et al., 2003). Sleep spindle density was calculated as total number of sleep spindles per minute during Stages II–IV. In order to investigate a locality of rTMS-induced changes of the sleep spindle density over time, the following four electrode sites were selected for analysis: F3 (frontal spindle near the stimulation site of rTMS), F4 (contralateral homologous frontal region), P3 (parietal spindle in the hemisphere ipsilateral to the stimulation site), and P4 (contralateral parietal region). Spindle waveforms were visually identified based on the above definition at each electrode in Stages II–IV, after EEG signal was processed by the sigma band-pass filter (11–15 Hz). Intra-rater reliability of sleep spindle detection was evaluated in order to confirm its methodological consistency. To this end, an independent dataset was created by a database manager (SO). In this dataset, PSG data were renamed so that the subject name and test timing information would not be known to the rater (TI). The randomly selected eight PSG recordings were duplicated with different names as two distinct data. For each dataset, the sleep spindle waves of the F3, F4, P3, and P4 electrodes were visually identified. Thus, this dataset provided 32 pairs of spindle density values. The intra-rater reliability of sleep spindle density in the 32 pairs was 0.95 as assessed using Cronbach's alpha, which was reasonably high. Additionally, the validity of the visually detected sleep spindles was estimated by determining the correlation between the averaged spindle density and the automatically calculated sigma power at corresponding electrode sites. Observed significant cross-sectional correlations ($r = 0.576$, $p < 0.0001$, $N = 35$) between the spindle density and sigma power density may indirectly validate the use of the present manual method to assess sleep spindle density.

Statistical Analysis

Using SPSS software (version 23.0; SPSS Inc., Chicago, IL), the averaged sleep spindle densities at the selected four electrode sites (F3, F4, P3, and P4) were analyzed by two-way repeated-measures analysis of variance (ANOVA) with "time" and "electrode site" as the within-subject factors. When main effects of time and/or time-by-site interaction were statistically significant in the two-way ANOVA model, one-way ANOVAs and subsequent paired *t*-tests were performed as *post hoc* tests. *Bonferroni* correction was applied to each *post hoc* test, setting alpha levels of 0.0125 for one-way ANOVAs and 0.0167 for paired *t*-tests. Physiological correlations among spindle densities and sigma/delta powers and clinical/cognitive correlations with spindle densities were analyzed by Pearson's or Spearman's correlation analyses, depending on the Shapiro-Wilk normality test. The alpha level of the exploratory correlation analyses was set at 0.05 without any correction for multivariate correlations.

RESULTS

The two-way ANOVA analysis of spindle density with the within-subject factors "time" (Baseline, Post-1, and Post-2) and "site" (for the visually analyzed four electrode sites; F3, F4, P3, and P4) revealed a significant main effect of site [$F_{(3,30)} = 5.542$, $p = 0.004$] and also a significant time-by-site interaction [$F_{(6,60)} = 3.193$, $p = 0.009$], while a main effect of time [$F_{(2,20)} = 2.295$, $p = 0.127$] was not statistically significant. As reflected by the significant main effect of site, parietal spindles were more frequently observed than frontal spindles, which is compatible with the findings form previous studies (Nakamura et al., 2003).

Considering that the time-by-site interaction was significant, *post hoc* one-way ANOVA was performed for each electrode

TABLE 1 | Sleep variables.

					P-value (paired *T* test)			
	Adaptation	**Baseline**	**Post-1**	**Post-2**	**Adaptation vs. Baseline**	**Baseline vs. Post-1**	**Baseline vs. Post-2**	**Post-1 vs. Post-2**
TST (SD) [minutes]	462.5 (48.6)	469.3 (53.6)	449.5 (63.2)	452.4 (42.8)	0.664	0.308	0.367	0.517
Stage I (SD) [minutes]	100.7 (41.8)	101.5 (43.0)	85.8 (34.5)	95.2 (25.6)	0.958	0.112	0.877	0.135
Stage II–IV (SD) [minutes]	268.4 (68.4)	259.9 (73.6)	270.5 (71.1)	273.9 (42.7)	0.345	0.359	0.344	0.814
REM (SD) [minutes]	96.1 (39.2)	111.8 (56.7)	96.1 (37.3)	83.3 (22.2)	0.227	0.410	0.106	0.246
WASO (SD) [times]	3.3 (2.6)	4.1 (3.8)	2.4 (3.2)	3.1 (2.4)	0.399	0.122	0.190	0.111
WASO (SD) [minutes]	11.3 (9.6)	13.2 (12.5)	11.0 (14.8)	23.3 (24.3)	0.563	0.591	0.156	0.103
%TST								
Stage I (SD) [%]	22.4 (8.9)	22.3 (9.5)	20.2 (8.5)	21.5 (5.4)	0.984	0.484	0.805	0.399
Stage II–IV (SD) [%]	59.0 (12.3)	55.6 (13.8)	60.9 (10.7)	61.8 (7.2)	0.231	0.033*	0.191	0.904
REM (SD) [%]	21.2 (8.3)	24.0 (12.8)	21.8 (7.4)	18.7 (4.5)	0.287	0.554	0.144	0.132

*TST, Total Sleep Time; SD, Standard Deviation; REM, Rapid Eye Movement; WASO, Wake After Sleep Onset; *: P < 0.05.*

TABLE 2 | Descriptive data.

	Baseline	**Post-1**	**Post-2**	*P*-value (paired *T* tests)		
				Baseline vs. Post-1	**Baseline vs. Post-2**	**Post-1 vs. Post-2**
total time of NREM (Stage II–IV) (SD) [minutes]	259.9 (73.6)	270.5 (71.1)	273.9 (42.7)	0.359	0.344	0.814
F3 total number of spindle (SD) [number]	874.9 (506.5)	1277.1 (747.9)	957.4 (620.6)	0.012*	0.390	0.077
F3 spindle density (SD) [number/time]	3.5 (1.7)	4.8 (2.5)	3.5 (2.2)	0.008*	0.961	0.044
F4 total number of spindle (SD) [number]	723.5 (429.1)	774.6 (406.8)	756.7 (404.3)	0.446	0.763	0.650
F4 spindle density (SD) [number/time]	2.9 (1.6)	2.9 (1.3)	2.7 (1.3)	0.905	0.479	0.183
P3 total number of spindle (SD) [number]	1003.3 (582.6)	1058.5 (580.4)	1134.4 (595.8)	0.538	0.192	0.258
P3 spindle density (SD) [number/time]	3.9 (1.9)	3.9 (2.0)	4.1 (2.0)	0.857	0.441	0.175
P4 total number of spindle (SD) [number]	1023.8 (554.4)	1126.3 (500.4)	1068.2 (543.6)	0.227	0.431	0.660
P4 spindle density (SD) [number/time]	4.0 (2.0)	4.1 (1.7)	3.9 (1.9)	0.730	0.671	0.589

*SD, Standard Deviation; number, total number of spindles; time, total minutes of Stage II–IV; NREM, Non-REM Stage II–IV; *: P < 0.0167.*

site. The main effect of time was significant at F3 electrode [$F_{(2,20)} = 5.519$, $p = 0.012$] but not significant at the three other sites. Subsequently, *post-hoc* paired-*t* tests at the F3 electrode showed that the spindle density increased significantly between Baseline and Post-1 ($t_{11} = -3.265$, $p = 0.008$, Cohen's $d = 0.58$) and exhibited a decreasing trend between Post-1 and Post-2 $t_{11} = 2.304$, $p = 0.044$, Cohen's $d = 0.53$ (**Table 2** and **Figure 2**). No significant difference in spindle density at F3 was found between the Baseline and Post-2 time points. **Figure 1B** illustrates the longitudinal changes of sleep spindle density measured at each electrode site, emphasizing the sleep spindle density increase for the F3 electrode, located nearby the stimulation site in the serial rTMS sessions. Descriptive statistics values are summarized in **Table 1** along with the percentages of sleep stages across the total sleep time. At Post-1, density of the frontal spindles from F3 electrode increased to reach the same level as the parietal spindles from P3/P4 electrodes before returning to the level of frontal spindles at Post-2.

The most important electrophysiological correlational finding from the present study was the positive correlation between the spindle density increase and the previously reported delta power increase of SWA at the F3 electrode between Baseline and Post-1 ($\rho = 0.587$, $p = 0.045$, $N = 12$) (**Figure 3A**). This finding suggests that the two rTMS-associated EEG changes during NREM stages may be concomitant within the thalamocortical network. Additionally, the frontal spindle density increase at F3 between Baseline and Post-1 was inversely correlated with its decrease between Post-1 and Post-2 ($r = 0.798$, $p = 0.003$, $N = 11$) (**Figure 3B**). This change may result from a homeostatic regulation of sleep spindle activity. Although the sleep spindle density was cross-sectionally correlated with the sigma power during NREM period as in the section "Materials and methods," their longitudinal changes between Baseline and Post-1 were not correlated at F3 ($r = 0.095$, $p = 0.77$, $N = 12$) and at other electrode sites.

To interpret the background underlying the discrepancy between the increased spindle density and unchanged sigma power density at Post-1, we measured the amplitude and duration of each spindle waveform at F3 electrode. As summarized in **Table 3**, the absolute number of sleep spindles at F3 increased at Post-1 and then decreased to the baseline level at Post-2, which is a basis of the observed

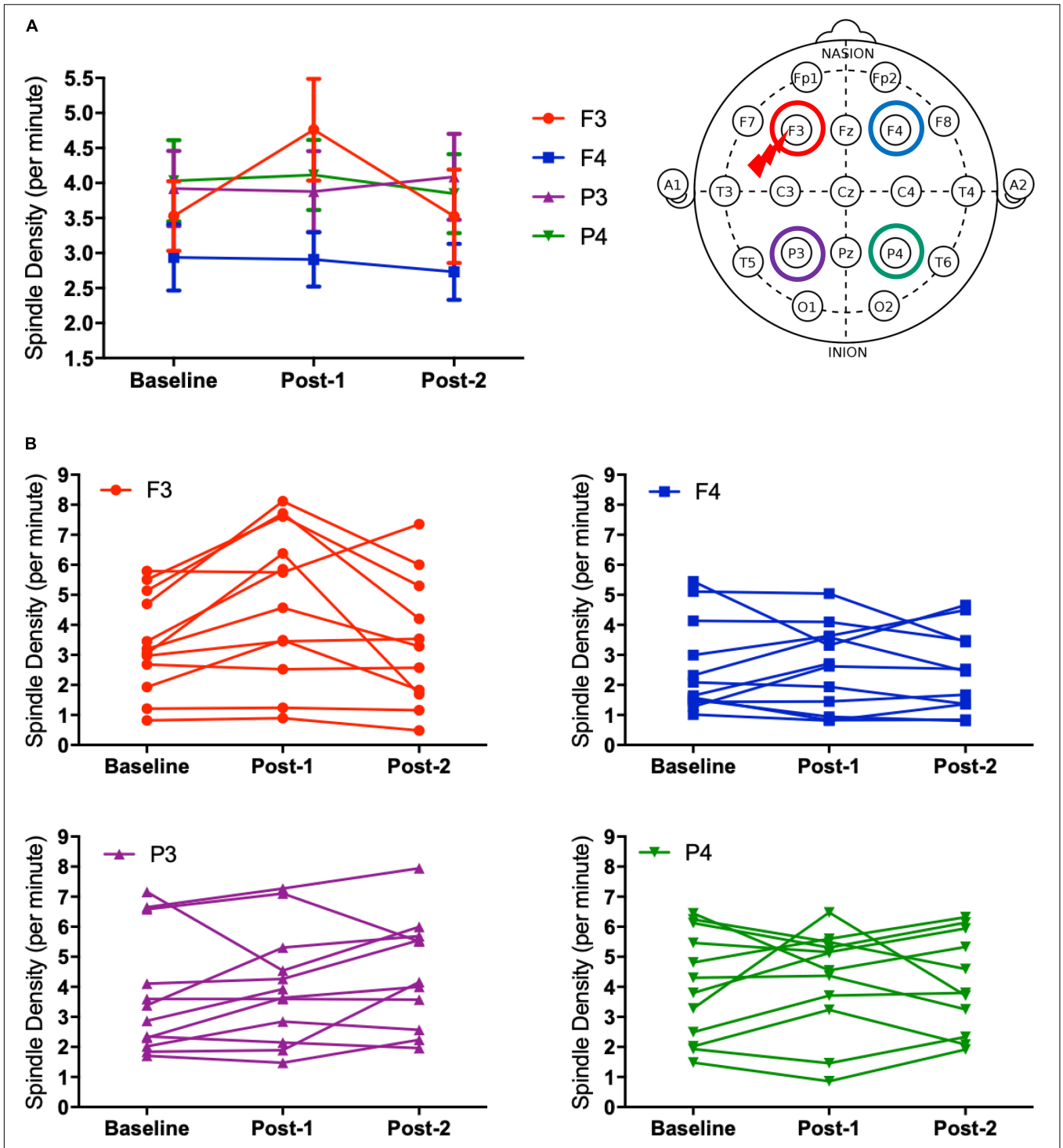

FIGURE 2 | Spindle density changes over time. **(A)** The graph at the left shows sleep spindle density, which is the number of spindles recorded per minute during NREM sleep Stages II–IV, from four derivations of F3, F4, P3, and P4. As illustrated at the right, the F3 electrode is closer to the stimulation site of rTMS sessions. Spindle density at F3 increased from Baseline to Post-1 ($P = 0.008$) and then decreased from Post-1 to Post-2 ($P = 0.044$). **(B)** Inter-individual differences in spindle density change over time. Individual data was presented in four figures of F3, F4, P3, and P4 electrodes.

changes of the spindle density. Notably, the mean amplitude of each spindle showed a trend-level ($p = 0.085$) decrease at Post-1, whereas the mean duration did not change over time ($p = 0.77$). Also, the sigma power of each spindle showed a trend-level ($p = 0.084$) decrease at Post-1, whereas the sigma power density did not significantly change over

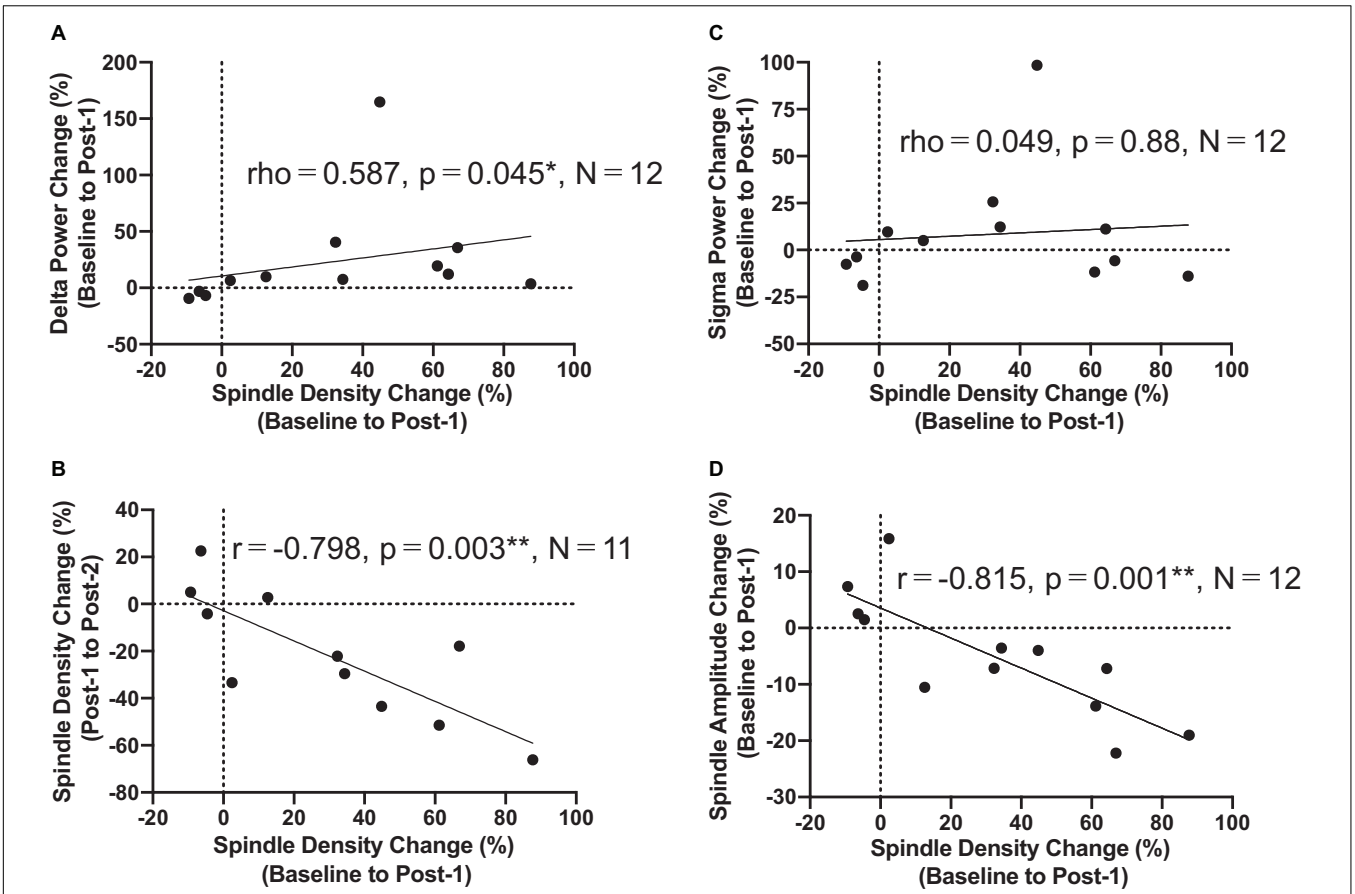

FIGURE 3 | Correlation findings. **(A)** Spindle density change from Baseline to Post-1 was positively correlated with the delta power change during the same period (rho = 0.587, $P = 0.045$, $N = 12$). **(B)** Spindle density change from Baseline to Post-1 was negatively correlated with the spindle density change from Post-1 to Post-2 ($r = -0.798$, $P = 0.003$, $N = 11$). **(C)** Spindle density change from Baseline to Post-1 was not correlated with sigma power change during the same period. **(D)** Spindle density change from Baseline to Post-1 was negatively correlated with the spindle amplitude change during the same period ($r = -0.815$, $P = 0.001$, $N = 12$). *: $P < 0.05$; **: $P < 0.01$.

TABLE 3 | Spindle density and morphology at F3.

	Baseline	Post-1	Post-2	*P*-value (paired *T* tests)		
				Baseline vs. Post-1	Baseline vs. Post-2	Post-1 vs. Post-2
F3 spindle density (SD) [number/time]	3.53 (1.7)	4.76 (2.5)	3.52 (2.2)	0.008**	0.961	0.044*
F3 spindle duration (SD) [seconds/number]	1.06 (0.1)	1.07 (0.1)	1.07 (0.1)	0.767	0.857	0.936
F3 spindle amplitude (SD) [μV/number]	6.63 (1.8)	6.17 (1.2)	6.68 (1.6)	0.085	0.792	0.131
F3 sigma power during NREM (SD) [μV^2/number]	3.84 (1.5)	3.19 (2.3)	4.28 (2.8)	0.084	0.477	0.177
F3 sigma power during NREM (SD) [μV^2/time]	11.59 (4.8)	10.92 (4.1)	10.65 (4.2)	0.249	0.412	0.839

*SD, Standard Deviation; number, total number of spindles; time, total minutes of Stage II–IV; NREM, Non-REM Stage II–IV; *: $P < 0.05$; **: $P < 0.01$.*

time as we have previously reported (Saeki et al., 2013). In addition, change rates of spindle density and spindle amplitude between Baseline and Post-1 are highly negatively correlated ($r = -0.815$, $p = 0.001$, $n = 12$) (**Figure 3D**). Given these findings, the discrepancy between the increased spindle density and unchanged sigma power density at F3 is potentially attributed to the decreasing trend in the amplitude of each spindle.

Clinical and cognitive correlation analyses with the spindle density change at F3 showed no significant correlation, even with an uncorrected alpha level. Though descriptive data of the clinical and cognitive measures were described in detail elsewhere (Saeki et al., 2013), it was briefly noted here that depression symptoms evaluated by HAM-D and BDI, daytime sleepiness by KSS, and executive function by WCST showed significant improvement from Baseline to Post-2.

DISCUSSION

The present study showed that the increase of the sleep spindle density during natural sleep was highly localized to the F3 electrode, following five sessions of high-frequency rTMS delivered to the left DLPFC of major depression patients. Moreover, this local increase of spindle density at F3 was significantly associated with the previously reported power increase of SWA localized also at F3 in major depression patients. By contrast to the first half period of rTMS sessions, the locally enhanced spindle density at F3 decreased to reach the baseline level during the last series of rTMS sessions. To our knowledge, this is the first study showing a modulation of sleep spindle following rTMS.

Given these findings, it is reasonable to suggest that the localized increases of the sleep spindle density and SWA power could be derived from a common rTMS-induced neuromodulation of the thalamocortical network activity during NREM sleep. The high-frequency rTMS-induced action potentials within cortical pyramidal cells of DLPFC could stimulate not only thalamocortical neurons but also the reticular nucleus of the thalamus, which serve as delta and spindle oscillators, respectively (Gross et al., 2007). It should be noted here that all rTMS sessions were carried out in the morning, to explore long-lasting cumulative effects on PSG data during night rather than the acute after effects of the last rTMS session, which can last for about half an hour (Peinemann et al., 2004).

In our previous work (Saeki et al., 2013), the sigma band power during NREM stages II–IV, which represents an aspect of the sleep spindle activity, was not significantly changed following rTMS sessions in contrast to the localized enhancement of SWA power. The sleep spindle density is likely distinct from a sigma band power, reflecting different aspects of sleep spindle activity. Although both measures were significantly correlated in the cross-sectional dataset, their longitudinal changes did not correlate. The observed discrepancy in the rTMS-induced changes between the spindle density and sigma power density seems attributable to the decreasing trend of amplitude of each spindle waveform during the first half period. Along the lines of this discussion, it can be speculated that the sleep spindle density may be a more sensitive measure to assess rTMS-induced neuromodulation than a sigma power density during NREM stages II–IV.

It should be noted that the observed rise and fall phenomenon of sleep spindle density during a series of rTMS sessions is quite similar for the averaged SWA power, as previously reported (Saeki et al., 2013). Both NREM sleep-related phenomena were localized to the stimulation site of rTMS, and may commonly result from rTMS-induced facilitatory neuroplasticity and subsequent homeostatic downregulation of the locally enhanced thalamocortical synchronization during NREM sleep. Such intrinsic downregulation of NREM sleep may occur within 2 weeks, even during high-frequency rTMS sessions, which should be considered when evaluating direct effects of rTMS on NREM sleep-related phenomena. For instance, a previous study (Pellicciari et al., 2013) failed to detect NREM sleep changes with a 2-week interval of PSG assessments. Accordingly, it could be concluded that an initial follow-up assessment of local NREM sleep activity needs to be scheduled within a week or so after the onset of an rTMS intervention.

With regard to the clinical and cognitive correlation analyses, our basic assumption was that potential rTMS-associated physiological changes of sleep spindle activity can result in clinical or cognitive improvements, especially for executive function, insomnia, and excessive daytime sleepiness. However, exploratory correlation analyses did not suggest any significant association, even with an uncorrected alpha level. Further research with a larger sample size is warranted to determine the clinical/cognitive significance of the rTMS-induced changes of NREM sleep.

The present study has some drawbacks to disclose. First, in an open-label study design, we did not evaluate non-specific effects of a sham stimulation on all-night PSG data, albeit we found a significant change of the sleep spindle density exclusively localized to the stimulation site of the high-frequency rTMS. Second, the present method to identify sleep spindles visually is totally manual and thus could be arbitrary, as compared with an automatic detection algorithm of sleep spindle waveform. Hence, we paid a maximum attention to keeping the single rater (TI) blind to subject profiles particularly for time points of the PSG recording such as Baseline, Post-1 and Post-2. Third, concomitant medication might have impacted on all-night PSG data. As individual medication was fixed throughout the study period, it is less likely that medication could affect longitudinal changes of PSG data. Finally, in this study design, we employed a one-week interval of PSG measurements to avoid excessive burden on depressed patients. However, more frequent PSG measurements enable us to reveal more exact trajectories of the spindle density and associated sigma power during a series of rTMS sessions.

In conclusion, the present study showed a locally and transiently enhanced density of the frontal sleep spindle activity in patients with major depressive episodes, possibly induced by a series of high-frequency rTMS sessions over the left DLPFC. The observed local facilitation of frontal spindle density was transient and downregulated to the baseline level during the last half period of the consecutive 10 rTMS sessions, potentially due to an intrinsic homeostatic regulatory system. Such rise and fall phenomenon of sleep spindle activity is very similar to that observed in SWA and both may be complementary to each other within a framework of thalamocortical synchronization during NREM sleep. Although the clinical/cognitive association with the rTMS-induced changes of sleep spindle density awaits further investigation, the present findings shed light on the neuromodulatory impact of diurnal rTMS sessions on the nocturnal sleep spindle activity.

DATA AVAILABILITY STATEMENT

The data analyzed in this study is subject to the following licenses/restrictions: Kanagawa Psychiatric Center's restrictions. Requests to access these datasets should be directed to MN motoaki@motoaki.com.

ETHICS STATEMENT

The studies involving human participants were reviewed and approved by Ethics Committee of the Kanagawa Psychiatric Center (KPC201107). The patients/participants provided their written informed consent to participate in this study.

AUTHOR CONTRIBUTIONS

TI, TS, TY, and MN contributed to conception and design of the study. TI analyzed the sleep EEG data using a software developed by NH. TI, MS, and MN performed the statistical analysis. TI and MN wrote the first draft of the manuscript. TI, NH, and MN wrote sections of the manuscript. All authors contributed to manuscript revision, read, and approved the submitted version.

FUNDING

This work was supported by grants-in-aid for Young Scientists B (23791345), and Scientific Research C (17K10326, 20K07954) from the Ministry of Education, Culture, Sports, Science and Technology of Japan (MEXT) and Japan Society for the Promotion of Science.

ACKNOWLEDGMENTS

The authors gratefully acknowledge the technical support of Toshiaki Tomioka and Kinya Obata, and the research assistance of Susumu Okada.

SUPPLEMENTARY MATERIAL

The Supplementary Material for this article can be found online at: https://www.frontiersin.org/articles/10.3389/fnhum.2021.738605/full#supplementary-material

Supplementary Figure 1 | Spindle morphology and sigma power changes at F3 over time. **(A)** Spindle duration changes from Baseline to Post-2. **(B)** Spindle amplitude changes from Baseline to Post-2. There was a trend-level decrease ($P = 0.085$) between Baseline and Post-1. **(C)** Sigma power per each spindle changes from Baseline to Post-2. There was a trend-level decrease ($P = 0.084$) between Baseline and Post-1. **(D)** Sigma power per minute changes from Baseline to Post-2.

REFERENCES

AASM (2005). *ICSD – 2 The International Classification of Sleep Disorders, Diagnostic and Coding Manual*, 2nd Edn. Westchester, IL: American Academy of Sleep Medicine.

APA (2000). *Diagnostic and Statistical Manual of Mental Disorders – Text Revision*, 4th Edn. Washington, DC: American Psychiatric Association Press.

Armitage, R. (2007). Sleep and circadian rhythms in mood disorders. *Acta Psychiatr. Scand. Suppl.* 433, 104–115. doi: 10.1111/j.1600-0447.2007.00968.x

Baglioni, C., Battagliese, G., Feige, B., Spiegelhalder, K., Nissen, C., Voderholzer, U., et al. (2011). Insomnia as a predictor of depression: a meta-analytic evaluation of longitudinal epidemiological studies. *J. Affect. Disord.* 135, 10–19. doi: 10.1016/j.jad.2011.01.011

Beck, A., Ward, C. H., Mendelson, M., Mock, J., and Erbaugh, J. (1961). An inventory for measuring depression. *Arch. Gen. Psychiatry* 4, 561–571. doi: 10.1001/archpsyc.1961.01710120031004

Benca, R. M., Okawa, M., Uchiyama, M., Ozaki, S., Nakajima, T., Shibui, K., et al. (1997). Sleep and mood disorders. *Sleep Med. Rev.* 1, 45–56. doi: 10.1016/s1087-0792(97)90005-8

Benton, A., and Hamsher, K. (1976). *Multilingual Aphasia Examination*. Iowa City, IA: University of Iowa.

Chen, C. N. (1979). Sleep, depression and antidepressants. *Br. J. Psychiatry* 135, 385–402. doi: 10.1192/bjp.135.5.385

Dunleavy, D. L., Brezinova, V., Oswald, I., Maclean, A. W., and Tinker, M. (1972). Changes during weeks in effects of tricyclic drugs on the human sleeping brain. *Br. J. Psychiatry* 120, 663–672. doi: 10.1192/bjp.120.559.663

Goder, R., Hinrichsen, I., Seeck-Hirschner, M., Pfeiffer, R., Weinhold, S. L., Baier, P. C., et al. (2016). Sleep at baseline and after electroconvulsive therapy in patients with major depression. *Psychiatry Res.* 246, 683–687. doi: 10.1016/j.psychres.2016.10.064

Grant, D., and Berg, E. A. (1948). A behavioral analysis of degree of reinforcement and ease of shifting to new responses in a Weigl-type card-sorting problem. *J. Exp. Psychol.* 38, 404–411. doi: 10.1037/h0059831

Gross, M., Nakamura, L., Pascual-Leone, A., and Fregni, F. (2007). Has repetitive transcranial magnetic stimulation (rTMS) treatment for depression improved? A systematic review and meta-analysis comparing the recent vs. the earlier rTMS studies. *Acta Psychiatr. Scand.* 116, 165–173. doi: 10.1111/j.1600-0447.2007.01049.x

Hamilton, M. (1960). A rating scale for depression. *J. Neurol. Neurosurg. Psychiatry* 23, 56–62. doi: 10.1136/jnnp.23.1.56

Hoffmann, G., Linkowski, P., Kerkhofs, M., Desmedt, D., and Mendlewicz, J. (1985). Effects of ECT on sleep and CSF biogenic amines in affective illness. *Psychiatry Res.* 16, 199–206. doi: 10.1016/0165-1781(85)90107-6

Huber, R., Esser, S. K., Ferrarelli, F., Massimini, M., Peterson, M. J., and Tononi, G. (2007). TMS-induced cortical potentiation during wakefulness locally increases slow wave activity during sleep. *PLoS One* 2:e276. doi: 10.1371/journal.pone.0000276

Ishihara, K., Saito, T., and Miyata, Y. (1982). Sleepiness scale and an experimental approach. *Shinrigaku Kenkyu* 52, 362–365.

Jalinous, R. (1991). Technical and practical aspects of magnetic nerve stimulation. *J. Clin. Neurophysiol.* 8, 10–25. doi: 10.1097/00004691-199101000-00004

Kluge, M., Schussler, P., and Steiger, A. (2007). Duloxetine increases stage 3 sleep and suppresses rapid eye movement (REM) sleep in patients with major depression. *Eur. Neuropsychopharmacol.* 17, 527–531. doi: 10.1016/j.euroneuro.2007.01.006

Mazure, C., Nelson, J. C., and Price, L. H. (1986). Reliability and validity of the symptoms of major depressive illness. *Arch. Gen. Psychiatry* 43, 451–456. doi: 10.1001/archpsyc.1986.01800050053006

Milak, M., Parsey, R. V., Keilp, J., Oquendo, M. A., Malone, K. M., and Mann, J. J. (2005). Neuroanatomic correlates of psychopathologic components of major depressive disorder. *Arch. Gen. Psychiatry* 62, 397–408. doi: 10.1001/archpsyc.62.4.397

Nakamura, M., Uchida, S., Maehara, T., Kawai, K., Hirai, N., Nakabayashi, T., et al. (2003). Sleep spindles in human prefrontal cortex: an electrocorticographic study. *Neurosci. Res.* 45, 419–427. doi: 10.1016/s0168-0102(03)00007-5

Pascual-Leone, A., Freitas, C., Oberman, L., Horvath, J. C., Halko, M., Eldaief, M., et al. (2011). Characterizing brain cortical plasticity and network dynamics across the age-span in health and disease with TMS-EEG and TMS-fMRI. *Brain Topogr.* 24, 302–315. doi: 10.1007/s10548-011-0196-8

Peinemann, A., Reimer, B., Loer, C., Quartarone, A., Munchau, A., Conrad, B., et al. (2004). Long-lasting increase in corticospinal excitability after 1800 pulses of subthreshold 5 Hz repetitive TMS to the primary motor cortex. *Clin. Neurophysiol.* 115, 1519–1526. doi: 10.1016/j.clinph.2004.02.005

Pellicciari, M. C., Cordone, S., Marzano, C., Bignotti, S., Gazzoli, A., Miniussi, C., et al. (2013). Dorsolateral prefrontal transcranial magnetic stimulation in

patients with major depression locally affects alpha power of REM sleep. *Front. Hum. Neurosci.* 7:433. doi: 10.3389/fnhum.2013.00433

Rechtschaffen, A., and Kales, A. (1968). *A Manual of Standardized Terminology, Techniques and Scoring System for Sleep Stages of Human Subjects*. Washington, DC: Government printing office.

Saeki, T., Nakamura, M., Hirai, N., Noda, Y., Hayasaka, S., Iwanari, H., et al. (2013). Localized potentiation of sleep slow-wave activity induced by prefrontal repetitive transcranial magnetic stimulation in patients with a major depressive episode. *Brain Stimul.* 6, 390–396. doi: 10.1016/j.brs.2012.08.004

Steiger, A., and Pawlowski, M. (2019). Depression and sleep. *Int. J. Mol. Sci.* 20:607. doi: 10.3390/ijms20030607

Steriade, M., McCormick, D. A., and Sejnowski, T. J. (1993). Thalamocortical oscillations in the sleeping and aroused brain. *Science* 262, 679–685. doi: 10.1126/science.8235588

Vogel, G. W., Thurmond, A., Gibbons, P., Sloan, K., and Walker, M. (1975). REM sleep reduction effects on depression syndromes. *Arch. Gen. Psychiatry* 32, 765–777. doi: 10.1001/archpsyc.1975.01760240093007

von Bardeleben, U., Steiger, A., Gerken, A., and Holsboer, F. (1989). Effects of fluoxetine upon pharmacoendocrine and sleep-EEG parameters in normal controls. *Int. Clin. Psychopharmacol.* 4(Suppl. 1), 1–5.

Yoshiike, T., Kuriyama, K., Nakasato, Y., and Nakamura, M. (2020). Mutual relationship between somatic anxiety and insomnia in maintaining residual symptoms of depression. *J. Behav. Cogn. Ther.* 30, 83–93.

Yoshiike, T., Kuriyama, K., Nakasato, Y., Yamada, N., and Nakamura, M. (2017). Insomnia as a somatic representation of anxiety in the symptomatology of depression. *Sleep Med.* 40:e357. doi: 10.1016/j.sleep.2017.11.1054

Conflict of Interest: The authors declare that the research was conducted in the absence of any commercial or financial relationships that could be construed as a potential conflict of interest.

frontiers in Behavioral Neuroscience

REVIEW
published: 18 January 2022
doi: 10.3389/fnbeh.2021.820017

Review of Noninvasive or Minimally Invasive Deep Brain Stimulation

Xiaodong Liu[1], *Fang Qiu*[2], *Lijuan Hou*[3]* *and Xiaohui Wang*[1]*

[1]School of Kinesiology, Shanghai University of Sport, Shanghai, China, [2]Department of Exercise Physiology, Beijing Sport University, Beijing, China, [3]College of Physical Education and Sports, Beijing Normal University, Beijing, China

Brain stimulation is a critical technique in neuroscience research and clinical application. Traditional transcranial brain stimulation techniques, such as transcranial magnetic stimulation (TMS), transcranial direct current stimulation (tDCS), and deep brain stimulation (DBS) have been widely investigated in neuroscience for decades. However, TMS and tDCS have poor spatial resolution and penetration depth, and DBS requires electrode implantation in deep brain structures. These disadvantages have limited the clinical applications of these techniques. Owing to developments in science and technology, substantial advances in noninvasive and precise deep stimulation have been achieved by neuromodulation studies. Second-generation brain stimulation techniques that mainly rely on acoustic, electronic, optical, and magnetic signals, such as focused ultrasound, temporal interference, near-infrared optogenetic, and nanomaterial-enabled magnetic stimulation, offer great prospects for neuromodulation. This review summarized the mechanisms, development, applications, and strengths of these techniques and the prospects and challenges in their development. We believe that these second-generation brain stimulation techniques pave the way for brain disorder therapy.

Keywords: deep brain stimulation, focused ultrasound, temporal interference, nanoparticle, neuromodulation

OPEN ACCESS

Edited by:
Masaki Sekino,
The University of Tokyo, Japan

Reviewed by:
Jong-Cheol Rah,
Korea Brain Research Institute, South Korea
Shan Huang,
University of California, Los Angeles, United States

***Correspondence:**
Lijuan Hou
houlj@bnu.edu.cn
Xiaohui Wang
wangpan96@126.com

Specialty section:
This article was submitted to Pathological Conditions, a section of the journal Frontiers in Behavioral Neuroscience

Received: *22 November 2021*
Accepted: *27 December 2021*
Published: *18 January 2022*

Citation:
Liu X, Qiu F, Hou L and Wang X (2022) Review of Noninvasive or Minimally Invasive Deep Brain Stimulation. Front. Behav. Neurosci. 15:820017. doi: 10.3389/fnbeh.2021.820017

INTRODUCTION

Neuromodulation has attracted considerable attention worldwide for its value in treating neurodegenerative diseases and increasing human performance, and many countries have increased investment and built their brain projects to accelerate the development process of neuromodulation. Brain stimulation, a part of the brain project, plays a crucial role in neuroscience research and clinical application and has an advantage over pharmacotherapy because of its fast, direct, and focal effects. Brain stimulation can alter neuronal activities through the delivery of a stimulus to targeted brain areas, thus alleviating brain disorders or enhancing brain functions. Brain stimulation is a multidisciplinary research field, which involves neurophysiology, bioengineering, and material and computer science (Tatti et al., 2016; Antal et al., 2017).

The most commonly employed transcranial brain stimulation techniques include transcranial magnetic stimulation (TMS), transcranial direct current stimulation (tDCS), and deep brain stimulation (DBS; Adair et al., 2020). TMS and tDCS represent major noninvasive neurostimulation techniques, which have been widely used in clinical research for decades (Begemann et al., 2020). However, the effects of noninvasive brain stimulation through TMS and tDCS on neurons vary and are difficult to assess. Furthermore, magnetic and electric signals show absorption and scattering properties within brain tissues, limiting spatial resolution and penetration depth (Woods et al., 2016; Airan, 2017).

DBS is an invasive neuromodulation that requires the implantation of stimulating electrodes to deep brain structures; these electrodes can precisely target deep brain nuclei through the direct control of brain circuit dynamics (Parker et al., 2020). DBS has been widely used in alleviating neurological disorders, such as motor and cognitive dysfunctions, which cannot be alleviated by traditional therapies (Lozano and Lipsman, 2013). In particular, DBS of the subthalamic nucleus (STN) is one of the most effective treatments for Parkinson's disease (Habets et al., 2018). However, DBS requires chronic implantation deep in the brain, which may eventually suffer from bleeding and infection (Kim et al., 2016). The above techniques lack cell specificity and thus have limited efficacy (Dayan et al., 2013). Thus, noninvasive and precisely deep stimulation represents a major breakthrough in neuroscience.

For this problem, exploring novel brain modulation techniques that satisfy the requirements of research and clinical application should be explored. Ideal brain stimulation targeting deep brain regions should be noninvasive or minimally invasive and have a high spatiotemporal resolution and negligible inflammatory or complications in different animal models, including rodents, large mammals, non-human primates, and humans (Li et al., 2021). Great advances have been achieved by neuromodulation studies in the past decade, driven by improvements in methods and devices. In particular, second-generation brain stimulation techniques that mainly rely on acoustic, electronic, optical, and magnetic signals exhibit great promise for neuromodulation (Lewis, 2016; Lozano, 2017; Chen, 2019; Darrow, 2019). These novel techniques are aimed at surpassing the limitations of conventional brain stimulation approaches. Some current approaches are limited to laboratory research. Nevertheless, some methods have already been used in clinical applications. Here, we provide an overview of these techniques and outline the prospects and challenges in future development.

FOCUSED ULTRASOUND

Focused ultrasound (FUS) is a noninvasive neuromodulation technique with high spatial resolution and penetration depth (**Figure 1**; Fini and Tyler, 2017). FUS can deliver mechanical forces, penetrate biological tissues in small deep brain regions, and form a focal spot that can result in thermal and mechanical bioeffects (Kubanek, 2018; Blackmore et al., 2019). Ultrasound is a mechanical pressure wave with frequencies above the human audible range. As a propagating wave, ultrasound can alter neuronal activity by stimulating nerves and muscles (Harvey, 1929). Fry et al. (1958) first reported that ultrasound considerably affects brain activity, and they used high-intensity focused ultrasound (HIFU) for movement disorders and chronic pain (Fry, 1958). After decades of development in basic FUS technology, FUS especially Low-intensity ultrasound (LIFU) has burst a great breakthrough in scientific research and clinical treatment, continuously creating new possibilities in neuroscience (Rabut et al., 2020).

Mechanisms of FUS

FUS has many interaction modes for tissues, and these modes depend on FUS parameters, including thermal, cavitation, and mechanical mechanisms. Ultrasound can be defined as high intensity (>1 W/cm^2) or low intensity (<300 mW/cm^2; Tufail et al., 2010). The biological effects of HIFU are mainly local heating effects. The heating effects homogenize tissues and denatured proteins (Ishibashi et al., 2010). LIFU has been reported to have a great number of effects on neuromodulation. LIFU can create minimal temperature elevation. Even a small variation in temperature affects ion channels and enzymatic and potential activities (Darrow, 2019). Most studies indicated that the neuromodulation of LIFU is due to nonthermal mechanical mechanisms. Mechanosensitive ion channels, which can respond to mechanical stimuli, may mediate neural response to FUS (Ye et al., 2018). Mechanical forces exerted by FUS induce membrane displacement and mediate conformational change in embedded ion channels (Kubanek, 2018). In addition, cavitation elicited by LIFU is considered a mechanism of neuromodulation. Cavitation produces microbubbles that cause the collapse of soft tissues, and shear stress temporarily alters tight junctions and increases the permeability of the blood–brain barrier (BBB; Chu et al., 2015; Kubanek, 2018).

Development and Applications of FUS

FUS is valuable to neuroscience research and clinical applications. A large number of studies used FUS in different models, including neural tissues, rodents, non-human primates, and humans. In *in vitro* studies, FUS was first applied to brain modulation in the 1950s. It caused reversible suppression for sensory-evoked potential in the primary visual cortices of cats through the lateral geniculate nucleus (Fry et al., 1958). Mihran et al. (1996) determined whether or not the mechanical vibration of FUS applied to neural and cardiac cells can modify cellular excitability. Low-energy FUS increased conduction velocity and compound action potential in the excised sciatic nerves of a bullfrog (Tsui et al., 2005). In microelectrode arrays for observing the spatiotemporal dynamics of extracellular neuronal activities after FUS, local field potential spread across hippocampal sections (Suarez-Castellanos et al., 2021).

Following the initial discovery using FUS *in vitro*, animal behavioral effects and network activity changes have been investigated *in vivo* (King et al., 2013; Yu et al., 2016; Yuan et al., 2020). Tufail et al. (2010, 2011) reported that LIFU can promote sharp-wave ripple oscillations and trigger electromyogram (EMG) activities and forepaw and tail movements. Yuan et al. (2020) found that LIFU induces rapid hemodynamic responses at stimulation sites and demonstrated linear coupling relationships among cortical blood flow, local field potential, and EMG amplitude. Baek et al. (2018) revealed that LIFU generates motor-evoked potential (MEP) and enhances sensorimotor recovery in stoke mice and found that cerebellar LIFU leads to a symmetrical decrease in pathological neural activities and enhances recovery in stoke mice. Yoo et al. (2011) demonstrated that FUS can be applied to rabbit deep brain structures and neuronal activities can be activated or suppressed depending on FUS parameters. FUS effects in large animals were further investigated, and the

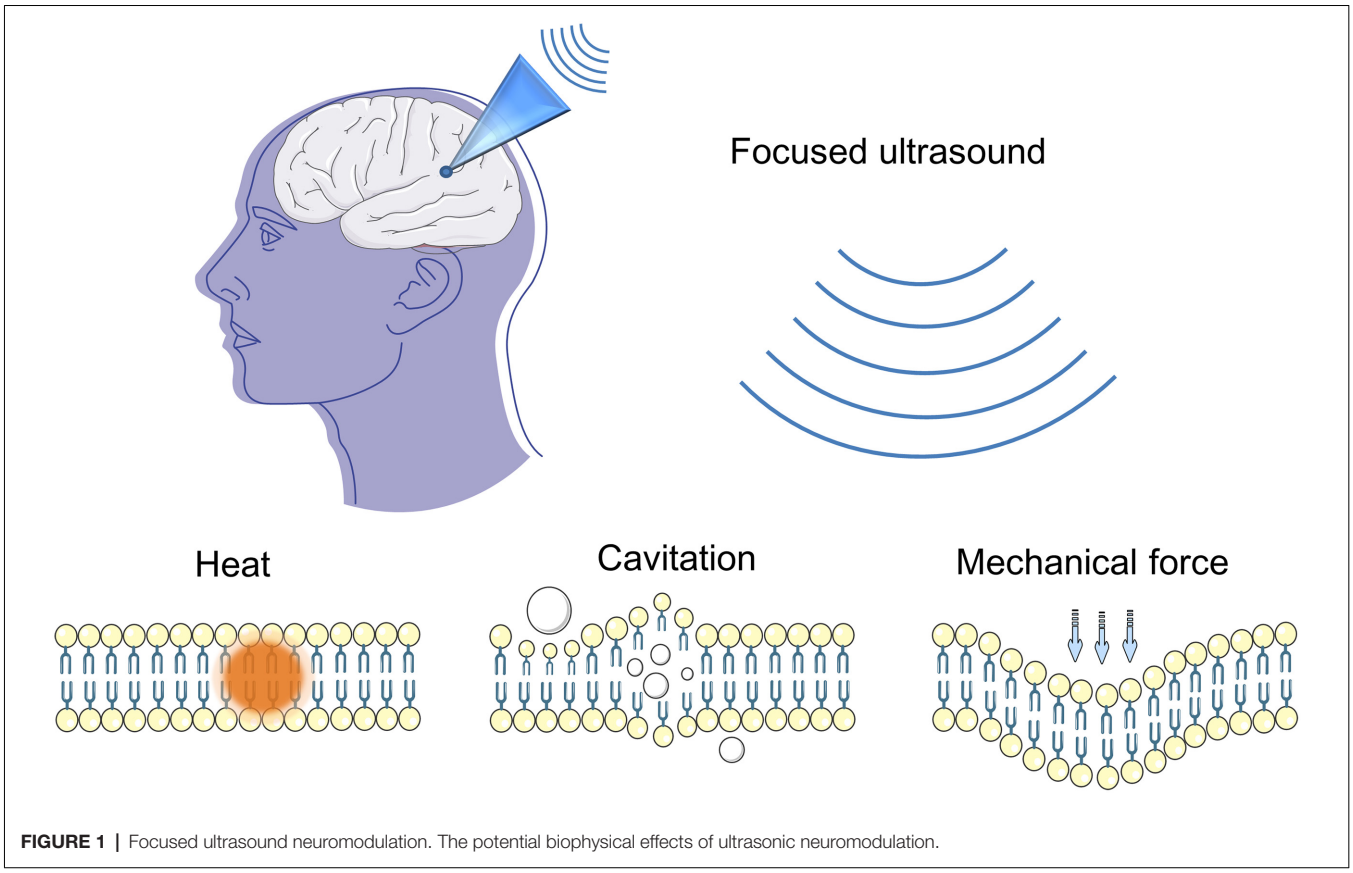

FIGURE 1 | Focused ultrasound neuromodulation. The potential biophysical effects of ultrasonic neuromodulation.

results suggested that FUS-mediated brain stimulation can be precise, effective, and safe in ovine models (Yoon et al., 2019). Deffieux et al. (2013) examined awake macaque rhesus monkeys; they showed that LIFU significantly modulates antisaccade task latencies; and they demonstrated the feasibility of using LIFU in modulating high-level cognitive behavior. What is more, FUS transiently and reversibly changes brain activities in deep cortical and subcortical regions with high spatial resolution, and modulatory effects on active and resting neurons vary (Folloni et al., 2019; Yang et al., 2021).

Moreover, the molecular responses of FUS have been recently reported. Data has shown that LIFU can stimulate brain activities involved in the activation of voltage-gated sodium and calcium channels (Tyler et al., 2008). LIFU modulates the level of neurotransmitters, Min observed a significant increase of the extracellular levels of dopamine and serotonin (Min et al., 2011). Oh et al. (2019) found that ultrasound-induced neuromodulation is initiated by transient receptor potential A1 (TRPA1) in astrocytes; TRPA1 causes a release of glutamate; finally activates N-methyl-D-aspartic acid receptors in neighboring neurons. The expression levels of neurotrophic factors, such as brain-derived neurotrophic factor (BDNF), glial cell line-derived neurotrophic factor, and vascular endothelial growth factor, can be increased by LIFU in the rat models of Alzheimer's disease (Lin et al., 2015). BDNF expression is upregulated through the activation of tropomyosin-related kinase B, phosphatidylinositol-3-kinase (PI3K), protein kinase B (Akt), and calmodulin kinase signaling pathways (Liu et al., 2017). FUS exposure suppresses epileptic activities in acute epilepsy rat models, and this effect seems to be mediated by the PI3K-Akt-mammalian target of rapamycin (mTOR) signaling pathway (Chen S.-G. et al., 2020).

In addition to the animal results, many researchers targeted human studies. FUS on the motor cortex transiently increases motor cortex excitability and decreases reaction time during visual motor tasks (Gibson et al., 2018; Fomenko et al., 2020). Legon et al. (2018) successfully combined electroencephalographic, computed tomography (CT), and magnetic resonance imaging (MRI) to assess the effects of FUS neuromodulation on humans. The study revealed that FUS shows perfect spatial precision and resolution when used in modulating human subcortical deep brain regions, such as the unilateral thalamus (Legon et al., 2018).

Strengths and Challenges of FUS

FUS is a promising noninvasive deep brain neuromodulation approach with high spatial precision, resolution, and safety and can reversibly modulate brain activities in subcortical and deep cortical regions with millimetric range neurostimulation (Tufail et al., 2010; Deffieux et al., 2013). Portable, wearable, and array transducer FUS has been used in research, so as to better perform its function (Li et al., 2018, 2019). FUS devices are constantly developed to be more suitable for clinical practice. Using nanoparticles that specifically target drugs in specific brain areas have been used as mediators to improve the targetability

of FUS (Ozdas et al., 2020; Hou et al., 2021). FUS has been used effectively and safely for neuromodulation in small animals, non-human primates, and humans (Legon et al., 2018; Folloni et al., 2019; Baek et al., 2020) and is compatible with MRI and CT imaging techniques, showing considerable potential as a neuromodulation method for disabling neurological disorders. Clinical trials using FUS have been conducted for the treatment of Alzheimer's disease, Parkinson's disease, epilepsy, and stroke (Meng et al., 2017; Fomenko et al., 2020).

Although a number of studies have shown that FUS is safe and effective, further prospective work is needed to elucidate parameters for safety and effectivity threshold. The short- and long-term effects of FUS need to be treated differently. Basic experiments should focus on illuminating the potential cellular, molecular, synaptic, and ionic mechanisms of FUS neuromodulation.

TEMPORAL INTERFERENCE STIMULATION

Temporal interference (TI) stimulation is a novel noninvasive transcranial electrical stimulation (TES) technique that can reach deep brain regions (**Figure 2**). It utilizes multigroup high frequency (≥1,000 Hz) and oscillating electric fields in modulating neural activities. In 1965, The TI concept was proposed by Russian scientists and applied to peripheral stimulation (Beatti et al., 2011; Guleyupoglu et al., 2013; Li et al., 2020). Then, Grossman et al. (2017) used TI stimulation in brain research in 2017. Since then, TI has attracted the attention of neuroscientists because it may achieve noninvasive deep brain stimulation. The position of TI stimulation can be changed by adjusting electrode location and current amplitude ratio. It can target deep brain regions and prevent the activation of the neighboring and overlying cortex. TI stimulation offers a means to precisely regulate subcortical structures.

Mechanisms of TI Stimulation

TI stimulation consists of two sets of high frequency sinusoidal waveform currents with slightly different frequencies (f_1 = 2,000 Hz; f_2 = 2,010 Hz; Δf = 10 Hz). Two high frequency oscillating electric fields interact and produce an envelope that is equal to Δf in current intersection regions. Owing to neural biophysical properties, neural membranes respond to low-frequency electrical signals, and high-frequency oscillation does not recruit effective neural firing (Hutcheon and Yarom, 2000). Cao et al. (2018) demonstrated that neurons exhibit TI stimulation in a single neuron computational model. Esmaeilpour et al. (2021) investigated that the spatial selectivity of TI stimulation in deep brain areas depends on the phasic modulation of neural oscillations. TI stimulation can modulate spiking activity and facilitate phase synchronization, similar to transcranial alternating current stimulation (tACS; Howell and McIntyre, 2021). At similar field intensities, TI stimulation has less potent modulatory effects than other conventional TES (Negahbani et al., 2018). Mirzakhalili et al. (2020) found that TI stimulation requires a signal rectification process mediated by ion channels. The subthreshold neuromodulation of TI stimulation may be the most important effect (Chakraborty et al., 2018), and polarization effects can alter neural firing and synaptic transmission. Moreover, the potential mechanisms of TI stimulation may involve neurons, glial cells, and cerebral blood flow (Wachter et al., 2011; Monai et al., 2016). More studies are needed to explore and clarify the possible mechanisms.

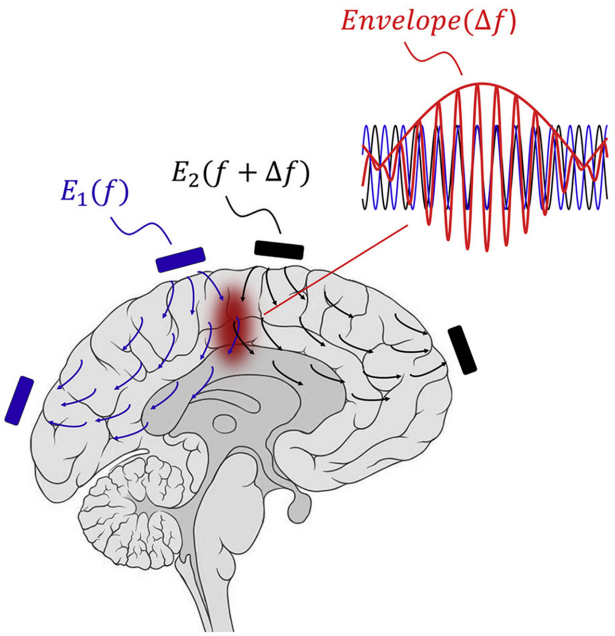

FIGURE 2 | Concept of TI stimulation. The interference of two oscillating electric fields with slightly different frequencies (f1 = 2,000 Hz; f2 = 2,010 Hz; Δf = 10 Hz) produces an envelope equal to Δf in current intersection regions (Copyright permission was obtained from the publisher; Grossman et al., 2017). TI, Temporal interference.

Development and Applications of TI Stimulation

Grossman et al. (2017) proposed that TI stimulation is noninvasive deep brain stimulation and carried out a series of experiments to validate the approach (Bouthour et al., 2017). Mouse neurons were fired with the Δf envelopes of electric fields with a patch clamp electrophysiological recording technique. To assess the focality and depth of TI stimulation, they applied 10 Hz of transcranial stimulation and 2,000 Hz + 2,010 Hz TI stimulation to the hippocampi of anesthetized mice and then measured the expression of the immediate early gene *c-fos* (an indicator of activated neurons). Transcranial stimulation at 10 Hz results in widespread expression in the cortex and hippocampus. By contrast, 2,000 Hz + 2,010 Hz of TI stimulation activates hippocampus regions without activating the cortex. They also explored behavioral responses to TI stimulation and found that TI stimulation can evoke forepaw movement. Stimulation regions can be altered by changing the ratios of currents without electrode movement. No pathophysiological activities and neural damage were observed (Grossman et al., 2017). Using the finite element method, Lee et al. (2020)

found that optimized TI stimulation can successfully reach the hippocampus while reducing the effect of neocortical regions. Another study designed a TI stimulation method and validated its steerability through finite element analysis by using an action potential model and measuring waveforms in a saline solution (Xiao et al., 2019). The simulations of TI stimulation in a mouse head model achieved field strength in deep brain areas but less field strength in superficial areas (Grossman et al., 2017). Furthermore, the field strengths in a human model were much lower, and no direct stimulation effects were found; current higher than that in a mouse model might be required (Rampersad et al., 2019). Computational results indicated that the activation threshold increased with frequency and the envelope frequency had no association with the threshold. Moreover, the current intensity ratio altered the position of responding neurons. The characteristics of an envelope may predict the regions of TI stimulation (Gomez-Tames et al., 2021). Multichannel array electrodes for TI stimulation enhance focality and reduce scalp sensation in computational modeling and mouse experiments (Song et al., 2020). Wang H. et al. (2020) fabricated a TI stimulator that measures bioimpedance in real time and proposed an approach that can easily locate the target position. Current investigations on TI stimulation mainly use computational simulations and small animal experiments. A study investigated the variability in the electric field during TI stimulation and compared it to tACS. The results showed that the electric fields of TI stimulation are variable and more focal than those of tACS (von Conta et al., 2021). Hence, experiments on human subjects are necessary. Further human investigations on TI stimulation needs to be validated.

Strengths and Challenges of TI Stimulation

In summary, the prospects of TI stimulation using noninvasive techniques are exciting. Conventional noninvasive TES usually generates scalp pain when exposing stimulation and limits the intensity of injection currents (Wu et al., 2021). TI stimulation can selectively stimulate specific brain regions, such as cortical and subcortical areas, thus preventing the stimulation of scalp nerves and scalp pain (Gomez-Tames et al., 2021). Given that DBS has remarkable therapeutic benefits for the treatment of Parkinson's disease, tremor, and dystonia (Kringelbach et al., 2007), TI stimulation as a noninvasive DBS offers exciting prospects for the treatment of various brain disorders.

Most TI stimulation studies focus on computation and animal models, and thus human trials need to be further investigated. Given that anatomical differences affect electric field distributions, optimal TI stimulation parameters need to be further validated using various models. Furthermore, a specific positioning scheme for target regions is currently unavailable. An optimization algorithm focusing on the electric field in a target region should be established. Electrode fixation and interference location calculation should be accurate and convenient to facilitate clinical translation (Gunduz and Okun, 2017). TI stimulation currently cannot match the spatial resolution of implantable DBS. Deep small brain structures may not be specifically stimulated, such as the subthalamic nucleus (Grossman, 2018). Further studies are necessary to elucidate the related mechanism, which may involve neurons, synaptic plasticity, cerebral blood flow, and glial cells (Mirzakhalili et al., 2020). More importantly, the safety of TI stimulation needs to be examined and monitored. Finally, the prospect of TI stimulation neuromodulation method is highly promising, but the method requires further research before it can be applied to clinical processes.

NEAR-INFRARED OPTOGENETIC STIMULATION

Near-infrared (NIR) optogenetic stimulation is a mode of optogenetic stimulation that does not require optical fiber implantation and has minimal invasiveness. Optogenetics is widely used in exploring neural circuits that govern sensory, memory, and motor behavior (Hausser, 2014). However, optogenetics requires the insertion of invasive optical fibers to target areas because the penetration depth of visible light is shallow. Blue-green wavelength penetration is limited because of the scattering and absorption by endogenous chromophores (Lin et al., 2013). NIR light (650–1,350 nm), which is much less scattered, can easily penetrate tissues and reach deep brain areas (Shi et al., 2016). NIR light-based photoregulation strategies offer means to modulate specific cells in deep brain structures (Chen G. et al., 2020). However, NIR light cannot be used directly and requires special processing. NIR optogenetic approaches stimulate deep brain regions by activating channel rhodopsin-expressing neurons, where NIR light is converted to visible light (**Figure 3**). By using this approach, researchers can control behavioral patterns simply by NIR illumination without performing optical fiber implantation (Chen et al., 2018). This approach shows great potential in bioimaging and neuromodulation because of its low imaging background and deep penetration (Wu et al., 2015).

Mechanisms of NIR Optogenetic Stimulation

NIR optogenetic stimulation needs NIR light nanotransducers to exert its function. Typically, lanthanide-doped upconversion nanoparticles (UCNPs) can be modulated to a particular wavelength because of the special ladder-like electronic energy structures of trivalent lanthanide ions (Zhou et al., 2015). Dopant–host combination can control the emission wavelengths of UCNPs (Wang and Liu, 2009). The different site symmetries of dopant ions affect emission wavelength and emission peak intensity. The output color of UCNPs can be adjusted into a specific wavelength for optogenetic stimulation (All et al., 2019). UCNPs can convert low-energy NIR light to high-energy visible light (Prodi et al., 2015). UCNPs can be implanted close to optogenetic opsin neurons, and NIR illumination can be converted into visible light, which in turn activates optogenetic opsins, regulates light-gated ion channels that control the, and outflow of ions, and induces cell activation or suppression (Yu et al., 2019). Moreover, blended UCNPs with distinct excitation and emission wavelengths may result in neuron excitation and inhibition simultaneously within one region or multiple deep brain areas (Chen, 2019).

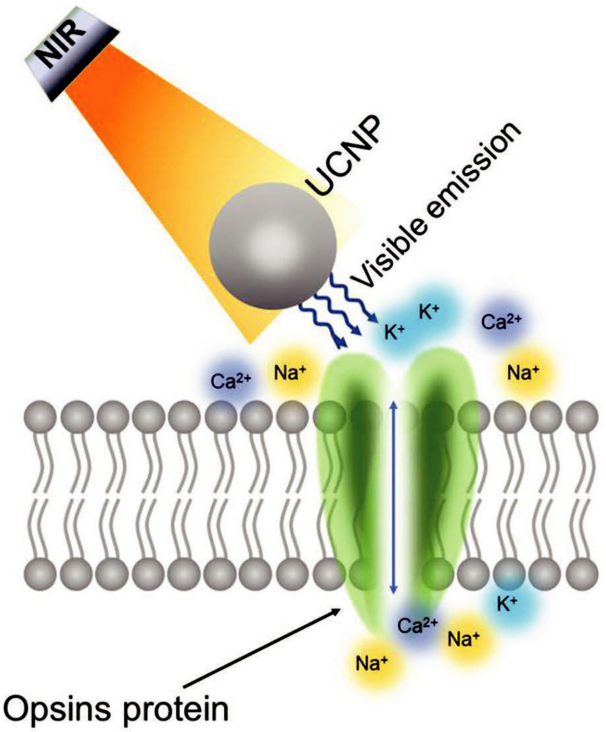

FIGURE 3 | Near-infrared optogenetic stimulation. Schematic principle of lanthanide-doped upconversion nanoparticle (UCNP) mediated NIR optogenetic stimulation (Copyright permission was obtained from the publisher; Yu et al., 2019).

Development and Applications of NIR Optogenetic Stimulation

UCNP-mediated optogenetics was first proposed by Deisseroth in 2011 (Chen S. et al., 2020). After a decade of research and development, NIR optogenetic stimulation has been investigated using different models (Ai et al., 2017; Wang et al., 2017; Ding et al., 2018). Hososhima et al. (2015) first used cultured cells containing UCNPs to observe the photoreactive responses that express channelrhodopsin. Neurons are triggered by NIR laser irradiation and generate action potential (Hososhima et al., 2015). Wu et al. (2016) synergized two unconversion booster effectors (dye-sensitizing and core/shell enhancement) to enhance upconversion efficiency; they successfully altered optogenetic neuron excitation to a biocompatible, water-solubilized, and deep-tissue penetrable 800 nm wavelength. The first *in vivo* study was investigated with *Caenorhabditis elegans* (*C. elegans*). *C. elegans* is widely used in optogenetic manipulation because of its small nervous system and quantifiable motor behavior (Zhen and Samuel, 2015). Bansal et al. (2016) implemented NIR optogenetic stimulation in *C. elegans* and found that it can activate channelrhodopsin-2 ion channels in mechanosensory neurons at a low average power with a quasi-continuous wave excitation approach. Further study showed that UCNPs can effectively activate inhibitory GABAergic motor neurons and excitatory glutamatergic DVC interneurons, leading to locomotion inhibition and activation (Ao et al., 2019). A recent study on zebrafish showed that NIR optogenetic stimulation can remotely activate channelrhodopsin-2 ion channels and effectively manipulate cation influx. This investigation provided a site-specific approach for regulating membrane-associated activities (Ai et al., 2017). More importantly, NIR optogenetic stimulation on live rodent animals was conducted in a number of experimental studies. Lin et al. (2017) packaged UCNPs in glass micropipettes and positioned them close to specific brain structures, such as the tegmental area, cortical striatum, and visual cortex. The results showed that NIR light remotely activated targeting brain structures and showed great biocompatibility (Lin et al., 2017). They then implanted a microscale upconversion-based device into a mouse brain and successfully controlled motor function in awake and freely moving animal (Wang et al., 2017; Lin et al., 2018). NIR optogenetic stimulation represented a major leap when Chen et al. published their findings in the Science journal (Feliu et al., 2018). They demonstrated that UCNP-mediated NIR approach regulated multiple neuronal activities in deep brain regions, specifically evoking dopamine release in the ventral tegmental area, inducing brain oscillations by activating the medial septum, and silencing seizure by inhibiting hippocampal cells and triggering memory recall. In addition, the study showed the excellent biocompatibility, flexibility, robust minimal invasiveness, long-term *in vivo* utility, low dispersion, and negligible cytotoxicity of the approach (Chen et al., 2018). One large timescale study demonstrated that NIR optogenetic stimulation successfully controlled animal locomotive behavior by manipulating neurons in the dorsal striatum and UCNPs remained functional for at least 8 weeks at the injection brain site; these results suggested that using this approach in long-term behavioral tests is highly feasible (Miyazaki et al., 2019). Ma et al. (2019) reported that injected UCNPs enable retinal photoreceptors to perceive NIR light and differentiate sophisticated NIR shape patterns. This type of vision is compatible with daylight vision, offering options for mammalian vision repair and enhancement (Ma et al., 2019). Liu et al. (2021) developed NIR multicolor optogenetics using trichromatic UCNPs, which can selectively activate three distinct neuronal populations and modulate motor behavior in awake mice.

Strengths and Challenges of NIR Optogenetic Stimulation

NIR optogenetic stimulation offers the possibility of delivering light to deep brain regions, is less invasiveness, and has a high spatial resolution and cell specificity (Chen S. et al., 2020). Compared with optogenetics, NIR optogenetic stimulation can be manipulated remotely in the brain without resulting in behavior restriction (All et al., 2019; Lin et al., 2021). This approach has been validated *in vitro* and *in vivo* in terms of its capability to modulate neural activities, and the results suggested potential neuroscience applications. Safety has been demonstrated in many studies, as well as good biocompatibility and negligible toxicity. Furthermore, advancements in NIR optogenetic stimulation require collaboration among physicists,

chemists, neuroscientists, and biologists. It is a big step toward the remote and noninvasive control of brain activities. Hence, transferring this approach to clinical trials is possible, and it may complement current neurological disorder therapies, such as DBS.

Some challenges encountered in NIR optogenetic stimulation need to be addressed here. The toxicity of UCNPs on the cellular, tissue, and organ levels should be comprehensively investigated in order that potential organ damage can be prevented, and long-term biocompatibility studies should be conducted given that UCNPs may change properties and are readily endocytosed by cells (Nazarenus et al., 2014). Effective nanostructures should be designed to satisfy different studies (Tao et al., 2020). In addition, further investigations using large animals are required before clinical trials. Despite such challenges, the recent discovery of NIR optogenetic stimulation is a significant breakthrough. We believe that this new technology has bright therapeutic prospects.

NANOMATERIAL-ENABLED MAGNETIC STIMULATION

Magnetic fields can penetrate tissues with less attenuation and harmless effects, thus having potential uses in wireless and noninvasive methods for modulating brain activities (Christiansen et al., 2019). Magnetic fields are considered intermediary and should be converted to localized secondary stimuli (Wang and Guo, 2016). Methods combining magnetic fields with magnetic nanoparticles (MNPs) converting magnetic signals have been investigated with different techniques (Huang et al., 2010; Wang G. et al., 2020; Kozielski et al., 2021). MNPs as transducers can be categorized into magnetothermal activation, magnetoelectric activation, and magnetomechanical activation (Roet et al., 2019). MNPs incorporate ion-transporting proteins, which can be transgenically expressed in neurons and respond to changes in heat, electricity, or force (Christiansen et al., 2019). It is commonly known as nanomaterial-enabled magnetic stimulation. This approach represents a more effective stimulation that can noninvasively modulate deep brain neural activities and selectively activate specific neural circuits.

Mechanisms of Nanomaterial-Enabled Magnetic Stimulation

Magnetothermal activation uses alternating magnetic fields (AMFs) to activate the temperature-gated ion channels of transient receptor potential vanilloid (TRPV) family (**Figure 4**). MNPs can fuse to TRPV and generate heat through hysteretic power loss and then induce calcium ion influx, membrane depolarization, and action potential firing (Huang et al., 2010; Munshi et al., 2017). TRPV1 is endogenously expressed in mammalian neurons (Starowicz et al., 2008; Terzian et al., 2014). Some studies used genetic tools to achieve the uniform expression of TRPV1 in specific brain areas in mice (Huang et al., 2010; Temel and Jahanshahi, 2015). Magnetoelectric activation uses magnetoelectric nanoparticles (MENs) to generate local electric fields under an external magnetic field. The electric field originates from the intrinsic coupling between electric and magnetic fields in MENs (Guduru et al., 2015). Magnetomechanical activation uses MNPs to convert the energy of magnetic fields into mechanical forces (Chen M. et al., 2020). These forces can activate pressure-sensitive receptors and subsequently modulate neurons (Shin and Cheon, 2017).

Development and Applications of Nanomaterial-Enabled Magnetic Stimulation

Huang et al. (2010) first demonstrated that superparamagnetic nanoparticles exposed to AMFs can locally generate heat and remotely activate TRPV1, eliciting responses from human embryonic kidney 293 cells and *C. elegans*. Another study showed that modified TRPV1 with MNPs can modulate calcium influx *in vivo* and *in vitro* when exposed to a magnetic field (Stanley et al., 2012). Further studies aimed to determine whether a magnetic field can regulate the behavior of rodents animals. Radio wave or magnetic field treatment for glucokinase–Cre (GK–Cre) mice that received ventromedial hypothalamus injection of Ad-FLEX-anti-GFP-TRPV1/GFP-ferritin alters blood glucose and food intake (Stanley et al., 2016). However, the above investigations did not discuss the mechanisms of neural modulation. Chen et al. (2015) exerted a considerable amount of effort into studying wireless magnetothermal activation. In mice, the hysteretic heating of MNPs activates hippocampal and ventral tegmental area neurons after the application of AMFs. To ensure the sustained and uniform levels of TRPV1 expression, the author designed a transgene across a cell membrane. Meanwhile, magnetothermal deep brain stimulation has minimal cytotoxicity, long-term, biocompatibility, and stability (Chen et al., 2015). Munshi et al. (2017) first reported magnetothermal activation using MNPs in awake and freely moving animals. Magnetothermal stimulation in the motor cortex or striatum evokes different types of motor behavior, and the duration of behavior correlates with magnetic field application (Munshi et al., 2017). In addition, they transfected rat hippocampal neurons to express thermosensitive chloride channel anoctamin 1 and silenced neuronal activity by applying a magnetic field to target neurons (Munshi et al., 2018). The behavioral responses evoked by magnetothermal activation result from optogenetic or chemogenetic neural modulation. Hescham et al. (2021) used a wireless magnetothermal approach for parkinsonian-like mice. The results revealed that magnetothermal neuromodulation in the STN can not only modulate the motor behavior of healthy mice remotely but also reverse motor deficits (Hescham et al., 2021). MNPs offer attractive methods for brain tumor therapies because magnetic fields can stimulate tumors through heating without damaging healthy hypodermal tissues (Thorat et al., 2016, 2019). This approach prevents the serious adverse effects of traditional chemotherapy. Compared with magnetothermal activation, magnetoelectric activation, and magnetomechanical activation have not been extensively explored. Nguyen et al. (2021) intravenously injected MENs

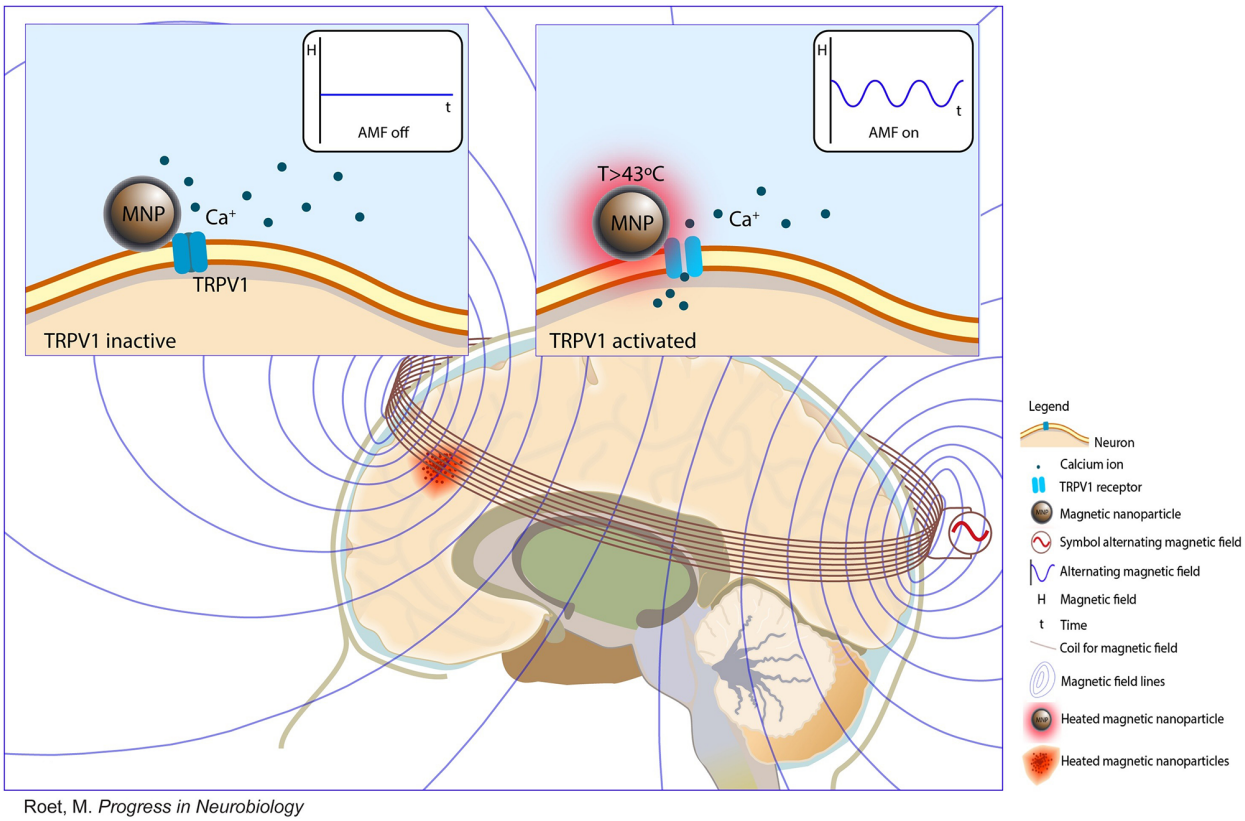

FIGURE 4 | Nanomaterial-enabled magnetic stimulation. A schematic view and schematic principle of nanomaterial-enabled magnetic stimulation in the human brain (Copyright permission was obtained from the publisher; Roet et al., 2019).

TABLE 1 | Overview of each type of neuromodulation.

	FUS	TI stimulation	NIR optogenetic stimulation	Nanomaterial-enabled magnetic stimulation
Energy delivery	Ultrasound	Electrical	Near-infrared	Magnetic
Invasiveness	Noninvasive	Noninvasive	Minimally invasive	Minimally invasive
Spatial resolution	∼1 mm	> mm	<1 mm	<1 mm
Depth of penetration	10–15 cm or more	5 cm or more	1 cm or more	Unlimited in theory
Gene delivery	No	No	Yes	Yes
Experiment animal models	Rodents, non-human primates, human	Rodents, human	Rodents	Rodents
Stimulation mode	Fixing transducer	Fixing electrodes	Remote	Remote
Complexity level	Moderate	Moderate	Complicated	Complicated
Reversible	Yes	Yes	No	No
Cost	Moderate	Low	High	High

FUS, focused ultrasound.

and forced them to cross the BBB and localize to the cortical areas by using a magnetic field gradient. The results showed that cortical neurons and cortical networks can be activated by an external magnetic field (Nguyen et al., 2021). Kozielski et al. (2021) demonstrated that the magnetic stimulation of MENs can modulate neuronal activities in the motor cortex and nonmotor thalamus and modulate mice behavior. Overall, nanomaterial-enabled magnetic stimulation may facilitate remote noninvasive deep brain stimulation without genetic manipulation.

Strengths and Challenges of Nanomaterial-Enabled Magnetic Stimulation

Nanomaterial-enabled magnetic stimulation has offered broad application prospects for noninvasive deep brain modulation. The approach provides high spatial resolution and cell specificity. Its feasibility, effectiveness, biocompatibility, stability, and safety have been validated *in vitro* and *in vivo* (Chen et al., 2015; Park et al., 2020; Wang G. et al., 2020; Kozielski et al., 2021). More importantly, nanomaterial-enabled magnetic stimulation

can utilize MNPs for the modulation of neurons with heat or electric or mechanical forces without genetically engineering. This feature is important and may ensure clinical trial approval (Starowicz et al., 2008). The chemical composition of MNPs is similar to that of MRI agents by having minimal cytotoxicity and long-term effectiveness (Petters et al., 2014; Roet et al., 2019). Meanwhile, with the development of nanotechnology, MNPs have huge biomedical application potential (Chen et al., 2017; Manescu Paltanea et al., 2021).

Studies on nanomaterial-enabled magnetic stimulation mainly focused on small animal models. The next step should be conducting studies on non-human primates and even clinical trials. Scaling AMF coils to human deep brain areas is a huge challenge. In addition, The heating side effects of MNPs should be considered because they may result in brain swelling and increase intracranial pressure (Maier-Hauff et al., 2007). Moreover, heating can promote MNP aggregation, which may cause occlusion in the blood vessel (Wegscheid et al., 2014) and ultimately lead to serious clinical consequences. Therefore, solving this problem is highly necessary. Lastly, the long-term toxicological effects and clearance of MNPs in the brain regions should be investigated.

FUTURE TRENDS

The above deep brain neuromodulation techniques mainly rely on acoustic, electronic, optical, and magnetic signals and show great promise as a high-spatiotemporal resolution and deep penetration platform. These approaches are noninvasive or minimally invasive. The characteristics of the four types of neuromodulation are summarized in **Table 1**.

FUS and TI stimulation are noninvasive neuromodulations without gene delivery. It is relatively easy to translate to the clinic. These techniques may serve as complementary neuromodulation for the treatment of brain disorders. We believe that FUS and TI could be an upgrade of traditional DBS to improve efficiency and safety. However, a similar situation as DBS, FUS, and TI stimulation may just alleviate the progression but cannot cure the disease. Furthermore, none of these approaches has cell type-specific to the brain target. Therefore, future research should explore the underlying mechanisms behind FUS and TI stimulation so that the results can be optimized for clinical application.

Compared to FUS and TI stimulation, NIR optogenetic stimulation and nanomaterial-enabled magnetic stimulation have a long way to go for clinical application. Both approaches need gene delivery. So there are a number of practical challenges before clinical application. First, the long-term safety of viral vectors used for genetic modification to the target neurons has yet to be fully illustrated. Second, maintaining the gene delivery effective and stable in different animal models especially non-human primates is also a potential challenge. Third, genetic therapy for primates is much more complicated, and high cost and long cycle are required for the research. Therefore, there remains much to be done before NIR optogenetic stimulation and nanomaterial-enabled magnetic stimulation can be delivered to the clinical arena. Promisingly, gene therapy has been increasingly applied to treat tumors, virus infection, and genetic disease. As gene delivery technologies develop, the application will be continuously updated. That would be of great significance in neuromodulation.

CONCLUSIONS

These techniques may represent next-generation neural interface tools for neuroscience and have huge potential as tools for advancing neuroscience research. Cross-disciplinary collaboration is needed to establish an optimal scheme given and confirm that these techniques are indeed next-generation noninvasive DBS technologies. We believe that advancements in these techniques will pave the way for novel therapeutic options for brain disorders.

AUTHOR CONTRIBUTIONS

XL and FQ wrote the manuscript. LH performed revision and improved the quality of the manuscript. XW edited and revised the manuscript. All authors contributed to the article and approved the submitted version.

FUNDING

This work was supported by a grant from the key program of National Natural Science Foundation of China (No. 11932013).

REFERENCES

Adair, D., Truong, D., Esmaeilpour, Z., Gebodh, N., Borges, H., Ho, L., et al. (2020). Electrical stimulation of cranial nerves in cognition and disease. *Brain Stimul.* 13, 717–750. doi: 10.1016/j.brs.2020.02.019

Ai, X., Lyu, L., Zhang, Y., Tang, Y., Mu, J., Liu, F., et al. (2017). Remote regulation of membrane channel activity by site-specific localization of lanthanide-doped upconversion nanocrystals. *Angew. Chem. Int. Ed. Engl.* 56, 3031–3035. doi: 10.1002/anie.201612142

Airan, R. (2017). Neuromodulation with nanoparticles. *Science* 357:465. doi: 10.1126/science.aao1200

All, A. H., Zeng, X., Teh, D. B. L., Yi, Z., Prasad, A., Ishizuka, T., et al. (2019). Expanding the toolbox of upconversion nanoparticles for in vivo optogenetics and neuromodulation. *Adv. Mater* 31:e1803474. doi: 10.1002/adma.201803474

Antal, A., Alekseichuk, I., Bikson, M., Brockmöller, J., Brunoni, A. R., Chen, R., et al. (2017). Low intensity transcranial electric stimulation: Safety, ethical, legal regulatory and application guidelines. *Clin. Neurophysiol.* 128, 1774–1809. doi: 10.1016/j.clinph.2017.06.001

Ao, Y., Zeng, K., Yu, B., Miao, Y., Hung, W., Yu, Z., et al. (2019). An upconversion nanoparticle enables near infrared-optogenetic manipulation of the caenorhabditis elegans motor circuit. *ACS Nano* 13, 3373–3386. doi: 10.1021/acsnano.8b09270

Baek, H., Pahk, K. J., Kim, M. J., Youn, I., and Kim, H. (2018). Modulation of cerebellar cortical plasticity using low-intensity focused ultrasound for poststroke sensorimotor function recovery. *Neurorehabil. Neural Repair* 32, 777–787. doi: 10.1177/1545968318790022

Baek, H., Sariev, A., Lee, S., Dong, S. Y., Royer, S., and Kim, H. (2020). Deep cerebellar low-intensity focused ultrasound stimulation restores

interhemispheric balance after ischemic stroke in mice. *IEEE Trans. Neural Syst. Rehabil. Eng.* 28, 2073–2079. doi: 10.1109/TNSRE.2020.3002207

Bansal, A., Liu, H., Jayakumar, M. K., Andersson-Engels, S., and Zhang, Y. (2016). Quasi-continuous wave near-infrared excitation of upconversion nanoparticles for optogenetic manipulation of *C. elegans*. *Small* 12, 1732–1743. doi: 10.1002/smll.201503792

Beatti, A., Rayner, A., Chipchase, L., and Souvlis, T. (2011). Penetration and spread of interferential current in cutaneous, subcutaneous and muscle tissues. *Physiotherapy* 97, 319–326. doi: 10.1016/j.physio.2011.01.008

Begemann, M. J., Brand, B. A., Curcic-Blake, B., Aleman, A., and Sommer, I. E. (2020). Efficacy of non-invasive brain stimulation on cognitive functioning in brain disorders: a meta-analysis. *Psychol. Med.* 50, 2465–2486. doi: 10.1017/S0033291720003670

Blackmore, J., Shrivastava, S., Sallet, J., Butler, C. R., and Cleveland, R. O. (2019). Ultrasound neuromodulation: a review of results, mechanisms and safety. *Ultrasound Med. Biol.* 45, 1509–1536. doi: 10.1016/j.ultrasmedbio.2018.12.015

Bouthour, W., Krack, P., and Luscher, C. (2017). A deeply superficial brain stimulation. *Mov. Disord.* 32:1326. doi: 10.1002/mds.27111

Cao, J., and Grover, P. (2018). "Do single neuron models exhibit temporal interference stimulation," in *2018 IEEE Biomedical Circuits and Systems Conference (BioCAS)*. doi: 10.1109/BIOCAS.2018.8584745

Chakraborty, D., Truong, D. Q., Bikson, M., and Kaphzan, H. (2018). Neuromodulation of axon terminals. *Cereb. Cortex* 28, 2786–2794. doi: 10.1093/cercor/bhx158

Chen, S. (2019). Optical modulation goes deep in the brain. *Science* 365, 456–457. doi: 10.1126/science.aay4350

Chen, G., Cao, Y., Tang, Y., Yang, X., Liu, Y., Huang, D., et al. (2020). Advanced near-infrared light for monitoring and modulating the spatiotemporal dynamics of cell functions in living systems. *Adv. Sci. (Weinh)* 7:1903783. doi: 10.1002/advs.201903783

Chen, R., Canales, A., and Anikeeva, P. (2017). Neural recording and modulation technologies. *Nat. Rev. Mater* 2:16093. doi: 10.1038/natrevmats.2016.93

Chen, R., Romero, G., Christiansen, M. G., Mohr, A., and Anikeeva, P. (2015). Wireless magnetothermal deep brain stimulation. *Science* 347, 1477–1480. doi: 10.1126/science.1261821

Chen, S.-G., Tsai, C.-H., Lin, C.-J., Lee, C.-C., Yu, H.-Y., Hsieh, T.-H., et al. (2020). Transcranial focused ultrasound pulsation suppresses pentylenetetrazol induced epilepsy *in vivo*. *Brain Stimul.* 13, 35–46. doi: 10.1016/j.brs.2019.09.011

Chen, S., Weitemier, A. Z., Zeng, X., He, L., Wang, X., Tao, Y., et al. (2018). Near-infrared deep brain stimulation *via* upconversion nanoparticle-mediated optogenetics. *Science* 359, 679–684. doi: 10.1126/science.aaq1144

Chen, S., Wu, J., Cai, A., Gonzalez, N., and Yin, R. (2020). Towards minimally invasive deep brain stimulation and imaging: a near-infrared upconversion approach. *Neurosci. Res.* 152, 59–65. doi: 10.1016/j.neures.2020.01.005

Chen, M., Wu, J., Ning, P., Wang, J., Ma, Z., Huang, L., et al. (2020). Remote control of mechanical forces *via* mitochondrial-targeted magnetic nanospinners for efficient cancer treatment. *Small* 16:e1905424. doi: 10.1002/smll.201905424

Christiansen, M. G., Senko, A. W., and Anikeeva, P. (2019). Magnetic strategies for nervous system control. *Annu. Rev. Neurosci.* 42, 271–293. doi: 10.1146/annurev-neuro-070918-050241

Chu, P. C., Liu, H. L., Lai, H. Y., Lin, C. Y., Tsai, H. C., and Pei, Y. C. (2015). Neuromodulation accompanying focused ultrasound-induced blood-brain barrier opening. *Sci. Rep.* 5:15477. doi: 10.1038/srep15477

Darrow, D. P. (2019). Focused ultrasound for neuromodulation. *Neurotherapeutics* 16, 88–99. doi: 10.1007/s13311-018-00691-3

Dayan, E., Censor, N., Buch, E. R., Sandrini, M., and Cohen, L. G. (2013). Noninvasive brain stimulation: from physiology to network dynamics and back. *Nat. Neurosci.* 16, 838–844. doi: 10.1038/nn.3422

Deffieux, T., Younan, Y., Wattiez, N., Tanter, M., Pouget, P., and Aubry, J. F. (2013). Low-intensity focused ultrasound modulates monkey visuomotor behavior. *Curr. Biol.* 23, 2430–2433. doi: 10.1016/j.cub.2013.10.029

Ding, H., Lu, L., Shi, Z., Wang, D., Li, L., Li, X., et al. (2018). Microscale optoelectronic infrared-to-visible upconversion devices and their use as injectable light sources. *Proc. Natl. Acad. Sci. U S A* 115, 6632–6637. doi: 10.1073/pnas.1802064115

Esmaeilpour, Z., Kronberg, G., Reato, D., Parra, L. C., and Bikson, M. (2021). Temporal interference stimulation targets deep brain regions by modulating neural oscillations. *Brain Stimul.* 14, 55–65. doi: 10.1016/j.brs.2020.11.007

Feliu, N., Neher, E., and Parak, W. J. (2018). Toward an optically controlled brain. *Science* 359, 633–634. doi: 10.1126/science.aar7379

Fini, M., and Tyler, W. J. (2017). Transcranial focused ultrasound: a new tool for non-invasive neuromodulation. *Int. Rev. Psychiatry* 29, 168–177. doi: 10.1080/09540261.2017.1302924

Folloni, D., Verhagen, L., Mars, R. B., Fouragnan, E., Constans, C., Aubry, J.-F., et al. (2019). Manipulation of subcortical and deep cortical activity in the primate brain using transcranial focused ultrasound stimulation. *Neuron* 101, 1109–1116.e5. doi: 10.1016/j.neuron.2019.01.019

Fomenko, A., Chen, K. S., Nankoo, J. F., Saravanamuttu, J., Wang, Y., El-Baba, M., et al. (2020). Systematic examination of low-intensity ultrasound parameters on human motor cortex excitability and behavior. *eLife* 9:e54497. doi: 10.7554/eLife.54497

Fry, F., Ades, H., and Fry, W. J. S. (1958). Production of reversible changes in the central nervous system by ultrasound. *Science* 127, 83–84. doi: 10.1126/science.127.3289.83

Fry, W. J. (1958). Use of intense ultrasound in neurological research. *Am. J. Phys. Med.* 37, 143–147.

Gibson, B. C., Sanguinetti, J. L., Badran, B. W., Yu, A. B., Klein, E. P., Abbott, C. C., et al. (2018). Increased excitability induced in the primary motor cortex by transcranial ultrasound stimulation. *Front. Neurol.* 9:1007. doi: 10.3389/fneur.2018.01007

Gomez-Tames, J., Asai, A., and Hirata, A. (2021). Multiscale computational model reveals nerve response in a mouse model for temporal interference brain stimulation. *Front. Neurosci.* 15:684465. doi: 10.3389/fnins.2021.684465

Grossman, N. (2018). Modulation without surgical intervention. *Science* 361, 461–462. doi: 10.1126/science.aau4915

Grossman, N., Bono, D., Dedic, N., Kodandaramaiah, S. B., Rudenko, A., Suk, H. J., et al. (2017). Noninvasive deep brain stimulation *via* temporally interfering electric fields. *Cell* 169, 1029–1041.e16. doi: 10.1016/j.cell.2017.05.024

Guduru, R., Liang, P., Hong, J., Rodzinski, A., Hadjikhani, A., Horstmyer, J., et al. (2015). Magnetoelectric "spin" on stimulating the brain. *Nanomedicine (Lond)* 10, 2051–2061. doi: 10.2217/nnm.15.52

Guleyupoglu, B., Schestatsky, P., Edwards, D., Fregni, F., and Bikson, M. (2013). Classification of methods in transcranial electrical stimulation (tES) and evolving strategy from historical approaches to contemporary innovations. *J. Neurosci. Methods* 219, 297–311. doi: 10.1016/j.jneumeth.2013.07.016

Gunduz, A., and Okun, M. S. (2017). A new non-surgical approach for deep-brain stimulation. *Lancet Neurol.* 16:e1. doi: 10.1016/S1474-4422(17)30224-7

Habets, J. G. V., Heijmans, M., Kuijf, M. L., Janssen, M. L. F., Temel, Y., and Kubben, P. L. (2018). An update on adaptive deep brain stimulation in Parkinson's disease. *Mov. Disord.* 33, 1834–1843. doi: 10.1002/mds.115

Harvey, E. N. (1929). The effect of high frequency sound waves on heart muscle and other irritable tissues. *Am. J. Physiol.* 91, 284–290. doi: 10.1152/ajplegacy.1929.91.1.284

Hausser, M. (2014). Optogenetics: the age of light. *Nat. Methods* 11, 1012–1014. doi: 10.1038/nmeth.3111

Hescham, S. A., Chiang, P. H., Gregurec, D., Moon, J., Christiansen, M. G., Jahanshahi, A., et al. (2021). Magnetothermal nanoparticle technology alleviates parkinsonian-like symptoms in mice. *Nat. Commun.* 12:5569. doi: 10.1038/s41467-021-25837-4

Hososhima, S., Yuasa, H., Ishizuka, T., Hoque, M. R., Yamashita, T., Yamanaka, A., et al. (2015). Near-infrared (NIR) up-conversion optogenetics. *Sci. Rep.* 5:16533. doi: 10.1038/srep16533

Hou, X., Qiu, Z., Xian, Q., Kala, S., Jing, J., Wong, K. F., et al. (2021). Precise ultrasound neuromodulation in a deep brain region using nano gas vesicles as actuators. *Adv. Sci. (Weinh)* 8:e2101934. doi: 10.1002/advs.202101934

Howell, B., and McIntyre, C. C. (2021). Feasibility of interferential and pulsed transcranial electrical stimulation for neuromodulation at the human scale. *Neuromodulation* 24, 843–853. doi: 10.1111/ner.13137

Huang, H., Delikanli, S., Zeng, H., Ferkey, D. M., and Pralle, A. (2010). Remote control of ion channels and neurons through magnetic-field heating of nanoparticles. *Nat. Nanotechnol.* 5, 602–606. doi: 10.1038/nnano.2010.125

Hutcheon, B., and Yarom, Y. (2000). Resonance, oscillation and the intrinsic frequency preferences of neurons. *Trends Neurosci.* 23, 216–222. doi: 10.1016/s0166-2236(00)01547-2

Ishibashi, K., Shimada, K., Kawato, T., Kaji, S., Maeno, M., Sato, S., et al. (2010). Inhibitory effects of low-energy pulsed ultrasonic stimulation on cell surface protein antigen C through heat shock proteins GroEL and DnaK in Streptococcus mutans. *Appl. Environ. Microbiol.* 76, 751–756. doi: 10.1128/AEM.02230-09

Kim, M.-R., Yun, J. Y., Jeon, B., Lim, Y. H., Kim, K. R., Yang, H.-J., et al. (2016). Patients' reluctance to undergo deep brain stimulation for Parkinson's disease. *Parkinsonism Relat. Disord.* 23, 91–94. doi: 10.1016/j.parkreldis.2015.11.010

King, R. L., Brown, J. R., Newsome, W. T., and Pauly, K. B. (2013). Effective parameters for ultrasound-induced *in vivo* neurostimulation. *Ultrasound Med. Biol.* 39, 312–331. doi: 10.1016/j.ultrasmedbio.2012.09.009

Kozielski, K. L., Jahanshahi, A., Gilbert, H. B., Yu, Y., Erin, Ö., Francisco, D., et al. (2021). Nonresonant powering of injectable nanoelectrodes enables wireless deep brain stimulation in freely moving mice. *Sci. Adv.* 7:eabc4189. doi: 10.1126/sciadv.abc4189

Kringelbach, M. L., Jenkinson, N., Owen, S. L. F., and Aziz, T. Z. (2007). Translational principles of deep brain stimulation. *Nat. Rev. Neurosci.* 8, 623–635. doi: 10.1038/nrn2196

Kubanek, J. (2018). Neuromodulation with transcranial focused ultrasound. *Neurosurg. Focus* 44:E14. doi: 10.3171/2017.11.FOCUS17621

Lee, S., Lee, C., Park, J., and Im, C. H. (2020). Individually customized transcranial temporal interference stimulation for focused modulation of deep brain structures: a simulation study with different head models. *Sci. Rep.* 10:11730. doi: 10.1038/s41598-020-68660-5

Legon, W., Ai, L., Bansal, P., and Mueller, J. K. (2018). Neuromodulation with single-element transcranial focused ultrasound in human thalamus. *Hum. Brain Mapp.* 39, 1995–2006. doi: 10.1002/hbm.23981

Lewis, S. (2016). Techniques: magnetic manipulation. *Nat. Rev. Neurosci.* 17, 262–263. doi: 10.1038/nrn.2016.42

Li, J., Lee, K. M., and Bai, K. (2020). Analytical and experimental investigation of temporal interference for selective neuromuscular activation. *IEEE Trans. Neural Syst. Rehabil. Eng.* 28, 3100–3112. doi: 10.1109/TNSRE.2020.3038025

Li, G., Qiu, W., Hong, J., Jiang, Q., Su, M., Mu, P., et al. (2018). Imaging-guided dual-target neuromodulation of the mouse brain using array ultrasound. *IEEE Trans. Ultrason. Ferroelectr. Freq. Control* 65, 1583–1589. doi: 10.1109/TUFFC.2018.2847252

Li, G., Qiu, W., Zhang, Z., Jiang, Q., Su, M., Cai, R., et al. (2019). Noninvasive ultrasonic neuromodulation in freely moving mice. *IEEE Trans. Biomed. Eng.* 66, 217–224. doi: 10.1109/TBME.2018.2821201

Li, X., Xiong, H., Rommelfanger, N., Xu, X., Youn, J., Slesinger, P. A., et al. (2021). Nanotransducers for wireless neuromodulation. *Matter* 4, 1484–1510. doi: 10.1016/j.matt.2021.02.012

Lin, W. T., Chen, R. C., Lu, W. W., Liu, S. H., and Yang, F. Y. (2015). Protective effects of low-intensity pulsed ultrasound on aluminum-induced cerebral damage in Alzheimer's disease rat model. *Sci. Rep.* 5:9671. doi: 10.1038/srep09671

Lin, X., Chen, X., Zhang, W., Sun, T., Fang, P., Liao, Q., et al. (2018). Core-shell-shell upconversion nanoparticles with enhanced emission for wireless optogenetic inhibition. *Nano. Lett.* 18, 948–956. doi: 10.1021/acs.nanolett.7b04339

Lin, J. Y., Knutsen, P. M., Muller, A., Kleinfeld, D., and Tsien, R. Y. (2013). ReaChR: a red-shifted variant of channelrhodopsin enables deep transcranial optogenetic excitation. *Nat. Neurosci.* 16, 1499–1508. doi: 10.1038/nn.3502

Lin, X., Wang, Y., Chen, X., Yang, R., Wang, Z., Feng, J., et al. (2017). Multiplexed optogenetic stimulation of neurons with spectrum-selective upconversion nanoparticles. *Adv. Healthc. Mater.* 6:1700446. doi: 10.1002/adhm.201700446

Lin, Y., Yao, Y., Zhang, W., Fang, Q., Zhang, L., Zhang, Y., et al. (2021). Applications of upconversion nanoparticles in cellular optogenetics. *Acta Biomater.* 135, 1–12. doi: 10.1016/j.actbio.2021.08.035

Liu, X., Chen, H., Wang, Y., Si, Y., Zhang, H., Li, X., et al. (2021). Near-infrared manipulation of multiple neuronal populations *via* trichromatic upconversion. *Nat. Commun.* 12:5662. doi: 10.1038/s41467-021-25993-7

Liu, S. H., Lai, Y. L., Chen, B. L., and Yang, F. Y. (2017). Ultrasound enhances the expression of brain-derived neurotrophic factor in astrocyte through activation of TrkB-Akt and Calcium-CaMK signaling pathways. *Cereb. Cortex* 27, 3152–3160. doi: 10.1093/cercor/bhw169

Lozano, A. M. (2017). Waving hello to noninvasive deep-brain stimulation. *N Engl. J. Med.* 377, 1096–1098. doi: 10.1056/NEJMcibr1707165

Lozano, A. M., and Lipsman, N. (2013). Probing and regulating dysfunctional circuits using deep brain stimulation. *Neuron* 77, 406–424. doi: 10.1016/j.neuron.2013.01.020

Ma, Y., Bao, J., Zhang, Y., Li, Z., Zhou, X., Wan, C., et al. (2019). Mammalian near-infrared image vision through injectable and self-powered retinal nanoantennae. *Cell* 177, 243–255.e15. doi: 10.1016/j.cell.2019.01.038

Maier-Hauff, K., Rothe, R., Scholz, R., Gneveckow, U., Wust, P., Thiesen, B., et al. (2007). Intracranial thermotherapy using magnetic nanoparticles combined with external beam radiotherapy: results of a feasibility study on patients with glioblastoma multiforme. *J. Neurooncol.* 81, 53–60. doi: 10.1007/s11060-006-9195-0

Manescu Paltanea, V., Paltanea, G., Antoniac, I., and Vasilescu, M. (2021). Magnetic nanoparticles used in oncology. *Materials (Basel, Switzerland)* 14:5948. doi: 10.3390/ma14205948

Meng, Y., Volpini, M., Black, S., Lozano, A. M., Hynynen, K., and Lipsman, N. (2017). Focused ultrasound as a novel strategy for Alzheimer disease therapeutics. *Ann. Neurol.* 81, 611–617. doi: 10.1002/ana.24933

Mihran, R. T., Lineaweaver, S. K., Barnes, F. S., and Wachtel, H. (1996). Effects of pulsed acoustic and mechanical stimuli on the excitability of isolated neuronal and cardiac cells. *Appl. Occup. Env. Hygiene* 11, 271–274. doi: 10.1080/1047322X.1996.10389322

Min, B.-K., Yang, P. S., Bohlke, M., Park, S., R.Vago, D., Maher, T. J., et al. (2011). Focused ultrasound modulates the level of cortical neurotransmitters: potential as a new functional brain mapping technique. *Int. J. Imaging Syst. Technol.* 21, 232–240. doi: 10.1002/ima.20284

Mirzakhalili, E., Barra, B., Capogrosso, M., and Lempka, S. F. (2020). Biophysics of temporal interference stimulation. *Cell Syst.* 11, 557–572.e5. doi: 10.1016/j.cels.2020.10.004

Miyazaki, T., Chowdhury, S., Yamashita, T., Matsubara, T., Yawo, H., Yuasa, H., et al. (2019). Large timescale interrogation of neuronal function by fiberless optogenetics using lanthanide micro-particles. *Cell Rep.* 26, 1033–1043.e5. doi: 10.1016/j.celrep.2019.01.001

Monai, H., Ohkura, M., Tanaka, M., Oe, Y., Konno, A., Hirai, H., et al. (2016). Calcium imaging reveals glial involvement in transcranial direct current stimulation-induced plasticity in mouse brain. *Nat. Commun.* 7:11100. doi: 10.1038/ncomms11100

Munshi, R., Qadri, S. M., and Pralle, A. (2018). Transient magnetothermal neuronal silencing using the chloride channel anoctamin 1 (TMEM16A). *Front. Neurosci.* 12:560. doi: 10.3389/fnins.2018.00560

Munshi, R., Qadri, S. M., Zhang, Q., Castellanos Rubio, I., Del Pino, P., and Pralle, A. (2017). Magnetothermal genetic deep brain stimulation of motor behaviors in awake, freely moving mice. *eLife* 6:e27069. doi: 10.7554/eLife.27069

Nazarenus, M., Zhang, Q., Soliman, M. G., Del Pino, P., Pelaz, B., Carregal-Romero, S., et al. (2014). in vitro interaction of colloidal nanoparticles with mammalian cells: what have we learned thus far. *Beilstein J. Nanotechnol.* 5, 1477–1490. doi: 10.3762/bjnano.5.161

Negahbani, E., Kasten, F. H., Herrmann, C. S., and Frohlich, F. (2018). Targeting alpha-band oscillations in a cortical model with amplitude-modulated high-frequency transcranial electric stimulation. *Neuroimage* 173, 3–12. doi: 10.1016/j.neuroimage.2018.02.005

Nguyen, T., Gao, J., Wang, P., Nagesetti, A., Andrews, P., Masood, S., et al. (2021). *In vivo* wireless brain stimulation *via* non-invasive and targeted delivery of magnetoelectric nanoparticles. *Neurotherapeutics* 18, 2091–2106. doi: 10.1007/s13311-021-01071-0

Oh, S. J., Lee, J. M., Kim, H. B., Lee, J., Han, S., Bae, J. Y., et al. (2019). Ultrasonic neuromodulation *via* astrocytic TRPA1. *Curr. Biol.* 29, 3386–3401.e8. doi: 10.1016/j.cub.2019.08.021

Ozdas, M. S., Shah, A. S., Johnson, P. M., Patel, N., Marks, M., Yasar, T. B., et al. (2020). Non-invasive molecularly-specific millimeter-resolution manipulation of brain circuits by ultrasound-mediated aggregation and

uncaging of drug carriers. *Nat. Commun.* 11:4929. doi: 10.1038/s41467-020-18059-7

Park, J., Tabet, A., Moon, J., Chiang, P. H., Koehler, F., Sahasrabudhe, A., et al. (2020). Remotely controlled proton generation for neuromodulation. *Nano Lett.* 20, 6535–6541. doi: 10.1021/acs.nanolett.0c02281

Parker, T., Raghu, A. L. B., FitzGerald, J. J., Green, A. L., and Aziz, T. Z. (2020). Multitarget deep brain stimulation for clinically complex movement disorders. *J. Neurosurg.* 134, 351–356. doi: 10.3171/2019.11.JNS192224

Petters, C., Irrsack, E., Koch, M., and Dringen, R. (2014). Uptake and metabolism of iron oxide nanoparticles in brain cells. *Neurochem. Res.* 39, 1648–1660. doi: 10.1007/s11064-014-1380-5

Prodi, L., Rampazzo, E., Rastrelli, F., Speghini, A., and Zaccheroni, N. (2015). Imaging agents based on lanthanide doped nanoparticles. *Chem. Soc. Rev.* 44, 4922–4952. doi: 10.1039/c4cs00394b

Rabut, C., Yoo, S., Hurt, R. C., Jin, Z., Li, H., Guo, H., et al. (2020). Ultrasound technologies for imaging and modulating neural activity. *Neuron* 108, 93–110. doi: 10.1016/j.neuron.2020.09.003

Rampersad, S., Roig-Solvas, B., Yarossi, M., Kulkarni, P. P., Santarnecchi, E., Dorval, A. D., et al. (2019). Prospects for transcranial temporal interference stimulation in humans: a computational study. *Neuroimage* 202:116124. doi: 10.1016/j.neuroimage.2019.116124

Roet, M., Hescham, S. A., Jahanshahi, A., Rutten, B. P. F., Anikeeva, P. O., and Temel, Y. (2019). Progress in neuromodulation of the brain: a role for magnetic nanoparticles. *Prog. Neurobiol.* 177, 1–14. doi: 10.1016/j.pneurobio.2019.03.002

Shi, L., Sordillo, L. A., Rodriguez-Contreras, A., and Alfano, R. (2016). Transmission in near-infrared optical windows for deep brain imaging. *J. Biophotonics* 9, 38–43. doi: 10.1002/jbio.201500192

Shin, T.-H., and Cheon, J. (2017). Synergism of nanomaterials with physical stimuli for biology and medicine. *Acc. Chem. Res.* 50, 567–572. doi: 10.1021/acs.accounts.6b00559

Song, X., Zhao, X., Li, X., Liu, S., and Ming, D. (2020). Multi-channel transcranial temporally interfering stimulation (tTIS): application to living mice brain. *J. Neural Eng.* doi: 10.1088/1741-2552/abd2c9. [Online ahead of print].

Stanley, S. A., Gagner, J. E., Damanpour, S., Yoshida, M., Dordick, J. S., and Friedman, J. M. (2012). Radio-wave heating of iron oxide nanoparticles can regulate plasma glucose in mice. *Science* 336, 604–608. doi: 10.1126/science.1216753

Stanley, S. A., Kelly, L., Latcha, K. N., Schmidt, S. F., Yu, X., Nectow, A. R., et al. (2016). Bidirectional electromagnetic control of the hypothalamus regulates feeding and metabolism. *Nature* 531, 647–650. doi: 10.1038/nature17183

Starowicz, K., Cristino, L., and Di Marzo, V. (2008). TRPV1 receptors in the central nervous system: potential for previously unforeseen therapeutic applications. *Curr. Pharm. Design* 14, 42–54. doi: 10.2174/138161208783330790

Suarez-Castellanos, I. M., Dossi, E., Vion-Bailly, J., Salette, L., Chapelon, J.-Y., Carpentier, A., et al. (2021). Spatio-temporal characterization of causal electrophysiological activity stimulated by single pulse Focused Ultrasound: an *ex vivo* study on hippocampal brain slices. *J. Neural Eng.* doi: 10.1088/1741-2552/abdfb1. [Online ahead of print].

Tao, Y., Chan, H. F., Shi, B., Li, M., and Leong, K. W. (2020). Light: a magical tool for controlled drug delivery. *Adv. Funct. Mater.* 30:2005029. doi: 10.1002/adfm.202005029

Tatti, E., Rossi, S., Innocenti, I., Rossi, A., and Santarnecchi, E. (2016). Non-invasive brain stimulation of the aging brain: State of the art and future perspectives. *Ageing Res. Rev.* 29, 66–89. doi: 10.1016/j.arr.2016.05.006

Temel, Y., and Jahanshahi, A. (2015). Neuroscience. treating brain disorders with neuromodulation. *Science* 347, 1418–1419. doi: 10.1126/science.aaa9610

Terzian, A. L., dos Reis, D. G., Guimaraes, F. S., Correa, F. M., and Resstel, L. B. (2014). Medial prefrontal cortex transient receptor potential vanilloid type 1 (TRPV1) in the expression of contextual fear conditioning in Wistar rats. *Psychopharmacology (Berl)* 231, 149–157. doi: 10.1007/s00213-013-3211-9

Thorat, N. D., Bohara, R. A., Malgras, V., Tofail, S. A. M., Ahamad, T., Alshehri, S. M., et al. (2016). Multimodal superparamagnetic nanoparticles with unusually enhanced specific absorption rate for synergetic cancer therapeutics and magnetic resonance imaging. *ACS Appl. Mater. Interfaces* 8, 14656–14664. doi: 10.1021/acsami.6b02616

Thorat, N. D., Townely, H., Brennan, G., Parchur, A. K., Silien, C., Bauer, J., et al. (2019). Progress in remotely triggered hybrid nanostructures for next-generation brain cancer theranostics. *ACS Biomater. Sci. Eng.* 5, 2669–2687. doi: 10.1021/acsbiomaterials.8b01173

Tsui, P. H., Wang, S. H., and Huang, C. C. (2005). in vitro effects of ultrasound with different energies on the conduction properties of neural tissue. *Ultrasonics* 43, 560–565. doi: 10.1016/j.ultras.2004.12.003

Tufail, Y., Matyushov, A., Baldwin, N., Tauchmann, M. L., Georges, J., Yoshihiro, A., et al. (2010). Transcranial pulsed ultrasound stimulates intact brain circuits. *Neuron* 66, 681–694. doi: 10.1016/j.neuron.2010.05.008

Tufail, Y., Yoshihiro, A., Pati, S., Li, M. M., and Tyler, W. J. (2011). Ultrasonic neuromodulation by brain stimulation with transcranial ultrasound. *Nat. Protoc.* 6, 1453–1470. doi: 10.1038/nprot.2011.371

Tyler, W. J., Tufail, Y., Finsterwald, M., Tauchmann, M. L., Olson, E. J., and Majestic, C. (2008). Remote excitation of neuronal circuits using low-intensity, low-frequency ultrasound. *PLoS One* 3:e3511. doi: 10.1371/journal.pone.0003511

von Conta, J., Kasten, F. H., Curcic-Blake, B., Aleman, A., Thielscher, A., and Herrmann, C.S. (2021). Interindividual variability of electric fields during transcranial temporal interference stimulation (tTIS). *Sci. Rep.* 11:20357. doi: 10.1038/s41598-021-99749-0

Wachter, D., Wrede, A., Schulz-Schaeffer, W., Taghizadeh-Waghefi, A., Nitsche, M. A., Kutschenko, A., et al. (2011). Transcranial direct current stimulation induces polarity-specific changes of cortical blood perfusion in the rat. *Exp. Neurol.* 227, 322–327. doi: 10.1016/j.expneurol.2010.12.005

Wang, Y., and Guo, L. (2016). Nanomaterial-enabled neural stimulation. *Front. Neurosci.* 10:69. doi: 10.3389/fnins.2016.00069

Wang, F., and Liu, X. (2009). Recent advances in the chemistry of lanthanide-doped upconversion nanocrystals. *Chem. Soc. Rev.* 38, 976–989. doi: 10.1039/b809132n

Wang, Y., Lin, X., Chen, X., Chen, X., Xu, Z., Zhang, W., et al. (2017). Tetherless near-infrared control of brain activity in behaving animals using fully implantable upconversion microdevices. *Biomaterials* 142, 136–148. doi: 10.1016/j.biomaterials.2017.07.017

Wang, H., Shi, Z., Sun, W., Zhang, J., Wang, J., Shi, Y., et al. (2020). Development of a non-invasive deep brain stimulator with precise positioning and real-time monitoring of bioimpedance. *Front. Neuroinform.* 14:574189. doi: 10.3389/fninf.2020.574189

Wang, G., Zhang, P., Mendu, S. K., Wang, Y., Zhang, Y., Kang, X., et al. (2020). Revaluation of magnetic properties of Magneto. *Nat. Neurosci.* 23, 1047–1050. doi: 10.1038/s41593-019-0473-5

Wegscheid, M. L., Morshed, R. A., Cheng, Y., and Lesniak, M. S. (2014). The art of attraction: applications of multifunctional magnetic nanomaterials for malignant glioma. *Exp. Opin. Drug Deliv.* 11, 957–975. doi: 10.1517/17425247.2014.912629

Woods, A. J., Antal, A., Bikson, M., Boggio, P. S., Brunoni, A. R., Celnik, P., et al. (2016). A technical guide to tDCS and related non-invasive brain stimulation tools. *Clin. Neurophysiol.* 127, 1031–1048. doi: 10.1016/j.clinph.2015.11.012

Wu, X., Chen, G., Shen, J., Li, Z., Zhang, Y., and Han, G. (2015). Upconversion nanoparticles: a versatile solution to multiscale biological imaging. *Bioconjug. Chem.* 26, 166–175. doi: 10.1021/bc5003967

Wu, L., Liu, T., and Wang, J. (2021). Improving the effect of transcranial alternating current stimulation (tACS): a systematic review. *Front. Hum. Neurosci.* 15:652393. doi: 10.3389/fnhum.2021.652393

Wu, X., Zhang, Y., Takle, K., Bilsel, O., Li, Z., Lee, H., et al. (2016). Dye-sensitized core/active shell upconversion nanoparticles for optogenetics and bioimaging applications. *ACS Nano* 10, 1060–1066. doi: 10.1021/acsnano.5b06383

Xiao, Q., Zhong, Z., Lai, X., and Qin, H. (2019). A multiple modulation synthesis method with high spatial resolution for noninvasive neurostimulation. *PLoS One* 14:e0218293. doi: 10.1371/journal.pone.0218293

Yang, P. F., Phipps, M. A., Jonathan, S., Newton, A. T., Byun, N., Gore, J. C., et al. (2021). Bidirectional and state-dependent modulation of brain activity by transcranial focused ultrasound in non-human primates. *Brain Stimul.* 14, 261–272. doi: 10.1016/j.brs.2021.01.006

Ye, J., Tang, S., Meng, L., Li, X., Wen, X., Chen, S., et al. (2018). Ultrasonic control of neural activity through activation of the mechanosensitive channel MscL. *Nano Lett.* 18, 4148–4155. doi: 10.1021/acs.nanolett.8b00935

Yoo, S. S., Bystritsky, A., Lee, J. H., Zhang, Y., Fischer, K., Min, B. K., et al. (2011). Focused ultrasound modulates region-specific brain activity. *Neuroimage* 56, 1267–1275. doi: 10.1016/j.neuroimage.2011.02.058

Yoon, K., Lee, W., Lee, J. E., Xu, L., Croce, P., Foley, L., et al. (2019). Effects of sonication parameters on transcranial focused ultrasound brain stimulation in an ovine model. *PLoS One* 14:e0224311. doi: 10.1371/journal.pone.0224311

Yu, N., Huang, L., Zhou, Y., Xue, T., Chen, Z., and Han, G. (2019). Near-infrared-light activatable nanoparticles for deep-tissue-penetrating wireless optogenetics. *Adv. Healthc. Mater.* 8:e1801132. doi: 10.1002/adhm.201801132

Yu, K., Sohrabpour, A., and He, B. (2016). Electrophysiological source imaging of brain networks perturbed by low-intensity transcranial focused ultrasound. *IEEE Trans. Biomed. Eng.* 63, 1787–1794. doi: 10.1109/TBME.2016.2591924

Yuan, Y., Wang, Z., Liu, M., and Shoham, S. (2020). Cortical hemodynamic responses induced by low-intensity transcranial ultrasound stimulation of mouse cortex. *Neuroimage* 211:116597. doi: 10.1016/j.neuroimage.2020.116597

Zhen, M., and Samuel, A. D. (2015). C. elegans locomotion: small circuits, complex functions. *Curr. Opin. Neurobiol.* 33, 117–126. doi: 10.1016/j.conb.2015.03.009

Zhou, B., Shi, B., Jin, D., and Liu, X. (2015). Controlling upconversion nanocrystals for emerging applications. *Nat. Nanotechnol.* 10, 924–936. doi: 10.1038/nnano.2015.251

Conflict of Interest: The authors declare that the research was conducted in the absence of any commercial or financial relationships that could be construed as a potential conflict of interest.

Publisher's Note: All claims expressed in this article are solely those of the authors and do not necessarily represent those of their affiliated organizations, or those of the publisher, the editors and the reviewers. Any product that may be evaluated in this article, or claim that may be made by its manufacturer, is not guaranteed or endorsed by the publisher.

frontiers in Behavioral Neuroscience

ORIGINAL RESEARCH
published: 24 February 2022
doi: 10.3389/fnbeh.2022.808789

Effect of Electro-Acupuncture on Lateralization of the Human Swallowing Motor Cortex Excitability by Navigation-Transcranial Magnetic Stimulation-Electromyography

Xiaorong Tang[1†], Mindong Xu[1†], Jiayi Zhao[1†], Jiahui Shi[1†], Yingyu Zi[2], Jianlu Wu[1], Jing Xu[1], Yanling Yu[1], LuLu Yao[1], Jiayin Ou[1], Yitong Li[3], Shuqi Yao[4], Hang Lv[2], Liming Lu[1], Nenggui Xu[1]* and Lin Wang[1]**

[1] South China Research Center for Acupuncture and Moxibustion, Medical College of Acu-Moxi and Rehabilitation, Guangzhou University of Chinese Medicine, Guangzhou, China, [2] Nanfang Hospital, Southern Medical University, Guangzhou, China, [3] Shenzhen Maternity and Child Healthcare Hospital, Shenzhen, China, [4] Department of Integration of Chinese and Western Medicine, School of Basic Medical Sciences, Peking University, Beijing, China

OPEN ACCESS

Edited by:
Masaki Sekino,
The University of Tokyo, Japan

Reviewed by:
David M. Niddam,
National Yang-Ming University, Taiwan
Travis Davidson,
University of Ottawa, Canada

***Correspondence:**
Liming Lu
lulimingleon@gzucm.edu.cn
Nenggui Xu
ngxu8018@163.com
Lin Wang
wanglin16@gzucm.edu.cn

[†] These authors have contributed equally to this work

Specialty section:
This article was submitted to Pathological Conditions, a section of the journal Frontiers in Behavioral Neuroscience

Received: 04 November 2021
Accepted: 24 January 2022
Published: 24 February 2022

Citation:
Tang X, Xu M, Zhao J, Shi J, Zi Y, Wu J, Xu J, Yu Y, Yao L, Ou J, Li Y, Yao S, Lv H, Lu L, Xu N and Wang L (2022) Effect of Electro-Acupuncture on Lateralization of the Human Swallowing Motor Cortex Excitability by Navigation-Transcranial Magnetic Stimulation-Electromyography. Front. Behav. Neurosci. 16:808789. doi: 10.3389/fnbeh.2022.808789

Background: The use of transcranial magnetic stimulation combined with electromyography for the functional evaluation of the cerebral cortex in both clinical and non-clinical populations is becoming increasingly common. Numerous studies have shown that electro-acupuncture (EA) can regulate cerebral cortical excitability. However, the effect of EA on the lateralization of the human swallowing motor cortex excitability is not yet fully understood.

Objective: The aim of this study was to assess whether lateralization is present in the swallowing motor cortex of healthy subjects, and to investigate the impact of EA at Lianquan (CV23) and Fengfu (GV16) on lateralization.

Methods: Forty subjects were randomized 1:1 into the EA group and the sham-EA group. The bilateral swallowing motor cortices was located by a neuroimaging navigation system. Then, the resting motor threshold (RMT) and motor evoked potential (MEP) of the mylohyoid of healthy subjects were recorded while applying combined transcranial magnetic stimulation and electromyography before and after EA or sham-EA.

Results: First, the RMT and MEP latency of the contralateral mylohyoid innervated by the right swallowing cortex (71.50 ± 1.67%, 8.30 ± 0.06 ms) were lower than those innervated by the left (79.38 ± 1.27%, 8.40 ± 0.06 ms). Second, EA at CV23 and GV16 reduced the bilateral RMT and enhanced the bilateral MEP latency and amplitude ($P = 0.005$, $P < 0.001$; $P = 0.002$, $P = 0.001$; $P = 0.002$, $P = 0.009$), while sham-EA did not ($P > 0.05$). Third, EA had an effect on the RMT and MEP latency in terms of lateralization changes, but this was not significant ($P = 0.067$, $P = 0.156$).

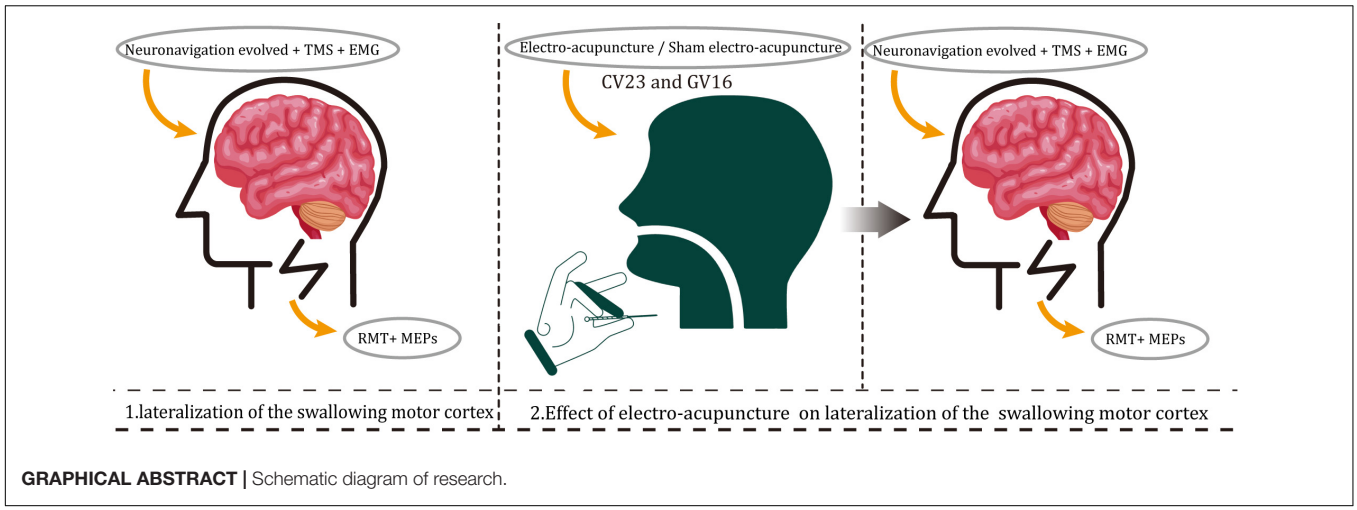

GRAPHICAL ABSTRACT | Schematic diagram of research.

Conclusion: The right swallowing motor cortex of healthy subjects is more excitable than that of the left at resting state. Thus, we found that lateralization is present in the swallowing motor cortex of healthy people, which might indicate a hemispheric dominance of swallowing predominates in the right swallowing motor cortex. In addition, EA at CV23 and GV16 can instantly promote the excitability of the bilateral swallowing motor cortices. But there was no significant difference in EA stimulation in terms of lateralization.

Keywords: lateralization, swallowing, single-pulse TMS, resting motor threshold, motor evoked potential, electro-acupuncture (EA)

HIGHLIGHTS

- The right swallowing motor cortex of healthy people is more excitable than the left.
- EA promoted swallowing motor cortex excitability, bilaterally.
- The above research results will help people understand the way of brain swallowing control more comprehensively, which may help clinicians formulate scientific rehabilitation treatment plans.

INTRODUCTION

We have a favorite hand for writing, a preferred foot for kicking a ball, and even a favorite way to turn our head when kissing (Carey et al., 2001; Gunturkun, 2003; Papadatou-Pastou and Tomprou, 2015). These are the result of structural or functional differences between the left and right hemispheres known as hemispheric lateralization, which is a feature found in almost all major nervous systems of the human brain (Gunturkun and Ocklenburg, 2017). At the structural level, hemispheric lateralization can manifest as asymmetric gene expression in specific brain regions, asymmetry in the size and shape of brain regions, and asymmetry in the shape and structure of functional networks and the two hemispheres themselves (Crow, 2013; Caeyenberghs and Leemans, 2014; Karlebach and Francks, 2015; Ocklenburg et al., 2016). At the functional level, the most significant asymmetry in brain activity is found in language systems, as well as visual spatial processing, auditory processing neurons, memory, motor systems, and emotional processing (Goodale, 1988; Cabeza, 2002; Tervaniemi and Hugdahl, 2003; Grimshaw and Carmel, 2014). Although hemispheric lateralization is ubiquitous in the human nervous system and body, bringing about a series of highly relevant behavioral and cognitive changes, this core principle has still not been thoroughly studied.

Swallowing is one of the most complex and closely coordinated physiological activities of humans. In contrast to most somatic functions, swallowing has bilateral cerebral representation. Previous studies had found that left hemisphere damage and right hemisphere damage may be associated with different types of swallowing behaviors (Robbins et al., 1993; Daniels et al., 1996). Dysphagia would occur if damage had affected the side of the brain with the largest or dominant projection (Singh and Hamdy, 2006). This means that the functional asymmetry of the swallowing motor cortex may be important for determining the severity of the dysphagia and the recovery of the dysphagia. Hamdy et al. (1996) and Scoppa et al. (2020) identified the sites of cortical activation during swallowing

Abbreviations: EA, electro-acupuncture; EMG, electromyography; MEP, motor evoked potential; MRI, magnetic resonance image; RMT, resting motor threshold; TMS, transcranial magnetic stimulation.

using functional magnetic resonance imaging (MRI) techniques, and they found it mainly concentrated in the precentral gyrus. Therefore, similar to previous studies, our study selected the swallowing area of the precentral gyrus to measure the excitability of the swallowing motor cortex (Hamdy et al., 1997, 1998; Singh and Hamdy, 2006).

Transcranial magnetic stimulation (TMS) is an approach that allows non-invasive stimulation of neurons using time-varying magnetic fields (Halko et al., 2013). TMS has been used to detect cerebral cortex excitability (Badawy et al., 2012). The MEP elicited in peripheral muscles by TMS over human motor cortex is one of the hallmark measures for non-invasive quantification of cortical and spinal excitability in cognitive and clinical neuroscience (Bestmann and Krakauer, 2015). A series of previous studies have shown that the threshold for producing an motor evoked potentials (MEPs) reflects the excitability of a central core of neurons and MEPs indicates the excitatory state changes in the cortex (Leocani et al., 2000; Hallett, 2007; Biabani et al., 2021). As for the area of the swallowing cortex, there are many previous studies using MEPs to assess the excitability of the contralateral swallowing cortex (Hamdy et al., 1997, 1998).

Electro-acupuncture (EA) is a technique based on the traditional acupuncture method combined with modern electrotherapy. EA can stimulate nerves, and the resulting nerve impulses can strengthen the corresponding neural reflexes (Deng and Wu, 2017). Systematic review and meta-analysis have supported the claim that acupuncture therapies cannot cure dysphagia, but it can partially improve the swallowing function of patients with dysphagia, and CV23 and GV16 were the most commonly used acupoints (Lu et al., 2021; Zhong et al., 2021). However, the mechanism underlying the curative effect of EA is unknown.

As for the lateralization, Hamdy et al. (1996) illustrated that the swallowing musculature is discretely and somatotopically represented on the motor and premotor cortex of both hemispheres and interhemispheric asymmetry varied among mylohyoid, pharynx and esophagus by TMS combined with EMG. Mosier et al. (1999) showed that right hemispheric dominance showed stronger swallowing lateralization than the left hemisphere with functional MRI imaging. Besides, Rotenberg et al. (2010) demonstrated that lateralized cortical stimulation resulting in selective activation of one forelimb contralateral to the site of stimulation could be achieved by TMS using MEPs in the rat. But, Ferrari et al. (2017) failed to demonstrate lateralization in the dorsolateral prefrontal cortex by using TMS. Khamnei et al. (2019) have discovered that the dominant chewing side may originate in the dominant hemisphere of the brain (dominant hemisphere is defined by handedness) by using surface electromyography recording from masseter muscles. However, researchers failed to identify a consistent pattern of lateralization from swallowing musculature. Thus, to further explore the hemispheric dominance of swallowing function at resting state, we investigated the lateralization of the human swallowing motor cortex excitability in healthy subjects using the Resting motor threshold (RMT) and MEPs induced by TMS. More importantly, we examined the effect of EA on swallowing motor cortex excitability.

MATERIALS AND METHODS

Study Design and Subjects

This was a single-blind randomized controlled trial. Recruitment of eligible healthy subjects was conducted at the South China Research Center for Acupuncture and Moxibustion. The protocol of this trial has been published previously (Li et al., 2019). This trial was following the Declaration of Helsinki and registered with the Chinese Clinical Trial Registry (ChiCTR-IOR-17011359). Ethical approval was obtained from the China Ethics Committee of Registering Clinical Trials (ChiECRCT-20170038). Forty healthy subjects (20 female and 20 males; age: 21.65 $\pm$ 0.28 years; body mass index: 20.40 $\pm$ 0.34; Mean Mini-mental State Examination score: 30; Kubota Water Swallow Test: Grade 1) were enrolled in the study. Subjects had no history of neurological or psychiatric disease and were not taking drugs that act on the central nervous system. Subjects gave written informed consent.

Randomization and Blinding

Eligible subjects were randomly assigned to receive either EA or sham-EA *via* a computer randomization program (PEMS3.1, Sichuan University, Sichuan, China) using a 1:1 ratio. Due to the specific nature of acupuncture, the acupuncturist was not blinded to treatment allocation. The participants, outcome assessors, and statisticians were blinded to treatment allocation.

Intervention

Lianquan (CV23) is an acupuncture point on the anterior part of the surface of the neck directly superior to the laryngeal prominence, in the depression at the upper margin of the hyoid bone. It is at the base of the tongue and level with the pharynx (Li et al., 2019). CV23 is also located where the mylohyoid (which is a paired muscle running from the hyoid bone to the mandible and which forms the floor of the mouth) inserts into the hyoid (Li et al., 2019; **Supplementary Appendix 1**). For the EA group, two sterile acupuncture needles (length: 25 mm, diameter: 0.30 mm; Huatuo, Suzhou Medical Supplies Factory Co., Ltd., Suzhou, China) were inserted into CV23 and GV16 to a depth of 0.5–1 cun. The acupuncture needles were connected to an acupuncture point nerve stimulator (HANS-200A) with a frequency of 2 Hz for 15 min, and the intensity of EA was set to the maximum-tolerated intensity of each subject (0.9–3.0 mA). For the sham-EA group, Streitberger placebo needles (Huatuo, Suzhou Medical Supplies Factory Co., Ltd., Suzhou, China) were inserted into CV23 and GV16. The Streitberger placebo needle set was invented by Streitberger and Kleinhenz (1998), and is a validated and reliable single-blind acupuncture needle used to investigate the effects of acupuncture.

Navigation

The subjects' brains were scanned using an MRI scanner (Signa EXCITE 3.0T HD, IGE, Milwaukee, United States) at Guangdong Provincial Hospital of Chinese Medicine. The MRI T1 file was imported into the Brainsight TMS Navigation system (Brainsight 2.3.3.dmg) and a three-dimensional brain was then

reconstructed. Targets with 3 × 3 square grid were built over the swallowing motor cortex of the three-dimensional brain. The Polaris System was used to collect cortical topographical landmarks from the head of subject, which allowed the external near-infrared system to follow the figure-of-eight TMS coil in real-time. Subjects sited on the treatment couch facing the neuroimaging navigation system and TMS machine to enable location of the correct brain regions. They were asked to remain as relaxed as possible and to avoid swallowing, coughing, or vocalizing during the stimulation procedure.

Transcranial Magnetic Stimulation and Electromyography

Transcranial magnetic stimulation was applied to the motor cortex in the bilateral hemisphere with a Magstim Super Rapid magnetic stimulator (Magstim Company, Dyfed, United Kingdom) equipped with a figure-of-eight coil (external wing diameter, 70 mm). The coil was orientated at 45°oblique to the sagittal plane. That was to ensure that the stimulus can be applied vertically to the swallowing area of the precentral gyrus. RMT and MEPs induced by TMS were recorded from the bilateral mylohyoid.

Motor evoked potentials were electromyographic signals produced by the peripheral muscles under transcranial magnetic stimulation (Peng et al., 2020). The recording electrodes were two pairs of bipolar silver-silver chloride electrodes (10 mm diameter 1.5 m cable 12/package, DIN Style, Nicolet, United States), which were placed bilaterally on each side of the mylohyoid after skin disinfection to record MEPs of the mylohyoid. The reference electrodes were placed directly next to them (1 cm). Two pairs of ground wire disk electrodes (1.25 m cable, 1/package, DIN Style) were placed 2 cm from both corners of the mouth to reduce interference to the electromyographic signal. All electrodes were checked every 15 min to ensure that they were in contact with the skin and underlying muscles.

Cortical stimulation was performed over the left and right swallowing motor cortices every 30 s according to the targets with 3 × 3 square grid, described above. First, a preliminary study was performed using initial stimulation intensities of 1.3–2.0 tesla (60–90% stimulator output) on the targets with 3*3 square grid according to tolerance degree of different subjects. This allowed the sites of square gird evoking maximal MEPs for the mylohyoid to be identified the optimal stimulation point. Next, cortical stimulation was reapplied at the optimal stimulation point using an intensity of 0.7 tesla and increased in 0.1 tesla steps until an intensity was found that MEPs of greater than 30 μV, on at least five of ten consecutive trials. The minimum stimulus intensity was defined as the RMT. Then, we used a stimulation intensity of 110% RMT to stimulate the optimal stimulation points of left and right swallowing motor cortices every 30 s during three stimulation trials, and recorded the MEPs amplitude/latency (Hamdy et al., 1996). Finally, we averaged the three MEPs recorded each time and used the averaged value as the final data for analysis (Hamdy et al., 1996).

Statistical Analysis

Statistical analysis were performed by using the Statistical Package for Social Science (SPSS) version 20.0 (SPSS Inc., Chicago, IL, United States). χ^2 test for categorical variables, *t*-test for continuous variables with normal distribution, and non-parametric test (Mann–Whitney *U* tests) for skewed distribution were used to detect difference in baseline characteristics between the two groups. For the outcome analysis, Mann–Whitney *U* tests was used to assess the difference between two groups, and Wilcoxon's tests was used to assess the changes of same groups after intervention. The level of significance was set at 5% in the comparison, and all statistical testing was 2-sided. RMT/MEP lateralization was calculated according to the following formula: RMT/MEP lateralization = left swallowing motor cortex RMT/MEP – right swallowing motor cortex RMT/MEP.

RESULTS

Forty subjects completed the study. None of the subjects reported any persistent complaints of weakness or paresthesia after the prolonged stimulus. The study process can be found in **Supplementary Appendix 2**.

Lateralization of Swallowing Motor Cortex Excitability

The RMT and MEPs of the contralateral mylohyoid innervated by the bilateral swallowing motor cortices of healthy subjects at resting state are shown in **Figure 1** and **Supplementary Appendix Table 3A**, respectively. The RMT of the contralateral mylohyoid innervated by the right swallowing motor cortex (71.50 ± 1.67) was lower than that innervated by the left (79.38 ± 1.27, Mann–Whitney *U* test, $Z = -3.859$, $P < 0.001$, **Figure 1A**). The MEP latency of the contralateral mylohyoid innervated by the right swallowing motor cortex (8.30 ± 0.06) was shorter than that innervated by the left (8.40 ± 0.06, Mann–Whitney *U* test, $Z = -2.041$, $P = 0.041$, **Figure 1B**). However, there was no significant difference in the MEP amplitude (R: 52.68 ± 1.76, L: 50.15 ± 1.23, Mann–Whitney *U* test, $Z = 0.804$, $P = 0.422$, **Figure 1C**). Thus, the excitability of the right swallowing motor cortex was higher than that of the left swallowing motor cortex.

Effect of Electro-Acupuncture on Swallowing Motor Cortex Excitability

The same sample was divided into an EA group and a sham-EA group to study the effects of EA on the brain. There were no significant between-group differences in sex, age, Kubota Water Swallow Test score, Mini-mental State Examination score, or body mass index (Details in **Supplementary Appendix 4**). The results of RMT, MEP latency, and MEP amplitude of the mylohyoid induced by bilateral stimulation of the swallowing motor cortex in the EA and sham-EA groups are shown in **Figures 2A–F** and **Supplementary Appendix Table 3B**, respectively. **Figures 2G,H** shows representative MEP from the bilateral swallowing motor cortices before and after the

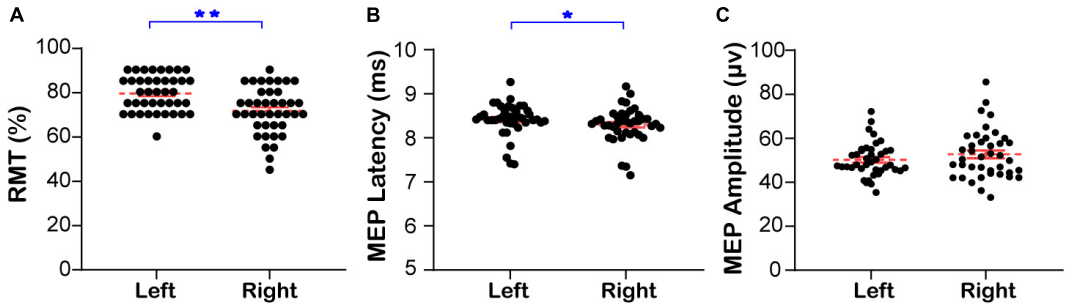

FIGURE 1 | The RMT and MEP of the contralateral mylohyoid innervated by the bilateral swallowing motor cortices. **(A)** The bilateral resting motor threshold. **(B)** The bilateral latency of motor evoked potential. **(C)** The bilateral amplitude of motor evoked potential. Left: The RMT and MEP of the contralateral mylohyoid innervated by the left swallowing motor cortex; Right: The RMT and MEP of the contralateral mylohyoid innervated by the right swallowing motor cortex; RMT, resting motor threshold; MEP, motor evoked potential;*$P < 0.05$, **$P < 0.01$.

intervention. On comparing the changes in the RMT, MEP latency, and MEP amplitude of the contralateral mylohyoid innervated by the right and left swallowing motor cortex, the RMT was diminished after EA (R: 73.00 ± 1.90 to 66.00 ± 2.22, L: 79.75 ± 1.60 to 76.00 ± 1.94, Wilcoxon's tests, $Z = -2.839$, $P = 0.005$; $Z = -3.866$, $P = 0.0001$, **Figure 2A**), the MEP latency was shortened after EA (R: 8.24 ± 0.10 to 8.10 ± 0.10, L: 8.36 ± 0.08 to 8.26 ± 0.08, Wilcoxon's tests, $Z = -3.041$, $P = 0.002$; $Z = -3.362$, $P = 0.001$, **Figure 2B**), and the MEP amplitude was enlarged after EA (R: 54.06 ± 2.73 to 65.29 ± 3.72, L: 49.53 ± 1.36 to 57.84 ± 2.43, Wilcoxon's tests, $Z = -3.192$, $P = 0.002$; $Z = -2.763$, $P = 0.009$, **Figure 2C**). However, these measures were not significantly different after sham-EA (Wilcoxon's tests, $P > 0.05$, **Figures 2D–F**). Thus, the excitability of right and left swallowing motor cortices was only increased after EA intervention.

Effect of Electro-Acupuncture on Lateralization of Swallowing Motor Cortex

Based on the above findings that the excitability of the right swallowing motor cortex was higher than that of the left side in healthy subjects, we investigated if EA can regulate the lateralization of swallowing motor cortex excitability. The changes in the RMT, MEP latency, and MEP amplitude of the mylohyoid induced by the bilateral swallowing motor cortices in the EA and sham-EA groups are shown in **Figure 3** and **Supplementary Appendix Table 3C**. There was no significant difference in the RMT (6.75 ± 2.27 to 10.00 ± 2.32, Wilcoxon's tests, $Z = -1.832$, $P = 0.067$, **Figure 3A**) or MEP latency (0.12 ± 0.04 to 0.16 ± 0.05, Wilcoxon's tests, $Z = -1.419$, $P = 0.156$, **Figure 3B**) of the contralateral mylohyoid innervated by the right swallowing motor cortex after EA, but there was a trend toward an increase in changes of RMT in the right swallowing motor cortex. In addition, since there is no significant change in the swallowing motor cortex excitability before and after the sham-EA, there was no significant difference in the lateralization of swallowing motor cortex excitability after the sham-EA (**Supplementary Appendix Table 3D**).

DISCUSSION

Our study revealed evidence of a dominant right-sided lateralization of swallowing motor cortex excitability in the healthy people at rest. We also found that EA at CV23 and GV16 can enhance excitability of the bilateral swallowing motor cortices, while the sham-EA could not. In addition, EA did not significantly change the lateralization of the swallowing motor cortex under physiological conditions.

Swallowing is a sensory-motor behavior regulated primarily by the brainstem and cerebral cortex (Ludlow, 2015). To date, the regulatory mechanism of human swallowing remains incompletely understood. With the development and wide application of many non-invasive human brain imaging techniques, positron emission tomography, functional MRI, magnetoencephalography, and TMS have been applied to study the cerebral motor cortex and swallowing (Hamdy et al., 1999; Suzuki et al., 2003). Some authors believe that the primary motor cortex is the initiating region for swallowing, whereas others believe that while the primary motor cortex is active during swallowing, it may play a more executive role, perhaps by balancing the excitatory and inhibitory mechanisms of the brainstem (Zald and Pardo, 1999; Mosier and Bereznaya, 2001; Furlong et al., 2004). Other studies have suggested that the motor cortex is involved in triggering the swallowing mechanism, and the motor cortex representation for swallowing displays territorial asymmetry (Mistry et al., 2007). These findings have led many researchers to infer a possible swallowing functional hemispheric dominance. Our study revealed that the excitability of the swallowing cortex is greater on the right side than on the left side by observing RMT and MEP, which indicates that the motor swallowing cortex is right-sided dominant.

Acupuncture originated in China 2,000 years ago as part of traditional Chinese medicine and is a minimally invasive therapy that regulates the human body (Kaptchuk, 2002). EA is an improved acupuncture therapy that stimulates acupoints by an electric current rather than manually. EA is widely used in clinical treatment and basic acupuncture research because of its controllable stimulation parameters and repeatability (Syuu et al., 2001; Elbasiouny et al., 2010). Acupuncture at CV23

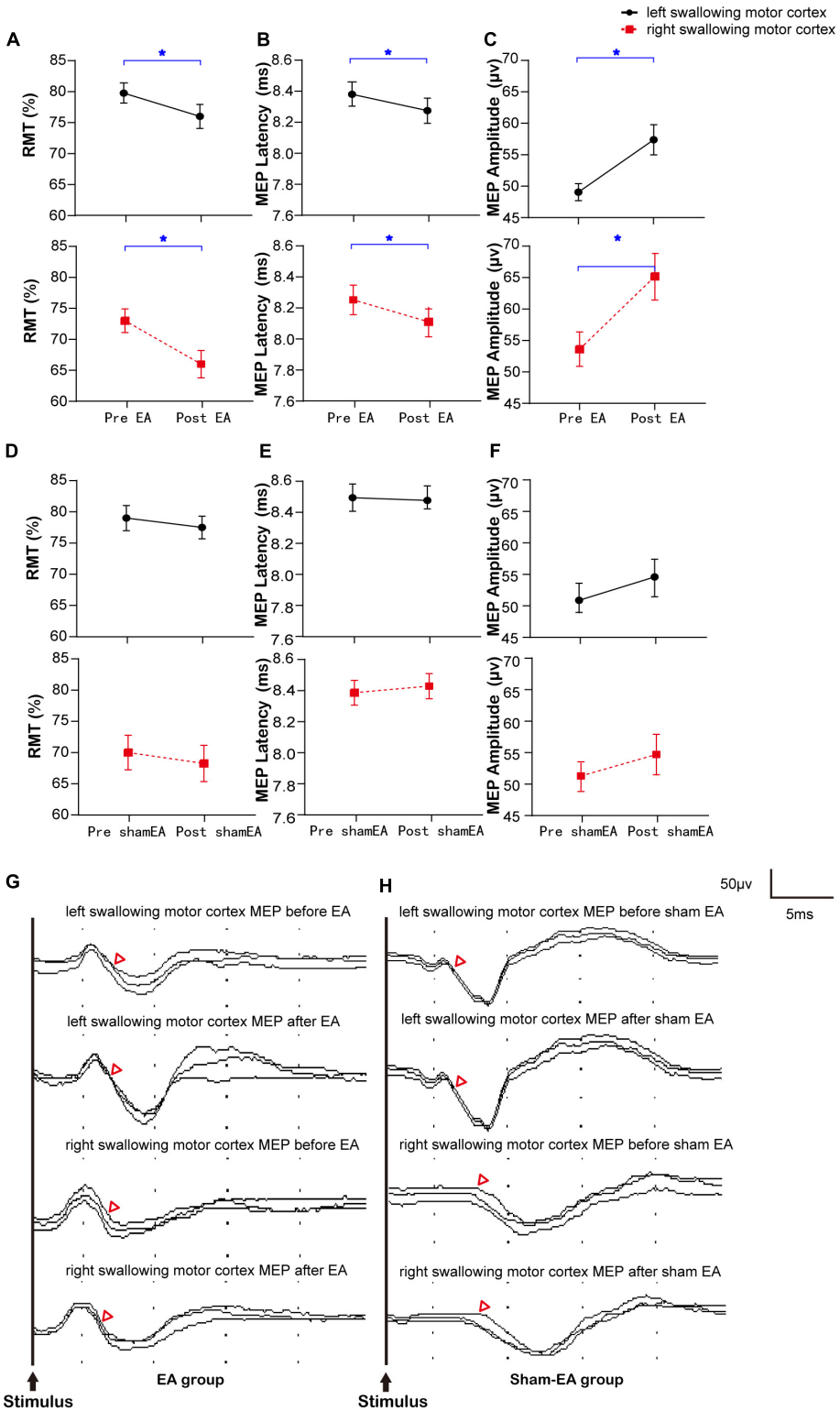

FIGURE 2 | Bilateral RMT and MEP of the swallowing motor cortex before and after the intervention and representative MEP. **(A–C)** The RMT and MEP of the cerebral swallowing motor cortex before and after EA. **(D–F)** The RMT and MEP of the cerebral swallowing motor cortex before and after sham-EA. **(G,H)** Representative EMG from the bilateral swallowing motor cortices before and after the intervention. RMT, resting motor threshold; MEP, motor evoked potential; EA, electro-acupuncture; $^{*}P < 0.05$; △ represents the latency of motor evoked potential.

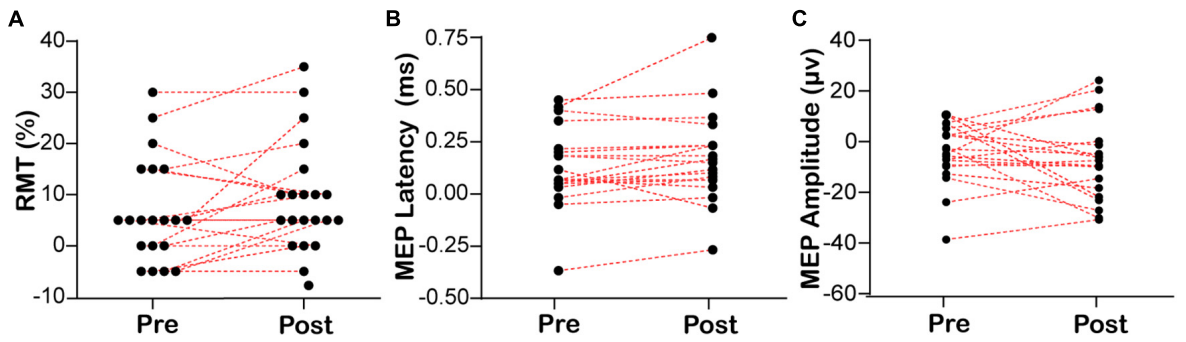

FIGURE 3 | Lateralization of bilateral RMT and MEP before and after EA. **(A)** The lateralization of resting motor threshold. **(B,C)** The lateralization of motor evoked potential. RMT, resting motor threshold; MEP, motor evoked potential. RMT/MEP lateralization was calculated according to the following formula: RMT/MEP lateralization = left swallowing motor cortex RMT/MEP – right swallowing motor cortex RMT/MEP.

and GV16 has been used to regulate swallowing function for thousands of years in China. CV23 is located between the thyroid cartilage and the hyoid bone, and deep tissue is innervated by branches of the hypoglossal and glossopharyngeal nerves (Shi et al., 2019). Human anatomy studies have confirmed that GV16 is located directly above the medulla oblongata and is innervated by the greater occipital nerve, accessory nerve, and cervical nerve (C1–C3). Some studies have shown that the afferent nerve of swallowing overlaps with the afferent nerve of CV23 and GV16 (Shi et al., 2019). It is believed that EA at CV23 and GV16 can stimulate the cervical nerve and hypoglossal nerve related to swallowing activities, enhance the excitability of swallowing afferent fibers, transmit impulses, and provide sensory feedback to the central nervous system (Ye et al., 2019). With the enhancement of sensory consciousness, the deglutition central pattern generator converts the excitatory information from the central and peripheral input into burst activity of motor neurons, which allows more new motion-projection areas to be created that evoke resting synapses to transmit nerve impulses (Guertin, 2013).

Our study confirmed that EA at CV23 and GV16 enhanced the excitability of the swallowing motor cortex at resting state by observing RMT and MEP, whereby there was an instantaneous increase of bilateral swallowing motor cortices excitability. Consistent with our study results, another study indicated that acupuncture therapy can modulate the corticomotoneuronal excitability and interhemispheric competition on healthy subjects, further enhance the excitability of the bilateral cortex (Yang et al., 2017). The symptoms of patients with dysphagia may be improved by increasing the excitability of the swallowing cortex, in other words, the changes in excitability would drive swallowing recovery (Hamdy et al., 1997; Sawan et al., 2020). Clinical studies have shown that acupuncture can effectively improve dysphagia (Lu et al., 2021), which may be related to EA at CV23 and GV16 enhanced the excitability of the swallowing motor cortex at resting state.

Concerning the lateralization of the swallowing motor cortex, we found that the lateralization of the latent period of RMT and MEPs of the swallowing motor cortex after the intervention of EA tended to further strengthen on the dominant side, but did not really change the inherent laterality of the swallowing motor cortex. McCambridge et al. (2019) demonstrated that EA has no significant regulatory effect on the cerebral cortex in healthy adults. Using TMS-EMG, Yang et al. (2017) found that acupuncture can increase the excitability of the primary motor cortex of the affected side of the brain in patients with stroke, while reducing contralateral primary motor cortex excitability. Our future work will focus on whether lateralization could influence the speed and degree of recovery in patients with post-stroke dysphagia, and the regulatory effect of EA on the bilateral swallowing cortex of these patients.

LIMITATIONS

Our study has some limitations that should be considered. First, the study subjects were healthy right-handed people, although some studies have proposed that handedness has no effect on lateralization of the cerebral cortex, this still needs to be formally proved by including more left-handed subjects in future studies. Second, the limited sample size could have restricted the detection of statistically significant effects. Third, the duration of excitability changes by EA were not examined. Fourth, due to the limitations of this technology, although we tried to ensure that the stimulation site was in the swallowing motor cortex of the precentral gyrus, strictly speaking, such positioning and stimulation methods were still relatively rough. Fifth, the physiological state of the cerebral cortex may not be consistent with pathological conditions. Thus, further studies are needed to demonstrate the relationship between excitability of the bilateral swallowing cortex and swallowing function.

CONCLUSION

The right swallowing motor cortex of healthy subjects is more excitable than that of the left at resting state. Thus, we found that lateralization is present in the swallowing motor cortex of healthy people, which indicates a hemispheric dominance of swallowing predominates in the right swallowing motor cortex. In addition, EA at CV23 and GV16 was found to

instantly promote excitability of the bilateral swallowing motor cortices. Moreover, although there was no significant difference in lateralization, we found an increasing trend that EA could regulate the lateralization of human swallowing motor cortex excitability. Our future work will investigate the effect of EA on lateralization of the swallowing motor cortex excitability in patients with dysphagia.

DATA AVAILABILITY STATEMENT

The raw data supporting the conclusions of this article will be made available by the correspondence authors, without undue reservation.

ETHICS STATEMENT

The studies involving human participants were reviewed and approved by China Ethics Committee for Registering Clinical Trials (reference number ChiECRCT-20170038). The patients/participants provided their written informed consent to participate in this study.

AUTHOR CONTRIBUTIONS

XT: conceptualization, methodology, software, formal analysis, investigation, writing – original draft, writing review and editing, and visualization. MX: methodology, formal analysis, writing original draft, and visualization. JZ and JW: investigation, writing – original draft, and writing – review and editing. JS: writing original draft, writing – review and editing, and visualization. YZ: software, investigation, writing – original draft, and writing – review and editing. JX, LY, and HL: investigation and writing – review and editing. YY: methodology, investigation, and writing – review and editing. JO and SY: writing – review and editing. YL: writing – original draft and writing – review and editing. LL: conceptualization and writing – review and editing. NX: conceptualization, writing – review and editing, and funding acquisition. LW: conceptualization, resources, writing – review and editing, supervision, and funding acquisition. All authors contributed to the article and approved the submitted version.

FUNDING

This research was partly supported by the Youth Program of the National Natural Science Foundation of China (Nos. 81904297, 82004469, and 81903836), General Program of the National Natural Science Foundation of China (No. 81774406), Opening Operation Program of Key Laboratory of Acupuncture and Moxibustion of Traditional Chinese Medicine in Guangdong (No. 2017B030314143), Special Project of "Lingnan Modernization of Traditional Chinese Medicine" in 2019 Guangdong Provincial R&D Program (No. 2020B1111100008), Foundation for distinguished Young Talents in Higher Education of Guangdong, China (No. 2016KQNCX027), "Elite Youth Education Program" of Guangzhou University of Chinese Medicine (No. QNYC20190106), Graduate Research Innovation Project of Guangzhou University of Chinese Medicine, and Qi-Huang Scholar of National Traditional Chinese Medicine Leading Talents Support Program, Fellowship of China Postdoctoral Science Foundation (No. 2020M672601). The funders had no influence on study design, data collection, analysis, decision to publish, or manuscript preparation.

ACKNOWLEDGMENTS

We acknowledge the support of the South China Research Center for Acupuncture and Moxibustion of Guangzhou University of Chinese Medicine. We thank all of the participants for their cooperation during the study.

SUPPLEMENTARY MATERIAL

The Supplementary Material for this article can be found online at: https://www.frontiersin.org/articles/10.3389/fnbeh.2022.808789/full#supplementary-material

REFERENCES

Badawy, R. A., Loetscher, T., Macdonell, R. A., and Brodtmann, A. (2012). Cortical excitability and neurology: insights into the pathophysiology. *Funct. Neurol.* 27, 131–145.

Bestmann, S., and Krakauer, J. W. (2015). The uses and interpretations of the motor-evoked potential for understanding behaviour. *Exp. Brain Res.* 233, 679–689. doi: 10.1007/s00221-014-4183-7

Biabani, M., Fornito, A., Coxon, J. P., Fulcher, B. D., and Rogasch, N. C. (2021). The correspondence between EMG and EEG measures of changes in cortical excitability following transcranial magnetic stimulation. *J. Physiol.* 599, 2907–2932. doi: 10.1113/JP280966

Cabeza, R. (2002). Hemispheric asymmetry reduction in older adults: the HAROLD model. *Psychol. Aging* 17, 85–100.

Caeyenberghs, K., and Leemans, A. (2014). Hemispheric lateralization of topological organization in structural brain networks. *Hum. Brain Mapp.* 35, 4944–4957. doi: 10.1002/hbm.22524

Carey, D. P., Smith, G., Smith, D. T., Shepherd, J. W., Skriver, J., Ord, L., et al. (2001). Footedness in world soccer: an analysis of France '98. *J. Sports Sci.* 19, 855–864. doi: 10.1080/02640410175311 3804

Crow, T. J. (2013). The XY gene hypothesis of psychosis: origins and current status. *Am. J. Med. Genet. B Neuropsychiatr. Genet.* 162B, 800–824. doi: 10.1002/ajmg.b.32202

Daniels, S. K., Foundas, A. L., Iglesia, G. C., and Sullivan, M. A. (1996). Lesion site in unilateral stroke patients with dysphagia. *J. Stroke Cerebrovasc. Dis.* 6, 30–34. doi: 10.1016/s1052-3057(96)80023-1

Deng, X. X., and Wu, C. (2017). "Xingnao Kaiqiao" acupuncture therapy combined with vitalstim swallowing therapeutic apparatus in treatment of dysphagia of stroke. *J. Chin. Med.* 32, 466–469.

Elbasiouny, S. M., Moroz, D., Bakr, M. M., and Mushahwar, V. K. (2010). Management of spasticity after spinal cord injury: current techniques and

future directions. *Neurorehabil. Neural Repair* 24, 23–33. doi: 10.1177/1545968309343213

Ferrari, C., Gamond, L., Gallucci, M., Vecchi, T., and Cattaneo, Z. (2017). An exploratory TMS study on prefrontal lateralization in valence categorization of facial expressions. *Exp. Psychol.* 64, 282–289. doi: 10.1027/1618-3169/a000363

Furlong, P. L., Hobson, A. R., Aziz, Q., Barnes, G. R., Singh, K. D., Hillebrand, A., et al. (2004). Dissociating the spatio-temporal characteristics of cortical neuronal activity associated with human volitional swallowing in the healthy adult brain. *Neuroimage* 22, 1447–1455. doi: 10.1016/j.neuroimage.2004.02.041

Goodale, M. A. (1988). Hemispheric differences in motor control. *Behav. Brain Res.* 30, 203–214. doi: 10.1016/0166-4328(88)90149-0

Grimshaw, G. M., and Carmel, D. (2014). An asymmetric inhibition model of hemispheric differences in emotional processing. *Front. Psychol.* 5:489. doi: 10.3389/fpsyg.2014.00489

Guertin, P. A. (2013). Central pattern generator for locomotion: anatomical, physiological, and pathophysiological considerations. *Front. Neurol.* 3:183. doi: 10.3389/fneur.2012.00183

Gunturkun, O. (2003). Human behaviour: adult persistence of head-turning asymmetry. *Nature* 421:711. doi: 10.1038/421711a

Gunturkun, O., and Ocklenburg, S. (2017). Ontogenesis of lateralization. *Neuron* 94, 249–263. doi: 10.1016/j.neuron.2017.02.045

Halko, M. A., Eldaief, M. C., and Pascual-Leone, A. (2013). Noninvasive brain stimulation in the study of the human visual system. *J. Glaucoma* 22, S39–S41. doi: 10.1097/IJG.0b013e3182934b31

Hallett, M. (2007). Transcranial magnetic stimulation: a primer. *Neuron* 55, 187–199. doi: 10.1016/j.neuron.2007.06.026

Hamdy, S., Aziz, Q., Rothwell, J. C., Crone, R., Hughes, D., Tallis, R. C., et al. (1997). Explaining oropharyngeal dysphagia after unilateral hemispheric stroke. *Lancet* 350, 686–692. doi: 10.1016/S0140-6736(97)02068-0

Hamdy, S., Aziz, Q., Rothwell, J. C., Power, M., Singh, K. D., Nicholson, D. A., et al. (1998). Recovery of swallowing after dysphagic stroke relates to functional reorganization in the intact motor cortex. *Gastroenterology* 115, 1104–1112. doi: 10.1016/s0016-5085(98)70081-2

Hamdy, S., Aziz, Q., Rothwell, J. C., Singh, K. D., Barlow, J., Hughes, D. G., et al. (1996). The cortical topography of human swallowing musculature in health and disease. *Nat. Med.* 2, 1217–1224. doi: 10.1038/nm1196-1217

Hamdy, S., Mikulis, D. J., Crawley, A., Xue, S., Lau, H., Henry, S., et al. (1999). Cortical activation during human volitional swallowing: an event-related fMRI study. *Am. J. Physiol.* 277, G219–G225. doi: 10.1152/ajpgi.1999.277.1.G219

Kaptchuk, T. J. (2002). Acupuncture: theory, efficacy, and practice. *Ann. Intern. Med.* 136, 374–383. doi: 10.7326/0003-4819-136-5-200203050-00010

Karlebach, G., and Francks, C. (2015). Lateralization of gene expression in human language cortex. *Cortex* 67, 30–36. doi: 10.1016/j.cortex.2015.03.003

Khamnei, S., Sadat-Ebrahimi, S. R., Salarilak, S., Savadi Oskoee, S., Houshyar, Y., Shakouri, S. K., et al. (2019). Manifestation of hemispheric laterality in chewing side preference and handedness. *Bioimpacts* 9, 189–193. doi: 10.15171/bi.2019.23

Leocani, L., Cohen, L. G., Wassermann, E. M., Ikoma, K., and Hallett, M. (2000). Human corticospinal excitability evaluated with transcranial magnetic stimulation during different reaction time paradigms. *Brain* 123(Pt. 6), 1161–1173. doi: 10.1093/brain/123.6.1161

Li, M., Wang, L., Xu, N., Tang, X., Xu, M., Liu, J., et al. (2019). Effect of electro-acupuncture on lateralization of the human swallowing motor cortex excitability in healthy subjects: study protocol for a single-blind, randomized controlled trial. *Trials* 20:180. doi: 10.1186/s13063-019-3267-x

Lu, Y., Chen, Y., Huang, D., and Li, J. (2021). Efficacy of acupuncture for dysphagia after stroke: a systematic review and meta-analysis. *Ann. Palliat. Med.* 10, 3410–3422. doi: 10.21037/apm-21-499

Ludlow, C. L. (2015). Central nervous system control of voice and swallowing. *J. Clin. Neurophysiol.* 32, 294–303. doi: 10.1097/WNP.0000000000000186

McCambridge, A. B., Zaslawski, C., and Bradnam, L. V. (2019). Investigating the mechanisms of acupuncture on neural excitability in healthy adults. *NeuroReport* 30, 71–76. doi: 10.1097/WNR.0000000000001159

Mistry, S., Verin, E., Singh, S., Jefferson, S., Rothwell, J. C., Thompson, D. G., et al. (2007). Unilateral suppression of pharyngeal motor cortex to repetitive transcranial magnetic stimulation reveals functional asymmetry in the hemispheric projections to human swallowing. *J. Physiol.* 585, 525–538. doi: 10.1113/jphysiol.2007.144592

Mosier, K. M., Liu, W. C., Maldjian, J. A., Shah, R., and Modi, B. (1999). Lateralization of cortical function in swallowing: a functional MR imaging study. *AJNR Am. J. Neuroradiol.* 20, 1520–1526.

Mosier, K., and Bereznaya, I. (2001). Parallel cortical networks for volitional control of swallowing in humans. *Exp. Brain Res.* 140, 280–289. doi: 10.1007/s002210100813

Ocklenburg, S., Friedrich, P., Gunturkun, O., and Genc, E. (2016). Intrahemispheric white matter asymmetries: the missing link between brain structure and functional lateralization? *Rev. Neurosci.* 27, 465–480. doi: 10.1515/revneuro-2015-0052

Papadatou-Pastou, M., and Tomprou, D. M. (2015). Intelligence and handedness: meta-analyses of studies on intellectually disabled, typically developing, and gifted individuals. *Neurosci. Biobehav. Rev.* 56, 151–165. doi: 10.1016/j.neubiorev.2015.06.017

Peng, W., Yang, T., Yuan, J., Huang, J., and Liu, J. (2020). Electroacupuncture-induced plasticity between different representations in human motor cortex. *Neural Plast.* 2020:8856868. doi: 10.1155/2020/8856868

Robbins, J., Levine, R. L., Maser, A., Rosenbek, J. C., and Kempster, G. B. (1993). Swallowing after unilateral stroke of the cerebral cortex. *Arch. Phys. Med. Rehabil.* 74, 1295–1300. doi: 10.1016/0003-9993(93)90082-l

Rotenberg, A., Muller, P. A., Vahabzadeh-Hagh, A. M., Navarro, X., López-Vales, R., Pascual-Leone, A., et al. (2010). Lateralization of forelimb motor evoked potentials by transcranial magnetic stimulation in rats. *Clin. Neurophysiol.* 121, 104–108. doi: 10.1016/j.clinph.2009.09.008

Sawan, S. A. E., Reda, A. M., Kamel, A. H., and Ali, M. A. M. (2020). Transcranial direct current stimulation (tDCS): its effect on improving dysphagia in stroke patients. *Egypt. J. Neurol. Psychiatry Neurosurg.* 56:111.

Scoppa, F., Saccomanno, S., Bianco, G., and Pirino, A. (2020). Tongue posture, tongue movements, swallowing, and cerebral areas activation: a functional magnetic resonance imaging study. *Appl. Sci.* 10:6027. doi: 10.3390/app10176027

Shi, J., Ye, Q., Zhao, J., Liu, J., Xu, Z., Yi, W., et al. (2019). EA promotes swallowing *via* activating swallowing-related motor neurons in the nucleus ambiguus. *Brain Res.* 1718, 103–113. doi: 10.1016/j.brainres.2018.12.013

Singh, S., and Hamdy, S. (2006). Dysphagia in stroke patients. *Postgrad. Med. J.* 82, 383–391.

Streitberger, K., and Kleinhenz, J. (1998). Introducing a placebo needle into acupuncture research. *Lancet* 352, 364–365. doi: 10.1016/S0140-6736(97)10471-8

Suzuki, M., Asada, Y., Ito, J., Hayashi, K., Inoue, H., and Kitano, H. (2003). Activation of cerebellum and basal ganglia on volitional swallowing detected by functional magnetic resonance imaging. *Dysphagia* 18, 71–77. doi: 10.1007/s00455-002-0088-x

Syuu, Y., Matsubara, H., Kiyooka, T., Hosogi, S., Mohri, S., Araki, J., et al. (2001). Cardiovascular beneficial effects of electroacupuncture at Neiguan (PC-6) acupoint in anesthetized open-chest dog. *Jpn. J. Physiol.* 51, 231–238. doi: 10.2170/jjphysiol.51.231

Tervaniemi, M., and Hugdahl, K. (2003). Lateralization of auditory-cortex functions. *Brain Res. Brain Res. Rev.* 43, 231–246. doi: 10.1016/j.brainresrev.2003.08.004

Yang, Y., Eisner, I., Chen, S., Wang, S., Zhang, F., and Wang, L. (2017). Neuroplasticity changes on human motor cortex induced by acupuncture therapy: a preliminary study. *Neural Plast.* 2017:4716792. doi: 10.1155/2017/4716792

Ye, Q., Liu, C., Shi, J., You, H., Zhao, J., Liu, J., et al. (2019). Effect of electro-acupuncture on regulating the swallowing by activating the interneuron in

ventrolateral medulla (VLM). *Brain Res. Bull.* 144, 132–139. doi: 10.1016/j.brainresbull.2018.11.021

Zald, D. H., and Pardo, J. V. (1999). The functional neuroanatomy of voluntary swallowing. *Ann. Neurol.* 46, 281–286.

Zhong, L., Wang, J., Li, F., Bao, X., Liu, H., and Wang, P. (2021). The effectiveness of acupuncture for dysphagia after stroke: a systematic review and meta-analysis. *Evid. Based Complement. Alternat. Med.* 2021:8837625. doi: 10.1155/2021/8837625

Conflict of Interest: The authors declare that the research was conducted in the absence of any commercial or financial relationships that could be construed as a potential conflict of interest.

Publisher's Note: All claims expressed in this article are solely those of the authors and do not necessarily represent those of their affiliated organizations, or those of the publisher, the editors and the reviewers. Any product that may be evaluated in this article, or claim that may be made by its manufacturer, is not guaranteed or endorsed by the publisher.

frontiers in Human Neuroscience

CASE REPORT
published: 25 February 2022
doi: 10.3389/fnhum.2022.778347

Differential Diagnosis of Akinetic Mutism and Disorder of Consciousness Using Diffusion Tensor Tractography: A Case Report

*Dong Hyun Byun and Sung Ho Jang**

Department of Physical Medicine and Rehabilitation, College of Medicine, Yeungnam University, Daegu, South Korea

This paper presents a case in whom a differential diagnosis of akinetic mutism with a disorder of consciousness was made using diffusion tensor tractography (DTT). A 69-year-old female patient was diagnosed with subarachnoid hemorrhage, intraventricular hemorrhage, and intracerebral hemorrhage produced by the subarachnoid hemorrhage. She exhibited impaired consciousness with a Coma Recovery Scale-Revised score of 13 until 1 month after onset. Her impaired consciousness recovered slowly to a normal state according to the Coma Recovery Scale-Revised (23 points: full score) at 7 weeks after onset. On the other hand, she exhibited the typical clinical features of akinetic mutism (no spontaneous movement [akinesia] or speech [mutism]). On the DTT performed at 1-month, the upper, and lower dorsal ascending reticular activating systems, which are related to a disorder of consciousness, showed an almost normal state. In contrast, the prefronto-caudate and prefronto-thalamic tracts, which are related to akinetic mutism, showed severe injuries. These DTT results suggested that the patient's main clinical features were not a disorder of consciousness but akinetic mutism. Therefore, DTT for the ascending reticular activating system, and the prefronto-caudate and prefronto-thalamic tracts could provide additional evidence for a differential diagnosis of DOC and AM at the early stages of stroke.

Keywords: diffusion tensor tractography (DTT), akinetic mutism, disorder of consciousness (DOC), prefronto-caudate tract, prefronto-thalamic tract

OPEN ACCESS

Edited by:
Ken-Ichiro Tsutsui, Tohoku University, Japan

Reviewed by:
Edgar G. Ordóñez-Rubiano, Hospital Infantil Universitario de San José, Colombia
Hisse Arnts, Amsterdam University Medical Center, Netherlands

***Correspondence:**
Sung Ho Jang
strokerehab@hanmail.net

Specialty section:
This article was submitted to Brain Imaging and Stimulation, a section of the journal Frontiers in Human Neuroscience

Received: *16 September 2021*
Accepted: *21 January 2022*
Published: *25 February 2022*

Citation:
Byun DH and Jang SH (2022) Differential Diagnosis of Akinetic Mutism and Disorder of Consciousness Using Diffusion Tensor Tractography: A Case Report. Front. Hum. Neurosci. 16:778347. doi: 10.3389/fnhum.2022.778347

INTRODUCTION

A differential diagnosis of akinetic mutism (AM) and disorder of consciousness (DOC) can be clinically difficult at the early stages of a brain injury. AM is a rare neurological disorder of impaired initiation and motivation for behavior (Arnts et al., 2020). The representative clinical features of AM are a lack of voluntary movement (akinesia) and absence of speech (mutism), but eye-opening and spontaneous or environmentally induced visual tracking are maintained (Arnts et al., 2020). Bilateral disruption of the fronto-subcortical circuit has been suggested as an important pathophysiological mechanism of AM (Mega and Cohenour, 1997; Nagaratnam et al., 2004; Marin and Wilkosz, 2005; Jang and Kwon, 2017). In particular, an injury to the cortico-striatal-pallidal-thalamic circuit is considered the most plausible pathophysiological mechanism

(Mega and Cohenour, 1997; Nagaratnam et al., 2004; Marin and Wilkosz, 2005; Jang and Kwon, 2017). However, precise reconstruction of the fronto-subcortical circuit in a live human brain has been impossible. The introduction of diffusion tensor tractography (DTT), which is derived from diffusion tensor imaging, enables the estimation and visualization of some neural tracts of the fronto-subcortical circuit, including the prefronto-caudate and prefronto-thalamic (mediodorsal nucleus) tracts (Behrens et al., 2007; Leh et al., 2007; Jang and Yeo, 2014; Jang and Kwon, 2017). As a result, several DTT-based studies have reported that AM is related to injuries of the above two neural tracts, particularly the prefronto-caudate tract (Jang and Kwon, 2017; Jang et al., 2017a,b, 2018). On the other hand, DTT also allows a reconstruction of the ascending reticular activating system (ARAS), which is an important neural network for controlling consciousness (Jang et al., 2019a,b). Thus, this study hypothesized that reconstruction of the neural tracts related to AM and DOC using DTT could be useful in a differential diagnosis of AM and DOC.

This case study describes a case of AM, which was confirmed from DOC by the clinical features and DTT.

CASE DESCRIPTION

A 69-year-old female patient was diagnosed with subarachnoid hemorrhage caused by an aneurysm rupture in the anterior communicating artery and intraventricular hemorrhage, and intracerebral hemorrhage in both basal forebrains produced by a subarachnoid hemorrhage (Fisher grade 4) (Fisher et al., 1980). She underwent coiling and extraventricular drainage through the right prefrontal lobe on the day of onset and ventriculoperitoneal shunt for hydrocephalus 5 days after onset at the neurosurgery department of a general hospital. Approximately 1 month after onset, she was transferred to the rehabilitation department of a University hospital. The patient exhibited impaired consciousness (obedient to simple commands, such as eye closing, eye tracking to visual stimuli, and head turning to the side of auditory stimuli), with a Coma Recovery Scale-Revised (full score: 23; a higher score indicates higher consciousness) score of 13 (auditory function, 3 [reproducible movement to command]; visual function, 4 [object localization: reaching]; motor function, 2 [flexion withdrawal]; verbal function, 1 [oral reflexive movement]; communication, 1 [non-functional: intentional]; and arousal, and 2 [eye opening without stimulation] (Giacino et al., 2004).

Brain magnetic resonance images taken 1 month after onset revealed leukomalactic lesions in both basal forebrains (**Figure 1A**). Her impaired consciousness recovered slowly to a normal state as Coma Recovery Scale-Revised (23 points) (auditory function, 4 [consistent movement to commend]; visual function, 5 [object recognition]; motor function, 6 [functional object use]; verbal function, 3 [intelligible verbalization]; communication, 3 [oriented]; and arousal, and 3 [attention) at 7 weeks after onset (Giacino et al., 2004). However, she showed no spontaneous movement or speech and remained in a lying position all day with no spontaneous activity. However, she could execute movements and speak according to the clinician's order with some preservation of awareness. The patient's daughter provided signed, informed consent, and the institutional review board approved the study protocol.

The diffusion tensor imaging data were acquired 1 month after onset using a 1.5 T Philips Gyroscan Intera (Philips, Ltd., Best, Netherlands) with a six-channel head coil and single-shot echo-planar imaging. For each of the 32 non-collinear diffusion-sensitizing gradients, contiguous slices parallel to the anterior commissure–posterior commissure line were acquired. The imaging parameters were as follows: acquisition matrix = 96 × 96, reconstructed to matrix = 192 × 192 matrix, field of view = 240 mm × 240 mm, TR = 10,398 ms, TE = 72 ms, parallel imaging reduction factor (SENSE factor) = 2, EPI factor = 59, b = 1,000 s/mm^2, NEX = 1, and slice thickness = 2.5 mm. The diffusion-weighted imaging data were analyzed using tools within the Oxford Center for Functional Magnetic Resonance Imaging of the Brain (FMRIB) Software Library (FSL; www.fmrib.ox.ac.uk/fsl). Affine multi-scale two-dimensional registration was used to correct the head motion effects and image distortion due to eddy currents. Fiber tracking was performed using a probabilistic tractography method based on a multifiber model and was applied using the tractography routines implemented in FMRIB Diffusion software (5,000 streamline samples, 0.5 mm step lengths, curvature thresholds = 0.2; corresponding to a minimum angle of 80°). All regions of interest (ROIs) were applied manually based on the previous studies and atlas (Daube, 1986; Morel et al., 1997; Afifi and Bergman, 2005; Johansen-Berg et al., 2005; Kringelbach, 2005; Petrides, 2005; Brodmann and Gary, 2006; Leh et al., 2007; Morel, 2007; Klein et al., 2010; Yeo et al., 2013; Jang and Yeo, 2014; Jang et al., 2014; Mendoza and Eblen-Zajjur, 2019). Two portions of the ARAS were reconstructed by selecting the fibers passing through the following regions of interest (ROIs): lower dorsal ARAS (seed ROI, the pontine reticular formation [RF], target ROI, thalamic intralaminar nucleus [ILN] at the level of the inter-commissural plane between the anterior and posterior commissures), and the upper ARAS (neural connectivity of the ILN to the cerebral cortex) (Daube, 1986; Morel et al., 1997; Afifi and Bergman, 2005; Morel, 2007; Yeo et al., 2013; Jang et al., 2014). Based on 5,000 samples generated from the seed voxel, the results for contact were visualized at a minimum threshold of two for the lower dorsal ARAS and 10 for the neural connectivity of the ILN (upper ARAS). For the connectivity of the caudate nucleus (CN) to the prefrontal cortex (PFC), the seed region of interest (ROI) was placed on the caudate nucleus, which was isolated by the adjacent structures (medial boundary: the lateral ventricle, lateral boundary: the anterior limb of the internal capsule) (Leh et al., 2007; Yeo et al., 2013; Mendoza and Eblen-Zajjur, 2019). To reconstruct the prefronto-thalamic tracts (Johansen-Berg et al., 2005; Kringelbach, 2005; Petrides, 2005; Brodmann and Gary, 2006; Klein et al., 2010; Jang and Yeo, 2014), a seed ROI was placed on the known anatomical location of the mediodorsal nucleus of the thalamus on the coronal image (Johansen-Berg et al., 2005; Klein et al., 2010; Jang and Yeo, 2014). Each target ROI was as follows: (1) dorsolateral PFC as Brodmann areas (BAs) 8, 9, and 46 on the coronal image; (2)

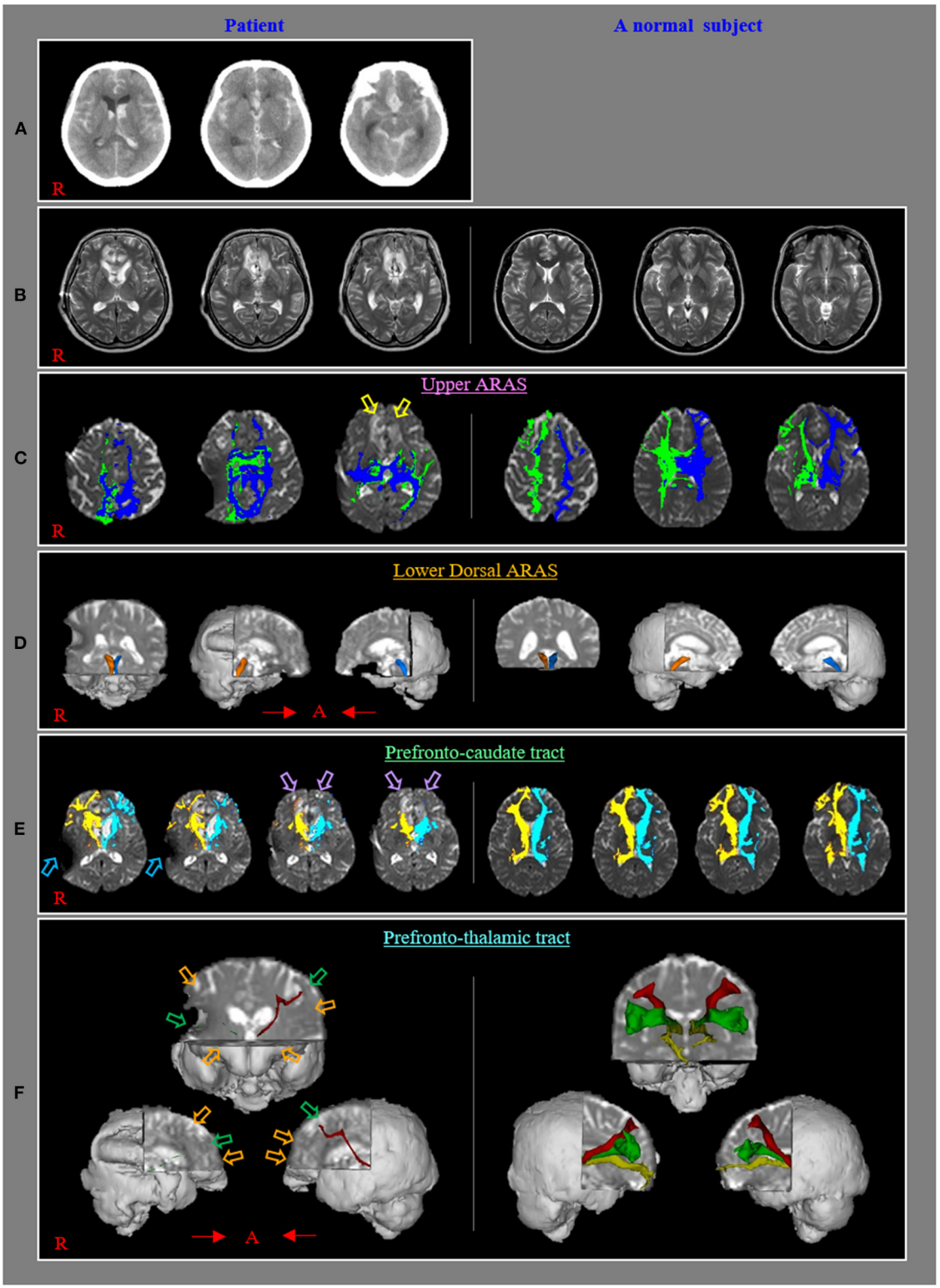

FIGURE 1 | (A) Brain CT images at onset reveal subarachnoid hemorrhage, intraventricular hemorrhage, and intracerebral hemorrhage in both basal forebrains. **(B)** T2-weighted brain MR images at 1 month after onset show leulomalactic lesions in both forebrains. **(C)** The upper ascending reticular activating system (ARAS) shows almost normal configurations in both hemispheres except for decreased neural connectivities to both basal forebrains (yellow arrows) compared with those of a

(Continued)

FIGURE 1 | normal control subject (50-year-old female). **(D)** The lower dorsal ARAS reveals almost normal configurations in both hemispheres compared with those of a normal control subject (62-year-old female). **(E)** The neural connectivity of the caudate nucleus to the prefrontal cortex decreased in both hemispheres (violet arrows) compared to those of a normal control subject (50-year-old female) (sky-blue arrows: artifact due to ventriculoperitoneal shunt, which was performed through the right parietal approach). **(F)** All prefronto-thalamic tracts are not reconstructed (orange arrows) except for the right ventrolateral and left dorsolateral tracts, which show severe thinning (green arrows) compared to those of a normal control subject (60-year-old female).

ventrolateral PFC as BAs 44, 45, and 47 on the coronal image; and (3) orbitofrontal cortex as BAs 47, 11, and 13 on the axial image (Kringelbach, 2005; Petrides, 2005; Brodmann and Gary, 2006; Klein et al., 2010; Jang and Yeo, 2014). The prefronto-thalamic tracts were determined by selecting the fibers passing through the seed and each target ROI.

The upper and lower dorsal ARAS showed almost normal configurations in both hemispheres except for decreased neural connectivities to both basal forebrains (**Figures 1B,C**). The neural connectivity of the CN to the prefrontal cortex was decreased in both hemispheres (**Figure 1D**). None of the prefronto-thalamic tracts were reconstructed except for the right ventrolateral and left dorsolateral tracts, which showed severe thinning (**Figures 1E,F**).

DISCUSSION

This patient showed a DOC until she was admitted to the rehabilitation department 1 month after onset. She also revealed the typical clinical features of AM (complete absence of spontaneous behavior [akinesia] and speech [mutism]) when her consciousness had recovered to a normal state 7 weeks after onset (Marin and Wilkosz, 2005). As a result, her main clinical features were not DOC but AM. In detail, it appeared that she had combined clinical features of AM (main) and DOC (minor) between 1 month and 7 weeks after onset because she could not execute movements and speak according to the clinician's order. Subsequently, at 7 weeks when her consciousness had recovered to a normal state, she presented typical clinical features of AM (akinesia and mutism) without clinical features of DOC because she could execute movements and speak according to the clinician's order. In addition, on 1-month DTT, the prefronto-caudate and prefronto-thalamic tracts showed severe injuries whereas the ARAS revealed mild injuries. Thus, when she was transferred to our hospital at 1 month after onset, we could assume that her main clinical features were not DOC but AM based on 1-month DTT findings.

Severe injury of the fronto-subcortical circuit (particularly, the prefronto-caudate, and prefronto-thalamic tracts) has been suggested as the pathophysiological mechanism of AM (Mega and Cohenour, 1997; Nagaratnam et al., 2004; Jang and Kwon, 2017; Jang et al., 2017a,b, 2018). The upper and lower dorsal ARAS showed an almost normal state in this patient, whereas the prefronto-caudate and prefronto-thalamic tracts revealed severe injuries. These DTT results appeared to coincide with the patient's main clinical features of AM. This study had some limitations. First, the whole fronto-subcortical circuit could not be reconstructed except for the prefronto-caudate and prefronto-thalamic tracts because a reconstruction method for the whole fronto-subcortical circuit has not been developed. Second, the results of DTT can be false positives or negatives due to crossing fibers and partial volume effects (Yamada et al., 2009). Third, follow up DTTs from the acute stage could provide better evidences. However, we could not scan the diffusion tensor imaging at the acute stage because she was transferred from other hospital.

In conclusion, a differential diagnosis of AK with DOC was made in this patient using the clinical features and DTT findings. The results suggest that DTT for the ARAS, prefronto-caudate tract, and prefronto-thalamic tract could be additional evidence for a differential diagnosis of DOC and AM at the early stages of a stroke. On the other hand, further studies will be needed to apply these DTT methods for other brain pathologies, such as hypoxic-ischemic brain injury, traumatic brain injury, and global ischemia.

DATA AVAILABILITY STATEMENT

The raw data supporting the conclusions of this article will be made available by the authors, without undue reservation.

ETHICS STATEMENT

The studies involving human participants were reviewed and approved by Yeungnam University Hospital. The patients/participants provided their written informed consent to participate in this study. Written informed consent was obtained from the individual(s) for the publication of any potentially identifiable images or data included in this article.

AUTHOR CONTRIBUTIONS

DB: study concept, design, and critical revision of manuscript for intellectual content. SJ: study concept and design, manuscript development, writing, funding, and critical revision of manuscript for intellectual content. All authors contributed to the article and approved the submitted version.

FUNDING

This work was supported by the National Research Foundation of Korea (NRF) grant funded by the Korean Government (MSIP) (No. 2021R1A2B5B01001386).

REFERENCES

Afifi, A. K., and Bergman, R. A. (2005). *Functional Neuroanatomy: Text and Atlas, 2nd Edn*. New York, NY: Lange Medical Books/McGraw-Hill.

Arnts, H., van Erp, W. S., Lavrijsen, J. C. M., van Gaal, S., Groenewegen, H. J., and van den Munckhof, P. (2020). On the pathophysiology and treatment of akinetic mutism. *Neurosci. Biobehav. Rev.* 112, 270–278. doi: 10.1016/j.neubiorev.2020.02.006

Behrens, T. E., Berg, H. J., Jbabdi, S., Rushworth, M. F., and Woolrich, M. W. (2007). Probabilistic diffusion tractography with multiple fibre orientations: what can we gain? *NeuroImage* 34, 144–155. doi: 10.1016/j.neuroimage.2006.09.018

Brodmann, K., and Gary, L. J. (2006). *Brodmann's Localization in the Cerebral Cortex: The Principles of Comparative Localisation in the Cerebral Cortex Based on Cytoarchitectonics*. New York, NY: Springer, 298.

Daube, J. R. (1986). *Medical Neurosciences: An Approach to Anatomy, Pathology, and Physiology by Systems and Levels*. Boston, MA: Little, Brown and Co.

Fisher, C. M., Kistler, J. P., and Davis, J. M. (1980). Relation of cerebral vasospasm to subarachnoid hemorrhage visualized by computerized tomographic scanning. *Neurosurgery* 6, 1–9. doi: 10.1227/00006123-198001000-00001

Giacino, J. T., Kalmar, K., and Whyte, J. (2004). The JFK coma recovery scale-revised: measurement characteristics and diagnostic utility. *Arch. Phys. Med. Rehabil.* 85, 2020–2029. doi: 10.1016/j.apmr.2004.02.033

Jang, S. H., Chang, C. H., Jung, Y. J., Kim, J. H., and Kwon, Y. H. (2019a). Relationship between impaired consciousness and injury of ascending reticular activating system in patients with intracerebral hemorrhage. *Stroke* 50, 2234–2237. doi: 10.1161/STROKEAHA.118.023710

Jang, S. H., Chang, C. H., Jung, Y. J., and Lee, H. D. (2017a). Recovery of akinetic mutism and injured prefronto-caudate tract following shunt operation for hydrocephalus and rehabilitation: a case report. *Medicine (Baltimore)* 96:e9117. doi: 10.1097/MD.0000000000009117

Jang, S. H., Kim, S. H., and Lee, H. D. (2017b). Recovery of an injured prefronto-caudate tract in a patient with traumatic brain injury: a diffusion tensor tractography study. *Brain Inj.* 31, 1548–1551. doi: 10.1080/02699052.2017.1376761

Jang, S. H., Kim, S. H., and Lee, H. D. (2018). Akinetic mutism following prefrontal injury by an electrical grinder a case report: a diffusion tensor tractography study. *Medicine (Baltimore)* 97:e9845. doi: 10.1097/MD.0000000000009845

Jang, S. H., and Kwon, H. G. (2017). Akinetic mutism in a patient with mild traumatic brain injury: a diffusion tensor tractography study. *Brain Inj.* 31, 1159–1163. doi: 10.1080/02699052.2017.1288265

Jang, S. H., Lim, H. W., and Yeo, S. S. (2014). The neural connectivity of the intralaminar thalamic nuclei in the human brain: a diffusion tensor tractography study. *Neurosci. Lett.* 579, 140–144. doi: 10.1016/j.neulet.2014.07.024

Jang, S. H., Park, J. S., Shin, D. G., Kim, S. H., and Kim, M. S. (2019b). Relationship between consciousness and injury of ascending reticular activating system in patients with hypoxic ischaemic brain injury. *J. Neurol. Neurosurg. Psychiatry*. 90, 493–494. doi: 10.1136/jnnp-2018-318366

Jang, S. H., and Yeo, S. S. (2014). Thalamocortical connections between the mediodorsal nucleus of the thalamus and prefrontal cortex in the human brain: a diffusion tensor tractographic study. *Yonsei Med. J.* 55, 709–714. doi: 10.3349/ymj.2014.55.3.709

Johansen-Berg, H., Behrens, T. E., Sillery, E., Ciccarelli, O., Thompson, A. J., Smith, S. M., et al. (2005). Functional-anatomical validation and individual variation of diffusion tractography-based segmentation of the human thalamus. *Cereb. Cortex* 15, 31–39. doi: 10.1093/cercor/bhh105

Klein, J. C., Rushworth, M. F., Behrens, T. E., Mackay, C. E., de Crespigny, A. J., D'Arceuil, H., et al. (2010). Topography of connections between human prefrontal cortex and mediodorsal thalamus studied with diffusion tractography. *Neuroimage* 51, 555–564. doi: 10.1016/j.neuroimage.2010.02.062

Kringelbach, M. L. (2005). The human orbitofrontal cortex: linking reward to hedonic experience. *Nat. Rev. Neurosci.* 6, 691–702. doi: 10.1038/nrn1747

Leh, S. E., Ptito, A., Chakravarty, M. M., and Strafella, A. P. (2007). Fronto-striatal connections in the human brain: a probabilistic diffusion tractography study. *Neurosci. Lett.* 419, 113–118. doi: 10.1016/j.neulet.2007.04.049

Marin, R. S., and Wilkosz, P. A. (2005). Disorders of diminished motivation. *J. Head Trauma Rehabil.* 20, 377–388. doi: 10.1097/00001199-200507000-00009

Mega, M. S., and Cohenour, R. C. (1997). Akinetic mutism: disconnection of frontal-subcortical circuits. *Neuropsychiatry Neuropsychol. Behav. Neurol.* 10, 254–259.

Mendoza, M., and Eblen-Zajjur, A. (2019). Age related T2-FSE-MRI basal ganglia and inter-nuclei changes in normal aging. *Neurol. Psychiatry Brain Res.* 32, 55–62. doi: 10.1016/j.npbr.2019.03.002

Morel, A. (2007). *Stereotactic Atlas of the Human Thalamus and Basal Ganglia*. New York, ny: Informa Healthcare.

Morel, A., Magnin, M., and Jeanmonod, D. (1997). Multiarchitectonic and stereotactic atlas of the human thalamus. *J. Comp. Neurol.* 387, 588–630. doi: 10.1002/(SICI)1096-9861(19971103)387:4<588::AID-CNE8>3.0.CO;2-Z

Nagaratnam, N., Nagaratnam, K., Ng, K., and Diu, P. (2004). Akinetic mutism following stroke. *J. Clin. Neurosci.* 11, 25–30. doi: 10.1016/j.jocn.2003.04.002

Petrides, M. (2005). Lateral prefrontal cortex: architectonic and functional organization. *Philos. Trans. R. Soc. Lond. B Biol. Sci.* 360, 781–795. doi: 10.1098/rstb.2005.1631

Yamada, K., Sakai, K., Akazawa, K., Yuen, S., and Nishimura, T. (2009). MR tractography: a review of its clinical applications. *Magn. Reson. Med. Sci.* 8, 165–174. doi: 10.2463/mrms.8.165

Yeo, S. S., Chang, P. H., and Jang, S. H. (2013). The ascending reticular activating system from pontine reticular formation to the thalamus in the human brain. *Front. Hum. Neurosci.* 7:416. doi: 10.3389/fnhum.2013.00416

Conflict of Interest: The authors declare that the research was conducted in the absence of any commercial or financial relationships that could be construed as a potential conflict of interest.

frontiers in Human Neuroscience

BRIEF RESEARCH REPORT
published: 22 March 2022
doi: 10.3389/fnhum.2022.845476

The Effect of Inter-pulse Interval on TMS Motor Evoked Potentials in Active Muscles

Noora Matilainen[1]*, *Marco Soldati*[1] and *Ilkka Laakso*[1,2]

[1] Department of Electrical Engineering and Automation, Aalto University, Espoo, Finland, [2] Aalto Neuroimaging, Aalto University, Espoo, Finland

Objective: The time interval between transcranial magnetic stimulation (TMS) pulses affects evoked muscle responses when the targeted muscle is resting. This necessitates using sufficiently long inter-pulse intervals (IPIs). However, there is some evidence that the IPI has no effect on the responses evoked in active muscles. Thus, we tested whether voluntary contraction could remove the effect of the IPI on TMS motor evoked potentials (MEPs).

Methods: In our study, we delivered sets of 30 TMS pulses with three different IPIs (2, 5, and 10 s) to the left primary motor cortex. These measurements were performed with the resting and active right hand first dorsal interosseous muscle in healthy participants (N = 9 and N = 10). MEP amplitudes were recorded through electromyography.

Results: We found that the IPI had no significant effect on the MEP amplitudes in the active muscle (p = 0.36), whereas in the resting muscle, the IPI significantly affected the MEP amplitudes ($p < 0.001$), decreasing the MEP amplitude of the 2 s IPI.

Conclusions: These results show that active muscle contraction removes the effect of the IPI on the MEP amplitude. Therefore, using active muscles in TMS motor mapping enables faster delivery of TMS pulses, reducing measurement time in novel TMS motor mapping studies.

Keywords: TMS, inter-pulse interval, motor evoked potential, motor mapping, active muscle contraction, motor threshold

OPEN ACCESS

Edited by:
Masaki Sekino,
The University of Tokyo, Japan

Reviewed by:
Umit Aydin,
King's College London, United Kingdom
Toshiaki Wasaka,
Nagoya Institute of Technology, Japan

***Correspondence:**
Noora Matilainen
noora.matilainen@aalto.fi

Specialty section:
This article was submitted to Brain Imaging and Stimulation, a section of the journal Frontiers in Human Neuroscience

Received: *29 December 2021*
Accepted: *24 February 2022*
Published: *22 March 2022*

Citation:
Matilainen N, Soldati M and Laakso I (2022) The Effect of Inter-pulse Interval on TMS Motor Evoked Potentials in Active Muscles. Front. Hum. Neurosci. 16:845476. doi: 10.3389/fnhum.2022.845476

1. INTRODUCTION

Transcranial magnetic stimulation (TMS) is a useful tool for motor mapping. Cortical motor maps help identifying lesions or plasticity changes in the motor system (Lefaucheur, 2019), and they are also used for presurgical assessment of brain tumor surgery (Lefaucheur and Picht, 2016).

Recently developed methods aim to localize the effect of TMS in the cerebral cortex using computer simulations of the induced electric fields (Bungert et al., 2017; Laakso et al., 2018; Weise et al., 2020). These methods, however, require a large number of pulses lengthening the measurement time. A common practice is to use fairly long inter-pulse intervals (IPIs) in order

to avoid the effect of the IPI on motor evoked potential (MEP) amplitudes (Julkunen et al., 2012; Vaseghi et al., 2015; Pellicciari et al., 2016; Hassanzahraee et al., 2019). However, the effect is reported only for resting muscles. For example, Bungert et al. (2017), Laakso et al. (2018) and Kataja et al. (2021) used active muscle contraction in their studies. Furthermore, there is some indication that the IPI has no effect on responses evoked in active muscles (Möller et al., 2009). Möller et al. discovered that the hysteresis effect, which was observed with a resting muscle, did not occur when the muscle was active. In addition, previous studies have suggested more thorough investigation of the effect on MEP amplitude when using an active muscle, as it has not been studied before (Vaseghi et al., 2015; Hassanzahraee et al., 2019).

Future research would benefit from the use of a shorter IPI for active muscles. Therefore, the objective of this study is to investigate the possibility of using active muscle contraction in TMS motor mapping with a shorter IPI in order to reduce the measurement time.

2. MATERIALS AND METHODS

2.1. Participants

The data was collected from 13 healthy participants who were right handed by self report and participated in two experimental conditions, active and resting. One participant was excluded from the study because of a high motor threshold. Two participants were excluded from the active condition as the baseline muscle activity was not sufficient. The resting condition was not performed for three participants. Altogether, seven participants were included in both the active and resting condition. Finally, the analysis of the active condition data included 10 participants (7 male, 3 female, mean age $\pm$ SD $=$ 30.8 $\pm$ 5.8, age range: 25–40) and the analysis of the resting condition data included 9 participants (7 male, 2 female, mean age $\pm$ SD $=$ 30.1 $\pm$ 5.6, age range: 22–40). All participants gave their written consent for participation. The study was approved by the Aalto University Research Ethics Committee.

2.2. Magnetic Resonance Imaging

T1 and T2 weighted magnetic resonance (MR) images were acquired using a 3 T MRI scanner (Magnetom Skyra; Siemens, Ltd., Erlangen, Germany). The imaging parameters are listed as follows. T1: TR/TE/TI/FA/FOV/voxel size/slice number $=$ 1,800/1.99/800 ms/9°/256/1 $\times$ 1 $\times$ 1 mm/176; and T2: TR/TE/FOV/voxel size/slice number $=$ 3,200/412 ms/256/1 $\times$ 1 $\times$ 1 mm /176. The data have been measured at AMI Centre, Aalto NeuroImaging, Aalto University School of Science.

2.3. Cortical Reconstruction and TMS Coil Location

The coil locations for the experiments were determined in advance to target the stimulation to the first dorsal interosseus (FDI) target location in the hand area of the left hemisphere.

First, cortical reconstructions were generated from the T1-weighted MR images using the FreeSurfer image analysis software (Dale et al., 1999; Fischl et al., 1999). After reconstruction, FreeSurfer was used to generate a mapping between the reconstructed surface of the individual brain and the surface reconstruction of the Montreal Neurological Institute (MNI) ICBM 2009a nonlinear asymmetric template brain (Fonov et al., 2009, 2011).

For each participant, the mapping was used to obtain an individual cortical target location that corresponded to $[-41, -7, 63]$ in MNI coordinates, which was previously estimated to be the group-average activation site for the FDI muscle (Laakso et al., 2018). The coil was positioned on the scalp at the closest point to the selected target cortical location. The coil orientation was selected so that the induced current direction was approximately perpendicular to the course of the central sulcus in the posterior-anterior direction at the target location. Finally, the predetermined coil locations and directions were marked on the MR images, which were used for neuronavigation (**Figures 1B,C**).

2.4. TMS and EMG Recordings

TMS was performed with a monophasic Magstim 200^2 stimulator (Magstim Company, UK) using an eight-shaped coil, which consists of two adjacent round wings of 9 cm diameter. The location and orientation of the coil were tracked and recorded with the Visor2 TMS neuronavigation system (ANT Neuro, Enschede, the Netherlands). The data have been measured at Aalto TMS, Aalto NeuroImaging, Aalto University School of Science.

Resting and active motor threshold (RMT and AMT) intensities were defined as the lowest intensities required to elicit TMS MEPs (peak-to-peak amplitude of >50 μV with resting and 100 μV with active condition) in at least 50% of successive trials (Rossini et al., 2015). MEPs were recorded from the right hand FDI muscle with the NeurOne EMG system (NeurOne, MEGA Electronics Ltd, Finland) and disposable Ag/AgCl surface electrodes. The EMG signal was sampled at 5 kHz and high-pass filtered with a 10 Hz cutoff frequency.

2.5. Experimental Setup

We studied the MEPs measured from the right hand FDI muscle when the primary motor cortex was stimulated by TMS. Three different IPIs (2, 5, and 10 s) with two different conditions, active and resting muscle, were used. Thirty pulses were delivered for each IPI for both conditions using a stimulation intensity approximately 20% above the motor threshold intensity. The order of the IPIs and conditions were pseudo-randomized. The experimental setup is illustrated in **Figure 1**.

During the measurement, the participant was sitting on a chair with the magnetic coil positioned using a mechanical holder on the predetermined scalp location above their left cerebral hemisphere. Their right arm was resting on a pillow placed on their lap. In the resting condition, the participant kept their hand resting on a pillow. In the active condition, their task was to contract their FDI muscle by applying a constant pressure on a small object with their index finger and thumb while their hand was still. Participants were instructed to observe their EMG activation from the screen in front of them and keep the peak-to-peak amplitude close to 200 μV.

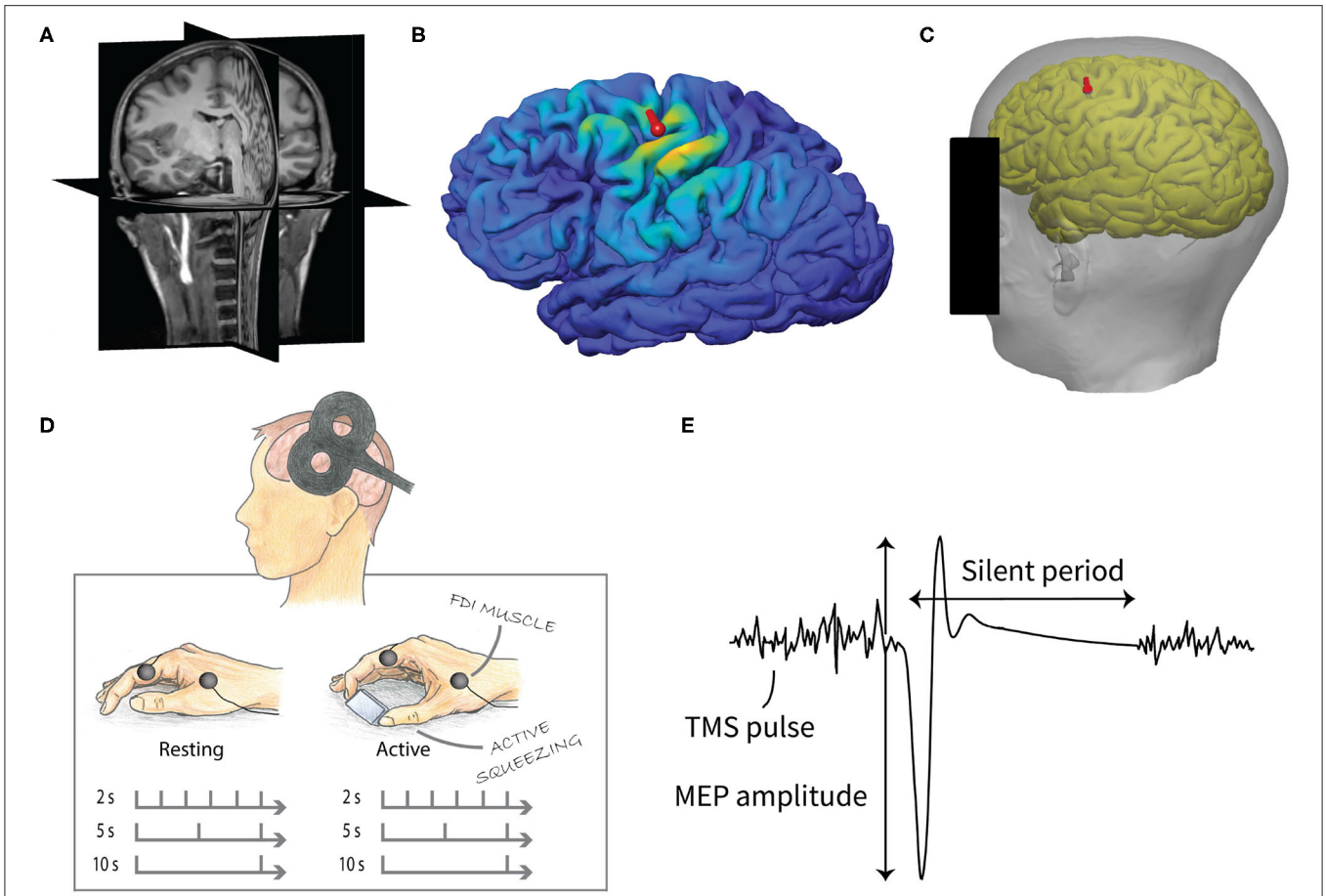

FIGURE 1 | Experimental design of the study. **(A)** T1- (pictured) and T2-weighted MR images were used to create individual cortical reconstructions. **(B)** The induced electric fields were calculated based on computer simulations. **(C)** The location of the TMS coil (red mark) for the experiment was predetermined from the cortical reconstruction in order to obtain the optimal cortical location for the FDI muscle. **(D)** TMS measurement consisted of two parts, resting and active condition. Both included three sets of 30 stimuli with 2, 5, and 10 s IPI. The order of the conditions and IPIs were pseudo-randomized. **(E)** MEPs were recorded from the FDI muscle of the right hand. The peak-to-peak amplitude of the MEPs was used in the analysis. The silent period was defined as the duration between the MEP onset and the resumption of the voluntary EMG.

2.6. Calculation of the Induced Electric Field

The finite-element method was used to computationally estimate the induced electric field at the cortical target location. The details of the computer simulations were similar to our previous study (Laakso et al., 2018). Briefly, volume conductor models were generated from the cortical reconstructions generated using FreeSurfer and the segmentation of the T1- and T2-weighted MR images. The following electric conductivity values were assigned to the segmented tissues and bodily fluids (unit: S/m): gray matter (0.215), white matter (0.142), cerebrospinal fluid (1.79), compact and spongy bone (0.009 and 0.034), subcutaneous fat (0.15), scalp (0.43), muscle (0.18), dura mater (0.18), and blood (0.7).

A model of the figure-8 coil (Çan et al., 2018) was placed on the location recorded in the experiments using the neuronavigation system. We note that the recorded location might differ slightly from the predetermined scalp location. The induced electric field was determined using the FEM with a uniform grid of first-order cubical elements with a side length of 0.5 mm (Laakso and Hirata, 2012). Finally, the electric field magnitude was calculated at the individual target cortical location. In addition, we calculated the maximum value of the electric field magnitude in the cortical gray matter at a depth of 2 mm below the pial surface.

2.7. Data Processing and Statistical Analysis

The MEP amplitude was defined as the peak-to-peak distance between the negative and positive peak in the waveform. The EMG baseline value for active condition was defined as the root mean square of the EMG signal in one second interval before the stimulus. The length of the silent period was defined as the duration between the MEP onset and the resumption of the voluntary EMG.

A linear mixed-effects model was used to predict the relationship between the MEP amplitude and the IPI. This model allows non-independent observations and considers

inter-subject variability as well as the EMG baseline level. For the analysis, the MEP amplitude was log transformed in order to ensure the normality of the residuals. Analyses were performed with the open-source programming language R (R Core Team, 2013), separately for the resting and active conditions.

For the resting condition, the model included the IPI (2, 5, and 10 s), pulse number (1–30) and their interaction as fixed effects. Participants were treated as a random effect. The order of the IPI measurement appeared non-significant when included in the model and did not result in a better model fit using the Akaike information criterion. Therefore, it was excluded from the model making the final model simpler. For the active condition, an additional fixed effect, EMG baseline, was included in the model, as the active muscle contraction causes a slightly varying baseline level that can affect the MEP. Maximum likelihood was used as the estimation method for the model coefficients. *P*-values were obtained by likelihood ratio tests of the full models with the effect of the IPI against the null model (without the IPI).

Post-hoc analyses were conducted to compare the different IPIs by the means of a Wilcoxon signed-rank test (as the data is dependent) with a Bonferroni adjustment of the p-values. A p-value smaller than 0.05 was considered significant for all statistical tests. For visualization and *post-hoc* analyses, the participant specific intercepts were removed from the data using the linear mixed-effects model.

To study whether the IPI affected the variability of the MEP amplitudes between trials, the coefficient of variation (CV = 100 × SD/mean) of the log transformed MEP amplitudes was computed for each participant at each IPI and condition (active and resting).

Additionally, a linear mixed-effects model was used to predict the relationship between the length of the silent period and the IPI. For the analysis, the length was log transformed in order to ensure the normality of the residuals.

3. RESULTS

3.1. Motor Threshold and Induced Electric Field

Intensities for the RMT and AMT were 43.2 ± 5.2% and 38.8 ± 7.2% (mean ± SD) of the maximum stimulator output, respectively. The corresponding induced electric field magnitudes in the gray matter at the predetermined FDI target location were 135 ± 40 and 108 ± 37 V/m (mean ± SD) for the resting and active conditions, respectively.

The corresponding maximum values of the electric field magnitude in the gray matter were 188 ± 46 and 151 ± 37 V/m (mean ± SD). The maximum values did not differ significantly from those reported in an earlier study (Laakso et al., 2018) (Student's *t*-tests, $p = 0.2$ and $p = 0.07$, respectively), where the magnetic coil was manually positioned by searching the "hotspot" for the FDI muscle. This indicated that the coil location used in the experiments was comparable to that obtained using the conventional method.

3.2. Effects of Inter-pulse Interval on MEP Amplitude

A linear mixed-effects model with a likelihood ratio test showed that the IPI had a significant effect on the MEP amplitude for the resting [$\chi^2(2) = 18.91$, $p < 0.001$] but not for the active muscle [$\chi^2(2) = 2.02$, $p = 0.36$]. The only fixed effect significantly affecting the MEP amplitudes during active muscle contraction was the baseline EMG magnitude before the pulse [$\chi^2(1) = 85.20$, $p < 0.001$], a higher baseline producing higher amplitudes. The relationship between the MEP amplitude and the EMG baseline is visualized in **Figure 2A**.

Mean coefficient of variation (CV) of the log transformed MEP amplitude is presented in **Figure 2B**. *Post-hoc* testing showed that the CVs were significantly lower at active condition than at resting condition (pairwise Wilcoxon signed-rank tests, $p < 0.01$, Bonferroni corrected), but there was no support for significant differences in CVs between the IPI groups (pairwise Wilcoxon signed-rank tests, all $p > 0.32$, Bonferroni corrected).

The effect of the pulse number on the MEP amplitude for each IPI is illustrated in **Figure 3**. For the resting condition, the MEP amplitude of the first pulses appear to be higher than the MEP amplitude of the later pulses in the 2 and 5 s IPIs. For the 2 s IPI, *post-hoc* analysis shows a significant difference (pairwise Wilcoxon signed-rank tests, $p < 0.05$, Bonferroni corrected) between the first pulse and the participant-specific median of the later pulses (pulse numbers 2–30). For the active muscle, the level of the first pulse appears similar to the other pulses, and no significant difference could be demonstrated.

For later pulses (pulse numbers 2–30), there was a significant difference between the amplitudes of the 2 s IPI and the others (pairwise Wilcoxon signed-rank tests, $p < 0.001$, Bonferroni corrected) for the resting muscle (**Figure 4A**). On average, stimulation with the 2 s IPI decreased the median MEP amplitude by 14% compared to the 10 s IPI. For the active muscle, no significant differences (pairwise Wilcoxon signed-rank tests, all $p > 0.1$) were found between the IPI groups of later pulses.

3.3. Effects of Inter-pulse Interval on Silent Period

A linear mixed-effects model with a likelihood ratio test for a silent period indicated that the IPI did not significantly affect the length of the silent period for the active muscle [$\chi^2(2) = 0.11$, $p = 0.95$]. Data is demonstrated in **Figure 4B** with *post-hoc* analysis showing no support for significant differences (pairwise Wilcoxon signed-rank tests, all $p = 1$, Bonferroni corrected) between the IPI groups.

4. DISCUSSION

The current study investigated the effect of the TMS IPI on the MEP amplitude with the active and resting muscle. The objective was to find whether active muscle contraction could remove the

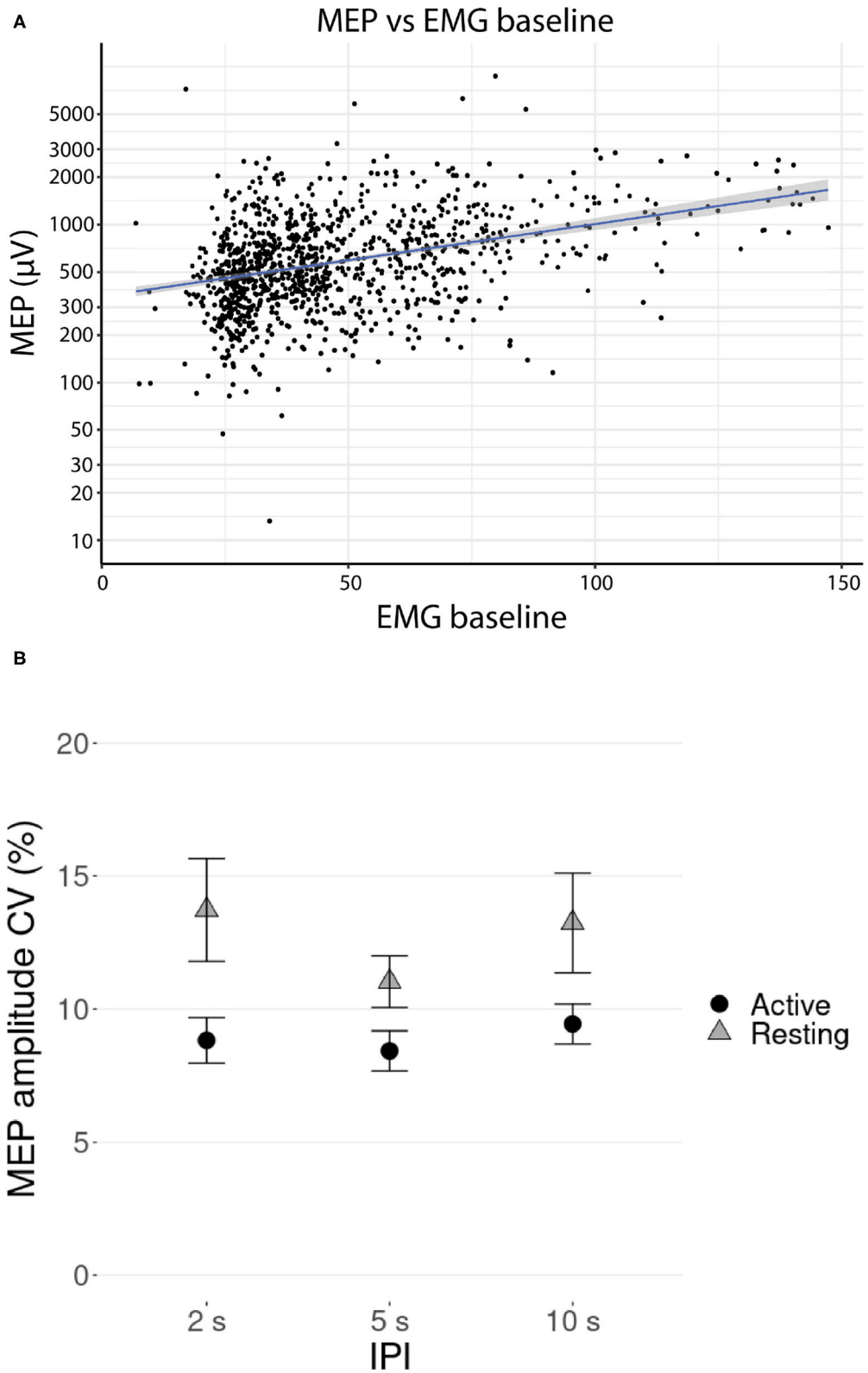

FIGURE 2 | (A) Relationship between the MEP amplitudes and the EMG baseline (RMS value over 1 s before the stimulus) during TMS stimulation with active contraction on logarithmic scale. Participant-specific intercepts have been removed from the data using a linear mixed effects model. The gray shaded area around the regression line represents the 95% confidence interval. **(B)** Mean coefficient of variation (CV) of the log transformed MEP amplitude versus IPI at active and resting conditions. Error bars represent the standard errors.

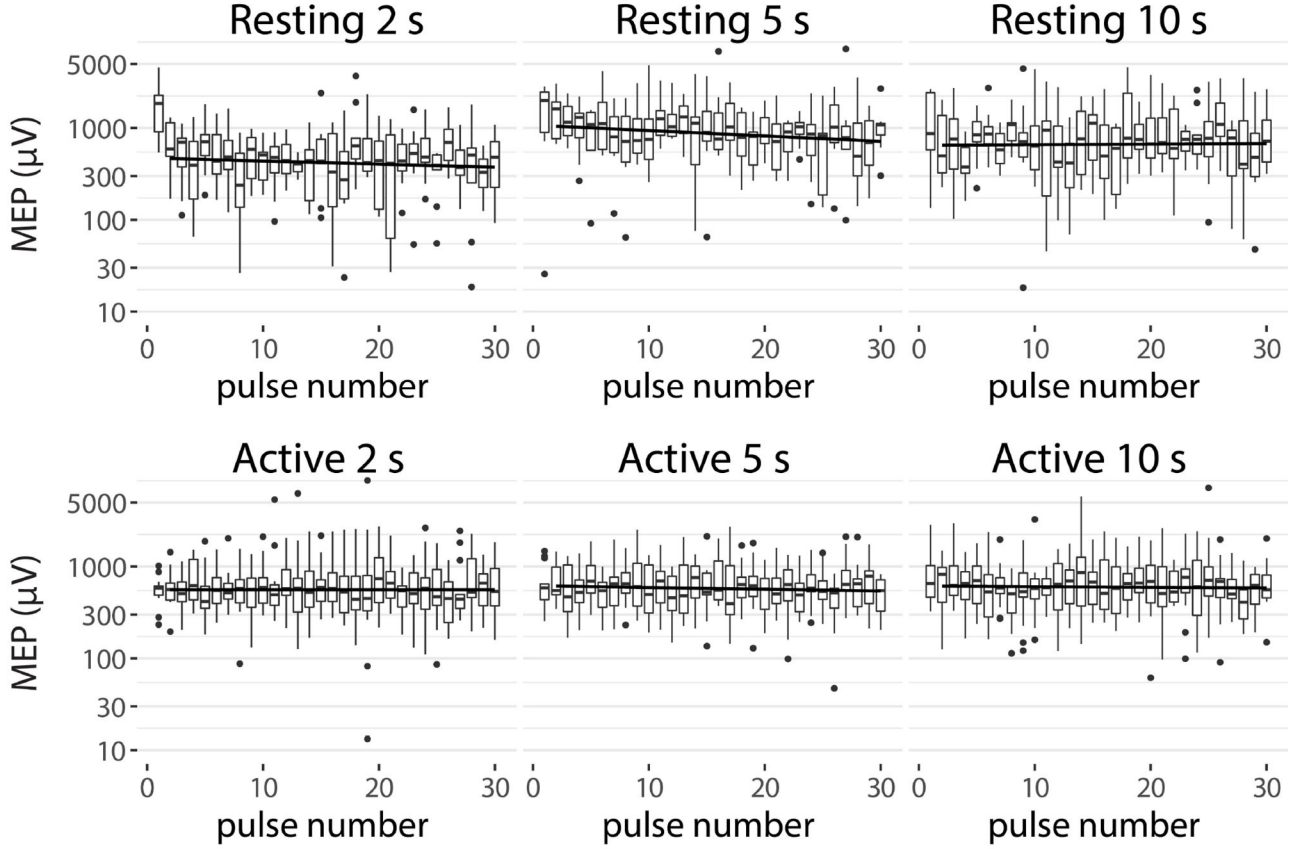

FIGURE 3 | MEP amplitudes of each IPI (2, 5, and 10 s) for resting and active condition. Participant-specific intercepts have been removed from the data using a linear mixed effects model. Graphs represent the minimum, maximum, median, first quartile, and third quartile in the data set on a logarithmic scale. The trend line is drawn from the second to the last pulse.

modulatory effect of the IPI on the MEP amplitude, and therefore reduce the time used in TMS motor mapping.

Previous studies have found that, with a resting muscle, the MEP amplitudes were greatly dependent on the IPI (Möller et al., 2009; Julkunen et al., 2012; Vaseghi et al., 2015; Pellicciari et al., 2016; Hassanzahraee et al., 2019). The MEP amplitude was shown to increase as the IPI increased from 5 to 20 s (Möller et al., 2009), from 2 to 10 s (Julkunen et al., 2012), from 4 to 10 s (Vaseghi et al., 2015), and from 5 to 15 s (Hassanzahraee et al., 2019). Hassanzahraee et al. (2019) also showed that IPIs longer than 12 s did not differ in amplitude, as their IPI was sufficient for the recovery of the cerebral perfusion. Because of the recovery time, it is suggested to use a longer IPI when giving TMS with a resting muscle. Our findings support these previous results, as the shortest 2 s IPI significantly decreased the MEP amplitude compared to both 10 and 5 s IPIs. However, we could not show a significant difference between the 5 and 10 s IPIs, but the difference between them has been smaller than their difference with the 2 s IPI in previous studies as well. Furthermore, several rTMS studies (Chen et al., 1997; Siebner et al., 1999; Muellbacher et al., 2000) have reported that low-frequency rTMS on the motor cortex reduces cortical excitability with a resting muscle, which can be observed as a reduction of MEP amplitudes. This could also underlie the reduction of MEP amplitudes we observed with 2 s IPI, as the 2 s IPI is close to commonly used frequencies in low-frequency rTMS.

To our knowledge, there are no previous studies that have researched whether the IPI has an effect on the silent period. Our results indicate that there is no significant effect. Furthermore, we did not find significant effects of the IPI on the inter-trial variability of the MEP amplitude. However, the variability in the MEPs was significantly smaller with the active muscle compared to the resting muscle, which is due to the stabilization of corticospinal excitability through slight voluntary muscle contraction (Darling et al., 2006).

Our main finding indicates that MEPs with active muscle contraction during TMS are not affected by the IPI. A possible cause is that constant muscle contraction saturates the excitability of the corticomotorneurons, which prevents the recovery of the cerebral perfusion that is present with a resting muscle.

Our result allows the use of shorter IPIs in TMS studies in active muscles. This can significantly shorten the recording time, making measurement sessions more effective. Shortening the recording time is especially beneficial in studies where a large

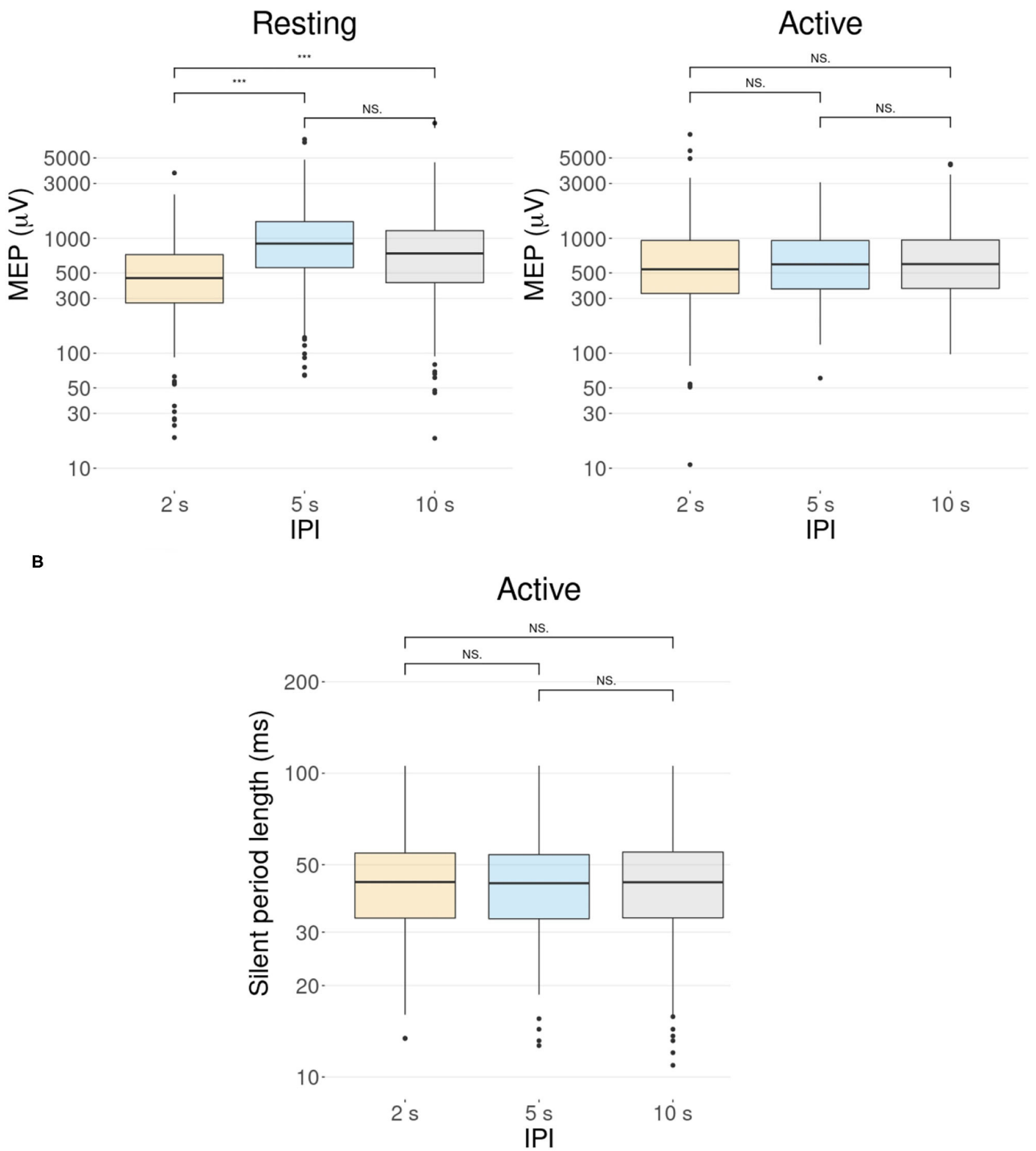

FIGURE 4 | The effect of the IPI. Participant-specific intercepts have been removed from the data using a linear mixed effects model. Graphs represent the minimum, maximum, median, first quartile, and third quartile in the data set on a logarithmic scale. ***$p \leq 0.001$, Ns, non-significance. **(A)** Pulses after the first pulse (pulse numbers 2–30) show a difference in the MEP amplitudes in the resting condition but not in the active condition. In the resting condition, the MEP amplitude of the 2 s IPI differs significantly from those of the 5 and 10 s IPIs ($p < 0.001$). In the active condition, there is no significant difference between the MEP amplitudes of different IPIs ($p > 0.1$). **(B)** Boxplot illustration of the length of the silent period for different IPIs in the active condition. A Wilcoxon signed-rank test with a Bonferroni adjustment shows no support for significant differences between the different IPIs (all $p = 1$).

number of TMS pulses are used, such as novel computational–experimental techniques that have been developed for accurate localization of the activation sites of TMS (Bungert et al., 2017; Laakso et al., 2018; Weise et al., 2020; Kataja et al., 2021). These techniques rely on the computational analysis of the induced electric field and may require the application of more than a thousand TMS pulses. The use of a shorter IPI in active muscles could significantly improve the applicability of such methods.

The main drawback with all active muscle TMS studies is the inaccuracy of the constant muscle contraction force. This was also indicated by our results, which showed an effect of the baseline EMG signal magnitude on the MEP size, higher baselines producing larger MEPs. In order to secure a reliable muscle contraction of required level during stimulation, it is necessary to have a sufficient feedback method to ensure that the participant can maintain the correct contraction level. However, these methods are not feasible if the participant is not able for constant contraction of muscle or unable to contract the muscle at all. Additionally, active muscle contraction might be unsuitable for studies aiming to measure brain activity in combination with TMS, such as TMS-EEG studies (Ilmoniemi and Kičić, 2010), because the active contraction in itself affects the EEG. Moreover, we did not study the effect of IPIs shorter than 2 s, and therefore our result may not be applicable with shorter IPIs. Furthermore, the current study was mainly conducted in young adults and cannot be generalized to the entire population without critical judgement. It should also be noted that there where few participants who were different between the study conditions.

In conclusion, the present study revealed that active muscle contraction eliminates the modulating effect of the IPI that is present with a resting muscle. This result indicates that IPIs as short as 2 s can be used to speed up TMS motor mapping in active muscles. To our knowledge, this is the first study to compare the effects of three different IPIs on the MEP amplitude in both active and resting muscles.

DATA AVAILABILITY STATEMENT

The raw data supporting the conclusions of this article will be made available by the authors, without undue reservation.

ETHICS STATEMENT

The studies involving human participants were reviewed and approved by Aalto University Research Ethics Committee. The patients/participants provided their written informed consent to participate in this study.

AUTHOR CONTRIBUTIONS

NM and IL designed the study. NM and MS performed the experiments. NM processed and analyzed the data and initially wrote the manuscript. IL obtained funding for the project. All authors reviewed, edited, and approved the final manuscript.

FUNDING

This work was supported by the Academy of Finland (Grant Number 325326).

REFERENCES

Bungert, A., Antunes, A., Espenhahn, S., and Thielscher, A. (2017). Where does TMS stimulate the motor cortex? combining electrophysiological measurements and realistic field estimates to reveal the affected cortex position. *Cereb. Cortex* 27, 5083–5094. doi: 10.1093/cercor/bhw292

Çan, M. K., Laakso, I., Nieminen, J. O., Murakami, T., and Ugawa, Y. (2018). Coil model comparison for cerebellar transcranial magnetic stimulation. *Biomed. Phys. Eng. Exp.* 5, 015020. doi: 10.1088/2057-1976/aaee5b

Chen, R., Classen, J., Gerloff, C., Celnik, P., Wassermann, E., Hallett, M., et al. (1997). Depression of motor cortex excitability by low-frequency transcranial magnetic stimulation. *Neurology* 48, 1398–1403.

Dale, A. M., Fischl, B., and Sereno, M. I. (1999). Cortical surface-based analysis: I. segmentation and surface reconstruction. *NeuroImage* 9, 179–194.

Darling, W. G., Wolf, S. L., and Butler, A. J. (2006). Variability of motor potentials evoked by transcranial magnetic stimulation depends on muscle activation. *Exp. Brain Res.* 174, 376–385. doi: 10.1007/s00221-006-0468-9

Fischl, B., Sereno, M. I., and Dale, A. M. (1999). Cortical surface-based analysis: II: inflation, flattening, and a surface-based coordinate system. *NeuroImage* 9, 195–207.

Fonov, V., Evans, A. C., Botteron, K., Almli, C. R., McKinstry, R. C., Collins, D. L., et al. (2011). Unbiased average age-appropriate atlases for pediatric studies. *NeuroImage* 54, 313–327. doi: 10.1016/j.neuroimage.2010.07.033

Fonov, V. S., Evans, A. C., McKinstry, R. C., Almli, C., and Collins, D. (2009). Unbiased nonlinear average age-appropriate brain templates from birth to adulthood. *NeuroImage* 47, S102. doi: 10.1016/S1053-8119(09)70884-5

Hassanzahraee, M., Zoghi, M., and Jaberzadeh, S. (2019). Longer transcranial magnetic stimulation intertrial interval increases size, reduces variability, and improves the reliability of motor evoked potentials. *Brain Connect.* 9, 770–776. doi: 10.1089/brain.2019.0714

Ilmoniemi, R. J., and Kičić, D. (2010). Methodology for combined tms and eeg. *Brain Topography* 22, 233–248. doi: 10.1007/s10548-009-0123-4

Julkunen, P., Säisänen, L., Hukkanen, T., Danner, N., and Könönen, M. (2012). Does second-scale intertrial interval affect motor evoked potentials induced by single-pulse transcranial magnetic stimulation? *Brain Stimulat.* 5, 526–532. doi: 10.1016/j.brs.2011.07.006

Kataja, J., Soldati, M., Matilainen, N., and Laakso, I. (2021). A probabilistic transcranial magnetic stimulation localization method. *J. Neural Eng.* 18, 0460f3. doi: 10.1088/1741-2552/ac1f2b

Laakso, I., and Hirata, A. (2012). Fast multigrid-based computation of the induced electric field for transcranial magnetic stimulation. *Phys. Med. Biol.* 57, 7753–7765. doi: 10.1088/0031-9155/57/23/7753

Laakso, I., Murakami, T., Hirata, A., and Ugawa, Y. (2018). Where and what TMS activates: experiments and modeling. *Brain Stimulat.* 11, 166–174. doi: 10.1016/j.brs.2017.09.011

Lefaucheur, J.-P. (2019). "Chapter 37 - transcranial magnetic stimulation," in *Clinical Neurophysiology: Basis and Technical Aspects, Handbook of Clinical Neurology*, eds K. H. Levin and P. Chauvel, vol. 160 (Elsevier), 559–580.

Lefaucheur, J.-P., and Picht, T. (2016). The value of preoperative functional cortical mapping using navigated TMS. *Neurophysiologie Clinique/Clin. Neurophysiol.* 46, 125–133. doi: 10.1016/j.neucli.2016.05.001

Möller, C., Arai, N., Lücke, J., and Ziemann, U. (2009). Hysteresis effects on the input–output curve of motor evoked potentials. *Clin. Neurophysiol.* 120, 1003–1008. doi: 10.1016/j.clinph.2009.03.001

Muellbacher, W., Ziemann, U., Boroojerdi, B., and Hallett, M. (2000). Effects of low-frequency transcranial magnetic stimulation on motor

excitability and basic motor behavior. *Clin. Neurophysiol.* 111, 1002–1007. doi: 10.1016/s1388-2457(00)00284-4

Pellicciari, M. C., Miniussi, C., Ferrari, C., Koch, G., and Bortoletto, M. (2016). Ongoing cumulative effects of single TMS pulses on corticospinal excitability: an intra-and inter-block investigation. *Clin. Neurophysiol.* 127, 621–628. doi: 10.1016/j.clinph.2015.03.002

R Core Team (2013). *R: A Language and Environment for Statistical Computing*. Vienna: R Foundation for Statistical Computing.

Rossini, P. M., Burke, D., Chen, R., Cohen, L., Daskalakis, Z., Di Iorio, R., et al. (2015). Non-invasive electrical and magnetic stimulation of the brain, spinal cord, roots and peripheral nerves: basic principles and procedures for routine clinical and research application. an updated report from an IFCN committee. *Clin. Neurophysiol.* 126, 1071–1107. doi: 10.1016/j.clinph.2015.02.001

Siebner, H. R., Auer, C., and Conrad, B. (1999). Abnormal increase in the corticomotor output to the affected hand during repetitive transcranial magnetic stimulation of the primary motor cortex in patients with writer's cramp. *Neurosci. Lett.* 262, 133–136.

Vaseghi, B., Zoghi, M., and Jaberzadeh, S. (2015). Inter-pulse interval affects the size of single-pulse TMS-induced motor evoked potentials: a reliability study. *Basic Clin. Neurosci.* 6, 44.

Weise, K., Numssen, O., Thielscher, A., Hartwigsen, G., and Knösche, T. R. (2020). A novel approach to localize cortical TMS effects. *NeuroImage* 209, 116486. doi: 10.1016/j.neuroimage.2019.116486

Conflict of Interest: The authors declare that the research was conducted in the absence of any commercial or financial relationships that could be construed as a potential conflict of interest.

Publisher's Note: All claims expressed in this article are solely those of the authors and do not necessarily represent those of their affiliated organizations, or those of the publisher, the editors and the reviewers. Any product that may be evaluated in this article, or claim that may be made by its manufacturer, is not guaranteed or endorsed by the publisher.

frontiers in Behavioral Neuroscience

ORIGINAL RESEARCH
published: 22 March 2022
doi: 10.3389/fnbeh.2022.805178

Local Neuronal Responses to Intracortical Microstimulation in Rats' Barrel Cortex Are Dependent on Behavioral Context

*Sergejus Butovas and Cornelius Schwarz**

Systems Neurophysiology, Werner Reichardt Center for Integrative Neuroscience, Hertie-Institute for Clinical Brain Research, University Tübingen, Tübingen, Germany

The goal of cortical neuroprosthetics is to imprint sensory information as precisely as possible directly into cortical networks. Sensory processing, however, is dependent on the behavioral context. Therefore, a specific behavioral context may alter stimulation effects and, thus, perception. In this study, we reported how passive vs. active touch, i.e., the presence or absence of whisker movements, affects local field potential (LFP) responses to microstimulation in the barrel cortex in head-fixed behaving rats trained to move their whiskers voluntarily. The LFP responses to single-current pulses consisted of a short negative deflection corresponding to a volley of spike activity followed by a positive deflection lasting ∼100 ms, corresponding to long-lasting suppression of spikes. Active touch had a characteristic effect on this response pattern. While the first phase including the negative peak remained stable, the later parts consisting of the positive peak were considerably suppressed. The stable phase varied systematically with the distance of the electrode from the stimulation site, pointing to saturation of neuronal responses to electrical stimulation in an intensity-dependent way. Our results suggest that modulatory effects known from normal sensory processing affect the response to cortical microstimulation as well. The network response to microstimulation is highly amenable to the behavioral state and must be considered for future approaches to imprint sensory signals into cortical circuits with neuroprostheses.

Keywords: intracortical electrical stimulation, behavioral modification, head-restraint rat, barrel cortex, sensory cortical prosthesis

OPEN ACCESS

Edited by:
Ken-Ichiro Tsutsui, Tohoku University, Japan

Reviewed by:
Joshua C. Brumberg, Queens College (CUNY), United States
Alison L. Barth, Carnegie Mellon University, United States

****Correspondence:***
Cornelius Schwarz
cornelius.schwarz@uni-tuebingen.de

Specialty section:
This article was submitted to Pathological Conditions, a section of the journal Frontiers in Behavioral Neuroscience

Received: *29 October 2021*
Accepted: *09 February 2022*
Published: *22 March 2022*

Citation:
Butovas S and Schwarz C (2022) Local Neuronal Responses to Intracortical Microstimulation in Rats' Barrel Cortex Are Dependent on Behavioral Context. Front. Behav. Neurosci. 16:805178. doi: 10.3389/fnbeh.2022.805178

INTRODUCTION

The whisker-related tactile sense in rodents is an exquisite example of active sensing and perception. Rats typically acquire tactile information about their environment by actively sweeping their array of whiskers across the object of interest (i.e., active touch). Sometimes, however, they make contact with a moving object when the whiskers are at rest (i.e., passive touch). These two modes of tactile processing are characterized by different modulation of signal representation in the barrel cortex (whisker representation of the primary somatosensory cortex in rodents) (Fanselow and Nicolelis, 1999; Crochet and Petersen, 2006; Ferezou et al., 2006; Hentschke et al., 2006; Lee et al., 2008; Chakrabarti and Schwarz, 2018). The phenomenon has been observed in several animal species and humans and is often called "sensory gating"

(Chapman et al., 1987, 1988; Gertz et al., 2017). The cardinal response of barrel cortex neurons to a transient whisker deflection is an action potential or two followed by a strong inhibitory period (Simons, 1978; Stüttgen and Schwarz, 2008). The abovementioned studies of sensory gating in the whisker system have uniquely shown that both phases of the sensory response in the barrel cortex are suppressed when the whiskers are actively moved ("gating"). Sensory gating is independent of the activity that may be evoked in the whisker follicle during whisking (Leiser and Moxon, 2007; Khatri et al., 2009) and persists after interruption of the infraorbital nerve (Hentschke et al., 2006; Poulet and Petersen, 2008). It is further presented on the tactile pathway as early as the trigeminal nuclei, holding its first synaptic station. Sensory gating has been shown to be selective for ascending channels, being prominent in the lemniscal pathway, while absent in the extralemniscal pathway (Chakrabarti and Schwarz, 2018 for review of pathways see Feldmeyer et al., 2013). The same study has shown that corticofugal projections play a critical role for sensory gating on subcortical stations of the tactile pathway. A lesion of primary somatosensory cortex and surrounding parietal cortical areas abolishes sensory gating.

In future cortical neuroprostheses, microstimulation is intended to substitute for ascending sensory signals. The question, therefore, arises whether and how the activity imprinted directly into the neocortex is affected by context-dependent changes. In this study, we used sensory gating as a model case to manipulate the behavioral context and concomitant neuronal activity of the cortical origin to study how the short latency, local cortical effects of intracortical microstimulation are modified. To this end, we used head-fixed rats that were operantly conditioned to move a whisker in a goal-oriented way. We found that the short-latency parts of the local response, including the first excitatory volley of spikes, corresponding to a short-latency negative deflection of the local field potential (LFP), is stable across context, while the parts of the response with longer latency, characterized by strong firing rate suppression, is amenable to modulation by active touch.

MATERIALS AND METHODS

Surgical Procedures and Behavioral Training

Three male Long Evans rats (12–14 weeks old, bodyweight 350–450 g) were used in this study. All experimental and surgical procedures were performed in accordance with the guidelines of animal use of the Society for Neuroscience and German Law (approval of Regierungspräsidium Tübingen). All the animals were accustomed to the experimenter and behavioral setup for at least 2 weeks before surgery. Surgery was performed to implant electrode arrays and the post for head fixation. Anesthesia was initialized with ketamine/xylazine (100 mg/kg/15 mg/kg i.p.) and was continued with isoflurane. Isoflurane concentration (1–2.5%) was adjusted to keep the painful hind paw reflex below the threshold. The animal's body temperature was held at 37°C by a feedback-controlled heating pad (Fine Science Tools, Heidelberg, Germany). The rat was mounted on a stereotaxic apparatus, and craniotomy over the barrel cortex was performed (coordinates P2–3/L4.5–5.5). A set of stainless-steel microscrews (Morris Co., Southbridge, MA, USA, part number 0x1/8 flat) were placed in the skull. The electrode array with vertically movable electrodes (refer to the Section Results) was implanted into the barrel column of whisker C1 (determined by mapping out the surface of the cortex by deflecting the whisker with a handheld cotton swab and recording spike and LFP responses *via* a single microelectrode) and embedded together with the skull screws into light-curing dental cement (Flowline, Heraeus Kulzer, Hanau, Germany). The wound was cleaned and disinfected with hydrogen peroxide at the end of the surgery. The open skin was sutured and carefully attached to the implant. In one animal, the infraorbital nerves on both sides of the head were cut as done before (Hentschke et al., 2006). To this end, the skin was shaved in the region of the face below the eyes. The skin was incised, and the nerve which is hidden below the musculature was prepared. The nerve was isolated from the underlying tissue and cut in its entirety after two sutures had been noosed around it. The nerve stumps were sutured in place leaving a gap of minimally 1 mm to prevent regeneration. The skin in the face was disinfected and sutured carefully. After the surgery, animals were kept warm and treated with analgesics (2 injections caprophen, 5 mg/kg, s.c.), they were allowed to recover for 14 days.

Rat housing, handling, accommodation to head fixation, and water control were performed as described before (Schwarz et al., 2010). Training sessions were scheduled two times a day for 5 days a week followed by 2 days of free access to water. All behavioral experiments were conducted inside a dark experimental box clad with sound-absorbing foam. The animals were monitored using infrared cameras. The behavioral training consisted of two phases. At first, the subjects were conditioned to respond to intracortical electrical stimulation by emitting a lick within an interval of 0.5 s after stimulus presentation to obtain a drop of water as a reward. Initially, the animals received a train of stimuli consisting of 15 pulses (at 320 Hz) at a suprathreshold intensity of 3.2–4.8 nC (Butovas and Schwarz, 2007). Interstimulus intervals were randomly varied from 3.25 to 6.25 s (mean 5 s, flat probability distribution). As soon as the animals responded well to the high-intensity stimuli, the number of pulses was reduced, guided by their performance until the animals were able to respond reliably to single pulses. To discourage premature responses, a 1 s interval before stimulus presentation was introduced, in which, a lick would delay the stimulus presentation by a new randomly drawn interstimulus interval.

Before the second phase of behavioral training, whiskers on both sides were cut to a length of 2 cm. Before each session, a polyimide tubing (250 μm in diameter, 3 cm length, and 0.7 mg weight) was slipped onto whisker C1. The movement of the whisker at ∼2.5 cm distance from the face was monitored using laser illumination from above, and the detection of the whisker's shadow on a linear CCD (**Figure 1A**) located below the whisker (Bermejo et al., 1998) was carried out. The rostro-caudal component of whisker movements was tracked at a temporal resolution of 2.5 kHz and a spatial resolution of 0.4 μm

(Metralight Inc., San Mateo, CA, USA). The rats were trained on a motor task that consisted in moving the C1 vibrissa in the rostro-caudal direction to find a virtual object (VO). The VO was computer-simulated at a resolution of 1 kHz and could be made to move on any arbitrary trajectory in the rostro-caudal direction. Online comparison of the real trajectory of the whisker and virtual trajectory of the VO yielded virtual contacts (VC, i.e., crossing of the two trajectories), leading to a water reward. The whisker movement was exclusively in the air without any "real" contact with objects. Thus, from the view point of the animal, a VC and water reward happened at varying times and positions, and its probability would be greatly increased by active whisker movements. To shape the rats' behavior, we started with a stationary VO—first positioned just rostral to the resting point of the whisker. With an increasing success rate of the rat to generate VCs, the stationary VO was gradually moved in the rostral direction. At this stage, the rat had to move the whisker forward from the resting point to generate a VC. Once VCs were regularly generated, the VO was set in motion and moved on a trajectory of low-pass-filtered Gaussian noise (limiting frequency 10 Hz) and maximal amplitude of ∼3 cm (just reaching the resting point of the whisker). At this stage, therefore, "passive" VCs, with a stationary whisker positioned at the resting point was possible. VCs of the whisker with the VO triggered an immediate barrel cortex microstimulation, given the last lick and the last VC both occurred more than 1 s ago.

When rats regularly achieved VCs, they were moved to the data acquisition stage, in which all data presented here were sampled. During the data acquisition stage, we exclusively used a moving VO and single-pulse bipolar stimulation (i.e., negative first) at an intensity of 4.8 nC. The whisker trace, the VO, and the behavioral data (i.e., timestamps of stimuli, licks, VCs, and rewards) were computed, controlled, and recorded by a custom-made software running on a LabView Real Time System (National Instruments, Texas, USA).

Microstimulation and Electrophysiology

Mobile microelectrode arrays were custom-made (Haiss et al., 2010). Shortly, nine pulled glass-coated platinum tungsten electrodes (i.e., 80 μm shank diameter, 25 μm diameter of the metal core, free tip length of 10 μm, and impedance > 1 MΩ; Thomas Recording, Giessen, Germany) were placed inside a 3 $\times$ 3 array of polyimide tubing with a distance of 300 μm (HV Technologies, Trenton, GA, USA). The electrodes were soldered to Teflon-insulated silver wires (Science Products, Hofheim, Germany), which, in turn, were connected to a microplug (Bürklin, Munich, Germany). The electrodes were attached to a rider that moved along the thread of a screw and, thus, allowed moving them into the cortex. The electrode array was inserted over barrel C1 of posteromedial barrel subfield, initially at the depth of 250 μm below the pia mater. All recordings presented in this study were carried out at a depth of 1,200 μm, roughly corresponding to layer 5. In all three rats, we assured that tactile responses in LFP (and if available spike responses) to rapid whisker deflections of whisker C1 were present throughout the array. Histological verification of stimulation sites was not performed. Electrical stimulation pulses were generated using a programmable stimulator (model number: STG 2008; MultiChannelSystems, Reutlingen, Germany). For microstimulation, a low-impedance electrode on one of the corners of the quadratic array was selected and used throughout training and experimental sessions. Simultaneous LFP signal recordings were performed using a multichannel extracellular amplifier (MultiChannelSystems, Reutlingen, Germany; gain 5,000, sampling rate 20 kHz).

Whisker "Virtual Contact" Classification and Data Analysis

All analyses were performed using custom-written MATLAB (Mathworks Inc., Natick, MA, USA) scripts. A VC was defined as the crossing point of whisker and VO trace as performed earlier (Gerdjikov et al., 2013). Each VC was classified into the "active" (A) or "passive" (P) class depending on the precontact whisker trace. A detailed description of the analysis is presented elsewhere. In brief, we first differentiated the whisker movement trajectory to calculate a velocity trace. The first criterion was the instantaneous velocity. It had to exceed a threshold derived from the bimodal distribution of whisker velocities 5 ms preceding contact (refer to **Figure 1C**, Hentschke et al., 2006). The peak of whisker velocities around zero mirrors the spurious whisker movements at rest for each individual (denoted in green in **Figure 1C**). We fitted a Gaussian to the peak around zero and defined the velocities defining the double of its half-peak width as criteria, which when surpassed in positive or negative direction would indicate an active VC. Before classifying a VC as passive, a second criterion had to be matched: root mean square of whisker velocity during 75 ms before the contact had to be below 0.03 m/s (Hentschke et al., 2006).

The excitatory cortical response was imposed as a negative peak with a very stable latency of 2 ms after the stimulation (**Figure 2A**). To measure its amplitude, the negative peak was cut out from the LFP trace and substituted by linear interpolation. The difference between the maximum negative-peak amplitude and the corresponding value of the interpolation line was then taken as the measure of the peak amplitude (as shown in the inset in **Figure 2A**). Since the excitatory peak amplitudes varied considerably from animal to animal, the measurements were normalized to mean amplitude as observed after passive VC in each animal. The amplitude of the positive evoked LFP wave was simply its maximum peak value (**Figure 2A**).

Statistical inference was performed using a bootstrap procedure (1,000 resamples) that output 95% confidence intervals (CI95) of the distributions to be compared. For the comparison of LFP distributions along poststimulus time, we calculated the effect size of the two distributions as given by the area under the ROC curve (AUC). The AUC measures the probability of an ideal observer confronted with a random pick from the two response distributions to correctly classify it. AUC is 0.5 if the two distributions are identical and 1, if the two distributions are perfectly discriminable (Green and Swets, 1966). CI95 of the AUC readings were calculated by bootstrapping LFP amplitude distributions (1,000 resamples). All data are presented as mean [lower CI95, upper CI95], if not indicated otherwise.

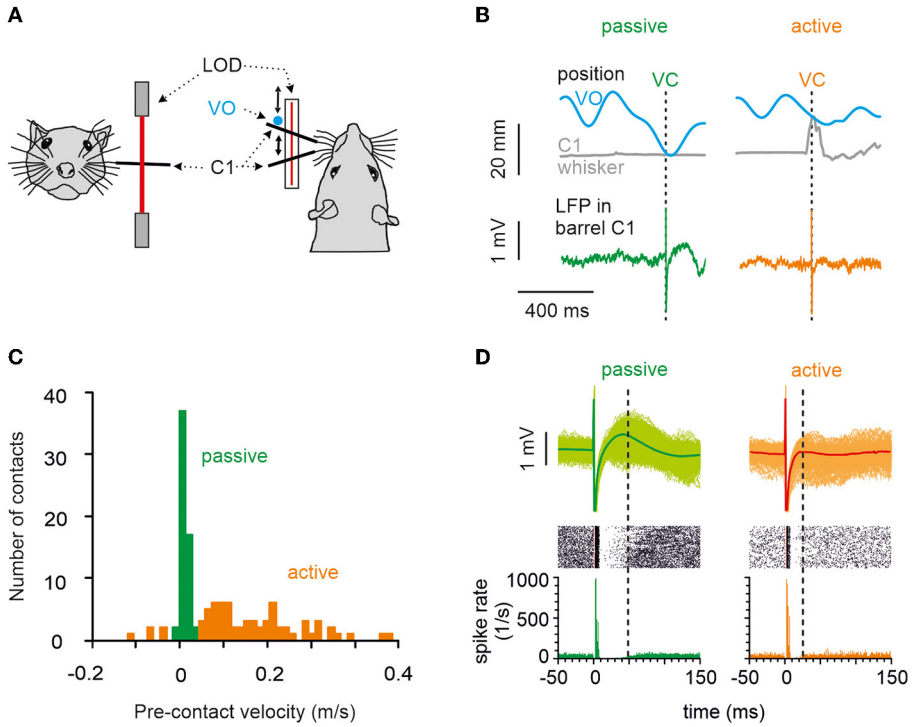

FIGURE 1 | Behavior, the principal measurements, and classification of touches into active vs. passive. **(A)** A head-fixed rat's whisker C1 was equipped with a light polyimide tube and tracked in real-time using a laser optical device. The movement of a virtual object (VO) was modeled in a computer and compared in real-time to the whisker position. **(B)** When measured whisker trajectory and modeled VO movement trajectory crossed, a VC occurred (realized as microstimulation in barrel column C1). Two VCs (arrows), one passive (left) and one active (right), are shown. Gray: the trajectory of whisker C1. Blue: the trajectory of the VO. Bottom: examples of LFP responses in barrel cortex with passive (green) and active (orange) VO contacts. **(C)** Histogram of whisker mean velocity distribution, measured within the 10 ms interval preceding the VCs obtained from an example session. Precontact velocities, classified as passive and active, are marked in green and orange, respectively. **(D)** Circumstantial observation of spikes (obtained in one animal in one session) allows a glimpse of how features in LFP signals relate to those in cortical spikes rates. Bottom: Spike density of spike responses to passive (green) and active (orange) contacts. Note that the inhibitory period was longer and more pronounced after passive contacts, while excitation remained unaffected (marked by the vertical broken line on the right of each plot). Center: Raster display. Top: Overlay of cutouts of the LFP responses to passive (green traces) and active (orange traces) contacts recorded from the same electrode as the spikes shown below. The thick trace is the average evoked LFP. The slow positive deflection amplitude reflects the strength and duration of the inhibitory response as seen in the spike density. Time of virtual contact is at time 0.

RESULTS

We trained head-fixed rats to move their whiskers to find a nonstationary, computer-simulated VO. The rostro-caudal whisker movement was tracked and compared with the location of the VO. A crossing of the two trajectories was called a VC, which was immediately followed by the delivery of a drop of water and a microstimulation pulse in the rat's barrel cortex, given the rat did not lick at the spout in a time interval 1 s before the VC (**Figure 1A**). The result was that the rat whisked voluntarily in free air at its own pace and got stimulated—unpredictably for the rat—at different whisker positions and velocities that covered the entire kinematic range including rest. A VC was identified as "active," if whisker movement preceded the contact and "passive" if the whisker was at rest. **Figure 1B** shows single trials, and **Figure 1C** shows an example session of passive and active contacts (refer to the Section Materials and methods for details). The quantitative analysis in this report is based on LFP recordings. Occasionally, however, we were able to record multiunit spike data along with the LFPs from the same electrodes. To show the correspondence of LFP recordings to spike recordings, **Figure 1D** plots an example session (n = 687 passive, n = 176 active trials) with LFP traces, raster plot, and peristimulus-time histograms (PSTHs). Spike responses in our awake rats showed the stereotypical cortical spike response pattern to electrical stimulus composed of a short excitatory peak followed by a long-lasting inhibition of tens of millisecond duration (as shown before under ketamine anesthesia: Butovas and Schwarz, 2003; Butovas et al., 2006). The corresponding LFP pattern was a short-latency negative LFP wave (not well seen in the average LFP of **Figure 1D**, refer to next paragraph and **Figure 2**) and a long-lasting LFP wave of positive polarity. Comparison of active vs. passive VCs (left vs. right side in **Figure 1D**) clearly shows a shortening of the spike suppression in the active case, which was reflected in the near-abolishment of the positive LFP wave (the right vertical broken line in each plot points to the end of the suppression period where spiking resumes again).

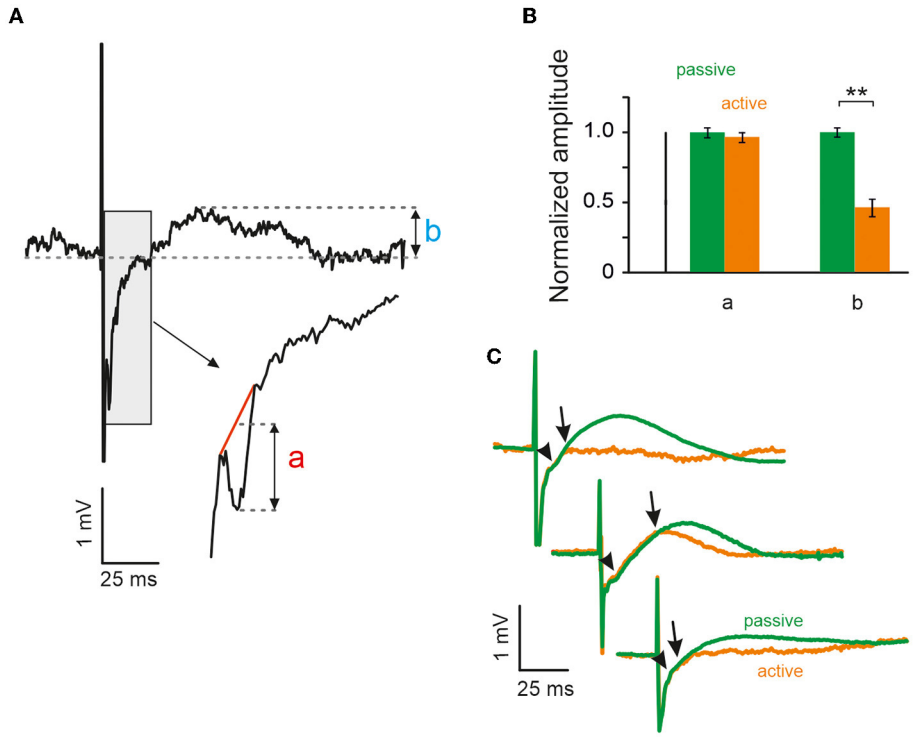

FIGURE 2 | Whisking reduces evoked local field potential (LFP) activity during the inhibitory period but not during the excitatory period. **(A)** Example of LFP response, which demonstrates sharp negative deflection (a) followed by long positive wave (b), presumably corresponding to electrically evoked excitation and inhibition respectively (cf. **Figure 1D**). **(B)** Peak amplitudes of excitatory LFP response (a) to both active and passive contacts yielded no difference, unlike amplitude of the inhibitory period (b), which had higher maximum amplitude during passive contacts in all three animals (**significant using Mann-Whitney *U*-test, error bars CI95, see text). **(C)** Mean LFP responses to both passive (green) and active (orange) contacts in all three animals (the infraorbital nerve was cut in the animal shown on top).

To assess the negative LFP deflection in quantitative detail, **Figure 2A** shows a single trace at higher temporal resolution. Typically, the negative peak was located on the part of the voltage trace that was on its upward rise after the strong negativity imposed by the stimulus artifact (gray box). The gray box is shown again at a shorter time scale and demonstrates how the amplitude (a) of the negative peak was quantified. Negative peak amplitudes (a) during active and passive VCs were very similar and, in fact, did not differ significantly. In contrast, the amplitude of the slow positive deflection (b) was markedly and significantly different between the two conditions. Population data ($n = 3$ rats) from the three recording electrodes neighboring the stimulation electrode are shown in **Figure 2B**. All data shown in this panel were normalized and rendered unitless by dividing each measured amplitude by the average amplitude observed in the passive condition (carried out separately for measures a and b). For the short-delay negative peak, (a) we analyzed $n = 820$ passive VCs (amplitude of 1 [0.038, 0.03]), and $n = 289$ active VCs (amplitude of 0.965 [0.037 0.036]). Testing the two means did not reveal a significant difference (Mann-Whitney *U*-test, $p > 0.05$). For the long-delay positive peak, (b) we analyzed $n = 846$ passive VCs (amplitude of 1 [0.034 0.034]) and $n = 354$ active VCs (amplitudes of 0.46 [0.067 0.060]). This difference turned out to be highly significant (Mann-Whitney *U*-test, $p < 0.01$). **Figure 2C** shows the mean evoked LFPs for active vs. passive cases separately for the three animals. The short-latency negative deflection appears as a kink in the average evoked LFP trace (arrow heads). Also, note that average-evoked LFP traces observed in active vs. passive cases overlap for a few milliseconds following stimulation (end of overlap is pointed to by arrows).

The analysis presented up to here seems to indicate that the different parts of the response, short-latency excitatory vs. long-lasting inhibition, display different susceptibilities for the movement-dependent modulation. This is distinct from experiments performed with more naturalistic whisker touch with an object, where the short-latency neuronal activation volley conveyed *via* the ascending tactile pathway is already susceptible to modulation, and the modulatory signal is related to whisker movement setting some tens of milliseconds before the touch (Hentschke et al., 2006; Chakrabarti and Schwarz, 2018). As electrical stimulation may drive network activity into saturation, modulation may not be possible shortly after electrical activation. We investigated this possibility by calculating the time course of the discriminability of evoked LFP responses in active vs. passive cases across time. Discriminability was quantified as the effect size AUC (same data as in **Figure 2C**). The result for the three animals is depicted in **Figure 3A** (1,000 resamples for each time point after stimulation; time resolution 1 ms). In all three animals, the AUC trace was around 0.5 at the time

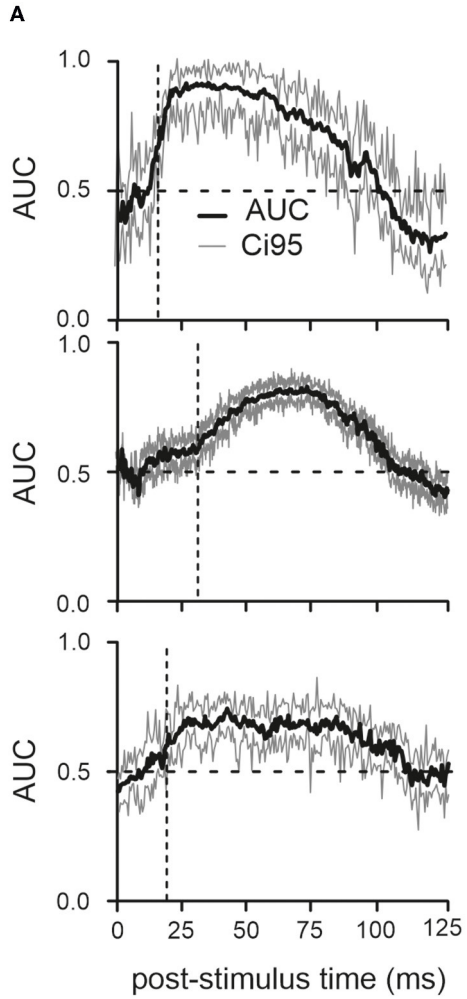

FIGURE 3 | Poststimulus period of nondiscriminability. **(A)** Corresponding mean and CI95 (1,000 bootstraps) of AUC traces computed from the LFP responses in the three animals (the one with the cut infraorbital nerve is shown on top). **(B)** Dwell time of lower confidence border below 0.5 (the time from stimulation time to the first occurrence of lower CI > 0.5 is plotted here). Results from recordings from eight electrodes across all three animals are shown. The stimulation electrode ("stim") is marked black.

of stimulation. The time point when active and passive traces became discriminable was defined as the time the lower bound of the CI settles above 0.5 at 16, 32, and 18 ms (i.e., vertical broken lines) to give rise to the positive LFP wave (i.e., in the passive case). Although these periods of insensitivity to modulation were different in the three animals, they always included the short-latency negative LFP deflection, consistent with our analysis shown in **Figure 2B**. We reasoned that if the phenomenon of discriminability is due to network saturation, then the effect should be dependent on the distance of the recording site to the stimulation site. In this case, we would expect that the period of nondiscriminability would be shorter farther away from the stimulation site. This was the case, as shown by the decrement of the time point, the CI first rose above 0.5 with distance from the stimulation electrode (**Figure 3B**).

DISCUSSION

In this study, we presented evidence that the local effects of cortical microstimulation are readily modulated by the behavioral state of the animal. There was, however, a clear difference to the modulation as seen with sensory stimulation in previous studies. Immediately after the stimulation including the period of the excitatory burst of spikes (or the short-latency negative peak in the LFP respectively), no modulation by the behavioral state could be observed. Only after a couple of ms, the difference in LFP evoked during active vs. passive cases was manifested. This period of nondiscriminability is best explained by saturation of neuronal circuits as it was decreased with the distance of the recording electrode from the stimulation site and, thus, the amplitude of the evoked LFP response.

Modulation Dynamics of Stimulation-Evoked Activity

Modulation of the electrically evoked signal, different from sensory signals originating from whisker deflections, only occurs sometime after the first volley of evoked spikes: A period of tens of milliseconds after microstimulation was devoid of signs of gating. Only thereafter, response features were affected. This is consistent with the previous finding that neuronal oscillations, arriving at much longer latencies after stimulation, are suppressed as well (Venkatraman and Carmena, 2009). A possible reason for these dynamics is a saturation of axons and synapses close to the stimulation site. However, before discussing this scenario, we first wish to mention an alternative possibility, namely, that modulation dynamics arise from latencies in neuronal loops. If modulation does not originate from the barrel cortex but happens at a remote site, to which barrel cortex is reciprocally connected, the evoked signals may first be conveyed to the site of modulation and then travel back in a modulated form to the barrel cortex. The latency of such a neuronal loop may then be the basis of the modulation dynamics as observed here. We think this mechanism is rather unlikely mainly because it has been shown that motor signals (or movement-related signals) are present in basically all ascending

tactile neuronal structures (Ferezou et al., 2006; Hentschke et al., 2006; Lee et al., 2008; Chakrabarti and Schwarz, 2018). Therefore, the principal mechanistic elements to do sensory gating (i.e., convergent presence of motor or movement-related signals and sensory signals) are present throughout the ascending pathway. On the level of the trigeminal nuclei, the earliest central tactile structure, such movement-related signals stem mainly from the parietal cortex. Once these connections are inactivated, sensory gating is impaired (Chakrabarti and Schwarz, 2018). In ventero-posterior-medial thalamus (VPM), gating is absent if sensory signals are electrically evoked from the lemniscal tract (the direct inputs to VPM) (Lee et al., 2008). Together, these experimental observations strongly suggest that the origin of gating signals is located on the cortical level. One obvious source of movement-related signals is the whisker-related motor cortex (Hill et al., 2011; Gerdjikov et al., 2013), which, in terms of axonal projections, is tightly interconnected with the barrel cortex (Mao et al., 2011). In sensory gating (i.e., active touch), movement-related signals are known to arrive long before any active touch event. That is why sensory gating in the whisker and arm-related tactile systems in rodents and monkeys have been observed to be immediate (relative to the sensory input). That is, even the earliest component of the ascending tactile signal was modulated (Chapman et al., 1988; Hentschke et al., 2006). One of our rats was subjected to the cutting of infraorbital nerves to confirm that we dealt here with the same central gating signals as reported earlier.

In the earlier text, we have discussed the "gating signal" typically arriving together with the movement (i.e., likely consisting of either a motor command or a motor-related signal). Using ICMS in this study, we observed that the gating signal is inactivated shortly after the stimulation. At this point, it is important to differentiate and clarify possible roles of motor structures (e.g., primary motor cortex) beyond gating. Independent of the generation of gating signals, the stimulation-evoked long-latency inhibition (i.e., positive LFP wave) could also be caused by the motor cortex. The motor cortex is known to be intricately interconnected with the barrel cortex, and it has been shown that motor cortex-evoked inhibition of barrel cortex circuitry is possible *via* direct and indirect connections (Kinnischtzke et al., 2014; Audette et al., 2018; Sermet et al., 2019). However, an important observation is that slow inhibition is also observed after electrical stimulation in *in vitro* preparations. The exact origin of the positive LFP wave (or corresponding spike suppression) is therefore not clear. Motor structures are likely to contribute, but local network components alone already give rise to the basic phenomenon (refer to the detailed discussion of this issue in Butovas and Schwarz, 2003, and Butovas et al., 2006).

This finding of modulation kicking in only tens of milliseconds after barrel cortex stimulation thus strongly contrasts the properties of gating found with peripheral sensory signals. Importantly, the absence and presence of modulation is a function of poststimulus time rather than of polarity of the LFP. The time series of AUC values clearly show that the nondiscriminability of LFP signals extends beyond the negative peak well into the positive phase. To understand the phenomenon, it seems important to consider that the fast-excitatory response after peripheral sensory stimulation is generated by the ascending activity in the tactile pathway, while the one of similar appearance observed with microstimulation is due to the little understood mechanism by which neurons are activated using extracellular current in the cortical tissue (Butovas and Schwarz, 2003). It is very likely that neurons in the vicinity of the electrode are activated by direct (i.e., antidromic) as well as indirect (i.e., orthodromic) trans-synaptic mechanisms. Two-photon calcium imaging of spike-related calcium transients revealed that directly activated neurons are distributed sparsely, and the group of activated neurons changes dramatically when the tip of the stimulation electrode moves a small distance of some tens of micrometers (Histed et al., 2009). This result pointed to a few axons around the electrode tip that are initially activated supporting a long-held notion from chronaxie measurements that it is axonal structures and not somas that are the immediate targets of microstimulation (Ranck, 1975; Tehovnik, 1996; Nowak and Bullier, 1998a,b). As axonal membranes are unlikely to be influenced by top-down signals, the predominant role of axons in direct activation by microstimulation may partly explain our observation that immediately after the stimulation, the response is unaffected by top-down responses.

However, direct activation only accounts for a very short period, presumably not exceeding a millisecond after the stimulation pulse. The rest of the neuronal (and behavioral) response is likely based on trans-synaptic conveyance of the activity. Postsynaptic potentials in the vicinity of cortical microstimulation have been measured to arrive at latencies up to 2 ms in the motor cortex of halothane-anesthetized cats (Asanuma and Rosen, 1973), and similar latencies were measured from evoked spikes in the somatosensory cortex of ketamine anesthetized rats (Butovas and Schwarz, 2003). In the latter study, the peak of the spike density was very narrow (<2 ms), and around 90% of neurons responded to the stimulation in an area of 900 μm around the stimulation site, indicating the presence of a massive and highly synchronous volley of trans-synaptic excitation.

The short-latency negative peak observed in LFP measurements in this study corresponds in latency and duration very well to the trans-synaptic excitatory activation of local neurons. In view of the high temporal precision of the evoked spikes it, most likely, corresponds to a population spike, as supported by occasional spike recordings (cf. **Figure 1D**). The massive nature of the trans-synaptic response renders it likely that the absence of modulation a few milliseconds after the microstimulation reflects a transient saturation of the neurons' responses. Strong evidence in favor of this idea has been obtained by repetitive intracortical microstimulation. The excitatory spike response evoked by repetitive stimulus pulses is not diminished compared with that of single-pulse stimulation, despite the presence of massive inhibitory activity in the repetitive case, arguing strongly for a saturation phenomenon at the time of the short-latency excitatory peak (Butovas and Schwarz, 2003, their Figure 11). In this study, using LFP signals, we found that the period of nonmodulation persists beyond the excitatory response and that it is dependent on distance and, thus response

intensity, from the stimulation site. It is therefore likely that the presumed saturation process involves the initial parts of inhibitory action following the first wave of excitation as well (Butovas and Schwarz, 2003; Butovas et al., 2006; Logothetis et al., 2010).

Implications for the Development of Cortical Neuroprostheses

Behavior-dependent modulation of cortical responses as demonstrated here certainly has to be considered when applying cortical microstimulation for cortical neuroprostheses. If context matters, its neuronal reflections have to be assessed before precise stimulation can be achieved. However, monitoring all possibly relevant signals in the brain is unattainable. In a recent study, we have provided proof of principle that using the local LFP as an estimate of the relevant context may be feasible (Brugger et al., 2011). This study has shown that local LFP in a 20 ms prestimulation interval contains enough information to adapt the stimulus in real-time, such that response variability across trials could be reduced as compared with "blind" stimulation with constant intensity. These previous results together with the present ones point to context-dependent microstimulation as a promising novel way to imprint sensory signals into cortical networks. An important next step is to demonstrate the perceptual effects of context-dependent modulations and demonstrate that context-sensitive dynamic brain stimulation improves it.

DATA AVAILABILITY STATEMENT

The datasets presented in this article are not readily available because they consist in multichannel systems files, and custom Matlab files. Requests to access the datasets should be directed to cornelius.schwarz@uni-tuebingen.de.

ETHICS STATEMENT

The animal study was reviewed and approved by Regierungspräsidium Tübingen.

AUTHOR CONTRIBUTIONS

SB and CS conceived the project and designed experiments, did the analysis, and wrote the article. SB performed the experiments. Both authors contributed to the article and approved the submitted version.

FUNDING

This work was supported by DFG SCH577/9-1 and SCH577/16-1.

ACKNOWLEDGMENTS

We thank Uschi Pascht for their excellent technical assistance.

REFERENCES

Asanuma, H., and Rosen, I. (1973). Spread of mono- and polysynaptic connections within cat's motor cortex. *Exp. Brain Res.* 16, 507–520. doi: 10.1007/BF00234477

Audette, N. J., Urban-Ciecko, J., Matsushita, M., and Barth, A. L. (2018). POm thalamocortical input drives layer-specific microcircuits in somatosensory cortex. *Cereb. Cortex.* 28, 1312–1328. doi: 10.1093/cercor/bhx044

Bermejo, R., Houben, D., and Zeigler, H. P. (1998). Optoelectronic monitoring of individual whisker movements in rats. *J. Neurosci. Methods.* 83, 89–96. doi: 10.1016/S0165-0270(98)00050-8

Brugger, D., Butovas, S., Bogdan, M., and Schwarz, C. (2011). Real-time adaptive microstimulation increases reliability of electrically evoked cortical potentials. *IEEE Trans. Biomed. Eng.* 58, 1483–1491. doi: 10.1109/TBME.2011.2107512

Butovas, S., Hormuzdi, S. G., Monyer, H., and Schwarz, C. (2006). Effects of electrically coupled inhibitory networks on local neuronal responses to intracortical microstimulation. *J Neurophysiol.* 96, 1227–1236. doi: 10.1152/jn.01170.2005

Butovas, S., and Schwarz, C. (2003). Spatiotemporal effects of microstimulation in rat neocortex: A parametric study using multielectrode recordings. *J. Neurophysiol.* 90, 3024–3039. doi: 10.1152/jn.00245.2003

Butovas, S., and Schwarz, C. (2007). Detection psychophysics of intracortical microstimulation in rat primary somatosensory cortex. *Eur. J. Neurosci.* 25, 2161–2169. doi: 10.1111/j.1460-9568.2007.05449.x

Chakrabarti, S., and Schwarz, C. (2018). Cortical modulation of sensory flow during active touch in the rat whisker system. *Nat. Commun.* 9, 3907. doi: 10.1038/s41467-018-06200-6

Chapman, C. E., Bushnell, M. C., Miron, D., Duncan, G. H., and Lund, J. P. (1987). Sensory perception during movement in man. *Exp. Brain Res.* 68, 516–524. doi: 10.1007/BF00249795

Chapman, C. E., Jiang, W., and Lamarre, Y. (1988). Modulation of lemniscal input during conditioned are movements in the monkey. *Exp. Brain Res.* 72, 316–334. doi: 10.1007/BF00250254

Crochet, S., and Petersen, C. C. (2006). Correlating whisker behavior with membrane potential in barrel cortex of awake mice. *Nat Neurosci* 9, 608–610. doi: 10.1038/nn1690

Fanselow, E. E., and Nicolelis, M. A. (1999). Behavioral modulation of tactile responses in the rat somatosensory system. *J. Neurosci.* 19, 7603–7616. doi: 10.1523/JNEUROSCI.19-17-07603.1999

Feldmeyer, D., Brecht, M., Helmchen, F., Petersen, C. C. H., Poulet, J. F. A., Staiger, J. F., et al. (2013). Barrel cortex function. *Prog. Neurobiol.* 103, 3–27. doi: 10.1016/j.pneurobio.2012.11.002

Ferezou, I., Bolea, S., and Petersen, C. C. (2006). Visualizing the cortical representation of whisker touch: voltage-sensitive dye imaging in freely moving mice. *Neuron.* 50, 617–629. doi: 10.1016/j.neuron.2006.03.043

Gerdjikov, T. V., Haiss, F., Rodriguez-Sierra, O. E., and Schwarz, C. (2013). Rhythmic whisking area (RW) in rat primary motor cortex: an internal monitor of movement-related signals? *J. Neurosci.* 33, 14193–14204. doi: 10.1523/JNEUROSCI.0337-1.2013

Gertz, H., Voudouris, D., and Fiehler, K. (2017). Reach-relevant somatosensory signals modulate tactile suppression. *J. Neurophysiol.* 117, 2262–2268. doi: 10.1152/jn.00052.2017

Green, D. M., and Swets, J. A. (1966). *Signal detection theory and psychophysics*. New York: Wiley.

Haiss, F., Butovas, S., and Schwarz, C. (2010). A miniaturized chronic microelectrode drive for awake behaving head restrained mice and rats. *J. Neurosci. Methods.* 187, 67–72. doi: 10.1016/j.jneumeth.2009.12.015

Hentschke, H., Haiss, F., and Schwarz, C. (2006). Central signals rapidly switch tactile processing in rat barrel cortex during whisker movements. *Cereb. Cortex.* 16, 1142–1156. doi: 10.1093/cercor/bhj056

Hill, D. N., Curtis, J. C., Moore, J. D., and Kleinfeld, D. (2011). Primary motor cortex reports efferent control of vibrissa motion on multiple timescales. *Neuron.* 72, 344–356. doi: 10.1016/j.neuron.2011.09.020

Histed, M. H., Bonin, V., and Reid, R. C. (2009). Direct activation of sparse, distributed populations of cortical neurons by electrical microstimulation. *Neuron.* 63, 508–522. doi: 10.1016/j.neuron.2009.07.016

Khatri, V., Bermejo, R., Brumberg, J. C., Keller, A., and Zeigler, H. P. (2009). Whisking in air: encoding of kinematics by trigeminal ganglion neurons in awake rats. *J. Neurophysiol.* 101, 1836–1846. doi: 10.1152/jn.90655.2008

Kinnischtzke, A. K., Simons, D. J., and Fanselow, E. E. (2014). Motor cortex broadly engages excitatory and inhibitory neurons in somatosensory barrel cortex. *Cereb. Cortex.* 24, 2237–2248. doi: 10.1093/cercor/bht085

Lee, S., Carvell, G. E., and Simons, D. J. (2008). Motor modulation of afferent somatosensory circuits. *Nat. Neurosci.* 11, 1430–1438. doi: 10.1038/nn.2227

Leiser, S. C., and Moxon, K. A. (2007). Responses of trigeminal ganglion neurons during natural whisking behaviors in the awake rat. *Neuron.* 53, 117–133. doi: 10.1016/j.neuron.2006.10.036

Logothetis, N. K., Augath, M., Murayama, Y., Rauch, A., Sultan, F., Goense, J., et al. (2010). The effects of electrical microstimulation on cortical signal propagation. *Nat. Neurosci.* 13, 1283–1291. doi: 10.1038/nn.2631

Mao, T., Kusefoglu, D., Hooks, B. M., Huber, D., Petreanu, L., and Svoboda, K. (2011). Long-range neuronal circuits underlying the interaction between sensory and motor cortex. *Neuron.* 72, 111–123. doi: 10.1016/j.neuron.2011.07.029

Nowak, L. G., and Bullier, J. (1998a). Axons, but not cell bodies, are activated by electrical stimulation in cortical gray matter. I. Evidence from chronaxie measurements. *Exp. Brain Res.* 118, 477–488. doi: 10.1007/s002210050304

Nowak, L. G., and Bullier, J. (1998b). Axons, but not cell bodies, are activated by electrical stimulation in cortical gray matter. II. evidence from selective inactivation of cell bodies and axon initial segments. *Exp. Brain Res.* 118, 489–500. doi: 10.1007/s002210050305

Poulet, J. F., and Petersen, C. C. (2008). Internal brain state regulates membrane potential synchrony in barrel cortex of behaving mice. *Nature.* 454, 881–885. doi: 10.1038/nature07150

Ranck, J. B. (1975). Which elements are excited in electrical stimulation of mammalian central nervous system: a review. *Brain Res.* 98, 417–440. doi: 10.1016/0006-8993(75)90364-9

Schwarz, C., Hentschke, H., Butovas, S., Haiss, F., Stüttgen, M. C., Gerdjikov, T., et al. (2010). The head-fixed behaving rat - procedures and pitfalls. *Somatosens. Mot. Res.* 27, 131–148. doi: 10.3109/08990220.2010.513111

Sermet, B. S., Truschow, P., Feyerabend, M., Mayrhofer, J. M., Oram, T. B., Yizhar, O., et al. (2019). Pathway-, layer-and cell-type-specific thalamic input to mouse barrel cortex. *Elife.* 8, 1–28. doi: 10.7554/eLife.52665

Simons, D. J. (1978). Response properties of vibrissa units in rat S1 somatosensory neocortex. *J. Neurophysiol.* 41, 798–820. doi: 10.1152/jn.1978.41.3.798

Stüttgen, M. C., and Schwarz, C. (2008). Psychophysical and neurometric detection performance under stimulus uncertainty. *Nat. Neurosci.* 11, 1091–1099. doi: 10.1038/nn.2162

Tehovnik, E. J. (1996). Electrical stimulation of neural tissue to evoke behavioral responses. *J. Neurosci. Methods.* 65, 1–17. doi: 10.1016/0165-0270(95)00131-X

Venkatraman, S., and Carmena, J. M. (2009). Behavioral modulation of stimulus-evoked oscillations in barrel cortex of alert rats. *Front. Integr. Neurosci.* 3, 10. doi: 10.3389/neuro.07.010.2009

Conflict of Interest: The authors declare that the research was conducted in the absence of any commercial or financial relationships that could be construed as a potential conflict of interest.

Publisher's Note: All claims expressed in this article are solely those of the authors and do not necessarily represent those of their affiliated organizations, or those of the publisher, the editors and the reviewers. Any product that may be evaluated in this article, or claim that may be made by its manufacturer, is not guaranteed or endorsed by the publisher.

frontiers | Frontiers in Behavioral Neuroscience

ORIGINAL RESEARCH
published: 04 April 2022
doi: 10.3389/fnbeh.2022.811419

Transcutaneous Auricular Vagus Nerve Stimulation Promotes White Matter Repair and Improves Dysphagia Symptoms in Cerebral Ischemia Model Rats

*Lu Long[1], Qianwen Zang[1], Gongwei Jia[1], Meng Fan[2], Liping Zhang[1], Yingqiang Qi[3], Yilin Liu[1], Lehua Yu[1] and Sanrong Wang[1]**

[1]Department of Rehabilitation Medicine, The Second Affiliated Hospital of Chongqing Medical University, Chongqing, China, [2]Department of Traditional Chinese Medicine, Weinan Central Hospital, Weinan, China, [3]Center of Electron Microscope, Institute of Life Science of Chongqing Medical University, Chongqing, China

Background: Clinical and animal studies have shown that transcutaneous auricular vagus nerve stimulation (ta-VNS) exerts neuroprotection following cerebral ischemia. Studies have revealed that white matter damage after ischemia is related to swallowing defects, and the degree of white matter damage is related to the severity of dysphagia. However, the effect of ta-VNS on dysphagia symptoms and white matter damage in dysphagic animals after an ischemic stroke has not been investigated.

Methods: Middle cerebral artery occlusion (MCAO) rats were randomly divided into the sham, control and vagus nerve stimulation (VNS) group, which subsequently received ta-VNS for 3 weeks. The swallowing reflex was measured once weekly by electromyography (EMG). White matter remyelination, volume, angiogenesis and the inflammatory response in the white matter were assessed by electron microscopy, immunohistochemistry, stereology, enzyme-linked immunosorbent assay (ELISA) and Western blotting.

Results: ta-VNS significantly increased the number of swallows within 20 s and reduced the onset latency to the first swallow. ta-VNS significantly improved remyelination but did not alleviate white matter shrinkage after MCAO. Stereology revealed that ta-VNS significantly increased the density of capillaries and increased vascular endothelial growth factor (VEGF) and basic fibroblast growth factor (FGF2) expression in the white matter. ta-VNS significantly alleviated the increase inTLR4, MyD88, phosphorylated MAPK, and NF-κB protein levels and suppressed the expression of the proinflammatory factors IL-1β and TNF-α.

Conclusion: These results indicated ta-VNS slightly improved dysphagia symptoms after ischemic stroke, possibly by increasing remyelination, inducing angiogenesis, and inhibiting the inflammatory response in the white matter of cerebral ischaemia model rats, implying that ta-VNS may be an effective therapeutic strategy for the treatment of dysphagia after ischemic stroke.

Keywords: ta-VNS, white matter, dysphagia after stroke, angiogenesis, inflammation

OPEN ACCESS

Edited by:
Ken-Ichiro Tsutsui, Tohoku University, Japan

Reviewed by:
Mustapha Muzaimi, Universiti Sains Malaysia, Malaysia
He Liu, Zhejiang University School of Medicine & Huzhou Central Hospital, China

****Correspondence:***
Sanrong Wang
303953@hospital.cqmu.edu.cn

Specialty section:
This article was submitted to Pathological Conditions, a section of the journal Frontiers in Behavioral Neuroscience

Received: *08 November 2021*
Accepted: *02 March 2022*
Published: *04 April 2022*

Citation:
Long L, Zang Q, Jia G, Fan M, Zhang L, Qi Y, Liu Y, Yu L and Wang S (2022) Transcutaneous Auricular Vagus Nerve Stimulation Promotes White Matter Repair and Improves Dysphagia Symptoms in Cerebral Ischemia Model Rats. Front. Behav. Neurosci. 16:811419. doi: 10.3389/fnbeh.2022.811419

INTRODUCTION

Ischemic stroke, a very common health problem worldwide, leads to a decline in quality of life and is associated with a high mortality rate (Khoshnam et al., 2017). Dysphagia is a common morbidity of stroke, as approximately 78% of people with acute stroke have varying degrees of dysphagia (Martino et al., 2005). In addition, the occurrence of dysphagia after stroke results in various complications, such as aspiration pneumonia, malnutrition, dehydration, and even mortality, indicating that identifying effective treatments for dysphagia is critical (Cohen et al., 2016). Terré (2020) indicated that early detection and effective management of dysphagia in patients with acute stroke reduces not only the incidence of these complications but also the length of hospital stay and overall healthcare expenditures.

The white matter comprises nearly half of the volume of the brain and plays a key role in development, ageing, and many neurologic and psychiatric disorders. Thousands of myelinated fibers in the white matter allow the transfer of information, which links all brain regions into functional ensembles (Filley, 2005; Filley and Fields, 2016). Experimental evidence has demonstrated that white matter areas, including the pyramidal tract, internal capsule, corona radiata, superior longitudinal fasciculus, external capsule, and corpus callosum, are commonly implicated in swallowing control (Alvar et al., 2021). Moreover, cerebral ischaemia usually results in damage to white matter regions, especially the corpus callosum and the optic tract (Li et al., 2014a). Rodents subjected to cerebral hypoperfusion showed disintegration of the white matter tracts, as indicated by neuroinflammation, loss of oligodendrocytes, attenuation of myelin density, and structural derangement at the nodes of Ranvier (Choi et al., 2016). Patients with white matter focal vascular lesions of the white matter tend to exhibit neurobehavioral syndromes such as conduction aphasia, pure alexia, and ideomotor apraxia (Catani et al., 2012). Therefore, it is very important to investigate the white matter changes that occur in rats with dysphagia symptoms after ischemic stroke.

Once ischaemia is caused by obstruction of cerebral blood flow, angiogenesis is activated immediately in response to the loss of blood supply (Kanazawa et al., 2019). Angiogenesis, which is closely associated with factors such as vascular endothelial growth factor (VEGF), angiopoietin (Ang), and basic fibroblast growth factor (FGF2), provides not only a sufficient supply of oxygen and nutrients but also a good environment for neurons regeneration after brain injury (Sun et al., 2003; Petcu et al., 2010; Zhang et al., 2020). In recent years, with the emphasis on the neurovascular unit (NVU; which includes neurons, capillaries, astrocytes, supporting cells, and extracellular matrix), a large amount of evidence has indicated a complex link between angiogenesis and ischemic stroke (Goldman and Chen, 2011; Zhao et al., 2018). Therefore, enhancing angiogenesis may be an effective therapeutic strategy for protecting against demyelination injury and improving swallowing function after ischemic stroke.

An inflammatory response is activated in brain tissue after central nervous system injury and aggravates brain tissue injury following ischemic stroke (Cao et al., 2014). Toll-like receptor (TLR) 4, a key member of the TLR family, plays a pivotal role in the initiation of the innate immune response. TLR4 binds and interacts with downstream mitogen-activated protein kinases (MAPKs) and nuclear transcription factor-kappa B (NF-kB) to regulate inflammation by promoting the expression of interleukin (IL)-1β, IL-6, tumor necrosis factor-α (TNF-α), and other proinflammatory cytokines (Lee et al., 1999; Kyriakis and Avruch, 2001). A previous study reported that specifically inhibiting MAPK with SB203580 can reduce the increase in TNF-α, IL-1β and IL-6 expression in the hippocampus induced by mitotic factor-induced inflammation (Chaparro-Huerta et al., 2005). Studies have shown that neuroinflammation plays a key role in the pathophysiology of white matter injury in animal models of chronic cerebral hypoperfusion. Acute inflammation induced by cerebral ischaemia exacerbates tissue damage by increasing the production and release of inflammatory cytokines (Deng et al., 2014; Theus et al., 2017). Therefore, resolving inflammation is critical for protecting against brain injury after ischemic hypoperfusion.

Vagus nerve stimulation (VNS) was clinically approved by the European Commission and the US Food and Drug Administration (FDA) for the treatment of drug-resistant epilepsy and depression (Nemeroff et al., 2006; Panebianco et al., 2015). Transcutaneous auricular vagus nerve stimulation (ta-VNS) has been proven to be a novel and effective neuroprotective treatment strategy for cerebral ischaemia. A large number of studies have demonstrated that ta-VNS can reduce the infarct volume, induce angiogenesis, and improve neurological functions in a rat model of middle cerebral artery occlusion (MCAO; Jiang et al., 2016; Ma et al., 2016; Redgrave et al., 2018; Li et al., 2020b; Dawson et al., 2021). More importantly, the vagus nerve is responsible for afferent and efferent nerve signals and is closely related to swallowing movement. A systematic review reported that stimulation of the vagus nerve in cavum concha results in the activation of the nucleus tractus solitarii (NTS) and the locus coeruleus (LC; Ay et al., 2015). As the main target of VNS, the NTS, with its surrounding reticular structure and nucleus suspicion (NA), which is located in the ventral medulla oblongata, constitute the "central pattern generator" of the swallowing reflex (Broussard and Altschuler, 2000). However, the effect of ta-VNS on dysphagia symptoms after an ischemic stroke is unclear, and the exact underlying mechanisms are still undefined if ta-VNS may improve dysphagia symptoms. Therefore, in the present study, an MCAO rat model and electromyography (EMG) were used to investigate the effect of ta-VNS on dysphagia symptoms after ischemic stroke. Then, remyelination, angiogenesis, and the inflammatory response in the white matter were investigated by electron microscopy, immunohistochemistry, stereological methods, enzyme-linked immunosorbent assay (ELISA) and Western blotting. We found that ta-VNS treatment for 3 weeks improved dysphagia symptoms, increased remyelination and angiogenesis and inhibited the inflammatory response in the white matter after ischaemia.

MATERIAL AND METHODS

Animals and Experimental Design

All animal procedures were approved by the Institutional Ethics Committee of Chongqing Medical University and performed strictly in accordance with the Guidelines for the Care and Use of Laboratory Animals. The experimental design is shown in **Figure 1A**. Six-week-old male Sprague–Dawley rats (200–230 g), which correspond to a weight range (6–8 weeks) frequently used for dysphagia studies on ischemic stroke, were used in the present study (Sugiyama et al., 2014; Cullins and Connor, 2019). The rats were obtained from the Experimental Animal Center of Chongqing Medical University and housed in a quiet room maintained at 21–22°C (60% humidity on a 12 h light/12 h dark cycle) and provided free access to food and water throughout the experiment. Sixty-five rats were randomly divided into three groups, i.e., the sham group ($n = 15$), control group ($n = 25$), and VNS group ($n = 25$), which received ta-VNS treatment. Changes in the swallowing reflex were measured every week (day 7 for week 1; day 14 for week 2 and day 21 for week 3). ta-VNS treatment was not given on the day of measuring the swallowing reflex, and tissues of the rats were processed after 3 weeks of ta-VNS treatment.

Induction of Dysphagia by MCAO

We used a rat model of transient MCAO, which exhibit some symptoms of human dysphagia following an ischemic stroke in cerebral areas (Sugiyama et al., 2014). The MCAO procedure was the same as that reported previously (Belayev et al., 1996). Briefly, food intake was limited 12 h before the surgery, and the rats were anesthetized with phenobarbital sodium (40 mg/kg, intraperitoneal injection). The left common carotid artery (CCA), external carotid artery (ECA), and internal carotid artery (ICA) were carefully sequentially exposed so that the vagus and superior laryngeal nerves were kept intact. The proximal end of the ECA and CCA was ligated, and a slip knot was reserved near the bifurcation of the ICA and ECA to fix the nylon thread bolt. Nylon thread (0.32 mm; Cinontech, A5, China) was introduced into the left CCA through a small incision and gently advanced through the ICA until the black mark reached the bifurcation of the ICA and ECA. After 90 min of ischaemia, the thread was removed, and the incision was closed with sutures. Body temperature was maintained at approximately 37°C with an electrothermal pad during the experimental process. The sham rats underwent the same surgical procedures as the MCAO rats except for ligation of the CCA and ECA and introduction of the thread. Zea-Longa scores were used to evaluate the neurological deficits of the rats 24 h after MCAO, and rats with a score of 2–3 were considered successful models and were included in the follow-up experiment (Longa et al., 1989).

ta-VNS Treatment

For ta-VNS treatment, the rats were anesthetized with 2% isoflurane, and two oppositely charged magnetic electrodes were placed inside and outside each ear over the auricular concha region. Transcutaneous electrical stimulation at a frequency of 20 Hz and an intensity of 2 mA square pulses (pulse width, 0.5 ms) was applied for a single stimulation of 30 min *via* an electrical stimulator (HANS-100, Nanjing, China). The

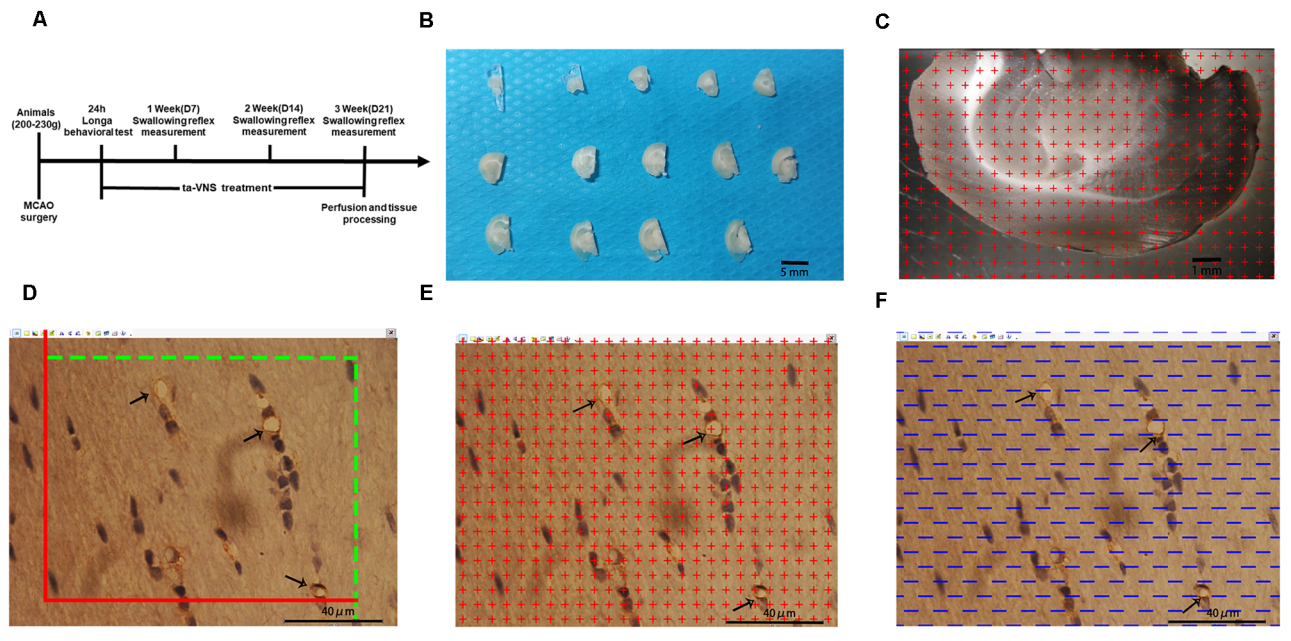

FIGURE 1 | Illustrations of the methods used to quantify the white matter volume and the density of capillaries in the white matter. **(A)** Diagram of the whole experiment. **(B)** One-millimetre-thick coronal sections of the left hemisphere of rats; scale bar = 5 mm. **(C)** Illustration of the stereological counting methods used for estimating the volume of the white matter; scale bar = 1 mm. **(D–F)** Illustration of the stereological methods used for quantifying capillaries in the white matter, scale bar = 40 μm.

stimulation parameters were already proven to effectively activate the vagus nerve by previous studies (Li et al., 2014b; Li S. et al., 2020). The ta-VNS procedure was administered daily at the same time between 9 a.m. and 12 a.m. to weaken the influence of biological rhythm. The animals received ta-VNS treatment daily for 3 weeks except on the days that the swallow reflex was tested. The rats in the control group and the sham group underwent the same procedure, but the stimulator was not turned on for electrical stimulation (Jiang et al., 2016).

Measurement of the Swallowing Reflex

Rats were anesthetized with phenobarbital sodium (40 mg/kg, intraperitoneal injection) and then fixed in the supine position on a heated pad to maintain the body temperature at 37°C. A 0.5 mm catheter was inserted through the mouth, with its tip placed in the pharynx. The other end of the catheter was connected to a microsyringe pump (RWD, KDS LEGATO 130, China). Distilled water (DW) was automatically infused *via* the microsyringe pump at a flow rate of 2.0 μl/s for 20 s. The infusion was repeated three times at intervals of 3 min. Meanwhile, a midline incision was made on the ventral surface of the neck, and a pair of needle electrodes made of enamel nichrome wire was inserted into the swallowing muscles to record EMG activity. The swallowing reflex elicited by infusions of DW was assessed by EMG activity, and the number of swallows during infusion and the onset latency to the first swallow were analyzed. The number of swallows within 20 s was defined as the swallowing frequency. The onset latency to the first swallow was defined as the time required to elicit the first swallow from the onset of DW infusion. For rats in the sham group, the number of swallows and onset latency to the first swallow were measured only once throughout the whole experiment (Kajii et al., 2002).

Perfusion and Tissue Processing

After measurement of the swallowing reflex in the 3rd week, the animals were deeply anesthetized by intraperitoneal injection of 60 mg/kg pentobarbital sodium. Then, five rats from each experimental group were randomly selected and perfused with saline followed by 4% paraformaldehyde. The cerebrum was removed from the brain and divided into two hemispheres along the sagittal suture, and the tissue was postfixed for at least 24 h after perfusion. The left hemispheres were embedded in a brain mould filled with 6% agar and cut into consecutive 1-mm-thick coronal slabs (**Figure 1B**). An average of 10–12 slabs were cut from the left cerebral hemispheres of each rat. Ten slabs containing white matter from the left cerebral hemisphere of each rat were randomly selected and imaged under a dissecting microscope at low magnification with a 10× objective. Then, tissue blocks approximately 1 mm^3 in size were cut from five slabs randomly selected from each rat where the plastic sheet touched the white matter. The randomly selected blocks of white matter were subsequently placed in 10%, 20%, and 30% sucrose solutions for 1 day each. After dehydration for 3 days, the embedded samples were subjected to the isector method (CM1860, Leica) to obtain isotropic and uniform random (IUR) slices (Tang et al., 2009; Qi et al., 2020). One 4-μm-thick slice was cut from each block along the direction parallel to the IUR surface to generate sections hereafter referred to as IUR sections. The isector method ensures that capillaries of the white matter in each direction of the three-dimensional space have the same probability of being sampled.

Immunohistochemical Staining

Briefly, frozen IUR slices were washed three times for 5 min each time in PBS (0.01 M, pH 7.4) after being warmed at room temperature. Then, the slices were immersed in acetone at 4°C for 10 min and washed three times in 0.01 M PBS. Then, the sections were incubated with 0.01 mol/L citrate buffer (pH 6.0) for 10 min at 99°C for antigen retrieval. Next, endogenous peroxidase activity in the slices was blocked with 3% hydrogen peroxide for 20 min at 37°C. After being washed three times in 0.01 M PBS for 5 min, the slices were incubated with a serum mixture (10% normal goat serum and 5% fetal bovine serum in 0.01 M PBS) for 40 min at 37°C to block nonspecific staining. Then, the slices were incubated with a mouse monoclonal anti-CD31 primary antibody (ab64543; Abcam, Cambridge, UK) diluted 1:400 in PBS at 4°C for 24 h. The slices were washed three times in PBS for 10 min each and were incubated with biotinylated goat anti-mouse immunoglobulin G secondary antibody in PBS for 2 h at 37°C. After being washed three times in PBS for 15 min each, the slices were then transferred to diaminobenzidine (DAB) solution (ZLL-9032; ZSGB, China) as a chromogen for approximately 3 min. After extensive washes with water, the cell nuclei in the slices were counterstained with Mayor's hematoxylin (AR005; Boster Biological Engineering Co. Ltd., Wuhan, China) for 2 min. The slices were dehydrated in gradient alcohol solutions, cleared with xylene and then mounted with neutral gum.

Stereological Analysis

Sampling and Image Acquisition

The slice boundary was delineated under a 4× objective lens and observed under a 100× oil lens using stereology equipment. The system randomly selected equidistant white matter areas. A total of 25 fields of view were selected from each slice, and a total of approximately 400–500 fields of view were selected for each animal. All marked blood vessels with a diameter of ≤10 μm according to a ruler were defined as capillaries (Chen et al., 2016).

Volume of the White Matter of the Left Hemisphere

Ten randomly selected slabs containing brain white matter from the left cerebral hemisphere of each rat were imaged under a dissecting microscope at a magnification of 10×. Then, equidistant points of light were randomly projected on every captured photograph, and the number of test points that hit the white matter was counted (**Figure 1C**). The total white matter volume was calculated according to Cavalieri's principle as follows:

$Vwm = t \times a(p) \times \Sigma P(wm)$ [Vwm represents the total volume of the white matter in the left hemisphere, a(p) is the area corresponding to each measurement point (0.59 mm^2), t is the sample thickness (1 mm), and ΣP(wm) is the total number of test points hitting the white matter].

Length Density and the Total Length of Capillaries in the White Matter of the Left Hemisphere

An unbiased counting frame was randomly superimposed on every captured photograph of the 4-μm-thick slices. According to the forbidden line method, the number of cross-sections containing blood vessels with a diameter ≤10 μm (Q (cap)) was counted (**Figure 1D**). Capillary profiles inside the counting frame or touching the top line and the right line (inclusion lines) were included in the counts, and capillary profiles touching the left line, the bottom line, and the extensions of the right line and the left line (exclusion lines) were excluded from the counts. The length density of the capillaries in the white matter and the total length of the capillaries were calculated with the following stereological formulas (Qi et al., 2020):

$$\mathrm{Lv\ (cap/wm)} = \Sigma \mathrm{Q(cap)} / \Sigma \mathrm{A}$$
$$\mathrm{L\ (cap/wm)} = \mathrm{Lv\ (cap/wm)} \times \mathrm{Vwm}$$

[ΣQ (cap) denotes the total number of capillary profiles in the white matter, and ΣA (0.0159 mm^2) is the total area of the counting frame used for each rat].

Volume Density and the Total Volume of Capillaries in the White Matter of the Left Hemisphere

Equidistant points of light were randomly projected on every captured photograph of the 4-μm-thick slices. The number of test points that hit the capillaries was counted (**Figure 1E**). The volume density of the capillaries and the total volume of capillaries in the white matter were calculated with the following stereological formulas:

$$\mathrm{Vv\ (cap/wm)} = \Sigma \mathrm{P(cap)} / \Sigma \mathrm{P(wm)}$$
$$\mathrm{V\ (cap/wm)} = \mathrm{Vv\ (cap/wm)} \times \mathrm{Vwm}$$

[Vv (cap/wm) is the volume density of the capillary in the white matter, ΣP (cap) is the total number of points in the capillary section, and ΣP (wm) is the total number of points in the whole field of view].

Surface Area Density and the Total Surface Area of Capillaries in the White Matter of the Left Hemisphere

Test lines were randomly placed on each photograph (**Figure 1F**). The number of intersecting points between the test lines and the capillary luminal surface were counted. The surface area density of the capillaries and the total surface area of capillaries in the white matter were calculated with the following stereological formulas:

$$\mathrm{Sv\ (cap/wm)} = \Sigma \mathrm{PI\ (cap)} / \Sigma \mathrm{L}$$
$$\mathrm{S\ (cap/wm)} = \mathrm{Sv\ (cap/wm)} \times \mathrm{Vwm}$$

[ΣPI (cap) is the number of intersecting points between the test lines and the capillary luminal surface, and ΣL is the total length of all the test lines in each field of view].

Electron Microscopy

For electron microscopy, three rats from each experimental group were randomly selected and perfused with 4% paraformaldehyde mixed with 2.5% glutaraldehyde in 0.1 M PBS. Then, the corpus callosum tissues were collected and post fixed in 4% glutaraldehyde solution for further processing. The left corpus callosum tissues were cut into 100-μm-thick slices and stained with Reynold's lead citrate and uranyl acetate. Images were obtained at a magnification of 20,000× under a transmission microscope (TEM; Hitachi-7500, Hitachi, Ltd., Tokyo, Japan).

ELISA

White matter tissue in the left cerebral hemisphere was rapidly removed from rats in the three groups, and a nine-fold volume of homogenate medium (0.9% normal saline) was added. Mechanical homogenization was carried out in an ice water bath to prepare 10% homogenates. The expression levels of IL-1β, TNFα, VEGF, and FGF2 were measured using rat ELISA kits (MULTI Science, China) according to the manufacturer's protocols.

Western Blotting

White matter tissue in the left cerebral hemisphere was collected from rats in the three groups, and protein was extracted using RIPA lysis buffer containing 1% PMSF, a phosphatase inhibitor (Beyotime Biotechnology, China). After the protein concentration was determined using a BCA kit (Beyotime Biotechnology, China), sodium dodecyl sulphate–polyacrylamide gel electrophoresis and Western blotting were carried out to measure the protein levels of TLR4, MyD88, MAPK, NF-κB, phosphorylated MAPK, and phosphorylated NF-κB.

Statistical Analyses

All statistical analyses were performed with SPSS (version 23, IBM Corp., Armonk, NY, USA). The general condition of each rat (body weight and 24-h food/water intake), the onset latency to the first swallow and the number of swallows within 20 s were statistically analyzed using repeated measures analysis of variance (ANOVA) followed by the least significant difference (LSD) test. Electron microscopy data, quantitative stereological data, Western blot data, and ELISA data were analyzed by one-way ANOVA followed by the least LSD test. $p < 0.05$ was considered significant for all tests.

RESULTS

A Rat Model of MCAO With Dysphagia Was Established, and ta-VNS Improved Dysphagia Symptoms

To determine whether MCAO can affect swallowing behavior in rats, we measured growth, the onset latency to the first swallow and the number of swallows within 20 s. Before the experiment, there were no significant differences in body weight between the three groups. However, the bodyweight of the three groups of rats decreased sharply within 3 days after MCAO. From the 3rd day,

the body weight gain of the VNS group was higher than that of the control group, and the body weights of the control group and VNS group were significantly lower than the body weights of the sham group (**Figure 2A**, $p < 0.05$). In addition, 24-h food intake, which was measured every 3 days, was lower in the VNS group and the control group than that in the sham group, but the 24-h food intake of the VNS group was higher than that of the control group (**Figure 2B**, $p < 0.05$). Furthermore, 24-h water intake, which was measured every 3 days after MCAO, was higher in the VNS group than in the control group (**Figure 2C**, $p < 0.05$).

EMG showed that infusion of DW elicited a swallowing reflex, and **Figure 2D** shows representative EMG activity recorded from the swallowing muscles during swallowing elicited by DW infusion each week after MCAO. In the 1st week, there was no significant difference in the onset latency to the first swallow or the number of swallows within 20 s elicited by infusion of DW between the three groups (**Figures 2D,E**, $p > 0.05$). The latency to the first swallow was significantly prolonged and the number of swallows was significantly decreased in the VNS group and the control group compared with the sham group in the 2nd week, but there was no significant difference between the VNS and the control group (**Figures 2D,E**, $p > 0.05$). These results seem to indicate that MCAO rats showed impairment of swallowing function and some symptoms of swallowing disorders observed in humans. In the third week, the onset latency to the first swallow was still significantly prolonged and the number of swallows was significantly decreased in the VNS group and the control group compared with the sham group. The number of swallows was significantly increased and the onset latency to the first swallow was significantly shortened in the VNS group compared to the control group (**Figures 2D,E**, $p < 0.05$).

ta-VNS Induced Remyelination but Did Not Alleviate White Matter Shrinkage Induced by MCAO

In the present study, stereology was used to accurately estimate the white matter volume in the three groups of rats. **Figure 3A** shows representative photographs containing white matter under a dissecting microscope at low magnification with a 10× objective. The white matter volume in the left hemisphere was 27.47 ± 1.40, 22.72 ± 0.86, and 22.99 ± 0.57 (mm^3) in the sham group, the control group and the VNS group, respectively. The white matter volume in the left hemisphere in the control group and the VNS group was significantly smaller than that in the sham group (**Figure 3C**, $p < 0.05$), which indicated that the white matter of the brain shrank in the rats subjected to MCAO. There was no significant difference in the white matter volume in the left hemisphere between the VNS group and the control group after 3 weeks of stimulation (**Figure 3C**, $p > 0.05$).

Figure 3B shows representative photographs containing myelin sheathes in the corpus callosum at a magnification of 20,000× under a transmission microscope. In contrast, transmission electron microscopy of the left corpus callosum showed that the myelin sheaths were significantly thinner in the VNS group and the control group compared with the sham group, and demyelination changes were the greatest in the control group (**Figure 3D**, $p < 0.01$). However, the myelin sheaths in the VNS group were significantly thicker than those in the control group (**Figure 3D**, $p < 0.01$). Although there was no significant difference in white matter volume, the present results demonstrated that MCAO resulted in white matter demyelination and that ta-VNS treatment significantly induced remyelination in the white matter.

ta-VNS Protected Against White Matter Damage by Inducing Angiogenesis

There was a significant difference in angiogenesis in the injured white matter. Immunohistochemical staining of capillaries in the left white matter of the three groups of rats is shown in **Figure 4A**. The length density of the capillaries in the white matter of the left hemisphere was significantly higher in the VNS group (0.053 ± 0.002; m/mm^3) and the control group (0.045 ± 0.003; m/mm^3) than in the sham group (0.03 ± 0.017; m/mm^3; **Figure 4B**, $p < 0.01$). The length density of capillaries in the VNS group was higher than that in the control group (**Figure 4B**, $p < 0.05$). Similarly, the total length of the capillaries in the white matter in the VNS group (1.262 ± 0.667; m) and the control group (1.009 ± 0.686; m) was significantly longer than that in the sham group (0.797 ± 0.039; m; **Figure 4F**, $p < 0.05$), and the total length of capillaries in the VNS group was longer than that in the control group (**Figure 4F**, $p < 0.05$). The volume density of capillaries in the white matter in the VNS group (1.59 ± 0.10; mm^3/mm^3) and the control group (1.40 ± 0.11; mm^3/mm^3) was significantly higher than that in the sham group (1.00 ± 0.04; mm^3/mm^3; **Figure 4C**, $p < 0.01$), but there was no significant difference in volume density between the VNS group and the control group (**Figure 4C**, $p > 0.05$). The total volume of capillaries in the white matter of the left hemisphere in the VNS group (38.00 ± 2.10; mm^3) was significantly larger than that in the control group (31.81 ± 2.58; mm^3) and the sham group (27.25 ± 0.20; mm^3; **Figure 4G**, $p < 0.05$). There was no significant difference in the total volume of the capillaries between the control group and the sham group (**Figure 4G**, $p > 0.05$). The surface area density of capillaries in the white matter of the left hemisphere in the VNS group (3.85 ± 0.02; mm^2/mm^3) and the control group (3.13 ± 0.31; mm^2/mm^3) was significantly higher than that in the sham group (2.21 ± 0.20; mm^2/mm^3; **Figure 4D**, $p < 0.05$). There was no significant difference in the surface area density of capillaries between the VNS group and the control group (**Figure 4D**, $p > 0.05$). The total surface area was significantly increased in the VNS group (92.23 ± 5.67; mm^2) compared with the control group (70.71 ± 6.74; mm^2; **Figure 4H**, $p < 0.01$), but there was no significant difference in total surface area between the control group and the sham group (58.58 ± 2.44 mm^2; **Figure 4H**, $p > 0.05$).

Moreover, ELISA revealed no statistically significant differences in VEGF levels in the white matter of the left hemisphere between the VNS group and the sham group ($p > 0.05$) but a significantly higher concentration of VEGF in the VNS group than in the control group (**Figure 4E**, $p < 0.05$). FGF2 levels in the white matter of the left hemisphere were significantly increased both in the VNS group and the control group after 3 weeks of ta-VNS stimulation ($p < 0.05$). Compared

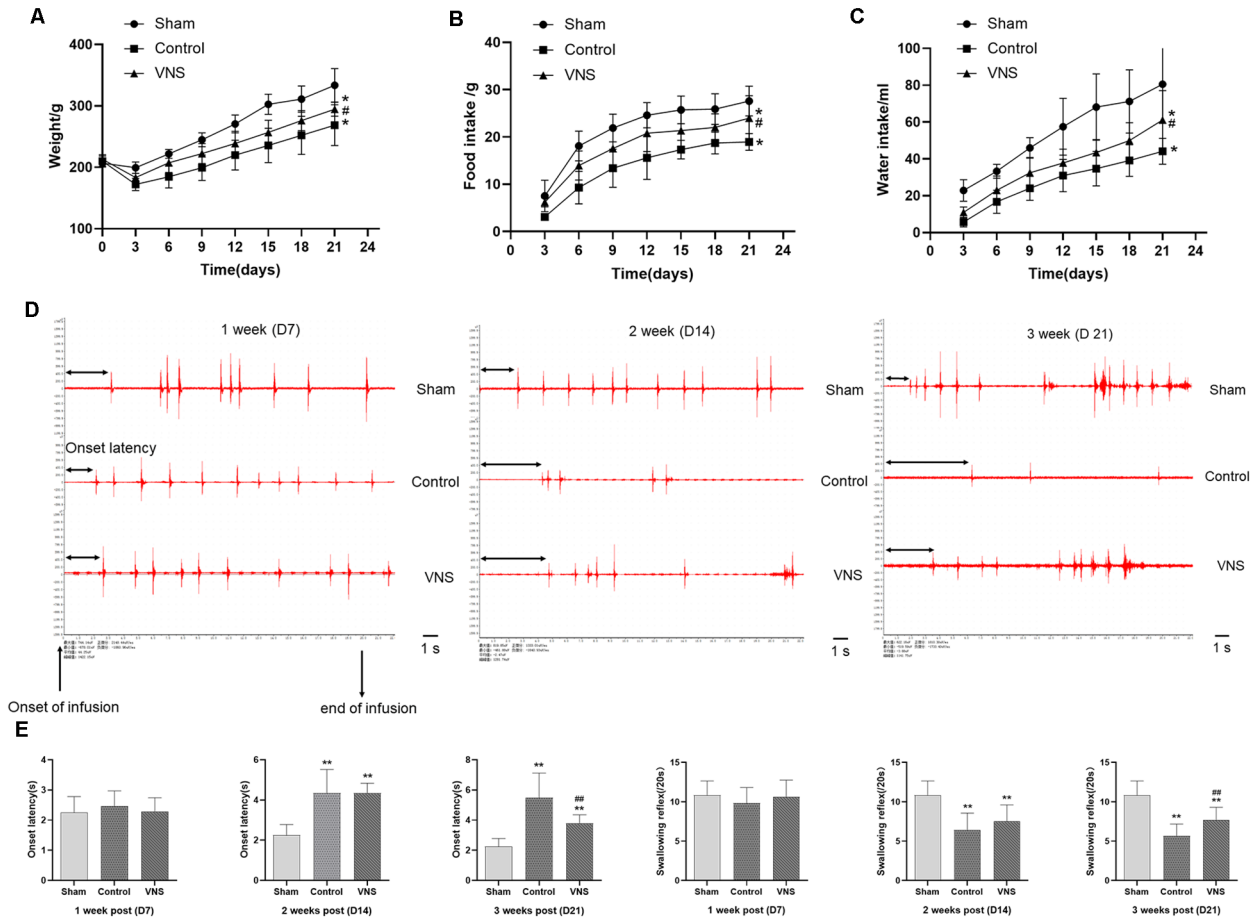

FIGURE 2 | The effects of ta-VNS on dysphagia symptoms in MCAO rats. **(A–C)** Changes in the body weight and food or water intake of each group rats (mean ± SD, $n = 10$). **(D)** Representative EMG activity recorded from the swallowing muscles during swallowing elicited by infusions of DW in each group at different weeks after MCAO; scale bar = 1 s. **(E)** Changes in the onset latency to the first swallow and the number of swallows within 20 s in each group (mean ± SD, $n = 10$); $^{*}p < 0.05$, $^{**}p < 0.01$, the VNS group or the control group compared with the sham group; $^{\#}p < 0.05$, $^{\#\#}p < 0.01$, the VNS group compared with the control group.

with those in the control group, the FGF2 levels in the VNS group were significantly higher (**Figure 4I**, $p > 0.05$).

In summary, the present results indicate that ischemic damage induces a certain degree of angiogenesis and that ta-VNS treatment significantly promotes angiogenesis in the white matter.

ta-VNS Alleviated the Increase in the Expression of Inflammatory Mediators and Inhibited TLR4/NF-κB Signaling and MAPK/NF-κB Signaling in the White Matter

In the present study, we investigated the levels of TNF-α and IL-1β in the injured white matter to determine the effect of ta-VNS. Statistical analysis revealed significant group effects on the white matter levels of these two inflammatory mediators after 3 weeks of ta-VNS treatment. We found that rats in the VNS group and the control group showed significantly increased white matter levels of IL-1β and TNF-α compared with the sham group rats. The concentrations of these inflammatory mediators in the white matter of the left hemisphere were significantly lower in the VNS group than in the control group (**Figures 5B,C**, $p < 0.05$). These results indicate that the increase in the expression of proinflammatory markers induced by MCAO was significantly decreased by ta-VNS treatment.

According to previous studies, TLR4/NF-κB signaling and MAPK/NF-κB signaling are important for the production of proinflammatory mediators (Chaparro-Huerta et al., 2005; Theus et al., 2017). Western blotting was used to measure the expression of TLR4, MyD88, MAPK, phosphorylated MAPK, NF-κB, and phosphorylated NF-κB in the white matter of the left hemisphere. The expression levels of TLR4 and MyD88 were significantly increased in rats both in the ta-VNS group and the control group compared with the sham group rats (**Figures 5A,D,E**, $p < 0.05$). The TLR4 intensity and MyD88 intensity in the VNS group were significantly lower than those in the control group (**Figures 5A,D,E**, $p < 0.05$). Similarly, the phosphorylation levels of MAPK and NF-κB were increased in the white matter of rats in the VNS group and

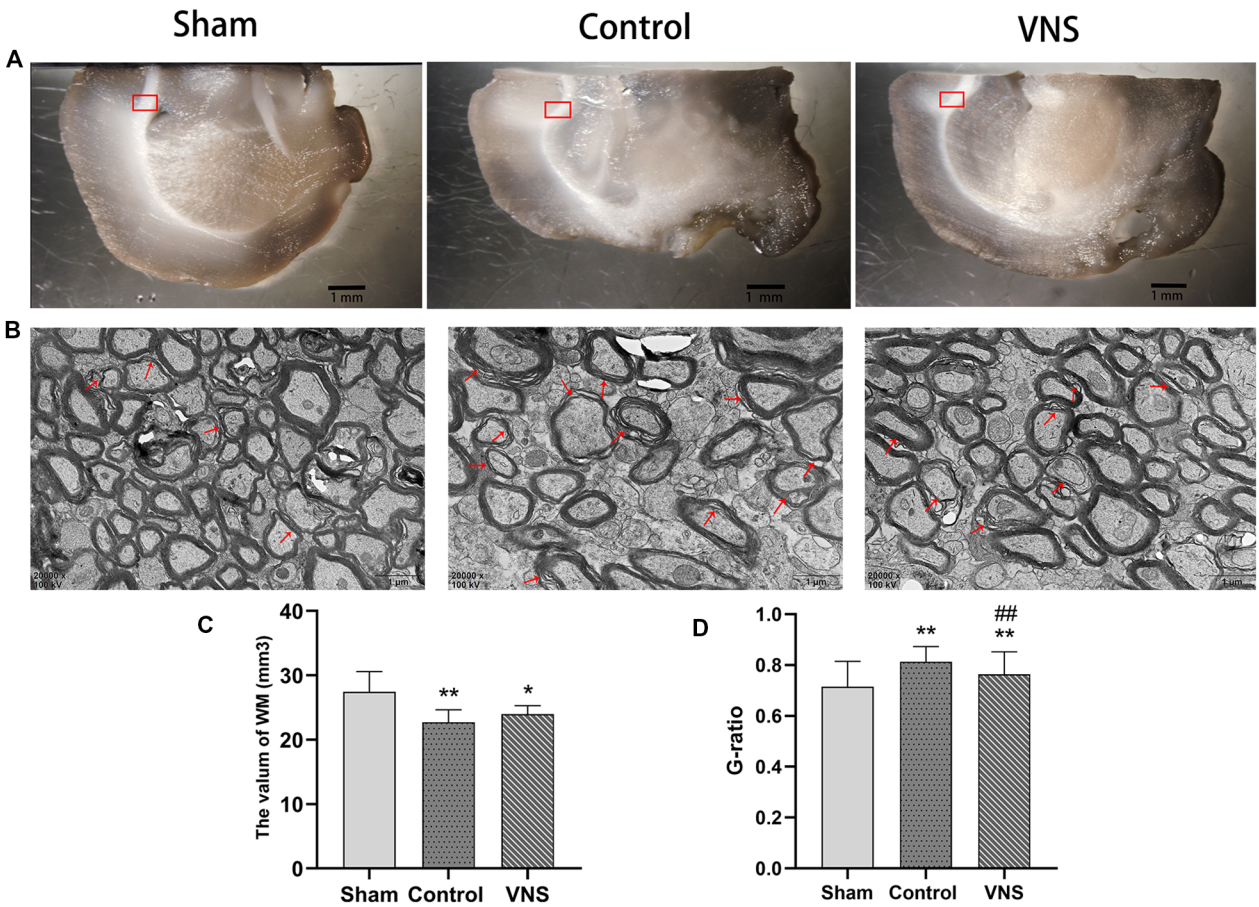

FIGURE 3 | The effects of ta-VNS on the volume and remyelination of the white matter of the MCAO rats. **(A)** Representative images of white matter of rats taken under a dissecting microscope; scale bar = 1 mm. **(B)** Representative transmission electron micrographs of the left white matter in each group at a magnification of 20,000×; the red arrows indicate demyelinated axons; scale bars = 1 μm. **(C)** Total volume of the left white matter in each group (mean ± SD, $n = 5$). **(D)** Quantitative analysis of G-ratio values for all three group rats (mean ± SD, $n = 3$). $^{*}p < 0.05$, $^{**}p < 0.01$, the VNS group or the control group compared with the sham group; $^{\#\#}p < 0.01$, the VNS group compared with the control group.

the control group compared to the white matter of sham group rats (**Figures 5A,F,G**, $p < 0.05$). The increase in the levels of phosphorylated MAPK and phosphorylated NF-κB in the white matter induced by MCAO were significantly alleviated in rats treated with ta-VNS (**Figures 5A,F,G**, $p < 0.05$). Our results revealed the presence of a significant inflammatory response in the injured white matter and that ta-VNS may have an anti-inflammatory effect *via* TLR4/NF-κB signaling and MAPK/NF-κB signaling.

DISCUSSION

Stroke-associated dysphagia is suggested to be the most important factor contributing to the risks of aspiration pneumonia, malnutrition, dehydration, and even mortality in patients (Cohen et al., 2016). In the present study, we evaluated the effects of ta-VNS on dysphagia symptoms and white matter damage, we found that ta-VNS was effective for improving the dysphagia symptoms, increasing remyelination, inducing angiogenesis, and inhibiting the inflammatory response in the white matter of cerebral ischaemia model rats.

The MCAO rat model of stroke has been widely used for decades to study the neural effects of ischaemia and has been increasingly used in recent years as an animal model to study dysphagia after stroke. Researchers found that MCAO caused a dramatic reduction in tongue protrusion (TP) and that TP values were correlated with the infarct size 7 and 24 days following MCAO (Gulyaeva et al., 2003). Impairments in licking efficiency and a compensatory increase in the number of drinking clusters were observed in MCAO rats compared with control rats (Ahmed et al., 2017). However, these studies did not use clinically relevant measures to allow translation from animal models to human studies. Cullins and Connor (2019) used video fluoroscopic swallowing studies (VFSS) to validate the unilateral transient MCAO rat model of an ischemic stroke as a translational model of poststroke dysphagia. They found clinically relevant changes in swallowing and tongue force, supporting the use of the MCAO rat model as a translational

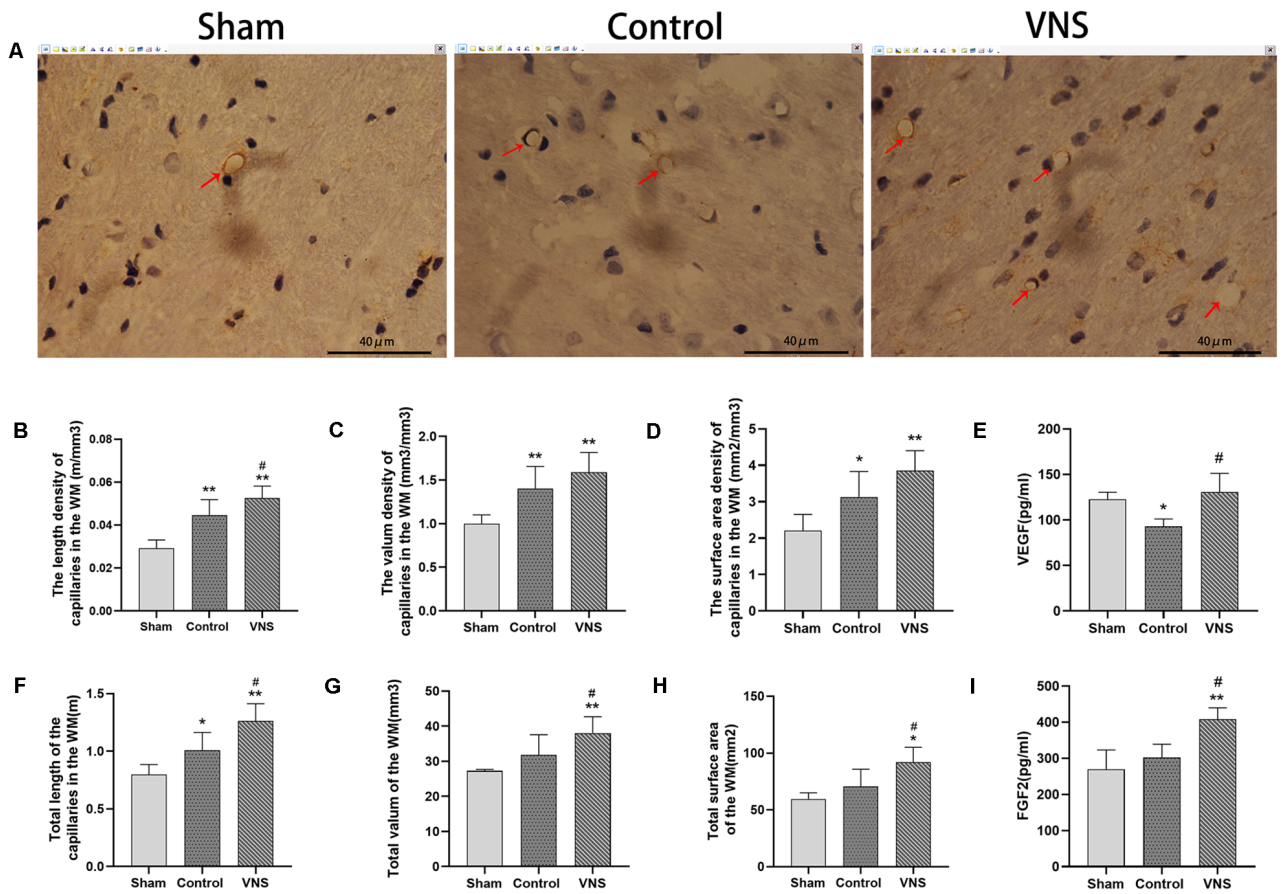

FIGURE 4 | The effects of ta-VNS on angiogenesis in the white matter of MCAO rats. **(A–C)** Representative immunohistochemical staining images of white matter capillaries of rats from each group; scale bar = 40 μm/**(B–D,F–H)**. The length density (m/mm^3), volume density (mm^3/mm^3), surface area density (mm^2/mm^3), total length (m), total volume (mm^3) and total surface area (mm^2) of the capillaries in the left white matter in each group (mean ± SD, $n = 5$). **(E)** The expression level of VEGF in the left white matter of rats in each group was assessed by using ELISA (mean ± SD, $n = 3$). **(I)** The expression level of FGF2 in the left white matter of rats in each group was assessed by using ELISA (mean ± SD, $n = 3$); $^*p < 0.05$, $^{**}p < 0.01$, the VNS group or the control group compared with the sham group; $^{\#}p < 0.05$, the VNS group compared with the control group.

model of poststroke dysphagia (Cullins and Connor, 2019). In a recent study, Sugiyama et al. (2014) reported that an MCAO rat model can be used to study dysphagia after stroke because MCAO rats show delayed initiation of swallowing and reduced swallowing times in response to water infusion under anesthesia. Although many studies have explored the impact of different stroke locations on swallowing function, there is no common opinion in the current studies. The autonomic disturbance and hemispheric stroke difference is a recognized phenomenon, and the MCAO model involving the left hemisphere could minimize the likely autonomic disturbances, unlike the right hemisphere stroke (Oppenheimer et al., 1992; Hilz et al., 2001). Therefore, in the present study, rats subjected to MCAO involving the left hemisphere were used to model poststroke dysphagia. Consistent with previous studies, the rats subjected to MCAO exhibited swallowing deficits, and the growth of the VNS group was better than that of the control group. We observed that the number of swallows was significantly decreased and that the onset latency to the first swallow was significantly prolonged 2 weeks after MCAO. The results from the third week indicated that ta-VNS treatment relieved the symptoms of dysphagia after stroke. These results demonstrate the usefulness of the MCAO rat model for studying dysphagia after ischemic stroke, as well as the effectiveness of ta-VNS on dysphagia after an ischemic stroke.

We chose 2 mA as the stimulus parameter in the present study for ta-VNS treatment, which was not the same as those in previous invasive VNS reports. Previous studies frequently used an intensity range of 0.5 mA to 1 mA in the treatment of invasive VNS or ta-VNS. In the clinical studies of Dawson et al. (2016, 2021), patients with an ischemic stroke were implanted with a VNS stimulation device on the vagus nerve in the left carotid sheath, and then the researchers investigated the effect of 0.8 mA VNS stimulation paired with upper-limb rehabilitation on upper limb function. They found that an intensity of 0.8 mA VNS stimulation paired with rehabilitation is a novel potential treatment option for an ischemic stroke patients and has not raised safety concerns (Dawson et al., 2016, 2021). Similarly, VNS in rats which implanted with a stimulating cuff

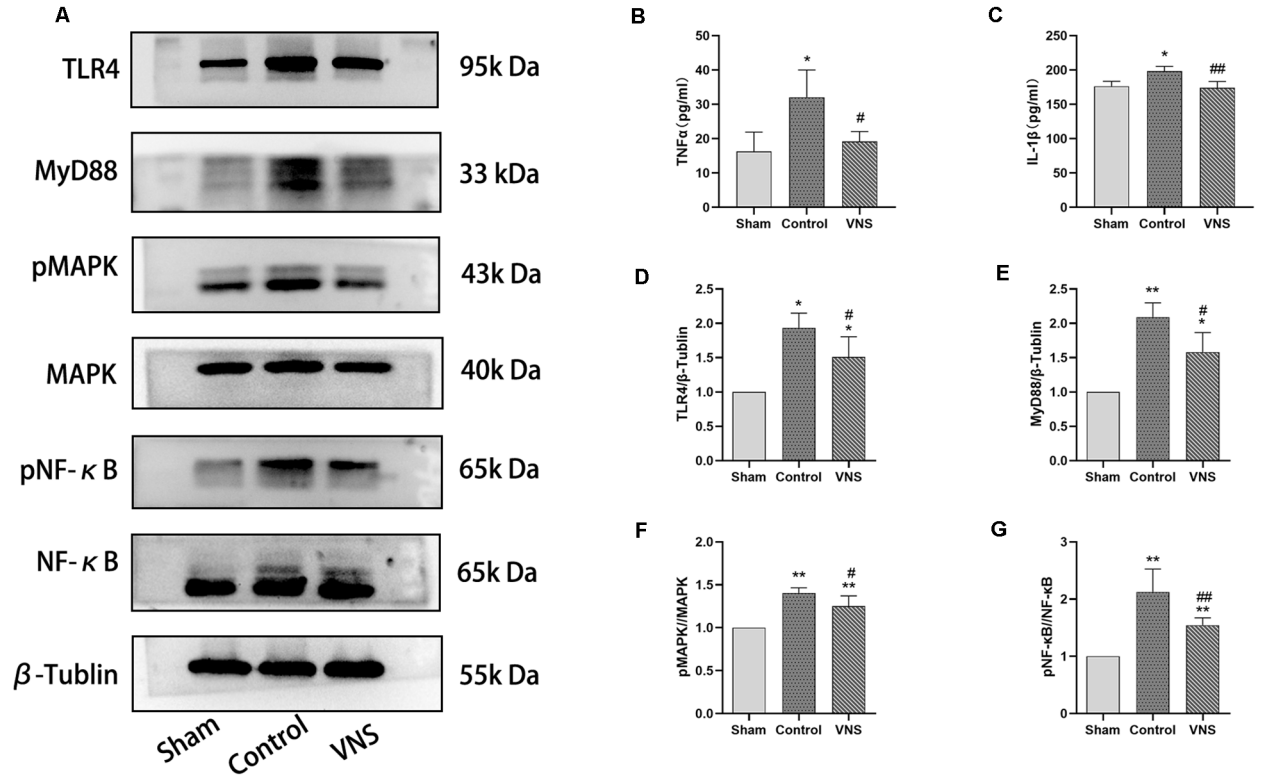

FIGURE 5 | The effects of ta-VNS on the inflammatory response in the white matter of MCAO rats. **(A)** The protein expression of TLR4, MyD88, MAPK, phosphorylated MAPK, NF-κB, and phosphorylated NF-κB in the left white matter of rats in each group was measured by using Western blotting. **(B)** The expression level of TNF-α in the left white matter of rats in each group was assessed by using ELISA (mean ± SD, $n = 3$). **(C)** The expression level of IL-1β in the left white matter of rats in each group was assessed by using ELISA (mean ± SD, $n = 3$). **(D–G)** Quantitative analysis of the protein expression of these TLR4/NF-κB signaling and MAPK/NF-κB signaling in the left white matter of rats in each group (mean ± SD, $n = 3$); $^{*}p < 0.05$, $^{**}p < 0.01$, the VNS group or the control group compared with the sham group; $^{\#}p < 0.05$, $^{\#\#}p < 0.01$, the VNS group compared with the control group.

on the left cervical vagus nerve at 0.8 mA paired with chewing training significantly increased motor cortex jaw representation compared to equivalent behavioral training without stimulation (Morrison et al., 2020). Different from invasive vagus nerve stimulation, transcutaneous auricular vagus nerve stimulation effectively avoids the possible trauma that may be caused by the intervention. On the one hand, the auricular concha is the only area on the body surface that is distributed with ear vagus nerve fiber endings; on the other hand, the plasticity enhancement of VNS follows an inverted-U response of stimulation current that is influenced by pulse width, so the stimulation parameters of ta-VNS that can activate the vagus nerve have become a pivotal issue, which can directly affect the curative efficacy of the interventions (Ellrich, 2019; Liu et al., 2020). In a study by Liu et al. (2020), stimulation parameters of ta-VNS (frequency, 20 Hz; pulse width, 0.5 ms; intensity, 1.0 mA) were demonstrated to suppress epileptiform activity by activating the firing of NTS neurons (Liu et al., 2020). It has been proven that ta-VNS at 0.5 mA at 20 Hz for 1 h can promote postischemic functional recovery and angiogenesis (Jiang et al., 2016; Li et al., 2020b). However, this way of activating the vagus nerve was achieved by inserting acupuncture needles into the concha area to deliver electrical stimulation. Unlike invasive acupuncture, Li et al. (2014b) and Li S. et al. (2020) ensured the passage of the electric current by using two positive and negative electrodes placed over the skin inside and outside of the rauricular concha region, and they found that a higher intensity of 2 mA at 20 Hz can activate the vagus nerve and neuro modulation pathways (cholinergic and noradrenergic). Compared with invasive activation of the vagus nerve, it is advisable to use a higher intensity of 2 mA to activate the vagus nerve in the concha region. We finally selected an intensity of 2 mA in the present study for ta-VNS treatment and proved that ta-VNS at the parameters used in the present study exert a therapeutic effect on dysphagia symptoms.

White matter connectivity is crucial for advanced brain functions. Numerous studies have shown the presence of white matter lesions in patients with stroke, but there is limited evidence linking the white matter to swallowing control. A systematic review revealed that white matter damage can be directly tied to swallowing deficits after ischemic stroke (Alvar et al., 2021). In a clinical study, Li et al. (2014a) found that the mean fractional anisotropy of the white matter tract was significantly reduced in patients with middle artery infarction and dysphagia. A retrospective analysis suggested that white matter lesion observed on brain magnetic resonance imaging scans was an independent factor affecting various

swallowing parameters; specifically, prolonged oral transit time and penetration were predicted by the severity of the white matter lesion (Moon et al., 2017). In the present study, we suspected that white matter damage is partly responsible for swallowing disorders in animals subjected to MCAO, and we used the white matter as a target for improving brain structure and function in the treatment of swallowing disorders by ta-VNS. We used electron microscopy to investigate changes in the myelin sheath in the white matter and stereological methods to accurately estimate the volume of the white matter. We found that MCAO caused significant shrinkage of the white matter. However, ta-VNS treatment for 3 weeks did not alleviate the white matter shrinkage. Interestingly, our results provided quantitative evidence that ta-VNS significantly induced remyelination in the white matter.

Both clinical and animal studies have demonstrated that VNS can promote functional recovery and exert neuroprotection against ischemic stroke (Jiang et al., 2016; Ma et al., 2016). In addition, ta-VNS paired with physical rehabilitation can improve upper limb motor function after an ischemic stroke in clinical practice (Redgrave et al., 2018; Dawson et al., 2021). However, the underlying mechanisms that mediate this beneficial therapeutic effect are unclear, and there is no unified view regarding the mechanism by which VNS treatment promotes recovery. Angiogenesis, as an important basis of neurological repair following an ischemic stroke and a novel target for stroke treatment, attracted our attention in the present study. Endogenous angiogenesis occurs 3 days after MCAO and persists for at least 21 days, resulting in improvements in functional prognosis due to increased cerebral blood flow (Sun et al., 2003). We used immunohistochemistry combined with stereology to quantitatively study capillaries in the white matter and found that ta-VNS treatment for 3 weeks induced a significant increase in angiogenesis, as indicated by an elevated capillary density. Consistent with this evidence, the white matter expression levels of VEGF and FGF2 were also significantly elevated in ta-VNS-treated rats. The results of the present study are similar to those of previous studies to some extent. For instance, a previous study revealed that ta-VNS promotes functional recovery and enhances the postischemic angiogenic response and this angiogenic response is associated with higher expression levels of brain-derived neurotrophic factor (BDNF), endothelial nitric oxide synthase (eNOS) and VEGF in the ischemic penumbra (Jiang et al., 2016). Li et al. (2020b) performed a series of experiments indicating that ta-VNS is capable of promoting angiogenesis and improving neurofunctional recovery in the chronic stage of ischemic stroke. They revealed that PPAR-γ might be involved in the promotion of angiogenesis by ta-VNS (Li et al., 2020b). However, in all previous studies, the researchers obtained indirect information from neuroimaging and molecular biology experiments and did not accurately measure capillary-related parameters. Our results accurately demonstrated that angiogenesis was promoted by ta-VNS treatment and this enhancement effect may be positively associated with VEGF and FGF2 expression in the white matter of rats subjected to MCAO by using quantitative stereology, laying a structural foundation for the improvement of dysphagia symptoms after ischemic stroke. Furthermore, the present study provided evidence that blood vessels and nerve fibers in white matter may be improved or strengthened as a whole during treated by ta-VNS stimulation after ischemic stroke.

The cerebral microvascular system plays an extremely important role in maintaining normal brain and nerve function. Enhancement of angiogenesis induced by an ischemic stroke is crucial to the modulation of neural circuits and brain function, further creating a favorable environment for neurogenesis (Li Y. et al., 2020). As an important part of the blood-brain barrier, cerebrovascular endothelial cells participate in the inflammatory response during neurovascular inflammation. The degradation of extracellular matrix and basement membrane caused by impaired endothelial function usually leads to increased vascular permeability and vascular inflammation further drives inflammation and neuronal destruction in the central nervous system after cerebral ischaemia (Frankowski et al., 2015; Ludewig et al., 2019). Researchers have found that an inflammatory environment also hinders angiogenesis. In an *in vitro* experiment, Shang et al. (2020) found that the proliferation of endothelial cells in a simulated proinflammatory microenvironment was significantly lower than that in an anti-inflammatory microenvironment and that apoptosis of endothelial cells was increased in an inflammatory microenvironment. A clinical study showed that several inflammatory mediators including TNF-α are associated with poor clinical outcomes in peripheral artery disease (Pande et al., 2015). Therefore, resolving inflammation is critical for promoting angiogenesis and protecting against brain injury after ischemic perfusion. Zhang et al. (2016) found that resolving D2 enhances postischemic angiogenesis while resolving inflammation. However, they did not provide evidence for the mechanism underlying this effect. Moreover, accumulating evidence indicates that ta-VNS causes obvious attenuation of the systemic inflammatory response evoked by endotoxin in experimental animals and that this effect is mediated by stimulation of nicotinic receptors on splenic macrophages by acetylcholine (ACh). Hence, the circuit was dubbed the "cholinergic anti-inflammatory pathway" (Hoover, 2017). Based on these results, Li et al. (2020a) found that ta-VNS treatment inhibits excessive post reperfusion inflammatory responses by enhancing α7nAChR mRNA and protein expression after brain injury. Li Y. et al. (2020) demonstrated that RenshenShouwu (RSSW) extract enhances neurogenesis and angiogenesis and this effect may be mediated by inhibition of the TLR4/NF-κB/NLRP3 inflammatory signaling pathway following an ischemic stroke in rats. In the present study, Western blot analysis revealed that the expression of proteins involved in the TLR4/NF-κB signaling pathway and MAPK signaling pathways, such as TLR4, MyD88, phosphorylated MAPK and phosphorylated NF-κB, was significantly increased in the white matter of rats subjected to MCAO. The levels of the inflammatory cytokines TNF-α and IL-1β, which are downstream of the NF-κB pathway, also increased in the left white matter of rats subjected to MCAO. Surprisingly, this increase was alleviated in rats treated

with ta-VNS. Therefore, we proposed that ta-VNS might improve the inflammatory environment of the white matter by inhibiting the activation of the TLR4/NF-κB and MAPK/NF-κB signaling pathways, thus affecting endothelial cell function and promoting neurovascular unit (NVU) regeneration in the white matter and promoting swallowing function recovery after ischemic stroke.

The need for sensitive, easy-to-implement assessment methods of dysphagia symptoms after stroke is crucial in preclinical stroke research. Although VFSS is the gold standard for swallowing disorders in clinical research, it is much more difficult to do so in an awake rat, and VFSS was not sensitive enough to changes in swallowing duration in basic research under the same conditions as those used in humans (Lever et al., 2015; Cullins and Connor, 2019). EMG as an evaluation tool is widely used in the study of dysphagia after an ischemic stroke, we used the EMG signals of swallowing muscles to reflect the swallowing reflex of rats induced by DW and we found time changes in the swallowing reflex of rats in each group in the present study (Sugiyama et al., 2014; Ikeda et al., 2015). As we can see in the current cerebral ischaemia studies, VNS paired with rehabilitation training could enhance synaptic plasticity and promote recovery after stroke. It is worth noting that the assessment of the swallowing reflex in the present study may also be a form of rehabilitation training for rats with dysphagia. However, we only performed the swallowing test once a week for a total of three times, which is not enough to prove that the assessment procedure can produce a therapeutic effect compared with studies including VNS paired with up to 6 weeks of exercise training (Dawson et al., 2016, 2021; Redgrave et al., 2018). Of course, we supposed that VNS combined with swallowing training (inducing swallowing reflex to occur spontaneously by infusion of DW like the assessment method) can be considered an intervention to better explore new dysphagia treatment in future studies.

The occurrence of dysphagia after an ischemic stroke not only affects the food and water intake of patients, causes malnutrition, and affects the quality of life of patients but also increases the incidence of aspiration and pulmonary infection, which greatly increase the mortality of patients. However, treatment options for dysphagia after stroke are very limited, and swallowing is a complex, sequential movement with a fixed pattern. The relative dispersion of the swallowing center in the cortex undoubtedly increases the difficulty of dysphagia research. Identifying the key target molecules or structures for alleviating dysphagia will provide new inspiration for the clinical treatment of dysphagia. In the present study, we demonstrated that 3 weeks of ta-VNS treatment can improve dysphagia symptoms in rats subjected to MCAO. We provided evidence that ta-VNS treatment promotes angiogenesis and inhibits inflammatory response in the white matter. This finding may clarify the partial neuroprotection exerted by ta-VNS.

Limitations

The limitations of the present study are that we did not study the effect of the intervention in the acute phase but administered ta-VNS treatment for 3 weeks beginning 24 h after MCAO. More precise intervention time points should be included in future studies. The stimulus parameters used throughout the experiment were based on previous studies, and the effects of different stimulus parameters should be compared and tested to maximize the therapeutic effect of ta-VNS. In addition, the status of the rats was also a limitation of the present study. It is known that other comorbid cardiovascular risk factors (e.g., hypertension, hyperlipidemia, diabetes, etc.) could influence prestroke autonomic disturbance and may worsen the recovery of poststroke dysphagia. From a translational research perspective, the healthy rat MCAO model cannot simulate actual clinical stroke patients. Future studies should include MCAO animal models in various disease states to elucidate the mechanisms that mediate this therapeutic effect of ta-VNS.

DATA AVAILABILITY STATEMENT

The original contributions presented in the study are included in the article, further inquiries can be directed to the corresponding author.

ETHICS STATEMENT

The animal study was reviewed and approved by the Institutional Ethics Committee of Chongqing Medical University.

AUTHOR CONTRIBUTIONS

Conception and design: SW, GJ, and LY. Administrative support: SW, MF, and GJ. Collection and assembly of data: LL, QZ, MF, LZ, YQ, and YL. Data analysis and interpretation: All authors. Manuscript writing: LL and SW. All authors contributed to the article and approved the submitted version.

FUNDING

This work was supported by the National Natural Science Foundation of China (NSFC, 81601967), Chongqing Health Joint Medical Research Project, Kuanren Talents Program of The Second Affiliated Hospital of Chongqing Medical University (2021MSXM144).

REFERENCES

Ahmed, J., Dwyer, D. M., Farr, T. D., Harrison, D. J., Dunnett, S. B., and Trueman, R. C. (2017). Lickometry: a novel and sensitive method for assessing functional deficits in rats after stroke. *J. Cereb. Blood Flow Metab.* 37, 755–761. doi: 10.1177/0271678X16684141

Alvar, A., Hahn Arkenberg, R., McGowan, B., Cheng, H., and Malandraki, G. A. (2021). The role of white matter in the neural control of swallowing: a systematic review. *Front. Hum. Neurosci.* 15:628424. doi: 10.3389/fnhum.2021.628424

Ay, I., Napadow, V., and Ay, H. (2015). Electrical stimulation of the vagus nerve dermatome in the external ear is protective in rat

cerebral ischemia. *Brain Stimul.* 8, 7–12. doi: 10.1016/j.brs.2014.09.009

Belayev, L., Alonso, O. F., Busto, R., Zhao, W., and Ginsberg, M. D. (1996). Middle cerebral artery occlusion in the rat by intraluminal suture. Neurological and pathological evaluation of an improved model. *Stroke* 27, 1616–1622. doi: 10.1161/01.str.27.9.1616

Broussard, D. L., and Altschuler, S. M. (2000). Brainstem viscerotopic organization of afferents and efferents involved in the control of swallowing. *Am. J. Med.* 108, 79S–86S. doi: 10.1016/s0002-9343(99)00343-5

Cao, Z. J., Balasubramanian, A., and Marrelli, S. P. (2014). Pharmacologically induced hypothermia *via* TRPV1 channel agonism provides neuroprotection following ischemic stroke when initiated 90 min after reperfusion. *Am. J. Physiol. Regul. Integr. Comp. Physiol.* 306, R149–R156. doi: 10.1152/ajpregu.00329.2013

Catani, M., Dell'acqua, F., Bizzi, A., Forkel, S. J., Williams, S. C., Simmons, A., et al. (2012). Beyond cortical localization in clinico-anatomical correlation. *Cortex* 48, 1262–1287. doi: 10.1016/j.cortex.2012.07.001

Chaparro-Huerta, V., Rivera-Cervantes, M. C., Flores-Soto, M. E., Gomez-Pinedo, U., and Beas-Zarate, C. (2005). Proinflammatory cytokines and apoptosis following glutamate-induced excitotoxicity mediated by p38 MAPK in the hippocampus of neonatal rats. *J. Neuroimmunol.* 165, 53–62. doi: 10.1016/j.jneuroim.2005.04.025

Chen, L. M., Zhang, A. P., Wang, F. F., Tan, C. X., Gao, Y., Huang, C. X., et al. (2016). Running exercise protects the capillaries in white matter in a rat model of depression. *J. Comp. Neurol.* 524, 3577–3586. doi: 10.1002/cne.24017

Choi, B. R., Kim, D. H., Back, D. B., Kang, C. H., Moon, W. J., Han, J. S., et al. (2016). Characterization of white matter injury in a rat model of chronic cerebral hypoperfusion. *Stroke* 47, 542–547. doi: 10.1161/STROKEAHA.115.011679

Cohen, D. L., Roffe, C., Beavan, J., Blackett, B., Fairfield, C. A., Hamdy, S., et al. (2016). Post-stroke dysphagia: a review and design considerations for future trials. *Int. J. Stroke* 11, 399–411. doi: 10.1177/1747493016639057

Cullins, M. J., and Connor, N. P. (2019). Reduced tongue force and functional swallowing changes in a rat model of post stroke dysphagia. *Brain Res.* 1717, 160–166. doi: 10.1016/j.brainres.2019.04.023

Dawson, J., Liu, C. Y., Francisco, G. E., Cramer, S. C., Wolf, S. L., Dixit, A., et al. (2021). Vagus nerve stimulation paired with rehabilitation for upper limb motor function after ischaemic stroke (VNS-REHAB): a randomised, blinded, pivotal, device trial. *Lancet* 397, 1545–1553. doi: 10.1016/S0140-6736(21)00475-X

Dawson, J., Pierce, D., Dixit, A., Kimberley, T. J., Robertson, M., Tarver, B., et al. (2016). Safety, feasibility and efficacy of vagus nerve stimulation paired with upper-limb rehabilitation after ischemic stroke. *Stroke* 47, 143–150. doi: 10.1161/STROKEAHA.115.010477

Deng, Y., Xie, D., Fang, M., Zhu, G., Chen, C., Zeng, H., et al. (2014). Astrocyte-derived proinflammatory cytokines induce hypomyelination in the periventricular white matter in the hypoxic neonatal brain. *PLoS One* 9:e87420. doi: 10.1371/journal.pone.0087420

Ellrich, J. (2019). Transcutaneous auricular vagus nerve stimulation. *J. Clin. Neurophysiol.* 36, 437–442. doi: 10.1097/WNP.0000000000000576

Filley, C. M. (2005). White matter and behavioral neurology. *Ann. N Y Acad. Sci.* 1064, 162–183. doi: 10.1196/annals.1340.028

Filley, C. M., and Fields, R. D. (2016). White matter and cognition: making the connection. *J. Neurophysiol.* 116, 2093–2104. doi: 10.1152/jn.00221.2016

Frankowski, J. C., DeMars, K. M., Ahmad, A. S., Hawkins, K. E., Yang, C., Leclerc, J. L., et al. (2015). Detrimental role of the EP1 prostanoid receptor in blood-brain barrier damage following experimental ischemic stroke. *Sci. Rep.* 5:17956. doi: 10.1038/srep17956

Goldman, S. A., and Chen, Z. (2011). Perivascular instruction of cell genesis and fate in the adult brain. *Nat. Neurosci.* 14, 1382–1389. doi: 10.1038/nn.2963

Gulyaeva, N., Thompson, C., Shinohara, N., Lazareva, N., Onufriev, M., Stepanichev, M., et al. (2003). Tongue protrusion: a simple test for neurological recovery in rats following focal cerebral ischemia. *J. Neurosci. Methods* 125, 183–193. doi: 10.1016/s0165-0270(03)00056-6

Hilz, M. J., Dutsch, M., Perrine, K., Nelson, P. K., Rauhut, U., and Devinsky, O. (2001). Hemispheric influence on autonomic modulation and baroreflex sensitivity. *Ann. Neurol.* 49, 575–584. doi: 10.1002/ana.1006.abs

Hoover, D. B. (2017). Cholinergic modulation of the immune system presents new approaches for treating inflammation. *Pharmacol. Ther.* 179, 1–16. doi: 10.1016/j.pharmthera.2017.05.002

Ikeda, J., Kojima, N., Saeki, K., Ishihara, M., and Takayama, M. (2015). Perindopril increases the swallowing reflex by inhibiting substance P degradation and tyrosine hydroxylase activation in a rat model of dysphagia. *Eur. J. Pharmacol.* 746, 126–131. doi: 10.1016/j.ejphar.2014.11.002

Jiang, Y., Li, L., Ma, J., Zhang, L., Niu, F., Feng, T., et al. (2016). Auricular vagus nerve stimulation promotes functional recovery and enhances the post-ischemic angiogenic response in an ischemia/reperfusion rat model. *Neurochem. Int.* 97, 73–82. doi: 10.1016/j.neuint.2016.02.009

Kajii, Y., Shingai, T., Kitagawa, J., Takahashi, Y., Taguchi, Y., Noda, T., et al. (2002). Sour taste stimulation facilitates reflex swallowing from the pharynx and larynx in the rat. *Physiol. Behav.* 77, 321–325. doi: 10.1016/s0031-9384(02)00854-5

Kanazawa, M., Takahashi, T., Ishikawa, M., Onodera, O., Shimohata, T., and Del Zoppo, G. J. (2019). Angiogenesis in the ischemic core: a potential treatment target? *J. Cereb. Blood Flow Metab.* 39, 753–769. doi: 10.1177/0271678X19834158

Khoshnam, S. E., Winlow, W., Farzaneh, M., Farbood, Y., and Moghaddam, H. F. (2017). Pathogenic mechanisms following ischemic stroke. *Neurol. Sci.* 38, 1167–1186. doi: 10.1007/s10072-017-2938-1

Kyriakis, J. M., and Avruch, J. (2001). Mammalian mitogen-activated protein kinase signal transduction pathways activated by stress and inflammation. *Physiol. Rev.* 81, 807–869. doi: 10.1152/physrev.2001.81.2.807

Lee, J. C., Kassis, S., Kumar, S., Badger, A., and Adams, J. L. (1999). p38 mitogen-activated protein kinase inhibitors--mechanisms and therapeutic potentials. *Pharmacol. Ther.* 82, 389–397. doi: 10.1016/s0163-7258(99)00008-x

Lever, T. E., Brooks, R. T., Thombs, L. A., Littrell, L. L., Harris, R. A., Allen, M. J., et al. (2015). Videofluoroscopic validation of a translational murine model of presbyphagia. *Dysphagia* 30, 328–342. doi: 10.1007/s00455-015-9604-7

Li, S., Ma, Z., Tu, S., Zhou, M., Chen, S., Guo, Z., et al. (2014a). Altered resting-state functional and white matter tract connectivity in stroke patients with dysphagia. *Neurorehabil. Neural Repair* 28, 260–272. doi: 10.1177/1545968313508227

Li, S., Zhai, X., Rong, P., McCabe, M. F., Wang, X., Zhao, J., et al. (2014b). Therapeutic effect of vagus nerve stimulation on depressive-like behavior, hyperglycemia and insulin receptor expression in Zucker fatty rats. *PLoS One* 9:e112066. doi: 10.1371/journal.pone.0112066

Li, Y., Liang, W., Guo, C., Chen, X., Huang, Y., Wang, H., et al. (2020). Renshen Shouwu extract enhances neurogenesis and angiogenesis *via* inhibition of TLR4/NF-κB/NLRP3 signaling pathway following ischemic stroke in rats. *J. Ethnopharmacol.* 253:112616. doi: 10.1016/j.jep.2020.112616

Li, J., Zhang, Q., Li, S., Niu, L., Ma, J., Wen, L., et al. (2020a). α7nAchR mediates transcutaneous auricular vagus nerve stimulation-induced neuroprotection in a rat model of ischemic stroke by enhancing axonal plasticity. *Neurosci. Lett.* 730:135031. doi: 10.1016/j.neulet.2020.135031

Li, J., Zhang, K., Zhang, Q., Zhou, X., Wen, L., Ma, J., et al. (2020b). PPAR-γ mediates Ta-VNS-induced angiogenesis and subsequent functional recovery after experimental stroke in rats. *Biomed Res. Int.* 2020:8163789. doi: 10.1155/2020/8163789

Li, S., Wang, Y., Gao, G., Guo, X., Zhang, Y., Zhang, Z., et al. (2020). Transcutaneous auricular vagus nerve stimulation at 20 Hz improves depression-like behaviors and down-regulates the hyperactivity of HPA axis in chronic unpredictable mild stress model rats. *Front. Neurosci.* 14:680. doi: 10.3389/fnins.2020.00680

Liu, C. H., Yang, M. H., Zhang, G. Z., Wang, X. X., Li, B., Li, M., et al. (2020). Neural networks and the anti-inflammatory effect of transcutaneous auricular vagus nerve stimulation in depression. *J. Neuroinflammation* 17:54. doi: 10.1186/s12974-020-01732-5

Longa, E. Z., Weinstein, P. R., Carlson, S., and Cummins, R. (1989). Reversible middle cerebral artery occlusion without craniectomy in rats. *Stroke* 20, 84–91. doi: 10.1161/01.str.20.1.84

Ludewig, P., Winneberger, J., and Magnus, T. (2019). The cerebral endothelial cell as a key regulator of inflammatory processes in sterile inflammation. *J. Neuroimmunol.* 326, 38–44. doi: 10.1016/j.jneuroim.2018.10.012

Ma, J., Zhang, L., He, G., Tan, X., Jin, X., and Li, C. (2016). Transcutaneous auricular vagus nerve stimulation regulates expression of growth differentiation factor 11 and activin-like kinase 5 in cerebral ischemia/reperfusion rats. *J. Neurol. Sci.* 369, 27–35. doi: 10.1016/j.jns.2016.08.004

Martino, R., Foley, N., Bhogal, S., Diamant, N., Speechley, M., and Teasell, R. (2005). Dysphagia after stroke: incidence, diagnosis and pulmonary complications. *Stroke* 36, 2756–2763. doi: 10.1161/01.STR.0000190056.76543.eb

Moon, H. I., Nam, J. S., Leem, M. J., and Kim, K. H. (2017). Periventricular white matter lesions as a prognostic factor of swallowing function in older patients with mild stroke. *Dysphagia* 32, 480–486. doi: 10.1007/s00455-017-9788-0

Morrison, R. A., Danaphongse, T. T., Pruitt, D. T., Adcock, K. S., Mathew, J. K., Abe, S. T., et al. (2020). A limited range of vagus nerve stimulation intensities produce motor cortex reorganization when delivered during training. *Behav. Brain Res.* 391:112705. doi: 10.1016/j.bbr.2020.112705

Nemeroff, C. B., Mayberg, H. S., Krahl, S. E., McNamara, J., Frazer, A., Henry, T. R., et al. (2006). VNS therapy in treatment-resistant depression: clinical evidence and putative neurobiological mechanisms. *Neuropsychopharmacology* 31, 1345–1355. doi: 10.1038/sj.npp.1301082

Oppenheimer, S. M., Gelb, A., Girvin, J. P., and Hachinski, V. C. (1992). Cardiovascular effects of human insular cortex stimulation. *Neurology* 42, 1727–1732. doi: 10.1212/wnl.42.9.1727

Pande, R. L., Brown, J., Buck, S., Redline, W., Doyle, J., Plutzky, J., et al. (2015). Association of monocyte tumor necrosis factor α expression and serum inflammatory biomarkers with walking impairment in peripheral artery disease. *J. Vasc. Surg.* 61, 155–161. doi: 10.1016/j.jvs.2014.06.116

Panebianco, M., Rigby, A., Weston, J., and Marson, A. G. (2015). Vagus nerve stimulation for partial seizures. *Cochrane Database Syst. Rev.* 2015:CD002896. doi: 10.1002/14651858.CD002896.pub2

Petcu, E. B., Smith, R. A., Miroiu, R. I., and Opris, M. M. (2010). Angiogenesis in old-aged subjects after ischemic stroke: a cautionary note for investigators. *J. Angiogenesis Res.* 2:26. doi: 10.1186/2040-2384-2-26

Qi, Y., Wang, S., Luo, Y., Huang, W., Chen, L., Zhang, Y., et al. (2020). Exercise-induced nitric oxide contributes to spatial memory and hippocampal capillaries in rats. *Int. J. Sports Med.* 41, 951–961. doi: 10.1055/a-1195-2737

Redgrave, J. N., Moore, L., Oyekunle, T., Ebrahim, M., Falidas, K., Snowdon, N., et al. (2018). Transcutaneous auricular vagus nerve stimulation with concurrent upper limb repetitive task practice for poststroke motor recovery: a pilot study. *J. Stroke Cerebrovasc. Dis.* 27, 1998–2005. doi: 10.1016/j.jstrokecerebrovasdis.2018.02.056

Shang, K., He, J., Zou, J., Qin, C., Lin, L., Zhou, L. Q., et al. (2020). Fingolimod promotes angiogenesis and attenuates ischemic brain damage *via* modulating microglial polarization. *Brain Res.* 1726:146509. doi: 10.1016/j.brainres.2019.146509

Sugiyama, N., Nishiyama, E., Nishikawa, Y., Sasamura, T., Nakade, S., Okawa, K., et al. (2014). A novel animal model of dysphagia following stroke. *Dysphagia* 29, 61–67. doi: 10.1007/s00455-013-9481-x

Sun, Y., Jin, K., Xie, L., Childs, J., Mao, X. O., Logvinova, A., et al. (2003). VEGF-induced neuroprotection, neurogenesis and angiogenesis after focal cerebral ischemia. *J. Clin. Invest.* 111, 1843–1851. doi: 10.1172/JCI17977

Tang, Y., Nyengaard, J. R., Andersen, J. B., Baandrup, U., and Gundersen, H. J. (2009). The application of stereological methods for estimating structural parameters in the human heart. *Anat. Rec. (Hoboken)* 292, 1630–1647. doi: 10.1002/ar.20952

Terré, R. (2020). Oropharyngeal dysphagia in stroke: diagnostic and therapeutic aspects. *Rev. Neurol.* 70, 444–452. doi: 10.33588/rn.7012.2019447

Theus, M. A.-O., Brickler, T. A.-O., Meza, A. L., Coutermarsh-Ott, S., Hazy, A., Gris, D., et al. (2017). Loss of NLRX1 exacerbates neural tissue damage and NF-κB signaling following brain injury. *J. Immunol.* 199, 3547–3558. doi: 10.4049/jimmunol.1700251

Zhang, L., Deng, Y., Zhang, Y., Liu, C., Zhang, S., Zhu, W., et al. (2020). The design, characterizations and tumor angiogenesis inhibition of a multi-epitope peptibody With bFGF/VEGFA. *Front. Oncol.* 10:1190. doi: 10.3389/fonc.2020.01190

Zhang, M. J., Sansbury, B. E., Hellmann, J., Baker, J. F., Guo, L. P., Parmer, C. M., et al. (2016). Resolvin D2 enhances postischemic revascularization while resolving inflammation. *Circulation* 134, 666–680. doi: 10.1161/CIRCULATIONAHA.116.021894

Zhao, M., Wang, J., Xi, X., Tan, N., and Zhang, L. (2018). SNHG12 promotes angiogenesis following ischemic stroke *via* regulating miR-150/VEGF pathway. *Neuroscience* 390, 231–240. doi: 10.1016/j.neuroscience.2018.08.029

Conflict of Interest: The authors declare that the research was conducted in the absence of any commercial or financial relationships that could be construed as a potential conflict of interest.

Publisher's Note: All claims expressed in this article are solely those of the authors and do not necessarily represent those of their affiliated organizations, or those of the publisher, the editors and the reviewers. Any product that may be evaluated in this article, or claim that may be made by its manufacturer, is not guaranteed or endorsed by the publisher.

frontiers | Frontiers in Human Neuroscience

REVIEW
published: 07 April 2022
doi: 10.3389/fnhum.2022.800349

Stimulation Parameters Used During Repetitive Transcranial Magnetic Stimulation for Motor Recovery and Corticospinal Excitability Modulation in SCI: A Scoping Review

Nabila Brihmat[1,2], *Didier Allexandre*[2,3], *Soha Saleh*[2,3], *Jian Zhong*[4], *Guang H. Yue*[2,3] *and Gail F. Forrest*[1,2,3]*

[1]*Tim and Caroline Reynolds Center for Spinal Stimulation, Kessler Foundation, West Orange, NJ, United States,* [2]*Department of Physical Medicine and Rehabilitation, Rutgers—New Jersey Medical School, Newark, NJ, United States,* [3]*Center for Mobility and Rehabilitation Engineering Research, Kessler Foundation, West Orange, NJ, United States,* [4]*Burke Neurological Institute and Feil Family Brain and Mind Research Institute, Weill Cornell Medicine, White Plains, NY, United States*

OPEN ACCESS

Edited by:
Alia Benali,
Hertie Institute for Clinical Brain Research, Germany

Reviewed by:
Ricardo Nuno Braço Forte Salvador, Neuroelectrics (Spain), Spain
Toshiki Tazoe, Tokyo Metropolitan Institute of Medical Science, Japan

***Correspondence:**
Gail F. Forrest
gforrest@kesslerfoundation.org

Specialty section:
This article was submitted to Brain Imaging and Stimulation, a section of the journal Frontiers in Human Neuroscience

Received: *22 October 2021*
Accepted: *24 February 2022*
Published: *07 April 2022*

Citation:
Brihmat N, Allexandre D, Saleh S, Zhong J, Yue GH and Forrest GF (2022) Stimulation Parameters Used During Repetitive Transcranial Magnetic Stimulation for Motor Recovery and Corticospinal Excitability Modulation in SCI: A Scoping Review. Front. Hum. Neurosci. 16:800349. doi: 10.3389/fnhum.2022.800349

There is a growing interest in non-invasive stimulation interventions as treatment strategies to improve functional outcomes and recovery after spinal cord injury (SCI). Repetitive transcranial magnetic stimulation (rTMS) is a neuromodulatory intervention which has the potential to reinforce the residual spinal and supraspinal pathways and induce plasticity. Recent reviews have highlighted the therapeutic potential and the beneficial effects of rTMS on motor function, spasticity, and corticospinal excitability modulation in SCI individuals. For this scoping review, we focus on the stimulation parameters used in 20 rTMS protocols. We extracted the rTMS parameters from 16 published rTMS studies involving SCI individuals and were able to infer preliminary associations between specific parameters and the effects observed. Future investigations will need to consider timing, intervention duration and dosage (in terms of number of sessions and number of pulses) that may depend on the stage, the level, and the severity of the injury. There is a need for more real vs. sham rTMS studies, reporting similar designs with sufficient information for replication, to achieve a significant level of evidence regarding the use of rTMS in SCI.

Keywords: neuromodulation, recovery, stimulation parameters, plasticity, variability, spasticity

INTRODUCTION

Spinal Cord Injury (SCI) is defined as a traumatic or non-traumatic event affecting the spinal cord that results in sensory, motor, and autonomic deficits reducing independence and quality of life (QOL). In 2020, the National Spinal Cord Injury Statistical Center reported 294,000 people currently living with SCI (National Spinal Cord Injury Statistical C, 2020). Worldwide, this represents 2–3 million people, predominantly young adults, living with SCI related disability (Quadri et al., 2020). Over the last decade, due to advancements in medical procedures and patient

care, survival rates after an SCI have increased (Alizadeh et al., 2019) and the length of acute stage hospitalization has dropped to 11 days as compared to 24 days in the 1970s (National Spinal Cord Injury Statistical C, 2020).

Improved understanding of the pathophysiological mechanisms underlying recovery after SCI have opened new perspectives for rehabilitation (Witiw and Fehlings, 2015; Fouad et al., 2020). Limited spontaneous motor function recovery after incomplete and complete lesions is at least partially due to cerebral and spinal plasticity processes involving spared and damaged circuitry (Raineteau and Schwab, 2001; Fink and Cafferty, 2016). At 1 year post-injury, 70% of cervical complete SCI individuals recovered one motor level, but only 30% recovered two or more motor levels (Steeves et al., 2011). The recovery rate is lower after complete compared to incomplete SCI (Ditunno et al., 2000). Most injured individuals remain burdened with significant SCI-related deficits.

SCI interrupts the connection between the brain and the body periphery; to restore lost functions, new connections need to be made, which necessarily involves axon growth and synaptogenesis. In rodent studies, actual axonal sprouting, and corticospinal tract (CST) regeneration has been shown following a lesion (Liu et al., 2010; O'Donovan et al., 2014). Regeneration can be promoted by existing neuromodulatory interventions such as high frequency repetitive transcranial magnetic stimulation (HF-rTMS). Indeed, studies have shown that HF-rTMS can increase the levels of brain derived neurotrophic molecule (BDNF) in rats' central nervous system (Gao et al., 2017; Fujiki et al., 2020). This increase is thought to reflect mechanisms of structural and synaptic plasticity (Bliss and Cooke, 2011).

rTMS is a non-invasive brain stimulation (NIBS) technique that relies on the principle of electromagnetic induction of Faraday. A rapidly changing magnetic field in the TMS coil induces a brief electric current in the brain which generates secondary currents responsible for spreading neuronal activation at the cortical and subcortical levels (Barker et al., 1985; Lefaucheur, 2019). The underlying effects are thought to be mediated by long-term potentiation (LTP) and depression (LTD) -like mechanisms. The repeated administration of the magnetic pulses, at a certain frequency, are thought to induce short- to long-term changes in corticospinal excitability (CSE) and affect plasticity mechanisms. Until recently, the frequency of stimulation was thought to be the main determinant of the after-effects, with low frequency rTMS (LF-rTMS, <1 Hz) inducing a decrease of CSE whereas HF-rTMS (≥ 5 Hz) induces its increase (Rossi et al., 2009, 2020).

A recent review evaluated real vs. sham rTMS protocols, covering decades of research on therapeutic rTMS efficacy for several neurological conditions including neuropathic pain, depression, and stroke (Lefaucheur et al., 2020). For SCI, this field is novel with limited published research. Preliminary results suggest potential benefits for motor and sensory recovery, as well as addressing secondary complications such as spasticity and chronic pain. Recent reviews have suggested that rTMS is a promising neuromodulatory therapeutic tool that may help recovery after SCI (Ellaway et al., 2014; Tazoe and Perez, 2015; Gunduz et al., 2017), however, there is still insufficient evidence supporting rTMS use in clinical settings. Moreover, standardized rTMS protocols defining optimal stimulation parameters (i.e., stimulation frequency, intensity, duration of trains, number of pulses, etc.), number of sessions and duration of each session, and potential combination with other rehabilitation interventions remain to be determined.

Outcome variability is a well-known issue in the rTMS field (Sale et al., 2007; López-Alonso et al., 2014; Schoisswohl et al., 2019; Xiang et al., 2019). In tinnitus (Schoisswohl et al., 2019), the authors addressed the problem using a reviewing methodology based on study frequency that helped them infer optimal stimulation parameters. In SCI, Leszczyńska et al. (2020) described the use of an algorithm to define individual stimulation parameters based on individual SCI participant response to TMS. The resulting individualized parameters were however not explicitly reported.

Thus, instead of addressing only the therapeutic potential of rTMS in SCI, a topic already covered in previous reviews with positive conclusions, our focus here is to describe and discuss rTMS protocol design, aiming to highlight stimulation parameters that are likely to induce beneficial effects on motor function recovery, spasticity, and/or CSE after SCI. We conclude by making some recommendations for future research studies involving SCI individuals.

METHODS

Search Methodology and Study Selection

To identify the most relevant studies, a literature search in PubMed, MEDLINE (OVID) SCOPUS, and Cochrane Library databases was performed in the abstracts and/or titles using two general key concept words "spinal cord injury (SCI)" and "repetitive transcranial magnetic stimulation (rTMS)". Articles studying the effect of rTMS intervention on upper- and lower-extremity motor function and deficits, spasticity, and CSE in SCI individuals were examined. In addition, studies related to pain and sensory deficits were considered when the *rTMS targeted the motor cortex* and reported *independent outcomes of CSE*. We included randomized controlled, as well as non-randomized, longitudinal trials and studies that investigated the effects of rTMS *when combined with other rehabilitation interventions* and *single-case reports*.

The exclusion criteria were studies focusing on effects of patterned rTMS stimulation interventions, [i.e., paired associative stimulation (PAS) or theta burst stimulation (TBS)] or other forms of NIBS (i.e., tDCS or electrical stimulation alone), and studies reporting rTMS effects on pain or sensory function exclusively.

All articles meeting the above inclusion/exclusion criteria published in English up to mid-January 2021 were included and reviewed. A gray literature search and reference lists of the selected articles were also scanned to identify potentially relevant sources and additional studies.

Additional Exploratory Analysis

Given the small number of randomized controlled trials (RCT) in the rTMS-SCI field and the difficulty of calculating the effect size from the included studies, we chose to conduct an exploratory analysis based on the frequency of studies reporting significant or non-significant outcomes after the rTMS interventions (Schoisswohl et al., 2019). The frequency analysis was performed for a selection of rTMS parameters and characteristics, each of which was divided into subcategories. An excel table was completed with the data extracted from the included articles. The parameters analyzed (columns) were entered for each specific reviewed article (rows). Most of the subcategories (numerical categories: i.e., *number of sessions*, *number of pulses*. . .) were defined and subdivided based on a cutoff value corresponding to the median value calculated for a specific study parameter. Regarding "*stimulation frequency*" parameter, given that most of the included articles used HF protocols, we have chosen to set the cutoff value at 10 Hz to separate those which used commonly used frequencies (high: 5–10 Hz) from those which used less common and higher frequencies (very high: 15–20–22 Hz) of stimulation and thus also obtaining a similar number of studies in both sub-categories. Two main categories of outcomes were defined, i.e., "clinical" (which includes measures related to motor deficits, spasticity, QOL, and activity of daily living, ADL) and "neurophysiological" (which includes only neuro-electrophysiological measures of CSE). A study was considered significant for a given effect category if two or more of the used outcomes of the main outcome category were reported as significant.

RESULTS

Description of Included Studies

This study follows the Preferred Reporting Items for Systematic Reviews and Meta-Analyses (PRISMA) Extension for Scoping Reviews (PRISMA-ScR) guidelines (Tricco et al., 2018; see flow diagram in **Figure 1**). The search strategy resulted in a total of 612 records (416 articles in PubMed, 59 in MEDLINE, 96 in SCOPUS, and 41 trials in the Cochrane library). A first step was to identify and remove duplicates (n = 156), as well as non-English (n = 23), animal (n = 40), and non-exploitable studies (such as poster, clinical trials design without sufficient information about protocol designs, and retracted studies, n = 16). Non-related studies (i.e., not using rTMS or focusing on other pathology, n = 272) and reviews (n = 48) were removed. The remaining articles (n = 57) were screened more carefully against the inclusion/exclusion (I/E) criteria. Studies using other patterned rTMS intervention (i.e., PAS, TBS) or those testing rTMS for other purposes (pain alone; n = 37) were excluded.

Thus, after full-text examination according to the I/E criteria, 20 articles were retained; four were single-case reports and three were one arm(s) longitudinal studies. The 13 remaining were randomized controlled studies, of which six were randomized double-blinded cross-over placebo-controlled [one is a published study protocol with enough information about the protocol design to be included (de Araújo et al., 2017), one randomized simple-blinded cross-over placebo-controlled study, and six randomized blinded parallel placebo-controlled studies]; 13 studies were combined with other rehabilitation interventions and seven studies were not. One study involved bilateral rTMS [right and left M1 successive stimulation during the same session (Leszczyńska et al., 2020)]. One tested two rTMS conditions (leg and hand motor areas stimulation) vs. sham (Jetté et al., 2013).

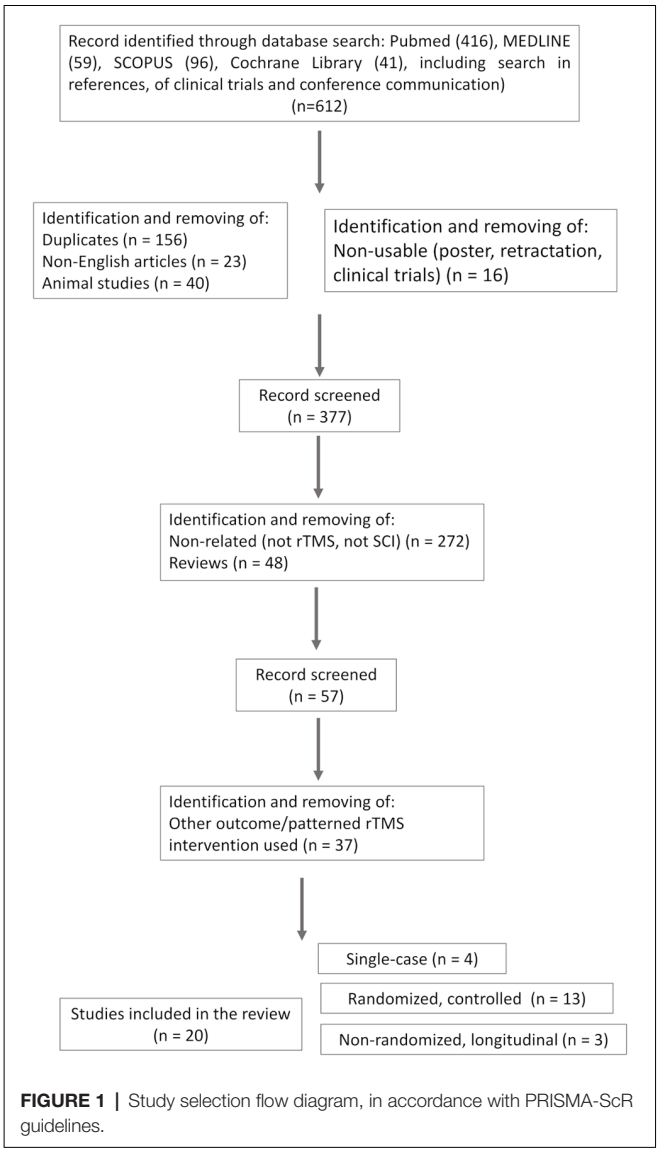

FIGURE 1 | Study selection flow diagram, in accordance with PRISMA-ScR guidelines.

The demographic and clinical information extracted were the *number of participants* in the study, SCI individuals' *deficit levels and severity* (as measured with the American Spinal Cord Injury Association (ASIA) impairment scale, AIS) and *time since injury* (in days, months, or years). Study-specific information included were the *study design*, the *associated intervention* (i.e., motor training, functional stimulation, robotic training), or the *control condition* (if present), and the *outcomes measures* used to assess to the intervention effects. The most common rTMS parameters identified and extracted were the *TMS device*, *coil type*, *targets of stimulation*, *TMS frequency*

(in Hz), *TMS intensity* (%) and the *method/muscle used to find the threshold*, the *number of pulses*, the *number of bursts per session* and its *duration*, the *number of total pulses*, the *duration of session*, the *number of sessions* and the *inter-trains interval (ITI)*. The pulse waveform and coil orientation were not reported explicitly and systematically in all studies and are therefore not included in the review. *Neuronavigation* was considered not used when not explicitly reported. **Table 1** summarizes specific information from all included articles on the population studied, the rTMS intervention design (i.e., duration, frequency, . . .etc.), the outcome measures and side effects.

Outcome Measures Used to Assess the rTMS Effects in SCI

Table 2 lists and describes the clinical and functional outcomes, as well as the spasticity and QOL/ADL measures, used in at least two studies.

Biological Substrates and Side/Adverse Effects

Other relevant outcomes include the *blood levels of BDNF (Brain-derived neurotrophic factor) and NGF (nerve growth factor)*. BDNF and NGF levels reflect rTMS effects on structural plasticity mechanisms (i.e., axon regeneration; Bliss and Cooke, 2011; Moxon et al., 2014). *Side effects (SE) and adverse events* (AE) related to TMS administration were also reported.

Main Observed Effects of rTMS in SCI

CSE Changes Associated With Analgesic Effects

One study applied a *single-session of HF-rTMS* tochronic SCI participants and included measures of pain and CSE (Jetté et al., 2013). The analgesic effects observed were associated with increase of CSE, as demonstrated with an increase of MEP amplitude. Similar effects on pain and CSE were observed in subacute SCI patients after repeated HF-rTMS over *18 sessions*, associated with an increase of biological markers levels (BDNF and NGF; Zhao et al., 2020). The other stimulation parameters (*frequency of 10 Hz, subthreshold stimulation intensity*) were similar in both studies.

Upper-Extremity Function and Associated CSE Changes

Modest to good and maintained effects on UE function and CSE seem to be associated with rTMS. Gomes-Osman and collaborators tested the effects of *three sessions* of HF-rTMS over the *hand M1*, *associated with repetitive task practice (RTP)* during the inter-train interval in 11 chronic iSCI (Gomes-Osman and Field-Fote, 2015). They showed improvement in grasp strength and the ability to perform the JTHFT (as showed with higher effect size in the active group) beyond those observed with RTP alone, with inter-manual transfer of the training effects observed. No changes in CSE were observed. Using a similar protocol but *repeated over 5 days (rather than 3)* and *without using any additional hand training* in 15 chronic SCI, Kuppuswamy et al. (2011) observed only modest, not maintained functional gain in ARAT score and increase in FDI' AMT at 72 and 120 h post-rTMS intervention. Both studies reported no between-condition (active vs. sham) difference in hand motor performance or CSE. Belci et al. (2004) were the first to test and administer a rTMS protocol to four SCI patients in the chronic stage, repeated over 5 days (Belci et al., 2004). They used a specific design of *high frequency double pulses* administered at low-frequency (0.1 Hz), at an intensity of 90% RMT for 5 days over the leg motor area *(leg M1, vertex)*. They demonstrated beneficial effects on motor and sensory function and dexterity, using the AIS and 9HPT respectively, and reduced CS inhibition and electrical perceptual threshold. The clinical changes were maintained for weeks whereas the electrophysiological changes returned to pretreatment levels at follow-up. Choi et al. (2019) specifically tested five *sessions* of HF-rTMS *(20 Hz)* in central cord syndrome patients, the most common type of SCI (Choi et al., 2019). They reported improved motor function with increased JTFHT time and scores and muscle strength thus demonstrating once again the potential of HF-rTMS to improve fine motor performance. With *10 sessions* of *10 Hz-rTMS associated with manual training program*, Fawaz et al. (2019) reported improvements in overall UE deficits and motor function associated with CSE increase.

Spasticity, Lower-Extremity Function, and CSE

The effect of *daily stimulation sessions over 1 week* on spasticity symptoms was explored. A modulation and improvement of knee spasticity symptoms were demonstrated after *20 Hz-rTMS* over the *leg M1* on 15 iSCI participants (Kumru et al., 2010). These changes were maintained at 1 week follow-up but were, however, not associated with neurophysiologic changes in iSCI. The same protocol was tested in 2014 in nine SCI at a more chronic stage of their injury (Nardone et al., 2014a). Real rTMS was observed to significantly reduce LE spasticity (decrease of MAS and SCAT scores), associated this time with neurophysiological effects, as reflected by a decrease of reciprocal inhibition. Both studies reported beneficial effects from the first session of the proposed rTMS protocol.

The effects on LE function and spasticity seem more significant and maintained when HF-rTMS is *associated with other rehabilitation interventions*. Improvements in LE muscle strength, spasticity, and gait were demonstrated following *15 sessions* of HF-rTMS at *20 Hz associated with rehabilitative training* in 17 iSCI participants (Benito et al., 2012). These improvements were maintained 2 weeks after the protocol ended. In 2016, Kumru tested the same protocol as Kumru et al. (2010) and Nardone et al. (2014a) in more severe and subacute patients, using *20 sessions* of *20 Hz-rTMS* protocol and *associated with a robotic treadmill training (Lokomat)* (Kumru et al., 2016). They observed significant improvement in limbs motor scores. These improvements were greater in the real compared to the sham group and were maintained at 4 weeks follow-up for gait performance. Similarly, Calabrò et al. (2017) reported improvements in clinical scores, kinetic parameters, and CSE as an increase in MEP amplitude and MUNE in one chronic iSCI participant after combining HF-rTMS sessions with *Lokomat gait training*. Improvements in walking independence, functional mobility, and QOL, as measured with the WISCI-III, MAS, SCIM-III, and SF-36 respectively, were reported after *12 sessions* of *15 Hz-rTMS combined with BWSTT* in one SCI

TABLE 1 | Descriptive table of the reviewed rTMS studies.

Study article	Number of participants n	Deficit level AIS	Time since injury d: days mo: months y: year	Trial protocol	Target Coil type TMS device	Control condition (if any)	TMS frequency (Hz)	TMS intensity (%)	Number of pulse/ session (total) Duration of one session Number of sessions	ITI	Measured outcomes Side/Adverse effects reported (n#, if any) NR : not reported
Jetté et al. (2013)	16	C1–L4 A—D	2–35 y	**rTMS** Real vs. sham (2 active sessions: hand M1/ leg M1) (RCT)	Hand and leg M1 (contralateral to the painful/ dominant side) F8C airfilm coil Magstim Super Rapid^2	Sham airfilm coil ~ hand M1	10	Hand 90% RMT (FDI) Leg 110% RMT (FDI)	2,000 pulses (5-s burst, 40 bursts; 2,000) 20 min 1 **(*2)**, 2 w WO	25 s	Before, after sham/treatment: **Corticospinal excitability**: FDI motor mapping: -Max MEP amplitude -Map area -Normalized map volume -Center of gravity (CoG) Mild discomfort, coil pressure, facial muscle twitching (7/16)
Gomes-Osman and Field-Fote (2015)	11 10AB	~C6 C, D	6.6 ± 8.2 y	**rTMS** Real vs. sham + RTP (RCT)	Hand M1 (thenar muscles of the weaker hand) F8C Magstim Super Rapid^2	Electric stimulation	10	80% RMT (BB)	800 pulses (2-s burst, 40 pulses; 2,400) ~11 min 3–3 d	30 s 9HPT	Before, after sham/treatment: **Motor**: -JTHFT -9HPT -Pinch and grasp strength **Corticospinal excitability**: -Active and resting MT -IO curve Transient headache (3/11)

(Continued)

TABLE 1 | Continued

Study article	Number of participants n	Deficit level AIS	Time since injury d: days mo: months y: year	Trial protocol	Target Coil type TMS device	Control condition (if any)	TMS frequency (Hz)	TMS intensity (%)	Number of pulse/ session (total) Duration of one session Number of sessions	ITI	Measured outcomes Side/Adverse effects reported (n#, if any) NR : not reported
de Araújo et al. (2017)	20	NR iSCI	>6 mo	**rTMS** Real vs. sham (RCT)	Leg M1 (vertex) F8C Neurosoft—Neuro-MS 5	Sham coil	5	100% RMT (APB)	600 (12 10-s trains of 50 pulses; 3,000) 4 min 5, 2 w WO	10 s	Before, after treatment: **Motor**: -ASIA: UEMS, LEMS -FMS: UE-FMS, LE-FMS **Spasticity**: -MAS **Corticospinal excitability**: -Surface EMG NA
Kuppuswamy et al. (2011)	15	C5–C8 A—D	3–28 y 7 mo	**rTMS** Real vs. sham (RCT)	Hand/arm M1 (right or left FDI, thenar or ECR) F8C Magstim Super Rapid^2	Circular sham (over vertex, 5% MSO)	5	80% AMT (Muscle with lower MT)	900 (2-s trains; 4,500 biphasic pulses) 15 min 5–5 d, 2 w WO	8 s	Before, after sham/treatment, 72/120 h: **Motor**: -ASIA for motor function -9HPT -ARAT **Corticospinal excitability**: -cSP -RMT -MEP amplitude -AMT NR
Belci et al. (2004)	4	C5 D	15 mo – 8 y	**rTMS** Real and sham (Longitudinal design)	Leg M1 (vertex) Circular Magstim 200	Coil over the occipital cortex	0.1 (10)	90% RMT (right thenar mucles)	360 double pulses (720*5 = 3,600) 1 h 5–5 d	10 s (100 ms)	Before, during sham/treatment, 3 w FO: **Motor**: -ASIA for motor function -9HPT **Corticospinal Excitability**: -cSP NR

(Continued)

TABLE 1 | Continued

Study article	Number of participants n	Deficit level AIS	Time since injury d: days mo: months y: year	Trial protocol	Target Coil type TMS device	Control condition (if any)	TMS frequency (Hz)	TMS intensity (%)	Number of pulse/ session (total) Duration of one session Number of sessions	ITI	Measured outcomes Side/Adverse effects reported (n#, if any) NR : not reported
Kumru et al. (2010)	14	C3–T11 C, D	7.3 ± 3.9 mo	**rTMS** Real and sham (RCT)	Leg M1 (vertex) Double cone coil Magstim Super Rapid	Coil disconnected on vertex Connected F8C under pillow	20	90% RMT (BB)	1,600 (2-s bursts, 40 pulses; 8,000) 20 min 5–5 d, 2 w WO	28 s	Before, after sham/treatment, 1w FO: **Spasticity**:- -MAS -VAS: spasms, stiffness and/or clonus -MPSFS -SCAT -SCI-SET **Corticospinal excitability**: -H reflex (soleus) -T reflex (soleus) -Withdrawal reflex (soleus, TA) Facial muscle twitching (3/14)
Nardone et al. (2014b)	9 8AB	C6–T10 C, D	4–17 y	**rTMS** Real/sham (RCT)	Leg M1 (vertex) Double cone coil Magstim Super Rapid	Double cone disconnected Connected F8C under pillow	20	90% RMT (rBB)	1,600 pulses (2-s burst; 8,000) 20 min 5–5 d, 4 w WO	28 s	Before, after sham/treatment, 1w FO: **Spasticity**:- -MAS -SCAT **Corticospinal excitability**: -H reflex (soleus) -Reciprocal inhibition NR

(Continued)

TABLE 1 | Continued

Study article	Number of participants n	Deficit level AIS	Time since injury d: days mo: months y: year	Trial protocol	Target Coil type TMS device	Control condition (if any)	TMS frequency (Hz)	TMS intensity (%)	Number of pulse/ session (total) Duration of one session Number of sessions	ITI	Measured outcomes Side/Adverse effects reported (n#, if any) NR : not reported
Choi et al. (2019)	19 20AB	C3–C7 C, D	9–83 d	**rTMS** +CRT	Hand M1 (left or right side randomly determined) F8C Magstim Super Rapid^2	Non-treated side	20	90% RMT (APB)	1,800 (2-s trains; 9,000) 30 min 5–5 d	28	Admission and 5w post: **Motor**: -NLI, AIS for UE and LE -Muscles Power: grasp strength, fingertip and lateral pich -JTHFT: WT (time) and total score -OFDT No side effect
Calabrò et al. (2017)	1	T10 C	20 mo	**rTMS** Real vs. sham + Lokomat (Single-case report)	Leg M1 (vertex) Double cone coil Magstim Super Rapid^2	(Lokomat alone: 40 sessions, 8 w)	10	90% RMT (TA)	1,200 pulses (60 2-s bursts, 20 pulses; 10,800) 12 min 9–3/w–3 w	10 s	Before, after treatment (post Lokomat): **Motor**: -ASIA -LEMS -Hip and knee F/E force and stiffness -LokomatPro guidance force **Corticospinal excitability**: -RMT -MEP amplitude (TA) -CCT -MUNE (vastuslateralis) No significant side effect

(Continued)

TABLE 1 | Continued

Study article	Number of participants n	Deficit level AIS	Time since injury d: days mo: months y: year	Trial protocol	Target Coil type TMS device	Control condition (if any)	TMS frequency (Hz)	TMS intensity (%)	Number of pulse/ session (total) Duration of one session Number of sessions	ITI	Measured outcomes Side/Adverse effects reported (n#, if any) NR : not reported
Fawaz et al. (2019)	22	C5–C7 NR	>6 mo	**rTMS** Real vs. sham + FES (RCT)	Hand M1 (APB) NR Magstim Super Rapid[2]	Coil angled at 90°, far from M1	10	90% RMT	1,500 (2-s trains, 30 trains; 15,000) 13 min 30 10–5 d–2 w (Different stimulation parameters for sham)	25 s	Before, after treatment: **Motor**: -AIS -MRC -ARAT -mSHFT -9HPT -Finger tapping test **Corticospinal excitability**: -MEP amplitude -Surface EMG **Independence**: -FIM NR
Hodaj et al. (2018)	1	T9-T10	24 y	**rTMS** (Single-case report)	Vertex F8C MagPro	NR	10	80% RMT (TA)	2,000 (5-s trains, 40 trains of 50 pulses; 24,000) 20 12–5d–2 w + 2d–3rd week + maintenance sessions at 4, 6, 8 w	25 s	Before and after, 6 w after last session: **Motor**: -Daily walking distance (pedometer) **Independence**: -SF-36 NR

(Continued)

TABLE 1 | Continued

Study article	Number of participants n	Deficit level AIS	Time since injury d: days mo: months y: year	Trial protocol	Target Coil type TMS device	Control condition (if any)	TMS frequency (Hz)	TMS intensity (%)	Number of pulse/ session (total) Duration of one session Number of sessions	ITI	Measured outcomes Side/Adverse effects reported (n#, if any) NR : not reported
Nogueira et al. (2020)	1	T8 D	8.5 y	**rTMS** rTMS+BWSTT (Single-case report)	Leg M1 (vertex) F8C Magstim Super Rapid	NR	15	90% RMT (FDI)	1,800 pulses (4-s trains; 21,600) 24 min 12	28 s	Before, after treatment: **Motor**: -AIS -LEMS -WISCI-II **Spasticity**: -MAS **Independence Measures** -Short-term form Health Survey -Patient Global Impression of change scale -SCIM III No significant side effect
Benito et al. (2012)	17	C4–T12 D	3–12 mo	**rTMS** Real and sham + CRT (RCT)	Leg M1 (vertex) Double cone coil Magstim Super Rapid	Double cone coil disconnected Connected F8C under pillow	20	90% RMT (UE muscle with the lower threshold)	1,800 pulses (2-s burst, 40 pulses; 27,000) 20 min 15–3 w, 3 w WO	28 s	Before, after sham/treatment, 2w FO: **Motor**: -LEMS (ASIA) -WISCI-II -10MWT: Gait velocity, step length, cadence -TUG **Spasticity**: **-**MAS Facial muscle twitching (6/10)

(Continued)

TABLE 1 | Continued

Study article	Number of participants n	Deficit level AIS	Time since injury d: days mo: months y: year	Trial protocol	Target Coil type TMS device	Control condition (if any)	TMS frequency (Hz)	TMS intensity (%)	Number of pulse/ session (total) Duration of one session Number of sessions	ITI	Measured outcomes Side/Adverse effects reported (n#, if any) NR : not reported
Zhao et al. (2020)	48	C4–L5 A—D	7d–2.3 mo	**rTMS** Real &vs. sham + CRT (RCT)	Hand M1 F8C CCY-1 stimulator	Sham coil	10	90% RMT (FDI)	1,500 (1.5-s trains, 15 pulses; 27,000) 7 min 30 18–6d/w–3 w	3 s	Before, after treatment: 3 d, 3 w **Biological measures**: -Levels of BDNF -Levels of NGF **Corticospinal excitability**: -MEP latency -MEP max amplitude Discomfort: reversible periods of numbness, facial muscle twitching (4/24)
Ji et al. (2015)	19	C4–T9 C, D	1–6 mo	**rTMS** Real vs. sham + CRT (RCT)	Leg M1 (left or right abductor hallucis muscle, with the lowest threshold) F8C Magstim Super Rapid^2	Sham coil	10	80% AMT (AH)	2,400 (2-s trains; 48,000 biphasic pulses) 20 min 20–5d/w–4 w	8 s	Before, after treatment (4w): **Corticospinal excitability**: -MNCV -MEP latency -MEP amplitude NR
Kim and Lee (2020)	16	T—L D	>6 mo 3.2 ± 1.23 mo 3.1 ± 1.3 mo	**rTMS** Real vs. sham + treadmill training (RCT)	Leg M1 (vertex) F8C Magstim Super Rapid^2	Tilted coil (90 degrees)	20	100% RMT (extensor hallucis longus)	12,000 (10-s bursts; 240,000) 20 min 20–5 d, 4 w	10 s	Before, after treatment: **Motor**: -10MWT -6MWT -CWT NR

(Continued)

TABLE 1 | Continued

Study article	Number of participants n	Deficit level AIS	Time since injury d: days mo: months y: year	Trial protocol	Target Coil type TMS device	Control condition (if any)	TMS frequency (Hz)	TMS intensity (%)	Number of pulse/ session (total) Duration of one session Number of sessions ITI	Measured outcomes Side/Adverse effects reported (n#, if any) NR : not reported
Leszczyńska et al. (2020)	15	C4–T2 B—D	5 mo–1 y	**rTMS** Bilateral rTMS + CRT (Longitudinal design)	Thumb and leg M1 Circular coil MagPro R30, R100 (MagOption)	NA	20–22	70–80% RMT	1,600 (2-s burst, 40 pulses, 800*2; 32,000) 10 min **(*2)** 20–3–5/w–5 mo Individually designed parameters 28 s	Before, after treatment **Corticospinal excitability**: -MEP amplitude -active and resting sEMG No significant side effect
Lee and Cha (2020)	14	C5–T12 D	>6 mo 4 ± 2.53 mo 5 ± 1.38 mo	**rTMS** Real vs. sham + CRT (RCT)	Leg M1 (vertex) F8C Magstim Super Rapid[2]	Tilted coil (90 degrees)	20	90% RMT (BB)	1,600 pulses (2-s bursts; 32,000) 20 min 20–5 d–4 w 28 s	Before, after treatment: **Motor**: -10MWT -CWT **Spasticity**: -MAS -SCAT NR

(Continued)

TABLE 1 | Continued

Study article	Number of participants n	Deficit level AIS	Time since injury d: days mo: months y: year	Trial protocol	Target Coil type TMS device	Control condition (if any)	TMS frequency (Hz)	TMS intensity (%)	Number of pulse/ session (total) Duration of one session Number of sessions	ITI	Measured outcomes Side/Adverse effects reported (n#, if any) NR : not reported
Kumru et al. (2016)	31	C2-T12 C, D	0.5–6 mo	**rTMS** Real &vs. sham + Lokomat training + CRT (RCT)	Leg M1 (vertex) Double cone coil Magstim Super Rapid	Double cone disconnected Connected F8C under pillow	20	90% RMT (FDI, APB/BB with the lowest threshold, less affected UE)	1,800 pulses (2-s burst, 40 pulses; 36,000) 20 min 20–20 d–4 w (Lokomat 4 w more after the end of rTMS)	28 s	Before, after treatment (4 w), 4 w FO: **Motor**: -LEMS -UEMS -10MWT Gait velocity, step length, cadence -WISCI-II **Spasticity**: **-**MAS Mild discomfort: facial twitching, difficulty to speak (8/15), mild headache (1/15)
Sato et al. (2018)	1	C6 D	67 d	**rTMS** Real + CRT (Single-case report)	Leg M1 (less affected TA) Double cone coil MagPro R30	NR	10	110% RMT (TA)	3,000 (1,500*2, 10-s trains, 100 pulses; 90,000) 15 min (*2) 30–15 d, 2 w	50 s	Before, after treatment **Motor**: -ASIA -muscle strength -calf circumference **Spasticity**: -MAS **Independence**: -SPPB -ABMS-2 -FIM No adverse effect reported

The studies are sorted by the number of rTMS sessions studied (smallest to largest). *Not explicitly reported parameters that may have been calculated from the available information are highlighted in yellow. Abbreviations: AB, able-bodied individuals; RCT, randomized controlled trial; FDI, first dorsal interossei; BB, biceps brachi; APB, abductor pollicis brevis; ECR, extensor capri radialis; A/RMT, active/resting motor threshold; w, weeks; WO, wash-out period; ITI, inter-train interval; UE, upper-extremity; RTP, repetitive task practice; CRT, conventional rehabilitation therapy; BWSTT, body weight-support treadmill; FO, follow-up period; NA, non-applicable. Those related to the outcomes used are outlined in* ***Table 2***.

TABLE 2 | List and description of the outcomes and measures used in the rTMS studies.

	Description and scoring	ICF Domain/ measurement domain
Clinical measures		
American spinal injury association (ASIA) scale (AIS)	Level and severity of the injury (A to D; ISNCSCI 2019 - American Spinal Injury Association, 2019) UE and LE measures: no contraction (0) to normal resistance (5) UEMS: /50 LEMS: /50	Body function Motor and Sensory
Walking index for spinal cord injury (WISCI, WISCI-II)	Walking independence, functional mobility, and walking. Type, amount of assistance and device needed (Ditunno et al., 2013). Scores: unable to walk (0) to independent walking (20)	Activity Motor
Upper-extremity function		
Nine-hole pegboard test (9HPT, NHPT)	Finger dexterity (Huertas-Hoyas et al., 2020). Time taken to complete the test activity (s) Number of pegs placed during 50 or 100 s.	Body function, activity Motor
Jebsen-Taylor hand function test (JTHFT)	Fine and gross motor hand function using simulated ADL (Huertas-Hoyas et al., 2020) Time taken to complete the test (s)	Participation Motor
Action Research Arm Test (ARAT)	Upper extremity performance (coordination, dexterity and functioning; Hsieh et al., 1998). A 4-point ordinal scale: (0) to maximum and better performance (57)	Activity Motor
Pinch, grasp strength test	Measure the maximum isometric strength of the hand and forearm muscles when doing a pinching/grasping action Testing is repeated 3 times and an average is calculated (kg, lbs)	
Lower-extremity function		
10-meter walk test (10-MWAT)	Functional mobility, gait and vestibular function (Amatachaya et al., 2014) Gait speed (m/s) during 10 meters walk.	Activity Motor
Community walk test (CWT)	LE functioning and mobility Time to walk 300 m in the community with no (1) or quadruped cane (6) aid	Activity Motor
Short physical performance battery (SPPB)	Balance, lower extremity strength, and functional capacity (Ronai and Gallo, 2019) 3 items: no (0) to maximum (12) Balance, gait speed test, chair stand test	Activity
Spasticity		
Modified Ashworth scale (MAS)	UE and LE spasticity and resistance to passive movement of a joint with varying degrees of velocity (Pandyan et al., 1999). No increase of muscle tone (0) to rigid parts in flexion or extension (4)	Body structure and function Motor
Spinal Cord Assessment Tool for Spastic reflexes (SCAT)	Spastic LE behavior (Akpinar et al., 2017) Clonus (0, no reaction to 3, severe lasting >10 s) Flexor spasms (0, no reaction to 4, severe with >30° of hip and knee flexion) Extensor spasms (0, no reaction to 4, severe with >30° of hip and knee flexion)	Body structure and function Motor
Quality of life (QOL) and daily living (DL)		
Short-term form Health Survey (SF-36)	Health status in the Medical Outcomes Study (Ware and Sherbourne, 1992) 36 questions, 8 domains of health Total score indicating a range of low to high QOL	Participation Quality of life
Patient Global Impression of change scale (PGICS)	All aspects of patients' health: improvement or decline in clinical status. no change (1) to considerable improvement (7)	ADL, quality of life
Functional independence measures (FIM)	level of patients' disability (level and function) and amount of assistance needed to carry out ADL (Sivan et al., 2011) 13 motor tasks and 5 cognitive tasks Independence: complete dependence (0) to complete independence (7) Level of function: lowest (18) to highest (126)	Activity ADL, motor, cognition
Corticospinal excitability		
RMT/AMT	Excitability of the central core of the corticomotor neurons and their membrane excitability (Nardone et al., 2015). %MSO	
MEP	Corticospinal excitability, cortico-muscular conduction (Nardone et al., 2015) At rest or during active muscle contraction Mean/max amplitude or area, latency	
Hoffmann reflex (H-reflex)	Spinal excitability. Modulation of monosynaptic reflex activity in the spinal cord (Knikou, 2008).	

Abbreviations: U/L EMS, upper/lower-extremity motor scores; QOL, quality of life; R/A MT, resting/active motor threshold; MSO, maximum stimulator output; MEP, motor evoked potential.

individual, 8.5 years after his injury (Nogueira et al., 2020). Definite beneficial effects of HF-rTMS on LE functions and spasticity were also confirmed in two randomized, placebo-controlled, and parallel trials (Kim and Lee, 2020; Lee and Cha, 2020) where significant clinical improvements were observed in chronic iSCI compared to sham group. Kim and collaborators study (Kim and Lee, 2020) study used a *higher intensity of stimulation (100% RMT)* and the *combination with treadmill training*.

Quality of Life and Side/Adverse Effects

Several studies were also interested in investigating HF-rTMS effects on ADL and QOL. Most of these were single-case studies (Hodaj et al., 2018; Sato et al., 2018; Nogueira et al., 2020) and reported beneficial effects with increases in SF-36 scores. A *high-frequency* and *intensity (10 Hz, 110% RMT)* protocol *associated with rehabilitative training* and *repeated over 30 sessions*, was demonstrated to be safe and to produce motor functional recovery in one subacute patient with incomplete, cervical injury (Sato et al., 2018). Fawaz et al. (2019) reported significant increases of FIM scores in 22 cervical and chronic SCI participants (Fawaz et al., 2019); increases reported to be significantly higher for the group for whom functional electrical stimulation (FES) was combined with real rTMS compared to the group where sham rTMS was used instead.

Globally, rTMS interventions were reported safe and well-tolerated by SCI participants with no serious and significant SE and AE. Only mild rTMS-related discomfort was reported (**Table 1**, 6 over 20 studies). The most common SE were facial muscle twitching during the real rTMS sessions (Kumru et al., 2010, 2016; Benito et al., 2012; Jetté et al., 2013; Zhao et al., 2020) and transient headaches (Gomes-Osman and Field-Fote, 2015; Kumru et al., 2016). These side effects were reported in a small number of participants.

rTMS Protocols Parameters Description

Each study used a specific combination of parameters for its rTMS intervention. The protocol designs are reported in **Table 1**. Some parameters were not explicitly reported (e.g., session duration), we thus reported and highlighted in yellow in **Table 1** the parameters that could be inferred or calculated from the available information. The frequency analysis in **Table 3** was performed for a selection of 10 rTMS protocol parameters and characteristics, each of which was divided into two or three subcategories. Among the 20 total included studies (N total), the single-case studies (3) (Calabrò et al., 2017; Hodaj et al., 2018; Sato et al., 2018; Nogueira et al., 2020) and the published clinical trial (1) (de Araújo et al., 2017) have not been considered. The study from Jetté et al. (2013) investigating both the leg and hand conditions separately was counted twice, bringing the number of studies included in the frequency analysis to 16 (N studies included). Eleven of the 16 studies assessed the clinical and/or neurophysiological effects of the intervention (assessed) and five did not assess either of the effects (not assessed; first row, **Table 3**). The same rationale was used for counting the number of relevant studies in all the subcategories. The study frequency calculation in each subcategory was described above (Methods—additional analysis). The results are presented in **Table 3**. The main purpose of this exploratory analysis is to clarify what has been done (or less done) in this emerging research field and to try to summarize the main results, according to the rTMS parameter used, which are discussed in more details in the section below.

DISCUSSION

Our review confirms previous work about the seeming effectiveness of HF-rTMS to promote motor improvements and CSE changes in SCI. All the group studies reported significant improvements for at least one of the outcomes considered (cf **Table 3**). Interestingly, beneficial effects were reported in most studies despite the multiplicity and variability of the protocol designs used.

The observed effects of rTMS on sensorimotor function and spasticity in SCI individuals are thought to be due mainly to the rTMS-induced changes in CSE and CS connectivity (Gomes-Osman, Belci, Kumru, Sato) together with effects on cortical inhibition (Belci et al., 2004) resulting in alteration of spinal and supraspinal circuits and excitability (Nardone et al., 2014a). The excitability changes and plasticity-related phenomena are thought to be mediated through NMDA receptors (Rossini et al., 2015) and to involve several biological mechanisms such as synaptic plasticity (sprouting of new axons, guidance of axons to targets), remyelination, and spinal plasticity modulation as well as cell death limitation, cell regeneration, and replacement. Such effects are supported by increases in serum levels of neurotrophic factors such as BDNF and NGF (Min Hwang et al., 2014; Fujiki et al., 2020; Zhao et al., 2020).

Most rTMS studies in SCI showed promising and lasting functional gains, associated or not with neurophysiological changes (**Table 3**). However, **the relative novelty of the field in SCI and** the limited number of RCTs and the wide range of rTMS protocol design and parameters used precluded us, at this time, from performing a meta-analysis and drawing definite conclusions. An exploratory frequency analysis allowed us however to have some insights on the parameter settings that may maximize a particular symptom recovery.

The inter- and intra-individual variability in response to TMS and to NIBS, in general, is widely reported and studied in the literature (Sale et al., 2007; López-Alonso et al., 2014; Ovadia-Caro et al., 2019; Guerra et al., 2020). In able-bodied individuals, key influence factors were identified such as baseline MEP amplitude stimulus intensity and target muscle (Corp et al., 2020, 2021). It is likely that an inter- and intra-individual variability of NIBS response also exists in SCI, and that specific stimulation parameter changes can have a critical effect on the generated plasticity processes and the neurophysiological and/or clinical effects observed. In the next section, we will discuss the potential key source influencing the rTMS response in SCI, focusing first on the technical parameters and then describing other parameters, more related to the design of the rTMS and associated-rehabilitation sessions or to the participants themselves. We conclude by making some recommendations for the design and reporting of future rTMS studies in SCI.

TABLE 3 | Study frequency table.

	Clinical Effect					Neurophysiological effect		
	N total (%)	N studies included	Assessed not assessed	Significant (%)	Not significant (%)	Assessed/ not assessed	Significant (%)	Not significant (%)
Overall	20	16	11/5	9 (82)	2 (18)	11/5	5 (45)	6 (55)
Number of sessions								
1–5 (<1 week)	8 (40)	8	6/2	5 (83)	1 (17)	7/1	2 (29)	5 (71)
9–30 (≥1 week)	12 (60)	8	5/3	4 (80)	1 (20)	4/4	3 (75)	1 (25)
Session duration								
<20 min	6 (30)	4	3/1	2 (67)	1 (33)	4/0	3 (75)	1 (25)
≥20 min	14 (70)	12	8/4	7 (88)	1 (22)	7/5	4 (57)	3 (43)
Number of Pulses								
<1,600	6 (30)	5	4/1	3 (75)	1 (25)	5/0	2 (40)	3 (60)
≥1,600	14 (70)	11	7/4	6 (86)	1 (14)	6/5	3 (50)	3 (50)
Inter-train interval								
<28 s	10 (50)	8	4/4	1 (25)	3 (75)	7/1	4 (57)	3 (43)
≥28 s	10 (50)	8	7/1	6 (86)	1 (14)	4/0	1 (25)	3 (75)
Stimulation Frequency								
HF (≤10 Hz)	11 (55)	8	4/4	3 (75)	1 (25)	8/0	4 (50)	4 (50)
vHF (>10 Hz)	9 (45)	8	7/1	6 (86)	1 (14)	3/5	1 (33)	2 (77)
Stimulation Intensity								
Below (<100% MT)	17 (85)	14	9/5	8 (89)	1 (21)	10/4	5 (50)	5 (50)
At/above (≥100% MT)	3 (15)	2	1/1	1 (100)	0 (0)	1/1	0 (0)	1 (100)
Coil Type								
F8C	11 (55)	9	5/4	4 (83)	1 (17)	6/3	2 (33)	4 (67)
Circular	2 (10)	1	1/0	1 (100)	0 (0)	2/0	2 (100)	0 (0)
Double	6 (30)	4	4/0	3 (75)	1 (25)	2/2	0 (0)	2 (100)
NR	1 (5)	-	-	-	-	-	-	-
TMS device								
Magstim Super Rapid^2	16 (80)	12	10/2	8 (80)	2 (20)	9/3	4 (44)	5 (56)
MagPro	3 (15)	1	0/1	-	-	1/0	1 (100)	0 (0)
CCY-1 Stimulator	1 (5)	1	0/1	-	-	1/0	0 (0)	1 (100)
Use of Neuronavigation								
No	18 (90)	13	11/2	9 (82)	2 (18)	8/5	4 (50)	4 (50)
Yes	2 (10)	3	0/3	na	na	3/0	1 (33)	2 (67)
Associated Rehabilitation								
No	8 (40)	6	4/2	3 (75)	1 (25)	6/0	2 (33)	4 (67)
Yes	12 (60)	10	7/3	6 (86)	1 (14)	5/5	3 (60)	2 (40)

N total: total number of studies reviewed (n =20). N studies included: total number of studies where the parameters could be extracted and effects were described (the clinical trial and single-case studies were excluded and the study with two separated conditions was counted twice, n = 16); among which assessed or not the cited effect (clinical/neurophysiological). HF, high-frequency; vHF, very high frequency; MT, motor threshold; F8C, figure-of-eight coil.

rTMS Technical Parameters

The **session duration** and the **number of sessions** are important factors to consider. Indeed, increased stimulation duration was shown to induce a more consistent increase in regional glucose metabolism and increase of neuronal activity in the stimulated area (Siebner et al., 2000; Thomson et al., 2011). Most studies (60% and 70%) used longer protocols (>1 week), with 20 min or higher duration per session. Increasing the number of sessions seems beneficial regarding both clinical and neurophysiological effects whereas, longer stimulation sessions had significant clinical effects (86%) with mixed results for neurophysiological effects (57%). However, few studies tested sessions shorter than 20 min (30%). Belci et al. (2004) used a 30 min rTMS protocol with significant and lasting effects on motor function and CS inhibition (Belci et al., 2004). One study out of the 20 reviewed reported the effect of single session of HF-rTMS on pain and CSE in chronic SCI (Jetté et al., 2013). Two others observed effects on spasticity and CSE after the first session of their repeated protocol (Kumru et al., 2010; Nardone et al., 2014a). No authors studied the effect of a single-session of HF-rTMS on motor function after SCI. Understandably, multiple sessions seem to be appropriate for maintaining the excitability and clinical effects (Benito et al., 2012; Kumru et al., 2016; Hodaj et al., 2018) and a higher number of training sessions with stimulation (≥1 week) is more likely to be associated with greater changes (Ji et al., 2015; Kim and Lee, 2020). However, quantifying the effect of a single session could provide important information on the mechanisms of effects obtained from multiple sessions.

The **number of pulses** and **duration of trains** delivered during a stimulation protocol is also critical to determine the after-effects of rTMS. Short trains were shown to decrease MEP whereas long trains increased MEP (Modugno et al., 2001; Peinemann et al., 2004). A small number of pulses (240) was also shown to produce less significant and consistent rTMS modulation effects in comparison with a larger number of pulses (1,600) (Maeda et al., 2000). The authors stated that 1,000 pulses or more might be needed to produce consistent rTMS effects. In SCI, three studies reported the use of a similar protocol in terms of daily stimulation pulses administration (720–900) and an overall number of sessions (3 to 4) on hand motor function

(Belci et al., 2004; Kuppuswamy et al., 2011; Gomes-Osman and Field-Fote, 2015). Kuppuswamy et al. (2011) and Gomes-Osman and Field-Fote (2015) reported only modest changes compared to baseline, which were not different from sham intervention. In Kuppuswamy et al. (2011) the modest improvement might be also explained by the more heterogeneous study population in terms of lesion severity and time since injury. Among the reviewed articles, 70% of the studies used a higher number of pulses (>1,600 pulses) with mostly beneficial clinical (86%) and neurophysiological effects (**Table 3**). Four of them (Kumru et al., 2010, 2016; Benito et al., 2012; Nardone et al., 2014a) used a high number of pulse rTMS protocols (1,600–1,800) at 20 Hz during a 20 min intervention at 90% RMT and reported significant improvements in LE function and spasticity in SCI.

The rTMS after-effects depend on the interval between bursts of pulses, i.e., the **inter-train interval (ITI)**. It was shown that rTMS delivered continuously can be responsible for the reversal of the net effect from increased to decreased CSE (Rothkegel et al., 2010), explained by a hysteresis phenomenon and neuronal excitability saturation. The included studies used non-continuous stimulation with a wide range of ITI ranging from 3 s to 50 s. Those with an ITI $\geq$ 28 s seemed to more likely result in significant clinical effects (86% vs. 25% for ITI <28 s) while surprisingly the opposite is true for the neurophysiological effect. Shorter ITIs were shown to result in greater disinhibitory effects whereas longer breaks between trains might lead to a normalization of CSE due to increased cortical inhibition before the occurrence of the next burst reducing the effect summation of repeated bursts (Cash et al., 2017; Pitkänen et al., 2017).

Regarding **stimulation intensity**, only a few studies (N = 3) tested intensity at or above the threshold (Jetté et al., 2013; Sato et al., 2018; Kim and Lee, 2020). Most of the studies (85%) used an intensity below the threshold at 80%–90% R/AMT. Sato and collaborators used a protocol with 3,000 pulses delivered at an intensity of 110% RMT over 15 sessions and reported the safety and feasibility of such high-intensity, HF-rTMS protocol in one subacute SCI patient. The more intense stimulation would produce more enhancement of spinal longitudinal neurons, would stimulate broader cortical regions, and elicit faster temporal-spatial summation on corticospinal-motoneuron connections (Fitzgerald et al., 2002; Rossini et al., 2015). A parallel RCT confirmed the benefit of stimulating at higher intensity, with a significantly greater effect of real HF-rTMS administered at 100% RMT compared to sham on LE function of 16 iSCI participants at 6 months post-injury (Kim and Lee, 2020). The tested protocol also used a higher total number of pulses (12,000) at very high frequency (20 Hz) and combined with treadmill training. The benefit of using suprathreshold intensity needs to be further investigated. Leszczyńska et al. (2020) developed an algorithm to decide the optimal stimulation intensity based on SCI participants' individual responses to TMS. Such individualized stimulation parameters may be an option to consider in the future; the procedure used to decide the parameters however needs to be detailed with accurate reporting of the results.

Pulse frequency was shown to be the major driver of the MEP change (Rodger et al., 2016). Also, high- (10 Hz; Dall'Agnol et al., 2014) but not low-frequency (1 Hz) rTMS was shown to increase BDNF levels (Mirowska-Guzel et al., 2013). This may explain why all the studies included in this review showed mostly beneficial effects. However, even if a wide range of high frequencies seems to provide consistent effects, the frequency-dependent increase in CSE due to rTMS at the group level was less clear at the individual level (Maeda et al., 2000). High- to very high-frequency rTMS (5–22 Hz) have generated both CSE and/or clinical beneficial effects in SCI individuals. However, to draw definite conclusions about the usefulness of rTMS in SCI, it may be worthwhile to also study the effects of LF-rTMS; especially given the possibly harmful hyperexcitability and increased inhibition that has been described after SCI (Petersen et al., 2012; Nardone et al., 2015) and that can be reversed by the administration of LF-rTMS protocols.

The **type of coil** influences the stimulated area. The double-cone coil seems to provide a deeper, stronger, and wider electric field (EF), but is also less focal compared to the one produced by a F8C (Lontis et al., 2006; Lefaucheur, 2019); which provides a deeper and more extensive magnetic field over the cerebral cortex than the usual circular coil (Lontis et al., 2006; Sato et al., 2018). A significant difference in MTs between F8C and double-cone coil for rTMS has been observed in patients with refractory depression, with systematically higher MT obtained with F8C (Miron et al., 2018). Targeting a wider area with a double-cone coil may be more appropriate for tetraplegic SCI patients. It is also important to keep in mind that when targeting the LE with a double-cone coil, one could also affect UE function (Kumru et al., 2016). In the literature surveyed here, F8C was the most used coil (55%) and the double cone coil was used in studies targeting LE and spasticity symptoms. Both were associated with mostly beneficial clinical effects in SCI. Modeling of the EF induced by different coil designs, achieved with newly developed tools (Saturnino et al., 2019; Aberra et al., 2020), may be useful to obtain additional information. Indeed, the head and EF modeling during brain stimulation can provide a better understanding of the rTMS underlying mechanisms, eventually, explaining the variability of the after-effects observed, and ultimately help to individually optimize the rTMS interventions (Konakanchi et al., 2020; Mosayebi-Samani et al., 2021). For example, it was demonstrated that the effect variability of a transcranial alternating current stimulation (tACS) intervention can be significantly predicted by measures derived from individual EF modeling (i.e., EF' strength and spatial distribution; Kasten et al., 2019). It is reasonable to expect similar results with other NIBS such as rTMS, hence the need to include EF modeling in stimulation studies, especially those involving people with an injured central nervous system (Rossi et al., 2020; Mosayebi-Samani et al., 2021).

Methods Used to Define and Assess rTMS Protocols

The **stimulation site**, or **hotspot of stimulation**, is a key factor that is chosen depending on the effect sought. The local neurophysiological changes and the associated clinical effects

depend on the targeted cerebral area. It is important to keep in mind that when targeting the motor cortex (hand, arm, or leg M1), it is very likely to impact additional adjacent and remote connections and areas such as S1 (Belci et al., 2004; Kuppuswamy et al., 2011), due to the extended EF induced by the stimulation. This may explain the effects observed on sensory function (Belci et al., 2004) and the non-targeted side (Gomes-Osman and Field-Fote, 2015; Choi et al., 2019). Such bilateral and sensory effects may be of interest in SCI, given that stimulating the sensory cortex could have also benefit recovery (Pleger et al., 2006).

The rTMS intensity is often based on and defined at a specified percentage level of the **participant's motor threshold** (e.g., 120% RMT). Resting or active (R/AMT, obtained with the muscle slightly contracted) MT determination is thus an important first step in the design of the rTMS protocol (Rossi et al., 2009; Lefaucheur, 2019). All the studies included in this review used this method to define their protocol. However, it can be difficult to measure the MT of the muscle to be targeted, particularly in individuals with disrupted motor pathways where MT may be very high or even absent. Researchers may then choose another **muscle for MT measurement** (in 15 studies, **Table 1**, column 9) which may lead to less optimal selection of stimulation intensity. Indeed, this procedure, although convenient for dealing with the MT problem, can result in insufficient (or too high) excitation of the CS specific projections of the targeted muscle leading to an absence or over-estimation of the effects which can bias the results. An alternative and standardized procedure needs to be defined for cases of absent MT.

The **targeted muscle** is chosen based on the specific population studied and the therapeutic goal. The optimal current direction on the stimulating site and thus coil orientation may vary based on the specific muscle targeted (Bashir et al., 2013; Corp et al., 2020). For example, the FDI muscle seems to be best activated with postero-anterior (PA) current (Corp et al., 2020).

Different methods were used to assess the rTMS effects in SCI (**Table 2**), which may explain the lack of consistency of some results. **Outcome measures** must be adapted to the study goal and be able to detect subtle changes. The clinical scale and functional outcomes commonly used in SCI studies are highly reliable (AIS, UEMS, ARAT) but may be not sensitive enough to highlight the complexity of the changes in response to modulatory interventions such as rTMS. Some neurophysiological parameters have shown poorer reliability in SCI individuals due to the injury induced-change in plasticity, especially in muscles with lower MRC (Medical Research Council, Muscle Scale) grade (Sydekum et al., 2014; Potter-Baker et al., 2016). Metrics measured from UE proximal muscle were also shown to be less reliable compared to distal ones, which may be due to the smaller cortical representation of proximal compared to distal muscle (Sankarasubramanian et al., 2015) making the latter a preferable target for rTMS. The collection of TMS metrics during a slight voluntary contraction is a known option to improve reliability. The reported dissociation between the clinical and neurophysiological changes reported by some studies (Kumru et al., 2010; Kuppuswamy et al., 2011) may be explained by the complex pathophysiology of the disease or symptom, the use of subthreshold rTMS and/or specific medication (Kumru et al., 2010) and/or the poor reliability of the neurophysiological metric, associated with a decrease of statistical power. However, such dissociation may also reveal the absence of a causal relationship between the local neuro-electrophysiological changes and the observed clinical improvements; these may be also mediated by distant effects. The relationship between neurophysiological changes and functional recovery induced by rTMS should be more consistently investigated.

The **combination of rTMS with training** or **other clinical interventions** was reported in 60% of the studied included in the review. The combination approach compared to clinical intervention alone demonstrated additional clinical and neurophysiological beneficial effects (**Table 3**). The added value of rTMS was demonstrated when combined with conventional rehabilitation therapy (CRT), repetitive task practice (Gomes-Osman and Field-Fote, 2015), FES (Fawaz et al., 2019), robotic (Lokomat) training (Kumru et al., 2016; Calabrò et al., 2017), and body weight-supported treadmill walking training (BWSTT; Kim and Lee, 2020; Nogueira et al., 2020). By priming the motor cortex, rTMS could be responsible for increased facilitation induced by specific motor training (Gunduz et al., 2017). These results confirm the potential of rTMS as an adjunct to the SCI rehabilitation therapy.

Participants' Characteristics

Many individual factors may influence the rTMS modulatory response (Ridding and Ziemann, 2010; López-Alonso et al., 2014). **Age** is the most common and widely described source of variability factor, with older participants known to show reduced potential for induced plasticity changes in response to NIBS. Individuals with SCI are usually young adults and thus exhibit a greater potential for response to rTMS and NIBS in general. The **stage and severity of the disease** may also have an influence (Jetté et al., 2013; Versace et al., 2018). Subacute and incomplete SCI individuals may have an increased potential for functional recovery and may respond better to rTMS protocols in comparison to chronic and stable SCI, who may show an activity-dependent cortical and maladaptive plasticity (Eckert and Martin, 2017). Six studies out of 20 investigated subacute SCI (1 week to 6 months; Benito et al., 2012; Ji et al., 2015; Kumru et al., 2016; Sato et al., 2018; Choi et al., 2019; Zhao et al., 2020) and three included motor and sensory complete SCI (AIS A). These studies reported the feasibility and tolerability of rTMS even at early stages and in case of severe deficits.

Individuals with different medical conditions and medications respond differently to rTMS (Leung et al., 2009). The inter-individual variability in the anatomy of the motor cortex may also reflect individual differences in the circuits activated by rTMS. All these can influence the **initial brain-state**, a well-known source of variability in response to TMS/rTMS (Bergmann, 2018). Indeed, it was observed that extreme baseline MEP values, a key factor in the TMS response,

could also be partly attributable to the initial state of MEP hyperexcitability during TMS sessions (Corp et al., 2021). This initial brain state depends on the **time of the day**, the **time taken to carry out some measures**, or the **previous administration of rehabilitation therapy**.

To address the inter-individual variability issue, one option is to recruit a homogeneous **participant population** in terms of injury location, severity, and time since injury. This was often the case of the articles included in the review (Benito et al., 2012; Nardone et al., 2014a; Choi et al., 2019; Lee and Cha, 2020). To address the issue in SCI, Leszczyńska et al. (2020) reported the use of an algorithm, based on specific participant responses to single pulse TMS, to determine the rTMS parameters to use for each participant. Although the individual parameters were not explicitly reported, investigators showed a decrease in APB hand muscle spasticity associated with CSE increase. These changes were not observed for the non-targeted TA muscle.

CONCLUSION AND REMAINING GAPS IN rTMS AND SCI RESEARCH

Almost all the rTMS protocols tested in SCI resulted in promising beneficial neurophysiological and/or clinical changes (**Table 3**). No serious side effects were reported (**Table 1**). Administered over several sessions (> 1week), rTMS with high number of pulses (≥1,600) administered non-continuously at subthreshold intensity and high or very-high frequency, and in combination with other rehabilitation interventions, seems appropriate to induce maintained changes in SCI. This can be explained by the cumulative plastic changes induced by repeated episodes of long-term potentiation which lead to a persistent remodeling and reorganization of the stimulated and remote areas. Future directions may extend the research field to investigate the effects of suprathreshold intensity and/or low frequency rTMS and in subacute SCI individuals. The more systematic use of neuronavigation and reporting of hotspot coordinates and rTMS induced electric fields during treatment may help increase the understanding and reproducibility of the effects observed.

A complete and detailed description of the used rTMS protocols is important. Progress has been made since the emergence of this study field and TMS experts continue to provide useful recommendations to improve reporting and ultimately designing of more effective rTMS interventions (Rodger et al., 2016; Corp et al., 2020, 2021; Lefaucheur et al., 2020; Rossi et al., 2020). However, some parameters such as the duration of the session, the number of pulses, the pulse waveform, the time of day at which sessions were administered, and the level of participant attention, have not been systematically reported in SCI studies. All these are known to influence the stimulated circuits (Di Lazzaro et al., 2001; Corp et al., 2020). Only two studies reported the use of a neuronavigation system despite its importance especially during repeated-sessions designs (Bashir et al., 2011). This may be due to the high cost of the currently available systems. Some easy-to-use and costless alternatives have been proposed and seem to provide reliable results (Cincotta et al., 2010; WashaBaugh and Krishnan, 2016; Rodseth et al., 2017; Ambrosini et al., 2018). These systems can help the systematic reporting of hotspot coordinates and monitor coil shifts across the session (Corp et al., 2020; Corp et al., 2021).

The heterogeneity of outcome measures, the lack of RCTs and the inconsistent reporting of data and statistics (means and SDs) prevented us from performing a meta-analysis. Among all the reviewed studies, no publication reported negative or complete absence of rTMS effects. Even if this is encouraging and may be explained by the use of high-frequency designs, it may also indicate publication bias (Moher et al., 2009). Despite the importance of reproducibility studies, the reporting of negative or null results could help avoid multiplication of unnecessary studies and improvement of current protocols (Bespalov et al., 2019). Explicitly specifying primary and secondary outcomes may avoid outcome reporting bias with for examples elective outcome reporting (Moher et al., 2009).

The "one-fits-all" approach in the design of rehabilitation interventions is a disputed concept, especially in the NIBS field. Some TMS stimulation parameters may need to be individually tailored based on clinical or neurophysiological state. This idea is not new (Maeda et al., 2000) and was successfully tested in one SCI study (Leszczyńska et al., 2020). The addition of neuroimaging outcomes may also be useful. A recent study reported significantly improved clinical response to rTMS when depressive patients were treated closer to personalized connectivity-guided targets (Cash et al., 2021). At the end, the stratification of the individuals in the rTMS studies could help the selection of SCI individuals more likely to respond to specific rTMS interventions.

Overall, rTMS is non-invasive, relatively easy to administer and well-tolerated intervention with promising beneficial effects on functional recovery after SCI. It is safe, with very rare to no serious side effects (**Table 1**; Rossi et al., 2020) and is ultimately easy to implement in clinical practice. Newly designed protocols need safety and tolerability studies, especially in the vulnerable SCI population. The best timing, intervention duration and dosage need to be clarified depending on the stage and severity of the injury. Future investigations may also focus on developing strategies to design individually-targeted rTMS interventions.

AUTHOR CONTRIBUTIONS

NB performed the literature review and wrote the manuscript. DA and GF were involved in the discussion of the findings and provided critical revisions. SS, GY, and JZ provided critical revisions of the final manuscript. All authors contributed to the article and approved the submitted version.

FUNDING

This work was supported by the New York State Department of Health (C34462GG, PI: JZ) and the Tim Reynolds Foundation.

REFERENCES

Aberra, A. S., Wang, B., Grill, W. M., and Peterchev, A. V. (2020). Simulation of transcranial magnetic stimulation in head model with morphologically-realistic cortical neurons. *Brain Stimul.* 13, 175–189. doi: 10.1016/j.brs.2019.10.002

Akpinar, P., Atici, A., Ozkan, F. U., Aktas, I., Kulcu, D. G., and Kurt, K. N. (2017). Reliability of the spinal cord assessment tool for spastic reflexes. *Arch. Phys. Med. Rehabil.* 98, 1113–1118. doi: 10.1016/j.apmr.2016.09.119

Alizadeh, A., Dyck, S. M., and Karimi-Abdolrezaee, S. (2019). Traumatic spinal cord injury: an overview of pathophysiology, models and acute injury mechanisms. *Front. Neurol.* 10, 1–25. doi: 10.3389/fneur.2019.00282

Amatachaya, S., Naewla, S., Srisim, K., Arrayawichanon, P., and Siritaratiwat, W. (2014). Concurrent validity of the 10-meter walk test as compared with the 6-minute walk test in patients with spinal cord injury at various levels of ability. *Spinal Cord* 52, 333–336. doi: 10.1038/sc.2013.171

Ambrosini, E., Ferrante, S., van de Ruit, M., Biguzzi, S., Colombo, V., Monticone, M., et al. (2018). StimTrack: an open-source software for manual transcranial magnetic stimulation coil positioning. *J. Neurosci. Methods* 293, 97–104. doi: 10.1016/j.jneumeth.2017.09.012

Barker, A. T., Jalinous, R., and Freeston, I. L. (1985). Non-invasive magnetic stimulation of human motor cortex. *Lancet* 1, 1106–1107. doi: 10.1016/s0140-6736(85)92413-4

Bashir, S., Edwards, D., and Pascual-Leone, A. (2011). Neuronavigation increases the physiologic and behavioral effects of low-frequency rTMS of primary motor cortex in healthy subjects. *Brain Topogr.* 24, 54–64. doi: 10.1007/s10548-010-0165-7

Bashir, S., Perez, J. M., Horvath, J. C., and Pascual-Leone, A. (2013). Differentiation of motor cortical representation of hand muscles by navigated mapping of optimal TMS current directions in healthy subjects. *J. Clin. Neurophysiol.* 30, 390–395. doi: 10.1097/WNP.0B013E31829DDA6B

Belci, M., Catley, M., Husain, M., Frankel, H. L., and Davey, N. J. (2004). Magnetic brain stimulation can improve clinical outcome in incomplete spinal cord injured patients. *Spinal Cord* 42, 417–419. doi: 10.1038/sj.sc.3101613

Benito, J., Kumru, H., Murillo, N., Costa, U., Medina, J., Tormos, J., et al. (2012). Motor and gait improvement in patients with incomplete spinal cord injury induced by high-frequency repetitive transcranial magnetic stimulation. *Top. Spinal Cord InJ. Rehabil.* 18, 106–112. doi: 10.1310/sci1802-106

Bergmann, T. O. (2018). Brain state-dependent brain stimulation. *Front. Psychol.* 9:2108. doi: 10.3389/fpsyg.2018.02108

Bespalov, A., Steckler, T., and Skolnick, P. (2019). Be positive about negatives-recommendations for the publication of negative (or null) results. *Eur. Neuropsychopharmacol.* 29, 1312–1320. doi: 10.1016/j.euroneuro.2019.10.007

Bliss, T. V. P., and Cooke, S. F. (2011). Long-term potentiation and long-term depression: a clinical perspective. *Clinics (Sao Paulo).* 66, 3–17. doi: 10.1590/s1807-59322011001300002

Calabrò, R. S., Naro, A., Leo, A., and Bramanti, P. (2017). Usefulness of robotic gait training plus neuromodulation in chronic spinal cord injury: a case report. *J. Spinal Cord Med.* 40, 118–121. doi: 10.1080/10790268.2016.1153275

Cash, R. F. H., Cocchi, L., Lv, J., Wu, Y., Fitzgerald, P. B., and Zalesky, A. (2021). Personalized connectivity-guided DLPFC-TMS for depression: advancing computational feasibility, precision and reproducibility. *Hum. Brain Mapp.* 42, 4155–4172. doi: 10.1002/hbm.25330

Cash, R. F. H., Dar, A., Hui, J., De Ruiter, L., Baarbé, J., Fettes, P., et al. (2017). Influence of inter-train interval on the plastic effects of rTMS. *Brain Stimul.* 10, 630–636. doi: 10.1016/j.brs.2017.02.012

Choi, H., Seo, K. C., Kim, T. U., Lee, S. J., and Hyun, J. K. (2019). Repetitive transcranial magnetic stimulation enhances recovery in central cord syndrome patients. *Ann. Rehabil. Med.* 43, 62–73. doi: 10.5535/arm.2019.43.1.62

Cincotta, M., Giovannelli, F., Borgheresi, A., Balestrieri, F., Toscani, L., Zaccara, G., et al. (2010). Optically tracked neuronavigation increases the stability of hand-held focal coil positioning: evidence from "transcranial" magnetic stimulation-induced electrical field measurements. *Brain Stimul.* 3, 119–123. doi: 10.1016/j.brs.2010.01.001

Corp, D. T., K Bereznicki, H. G., Clark, G. M., Fried, P. J., Jannati, A., Davies, C. B., et al. (2021). Large-scale analysis of interindividual variability in single and paired-1 pulse TMS data: results from the "Big TMS Data Collaboration". *bioRxiv* [Preprint]. doi: 10.1016/j.clinph.2021.06.014

Corp, D. T., Bereznicki, H. G. K., Clark, G. M., Youssef, G. J., Fried, P. J., Jannati, A., et al. (2020). Large-scale analysis of interindividual variability in theta-burst stimulation data: results from the "Big TMS data collaboration". *Brain Stimul.* 13, 1476–1488. doi: 10.1016/j.brs.2020.07.018

Dall'Agnol, L., Medeiros, L. F., Torres, I. L. S., Deitos, A., Brietzke, A., Laste, G., et al. (2014). Repetitive transcranial magnetic stimulation increases the corticospinal inhibition and the brain-derived neurotrophic factor in chronic myofascial pain syndrome: an explanatory double-blinded, randomized, sham-controlled trial. *J. Pain* 15, 845–855. doi: 10.1016/j.jpain.2014.05.001

de Araújo, A. V. L., Barbosa, V. R. N., Galdino, G. S., Fregni, F., Massetti, T., Fontes, S. L., et al. (2017). Effects of high-frequency transcranial magnetic stimulation on functional performance in individuals with incomplete spinal cord injury: study protocol for a randomized controlled trial. *Trials* 18:522. doi: 10.1186/s13063-017-2280-1

Di Lazzaro, V., Oliviero, A., Mazzone, P., Insola, A., Pilato, F., Saturno, E., et al. (2001). Comparison of descending volleys evoked by monophasic and biphasic magnetic stimulation of the motor cortex in conscious humans. *Exp. Brain Res.* 141, 121–127. doi: 10.1007/s002210100863

Ditunno, J. F., Cohen, M. E., Hauck, W. W., Jackson, A. B., and Sipski, M. L. (2000). Recovery of upper-extremity strength in complete and incomplete tetraplegia: a multicenter study. *Arch. Phys. Med. Rehabil.* 81, 389–393. doi: 10.1053/mr.2000.3779

Ditunno, J. F., Ditunno, P. L., Scivoletto, G., Patrick, M., Dijkers, M., Barbeau, H., et al. (2013). The walking index for spinal cord injury (WISCI/WISCI II): nature, metric properties, use and misuse. *Spinal Cord* 51, 346–355. doi: 10.1038/sc.2013.9

Eckert, M. J., and Martin, M. J.. (2017). Trauma: spinal cord injury. *Surg. Clin. North Am.* 97, 1031–1045. doi: 10.1016/j.suc.2017.06.008

Ellaway, P. H., Vásquez, N., and Craggs, M. (2014). Induction of central nervous system plasticity by repetitive transcranial magnetic stimulation to promote sensorimotor recovery in incomplete spinal cord injury. *Front. Integr. Neurosci.* 8, 1–12. doi: 10.3389/fnint.2014.00042

Fawaz, S., Kamel, F., El Yasaky, A., El Shishtawy, H., Genedy, A., Awad, R., et al. (2019). The therapeutic application of functional electrical stimulation and transcranial magnetic stimulation in rehabilitation of the hand function in incomplete cervical spinal cord injury. *Egypt. Rheumatol. Rehabil.* 46, 21–26. doi: 10.4103/err.err_48_18

Fink, K. L., and Cafferty, W. B. (2016). Reorganization of intact descending motor circuits to replace lost connections after injury. *Neurotherapeutics* 13, 370–381. doi: 10.1007/s13311-016-0422-x

Fitzgerald, P. B., Brown, T. L., Daskalakis, Z. J., Chen, R., and Kulkarni, J. (2002). Intensity-dependent effects of 1 Hz rTMS on human corticospinal excitability. *Clin. Neurophysiol.* 113, 1136–1141. doi: 10.1016/s1388-2457(02)00145-1

Fouad, K., Popovich, P. G., Kopp, M. A., and Schwab, J. M. (2020). The neuroanatomical-functional paradox in spinal cord injury. *Nat. Rev. Neurol.* 17, 53–62. doi: 10.1038/s41582-020-00436-x

Fujiki, M., Yee, K. M., and Steward, O. (2020). Non-invasive high frequency repetitive transcranial magnetic stimulation (hfrTMS) robustly activates molecular pathways implicated in neuronal growth and synaptic plasticity in select populations of neurons. *Front. Neurosci.* 14:32612497. .doi: 10.3389/fnins.2020.00558

Gao, W., Yu, L. g., Liu, Y. l., Chen, M., Wang, Y. z., and Huang, X. l. (2017). Effects of high frequency repetitive transcranial magnetic stimulation on KCC2 expression in rats with spasticity following spinal cord injury. *J. Huazhong Univ. Sci. Technol. Med. Sci.* 37, 777–781. doi: 10.1007/s11596-017-1804-y

Gomes-Osman, J., and Field-Fote, E. C. (2015). Improvements in hand function in adults with chronic tetraplegia following a multiday 10-Hz repetitive transcranial magnetic stimulation intervention combined with repetitive task practice. *J. Neurol. Phys. Ther.* 39, 23–30. doi: 10.1097/NPT.0000000000000062

Guerra, A., López-Alonso, V., Cheeran, B., and Suppa, A. (2020). Variability in non-invasive brain stimulation studies: reasons and results. *Neurosci. Lett.* 719:133330. doi: 10.1016/j.neulet.2017.12.058

Gunduz, A., Rothwell, J., Vidal, J., and Kumru, H. (2017). Non-invasive brain stimulation to promote motor and functional recovery following spinal cord injury. *Neural Regen. Res.* 12, 1933–1938. doi: 10.4103/1673-5374.221143

Hodaj, H., Payen, J. F., and Lefaucheur, J. P. (2018). Therapeutic impact of motor cortex rTMS in patients with chronic neuropathic pain even in the absence of an analgesic response. A case report. *Neurophysiol. Clin.* 48, 303–308. doi: 10.1016/j.neucli.2018.05.039

Hsieh, C., Hsueh, I.-P., Chiang, F., and Lin, P. (1998). Inter-rater reliability and validity of the action research arm test in stroke patients. *Age Ageing* 27, 107–113. doi: 10.1093/ageing/27.2.107

Huertas-Hoyas, E., Martínez-Piédrola, M. R., Sánchez-Herrera-Baeza, P., Serrada Tejeda, S., Máximo-Bocanegra, N., Sánchez Camarero, C., et al. (2020). Alterations in dexterity and manual function in patients with focal hand dystonia. *Neurologia (Engl Ed)* doi: 10.1016/j.nrl.2020.04.020. [Online ahead of print].

ISNCSCI 2019 - American Spinal Injury Association (2019). Available online at: https://asia-spinalinjury.org/isncsci-2019-revision-released/. Accessed May 1, 2021.

Jetté, F., Côté, I., Meziane, H. B., and Mercier, C. (2013). Effect of single-session repetitive transcranial magnetic stimulation applied over the hand versus leg motor area on pain after spinal cord injury. *Neurorehabil. Neural Repair* 27, 636–643. doi: 10.1177/1545968313484810

Ji, S. G., Cha, H. G., and Kim, M. K. (2015). Effects of repetitive transcranial magnetic stimulation on motor recovery in lower extremities of subacute stage incomplete spinal cord injury patients: a randomized controlled trial. *J. Magn.* 20, 427–431. doi: 10.4283/JMAG.2015.20.4.427

Kasten, F. H., Duecker, K., Maack, M. C., Meiser, A., and Herrmann, C. S. (2019). Integrating electric field modeling and neuroimaging to explain inter-individual variability of tACS effects. *Nat. Commun.* 10:5427. doi: 10.1038/s41467-019-13417-6

Kim, M. K., and Lee, S. A. (2020). The effect of high frequency repetitive transcranial magnetic stimulation on community ambulation ability in spinal cord injury patients: a randomized controlled trial. *J. Magn.* 25, 301–306. doi: 10.4283/jmag.2020.25.4.517

Knikou, M. (2008). The H-reflex as a probe: pathways and pitfalls. *J. Neurosci. Methods* 171, 1–12. doi: 10.1016/j.jneumeth.2008.02.012

Konakanchi, D., de Jongh Curry, A. L., Waters, R. S., and Narayana, S. (2020). Focality of the induced E-Field is a contributing factor in the choice of TMS parameters: evidence from a 3D computational model of the human brain. *Brain Sci.* 10, 1–17. doi: 10.3390/brainsci10121010

Kumru, H., Benito-Penalva, J., Valls-Sole, J., Murillo, N., Tormos, J. M., Flores, C., et al. (2016). Placebo-controlled study of rTMS combined with Lokomat®gait training for treatment in subjects with motor incomplete spinal cord injury. *Exp. Brain Res.* 234, 3447–3455. doi: 10.1007/s00221-016-4739-9

Kumru, H., Murillo, N., Samso, J. V., Valls-Solé, J., Edwards, D., Pelayo, R., et al. (2010). Reduction of spasticity with repetitive transcranial magnetic stimulation in patients with spinal cord injury. *Neurorehabil. Neural Repair* 24, 435–441. doi: 10.1177/1545968309356095

Kuppuswamy, A., Balasubramaniam, A. V., Maksimovic, R., Mathias, C. J., Gall, A., Craggs, M. D., et al. (2011). Action of 5 Hz repetitive transcranial magnetic stimulation on sensory, motor and autonomic function in human spinal cord injury. *Clin. Neurophysiol.* 122, 2452–2461. doi: 10.1016/j.clinph.2011.04.022

Lee, S. A., and Cha, H. G. (2020). The effect of high frequency repetitive transcranial magnetic stimulation on community ambulation ability in spinal cord injury patients: a randomized controlled trial. *J. Magn.* 25, 517–523. doi: 10.4283/jmag.2020.25.4.517

Lefaucheur, J. P. (2019). Transcranial magnetic stimulation. *Handb. Clin. Neurol.* 160, 559–580. doi: 10.1016/B978-0-444-64032-1.00037-0

Lefaucheur, J. P., Aleman, A., Baeken, C., Benninger, D. H., Brunelin, J., Di Lazzaro, V., et al. (2020). Evidence-based guidelines on the therapeutic use of repetitive transcranial magnetic stimulation (rTMS): an update (2014–2018). *Clin. Neurophysiol.* 131, 474–528. doi: 10.1016/j.clinph.2019.11002

Leszczyńska, K., Wincek, A., Fortuna, W., Huber, J., Łukaszek, J., Okurowski, S., et al. (2020). Treatment of patients with cervical and upper thoracic incomplete spinal cord injury using repetitive transcranial magnetic stimulation. *Int. J. Artif. Organs* 43, 323–331. doi: 10.1177/0391398819887754

Leung, A., Donohue, M., Xu, R., Lee, R., Lefaucheur, J.-P., Khedr, E. M., et al. (2009). Review article rTMS for suppressing neuropathic pain: a meta-analysis. *J. Pain* 10, 1205–1216. doi: 10.1016/j.jpain.2009.03.010

Liu, K., Lu, Y., Lee, J. K., Samara, R., Willenberg, R., Sears-Kraxberger, I., et al. (2010). PTEN deletion enhances the regenerative ability of adult corticospinal neurons. *Nat. Neurosci.* 13, 1075–1081. doi: 10.1038/nn.2603

Lontis, E. R., Voigt, M., and Struijk, J. J. (2006). Focality assessment in transcranial magnetic stimulation with double and cone coils. *J. Clin. Neurophysiol.* 23, 462–471. doi: 10.1097/01.wnp.0000229944.63011.a1

López-Alonso, V., Cheeran, B., Río-Rodríguez, D., and Fernández-Del-Olmo, M. (2014). Inter-individual variability in response to non-invasive brain stimulation paradigms. *Brain Stimul.* 7, 372–380. doi: 10.1016/j.brs.2014.02.004

Maeda, F., Keenan, J. P., Tormos, J. M., Topka, H., and Pascual-Leone, A. (2000). Interindividual variability of the modulatory effects of repetitive transcranial magnetic stimulation on cortical excitability. *Exp. Brain Res.* 133, 425–430. doi: 10.1007/s002210000432

Min Hwang, J., Kim, Y.-H., Jae Yoon, K., Eun Uhm, K., and Hyuk Chang, W. (2014). Different responses to facilitatory rTMS according to BDNF genotype. *Clin. Neurophysiol.* 126, 1348–1353. doi: 10.1016/j.clinph.2014.09.028

Miron, J. P., Desbeaumes Jodoin, V., Montplaisir, L., and Lespérance, P. (2018). Significant differences in motor threshold between figure-8 and double-cone coils for repetitive transcranial magnetic stimulation in patients with refractory depression. *Eur. J. Psychiatry* 32, 195–196. doi: 10.1016/j.ejpsy.2018.06.001

Mirowska-Guzel, D., Gromadzka, G., Seniow, J., Lesniak, M., Bilik, M., Waldowski, K., et al. (2013). Association between BDNF-196 G>A and BDNF-270 C>T polymorphisms, BDNF concentration and rTMS-supported long-term rehabilitation outcome after ischemic stroke. *NeuroRehabilitation* 32, 573–582. doi: 10.3233/NRE-130879

Modugno, N., Nakamura, Y., MacKinnon, C. D., Filipovic, S. R., Bestmann, S., Berardelli, A., et al. (2001). Motor cortex excitability following short trains of repetitive magnetic stimuli. *Exp. Brain Res.* 140, 453–459. doi: 10.1007/s002210100843

Moher, D., Liberati, A., Tetzlaff, J., and Altman, D. G. (2009). Reprint—preferred reporting items for systematic reviews and meta-analyses: the PRISMA statement. *Phys. Ther.* 89:. doi: 10.1093/ptj/89.9.873

Mosayebi-Samani, M., Jamil, A., Salvador, R., Ruffini, G., Haueisen, J., and Nitsche, M. A. (2021). The impact of individual electrical fields and anatomical factors on the neurophysiological outcomes of tDCS: a TMS-MEP and MRI study. *Brain Stimul.* 14, 316–326. doi: 10.1016/j.brs.2021.01.016

Moxon, K. A., Oliviero, A., Aguilar, J., and Foffani, G. (2014). Cortical reorganization after spinal cord injury: always for good. *Neuroscience* 283, 78–94. doi: 10.1016/j.neuroscience.2014.06.056

Nardone, R., Höller, Y., Thomschewski, A., Bathke, A. C., Ellis, A. R., Golaszewski, S. M., et al. (2015). Assessment of corticospinal excitability after traumatic spinal cord injury using MEP recruitment curves: a preliminary TMS study. *Spinal Cord* 53, 534–538. doi: 10.1038/sc.2015.12

Nardone, R., Höller, Y., Thomschewski, A., Brigo, F., Orioli, A., Höller, P., et al. (2014a). rTMS modulates reciprocal inhibition in patients with traumatic spinal cord injury. *Spinal Cord* 52, 831–835. doi: 10.1038/sc.2014.136

Nardone, R., Höller, Y., Thomschewski, A., Höller, P., Bergmann, J., Golaszewski, S., et al. (2014b). Central motor conduction studies in patients with spinal cord disorders: a review. *Spinal Cord* 52, 420–427. doi: 10.1038/sc.2014.48

National Spinal Cord Injury Statistical C (2020). *2020 Annual Report*.

Nogueira, F., Shirahige, L., Brito, R., and Monte-Silva, K. (2020). Independent community walking after a short protocol of repetitive transcranial magnetic stimulation associated with body weight-support treadmill training in a patient

with chronic spinal cord injury: a case report. *Physiother. Theory Pract.* doi: 10.1080/09593985.2020.1802797. [Online ahead of print].

O'Donovan, K. J., Ma, K., Guo, H., Wang, C., Sun, F., Han, S. B., et al. (2014). B-RAF kinase drives developmental axon growth and promotes axon regeneration in the injured mature CNS. *J. Exp. Med.* 211, 801–814. doi: 10.1084/jem.20131780

Ovadia-Caro, S., Khalil, A. A., Sehm, B., Villringer, A., Nikulin, V. V., and Nazarova, M. (2019). Predicting the response to noninvasive brain stimulation in stroke. *Front. Neurol.* 10:302. doi: 10.3389/fneur.2019.00302

Pandyan, A. D., Johnson, G. R., Price, C. I. M., Curless, R. H., Barnes, M., and Rodgers, H. (1999). A review of the properties and limitations of the Ashworth and modified Ashworth Scales as measures of spasticity. *Clin. Rehabil.* 13, 373–383. doi: 10.1191/026921599677595404

Peinemann, A., Reimer, B., Löer, C., Quartarone, A., Münchau, A., Conrad, B., et al. (2004). Long-lasting increase in corticospinal excitability after 1800 pulses of subthreshold 5 Hz repetitive TMS to the primary motor cortex. *Clin. Neurophysiol.* 115, 1519–1526. doi: 10.1016/j.clinph.2004.02.005

Petersen, J. A., Spiess, M., Curt, A., Dietz, V., and Schubert, M. N. (2012). Spinal cord injury: One-year evolution of motor-evoked potentials and recovery of leg motor function in 255 patients. *Neurorehabil. Neural Repair* 26, 939–948. doi: 10.1177/1545968312438437

Pitkänen, M., Kallioniemi, E., and Julkunen, P. (2017). Effect of inter-train interval on the induction of repetition suppression of motor-evoked potentials using transcranial magnetic stimulation. *PLoS One* 12:e0181663. doi: 10.1371/journal.pone.0181663

Pleger, B., Blankenburg, F., Bestmann, S., Ruff, C. C., Wiech, K., Stephan, K. E., et al. (2006). Repetitive transcranial magnetic stimulation-induced changes in sensorimotor coupling parallel improvements of somatosensation in humans. *J. Neurosci.* 26, 1945–1952. doi: 10.1523/JNEUROSCI.4097-05.2006

Potter-Baker, K. A., Janini, D. P., Frost, F. S., Chabra, P., Varnerin, N., Cunningham, D. A., et al. (2016). Reliability of TMS metrics in patients with chronic incomplete spinal cord injury. *Spinal Cord* 54, 980–990. doi: 10.1038/sc.2016.47

Quadri, S. A., Farooqui, M., Ikram, A., Zafar, A., and Muhammad, K. A. (2020). Recent update on basic mechanisms of spinal cord injury. *Neurosurg. Rev.* 43, 425–441. doi: 10.1007/s10143-018-1008-3

Raineteau, O., and Schwab, M. E. (2001). Plasticity of motor systems after incomplete spinal cord injury. *Nat. Rev. Neurosci.* 2, 263–273. doi: 10.1038/35067570

Ridding, M. C., and Ziemann, U. (2010). Determinants of the induction of cortical plasticity by non-invasive brain stimulation in healthy subjects. *J. Physiol.* 588, 2291–2304. doi: 10.1113/jphysiol.2010.190314

Rodger, J., Gandevia, S. C., Wilson, M. T., and St George, L. (2016). Repetitive transcranial magnetic stimulation: a call for better data. *Front. Neural Circuits* 1:57. doi: 10.3389/fncir.2016.00057

Rodseth, J., WashaBugh, E. P., and Krishnan, C. (2017). A novel low-cost approach for navigated transcranial magnetic stimulation. *Restor. Neurol. Neurosci.* 35, 601–609. doi: 10.3233/RNN-170751

Ronai, P., and Gallo, P. M. (2019). The short physical performance battery (ASSESSMENT). *ACSM's Health Fitness J.* 23, 52–56. doi: 10.1249/FIT.0000000000000519

Rossi, S., Antal, A., Bestmann, S., Bikson, M., Brewer, C., Brockmöller, J., et al. (2020). Safety and recommendations for TMS use in healthy subjects and patient populations, with updates on training, ethical and regulatory issues: expert guidelines. *Clin. Neurophysiol.* doi: 10.1016/j.clinph.2020.10.003

Rossi, S., Hallett, M., Rossini, P. M., Pascual-Leone, A., Avanzini, G., Bestmann, S., et al. (2009). Safety, ethical considerations and application guidelines for the use of transcranial magnetic stimulation in clinical practice and research. *Clin. Neurophysiol.* 120, 2008–2039. doi: 10.1016/j.clinph.2009.08.016

Rossini, P. M., Burke, D., Chen, R., Cohen, L. G., Daskalakis, Z., Di Iorio, R., et al. (2015). Non-invasive electrical and magnetic stimulation of the brain, spinal cord, roots and peripheral nerves: basic principles and procedures for routine clinical and research application: an updated report from an I.F.C.N. Committee. *Clin. Neurophysiol.* 126, 1071–1107. doi: 10.1016/j.clinph.2015.02.001

Rothkegel, H., Sommer, M., and Paulus, W. (2010). Breaks during 5 Hz rTMS are essential for facilitatory after effects. *Clin. Neurophysiol.* 121, 426–430. doi: 10.1016/j.clinph.2009.11.016

Sale, M. V., Ridding, M. C., and Nordstrom, M. A. (2007). Factors influencing the magnitude and reproducibility of corticomotor excitability changes induced by paired associative stimulation. *Exp. Brain Res.* 181, 615–626. doi: 10.1007/s00221-007-0960-x

Sankarasubramanian, V., Roelle, S. M., Bonnett, C. E., Janini, D., Varnerin, N. M., Cunningham, D. A., et al. (2015). Reproducibility of transcranial magnetic stimulation metrics in the study of proximal upper limb muscles. *J. Electromyogr. Kinesiol.* 25, 754–764. doi: 10.1016/j.jelekin.2015.05.006

Sato, S., Kakuda, W., Sano, M., Kitahara, T., and Kiko, R. (2018). Therapeutic application of transcranial magnetic stimulation combined with rehabilitative training for incomplete spinal cord injury: a case report. *Prog. Rehabil. Med.* 3:20180014. doi: 10.2490/prm.20180014

Saturnino, G. B., Puonti, O., Nielsen, J. D., Antonenko, D., Madsen, K. H., and Thielscher, A. (2019). "SimNIBS 2.1: a comprehensive pipeline for individualized electric field modelling for transcranial brain stimulation," in *Brain and Human Body Modeling: Computational Human Modeling at EMBC 2018 [Internet]*, eds S. Makarov, M. Horner, and G. Noetscher (Cham: Springer), 3–25. doi: 10.1007/978-3-030-21293-3_1

Schoisswohl, S., Agrawal, K., Simoes, J., Neff, P., Schlee, W., Langguth, B., et al. (2019). RTMS parameters in tinnitus trials: a systematic review. *Sci. Rep.* 9:12190. doi: 10.1038/s41598-019-48750-9

Siebner, H., Peller, M., Willoch, F., Minoshima, S., Boecker, H., Auer, C., et al. (2000). Lasting cortical activation after repetitive TMS of the motor cortex: a glucose metabolic study. *Neurology* 54, 956–963. doi: 10.1212/wnl.54.4.956

Sivan, M., O'Connor, R. J., Makower, S., Levesley, M., and Bhakta, B. (2011). Systematic review of outcome measures used in the evaluation of robot-assisted upper limb exercise in stroke. *J. Rehabil. Med.* 43, 181–189. doi: 10.2340/16501977-0674

Steeves, J. D., Kramer, J. K., Fawcett, J. W., Cragg, J., Lammertse, D. P., Blight, A. R., et al. (2011). Extent of spontaneous motor recovery after traumatic cervical sensorimotor complete spinal cord injury. *Spinal Cord* 49, 257–265. doi: 10.1038/sc.2010.99

Sydekum, E., Ghosh, A., Gullo, M., Baltes, C., Schwab, M., and Rudin, M. (2014). Rapid functional reorganization of the forelimb cortical representation after thoracic spinal cord injury in adult rats. *Neuroimage* 87, 72–79. doi: 10.1016/j.neuroimage.2013.10.045

Tazoe, T., and Perez, M. A. (2015). Effects of repetitive transcranial magnetic stimulation on recovery of function after spinal cord injury. *Arch. Phys. Med. Rehabil.* 96, S145–S155. doi: 10.1016/j.apmr.2014.07.418

Thomson, R. H., Rogasch, N. C., Maller, J. J., Daskalakis, Z. J., and Fitzgerald, P. B. (2011). Intensity dependent repetitive transcranial magnetic stimulation modulation of blood oxygenation. *J. Affect. Disord.* 136, 1243–1246. doi: 10.1016/j.jad.2011.08.005

Tricco, A. C., Lillie, E., Zarin, W., O'Brien, K. K., Colquhoun, H., Levac, D., et al. (2018). PRISMA extension for scoping reviews (PRISMA-ScR): Checklist and explanation. *Ann. Intern. Med.* 169, 467–473. doi: 10.7326/M18-0850

Versace, V., Langthaler, P. B., Höller, Y., Frey, V. N., Brigo, F., Sebastianelli, L., et al. (2018). Abnormal cortical neuroplasticity induced by paired associative stimulation after traumatic spinal cord injury: a preliminary study. *Neurosci. Lett.* 664, 167–171. doi: 10.1016/j.neulet.2017.11.003

Ware, J. E., and Sherbourne, C. D. (1992). The MOS 36-item short-form health survey (SF-36). I. conceptual framework and item selection. *Med. Care* 30, 473–483. Available online at: https://pubmed.ncbi.nlm.nih.gov/1593914/. Accessed July 19, 2021.

WashaBaugh, E. P., and Krishnan, C. (2016). A low-cost system for coil tracking during transcranial magnetic stimulation. *Restor. Neurol. Neurosci.* 34, 337–346. doi: 10.3233/RNN-150609

Witiw, C. D., and Fehlings, M. G. (2015). Acute spinal cord injury. *J. Spinal Disord. Tech.* 28, 202–210. doi: 10.1097/BSD.0000000000000287

Xiang, H., Sun, J., Tang, X., Zeng, K., and Wu, X. (2019). The effect and optimal parameters of repetitive transcranial magnetic stimulation on motor recovery in stroke patients: a systematic review and meta-analysis of randomized controlled trials. *Clin. Rehabil.* 33, 847–864. doi: 10.1177/0269215519829897

Zhao, C. G., Sun, W., Ju, F., Wang, H., Sun, X. L., Mou, X., et al. (2020). Analgesic effects of directed repetitive transcranial magnetic stimulation in acute neuropathic pain after spinal cord injury. *Pain Med.* 21, 1216–1223. doi: 10.1093/pm/pnz290

Conflict of Interest: The authors declare that the research was conducted in the absence of any commercial or financial relationships that could be construed as a potential conflict of interest.

Publisher's Note: All claims expressed in this article are solely those of the authors and do not necessarily represent those of their affiliated organizations, or those of the publisher, the editors and the reviewers. Any product that may be evaluated in this article, or claim that may be made by its manufacturer, is not guaranteed or endorsed by the publisher.

frontiers | Frontiers in Human Neuroscience

ORIGINAL RESEARCH
published: 23 June 2022
doi: 10.3389/fnhum.2022.867563

Transcutaneous Auricular Vagus Nerve Stimulation Differently Modifies Functional Brain Networks of Subjects With Different Epilepsy Types

Randi von Wrede[1], Thorsten Rings[1,2], Timo Bröhl[1,2], Jan Pukropski[1], Sophia Schach[1], Christoph Helmstaedter[1] and Klaus Lehnertz[1,2,3]*

[1] Department of Epileptology, University Hospital Bonn, Bonn, Germany, [2] Helmholtz-Institute for Radiation and Nuclear Physics, University of Bonn, Bonn, Germany, [3] Interdisciplinary Center for Complex Systems, University of Bonn, Bonn, Germany

OPEN ACCESS

Edited by:
Ken-Ichiro Tsutsui, Tohoku University, Japan

Reviewed by:
Jiliang Fang, China Academy of Chinese Medical Sciences, China
Masaki Iwasaki, National Center of Neurology and Psychiatry, Japan

***Correspondence:**
Randi von Wrede
randi.von.wrede@ukbonn.de

Specialty section:
This article was submitted to Brain Imaging and Stimulation, a section of the journal Frontiers in Human Neuroscience

Received: *01 February 2022*
Accepted: *24 May 2022*
Published: *23 June 2022*

Citation:
von Wrede R, Rings T, Bröhl T, Pukropski J, Schach S, Helmstaedter C and Lehnertz K (2022) Transcutaneous Auricular Vagus Nerve Stimulation Differently Modifies Functional Brain Networks of Subjects With Different Epilepsy Types. Front. Hum. Neurosci. 16:867563. doi: 10.3389/fnhum.2022.867563

Epilepsy types differ by pathophysiology and prognosis. Transcutaneous auricular vagus nerve stimulation (taVNS) is a non-invasive treatment option in epilepsy. Nevertheless, its mode of action and impact on different types of epilepsy are still unknown. We investigated whether short-term taVNS differently affects local and global characteristics of EEG-derived functional brain networks in different types of epilepsy. Thirty subjects (nine with focal epilepsy, 11 with generalized epilepsy, and 10 without epilepsy or seizures) underwent a 3-h continuous EEG-recording (1 h pre-stimulation, 1 h taVNS stimulation, 1 h post-stimulation) from which we derived evolving functional brain networks. We assessed—in a time-resolved manner—important global (topological, robustness, and stability properties) and local (centralities of vertices and edges) network characteristics. Compared to the subjects with focal epilepsies and without epilepsy, those with generalized epilepsies clearly presented with different topological properties of their functional brain network already at rest. Furthermore, subjects with focal and generalized epilepsies reacted differently to the stimulation, expressed as different taVNS-induced immediate and enduring reorganization of global network characteristics. On the local network scale, no discernible spatial pattern could be detected, which points to a rather unspecific and generalized modification of brain activity. Assessing functional brain network characteristics can provide additional information for differentiating between focal and generalized epilepsy. TaVNS-related modifications of global network characteristics clearly differ between epilepsy types. Impact of such a non–pharmaceutical intervention on clinical decision-making in the treatment of different epilepsy types needs to be assessed in future studies.

Keywords: epileptic brain networks, epilepsy, epilepsy type, transcutaneous vagal nerve stimulation (TVNS), functional networks

INTRODUCTION

Epilepsy is one of the most common neurological disorders with a prevalence of 0.5–1% and about 50 million affected subjects (people with epilepsy; PWE) worldwide (GBD 2016 Epilepsy Collaborators, 2019; Hauser and Hesdorffer, 2019; World Health Organization [WHO], 2019). According to the recent proposal of the International League against Epilepsy (ILAE), this disorder is a disease of the brain with at least two unprovoked (or reflex) seizures, or one unprovoked (or reflex) seizure and a probability of at least 60% for further seizures to occur over the next 10 years, or diagnosis of an epilepsy syndrome (Fisher et al., 2014). The most recent ILAE classification of epilepsy provides a very sophisticated schedule for seizure type, epilepsy type and, at each stage of classification, potential etiology of epilepsy (Scheffer et al., 2017). Therefore, the actual classified epilepsy might change over time in some PWE. Nevertheless, classification of epilepsies is substantial for clinical decisions, for clinical and basic epilepsy research as well as for the evaluation and development of new treatment options. Obviously, PWE with structural focal epilepsies might be candidates for epilepsy surgery, PWE with genetic epilepsies due to Glut-1 deficiency are candidates for ketogenic diet, and PWE with limbic encephalitis might profit from immunomodulation. What is more, studies on antiseizure medication (ASM) provide information on efficacy in different epilepsy types, thus providing useful and indispensable information for clinical consultation (Marson et al., 2007a,b, 2021).

The human brain can be understood as a complex network and epilepsy as a network disorder (Bullmore and Sporns, 2009; Berg and Scheffer, 2011). The study of network dynamics can be carried out in spatial as well as in temporal dimensions using different approaches. Electroencephalography is a non-invasive and easy-to-use method in terms of spatial and temporal scales. Tracking network characteristics over time can help to identify intervention-related alterations of brain activity as already been shown by the so-called "pharmaco-EEG" which has provided relevant insights in treatment response, ASM side effects and prediction of those (Höller et al., 2018). Namely, by using an analysis approach that investigates EEG-derived evolving functional brain networks, different global and local network characteristics can be assessed. It is conceivable that different epilepsy types display differences in network characteristics that might provide additional information for differentiating epilepsy types to support clinical evaluation.

ASM is the basis of any epilepsy treatment, but unfortunately for one third of PWE extensive pharmacotherapy attempts have to be undertaken for an at least acceptable seizure situation (Kwan and Brodie, 2000); even the newly developed ASM have not changed this situation significantly (Chen et al., 2018). Pharmacotherapy-resistance is a great burden for PWE and their caregivers. Thus, there is a strong need for alternative or complementary non-pharmaceutical treatment options. Brain stimulation techniques are well established in the treatment of epilepsy. Invasive vagus nerve stimulation (iVNS) is used for decades with more than 100,000 implanted systems (Fisher et al., 2020), and efficacy and safety are well documented over the years with responder (PWE in whom seizure frequency is reduced by more than 50%) rates of up to 50% (Elliott et al., 2011; Morris et al., 2013). Though generally well tolerated and even having a positive impact on mood, risk of anesthesia and surgery have to be considered with an overall complication rate of up to 12%, and surgical complication rate amounts up to 8.6% (Révész et al., 2016). Transcutaneous auricular vagus nerve stimulation (taVNS), the non-invasive external stimulation of the auricular branch of the vagus nerve, is an alternative worth of investigation. Good efficacy, tolerability and usability was previously shown for taVNS (Stefan et al., 2012; Bauer et al., 2016; Barbella et al., 2018; Liu et al., 2018; von Wrede et al., 2019). Most clinical trials have been conducted with PWE with focal epilepsy or in groups consisting of subjects with focal or generalized epilepsy. However, a thorough work up on differences in terms of efficacy in different epilepsy types is missing (Lampros et al., 2021). As the number of participants in above mentioned studies is quite low and only few data from randomized controlled trials is available, a final assessment of the efficacy is not yet available.

To date, the mode of action of vagus nerve stimulation is not fully understood, but may involve alterations of different metabolic pathways (for an overview see Farmer et al., 2021). Hence, it is supposed that VNS leads to a rather unspecific, global activation of various brain structures [including thalamus, limbic system, insular cortex (Rutecki, 1990; Ben-Menachem, 2002)]. Recently, modifications of brain network topology as well as modification of network stability and robustness were shown in a larger group of subjects with and without central nervous system diseases corroborating the idea of an unspecific global activation (Rings et al., 2021; von Wrede et al., 2021). As epilepsy types differ clinically and pathophysiologically, we hypothesized that effects of non-pharmaceutical interventions on functional brain networks in different epilepsy types differ as well. To test this hypothesis, we investigated short-term taVNS-induced immediate and enduring modifications of global and local characteristics of evolving functional brain networks in subjects with different types of epilepsy and non-epilepsy subjects.

MATERIALS AND METHODS

Subjects

Subjects who were admitted to our ward from March 2020 to February 2021 were screened for suitability for this study. Inclusion criteria were clinical necessity (differential diagnosis or electrophysiological follow-up) for long-term video-EEG-recording and age 18 years and older. Exclusion criteria were previous brain surgery, actual or previous neurostimulation such as invasive or non-invasive vagus nerve stimulation or deep brain stimulation, progressive disease, seizures occurring within 24 h before the start of the study, insufficient German language capability, mental disability and incompetence to follow instructions. Demographic data were derived from patient reports, and epilepsy type was classified according to Scheffer et al. (2017). Subjects were assigned to three different groups: focal epilepsy group (G1), generalized epilepsy group (G2), and non-epilepsy group (G3). After being provided with written

information and being given the opportunity to ask further questions, 35 subjects volunteered to participate and signed informed consent.

Transcutaneous Auricular Vagus Nerve Stimulation and Examination Schedule

Following previous studies (Rings et al., 2021; von Wrede et al., 2021), we applied transcutaneous auricular vagus nerve stimulation for 1 h in the early afternoon while the subjects underwent a 3 h continuous video-EEG-recording [1 h pre-stimulation baseline 1 (B1), 1 h taVNS (S) and 1 h post-stimulation baseline 2 (B2)]. During this 3-h block, subjects continued laid-back activities (awake, no other activation methods applied). Stimulation was carried out unilaterally (left cymba conchae) using two hemispheric titanium electrodes of a taVNS device (tVNS Technologies GmbH, Erlangen, Germany) with a set of non-adjustable parameters (biphasic signal form, impulse frequency 25 Hz, impulse duration 20 s, impulse pause 30 s) and individually adjusted intensity of stimulation until the subject experienced a "tingling," but no painful sensations. All subjects were under stable CNS medication (if taking any) and no activation methods (such as hyperventilation or sleep deprivation) were applied at least 24 h before start of the examination. In order to track possible changes of cognition and behavior, a standardized neuropsychological assessment [EpiTrack® and a modified version of the Adverse Events Profile (AEP)] preceded and followed the EEG-recording. After stimulation the subjects answered a questionnaire on the evaluation of the device usability and tolerability (for details of tests see **Supplementary Appendix A**).

Electroencephalogram Recordings and Data Pre-processing

We recorded electroencephalograms (EEG) from 19 electrodes (18 electrode sites according to the 10–20 system and Cz served as physical reference). EEG data were sampled at 256 Hz using a 16 bit analog-to-digital converter and were band-pass filtered offline between 1 and 45 Hz (4th order Butterworth characteristic). To suppress contributions at the line frequency (50 Hz) a notch filter (3rd order) was applied. All recordings were visually inspected for strong artifacts (subject movements, amplifier saturation, or stimulation artifacts) and such data were excluded from further analyses.

Characterizing Functional Brain Networks on Global and Local Scale

Functional networks consist of vertices and edges. We here associated network vertices with brain regions sampled by the EEG electrode contacts and network edges with time-varying estimates of the strength of interactions between the dynamics of pairs of those brain regions, regardless of their anatomical connections. Following previous studies, we derived evolving, fully connected and weighted networks from a time-resolved synchronization analysis of the above mentioned 3-h EEG-recording, assessed important global and local characteristics of the networks, and tracked their changes over time (for details see **Supplementary Appendix B**).

On the global network scale, we assessed the topological characteristics average clustering coefficient C and average shortest path length L. The average clustering coefficient C characterizes the network's functional segregation; the lower C, the more segregated is the weighted fully connected network. The average shortest path length L characterizes the network's functional integration; the lower L, the more integrated is the weighted fully connected network. In this model, functional segregation (integration) reflects independent (dependent) information processes between brain regions (Tononi et al., 1994).

Furthermore, we assessed the network's robustness and stability characteristics. Assortativity A reflects the tendency of edges to connect vertices with similar or equal properties. If edges preferentially connect vertices with dissimilar properties, such networks are called disassortative. Disassortative networks are more vulnerable to perturbations and appear to be easier to synchronize than assortative networks. Synchronisability S assesses the network's propensity (or vulnerability) to get synchronized by an admissible input activation: the higher S, the more easily can the synchronized state be perturbed.

On the local network scale, we assessed importance of vertices and edges using two different and opposing centrality concepts: a path-based and an interaction-strength-based one. Both of them provide non-redundant information about the role vertices and edges play in the larger network. As path-based centrality index, we employed betweenness centrality C^B. A vertex/edge with high C^B is central since it connects different regions of the network as a bridge. As interaction-strength-based centrality index, we employed eigenvector centrality C^E. A vertex/edge with high C^E is central since the vertices/edges connected to it are central as well, therefore it reflects the influence of the vertex/edge on the network as a whole (for details see **Supplementary Appendix C**).

Statistical Analyses

For each phase of the examination schedule (B1, S, and B2), we investigated whether the three subject groups (G1, G2, and G3) presented with different global and local network characteristics (Mann-Whitney U-test; $p < 0.05$). For each subject group, we investigated whether global and local network characteristics differed between the phases of the examination schedule (Mann-Whitney U-test; $p < 0.05$). In addition, and in order to distinguish cases that responded to the stimulation from non-responding cases, we repeated the latter analysis on a single subject level. All p-values were corrected for multiple comparisons using the Bonferroni method. Differences in taVNS intensities were investigated in the three subject groups (Kruskal-Wallis test; $p < 0.05$). Eventually, we tested for differences between neuropsychological variables assessed prior to and after the EEG-recording [repeated measures ANOVA; within-subject factor: EpiTrack® pre/post score; between-subject factor: group (G1, G2, and G3); $p < 0.05$]. Furthermore, we investigated whether the assessment of usability of the device differs between the three

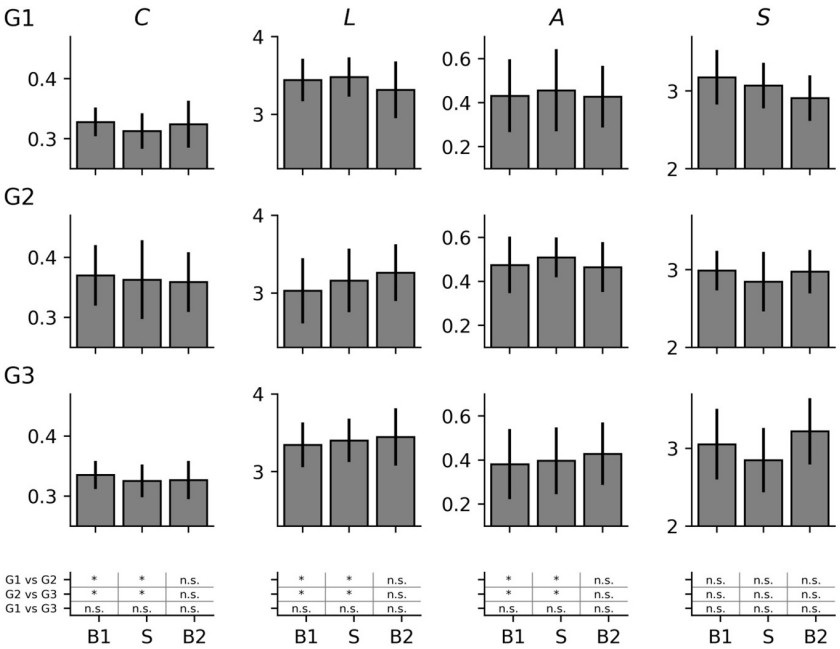

FIGURE 1 | Global network characteristics (average clustering coefficient *C*, average shortest path length *L*, synchronisability *S*, and assortativity *A*) of the investigated groups (G1 = focal epilepsy group, G2 = generalized epilepsy group, G3 = non-epilepsy group) in the three phases of the study (B1 = pre-stimulation baseline 1, S = stimulation, B2 = post-stimulation baseline 2). Mean values and standard deviation. *significant (Mann-Whitney *U*-test, $p < 0.05$), n.s. = non-significant.

subject groups (G1, G2, and G3) (Mann-Whitney *U*-test; $p < 0.05$).

RESULTS

From the thirty-five eligible subjects, five subjects had to be excluded due to EEG data quality. Data from thirty subjects (20 females; age 18–55 years, median 26.5 years) were included in the analyses. Twenty subjects suffered from epilepsy, 9 subjects from focal (G1: 5 females; age 18–55 years, median 26 years) and 11 subjects from generalized epilepsy (G2: 7 females; age 18–54 years, median 22 years). Fifteen of those 20 PWE (75%) had to be considered as drug-resistant according to the definition of the ILAE (Kwan et al., 2010), with 6 PWE with focal epilepsy and 9 PWE with generalized epilepsy. Ten subjects did not suffer from epilepsy and had never experienced seizures before (G3: 8 females; age 19–42 years, median 27.5 years). TaVNS stimulation intensities did not differ significantly between subject groups (G1: range: 0.9–3.5 mA, mean 2.5, *SD* ± 0.8; G2: range: 0.5–3.2 mA, mean 1.6, *SD* ± 0.9; G3: range: 1.0–5.0 mA, mean 2.3, *SD* ± 1.2).

Global Network Characteristics in Different Epilepsy Groups (G1 and G2) and Non-epilepsy Group (G3)

On the global network scale (see **Figure 1**), the focal epilepsy group (G1) and the non-epilepsy group (G3) presented with comparable topological network characteristics (average clustering coefficient *C* and average shortest path length *L*) during all phases of the examination schedule. Contrary to this, we observed the group of subjects with generalized epilepsies (G2) to possess topological characteristics that differed significantly from the characteristics seen in both the focal epilepsy group and the non-epilepsy group. Already before (phase B1) but also during stimulation (phase S), the networks of group G2 were less segregated (higher average clustering coefficient *C*) and more integrated (lower average shortest path length *L*) than the networks of groups G1 and G3. Interestingly, the vanishing differences seen after the stimulation (phase B2) possibly point to a taVNS-mediated topology-modifying effect in the group of subjects with generalized epilepsies. As regards the networks' stability and robustness characteristics (synchronisability *S* and assortativity *A*), the three subject groups presented with comparable findings during all phases of the examination schedule.

Testing for differences between network characteristics from each phase led to non-significant results in each subject group (data not shown). On this population sample level, taVNS thus appeared to not immediately affect the investigated global network characteristics. Nevertheless, since not all subjects may display taVNS-mediated changes of their functional brain network (Rings et al., 2021; von Wrede et al., 2021), we specifically investigated those subjects for whom we identified significant changes of their network characteristics (see **Figure 2**) and observed the subject groups to present with a different pattern of change. When the networks of both the focal epilepsy group (G1) and the non-epilepsy group (G3) transited from phase B1 to phase S, their average

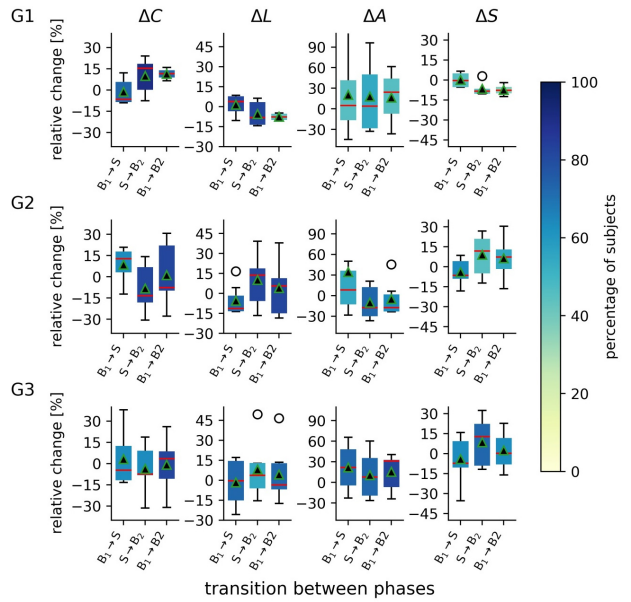

FIGURE 2 | Distributions of taVNS-related alterations in global network characteristics of the three investigated groups (G1 = focal epilepsy group, G2 = generalized epilepsy group, G3 = non-epilepsy group) between the three investigated phases (B1 = pre-stimulation baseline 1, S = stimulation, B2 = post-stimulation baseline 2). Boxplots of relative changes in network characteristics (average clustering coefficient *C*, average shortest path length *L*, synchronisability *S*, and assortativity *A*). Bottom and top of a box are the first and third quartiles, and the red band and the black triangle are the median and the mean of the distribution. The ends of the whiskers represent the interquartile range of the data. Outliers are marked by an o-sign. Boxes are color coded according to the percentage of subjects for whom significant changes in global network characteristics were observed on per subject base.

clustering coefficient *C* decreased (relative change of median values in G1: −6.5%; G3: −4.7%) while the average shortest path length *L* of G1 increased (+ 3.9%) and changes were negligible for G3 (−0.4%). This points to an immediate stimulation effect that renders these networks more segregated and, at least for G1 less integrated. When comparing network characteristics from the phases prior to (B1) and after the stimulation (B2), we could identify an enduring effect that rendered network less segregated (*C* increased; G1: + 11.4%, G3: + 3.6%) and more integrated (*L* decreased; G1: −7.8%; G3: −3.5%). Interestingly, for the networks of the generalized epilepsy group (G2), we observed these stimulation-mediated changes to present with an inverted pattern: the immediate stimulation effect resulted in less segregated (*C* increased by + 12.8%) and more integrated networks (*L* decreased by −11.3%), while the enduring effect presented with more segregated (*C* decreased; −7.6%) and less integrated networks (*L* increased; + 5.7%).

TaVNS exerted an immediate robustness-enhancing effect over the networks in all groups (changes in assortativity *A*; G1: + 4.9%; G2: + 8.4%; G3: + 21.8%). On the longer term (comparing phases B1 and B2), we observed a strong robustness-enhancing enduring effect for the focal epilepsy group and the non-epilepsy group (G1: + 24.4%; G3: 31.4%). In contrast, in the generalized epilepsy group appeared to have a robustness-decreasing enduring effect (G2: -17.4%).

As regards network stability, we observed taVNS to decrease the networks' vulnerability of the synchronized state to get perturbed when transiting from phase B1 to phase S in the generalized epilepsy group and the non-epilepsy groups (changes in synchronisability *S*: G2: −6.4%; G3: −7.3%) while this immediate effect in the focal epilepsy group was negligible (G1: −0.4%). Interestingly, in the focal epilepsy group this minor reduction increased into the post-stimulation phase (G1: −7.6%), while taVNS had an enduring vulnerability-enhancing effect on the networks in the generalized group (G2: + 7.4) and a negligible effect in the non-epilepsy group (G3: + 0.3%).

Local Network Characteristics in Different Epilepsy Groups (G1 and G2) and Non-epilepsy Group (G3)

On the local network scale (see **Figure 3**), we obtained different results on the population sample level depending on the employed vertex centrality concept. Betweenness centrality highlighted vertices associated with left fronto-centro-temporal brain regions as most important (high C^B values) in all subject groups. In contrast, eigenvector centrality highlighted a posterior-anterior gradient of vertex importance with the most important (high C^E values) vertices associated with posterior brain regions in all subject groups. Most important vertices differed significantly neither between groups nor between phases, apart from some few, locally mostly unspecific differences seen particularly for the generalized and non-epilepsy group. As regards the importance of edges, i.e., of interactions between brain regions, none of the employed edge centrality concepts highlighted a clear-cut spatial pattern of differences, neither between groups nor between phases. On the population sample level, taVNS thus appeared to have an only minor (if at all) immediate impact on the investigated local network characteristics.

Proceeding as above and investigating solely those subjects that presented with significant taVNS-mediated changes of their local network characteristics, we observed that most subjects displayed such changes (see **Figure 4**). Interestingly, the highest proportion of subjects showing significant changes was seen in the generalized epilepsy group, however, with no discernible spatial pattern of change. In contrast, for most subjects from the focal epilepsy group, taVNS-mediated changes of vertex importance (assessed with betweenness centrality) were confined to vertices associated with fronto-temporal brain areas. Other taVNS-mediated alterations of vertex or edge centralities presented as diffuse with no clear-cut spatial pattern.

Stimulation-Related Change of EpiTrack® Score and Subjective Measures

An improvement in attentional-executive functioning as measured with EpiTrack® from pre- to post-assessment (main effect time: $F = 28.97$, $p < 0.001$), but no interaction effect of time and group ($F = 1.31$, $p = 0.29$) was observed.

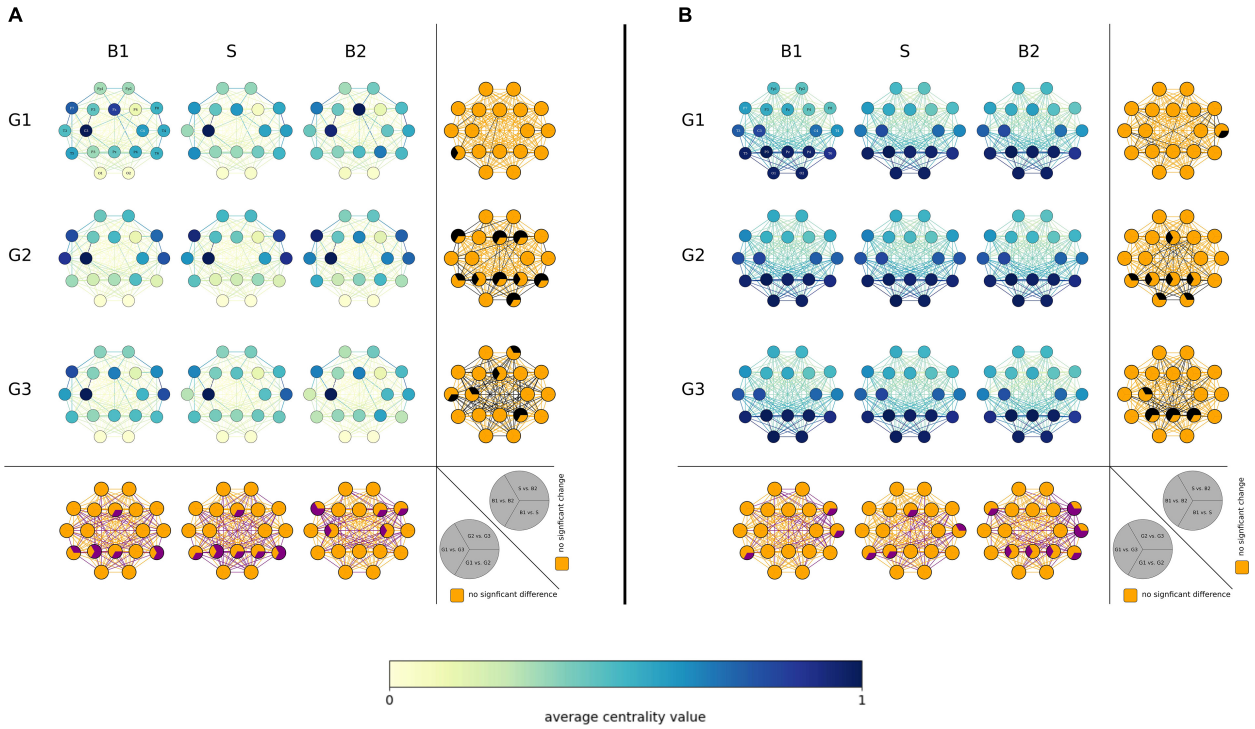

FIGURE 3 | Local network characteristics. [**(A)** Betweenness centrality C^B and **(B)** eigenvector centrality C^E] of the three investigated groups (G1 = focal epilepsy group, G2 = generalized epilepsy group, G3 = non-epilepsy group) in the three investigated phases (B1 = pre-stimulation baseline 1, S = stimulation, B2 = post-stimulation baseline 2). Network vertices arranged according the international 10–20 system for EEG-recording (electrode naming see first plot). Color coding of vertices and edges according to the average centrality values. Bottom: Difference between groups (G1, G2, G3) for local network characteristics in the three investigated phases. Orange: no significance, purple: significant difference ($p < 0.05$). Right side each plot: Differences between phases (B1, S, B2) for local network characteristics in the three investigated groups. Orange: no significance, black: significant change ($p < 0.05$).

Seven subjects (23.3%; 2 in G1, 1 in G2, 4 in G3) showed a significant intraindividual improvement (EpiTrack®; $\geq$ 4 points). None of the subjects worsened significantly. No significant self-perceived changes were observed regarding the total scores in the cognitive, behavioral, and physiological domains of the modified Adverse Events Profile ($p > 0.05$).

Usability, Tolerability and Side Effects of Transcutaneous Auricular Vagus Nerve Stimulation

Usability data were analyzed across all subjects as there were no differences between groups ($p > 0.05$). Handling of the device was rated as good or very good by all subjects. 93.1% felt that the continuation of their activities was not affected by the stimulation. Wearing comfort was rated as good or very good by 83.3% of the subjects. Most subjects stated that the device is well or very well suited for long-term use during the day (80%) or repeated use within 1 day (86.6%). Side effects were neither reported nor clinically observed.

DISCUSSION

In this study, we investigated whether global and local characteristics of functional brain networks differ between different types of epilepsy and non-epilepsy subjects and whether short-term taVNS differently modifies their global and local network characteristics. In the following, we discuss our findings in the light of the available research results.

Global and Local Network Characteristics Differ Between Different Epilepsy Types During Rest Phase

We observed significant differences between global characteristics (average clustering coefficient and average shortest path length) of networks from subjects with generalized epilepsies, focal epilepsies and from non-epilepsy subjects, which corroborates previous studies (Niso et al., 2015; Drenthen et al., 2020). Here, subjects with generalized epilepsies presented with less segregated and more integrated functional brain networks. These findings are in line with earlier studies (Chavez et al., 2010; Chowdhury et al., 2014), though contrast with another study (Zhang et al., 2011). Network studies in epilepsy and especially epilepsy syndromes is an evolving research field, and although results and knowledge are published at a tremendous pace, the applied methods differ and results are not easy to reconcile and might therefore explain opposing results. On the local scale and in par with previous studies (Lohmann et al.,

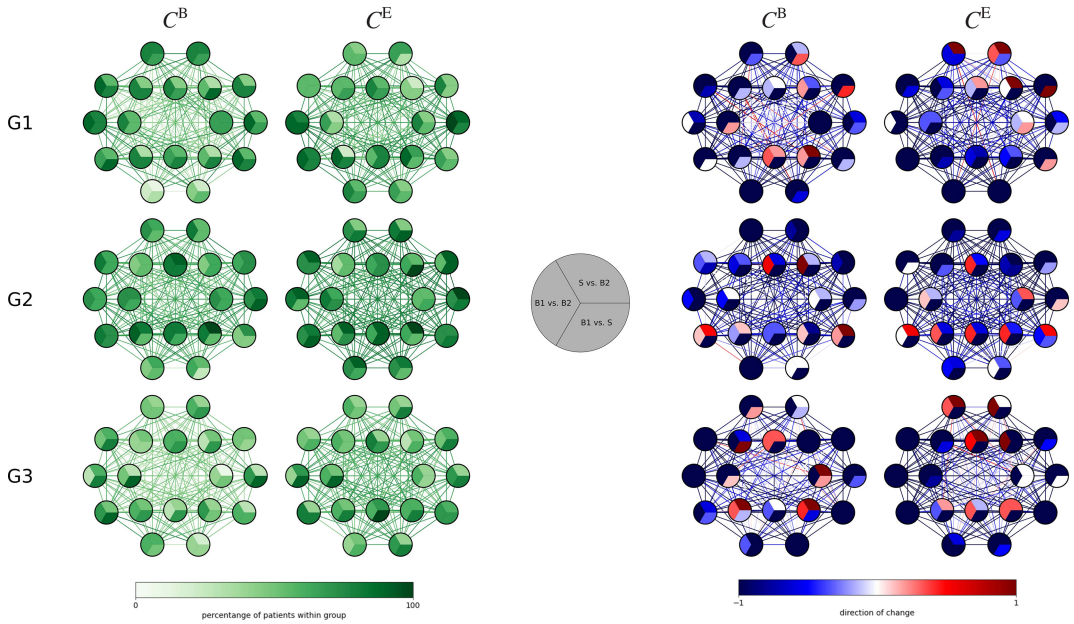

FIGURE 4 | (Left) Distributions of taVNS-related alterations in local network characteristics (betweenness centrality C^B and eigenvector centrality C^E) of the three investigated groups (G1 = focal epilepsy group, G2 = generalized epilepsy group, G3 = non-epilepsy group) between the three investigated phases (B1 = pre-stimulation baseline 1, S = stimulation, B2 = post-stimulation baseline 2). Network vertices arranged according the international 10–20 system for EEG-recording. Color coding of vertices and edges according to the percentage of subjects for whom significant changes in local network characteristics were observed on per subject base. **(Right)** Differences between phases (B1, S B2) for local network characteristics in the three investigated groups. Color coding of vertices and edges according to the direction of change of importance for vertices and edges (per subject base).

TABLE 1 | Synopsis of taVNS-induced immediate and enduring modifications of global and local characteristics of weighted fully connected functional brain networks in different epilepsy types.

		Focal epilepsy group	Generalized epilepsy group	Non-epilepsy group
Global network scale				
Topology	Immediate effect	Segregation ↑ integration ↓	Segregation ↓ integration ↑	Segregation ↑ integration ↔
	Enduring effect	Segregation ↓ integration ↑	Segregation ↑ integration ↓	Segregation ↓ integration ↑
Robustness	Immediate effect	↑	↑	↑↑
	Enduring effect	↑↑	↓↓	↑↑
Stability of the synchronized state	Immediate effect	↔	↑	↑
	Enduring effect	↑	↓	↔
Local network scale				
Path-based centrality index	Vertices	Diffuse	Diffuse	Diffuse
	Edges	Diffuse	Diffuse	Diffuse
Interaction-strength-based centrality index	Vertices	Diffuse	Diffuse	Diffuse
	Edges	Diffuse	Diffuse	Diffuse

↑, *increase;* ↑↑, *strong increase;* ↓, *decrease,* ↓↓, *strong decrease;* ↔, *negligible change.*

2010; van den Heuvel and Sporns, 2013; Rings et al., 2021), different brain regions were highlighted as important with the different centrality concepts. Our findings for the three subject groups, namely left fronto-central brain regions are characterized as most important with betweenness centrality and parieto-occipital regions with eigenvector centrality, are in line with previous observations (Lohmann et al., 2010; van den Heuvel and Sporns, 2013). Differences in functional connections between brain regions were negligible as no clear-cut spatial differences were observed between subjects with generalized epilepsies, focal epilepsies and non-epilepsy subjects.

Summarizing these findings, we could show that already during rest global but not local characteristics of functional

brain networks are different in generalized epilepsies compared to focal epilepsies and the non-epilepsy group. Results derived from brain network analyses might thus provide additional information for differentiating between different types of epilepsy, and thereby supporting a thorough work-up for classification of epilepsy type which is indispensable for optimal patients' care.

Transcutaneous Auricular Vagus Nerve Stimulation Differently Modifies Global and Local Network Characteristics in Different Epilepsy Types

As in previous studies (Redgrave et al., 2018; von Wrede et al., 2021), taVNS was easy to use, well tolerated and without negative impact on attention and executive function; in some subjects these even improved.

On the global network scale, short-term taVNS induced modifications of topology-, robustness-, and stability-associated network characteristics in the majority of investigated subjects as it was observed in previous studies (Rings et al., 2021; von Wrede et al., 2021). A taVNS-related enduring topological reorganization of functional brain networks in focal epilepsies in terms of a more integrated and less segregated network structure was shown recently (von Wrede et al., 2021). Extending this finding, we here observed modifications of functional brain network organization to differ between different epilepsy types. We found an inverted pattern of reorganization between focal and generalized epilepsies, with the latter displaying an immediate reorganization toward a more integrated/less segregated and an enduring reorganization toward a more segregated/less integrated network. The taVNS-mediated topological reorganization of functional brain networks in the non-epilepsy subjects resembled those of the focal epilepsy group though being less pronounced. These epilepsy-type-related findings might explain the differing results for immediate modifications of brain network reorganization by taVNS reported previously (Rings et al., 2021).

TaVNS induced a comparable immediate robustness-enhancing modification of the functional brain networks of subjects with focal and generalized epilepsies as well as non-epilepsy subjects. The enduring effect, however, clearly differed between epilepsy types: robustness increased in the focal epilepsy group (which is in par with a previous study (von Wrede et al., 2021), but decreased in the generalized epilepsy group. What is more, taVNS induced an enduring higher vulnerability for perturbation in generalized epilepsies and a lower one in focal epilepsies, leading to different network stability.

Interestingly, on a local network scale, more subjects with generalized epilepsy than with focal epilepsy displayed taVNS-induced modifications of importance of brain regions and functional connections. We hypothesize that in focal epilepsies important brain regions are more susceptible for modifications, whereas in generalized epilepsy the pattern of modified brain regions is more diffuse. No clear-cut spatial pattern could be observed for the importance of functional connections.

Summarizing these findings (see **Table 1**), we could provide first evidence that in subjects with generalized or focal epilepsy, short-term taVNS differently modified global characteristics of their functional brain networks. Local network characteristics remained largely unaffected as already reported on previously (Rings et al., 2021).

There are some limitations of our study; due to the special setting on the ward and the necessity of the longer EEG-recording as well as due to drop outs, the number of investigated subjects was rather low. What is more, though matched between groups, the span in age and epilepsy duration was rather high, which might have influenced our findings. Further studies in larger groups are thus necessary.

Using non–pharmaceutical interventions in epilepsy treatment often starts rather late in the course of treatment, especially since most of the current non–pharmaceutical interventions, such as epilepsy surgery or invasive stimulation methods, are accompanied by clearly defined risks. The non-invasive stimulation-based treatment is still in its infancy. The search for candidates who might profit from taVNS-based treatment should thus be extended, as it is common for epilepsy surgery and also ASM. Our experimental findings suggest, to our knowledge for the first time, different stimulation-mediated modifications of functional brain networks in different epilepsy types and point at potentially different responses of epileptic brain networks to taVNS in focal and generalized epilepsies. Further studies that investigate possible relationships between taVNS-induced modifications of functional brain networks and clinical efficacy are necessary to translate these experimental findings into clinical decision-making. The search for predictors of successful vagus nerve stimulation is a major challenge, for which first interesting insights have already been presented for iVNS (Workewych et al., 2020), but it is of importance to proceed and to install standardized protocols for experimental VNS research (Farmer et al., 2021) and also for future clinical applications.

DATA AVAILABILITY STATEMENT

The datasets presented in this article are not readily available because they contain information that could comprise the privacy of the participants. Requests to access the datastes should be directed to RW, randi.von.wrede@ukbonn.de.

ETHICS STATEMENT

The studies involving human participants were reviewed and approved by the Ethics Committee of the University of Bonn.

The patients/participants provided their written informed consent to participate in this study.

AUTHOR CONTRIBUTIONS

RW, CH, and KL: conceptualization. RW and KL: methodology, writing—original draft preparation, writing—review, editing, and supervision. RW, TR, TB, JP, SS, CH, and KL: validation, formal analysis, and data curation. All authors contributed to the article and approved the submitted version.

FUNDING

This work was supported by the Verein zur Foerderung der Epilepsieforschung e.V. (Bonn).

SUPPLEMENTARY MATERIAL

The Supplementary Material for this article can be found online at: https://www.frontiersin.org/articles/10.3389/fnhum.2022.867563/full#supplementary-material

REFERENCES

Barbella, G., Cocco, I., Freri, E., Marotta, G., Visani, E., Franceschetti, S., et al. (2018). Transcutaneous vagal nerve stimulatio (t-VNS): an adjunctive treatment option for refractory epilepsy. *Seizure* 60, 115–119. doi: 10.1016/j.seizure.2018.06.016

Bauer, S., Baier, H., Baumgartner, C., Bohlmann, K., Fauser, S., Graf, W., et al. (2016). Transcutaneous Vagus Nerve Stimulation (tVNS) for Treatment of Drug-Resistant Epilepsy: a Randomized, Double-Blind Clinical Trial (cMPsE02). *Brain Stimul.* 9, 356–363. doi: 10.1016/J.BRS.2015.11.003

Ben-Menachem, E. (2002). Vagus-nerve stimulation for the treatment of epilepsy. *Lancet Neurol.* 1, 477–482. doi: 10.1016/s1474-4422(02)00220-x

Berg, A. T., and Scheffer, I. E. (2011). New concepts in classification of the epilepsies: entering the 21st century. *Epilepsia* 52, 1058–1062. doi: 10.1111/j.1528-1167.2011.03101.x

Bullmore, E., and Sporns, O. (2009). Complex brain networks: graph theoretical analysis of structural and functional systems. *Nat. Rev. Neurosci.* 10, 186–198. doi: 10.1038/nrn2575

Chavez, M., Valencia, M., Navarro, V., Latora, V., and Martinerie, J. (2010). Functional modularity of background activities in normal and epileptic brain networks. *Phys. Rev. Lett.* 104:118701. doi: 10.1103/PhysRevLett.104.118701

Chen, Z., Brodie, M. J., Liew, D., and Kwan, P. (2018). Treatment outcomes in patients with newly diagnosed epilepsy treated with established and new antiepileptic drugs a 30-year longitudinal cohort study. *JAMA Neurol.* 75, 279–286. doi: 10.1001/jamaneurol.2017.3949

Chowdhury, F. A., Woldman, W., FitzGerald, T. H. B., Elwes, R. D. C., Nashef, L., Terry, J. R., et al. (2014). Revealing a brain network endophenotype in families with idiopathic generalised epilepsy. *PLoS One* 9:e110136. doi: 10.1371/journal.pone.0110136

Drenthen, G. S., Fasen, F., Fonseca Wald, E. L. A., Backes, W. H., Aldenkamp, A. P., Vermeulen, R. J., et al. (2020). Functional brain network characteristics are associated with epilepsy severity in childhood absence epilepsy. *NeuroImage Clin.* 27:102264. doi: 10.1016/j.nicl.2020.102264

Elliott, R. E., Morsi, A., Kalhorn, S. P., Marcus, J., Sellin, J., Kang, M., et al. (2011). Vagus nerve stimulation in 436 consecutive patients with treatment-resistant epilepsy: long-term outcomes and predictors of response. *Epilepsy Behav.* 20, 57–63. doi: 10.1016/j.yebeh.2010.10.017

Farmer, A. D., Strzelczyk, A., Finisguerra, A., Gourine, A. V., Gharabaghi, A., Hasan, A., et al. (2021). International Consensus Based Review and Recommendations for Minimum Reporting Standards in Research on Transcutaneous Vagus Nerve Stimulation (Version 2020). *Front. Hum. Neurosci.* 14:568051. doi: 10.3389/fnhum.2020.568051

Fisher, B., DesMarteau, J. A., Koontz, E. H., Wilks, S. J., and Melamed, S. E. (2020). Responsive Vagus Nerve Stimulation for Drug Resistant Epilepsy: a Review of New Features and Practical Guidance for Advanced Practice Providers. *Front. Neurol.* 11:610379. doi: 10.3389/fneur.2020.610379

Fisher, R. S., Acevedo, C., Arzimanoglou, A., Bogacz, A., Cross, J. H., Elger, C. E., et al. (2014). ILAE Official Report: a practical clinical definition of epilepsy. *Epilepsia* 55, 475–482. doi: 10.1111/epi.12550

GBD 2016 Epilepsy Collaborators (2019). Global, regional, and national burden of epilepsy, 1990-2016: a systematic analysis for the Global Burden of Disease Study 2016. *Lancet Neurol.* 18, 357–375. doi: 10.1016/S1474-4422(18)30454-X

Hauser, W., and Hesdorffer, D. (1991). "Epidemiology in Epilepsy," in *Neurepidemiology*, eds D. W. Anderson and D. G. Schoenberg (Boca Raton, FL: CRC Press).

Höller, Y., Helmstaedter, C., and Lehnertz, K. (2018). Quantitative Pharmaco-Electroencephalography in Antiepileptic Drug Research. *CNS Drugs* 32, 839–848. doi: 10.1007/s40263-018-0557-x

Kwan, P., and Brodie, M. J. (2000). Early Identification of Refractory Epilepsy. *N. Engl. J. Med.* 342, 314–319. doi: 10.1056/NEJM200002033420503

Kwan, P., Arzimanoglou, A., Berg, A. T., Brodie, M. J., Allen Hauser, W., Mathern, G., et al. (2010). Definition of drug resistant epilepsy: consensus proposal by the ad hoc Task Force of the ILAE Commission on Therapeutic Strategies. *Epilepsia* 51, 1069–1077. doi: 10.1111/j.1528-1167.2009.02397.x

Lampros, M., Vlachos, N., Zigouris, A., Voulgaris, S., and Alexiou, G. A. (2021). Transcutaneous Vagus Nerve Stimulation (t-VNS) and epilepsy: a systematic review of the literature. *Seizure* 91, 40–48. doi: 10.1016/j.seizure.2021.05.017

Liu, A., Song, L., Wang, X., Wang, Y., Gong, L., Li, L., et al. (2018). Efficacy and Safety of Treatment with Transcutaneous Vagus Nerve Stimulation in 17 Patients with Refractory Epilepsy Evaluated by Electroencephalogram, Seizure Frequency, and Quality of Life. *Med. Sci. Monit.* 24, 8439–8448. doi: 10.12659/msm.910689

Lohmann, G., Margulies, D., Horstmann, A., Pleger, B., Lepsien, J., Goldhahn, D., et al. (2010). Eigenvector Centrality Mapping for Analyzing Connectivity Patterns in fMRI Data of the Human Brain. *PLoS One* 5:e10232. doi: 10.1371/journal.pone.0010232

Marson, A. G., Al-Kharusi, A. M., Alwaidh, M., Appleton, R., Baker, G. A., Chadwick, D. W., et al. (2007a). The SANAD study of effectiveness of carbamazepine, gabapentin, lamotrigine, oxcarbazepine, or topiramate for treatment of partial epilepsy: an unblinded randomised controlled trial. *Lancet* 369, 1000–1015. doi: 10.1016/S0140-6736(07)60460-7

Marson, A. G., Al-Kharusi, A. M., Alwaidh, M., Appleton, R., Baker, G. A., Chadwick, D. W., et al. (2007b). The SANAD study of effectiveness of valproate, lamotrigine, or topiramate for generalised and unclassifiable epilepsy: an unblinded randomised controlled trial. *Lancet* 369, 1016–1026. doi: 10.1016/S0140-6736(07)60461-9

Marson, A., Burnside, G., Appleton, R., Smith, D., Leach, J. P., Sills, G., et al. (2021). The SANAD II study of the effectiveness and cost-effectiveness of levetiracetam, zonisamide, or lamotrigine for newly diagnosed focal epilepsy: an open-label, non-inferiority, multicentre, phase 4, randomised controlled trial. *Lancet* 397, 1363–1374. doi: 10.1016/S0140-6736(21)00247-6

Morris, G. L. III, Gloss, D., Buchhalter, J., Mack, K. J., Nickels, K., and Harden, C. (2013). Evidence-based guideline update: vagus nerve stimulation for the treatment of epilepsy: report of the Guideline Development Subcommittee of the American Academy of Neurology. *Neurology* 81, 1453–1459. doi: 10.1212/WNL.0b013e3182a393d1

Niso, G., Carrasco, S., Gudín, M., Maestú, F., Del-Pozo, F., and Pereda, E. (2015). What graph theory actually tells us about resting state interictal MEG epileptic activity. *NeuroImage Clin.* 8, 503–515. doi: 10.1016/j.nicl.2015.05.008

Redgrave, J., Day, D., Leung, H., Laud, P. J., Ali, A., Lindert, R., et al. (2018). Safety and tolerability of Transcutaneous Vagus Nerve stimulation in humans; a systematic review. *Brain Stimul.* 11, 1225–1238. doi: 10.1016/j.brs.2018.08.010

Révész, D., Rydenhag, B., and Ben-Menachem, E. (2016). Complications and safety of vagus nerve stimulation: 25 years of experience at a single center. *J. Neurosurg. Pediatr.* 18, 97–104. doi: 10.3171/2016.1.PEDS15534

Rings, T., von Wrede, R., Bröhl, T., Schach, S., Helmstaedter, C., and Lehnertz, K. (2021). Impact of Transcutaneous Auricular Vagus Nerve Stimulation on Large-Scale Functional Brain Networks: from Local to Global. *Front. Physiol.* 12:700261. doi: 10.3389/fphys.2021.700261

Rutecki, P. (1990). Anatomical, physiological, and theoretical basis for the antiepileptic effect of vagus nerve stimulation. *Epilepsia* 31, S1–S6. doi: 10.1111/j.1528-1157.1990.tb05843.x

Scheffer, I. E., Berkovic, S., Capovilla, G., Connolly, M. B., French, J., Guilhoto, L., et al. (2017). ILAE classification of the epilepsies: position paper of the ILAE Commission for Classification and Terminology. *Epilepsia* 58, 512–521. doi: 10.1111/epi.13709

Stefan, H., Kreiselmeyer, G., Kerling, F., Kurzbuch, K., Rauch, C., Heers, M., et al. (2012). Transcutaneous vagus nerve stimulation (t-VNS) in pharmacoresistant epilepsies: a proof of concept trial. *Epilepsia* 53, e115–e118. doi: 10.1111/j.1528-1167.2012.03492.x

Tononi, G., Sporns, O., and Edelman, G. M. (1994). A measure for brain complexity: relating functional segregation and integration in the nervous system. *Proc. Natl. Acad. Sci. U. S. A.* 91, 5033–5037. doi: 10.1073/pnas.91.11.5033

van den Heuvel, M. P., and Sporns, O. (2013). Network hubs in the human brain. *Trends Cogn. Sci.* 17, 683–696. doi: 10.1016/j.tics.2013.09.012

von Wrede, R., Moskau-Hartmann, S., Rüber, T., Helmstaedter, C., and Surges, R. (2019). Sustained seizure freedom with transcutaneous vagal nerve stimulation in drug-resistant epilepsy caused by subcortical band heterotopias. *Seizure* 70, 25–26. doi: 10.1016/j.seizure.2019.06.026

von Wrede, R., Rings, T., Schach, S., Helmstaedter, C., and Lehnertz, K. (2021). Transcutaneous auricular vagus nerve stimulation induces stabilizing modifications in large-scale functional brain networks: towards understanding the effects of taVNS in subjects with epilepsy. *Sci. Rep.* 11:7906. doi: 10.1038/s41598-021-87032-1

Workewych, A. M., Arski, O. N., Mithani, K., and Ibrahim, G. M. (2020). Biomarkers of seizure response to vagus nerve stimulation: a scoping review. *Epilepsia* 61, 2069–2085. doi: 10.1111/epi.16661

World Health Organization [WHO] (2019). *Epilepsy*. Geneva: World Health Organization.

Zhang, Z., Liao, W., Chen, H., Mantini, D., Ding, J.-R., Xu, Q., et al. (2011). Altered functional-structural coupling of large-scale brain networks in idiopathic generalized epilepsy. *Brain* 134, 2912–2928. doi: 10.1093/brain/awr223

Conflict of Interest: RW received once a fee for lecture from Cerbomed in 2016.

The remaining authors declare that the research was conducted in the absence of any commercial or financial relationships that could be construed as a potential conflict of interest.

Publisher's Note: All claims expressed in this article are solely those of the authors and do not necessarily represent those of their affiliated organizations, or those of the publisher, the editors and the reviewers. Any product that may be evaluated in this article, or claim that may be made by its manufacturer, is not guaranteed or endorsed by the publisher.

frontiers | Frontiers in Human Neuroscience

TYPE Case Report
PUBLISHED 28 July 2022
DOI 10.3389/fnhum.2022.815232

OPEN ACCESS

EDITED BY
Ken-Ichiro Tsutsui,
Tohoku University, Japan

REVIEWED BY
Brian A. Coffman,
University of Pittsburgh, United States
Zsuzsanna Kocsis,
The University of Iowa, United States

*CORRESPONDENCE
Lu Shen
lu.shen2013@gmail.com
Xingzhou Liu
sinclairliu@sina.cn

†These authors have contributed equally to this work

SPECIALTY SECTION
This article was submitted to Brain Imaging and Stimulation, a section of the journal Frontiers in Human Neuroscience

RECEIVED 15 November 2021
ACCEPTED 30 June 2022
PUBLISHED 28 July 2022

CITATION
Long Q, Li W, Zhang W, Han B, Chen Q, Shen L and Liu X (2022) Electrical stimulation mapping in the medial prefrontal cortex induced auditory hallucinations of episodic memory: A case report. *Front. Hum. Neurosci.* 16:815232. doi: 10.3389/fnhum.2022.815232

Electrical stimulation mapping in the medial prefrontal cortex induced auditory hallucinations of episodic memory: A case report

Qiting Long[1,2†], Wenjie Li[1,2†], Wei Zhang[3†], Biao Han[1,2], Qi Chen[1,2], Lu Shen[1,2*] and Xingzhou Liu[3*]

[1]Key Laboratory of Brain, Cognition and Education Sciences, Ministry of Education, Guangzhou, China, [2]Guangdong Key Laboratory of Mental Health and Cognitive Science, Center for Studies of Psychological Application, School of Psychology, South China Normal University, Guangzhou, China, [3]Department of Neurology, Beijing Tsinghua Changgung Hospital, Beijing, China

It has been well documented that the auditory system in the superior temporal cortex is responsible for processing basic auditory sound features, such as sound frequency and intensity, while the prefrontal cortex is involved in higher-order auditory functions, such as language processing and auditory episodic memory. The temporal auditory cortex has vast forward anatomical projections to the prefrontal auditory cortex, connecting with the lateral, medial, and orbital parts of the prefrontal cortex. The connections between the auditory cortex and the prefrontal cortex thus help in localizing, recognizing, and comprehending external auditory inputs. In addition, the medial prefrontal cortex (MPFC) is believed to be a core region of episodic memory retrieval and is one of the most important regions in the default mode network (DMN). However, previous neural evidence with regard to the comparison between basic auditory processing and auditory episodic memory retrieval mainly comes from fMRI studies. The specific neural networks and the corresponding critical frequency bands of neuronal oscillations underlying the two auditory functions remain unclear. In the present study, we reported results of direct cortical stimulations during stereo-electro-encephalography (SEEG) recording in a patient with drug-resistant epilepsy. Electrodes covered the superior temporal gyrus, the operculum and the insula cortex of bilateral hemispheres, the prefrontal cortex, the parietal lobe, the anterior and middle cingulate cortex, and the amygdala of the left hemisphere. Two types of auditory hallucinations were evoked with direct cortical stimulations, which were consistent with the habitual seizures. The noise hallucinations, i.e., "I could hear buzzing noises in my head," were evoked with the stimulation of the superior temporal gyrus. The episodic memory hallucinations "I could hear a young woman who was dressed in a red skirt saying: What is the matter with you?," were evoked with the stimulation of MPFC. The patient described how she had met this young

woman when she was young and that the woman said the same sentence to her. Furthermore, by analyzing the high gamma power (HGP) induced by direct electrical stimulation, two dissociable neural networks underlying the two types of auditory hallucinations were localized. Taken together, the present results confirm the hierarchical processing of auditory information by showing the different involvements of the primary auditory cortex vs. the prefrontal cortex in the two types of auditory hallucinations.

KEYWORDS

electrical stimulation mapping, auditory processing, episodic memory retrieval, default mode network, high gamma activity, case report

Introduction

The temporal auditory cortex, including the superior temporal gyrus and the sulcus, is divided into the core region, the belt region, the para-belt region, and the rostral superior temporal gyrus (Rauschecker et al., 1995, 1997; Rauschecker and Tian, 2004; Romanski and Averbeck, 2009). The prefrontal lobe is involved in various higher-order cognitive functions, such as decision-making, motor planning, and communication (Barbas, 1995; Petrides, 2005; Fuster, 2008; Kostopoulos and Petrides, 2008). The temporal auditory cortex has vast forward anatomical projections to the prefrontal auditory cortex, connecting with the lateral, medial, and orbital parts of the prefrontal cortex (Petrides and Pandya, 1988; Barbas et al., 1999; Romanski et al., 1999; Romanski and Goldman-Rakic, 2002; Romanski and Averbeck, 2009; Plakke and Romanski, 2014). Conversely, the prefrontal cortex has backward anatomical projections with the temporal auditory cortex (Barbas et al., 2011). The connections between the auditory cortex and the prefrontal cortex are involved in localizing, recognizing, and comprehending external auditory inputs. In addition, the vast and diverse interconnections between the temporal auditory cortex and the prefrontal cortex suggest a close relationship between auditory information processing and prefrontal functions. The temporal auditory cortex inputs all levels of sound information to the prefrontal cortex. Our brain processes the relevant acoustic information and ignores the irrelevant noises and further transforms the selected auditory information into spatial locations and semantics for object recognition, communication, and motor execution. Therefore, the prefrontal cortex is regarded as a higher-order "auditory field" in addition to the temporal cortex.

In addition, the medial prefrontal cortex (MPFC) plays an important role in social cognition and self-referential cognition. It is believed to be a core region during episodic memory retrieval, especially in the retrieval of autobiographical information (Svoboda et al., 2006; McDermott et al., 2009; Eichenbaum, 2017). Therefore, the prefrontal cortex involves dealing with memory retrieval with sounds. In an fMRI study, regions, such as the MPFC, the cingulate cortex, and the medial temporal structures, were associated with enhanced activity in the general recollection network (Rugg and Vilberg, 2013). Furthermore, MPFC is one of the major regions in the Default Mode Network (DMN) (Sestieri et al., 2011). The DMN includes three main regions: The MPFC, the posterior cingulate cortex, and the bilateral angular gyrus, and it can be divided into many sub-systems, including episodic memory and self-referential cognition (Andrews-Hanna et al., 2010). Previous studies pointed out that DMN is responsible for episodic memory retrieval (Buckner et al., 2008; Foster et al., 2012), and the frontoparietal network is also involved in episodic memory retrieval (St Jacques et al., 2011; Westphal et al., 2017). However, previous neural evidence with regard to the comparison between basic auditory processing and auditory episodic memory retrieval mainly comes from fMRI studies.

One optimal method to examine the functional roles of given regions in basic auditory processing and auditory episodic memory retrieval is direct electrical stimulation, in which a volley of electrical charge is delivered to a focal brain area to perturb its function (Selimbeyoglu and Parvizi, 2010). In the present study, we induced two different types of auditory hallucinations by applying electrical stimulation mapping (ESM) to an epilepsy patient who was undergoing stereo-electro-encephalography (SEEG) recording with implanted electrodes. One type of auditory hallucination was noise hallucination with only basic sound during stimulation of the superior temporal gyrus. The other type was an auditory hallucination that contained semantic auditory hallucinations and episodic memory retrieval during the stimulation of the MPFC. It has been suggested that the functional changes induced by electrical stimulation may reflect the dysfunction of a large-scale network but not just one site (Mandonnet et al., 2010, 2016). Therefore, in the present study, we aimed to identify the brain regions and networks associated with the two different auditory hallucinations.

It has been demonstrated that high gamma activity was extensively recorded in acoustic and speech processing (Edwards et al., 2005; Chang et al., 2011; Nourski et al., 2014), auditory verbal memory (Kaiser et al., 2003), and auditory language comprehension (Nakai et al., 2017; Ikegaya et al., 2019). A recent study showed that high-frequency activity induced by 50 Hz electrical stimulation during language disturbances may help to localize language-related regions (Perrone-Bertolotti et al., 2020). In the present study, we used a similar approach to identify brain areas and networks associated with two different auditory hallucinations by analyzing the high gamma band activity induced by 50 Hz electrical stimulation. We found that the temporal auditory network was primarily involved in the noise hallucinations, while the DMN and frontoparietal network were involved in the episodic memory hallucinations. These results shed light on the fact that the prefrontal cortex is involved in the auditory information processing and retrieval of episodic memory. These results were consistent with previous studies that MPFC is involved in the dual auditory processing networks and the episodic memory retrieval networks, such as DMN.

Materials and methods

Subject

The subject was a 30-year-old female patient implanted with intracranial electrodes to localize the source of drug-resistant seizures who provided informed consent to participate in this study. The procedure was approved by the Ethics Committee of the School of Psychology, South China Normal University. The patient also consented to the publication of the present case report. Detailed history, neurological examination, neuropsychological evaluation, neuroimaging, high-resolution structural magnetic resonance imaging, and positron emission tomography/computed tomography (PET/CT) were accessed during the non-invasive diagnostic evaluation. Detailed profiles of the patient are provided in **Supplementary Table 1**. The habitual seizure semiology was: aura (including rustling of leaves, or the voice of a young woman who was dressed in a red skirt saying "what is the matter with you") → chapeau de gendarme → automatic movement (hands) → hyperventilation. The duration of the seizure was about 10–30 s. In the first few years, the seizure frequency was 1–2 times a year, but it became more and more frequent, although, with appropriate and adequate anti-epileptic drugs, it became 3–10 times per day prior to surgery. There was no relevant family history of the patient. Additionally, she did not have any intracranial surgeries before SEEG implantation. After the invasive evaluation with SEEG, the epileptic zone was identified, and a tailored resection was made. The patient has been seizure-free for 3 years since the surgical treatment.

Intracranial implantation

During the pre-surgical SEEG evaluation, the clinical team gave a detailed and precise diagnosis of the anatomical location of the epileptogenic zone and its relationship with the eloquent cortex. The patient was implanted with 16 electrodes (left: 13 and right: 3). The depth electrodes were semi-rigid platinum/iridium with either 7 or 18 contacts (2 mm in length, 0.8 mm in diameter, and 1.5 mm apart). The distribution of all the electrodes in the brain is shown in **Supplementary Figure 1**. To locate the electrode contacts, a CT scan after the electrode implantation and a pre-operative MRI were co-registered in FSL,[1] and then, electrode coordinates were obtained using FreeSurfer scripts (FreeSurfer scripts:).[2] The electrodes were positioned in different areas based on the Destrieux Atlas (Destrieux et al., 2010).

Electrical stimulation mapping

The ESM was performed by a professional physician during the SEEG recording. SEEG was recorded with simultaneous video recording, using a 256-channel Nihon Kohden Neurofax 1200A Digital System. Bipolar electrical stimuli (50 Hz, pulse width 0.3 ms, intensity 0.6–5 mA, duration 3–5 s) were delivered by means of biphasic rectangular stimuli of alternating polarity. The patient was not informed of the stimulation onset/offset and was asked to describe any feelings she experienced. Both subjective reports of her and objective observations from the physician were noted down on the patient's medical record, which were ultimately reviewed on recording and confirmed by two neurologists and a neuroscientist.

Localization of responsive electrodes

Recording electrodes were considered to be responsive if HGP was within the post-stimulation period (0.2–2.8 s) against ($z > 2$) the pre-stimulation baseline period (–500 to –20 ms). HGP was computed by means of a continuous wavelet transform of data for the frequency range from 70 to 160 Hz. The length of the wavelets increased linearly from 10 cycles at 70 Hz to 26 cycles at 160 Hz. The wavelet analysis was performed with a Morlet wavelet by applying a Gaussian-shaped taper. The spectral resolution was chosen at 2 Hz. The start of the stimulation onset was based on the stimulation artifact. Then, the high gamma band power within the post-stimulation period was transformed into a z-score against the pre-stimulation baseline period in each stimulation

1 www.fmrib.ox.ac.uk/fsl

2 http://surfer.nmr.mgh.harvard.edu

condition. To eliminate any influence of stimulation artifacts in the predicted SEEG power changes, we masked out z-values above 10 along the frequency dimension and removed channels (less than 15 mm away from the stimulating electrodes). Bad recording electrodes were excluded from all analyses. Finally, to obtain responsive electrodes within each type of auditory hallucination, response electrodes under all relevant stimulation conditions were intersected.

High gamma power z-scores of electrodes within the networks of interest

All implanted electrodes (except electrodes in the epileptic zone, as seen in **Supplementary Figure 1**) were categorized into DMN and frontoparietal networks using Yeo Atlas (Yeo et al., 2011) and categorized into the auditory network (early auditory cortex and auditory association cortex) using the multimodal cortical parcellation (Glasser et al., 2016). The early auditory areas include A1, Lateral Belt (LBelt), Medial Belt (MBelt), Para-Belt (PBelt), and the retro-insular cortex (RI). The auditory association cortex includes A4, A5, STSdp, STSda, STSvp, STSva, STGa, and TA2. Electrodes of the MPFC within DMN were defined using the multimodal cortical parcellation, including a32pr, d32, and 9 m (Glasser et al., 2016). All these automatic labels were confirmed visually by two neurologists (anatomical locations of all network electrode sites as shown in **Figure 1**). The HGP z-scores of the recording electrodes in each network within each type of auditory hallucination were determined by averaging the HGP z-values from relevant stimulation conditions.

Statistical analyses

To examine whether the HGP z-values of a specific network showed a statistical difference between noise hallucinations and episodic memory hallucinations conditions, we performed a paired t-test for each network and corrected for multiple comparisons with the false discovery correction (FDR) procedure (Benjamini and Hochberg, 1995).

Results

Electrical stimulation in different sites induced different hallucinations symptoms

Electrical stimulation mapping could evoke a summation effect in a vast volume of the cortex and cause a transient

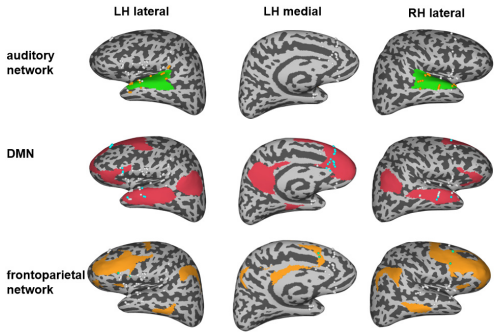

FIGURE 1
Distribution of electrodes in three different networks. The green region represents the auditory network and the orange electrodes indicate the electrodes in the auditory network. The red region represents the default mode network (DMN), and the blue electrodes indicate the electrodes in the DMN. The orange region represents the frontal network and the green electrodes indicate the electrodes in the frontal network. Note that the white electrodes represent electrodes that were implanted outside the corresponding network.

experience or changes in behavior. The subjective experiences or behavioral changes induced by ESM in the patient could be categorized into two main types of auditory hallucinations: noise hallucinations vs. episodic memory hallucinations. Noise hallucinations were described by the patient as "I could hear buzzing noises in my head." The episodic memory hallucinations were complex auditory hallucinations with specific contents, i.e., the patient reported that "I could hear a young woman's voice saying: what is the matter with you?" The latter type of auditory aura was her habitual seizure. The patient further described that she seemed to see her when she heard this voice. She had seen this girl before, wearing a red dress, and had said the same thing to her. Therefore, we believe that she recalled episodic memories during the stimulation. The noise hallucinations were evoked on the middle part of the superior temporal gyrus of the left hemisphere (**Figure 2** and **Supplementary Table 2**) while the episodic memory hallucinations symptoms were elicited on the left superior frontal gyrus (**Figure 2** and **Supplementary Table 2**) *via* ESM.

High gamma activity associated with hallucinations symptoms

The current applied to the stimulation sites not only affects the local activity but also affects the network areas connected with the stimulation sites (Perrone-Bertolotti et al., 2020). Therefore, the subjective experiences and behavioral changes elicited by the electrical stimulations were attributed to the functional changes of the large-scale distributed neural networks: both the noise and the episodic memory

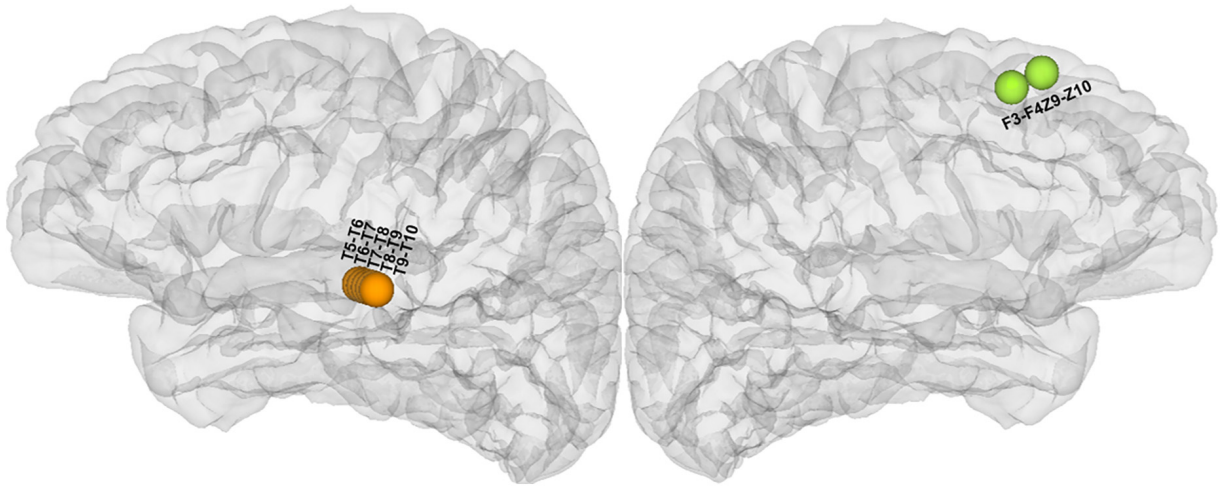

FIGURE 2
Anatomical location of all cortical stimulated sites responsible for hallucinations during electrical stimulation mapping (ESM) (the orange electrodes in the lateral view of the left hemisphere were responsible for noise hallucinations and the green electrodes in the medial view of the left hemisphere were responsible for episodic memory hallucinations).

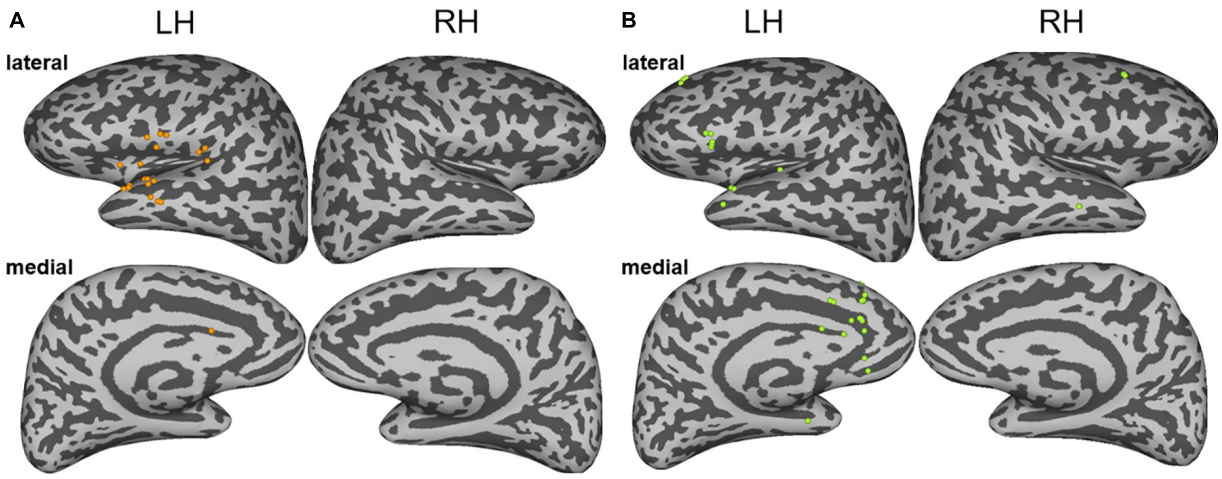

FIGURE 3
(A) The sites of stimulation-induced high gamma-band power during noise hallucinations. **(B)** The sites of stimulation-induced high gamma-band power during episodic memory hallucinations. Lateral and medial views of the left and right hemispheres are represented.

hallucinations during the ESM could be explained by large-scale brain regions or networks. To identify the brain regions related to different auditory hallucinations, we analyzed the changes in high gamma band activity, which has been considered a potential specific biological support of auditory processing (Edwards et al., 2005; Chang et al., 2011; Nourski et al., 2014). We identified brain regions in which the high gamma band power is higher than the baseline activity ($z > 2$) (as shown in detail in the "Materials and methods" section). The results showed that the two types of auditory hallucinations were associated with increased evoked high gamma activity in different responsive regions. Specifically, the noise hallucinations were associated with enhanced high gamma activity in the ventral auditory stream, including the superior temporal gyrus, the Heschel's gyrus, the central operculum, the parietal operculum, the frontal operculum, the anterior insula, and the cingulate electrodes (**Figure 3A**). Among these regions, the superior temporal gyrus and the middle temporal gyrus were the most representative regions, with 11 electrodes having enhanced high gamma activity, accounting for 38% of all response contacts. These representative regions are key regions of the auditory network.

However, episodic memory hallucinations were associated with the dorsal MPFC, the cingulate gyrus, the pars triangularis, the superior temporal gyrus, and the middle temporal gyrus (**Figure 3B**). Especially, the medial frontal cortex, the cingulate gyrus, and the inferior frontal gyrus were representative regions, with 19 electrodes having enhanced high gamma activity, accounting for 61% of all responsive electrodes. These representative regions are key regions of the DMN and the frontoparietal network.

Functional networks involved in different hallucinations symptoms

By analyzing the responsive brain areas associated with specific hallucinations, we found that the occurrence of the two hallucinations involved distinct regions, suggesting that the two hallucinations may be involved in different networks. Previous neural evidence suggested important roles of the auditory network, the frontoparietal network (St Jacques et al., 2011; Westphal et al., 2017), and the DMN (Buckner et al., 2008; Foster et al., 2012) in auditory processing and episodic memory retrieval. Therefore, we further directly confirmed the different roles of these different networks in noise and episodic memory hallucinations. We reanalyzed data from another perspective: We assigned all implanted electrodes (except the electrodes in the epileptic zone) into different functional networks of interest (as shown in **Figure 1**). Then, we investigated the HGP difference between noise and episodic memory hallucinations within each network. For the auditory network, mean HGP z-values in the noise hallucination condition were higher than that in the episodic memory hallucination condition [$t_{(35)} = 4.072$, $p < 0.001$, FDR corrected]. However, for the DMN [$t_{(31)} = -2.480$, $p < 0.05$, FDR corrected] and the frontoparietal network [$t_{(9)} = -5.192$, $p < 0.01$, FDR corrected], mean HGP z-values in the episodic memory hallucination condition were significantly higher than that in the noise hallucination condition (**Figure 4**).

Since the MPFC in the DMN has been considered a core region in episodic memory retrieval, to further directly show the role of the MPFC in episodic memory hallucinations, we divided the electrodes of the DMN into the MPFC and the others (as shown in section "Materials and Methods") and then analyzed the HGP difference between the two hallucinations for the different groups of DMN electrodes. For the electrodes of the MPFC within the DMN, the mean HGP z-values in the episodic memory hallucination condition were significantly higher than in the noise hallucination condition [$t_{(11)} = 3.365$, $p < 0.01$], while for electrodes within the DMN but outside the MPFC, there was no significant HGP difference between the two hallucination conditions [$t_{(19)} = 0.728$, $p = 0.48$] (as shown in **Supplementary Figure 2**].

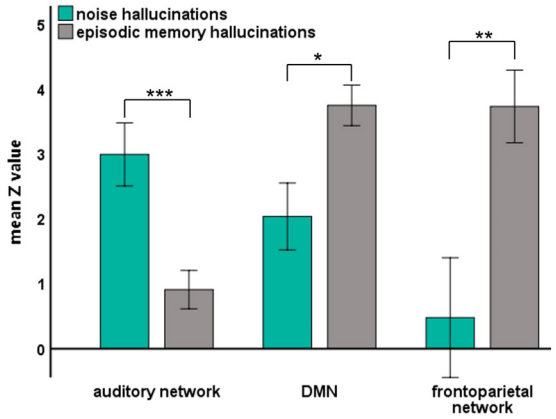

FIGURE 4
The mean HGP z-values of each auditory hallucinations condition in three brain networks. Significant group differences were denoted with asterisks (error bars indicate ± 1 SEM, $*p < 0.05$, $**p < 0.01$, and $***p < 0.001$).

Discussion

In this case study, with the use of the direct cortical stimulation method, we analyzed high gamma activity induced by 50 Hz electrical stimulation to identify brain regions and networks associated with two different auditory hallucinations. The patient had two types of habitual auditory auras, one type was noise hallucinations and the other type was episodic memory hallucinations. Both hallucinations included auditory experience, but episodic memory hallucinations recalled the experience the patient had before. The patient not only heard the voice of a young woman saying "what is the matter with you," but she also recalled the memory that she had seen the young woman before who was dressed in a red skirt. In contrast, the noise auditory aura was only the voices of many people (**Supplementary Table 2**). We found that episodic memory hallucinations were elicited in the medial prefrontal regions, and both the dorsal and ventral auditory streams were activated, including the involvement of the dorsal prefrontal cortices BA8 and BA9, the anterior cingulate cortex, the ventral lateral prefrontal cortices BA44 and BA45, and the superior temporal gyrus. The noise auditory experience was elicited in the superior temporal gyrus, and the ventral stream was activated, including the involvement of the ventral lateral prefrontal cortices BA44 and BA45, the central operculum, and the superior temporal gyrus (**Figures 2**, **3**). The results are consistent with previous auditory pathway studies (Romanski et al., 1999, 2005; Pedersen et al., 2000; Alain et al., 2001; Romanski and Goldman-Rakic, 2002). First, the auditory processing is hierarchically organized such that the "rustling of leaves" is induced in the auditory core region, and the "buzz voice" noise hallucinations were

induced in the belt or the parabelt auditory region. Second, when the auditory hallucinations were involved in semantic processing, the ventral stream was activated. In this case, the ventral auditory stream in episodic memory hallucinations was activated, suggesting that this stream is involved in processing episodic auditory hallucinations.

The difference between these two auras may be due to the medial and dorsal lateral prefrontal network involvement, with additional involvement of BA8B, BA9, and the anterior cingulate cortex (**Figure 3**). The MPFC has proved to be associated with the emotion, memory, and complex cognitive processes (Barbas et al., 2002). The anterior cingulate cortex receives higher processed auditory information from temporal auditory regions and interconnects with the prefrontal cortex to select relevant signals and suppress noise (Micheyl et al., 2007; Medalla and Barbas, 2010). The network of the cingulate-prefrontal-temporal cortical network may help in filtering auditory information in a noise environment. Therefore, in this case, the patient may hear the sentence instead of the noise hallucinations induced in temporal regions.

Our results further confirmed the different roles of the auditory network, the DMN, and the frontoparietal network in noise hallucinations and episodic memory hallucinations (**Figure 4**). Specifically, the auditory cortex showed higher gamma activity in noise hallucinations than episodic memory hallucinations. This is in line with previous studies showing that high gamma activity in the auditory cortex increases during auditory processing (Edwards et al., 2005; Chang et al., 2011; Nourski et al., 2014). More importantly, the DMN and the frontoparietal network showed higher gamma activity in episodic memory hallucinations than noise hallucinations. Compelling evidence supports the relationship between high gamma activity and episodic memory retrieval (Hanslmayr et al., 2016). For example, direct hippocampal recordings from patients with epilepsy showed that high gamma power increases correlation with successful memory encoding and retrieval (Long et al., 2014). Our results further suggest that increased high gamma activity in the DMN and the frontoparietal network are also associated with episodic memory retrieval. These results are also consistent with previous imaging findings demonstrating that the DMN and the frontoparietal network were involved in episodic memory retrieval (Buckner et al., 2008; Foster et al., 2012; St Jacques et al., 2011; Westphal et al., 2017). To note, the MPFC in the DMN has been considered a core region in the neocortex during the retrieval of episodic memory. Direct evidence comes from animal studies, where the performance of episodic memory tasks has been shown to be impaired by lesions or dysfunction in MPFC (DeVito and Eichenbaum, 2010; Barker et al., 2017). In the present study, we further confirmed the critical role of the MPFC in the DMN in auditory hallucinations involving episodic memory retrieval (**Supplementary Figure 2**).

Taken together, the present study supports hierarchical and dual pathways in auditory processing. Both the noise and episodic memory hallucinations involved the ventral stream, suggesting that the ventral stream is involved in language comprehensive processing. Besides, the stimulation of temporal auditory regions only evoked noise hallucinations without clear semantic content and without emotional expression. Moreover, the MPFC in the DMN and the dorsal frontal cortex in the frontoparietal network were associated with auditory episodic memory retrieval. These results suggest higher-level auditory processing in the prefrontal cortex and are consistent with previous studies demonstrating an essential role of the prefrontal cortex in episodic memory retrieval.

Data availability statement

The raw data supporting the conclusions of this article will be made available by the authors, without undue reservation.

Ethics statement

The studies involving human participants were reviewed and approved by the Ethics Committee of School of Psychology, South China Normal University. The patients/participants provided their written informed consent to participate in this study. Written informed consent was obtained from the individual(s) for the publication of any potentially identifiable images or data included in this article.

Author contributions

QL, LS, WZ, and XL contributed to the design of the work. QL contributed to the acquisition of data. WL and LS analyzed the data. WZ, BH, XL, and QC contributed to the interpretation of data. QL and WL wrote the first draft. WZ, BH, QC, LS, and XL edited the manuscript. All authors contributed to the article and approved the submitted version.

Funding

This work was supported by the National Natural Science Foundation of China (31871138, 32071052, and 32000785) and the Guangdong Natural Science Foundation (2021A1515011185).

Conflict of interest

The authors declare that the research was conducted in the absence of any commercial or financial relationships that could be construed as a potential conflict of interest.

Publisher's note

All claims expressed in this article are solely those of the authors and do not necessarily represent those of their affiliated organizations, or those of the publisher, the editors and the reviewers. Any product that may be evaluated in this article, or claim that may be made by its manufacturer, is not guaranteed or endorsed by the publisher.

Supplementary material

The Supplementary Material for this article can be found online at: https://www.frontiersin.org/articles/10.3389/fnhum.2022.815232/full#supplementary-material

References

Alain, C., Arnott, S. R., Hevenor, S., Graham, S., and Grady, C. L. (2001). "What" and "where" in the human auditory system. *Proc. Natl. Acad. Sci. U.S.A.* 98, 2301–2306. doi: 10.1073/pnas.211209098

Andrews-Hanna, J. R., Reidler, J. S., Sepulcre, J., Poulin, R., and Buckner, R. L. (2010). Functional-anatomic fractionation of the brain's default network. *Neuron* 65, 550–562. doi: 10.1016/j.neuron.2010.02.005

Barbas, H. (1995). Anatomic basis of cognitive-emotional interactions in the primate prefrontal cortex. *Neurosci. Biobehav. Rev.* 19, 499–510. doi: 10.1016/0149-7634(94)00053-4

Barbas, H., Ghashghaei, H., Dombrowski, S. M., and Rempel-Clower, N. L. (1999). Medial prefrontal cortices are unified by common connections with superior temporal cortices and distinguished by input from memory-related areas in the rhesus monkey. *J. Comp. Neurol.* 410, 343–367. doi: 10.1002/(sici)1096-9861(19990802)410:3<343::aid-cne1<3.0.co;2-1

Barbas, H., Ghashghaei, H., Rempel-Clower, N., and Xiao, D. (2002). "Anatomic basis of functional specialization in prefrontal cortices in primates," in *Handbook of Neuropsychology*, ed. J. Grafman (Amsterdam: Elsevier Science)

Barbas, H., Zikopoulos, B., and Timbie, C. (2011).). Sensory pathways and emotional context for action in primate prefrontal cortex. *Biol. Psychiatry* 69, 1133–1139. doi: 10.1016/j.biopsych.2010.08.008

Barker, G. R. I., Banks, P. J., Scott, H., Ralph, G. S., Mitrophanous, K. A., Wong, L. F., et al. (2017). Separate elements of episodic memory subserved by distinct hippocampal-prefrontal connections. *Nat. Neurosci.* 20, 242–250. doi: 10.1038/nn.4472

Benjamini, Y., and Hochberg, Y. (1995). Controlling the false discovery rate: a practical and powerful approach to multiple testing. *J. R. Stat. Soc. B.* 57, 289–300.

Buckner, R. L., Andrews-Hanna, J. R., and Schacter, D. L. (2008). The brain's default network: anatomy, function, and relevance to disease. *Ann. N. Y. Acad. Sci.* 1124, 1–38. doi: 10.1196/annals.1440.011

Chang, E. F., Edwards, E., Nagarajan, S. S., Fogelson, N., Dalal, S. S., Canolty, R. T., et al. (2011). Cortical spatio-temporal dynamics underlying phonological target detection in humans. *J. Cogn. Neurosci.* 23, 1437–1446. doi: 10.1162/jocn.2010.21466

Destrieux, C., Fischl, B., Dale, A., and Halgren, E. (2010). Automatic parcellation of human cortical gyri and sulci using standard anatomical nomenclature. *Neuroimage* 53, 1–15. doi: 10.1016/j.neuroimage.2010.06.010

DeVito, L. M., and Eichenbaum, H. (2010). Distinct contributions of the hippocampus and medial prefrontal cortex to the "what-where-when" components of episodic-like memory in mice. *Behav. Brain Res.* 215, 318–325. doi: 10.1016/j.bbr.2009.09.014

Edwards, E., Soltani, M., Deouell, L. Y., Berger, M. S., and Knight, R. T. (2005). High gamma activity in response to deviant auditory stimuli recorded directly from human cortex. *J. Neurophysiol.* 94, 4269–4280. doi: 10.1152/jn.00324.2005

Eichenbaum, H. (2017). Prefrontal-hippocampal interactions in episodic memory. *Nat. Rev. Neurosci.* 18, 547–558. doi: 10.1038/nrn.2017.74

Foster, B. L., Dastjerdi, M., and Parvizi, J. (2012). Neural populations in human posteromedial cortex display opposing responses during memory and numerical processing. *Proc. Natl. Acad. Sci.* 109, 15514–15519. doi: 10.1073/pnas.1206580109

Fuster, J. M. (2008). *The Prefrontal Cortex*. New York: Academic Press

Glasser, M. F., Coalson, T. S., Robinson, E. C., Hacker, C. D., Harwell, J., Yacoub, E., et al. (2016). A multi-modal parcellation of human cerebral cortex. *Nature* 536, 171–178. doi: 10.1038/nature18933

Hanslmayr, S., Staresina, B. P., and Bowman, H. (2016). Oscillations and Episodic Memory: addressing the Synchronization/Desynchronization Conundrum. *Trends Neurosci.* 39, 16–25. doi: 10.1016/j.tins.2015.11.004

Ikegaya, N., Motoi, H., Iijima, K., Takayama, Y., Kambara, T., Sugiura, A., et al. (2019). Spatiotemporal dynamics of auditory and picture naming-related high-gamma modulations: a study of Japanese-speaking patients. *Clin. Neurophysiol.* 130, 1446–1454. doi: 10.1016/j.clinph.2019.04.008

Kaiser, J., Ripper, B., Birbaumer, N., and Lutzenberger, W. (2003). Dynamics of gamma-band activity in human magnetoencephalogram during auditory pattern working memory. *Neuroimage* 20, 816–827. doi: 10.1016/S1053-8119(03)00350-1

Kostopoulos, P., and Petrides, M. (2008). Left mid-ventrolateral prefrontal cortex: underlying principles of function. *Eur. J. Neurosci.* 27, 1037–1049. x doi: 10.1111/j.1460-9568.2008.06066

Long, N. M., Burke, J. F., and Kahana, M. J. (2014). Subsequent memory effect in intracranial and scalp EEG. *Neuroimage* 84, 488–494. doi: 10.1016/j.neuroimage.2013.08.052

Mandonnet, E., Dadoun, Y., Poisson, I., Madadaki, C., Froelich, S., and Lozeron, P. (2016). Axono-cortical evoked potentials: a proof-of-concept study. *Neurochirurgie* 62, 67–71. doi: 10.1016/j.neuchi.2015.09.003

Mandonnet, E., Winkler, P. A., and Duffau, H. (2010). Direct electrical stimulation as an input gate into brain functional networks: principles, advantages and limitations. *Acta Neurochir.* 152, 185–193. doi: 10.1007/s00701-009-0469-0

McDermott, K. B., Szpunar, K. K., and Christ, S. E. (2009). Laboratory-based and autobiographical retrieval tasks differ substantially in their neural substrates. *Neuropsychologia* 47, 2290–2298. doi: 10.1016/j.neuropsychologia.2008.12.025

Medalla, M., and Barbas, H. (2010). Anterior cingulate synapses in prefrontal areas 10 and 46 suggest differential influence in cognitive control. *J. Neurosci.* 30, 16068–16081. doi: 10.1523/JNEUROSCI.1773-10.2010

Micheyl, C., Carlyon, R. P., Gutschalk, A., Melcher, J. R., Oxenham, A. J., Rauschecker, J. P., et al. (2007). The role of auditory cortex in the formation of auditory streams. *Hear. Res.* 229, 116–131. doi: 10.1016/j.heares.2007.01.007

Nakai, Y., Jeong, J. W., Brown, E. C., Rothermel, R., Kojima, K., Kambara, T., et al. (2017). Three- and four-dimensional mapping of speech and language in patients with epilepsy. *Brain* 140, 1351–1370. doi: 10.1093/brain/awx051

Nourski, K. V., Steinschneider, M., McMurray, B., Kovach, C. K., Oya, H., Kawasaki, H., et al. (2014). Functional organization of human auditory cortex: investigation of response latencies through direct recordings. *Neuroimage* 101, 598–609. doi: 10.1016/j.neuroimage.2014.07.004

Pedersen, C. B., Mirz, F., Ovesen, T., Ishizu, K., Johannsen, P., Madsen, S., et al. (2000). Cortical centres underlying auditory temporal processing in humans: a PET study. *Audiology* 39, 30–37. doi: 10.3109/00206090009073052

Perrone-Bertolotti, M., Alexandre, S., Jobb, A. S., De Palma, L., Baciu, M., Mairesse, M. P., et al. (2020). Probabilistic mapping of language networks from

high frequency activity induced by direct electrical stimulation. *Hum. Brain Mapp.* 41, 4113–4126. doi: 10.1002/hbm.25112

Petrides, M. (2005). Lateral prefrontal cortex: architectonic and functional organization. *Philos. Trans. R. Soc. Lond. B Biol. Sci.* 360, 781–795. doi: 10.1098/rstb.2005.1631

Petrides, M., and Pandya, D. N. (1988). Association fiber pathways to the frontal cortex from the superior temporal region in the rhesus monkey. *J. Comp. Neurol.* 273, 52–66. doi: 10.1002/cne.902730106

Plakke, B., and Romanski, L. M. (2014). Auditory connections and functions of prefrontal cortex. *Front. Neurosci.* 8:199. doi: 10.3389/fnins.2014.00199

Rauschecker, J. P., and Tian, B. (2004). Processing of band-passed noise in the lateral auditory belt cortex of the rhesus monkey. *J. Neurophysiol.* 91, 2578–2589. doi: 10.1152/jn.00834.2003

Rauschecker, J. P., Tian, B., and Hauser, M. (1995). Processing of complex sounds in the macaque nonprimary auditory cortex. *Science* 268, 111–114. doi: 10.1126/science.7701330

Rauschecker, J. P., Tian, B., Pons, T., and Mishkin, M. (1997). Serial and parallel processing in rhesus monkey auditory cortex. *J. Comp. Neurol.* 382, 89–103.

Romanski, L. M., and Averbeck, B. B. (2009). The primate cortical auditory system and neural representation of conspecific vocalizations. *Annu. Rev. Neurosci.* 32, 315–346. doi: 10.1146/annurev.neuro.051508.135431

Romanski, L. M., Averbeck, B. B., and Diltz, M. (2005). Neural representation of vocalizations in the primate ventrolateral prefrontal cortex. *J. Neurophysiol.* 93, 734–747. doi: 10.1152/jn.00675.2004

Romanski, L. M., Bates, J. F., and Goldman-Rakic, P. S. (1999). Auditory belt and parabelt projections to the prefrontal cortex in the rhesus monkey. *J. Comp. Neurol.* 403, 141–157. doi: 10.1002/(sici)1096-9861(19990111)403:2<141::aid-cne1>3.0.co;2-v

Romanski, L. M., and Goldman-Rakic, P. S. (2002). An auditory domain in primate prefrontal cortex. *Nat. Neurosci.* 5, 15–16. doi: 10.1038/nn781

Rugg, M. D., and Vilberg, K. L. (2013). Brain networks underlying episodic memory retrieval. *Curr. Opin. Neurobiol.* 23, 255–260. doi: 10.1016/j.conb.2012.11.005

Selimbeyoglu, A., and Parvizi, J. (2010). Electrical stimulation of the human brain: perceptual and behavioral phenomena reported in the old and new literature. *Front. Hum. Neurosci.* 4:46. doi: 10.3389/fnhum.2010.00046

Sestieri, C., Corbetta, M., Romani, G. L., and Shulman, G. L. (2011). Episodic memory retrieval, parietal cortex, and the default mode network: functional and topographic analyses. *J. Neurosci.* 31, 4407–4420. doi: 10.1523/JNEUROSCI.3335-10.2011

St Jacques, P. L., Kragel, P. A., and Rubin, D. C. (2011). Dynamic neural networks supporting memory retrieval. *Neuroimage* 57, 608–616. doi: 10.1016/j.neuroimage.2011.04.039

Svoboda, E., McKinnon, M. C., and Levine, B. (2006). The functional neuroanatomy of autobiographical memory: a meta-analysis. *Neuropsychologia* 44, 2189–2208. doi: 10.1016/j.neuropsychologia.2006.05.023

Westphal, A. J., Wang, S., and Rissman, J. (2017). Episodic Memory Retrieval Benefits from a Less Modular Brain Network Organization. *J. Neurosci.* 37, 3523–3531. doi: 10.1523/JNEUROSCI.2509-16.2017

Yeo, B. T., Krienen, F. M., Sepulcre, J., Sabuncu, M. R., Lashkari, D., Hollinshead, M., et al. (2011). The organization of the human cerebral cortex estimated by intrinsic functional connectivity. *J. Neurophysiol.* 106, 1125–1165. doi: 10.1152/jn.00338.2011

Frontiers in
Human Neuroscience

Bridges neuroscience and psychology to understand the human brain

The second most-cited journal in the field of psychology, that bridges research in psychology and neuroscience to advance our understanding of the human brain in both healthy and diseased states.

Discover the latest Research Topics

See more →

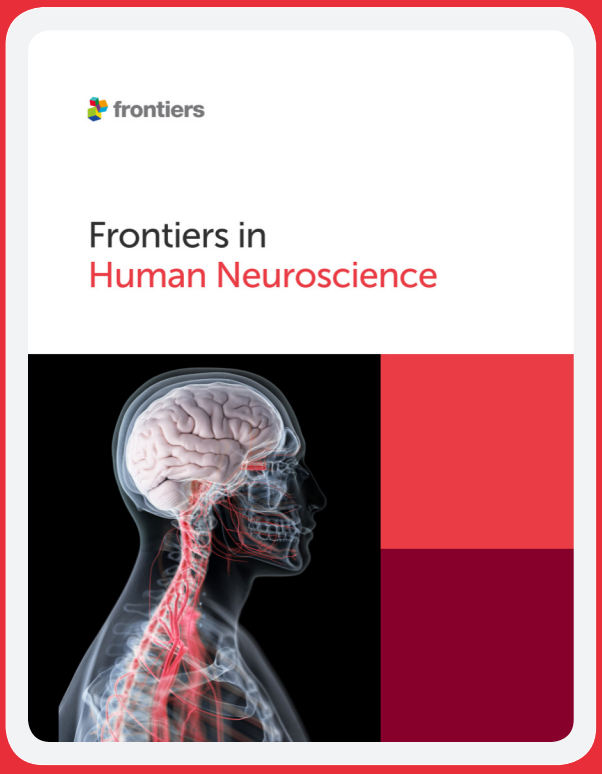

Frontiers

Avenue du Tribunal-Fédéral 34
1005 Lausanne, Swizerland
frontiersin.org

Contact us

+41 (0)21 510 17 00
frontiersin.org/about/contact